TELEVISION

Volume V

(1947-1948)

TELEVISION

Volume V

(1947-1948)

Edited by

ALFRED N. GOLDSMITH
ARTHUR F. VAN DYCK
ROBERT S. BURNAP
EDWARD T. DICKEY
GEORGE M. K. BAKER

AUGUST, 1950

Published by
RCA REVIEW
RADIO CORPORATION OF AMERICA
RCA LABORATORIES DIVISION
Princeton, New Jersey

Printed in U.S.A.

TELEVISION
RECEIVING
ANTENNA
(UHF)

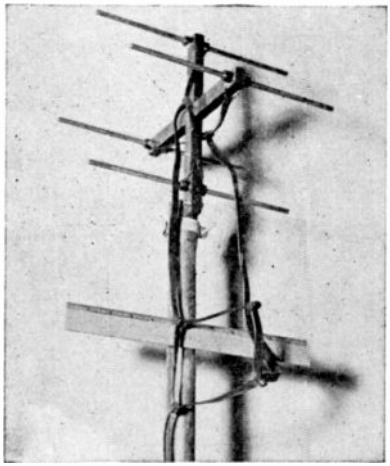

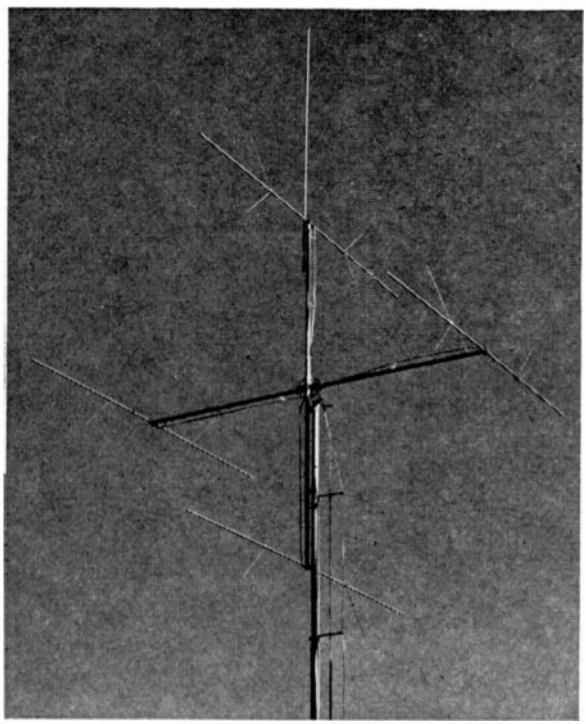

TELEVISION
RECEIVING
ANTENNA
(VHF)

TELEVISION, Volume V

PREFACE

TELEVISION, Volume V, covering the years 1947 and 1948, is the eleventh volume in the **RCA Technical Book Series**, and the fifth volume devoted exclusively to television. The first television volume was published in 1936 followed by Volume II in 1937. Volumes III and IV appeared in 1947.

Original plans called for the publication in 1950 of a volume covering the years 1947-1949. Because of the extraordinarily large amount of work done in television during this period, too many valuable papers would have had to be excluded for lack of space in a single volume. For this reason, two volumes are being published simultaneously, covering the periods 1947-1948 (TELEVISION, Vol. V) and 1949-June, 1950 (TELEVISION, Vol. VI).

Even with the two-volume presentation, the large number of excellent papers on the subject of television has made necessary a very stringent selection process. All the available material can not be included in full form. A number of papers are, therefore, presented herein in summary form only; it has been necessary to omit others entirely. Suitably balanced presentation of the various phases of television was the major criterion in deciding which papers to include in full and which in summary. The presentation of a paper in summary form (or the non-inclusion of any particular paper) is not intended to indicate any deficiency in technical accuracy, literary merit, or importance.

RCA Review gratefully acknowledges the courtesy of the Institute of Radio Engineers (*Proc. I.R.E.*), the Society of Motion Picture and Television Engineers (*Jour. Soc. Mot. Pic. Eng.*), the Byran-Davis Publishing Co., Inc. (*Communications*), Caldwell-Clements, Inc. (*Tele-Tech*), the Optical Society of America (*Jour. Opt. Soc. Amer.*), and the McGraw-Hill Publishing Co., Inc., (*Electronics*) in granting to RCA Review permission to republish material by RCA authors which has appeared in their publications. The appreciation of RCA Review is also extended to all authors whose papers appear herein.

The papers in this volume are presented in six sections: pickup, transmission, reception, color, UHF, and general.

RCA Laboratories
Princeton, N. J.
July 18, 1950

The Manager, RCA REVIEW

TELEVISION

Volume V

(1947-1948)

CONTENTS

Ultra-High-Frequencies

Color Television

Summary:

General

Summaries:

NEW TELEVISION FIELD-PICKUP EQUIPMENT EMPLOYING THE IMAGE ORTHICON*†

By

JOHN H. ROE

Engineering Products Department, RCA Victor Division, Camden, N. J.

Summary—A brief review of the characteristics of the more widely used types of electronic television pickup tubes traces the trend toward greater sensitivity, culminating in the image orthicon. This development results in the present-day ability to televise an unlimited variety of subject matter. Former restrictions imposed by requirements for large amounts of illumination have been almost entirely removed. An important by-product of higher sensitivity is the possible increase in depth of focus of the optical system.

Field or portable equipment has been designed to take advantage of the improved characteristics of the image orthicon. It is a design which lends itself to a maximum of flexibility for various types of operation, including use in studios and in mobile units. Most of the units are shaped like a medium-sized suitcase. The camera includes a four-position lens turret and an electronic view finder. Camera cables may be as much as 1000 feet long. Electrical interconnections are simple and few in number. Each of the major units is described in some detail, along with its function in the system. Discussion of some of the unusual circuits is included in the Appendix.

INTRODUCTION

IN EVERY ART, advances occur at intervals which serve as distinct milestones in the progress of that art. They are steps which overcome major limitations, and thus open up new fields which men have only dreamed about before. Such an advance has recently occurred in the art of television in the development of the image-orthicon pickup tube.

Television has made much progress in the past two decades in such things as higher definition, greater picture brilliance and size, greater immunity to interference in transmission, improved techniques in propagation, and the introduction of color on a laboratory scale. However, the requirement for intense illumination of the televised scene has dogged the industry from its inception up to the very recent past. This requirement has limited outdoor pickups to daylight hours with bright sunlight, and indoor pickups either to motion-picture film or to studios where enormous amounts of lighting on the order of 1000 to 1500 foot-candles could be provided.

* Decimal Classification: R583.6.
† Reprinted from *Proc. I.R.E.*, December, 1947.

The lighting equipment for such studios not only represents a large capital investment, but it entails excessive operating expense. Costly air-conditioning systems only partially alleviate the discomfort of performers, who literally have to "sweat it out" in scenes that cannot be retaken if things do not go right the first time. From the producer's point of view, such intense lighting produces flat, shadowless, uninteresting effects which greatly limit the artistic possibilities of the medium.

These conditions are always attendant on operation with the iconoscope as a pickup tube. The iconoscope itself is one of television's milestones because it introduced the storage principle to the art, made the system all-electronic, and thus brought television into a form which has commercial possibilities. It represented a big stride in sensitivity over previous nonstorage devices. However, its lack of sufficient sensitivity to operate satisfactorily outdoors in cloudy weather or in late-afternoon dusk, or indoors under moderate lighting, has been, and still is, its principal limitation.

The next step in the direction of greater sensitivity was the introduction in 1939 of low-velocity scanning in the RCA-1840 orthicon-type of pickup tube. It retained the storage principle and added a great improvement in efficiency with a corresponding improvement in sensitivity of the order of five times. This meant the possibility of reducing incident illumination to about 200 or 300 foot-candles.

Wartime development of military television equipment[1] accelerated work on a pickup tube which had its beginnings before the war started. The result of this work we know today as the image orthicon, a pickup tube which embodies the old principles of storage and low-velocity scanning, and, in addition, the principles of image-electron multiplication and signal-electron multiplication. The tube and the theories underlying its operation and incorporation into television cameras have been described in detail in recent literature.[2]

The image orthicon has as its most outstanding characteristic very great sensitivity, of the order of 100 times greater than that of the iconoscope. One of the most obvious and useful results of the high sensitivity of the tube is that, under medium or high illumination, the lens opening may be stopped down to a very small size, thus giving an enormous depth of focus. Even under relatively low illumination.

---

[1] A series of papers on military television developments appeared in *RCA Review*, Vol. 7, Nos. 3 and 4, September and December, 1946.

[2] A. Rose, P. K. Weimer, and H. B. Law, "The Image Orthicon—A Sensitive Television Pickup Tube", *Proc. I.R.E.*, Vol. 34, pp. 424-432, July, 1946.

the depth of focus of the image orthicon is much greater than that obtainable with less-sensitive tubes.

In contrast with the simple orthicon, the image orthicon has another outstanding characteristic; namely, its ability to accommodate a tremendous light range without serious loss of contrast. The scene illumination may be changed from dark shadows to bright sunlight and back again without losing essential picture information.

Other important characteristics are: (a) small target size, (b) small over-all tube size, and (c) high output signal level.

The small target area makes it possible to use relatively small lenses which lend themselves to a reasonable turret design. Lenses for such a field are readily available in a variety of focal lengths and apertures. The small size of the image orthicon is a factor of great importance in making the camera itself as compact and light as possible.

All previous types of standard pickup tubes have such low signal outputs that very high-gain amplifiers are required where shot noise in the first stage limits the signal-to-noise ratio. The image orthicon, in contrast to these, produces a high signal output, so that a comparatively low-gain amplifier may be used. Hence, shot noise in the amplifier is very low, compared with noise in the beam.

These characteristics have opened up a wide field of opportunities in television programming, such as night games under standard incandescent lighting, daytime athletic and other events lasting into late-afternoon shadows, and all sorts of special events at any time of day or night, as well as studio and theatrical shows with standard stage lighting, and a host of industrial and military applications.

Field-Pickup Equipment

First and most obvious application for the image orthicon is in field or remote-pickup equipment.[3] This type of equipment must be so designed that it can be transported quickly and easily and set up almost anywhere for operation with little more than a moment's notice. Usually, under such conditions, it is impossible to control the amount of illumination on the scene; hence, if it is to be truly useful, the pickup device must have sufficient sensitivity and range to function with the amount of light available at any time or place. The new field-pickup equipment being produced by the Radio Corporation of America has been designed to meet this need.

[3] R. E. Shelby and H. P. See, "Field Television", *RCA Review*, Vol. 7, pp. 77-93, March, 1946.

In the design, consideration has been given to the possible needs for using the field equipment under three different types of conditions. These are:

1. In temporary locations, inaccessible to vehicles, to which the equipment must be carried by hand.

2. In temporary locations accessible to vehicles where all of the equipment except the cameras may remain in a suitable mobile unit which serves as a control center.

3. In permanent locations where the equipment may be used for studio productions.

One of the first two of these conditions is encountered in every operation in the field. The third condition may exist in the case of a small broadcaster who wishes to begin studio operations with a minimum of capital investment. He may wish to use the same equipment for both field and studio work in case he is operating on a limited schedule which permits the necessary breaks for transporting the equipment. This third condition may also apply to the ambitious broadcaster who, like many in these times, is unable to obtain any other type of equipment immediately, and who, in spite of this, wishes to get the training of technical and program personnel under way for more extensive operations in the future.

These conditions, together with electrical considerations, dictate in large measure how the equipment should be divided into units. Each unit should be small and light enough to be carried by one man. On the other hand, the number of units must be kept to a reasonable minimum in order to facilitate assembling and disassembling in the field. The shape of the units must permit easy handling, and also permit setting them side by side on a bench or table so that the assembly of units has the general appearance and utility of a console. Simple and rapid means of electrical interconnection are a further requirement. To meet these requirements, most of the major units of the field equipment have been housed in cases resembling a medium-sized suitcase in both shape and dimensions. Cameras, view finders, and master monitors have special requirements which necessitate deviations from this standard shape.

The block diagram of Figure 1 shows the arrangement of major units required to make up a system of field-pickup equipment consisting of two or more cameras, with necessary switching facilities, radio relaying, and a mobile unit. It includes also a simplified schematic diagram of the interconnections. The two large upper-left-hand blocks show the actual camera equipment required for a standard two-camera system. The third block below (in dotted lines) illustrates how addi-

tional cameras, up to a total of four, may be included in the system. The blocks (in solid lines) in the center and right-hand side of the diagram show equipment which is common to the entire system, whether it be composed of two, three, or four cameras, and which need not be duplicated when cameras are added to the system. The dotted block in the lower center of the diagram shows additional monitoring equipment which may be added to provide a second viewing position for an announcer, for visitors, or for other special purposes. In the case of single-camera operation, the switching equipment and auxiliary monitoring equipment are omitted.

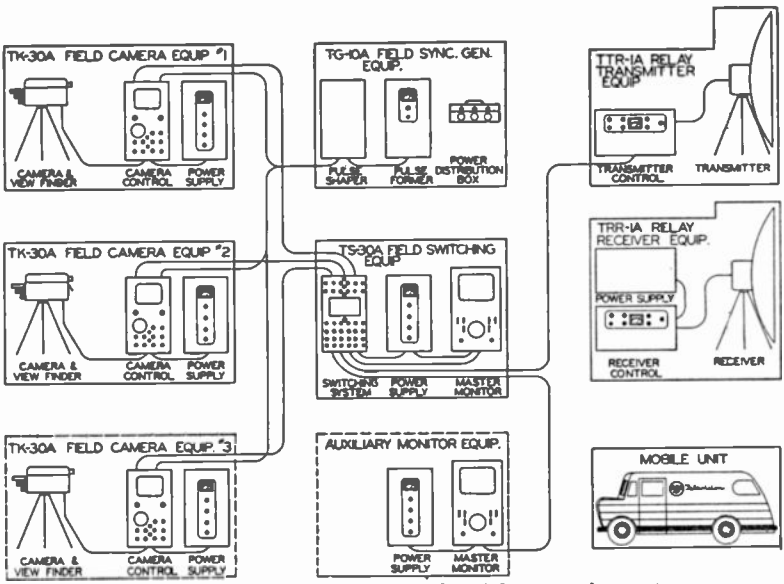

Fig. 1—Block diagram of field-pickup equipment.

The system illustrated provides a maximum of flexibility with a minimum number of separate units. As a system it provides many features which make for ease in operation and fine performance.

Figure 2 illustrates the equipment required for a two-camera setup, mounted on a desk such as may be used for studio operation. The units on top of the desk include two camera controls, a master monitor, and a switching system. These units contain all the controls normally required by the operators during the program. The other units under the desk are those which normally require little or no attention during program time. These units are the synchronizing generator and the power supplies.

Figure 3 shows the same equipment mounted in a similar manner in a mobile unit. Figure 4 is an external view of the mobile unit,

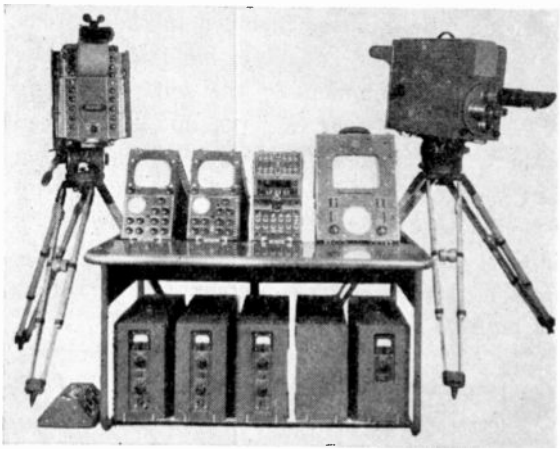

Fig. 2—Two-camera system including desk.

showing how access to the roof is provided through a hatch, and how a camera may be set up for operation on the roof. Sufficient space is also available on the roof for setting up a microwave relay transmitter. Storage space for a maximum of 1200 feet of camera cable is provided on reels with swing-out brackets at the rear of the mobile unit. The general plan of the mobile unit showing operating position and storage space for cameras, tripods, view finders, relay transmitter, sound-pickup equipment, and miscellaneous accessories, is illustrated in Figure 5.

CAMERA

Full advantage has been taken of the relatively small size of the image-orthicon tube in designing a compact camera. The dimensions of the case, including the cover, but without lenses or view finder,

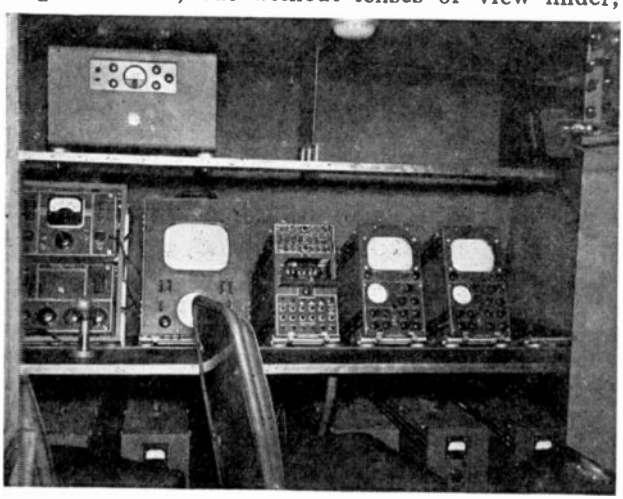

Fig. 3 — Installation of field equipment in the mobile unit.

Fig. 4 — Mobile unit in operation, with camera and relay transmitter on the roof.

are 20×10½×11¼ inches, and the weight is 65 pounds (see Figures 2 and 9).

The principal features of the camera are as follows:

1. Image-orthicon pickup tube.
2. Completely self-contained deflection circuits.
3. A four-position lens turret with rear control for quick change of lenses.
4. Miniature tubes in picture preamplifier.
5. Small, flexible camera cable.
6. Operation over a long cable (up to 1000 feet).
7. Forced-air ventilation.
8. Accessibility for servicing.
9. Rugged mechanical construction.

Though the use of lens turrets is well known on photographic cameras, their application to television cameras has not been attempted before, mainly because the lenses required for iconoscope and orthicon cameras are too large and heavy for a suitable turret mechanism. Furthermore, the use of optical viewfinders on many such cameras, requiring matched pairs of lenses, at least doubles the difficulties of turret design.

The useful photocathode area of the image orthicon is a rectangle 0.96 inch in height by 1.28 inches in width. Since this is approximately the same size as the frame of many miniature photographic cameras which use 35-millimeter film, it is possible to use lenses designed for such cameras. The Kodak Ektar lenses for the Ektar camera provide a useful series of focal length which has been applied to the image

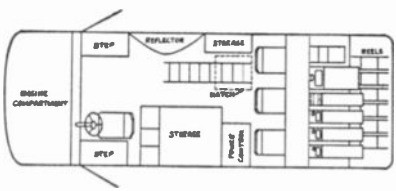

Fig. 5—Plan diagram of the mobile unit.

orthicon camera. Available lenses include 50-, 90-, and 135-millimeter focal lengths. These lenses are light in weight and are excellent for turret operation. Special lightweight lenses up to 25 inches in focal length and with *f*/5 apertures have been constructed using achromats in black bakelite barrels with quick-change slotted mountings. These weigh only 2 to 3 pounds and may be attached to the turret (see Figure 2).

The four-position turret is mounted on a hollow shaft which extends through the camera to a control handle and indexing mechanism in the rear at the operator's position. Releasing the indexing detent automatically cuts off the picture signal while the turret is being rotated to another position.

Optical focusing is accomplished in a novel manner by moving the pickup tube, along with its focus and deflection-coil assembly, instead of by motion of the lens. The mechanism is self-locking in any position

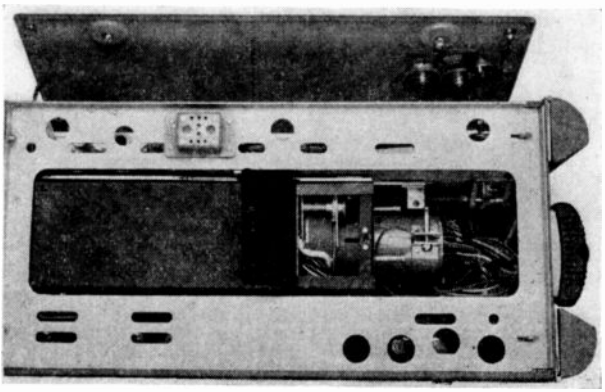

Fig. 6—Top view of camera, showing coil assembly.

of the camera. The greatest advantage in this system is the obvious simplification of the turret. A second important advantage is the increased range of focus obtainable when lenses with individual focusing mounts (such as the Ektar lenses) are used. The total available relative motion between lens and target is then the sum of the individual motions. A further advantage of the individual focusing mounts is that lenses of different focal lengths may be preset to focus on the same scene, thus eliminating the need for adjusting optical focus after rotation of the turret.

Figure 6 shows a top view of the camera in which the coil assembly and magnetic shield are exposed. The coil assembly is supported on a steel plate which moves on three rollers. At the rear of the compartment may be seen the focusing drive screw and the wiring to the base of the image orthicon. A small trap door at the rear end of the mag-

netic shield box exposes the cross field or alignment coil and the gear drive used for rotating this coil.

Figure 7 shows the focus coil alone. This is a simple, random-wound solenoid long enough to enclose both the deflecting coils and the image section of the image orthicon tube with an overhang of about one-half inch at the front and one inch at the rear. The deflecting coil assembly, which is mounted within the focusing coil, is illustrated in Figure 8.

The deflection circuits are included in the camera in order to reduce the number of major units in the field equipment. To make the camera

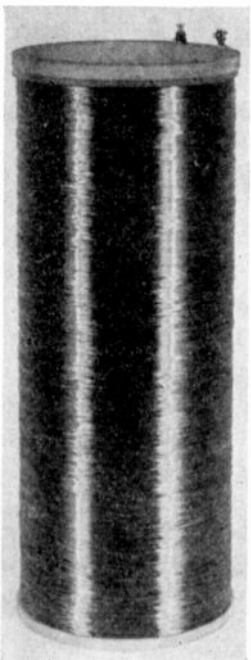

Fig. 7—Focus field coil for the image orthicon.

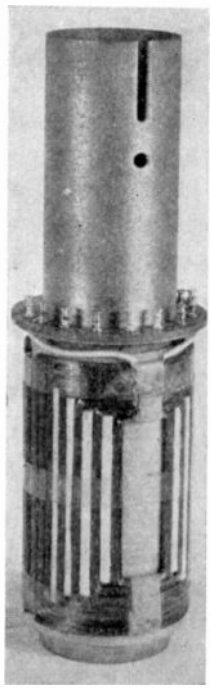

Fig. 8—Deflecting-coil assembly for the image orthicon (outer tube removed).

capable of operating over a long cable, it is necessary to locate the deflection generators either in the camera itself or in an auxiliary unit adjacent to the camera. Locating the deflection circuits and part of the picture preamplifier in an auxiliary unit makes it possible to keep the size and weight of the camera to a minimum. Such an arrangement, however, complicates the system by increasing the number of units, and hence the number of connecting cables and the time and effort required for setting up, dismantling, and transporting the equipment.

A further objection is that, in some field operations, an auxiliary unit is a serious nuisance, especially when the camera has to be set up on a small stage or platform where space is restricted. In the case of the image-orthicon camera, it is possible to include all of these circuits in the one unit without making the camera unreasonably large or heavy. With this arrangement, it is necessary to transmit over the cable only the timing information in the form of driving pulses. The transmission lines used for this purpose are easily terminated with resistors, and the pulses, which are not unduly critical as to wave form, are then easily amplified to usable levels.

The horizontal-deflection circuit, in common with similar circuits in other parts of the system, employs two new types of tubes, the 6BG6G and 6AS7G. The 6BG6G is similar to the 807, but has special characteristics for deflection output service. The 6AS7G is a twin triode, having very low plate resistance and large power capabilities. It is used as a damper or reversed-current output tube.

The horizontal retrace period is made about 10 per cent of the total horizontal scanning period, in order to avoid the necessity for artificial compensation for delay in long camera cables. The difference between the minimum kinescope blanking width (16 per cent) and this retrace is 6 per cent, or 3.8 microseconds. This is just slightly in excess of the time required for a round trip (2000 feet) in a 1000-foot cable.

The high voltage required for operating the image-orthicon tube totals about 2000 volts, —500 volts required in the image section and +1500 volts in the signal multiplier. This is generated by amplifying and rectifying the pulse signal that appears across the horizontal deflecting coils. Negative pulses are partially integrated and fed to the grid of a 6V6GT amplifier with its plate coupled to the primary of a special step-up transformer. The screen and cathode circuits of this amplifier are made degenerative in such a way as to compound the plate current. As a result, the peak plate current at the beginning of each retrace period is constant over a two-to-one range of pulse input to the grid. Thus the voltage fed to the rectifier is nearly independent of the horizontal scanning amplitude (width). The high-voltage transformer includes a small heater winding for the filament of a type 1B3/8016 rectifier. Suitable voltages for the various electrodes in the image orthicon are obtained from a filtered bleeder.

Negative feedback is employed in the vertical-deflection circuit by deriving a voltage from the drop across a small resistor in series with the deflecting coils and, after amplification, injecting the feedback signal into the plate circuit of the first sawtooth-amplifier stage. This feedback does two important things. It eliminates almost entirely the

effect of iron saturation in the transformer core and nonlinearities in the amplifiers. It also minimizes the effect of varying tube characteristics, and makes the vertical scanning linearity largely independent of amplitude.

Blanking signal for the target in the image orthicon is derived from the horizontal and vertical driving signals by mixing.

Controls associated with the scanning circuits are all located in the camera. These include height, width, centering, and linearity controls. Other controls also located in the camera are preamplifier gain, image accelerator, orthicon decelerator, and horizontal shading. None of these controls requires attention during actual operation, and hence the camera man is left free to aim the camera and focus the optical system.

The picture signal is amplified in a five-stage preamplifier built into the camera. The preamplifier employs miniature tubes and circuits compensated to give uniform output up to approximately 8 megacycles. The cathode follower in the final stage serves to feed the signal over a coaxial transmission line to the camera control, and also to provide signal for operation of an electronic view finder which may be used with the camera.

Components in all parts of the camera are accessible for servicing, and can be removed easily in case replacement becomes necessary.

A single camera cable contains all the electrical connections to the camera. It includes three 50-ohm coaxial transmission lines and 21 other conductors used for power, control, and communication. The cable is unusually small in diameter (0.84 inch) and light in weight.

View Finder

Television cameras have been equipped in the past with a wide variety of view finders, ranging from two screw heads used as rifle sights, through wire frames and double-lens systems, to electronic finders in which the scene is reproduced on small kinescopes mounted beside or above the cameras. Each type has advantages, but no one type has all the desired characteristics. In the cases of iconoscope and orthicon cameras, the optical view finder employing a second lens identical with the camera lens has enjoyed the greatest popularity because it not only serves to indicate focus, but is capable of including portions of the scene outside of those actually being televised. This has been considered important because the camera man can see and avoid unwanted objects before they intrude themselves in the picture.

In the case of the image-orthicon camera, the double-lens type of optical finder becomes completely useless when the equipment is used

under limiting low-light conditions. This is true because the image orthicon can operate with such low illumination that the image on a ground-glass screen is nearly invisible. Thus the electronic view finder is the only remaining type capable of indicating both focus and the outline of the scene. It has two distinct advantages over the optical system. It is entirely free of parallax errors, and it provides an erect image where a single-lens direct optical finder provides an inverted image. The electronic view finder has a disadvantage in that it cannot include anything outside of the televised scene.

The view finder designed to be used with the image-orthicon camera employs a flat-faced 5-inch kinescope tube (type 5FP4) with about 7000 volts on the second anode. This arrangement provides a picture with sufficient brilliance to be seen readily under bright ambient light. The view finder is constructed as a separate unit to be mounted on top

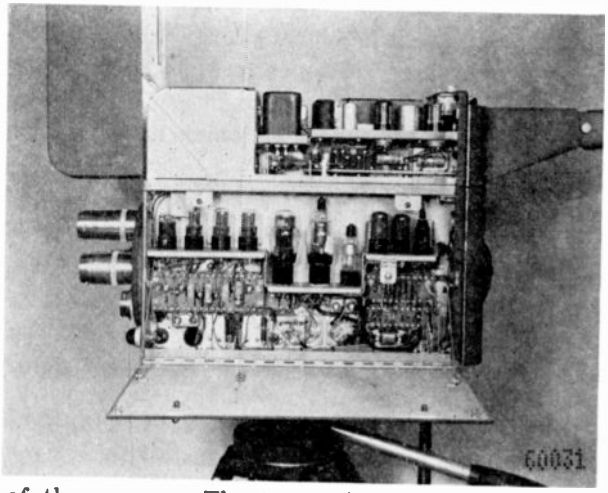

Fig. 9 — Deflection-amplifier side of the camera and view finder (internal view).

of the camera. The two units are styled to appear as a single unit when thus assembled.

The physical arrangement is such that the kinescope faces the operator at the rear of the camera. The face of the tube may be shaded with either of two types of viewing hoods. One of these includes two mirrors in a periscopic arrangement which may be reversed so that the operator's eye level is either above or below the kinescope, depending on the height of the camera. The other hood provides a direct view of the kinescope. A single cover opens on a hinge at the front, exposing the entire internal assembly (see Figure 9).

The circuits include the picture and blanking amplifiers required to drive the kinescope, and also the deflection generators and high-voltage supply. The latter is a pulse type of supply associated with the

horizontal-deflection circuit. Necessary controls are accessible at the rear in line with the operating controls on the camera. All electrical connections are made through a multicontact plug and receptacle (see Figure 6).

An auxiliary view finder in the form of a polaroid ring sight may be mounted on top of the periscope viewing hood (Figure 2), or, in the absence of the electronic view finder, on the camera itself. This ring sight produces a series of concentric spectral interference rings which appear to be at a considerable distance in front of the sight. Because they appear at a distance, the eye can observe the rings and the scene simultaneously with a minimum of strain. This device is useful in following action which moves too rapidly and too far to be followed readily on the kinescope. Its usefulness is limited, however, because it does not indicate either correct focus adjustment or the boundaries of the scene. It is simply an aiming device.

Camera Control

The camera control (Figure 1) is a unit which performs all of the functions not already performed in the camera itself that are necessary to the production of a complete composite picture signal. These functions include:

1. Amplification of the picture signal to the standard level required for feeding outgoing lines.
2. Addition of kinescope blanking signal.
3. Establishment and maintenance of the peaks of the blanking pulses at true "black" level.
4. Addition of the receiver synchronizing (sync.) signal in cases where only a single camera is in use.
5. Monitoring of the finished picture signal to check the accuracy of optical and electrical focus in the camera and the general quality of performance of the camera chain by means of the following:
   (a) A picture monitor tube (kinescope) which reproduces the scene being televised.
   (b) A wave-form monitor tube (cathode-ray oscilloscope) which shows the wave form of the picture signal and measures the amplitude of this signal.
6. Controlling electrical focus and other parameters involved in operation of the image-orthicon tube in the camera.

From consideration of these six functions it is apparent that the camera control is necessarily a complex unit, for it includes all the

circuits and components found in that part of a television receiver which follows the second detector, also those required for a wide-band cathode-ray oscilloscope, and, in addition, amplifiers, special circuits and controls, and cable connectors required directly for operation of the camera.

As indicated previously, the shape of the camera control is that of a medium-size suitcase, the dimensions being approximately 8×15×24 inches (Figures 2, 10, and 11), and the weight about 65 pounds. The chassis and case are spot-welded into a rigid, durable assembly. The kinescope (type 7CP4), the cathode-ray oscilloscope tube (type 3KP1), and the most important controls are mounted on the front end of the case. All small tubes, capacitors, and transformers are mounted on one

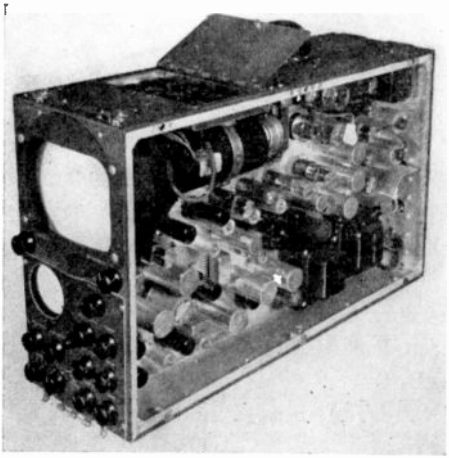

Fig. 10—Field-camera control.

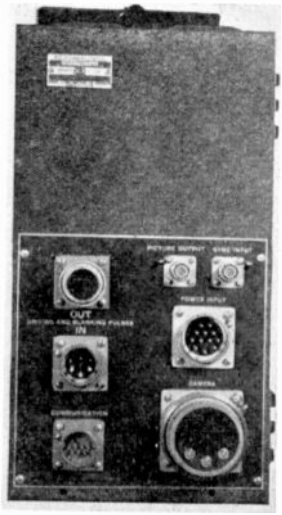

Fig. 11 — Rear of camera control.

side of the chassis, with wiring on the opposite side. Controls of secondary importance are mounted under a trap door in the top of the case. Past experience and a good deal of thought have produced a chassis layout which provides a maximum of accessibility for servicing, and at the same time a system for rigid, vibration-proof mounting of components which contributes much to trouble-free operation. A removable metal cover protects the cathode-ray tubes and controls during transportation. The two side panels or covers are easily removed by releasing three cowl fasteners at the top of each, and lifting them from three spring retainers at the bottom. All external electrical connections are made through plugs and receptacles on the rear of the case (Figure

11). This same general construction is followed in the other suitcase units described hereinafter.

The circuits in the camera control include:

1. The picture amplifier, with stages for mixing kinescope blanking and synchronizing pulses.
2. A picture amplifier for the monitor kinescope.
3. A picture amplifier for the cathode-ray oscilloscope tube (for vertical deflection).
4. Deflection circuits for both cathode-ray tubes.
5. Distribution amplifiers for feeding driving pulses to the camera.
6. A filament transformer.
7. A high-voltage transformer, rectifier, and filter for the cathode-ray tubes.
8. Camera circuit controls.
9. "On-the-air" tally and intercommunication system.
10. Remote power control.

The picture amplifier consists of several stages of types 6AC7 and 6AG7 tubes in conventional frequency-compensated circuits. One stage in this amplifier performs the very important function of establishing the peaks of blanking at "black level." To do this, the control grid is clamped at the end of each scanning line to an arbitrary reference potential. Because the target in the image orthicon is blanked during the scanning retrace (i.e., made sufficiently negative to repel the scanning beam) the picture signal from the camera during this retrace period is fixed with respect to black level, though it may vary continuously with respect to an arbitrary fixed reference because of the addition of hum, power-supply surges, or other spurious signals. The clamping action serves to set up a fixed relationship between the actual black level in the retrace periods of the picture signal and the arbitrary reference by connecting the control grid mentioned above to the reference potential through a very low impedance. At all times, except during the retrace periods, the grid is disconnected from the reference, and thus is free to follow the normal potential variations in the picture signal.

An important by-product of this clamping action is the elimination of the low-frequency components of any spurious signals, provided they do not have sufficient magnitude to cause amplitude modulation in any preceding stage. Hence, the clamp circuit removes power-supply surges and low-frequency hum, and minimizes microphonics. In fact, it limits the amplitude of any spurious additive signal to the amount which

occurs in the period of one scanning line. (For a more detailed description of clamping, see the Appendix.)

Kinescope blanking is mixed with the camera signal just ahead of the clamper. It provides undistorted, noise-free blanking intervals by the addition of independent, carefully controlled pulses. Since this added blanking is constant in amplitude, it does not affect the clamping action in any way except to shift the constant relationship between black level and the reference to a different constant value. After clamping, the combined camera and blanking signal is clipped near black level, thus producing a final signal in which the peaks of blanking bear a definite relationship to black level. The clipper makes use of a diode as a switch in series with the picture signal circuit. It depends for its accuracy in maintaining black level on the clamping which precedes it. This clipper is somewhat more complicated than the usual plate-current-cutoff type of clipper, but is justified because it cuts off very abruptly and is almost perfectly linear in the neighborhood of cutoff. (See Appendix.) A manual control (BLANKING) adjusts the clipping level to any desired point near black level, and thereafter the circuit maintains clipping at that level. Usually the clipper is adjusted so that the peaks of the blanking pulses are slightly "blacker than black," thus assuring complete removal of the retrace lines in receiver kinescopes.

DC restoring circuits maintain black level (or sync. peaks when sync. is present in the output) on the grid of the kinescope and on the grids of several stages where it is important to minimize distortion.

Deflection circuits for the kinescope are of the driven type. These circuits are of the same general kind as those used in the camera described previously, the only differences being in the deflecting-coil design and matching transformers.

Seven electrical controls, grouped on the front panel, provide for maintenance of proper operating conditions in the camera and associated picture-amplifier circuits in the camera control during the program. These are: (1) GAIN, (2) BLANKING, (3) BEAM CURRENT (ORTH.), (4) ORTHICON FOCUS, (5) IMAGE FOCUS, (6) TARGET POTENTIAL, and (7) MULTIPLIER FOCUS.

Only the first two of these require frequent checking during operation. However, the others are easily available to the operator at the camera control without the need of distracting the attention of the camera man, who is occupied with his normal duties. Location of these controls in the camera control is particularly useful in the process of making adjustments when a new image orthicon tube is installed in the camera, because the number of adjustments to be made in the

camera itself is reduced to a minimum. Controls of secondary importance, such as size and centering for the kinescope and cathode-ray oscilloscope, are located under a small trap door on top and near the front of the unit, easily accessible to the operator.

Plate current for all of the amplifier tubes is obtained from a regulated power supply entirely separate from the camera control. A power switch on the front panel of the camera control actuates a relay in the power supply which, in turn, opens or closes the power-input circuit for the entire camera chain.

Power Supply

The problem of providing the large amount of highly stabilized direct current required for the large number of amplifier tubes in a camera chain has been solved in a unique way in the field power supply. The problem resolves itself into one of finding means to reduce the weight of the unit to a point where one person can carry it. The difficulty may be understood when it is pointed out that the total plate-current drain in a single camera chain is approximately 1 ampere at 285 volts, regulated within limits of less than ±0.5 volt. The regulation does not constitute the major part of the problem, but simply adds to it by increasing the total voltage required from the rectifier.

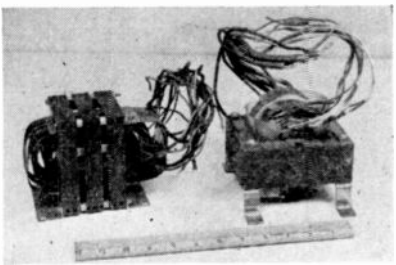

Fig. 12—(Left) Prewar design of a forced-air-cooled power transformer. (Right) New design.

The general attack on this problem was developed several years ago in the design of portable television equipment for the type-1840 orthicon.[4] A very lightweight transformer with the core divided into sections, with large openings in the end turns of the windings and with only a small fraction of the usual amount of iron and copper, was designed to be used with a continuous blast of air through the openings (Figure 12). This transformer, together with the blower and motor, weighed less than 20 pounds, and the entire power supply, including case, transformer, blower, tubes, and other components, weighed only 58 pounds. This design achieved the required objective, and gave reasonably good service in field use for several years.

In the field power supply for the image-orthicon equipment, a new

[4] M. A. Trainer, "Orthicon Portable Television Equipment", *Proc. I.R.E.*, Vol. 30, pp. 15-19, January, 1942.

and much improved transformer has been developed by making use of silicone enamel on the wire and glass fabric impregnated with silicone varnish for insulation between layers of the windings. The core is not sectionalized, and the windings are tight, as in conventional transformers (Figure 12). The running temperature may be as high as 180 degrees centigrade without danger of deterioration. As a result of this design, the over-all weight of the field power supply has been kept the same as in the earlier model, and the reliability has been increased.

New regulator tubes have made possible an improvement in efficiency. The type 6AS7G, a heavy-duty twin triode with extremely low plate resistance and the ability to dissipate 25 watts, is used for series regulation. This is the same tube that is used as a damper in the horizontal-deflection circuits. These tubes have appreciably less voltage drop than other types previously used in such service, and hence are more efficient. They also have very high transconductance, and therefore provide improved regulation control.

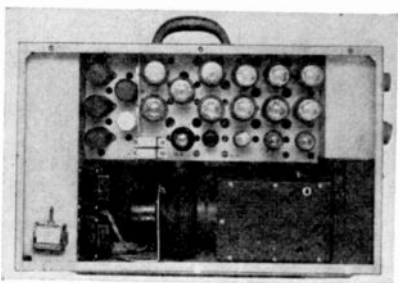

Fig. 13—Field power supply, tube side.

The rectifier is connected to a two-stage choke-input filter using electrolytic capacitors, through a thermal time-delay relay which prevents application of the high direct-current voltage until all tube heaters have attained operating temperature.

A 6SL7GT tube functions as a two-stage control amplifier, and two OD3/VR150 tubes serve as voltage references.

The field power supply is capable of delivering 950 milliamperes at 285 volts continuously to the main load, and, in addition, 75 milliamperes to the focusing field coil in the camera. This latter supply is current-stabilized so that changes in the resistance of the coil do not change the current. Figure 13 is a side view of the field power supply, showing the transformer housing, blower, and tubes.

The primary power circuit includes means for switching and metering of taps, so that a wide range of supply voltage may be accommodated. Provision is also made for metering currents and voltages in parts of the output system.

Synchronizing Generator

The new field synchronizing generator, which is part of the image-orthicon equipment, is designed on the same basic principles as earlier models, but improvements and new features have been added which make its performance the equal in every respect of that of the studio type of generator. Equality of performance is obviously necessary, especially in view of the increasing importance of field operations in television programming.

The field synchronizing generator comprises two suitcase units having the same size and shape as the field camera control. They are called the field pulse former and field pulse shaper, respectively. These two units generate four distinct signals for operation of the entire television system, including the receivers. All four signals, though different in wave shape, are accurately synchronized with each other by being derived from a single primary frequency source. Two of these signals appear directly in the composite picture signal which modulates the radio-frequency carrier. They are "kinescope blanking" and "synchronizing" (or "sync."), respectively. The wave shapes of these two signals are specified completely in standards recommended by the Radio Manufacturers Association.[5] The remaining two signals, "horizontal driving" and "vertical driving," respectively, are simple pulse signals used locally in the pickup equipment for triggering camera and monitor scanning circuits, and for target blanking and clamp-circuit keying.

The principles underlying the operation of this generator have been described fully in a previous publication.[6] No basic changes have been made in the arrangement of circuits, but refinements have been included to increase the stability of the primary frequency source and also to improve the steepness of wave fronts in the outputs. Among these, specifically, are a crystal oscillator which may be used in locations where the power supply frequency is unstable, an improved automatic-frequency-control circuit for lock-in with a 60-cycle power supply, an additional counter to reduce the maximum number of steps in any given counter, and a cathode-ray-tube indicator to provide a means of quickly checking the operation of the counters.

One of the two units includes a built-in regulated power supply, thus making the synchronizing generator completely self-contained in

---

[5] "Synchronizing Generator Waveforms", a drawing compiled by the Subcommittee on Studio Facilities of the RMA (revised, October 9, 1946).

[6] A. V. Bedford and J. P. Smith, "A Precision Television Synchronizing Signal Generator", *RCA Review*, Vol. 5, pp. 51-69, July, 1940.

the two units. Separation of the circuits occurs at a point where only three signals require connections between units. A single multiconductor cable connects the pulse former to the pulse shaper. The only input to the pulse former is alternating-current power. Output from the pulse shaper is split in two cables, one a single coaxial line for synchronizing signals and the other a multiple coaxial cable for the other three signals. The two suitcases appearing in the lower right hand corner of Figure 2 are the pulse shaper and pulse former.

Switching System

One of the most important operations in television programming is that of switching from one camera to another. Switching must be accomplished smoothly without either interrupting or disturbing the receiver synchronizing, even momentarily. If precautions are not taken to avoid surges in switching, it is possible that the sync. may be clipped later in the system during the period of the surge. Some receivers are very sensitive to such interruptions. Cases have been known in the past where switching surges have been so large as to overload the transmitter and throw it off the air. It is not possible to experience such difficulties in properly designed television systems today because means are used to maintain constant black level at all points where surges are harmful. Since switching is likely to produce surges, it is desirable to eliminate them at this point. A successful means for accomplishing this is the clamp circuit which was described previously in the section on the camera control. This circuit restores the picture signal to some arbitrary reference level at the end of each scanning line; i.e., during the retrace or blanking period. It is independent of anything that

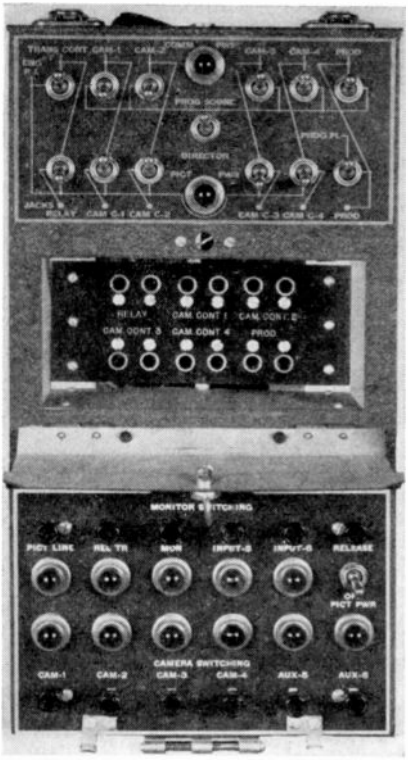

Fig. 14—Field switching system, front side.

takes place in the signal. Thus no surge can exist longer than the period of one line.

The field switching system is a suitcase unit of the same shape and size as the other units described previously (Figure 14). On the front panel are located two sets of push-button switches, the lower one of which provides for switching among four cameras and two auxiliary picture circuits. Each of these buttons has an associated tally light which operates in conjunction with tallies on the respective camera and camera control selected by it. These six switches connect six coaxial 75-ohm lines, one at a time, to the input of the picture amplifier contained in the unit.

The picture amplifier consists of three stages, the last one being a cathode follower which feeds the picture line to the relay transmitter, or a line directly to the main studio (75-ohm coaxial). A blocking capacitor separates the line from the cathode, so that no direct current flows in the line. The grid of this cathode follower is subjected to the action of the clamp circuit. Hence, no surges appear on the outgoing line.

Two other coaxial lines also provide signal to other parts of the system. One of these is connected to a line monitor, or field master monitor. It is fed through a separate unity-gain amplifier contained in the switching system. The input of this amplifier may be switched with the upper set of push buttons to any of several points in the pickup equipment. The second line may be used to feed an additional monitor for the use of spectators or an announcer, or it may feed a stand-by relay transmitter. All three output lines carry identical signals.

The synchronizing signal is mixed with the camera signal in the switching system to form the final composite picture signal. The synchronizing signal is supplied to the switching system directly from the pulse shaper, and is coupled to the picture output line through a two-stage amplifier. Thus, the synchronizing pulses are always transmitted independently of the camera switching. In cases where picture signal already including the synchronizing pulses is being received over one of the auxiliary input circuits, the local synchronizing signal may be disconnected by turning a special switch on the front panel.

Keying signal for the clamp circuit is derived from the sync. signal. In cases where the incoming signal includes sync., the sync. is separated, as in a receiver, and delayed so that keying is done on the "back porch," i.e., on the peaks of blanking just following the sync. pulses (see Appendix). In the usual case where the picture signal is received from a local camera chain, sync. is not present at the clamped grid;

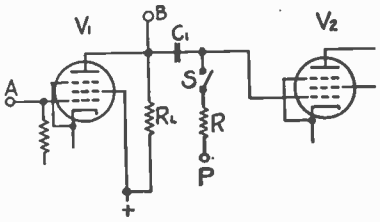

Fig. 16—Simplified schematic diagram of clamp circuit.

blanking in the receiver. This condition is illustrated in Figure 15(a). To provide clean-cut blanking pulses in the final signal, it is customary to add another blanking signal (Figure 15(b)) at a high-level point in the amplifier, giving the result shown in Figure 15(c). Then this composite signal is clipped at black level to give the signal shown in Figure 15(d). To insure proper operation of the receiver, the clipping must be done accurately at black level. Here the clamp circuit is an indispensable tool. It is used to bring about a firm correlation between the black level existing in the negative peaks of the camera blanking pulses and the grid bias on the clipper stage of the amplifier. It should be noted that the addition of a constant signal (such as the blanking signal shown in Figure 15(b)) does not affect the accuracy of the correlation between black level and clipper bias, but simply shifts the bias to a new value.

A simplified diagram of an amplifier controlled by a clamp circuit is shown in Figure 16. It consists of two amplifier tubes, V_1 and V_2, with a clamp circuit, consisting of the switch S in series with a small resistance R, connected to the control grid of V_2 on which it operates. Whenever the switch S closes, the grid of V_2 is established at the potential of terminal P (which is the arbitrary reference potential), provided that S is closed for a time interval that is long compared to the time constant $(R + R_L)C_1$. This latter condition is necessary for proper operation of the clamp circuit.

Assume that the camera signal of Figure 15(a) has been introduced at terminal A in Figure 16, and the blanking of Figure 15(b) at terminal B, but with polarities such that the resultant mixed signal as shown in Figure 15(c) appears on the plate of V_1. Now let the switch be closed for intervals such as m–m included within the peak of each camera blanking pulse, and let it be open the rest of the time.

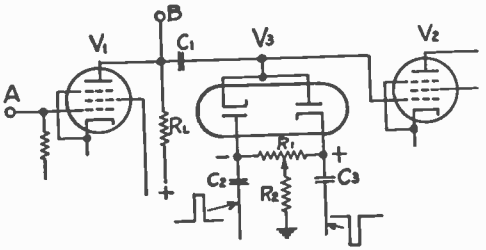

Fig. 17—Schematic diagram of clamp circuit.

Thus the grid of V_2 is established firmly at the potential P at each peak of the camera blanking. The tube, V_2, is made part of a clipper or limiter, hence, when P is set at the proper value with respect to the cutoff potential of the clipper grid, the clipping will take place at black level.

In actual practice, the switch is a pair of diodes (contained in the twin diode, V_3) which are keyed on and off by equal pulse signals of opposite polarity, as shown in Figure 17. These two pulse signals are coincident with each other and also with the time interval m–m in Figure 15(c). Thus, both diodes conduct simultaneously and provide a low-impedance path for current flow to change the charge on C_1. In this case, the critical time constant is

$$\left(R_L + \frac{R_D}{2} + R'\right) C_1$$

where R' is the effective resistance of the signal source which generates the keying pulses, and R_D is the effective resistance of one diode. In most cases, C_1 is made about 500 micromicrofarads and the total resistance about 2500 ohms. Hence, the time constant of the circuit is about 1.25 microseconds. Since the total keying interval is usually about 6 microseconds, there is time for the charge on C_1 to approach equilibrium.

In Figure 17, the reference potential is that which exists at the midpoint of R_1. This may be deduced as follows. During the keying-pulse intervals, both diodes conduct, and hence both terminals of R_1 are at the same potential. Because of this conduction, the equal capacitors, C_2 and C_3, receive opposite charges, each equal to the peak-to-peak voltage of the pulses. During the intervals between pulses, the diodes become nonconducting, and the charges placed on C_2 and C_3 cause a current to flow in R_1, producing a voltage drop equal to the sum of the pulse voltages on the two capacitors. The polarity of the voltage is shown in Figure 17. Since both the circuit and keying signals are balanced, it is then apparent that the diodes always arrive at a single potential during the pulse intervals which is the same as the potential existing at the midpoint of R_1 during the intervals between pulses. The time constant $C_2R_1 = C_3R_1$ is made very large compared to the period of the pulses, so that the current in R_1 is small; hence the charges on C_2 and C_3 remain essentially constant.

If R_1 is connected as a potentiometer, as shown in Figure 17, the reference potential (at the midpoint) may be shifted with respect to ground. For example, if the control is moved to the left, the midpoint

becomes positive with respect to ground. This control is an effective and useful means of adjusting the bias on the grid of the amplifier tube, V_2. Whenever the control is moved away from the midpoint, the circuit becomes unbalanced, and difficulty may be experienced in maintaining pulse shape, especially when the control is near one end of R_1. To minimize this effect, a resistor, R_2, may be inserted in the ground connection. Since the average current in such a resistor is always zero, it may have a very large resistance. Use of this control in no way disturbs the accuracy of the clamping action in establishing the grid of V_2 at the reference potential (midpoint of R_1).

The only path for charging current from the capacitor C_1 (in the absence of grid current in V_2), is through the clamp circuit. During the open-circuit intervals in the clamp circuit, it is therefore impossible for the charge on C_1 to change. Hence the low-frequency response of the coupling circuit between V_1 and V_2 is not attenuated even though the capacitance of C_1 be made very small.

It is important that the keying interval m-m shall come to an end *before* the end of the blanking pulse, so that the charge which is left on C_1 will always correspond to black level in the picture signal, and not to some other level existing in the signal after the blanking pulse.

A further consideration is necessary in determining the proper value for the time constant

$$\left(R_L + \frac{R_D}{2} + R'\right) C_1.$$

The peaks of the camera blanking pulses usually contain some high-frequency noise signal originating in the low-level parts of the signal system. The response of the charge on C_1 to the clamping action must be slow compared to the period of the noise signal, in order to avoid variations in the correlation between black level and the reference potential. Black level may be considered as the average of the noise signal. Hence the clamp must be slow enough to average out the noise. Since the resistive elements are usually determined by the requirements of the keying circuits, the value of C_1 is used to control the time constant. Values cited previously have been found to work well in most cases, though where the noise signal contains low-frequency components it may be necessary to use a larger value for C_1.

The chief advantage in the clamp circuit, as compared to other types of leveling or dc restoring circuits, is the fact that its action is entirely independent of the picture signal in the amplifier. It depends only on

the keying pulses. These may be controlled at will with respect to amplitude and timing. It should be noted that the amplitude of the keying pulses is usually made about twice the amplitude of the picture signal in the amplifier at the point where the clamp operates.

The ability to control the time at which the clamping is done is sometimes of great advantage. For example, in the field switching system, it is necessary to clamp the signal after the camera switching. At the point where the clamping is done, it is necessary to accommodate two types of picture signal: (a) from the cameras, in which case the sync. pulses are not present, since they are added subsequently, and (b) from an outside source which provides complete composite signal including the sync. pulses. Clamping must be done on the same level in both types of signal. Obviously, clamping cannot be done on the peaks of sync. in case (a); hence, it must be done on blanking peaks, or at true black level, which is present in both cases.

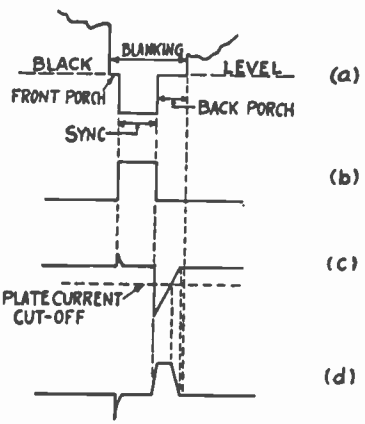

Fig. 18 — Derivation of keying pulses for back-porch clamping.

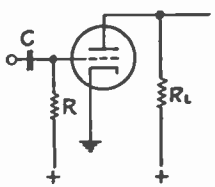

Fig. 19 — Schematic diagram of differentiating circuit.

In case (b), the only available space on which the clamp may operate at black level is that portion of the blanking pulse immediately following the sync. pulse, commonly called the "back porch" (see Figure 18). Keying pulses are derived from the sync. by separation as in a receiver, and subsequent forming. A sync. pulse after separation is shown in Figure 18(b). This separated signal is fed to the grid of a triode as in Figure 19. The capacitor C is made very small, about 20 micromicrofarads, and the grid leak R is connected to a positive voltage source. Before the leading edge of the pulse, it may be assumed that the grid is drawing current, hence is approximately at cathode potential. The positive excursion of the leading edge causes very little change in the grid potential because of the low impedance from grid to cathode. The resulting sharp exponential pulse is shown in Figure 18(c). After returning to its original potential, the grid is excited by the trailing

edge of the pulse in the negative direction. This excursion stops the flow of grid current and also swings far enough to go beyond plate-current cutoff, as illustrated. The signal voltage causes no further change, but the positive voltage on the grid leak immediately starts to recharge the capacitor C, and thus produces the positive slope shown in the diagram. The rise in grid voltage stops abruptly as soon as grid current starts to flow. The steepness of this slope is proportional to the positive bias voltage, and inversely proportional to the value of R. Hence the duration of this negative sawtooth may be adjusted by changing either the positive bias or the resistance of R.

The pulse of voltage appearing on the plate of the triode is shown in Figure 18(d). The leading edge of this pulse may be sloped a little to acquire some delay, by making R_L large and thus allowing the stray capacitance on the plate circuit to integrate the slope. Further clipping of this signal eliminates the negative "pip" caused by the leading edge of the original pulse, and makes it suitable for a keying signal in a clamp circuit to operate on the "back porch."

Examination of the functioning of this circuit during the serrated vertical pulse in the standard RMA sync. signal shows the formation of keying pulses which are timed to coincide with the slots in the vertical pulse. Thus keying of the clamp circuit at black level is carried on with no interruption throughout the vertical sync. pulse.

Use of this type of clamp circuit in the switching system eliminates surges introduced by switching, and also any surges and low-frequency additive cross talk from other sources which may have been introduced ahead of the clamping point. It further insures constant sync. output under all conditions of varying picture signal by confining the sync. pulses to a fixed portion of the e_g—i_p characteristic of the output stage.

Clipper Circuit

The clipping operation required in the process of correlating the peaks of blanking pulses with black level, illustrated in Figure 15, must be performed with rigid accuracy. In order to maintain the clipping level with the necessary accuracy, it is imperative that the critical electrode in the clipper stage be controlled by a clamp circuit, as described in the preceding paragraphs. When, as is usually the case, a screen-grid tube is used as a clipper, it is further necessary to supply current to the screen grid from a regulated source so that its potential does not change with variations in the average brightness of the scene. With these two precautions, any of the usual types of clipper will maintain the correct black level in the blanking pulses.

The clipper circuit used in the field equipment has unusual charac-

teristics which merit description. It is a circuit which was developed originally by K. R. Wendt[8] to overcome the inherent curvature near cutoff in the plate-current-cutoff type of clipper. Such curvature increases the gamma of the system. Since the orthicon type of camera tube has unity gamma, and the average kinescope has gamma in the neighborhood of 2, the resultant system gamma is higher than is ordinarily desired. Therefore, it is desirable to avoid increasing the gamma at any other point in the system.

The basic circuit (Figure 20) includes a pentode amplifier, V_2, which has for its principal plate load a resistor R_2 in series with a diode, V_4. An additional load, R_1, is connected in parallel with R_2 and V_4. R_1 is much larger than R_2. The diode acts as a peak limiter, pre-

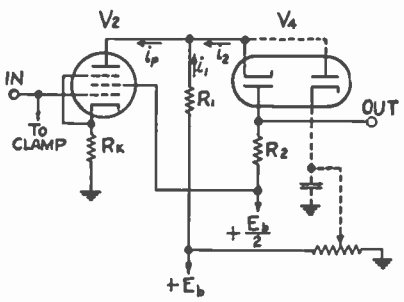

Fig. 20 — Schematic diagram of linear clipper.

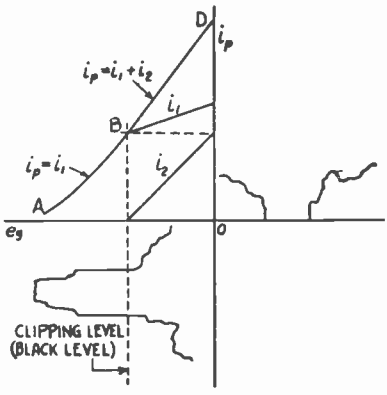

Fig. 21 — Characteristic curve of linear clipper.

venting the flow of current in R_2 whenever its cathode rises above the potential $E_b/2$. The tube, V_2, is the same as V_2 in the previous Figures 16 and 17, with its control grid connected to a clamp circuit. Both of the supply voltages shown, E_b and $E_b/2$, are closely regulated and have approximately the 2-to-1 relationship indicated. Under these conditions, black level will correspond to some definite value of plate current in V_2. By adjusting the clamp reference potential (equivalent to adjusting the bias on V_2) to the proper value, black level may be made to coincide with point B in Figure 21.

The curve A-B-D represents the normal e_g—i_p curve of V_2. From A to B, no current flows in R_2, and hence $i_p = i_1$. However, between B and D, current flows in V_4 and R_2, and hence i_p divides itself between R_1 and R_2. Therefore, $i_p = i_1 + i_2$ in this region of the curve. By proper

[8] RCA Laboratories, Princeton, N. J.

selection of the value of R_1, it is possible to place point B (cutoff point of the diode, V_4) so that B-D covers the linear portion of A-B-D. Then at all times the useful part of the picture signal swings only over this linear part of the tube characteristic. The curved portion of the characteristic from A to B is not used, and hence does not affect the gamma of the system.

It should be noted that the cutoff of this circuit is extremely abrupt. This arises from the fact that V_2 is a screen-grid tube having a very high plate resistance. In other words, the flow of plate current is not influenced appreciably when the external load resistance is changed by the opening of the diode. Therefore, as i_2 approaches zero, the ratio i_1/i_2 rises very rapidly, and, since R_1 is large (about 20 to 30 times R_2), the potential of the cathode of V_4 also rises very rapidly, carrying the diode abruptly through its cutoff region.

The diode limiter, V_4, has one serious fault; namely, its plate-cathode capacitance permits feed-through of unwanted parts of the signal — particularly, steep wavefronts involving high frequencies. This trouble may be largely nullified by the simple device of connecting a second diode (available in any of the twin diodes) across the plate circuit of V_2, as shown by the dotted lines in Figure 20. By proper adjustment of the bias control on this diode, it may be made to start conducting at a potential just above the cutoff potential of the limiter diode, thus causing a low-resistance shunt to appear across the signal source which effectively "squelches" the signal and prevents feed-through.

ACKNOWLEDGMENT

The equipment described in this paper is the result of the combined efforts of a large number of engineers with whom the writer has been associated during the past decade. Development of a workable system embracing so many complex circuits cannot be ascribed to the abilities and judgment of one or two, or even a few, persons. It is necessarily the product of the thinking of many individuals working collectively on the various problems. Among these are M. A. Trainer, W. J. Poch, H. N. Kozanowski, G. L. Beers, N. S. Bean, J. M. Brumbaugh, H. M. Potter, and F. E. Cone, of the RCA Victor Division, Radio Corporation of America, Camden, N. J., and R. D. Kell, A. V. Bedford, J. P. Smith, K. R. Wendt, and A. C. Schroeder of the RCA Laboratories Division, Radio Corporation of America, Princeton, N. J.

FILM PROJECTORS FOR TELEVISION*†

BY

RALPH V. LITTLE, JR.

RCA Victor Division,
Camden, N. J.

Summary

Television will make wide use of 35-mm and 16-mm motion picture film. The method of televising motion pictures using the storage-type pickup device is described. Theater and television projection practice are compared and methods of meeting proposed RMA Television Standards are discussed. Recently designed 16-mm and 35-mm RCA television projectors are described in detail.

(17 pages; 15 figures)

* Decimal Classification: R583.3.

† *Jour. Soc. Mot. Pic. Eng.*, February, 1947.

INTERLOCKED SCANNING FOR NETWORK TELEVISION*†

By

JAMES R. DE BAUN

Television Department, National Broadcasting Company, Inc., New York, N. Y.

Summary—The benefits of operating the scanning systems of two or more independent television broadcasting plants in locked coincidence are discussed. The problem of producing locked coincidence is explored, and methods of achieving the desired result are indicated. Some of the possible benefits of using stable (high inertia) frequency sources for scanning systems are noted.

BENEFITS OF INTERLOCKED SCANNING

THE desirability of maintaining continuity of synchronizing information on the television broadcast signal was recognized by the designers of early television plants, and the plants were so arranged that no interruption of the synchronizing signal occurred while switching between cameras or between local studios. However, no means for maintaining this continuity of synchronizing signal has evolved as yet for operational use when switching between local studios and remote pickup points or network programs where independent synchronizing signal generators are involved. To render less objectionable the attendant loss of synchronizing signal at receivers when such switches are made, it is usual practice to go to a dark screen before the switch is made and to fade up from a dark screen after the switch is completed. This allows time for synchronizing circuits in the receivers to lock in on the synchronizing signal transmitted after the switch before a picture reappears on the receiver, and hence the resultant disturbance of the image due to the momentary loss of the synchronizing signal is less noticeable. As an additional aid in bridging this gap in synchronizing signal continuity, it is good practice to have the 60-cycle components of the two synchronizing signals involved phased for approximate coincidence.

If complete time coincidence between the two signals (local and remote) could be maintained, it would be possible to preserve continuity of the transmitted synchronizing signal and thereby eliminate the necessity of going to a dark screen during switching, or, of checking and maintaining the vertical phasing of the two signals. From

* Decimal Classification: R583.13.
† Reprinted from *RCA Review*, December, 1947.

the standpoint of smooth program presentation, this is of importance because it is frequently necessary to switch between the local and remote pickups several times in the course of one program, particularly when presenting commercial announcements. In addition, if the local synchronizing signal is transmitted continuously on either the local or remote picture signal (this requires processing the remote signal to remove its synchronizing signal and adding the local synchronizing signal) the receivers are fed a relatively more noise-free synchronizing signal. Also made available between the local and remote signals are lap dissolves, super-impositions and all other processes normally available between local cameras or studios. As network television broadcasting grows, the foregoing aids to smooth presentation of programs assume increasing importance. Therefore, an analysis of what is involved in producing locked coincidence between a local and a remote signal is timely.

Requirements for Producing Interlocked Scanning

Complete coincidence is required between the local and remote signal to achieve the above benefits, and coincidence must therefore be on a line, field, and frame basis. This means that even fields must coincide with even fields, etc., and in the final analysis that each line of the 525 lines in a frame of one signal must coincide with its counterpart in the other signal. This complete matching is required before the local synchronizing signal can be used on the incoming signal and comply with FCC standards of transmission. If even and odd fields are matched and line blanking in the two signals coincide, the local synchronizing signal would align with the incoming signal as shown in Figure 1, where one line frequency synchronizing signal pulse (local) rests on the vertical blanking (remote), or one equalizing (2 times line frequency) pulse (local) rests on the last horizontal blanking (remote), or is lost in the video of the last line of alternate fields. When the required complete coincidence is obtained, the lock applied to maintain the coincidence must be quite rigid. Any hunting permitted by the lock would: first, render impossible the use of local synchronizing signal on the remote picture signal and hence, continuity of synchronizing signal transmission; and second, render ineffective the use of superimpositions and lap dissolves. The only gain in using a loosely-locked coincidence between the local and the remote signal lies in the fact that the vertical components of the two signals will remain approximately in phase and therefore the tendency for vertical scanning at receivers to lose synchronization momentarily following a switch will

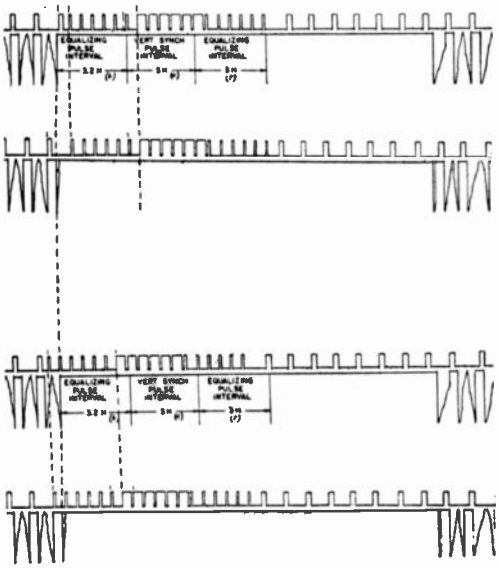

Fig. 1—Local synchronizing signal superimposed on a remote video signal showing the two possible conditions, both mis-matches, which can obtain when even vs. odd fields are locked in coincidence.

be reduced. Figure 2 serves to illustrate the coincidence required to achieve the desired results.

Methods of Achieving Interlocked Scanning

The block diagram of Figure 3 is an arrangement which has been used in "On the air" demonstrations of the operation of two independent television plants under conditions of "locked coincidence." While admittedly an experimental arrangement, it served to confirm the

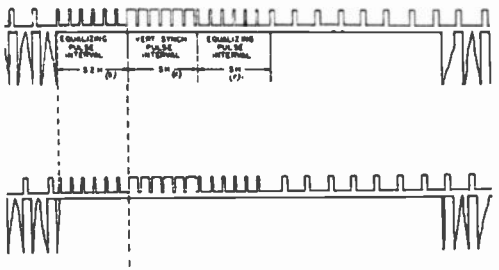

Fig. 2—Local synchronizing signal superimposed on a remote video signal showing the desired result which obtains when even vs. even fields are locked in coincidence.

possibility of realizing the benefits mentioned heretofore, and also to demonstrate effectively the program possibilities during the hours when election returns were coming in for a fall election, 1941. The regularly scheduled program on that occasion was wrestling from a sports arena via the Telemobile Unit. In the Radio City studios a camera was focused on a black-board upon which election returns were recorded. By using only the top of the black-board and by keeping the top of the picture from the Telemobile Unit relatively clear of action (normally the case) a superimposition of the election results upon the incoming sports picture provided the latest election returns without interrupting the sports event.

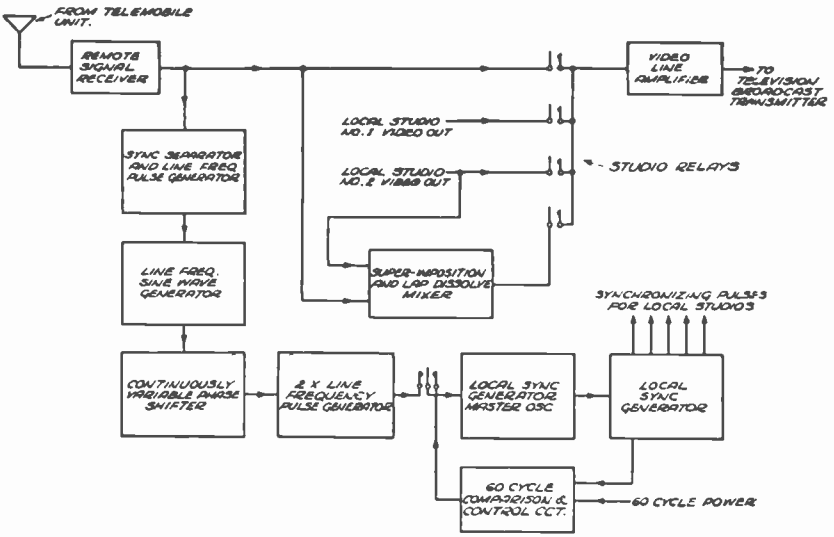

Fig. 3—Block diagram of equipment used to lock the local synchronizing signal generator with the incoming remote video signal.

Figure 4 is a schematic of the block diagram of Figure 3. The synchronizing signal separator and line frequency pulse generator are omitted, the former consisting merely of a conventional synchronizing signal separator, which drives a line frequency blocking oscillator. The line frequency sine wave generator has already been described.[1] The continuously-variable phase shifter made use of a rotating magnetic field and a pickup coil whose physical position could be advanced or retarded without limit in the rotating field. At the time of the demonstration the most convenient equipment for accomplishing this result

[1] R. A. Monfort and F. J. Somers, "Measurement of the Slope and Duration of Television Synchronizing Impulses," *RCA REVIEW*, Vol. VI, No. 3, pp. 370-389, January, 1942.

was a small Selsyn unit. The circuit for deriving the three-phase excitation for the Selsyn from the single phase output of the sine wave generator is shown in Figure 4. The resistance-capacitance components on the first grid of two of the legs are chosen to get the desired shift as indicated by the vectors. Following the continuously variable phase shifter the sine wave is processed to provide the locking information to the master oscillator of the local synchronizing generator. As stated before, the lock must be quite rigid before the desired benefits can be realized. In the demonstration referred to previously, the local synchronizing generator was a standard commercial unit.[2] The master

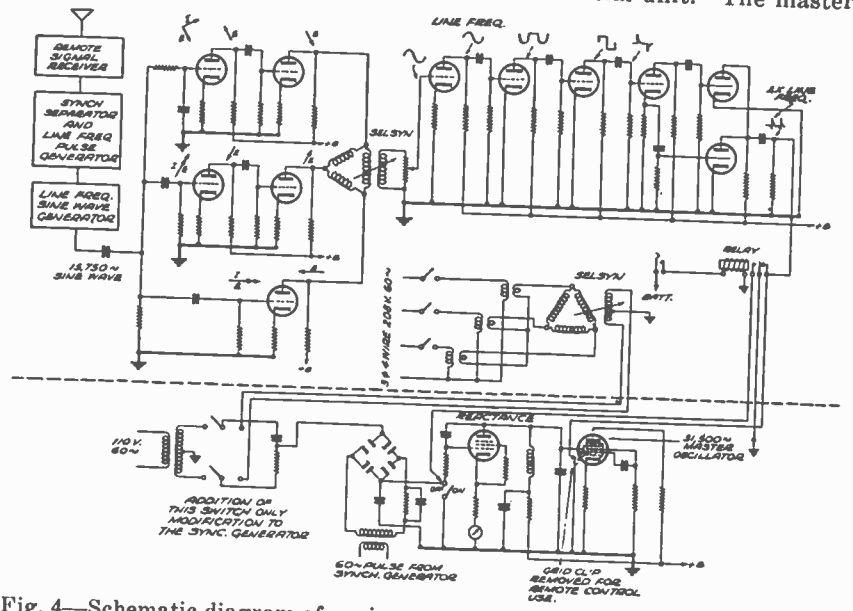

Fig. 4—Schematic diagram of equipment used to lock the local synchronizing ing signal generator against the incoming remote video signal.

oscillator in this unit is of the negative transconductance type and operates at twice line frequency. By trial and observation it was determined that control or lock of the desired degree of rigidity could be obtained by injecting a pulse of twice line frequency into the first grid of this master oscillator. Therefore, for the demonstration the processing required was the conversion of the line frequency sine wave output of the continuously variable phase shifter into twice line frequency pulses. This was accomplished by the symmetrical clipping of the sine wave to produce a symmetrical square wave which was in turn differentiated. A push-pull input into grid current biased grids

[2] A. V. Bedford and J. P. Smith, "A Precision Television Synchronizing Signal Generator", *RCA REVIEW*, Vol. V, No. 1, pp. 51-68, July, 1940.

of two tubes, the plates of which were in parallel, provided the desired result. An alternative and equally effective method would be the use of an unfiltered output from a full wave rectifier driven by the continuously-variable phase shifter.

The method of coupling this double frequency pulse into the master oscillator and of transferring the control of the local master oscillator from the 60-cycle power frequency to the incoming video signal is also indicated in Figure 4. No major modification of the local synchronizing generator was required, three clip leads from a relay clipped on at the proper points and the lifting of the grounded grid cap to the first grid of the master oscillator sufficing. However, it will be noted that the 60-cycle power into the comparison circuit which normally controls the master oscillator of the local generator was modified by the insertion of a continuously variable phase shifter. The same style Selsyn was used for both the 60-cycle and 15750-cycle phase shifters. The reason for this modification to the local generator is apparent when the task of securing coincidence between the two signals by the use of the line-frequency phase shifter alone is considered. A maximum of approximately 262½ revolutions of the line frequency phase shifter may be required if the control should be transferred to the remote signal when coincidence between an even field of one signal existed with an odd field of the other signal. It is much faster to use the 60-cycle phase shifter for rough setting of coincidence, transfer control, and finish the exact alignment of coincidence between the two signals by means of the line-frequency phase shifter.

For checking coincidence, the pulse cross unit, which was described in the paper on the sine wave generator,[1] provides an effective indicator. The local and incoming signals are mixed and applied to the pulse cross monitor and the phase shifters (60 and 15750 cycles) are adjusted to secure coincidence of the two signals on the pulse cross. Figure 5 shows blanking from one signal generator and synchronizing signal from another. There is lack of coincidence in terms of both line and field. Figure 6 shows coincidence for line but not for field. Figure 7 shows odd vs. even field coincidence. Note that one line frequency synchronizing signal pulse is sitting on the field frequency blanking. Figure 8 illustrates the same condition except the line frequency phase shifter has been rotated one revolution from the condition of Figure 7. Here an equalizing pulse is resting on the last line frequency blanking preceding field blanking. Figure 9 shows even field vs. even field coincidence.

Figure 9 is the same as Figures 7 and 8 except one signal is shifted through 262½ lines. Any hunting between signals is readily discerned

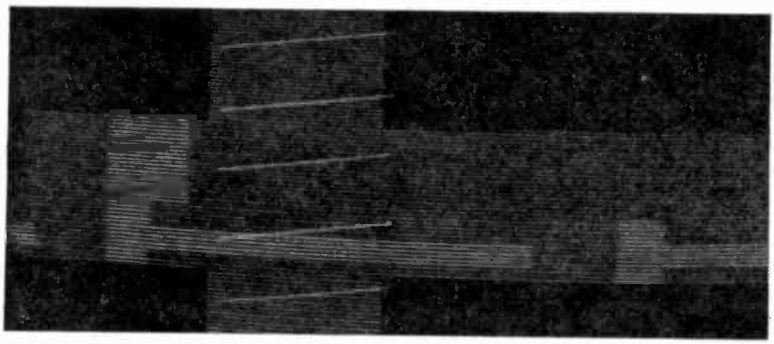

Fig. 5—Pulse cross pattern photograph showing complete lack of coincidence.

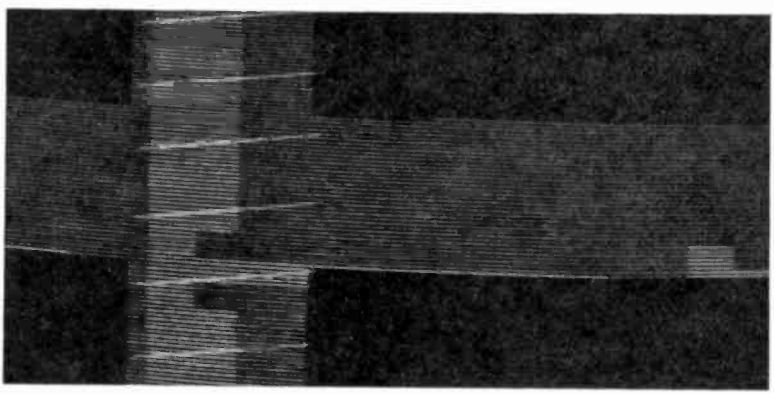

Fig. 6—Pulse cross pattern photograph showing coincidence at line frequency but not at field frequency.

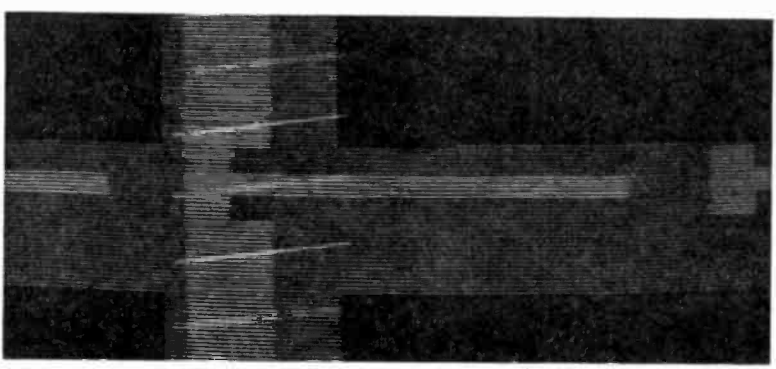

Fig. 7—Pulse cross pattern photograph showing odd vs. even field matching (the last line frequency synchronizing signal pulse is superimposed on the first line of the field frequency blanking.)

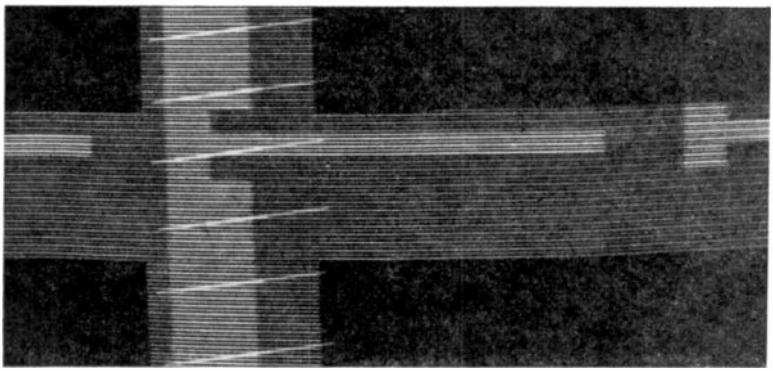

Fig. 8—Pulse cross pattern photograph showing odd vs. even field matching (the first equalizing pulse is superimposed on the last line frequency blanking pulse.)

on the pulse cross. Variations in the width of the "front porch," or delay of line-frequency synchronizing signal with respect to line-frequency blanking, are easily noted as shown in Figure 10.

The method and equipment outlined function satisfactorily and do not require excessive time in aligning the two signals for coincidence provided the continuity and stability of the received signal are good — i.e., provided one alignment will suffice for the transmission. For regular operational use, a means of quickly reverting to independent systems would be mandatory to cover the contingency of momentary interruption in the incoming signal. A means of automatically establishing coincidence and lock between the two signals as well as reverting to independent operation would of course be a highly desirable feature.

The results obtainable from interlocked scanning will be enhanced by the use of synchronizing generators that are not locked to local

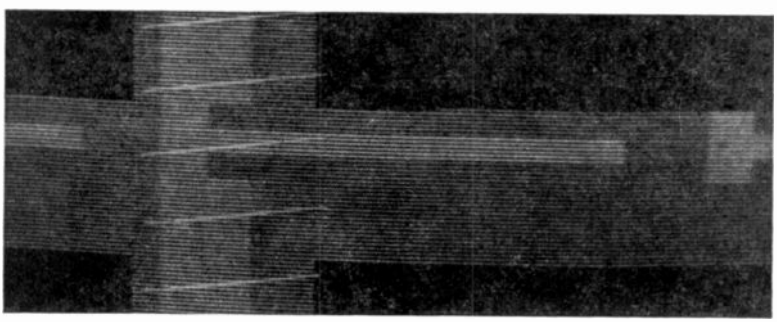

Fig. 9—Pulse cross pattern photograph showing even vs. even field matching

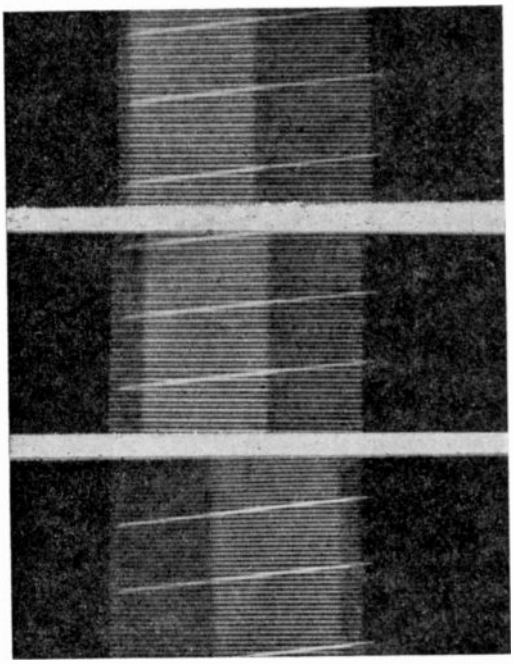

Fig. 10—Portions of pulse cross patterns showing variations in "front porch" or in the delay of line-frequency synchronizing signal with respect to the line-frequency blanking signal.

60-cycle power supplies, but which are controlled by high-inertia frequency sources. The most obvious benefit from the use of high-inertia systems lies in the fact that a momentary loss of the incoming signal would not ordinarily produce the same discontinuity of control of interlocked scanning that is inevitable with the system described. In fact, it appears possible to provide high-inertia controls for individual synchronizing generators of such excellence that appreciable discontinuity in incoming signal can be tolerated before, from an operational point of view, it would be necessary to sever the interlocked scanning tie-in.

A disadvantage in using the high-inertia frequency control system for synchronizing generator control lies in the fact that projector motors in film studios could no longer be synchronously driven from the local 60-cycle power.

Conclusions

The general direction of work toward one solution to the problem of interlocked scanning systems has been indicated. The work done has served more to show the nature and magnitude of the problems involved than to provide a complete answer. The use of the incoming signal for control is indicated by the economics of the problem.

NEW TECHNIQUES IN SYNCHRONIZING-SIGNAL GENERATORS*†

BY

EARL SCHOENFELD, WILLIAM BROWN, AND WILLIAM MILWITT

Industry Service Laboratory, RCA Laboratories Division,
New York, N. Y.

Summary

A generator of synchronizing and blanking signals has been developed in which the important pulse edges are established by means of a "stop watch", consisting of a terminated artificial transmission line carrying brief 31.5-kilocycle trigger impulses. The number of equalizing and vertical-synchronizing pulses appearing during each framing interval is determined by an electronic counter. The locked-in relationship between line and field scanning frequencies makes use of the cascaded-binary type of frequency divider wherein the divisor is established by the circuit connections rather than the value of a circuit element. The resulting apparatus lacks most of the screwdriver adjustments which usually have been associated with equipment of its type.

(14 pages, 13 figures)

* Decimal Classification: R583.13.
† *RCA Review*, June, 1947.

SPECIAL APPLICATIONS OF ULTRA-HIGH-FREQUENCY WIDE-BAND SWEEP GENERATORS*†

BY

JOHN A. BAUER

Engineering Products Department, RCA Victor Division,
Camden, N. J.

Summary

Three unusual uses of wide-band frequency-modulated signal generators are described. Instruments suitable for two uses immediately applicable to television receiver development are also shown.

These applications are as follows:—

1. *Radio-frequency impedance measurements;*
2. *Overall frequency response measurements of television receivers;*
3. *Microwave frequency measurements.*

Practicality has already been demonstrated with resulting large laboratory and factory test time savings.

(12 pages, 7 figures)

* Decimal Classification: R355.913.2×R200.
† *RCA Review*, September, 1947.

SYNC GENERATOR FREQUENCY STABILITY AND TV REMOTE PICKUPS*†

By

W. J. Poch

RCA Victor Division,
Camden, N. J.

Summary

An analysis of the relationship of synchronized generator control and field pickup setups in television is given.

(3 pages; no figures)

* Decimal Classification: R583.13.
† *Communications*, July, 1947.

TRIPLEX ANTENNA FOR TELEVISION AND F-M*†

By

L. J. Wolf

RCA Victor Division,
Camden, N. J.

Summary

Method of using a single four-bay Superturnstile antenna for simultaneous operation of an f-m transmitter and visual and aural transmitters of a television station, with power gain of 6.4 for f-m and 5 for television. Coupling between transmitters is negligible.

(4 pages; 6 figures)

* Decimal Classification: R326.6.
† *Electronics*, July, 1947.

TELEVISION HIGH VOLTAGE R-F SUPPLIES*#

By

ROBERT S. MAUTNER† AND O. H. SCHADE‡

Summary—The principles of operation and design of television high voltage r-f§ supplies have been previously described.[1] These are here reviewed and considered in greater detail. Constructional features of two typical units are shown and their performance is illustrated by curves indicating the magnitudes of current and voltage obtained under typical operating conditions. Sample calculations for the specific cases of a 75-watt, 90-kilovolt supply and a 10-watt, 30-kilovolt supply are included to illustrate the progressive steps in designing and calculating the circuit elements and operating conditions for a specified performance. A table of the symbols used is included at the end of the paper.

A TYPICAL r-f power supply circuit is shown in Figure 1. The oscillator voltage developed across the primary tank circuit, L_1C_1, is stepped up by the square root of the ratio of secondary to primary impedances, and then rectified. Because of the high voltage developed across the secondary, the principal portion of the network loss occurs in this part of the circuit requiring a high unloaded impedance for good efficiency. Such values of impedances are realized in practical supplies by the use of special coil configurations, and a minimum secondary tuning capacitance C_2. This capacitance is the sum of coil, wiring, and diode capacitances and is shown as a dotted capacitance in Figure 1.

In the following, the design of each portion of the circuit for satisfactory performance is considered in detail.

DESIGN

The design of r-f high voltage supplies may be divided into six consecutive steps:

1. Design the rectifier circuit and corona shielding

* Decimal Classification: R366 × R583.

Reprinted from *RCA Review*, March, 1947.

† Industry Service Laboratory, RCA Laboratories Division, New York, N. Y.

‡ Tube Department, RCA Victor Division, Harrison, N. J.

§ Throughout this paper, the abbreviation "r-f" is used for "radio-frequency."

[1] Schade, O. H., "Radio-Frequency Operated High-Voltage Supplies for Cathode-Ray Tubes", *Proc. I. R. E.*, Vol. 31, No. 4, pp. 158-163, April, 1943.

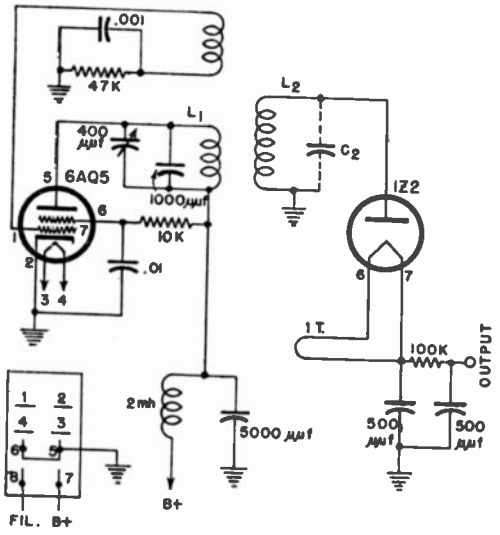

Fig. 1—Circuit of 4-kilovolt supply.

2. Determine the mechanical coil construction and compute the optimum winding and operating frequency for the high voltage coil
3. Estimate the required oscillator power; select the tube type and operating constants
4. Calculate the plate tank circuit and choke, if used
5. Calculate the diode filament transformers
6. Determine the regulation requirements of the supply.

Rectifier Circuit, Corona Shielding, and Capacitance

The basic circuit for voltage multiplication with diodes is shown in

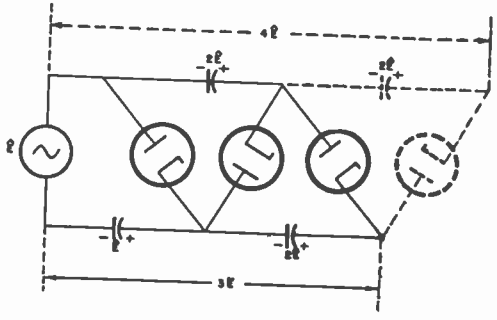

Fig. 2—Basic voltage multiplier circuit.

Figure 2. This circuit is particularly useful for 30 or 90 kilovolt operation. The focusing voltage for projection kinescopes, which generally runs about one-fifth of the second-anode voltage, can be conveniently obtained from the output of the first rectifier. The bleeder power loss is thus reduced to one-third of that otherwise dissipated in a bleeder connected to the full output voltage.

The choice of the number of rectifier stages depends on available rectifier types, the cost of circuit elements, and the impedance obtainable with practical high voltage coils.

The effective shunt load of the rectifier circuit on the tuned high voltage circuit is given by

$$R' = \bar{R}/2n^2 \qquad (1)$$

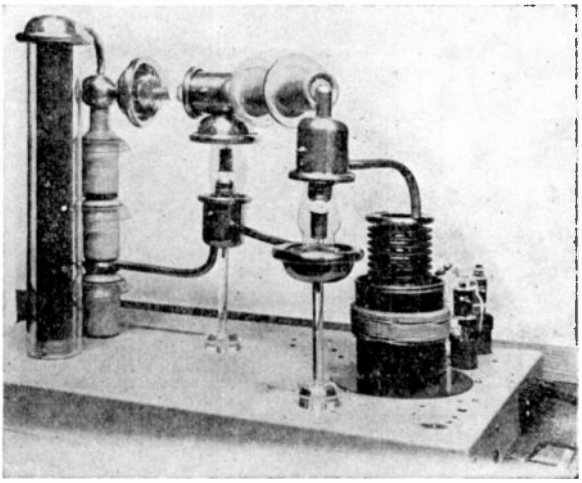

Fig. 3—Side view of 90-kilovolt tripler.

where $\bar{R}$ is the direct-current load resistance on the rectifier output terminals and n the number of cascaded rectifier stages.

For an output voltage $\bar{E} = 90$ kilovolts and $I = 0.8$ milliamperes, the direct current load is $\bar{R} = 110$ megohms. The inverse rating of 60 kilovolts for the R6194A experimental diode requires $n = 3$. Substitution in Equation (1) results in $R' = 6$ megohms. Similar computations for a 30-kilovolt supply with $n = 3$, $\bar{E} = 30$ kilovolts, and $I = 0.2$ milliamperes result in $R' = 8$ megohms.

Arrangement of parts and corona shielding for the 90KV tripler is shown in Figure 3. The 90-kilovolt unit requires considerably more elaborate corona shielding than the 30-kilovolt unit and will be treated in greater detail.

The minimum conductor diameter D (in inches) for a peak voltage $\hat{E}$ (kilovolts) is the diameter for which corona does not occur before spark-over occurs at a critical distance

$$D \approx \hat{E}/100 \text{ for } \hat{E} > 10\text{kv} \quad (60 \sim) \tag{2}$$

It decreases faster for potentials $\hat{E} < 10$kv. The required minimum spacing, i.e., the sparking distance between such conductors, is greater than the spheregap distance and is given by

$$S \approx 3D \tag{3}$$

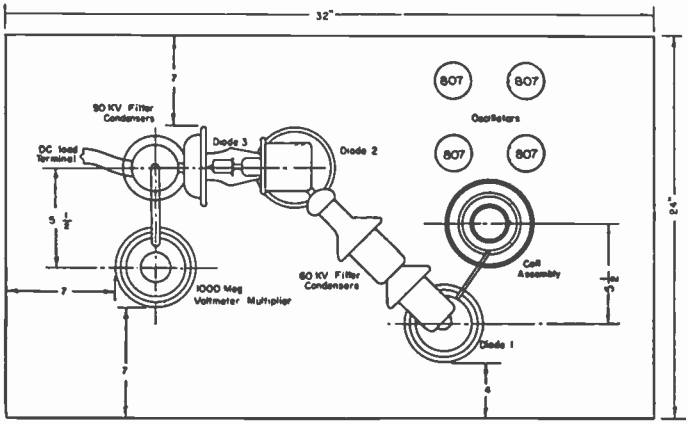

Fig. 4—Top view of chassis layout of 90-kilovolt supply.

For $\hat{E} = 90$ kilovolts, $D = 0.9''$ and $S = 2.7''$. It is good practice to use a somewhat larger diameter if feasible and provide spark-over clearances of double this value (triple at very high potentials; see Figure 4) to allow for the effects of scratches and dust particles on conductor surfaces. This is particularly advisable where conductors are exposed to, or at, r-f potentials as the power loss in air ionized by corona is much larger than that at low frequencies and serious loading of the power source results. All parts in the r-f fields as well as grounded objects must be given contours with a minimum radius $r \sim D/2$. Interconnecting leads at 60-kilovolt potential in the 90-kilovolt unit are thus made of one-half inch tubing while tightly wound phosphor bronze spring sections of one-quarter inch diameter are used in the 30-kilovolt unit. A clearance of 1.50 inches was used in this unit between output socket shell and shield wall. This spacing is the minimum recommended

and is a practical limit for safe operation, flashover occurring at slightly over 40 kilovolts.

Having determined the physical layout of the diode circuit, an estimate of its capacitance to ground is made to determine the secondary tuning capacitance C_2 of the high potential transformer winding.

The capacitance to ground of the circuit elements at r-f potential in the 30- or 90-kilovolts tripler circuits consists of three diode capacitances (3×2 micromicrofarad) and that of one condenser and two corona shield assemblies to ground. The latter may be estimated from its potential field contour which, for the 90-kilovolt unit, is similar to that of two spheres of roughly 12 centimeters diameter. As the space capacitance of a sphere is equal to its radius (in centimeters), the diode assembly at r-f potential has roughly $(12 + 6)$ micromicrofarad capacitance. Adding 2 micromicrofarads for the coil shield and 3.5 micromicrofarads for the winding capacitance (discussed later), the total shunt capacitance on the high voltage transformer winding of the 90-kilovolt unit will be in the order of $C_2 = 25$ micromicrofarads.

The High Voltage Secondary Circuit

The factors determining size, shape and type of winding used in the secondary of the transformer are:

1. Potential between layers and sections,
2. Distributed capacitance,
3. Corona,
4. Coil loss and temperature rise,
5. Coil impedance,
6. Coupling coefficient,
7. Coil form loss.

To minimize coil capacitance and voltage between layers it is practical to subdivide the winding into sections consisting of universal wound pies with five to ten turns per layer. Greater pie widths result in high distributed capacitance and increased voltage stress across layers. Narrower pies impose winding difficulties and result in weak coils. The voltage between layers should be less than indicated by the normal rating of the insulation inasmuch as the tendency of sections at the high potential end of the coil to produce corona as well as increased dielectric loss at r-f frequencies decreases the ability of the pie to resist breakdown. Values not exceeding 250 volts peak between layers have provided satisfactory operation. The space between pies should not be stressed with more than 12.5 kilovolts (peak) per inch (approximate double needle gap distance) to provide a safety factor for double

COIL DATA	4 KV COIL			10 KV (and 30 KV TRIP.)			30 KV UNBAL. DOUB.			90 KV TRIPLER		
	PRI.	SEC	TICK	PRI	SEC	TICK	PRI	SEC	TICK	PRI	SEC	TICK
FORM DIA	.750	.750	.750	1.25	1.25	1.25	3.75	2	3.75	4.375	2	4.375
FORM THICKNESS	.0625	.0625	.0625	.032	.032	.032	.125	.0625	.125	.125	.0625	.125
TURNS	100	1750	150	55	1400	75 – 100	2 parallel layers 35 t. ea.	2800	8	32	2800	9
PIE WIDTH	.1875	.0625	.0625	.1875	.0625	.0625		.125	close Solenoid		.125	close Solenoid
CROSS – OVERS PER TURN				6	10	10		6			6	
IND.	122 μh	56 mh		178 μh	43.5 mh	650 μh	145 μh	200 mh	18 μh	175 μh	220 mh	22 μh
WIRE (LITZ)	15/38	3/41	3/41	50/38	3/41	5/41	50/38	10/41	5/41	250/38	14/41	7/41
NO. π's	1	5	1	1	7	1	2 layer bank wound	10	single layer	3 layer bank	10	single layer
DISTANCE BETW. π's	.1875	.125	.3125	.25	.1875	.875		.1875			9/32	
SOLENOID LENGTH		.8125 TOT. SEC. LENGTH					1.375			1.5		

Fig. 5—Coil data for several practical coils.

voltage transients. A 30-kilovolt coil should thus have a total pie spacing of 2.4 inches. For a subdivision into 10 pies the clearance between pies should thus be a little over one-quarter inch. Lower voltage coils such as those used in the 30-kilovolt tripler can be designed with a somewhat greater safety factor, but are still subject to maintaining a form factor giving high Q and permitting sufficient coupling (see Figure 5).

The high voltage coil loss in r-f power supplies is a function of coil size and circuit capacitance. Larger power supplies require a high component-efficiency as high frequency power is relatively expensive. An over-all efficiency of 40 to 60 per cent requires the distribution of circuit losses as shown in Table I.

Table I—Circuit Efficiencies.

Circuit Element	30 kv–10w Eff. %	Power Loss Watts	90 kv–72w Eff. %	Power Loss Watts
Oscillator Tubes	70–75	6.5 – 8	75–80	30 –37.5
Primary Tank Circuit	94–96	1 – 2	95–97	4.5– 7.5
High Voltage Secondary Circuit	65–75	6 –10	88–90	15 –18
Rectifier Filament & Plate Loss	95–97	.75– 1.5	90–95	7.5–15
	40–48%	14.25–21.5	48–62%	57 –78

The overall efficiency of the 30-kilovolt tripler is less than 30 per cent at normal loads because of the small amount of power used compared with the power consumed in fixed losses such as that dissipated in the secondary coil and the minimum oscillator input. Higher efficiencies are obtained at higher load currents.

The figures in the second and fourth columns give design values. The required coupling is discussed later.

The necessary tuned impedance Z_{II} of the secondary is given by

$$Z_{II} = \frac{E_2^2}{2\,P_2} \tag{4}$$

where P_2 is power dissipated in that winding. To meet the requirements for the 90-kilovolt case (Table I) the r-f peak voltage $E_2 = 30$ kilovolts and the specified power loss required $Z_{II} = 25$ megohms.

The secondary coil used for the 30-kilovolt tripler was originally designed for a 10-kilovolt source, and resonated at approximately 280 kilocycles. When used in a tripler circuit the added shunt capacitance resulting from the additional diode and circuit capacitance lowered the resonant frequency to 180 kilocycles, reducing both coil Q and circuit impedance. However, both factors remain high enough to permit sufficient coupling for good regulation and satisfactory coil efficiency. The measured secondary impedance was over 9 megohms. From equation (4) the power loss for a 10-kilovolt peak voltage is $P_2 = 5.5$ watts which is within the rating of maximum dissipation (6.5 watts) for this particular coil.

Optimum wire size and number of turns are determined by a series of approximations. The coil inductance is given by

$$L = r^2N^2/[9r + 10\ (l + h)\,]\ 10^3 \text{ in millihenries} \tag{5}$$

where r = mean radius in inches

l = coil length in inches

h = pie height

N = number of turns

The frequency is computed with L and the estimated value C_2 ($C_2 = 20$ to 30 micromicrofarads) for the 90-kilovolt circuit and $C_2 = 17$ micromicrofarads for the 30-kilovolt circuit from the equation

$$\omega_0^2 = 1/L_2C_2 \tag{6}$$

The r-f resistance is then computed from

$$r = r_{\bullet}\ (1 + k^2) \tag{7}$$

with

$$k = \frac{0.04\ Nnd^3 f}{(l + h)}$$

where $r_{\bullet}$ = direct-current resistance of winding

N = number of turns

n = number of strands

d = wire diameter in inches

l, h, from Equation (5)

Also

$$Q = \frac{\omega L}{r} \tag{8}$$

and

$$Z = Q\omega L \tag{9}$$

The current density in the wire is expressed in circular mils per ampere of coil current, and should be

$$\text{Circular mils/Ampere} = 350\ (1 + k^2) \tag{10}$$

The secondary current is obtained with

$$I_{2\ (\text{rms})} = \hat{E}_2/\omega L_2 \sqrt{2} \tag{11}$$

The approximate total copper cross-section is obtained in first approximation with equation (10) and (11) setting $k = 1$. The coil loss for several coil designs was calculated for the 90-kilovolt unit. This data is summarized in Table II.

Table II—Coil Loss Data

#	N	n	L (mh)	C_p ($\mu\mu$f)	f (kc)	k^2	r_o	r	kilohms ωL	Q	Z (meg)	I_s (A)	c.m./a	P_s (w)
1	2800 (10 pies)	14	228	20	75	.31	194	254	107	422	45	.2	550	10
				30	61	.205		234	87	370	.32	.245	450	14
2	2000 (10 pies)	20	116	20	104	.62	98	159	76	477	.36	.28	560	12.5
				30	85	.41		138	62	450	28	.34	460	16
3	2500 (10 pies)	20	170	20	86	.65	122	201	92	456	42	.23	685	10.7
				30	70	.43		175	75	428	32	.283	555	14
4	3000 (12 pies)	20	250	20	71	.47	147	215	112	520	58	.19	880	7.8
				30	58	.31		192	91.5	475	43.5	.23	685	10.4

The first trial calculation with 2800 turns of 14×41 Litz wire happened to provide optimum design for its size as shown by a comparison with coils #2 and #3 using 20 strand Litz wire.

It is interesting to note that the power dissipated in a coil is a function of its size. This occurs as a result of being able to obtain both higher Q's by the use of more strands and higher inductance by the use of more turns. Thus a larger coil results in a higher tuned impedance and lower loss. However, if cost, physical size and other reasons restrict coil dimensions, the alternative is to vary the strands and number of turns, maintaining a constant copper cross-section (and resultant coil size) until a compromise is reached between coil loss and Q. If a fixed tuning capacitance is assumed and the coil resistance is considered equal to $r_\bullet$ regardless of frequency it can be shown that the power loss P_2 will be a constant. The effect of reducing the number of turns on a given coil to one half while maintaining a constant copper cross-section would then permit operation with the same coil loss at double the frequency, or $2f_\bullet$, the coil having half the inductive reactance it had previously, and twice the Q. However, actually the coil resistance will not drop to 25 per cent of its former value of r because of added eddy current losses at $2f_\bullet$ and the net result will be a coil of not quite $2Q_\bullet$ and of half the original value of $\omega_\bullet L$. It is, of course, desirable to maintain the product of Q and ωL as high as possible for minimum coil loss, but a high Q is also necessary, in order to permit sufficient energy transfer with obtainable coupling coefficients and good regulation, and further permit adequate spacing between primary and secondary for insulation.

Referring again to Table II it can be seen that a minimum coil loss requires a larger coil (#4). Coils #1 and #2 have about the same copper cross-section. It will be seen that loss in inductive reactance by using 20 strand Litz is not compensated by a proportionate rise in Q, resulting in a lower tuned secondary impedance. Even where coil size is slightly increased as in coil #3 by adding 50 additional turns per pie, the loss will still exceed that of coil #1.

Coil #1 will operate at 60 to 75 kilocycles depending on the exact circuit capacitance C_2, the degree of coupling, and the frequency to which the primary circuit is tuned.

The impedance of the secondary circuit will be somewhat lower than the computed value because of dielectric losses in the coil capacitance. The coil capacitance can be calculated from the capacitance between the two layers of one pie winding, which is approximately 1200 micromicrofarad (area $\frac{1}{8}'' \times 8''$, spacing 0.004", dielectric $\varepsilon = 3$). As one pie has about 35 layers of 8 turns, its capacitance is 34 micro-

microfarads and ten pies in series will then have 3.4 micromicrofarads. The reactance of this capacitance at 60 kilocycles is $1/\omega C_c = 0.75$ megohm. The impregnating compound must be of excellent quality as a 0.5 per cent power factor results in a shunt resistance loss of $200 \times 0.75 = 150$ megohms, which is equivalent to a 3-watt power loss at 30 kilovolts. The power factor of the insulating material should be excellent and the field strength low (long supports) to avoid power loss.

During early development of secondary windings, various types of coil forms and materials were tried. Many of the materials used, normally considered good insulators, showed considerable dielectric loss and a resultant heat rise. Even in cases where the coil form loss was low, the relatively poor thermal conductivity of the material used did not permit the heat generated by the copper loss to be dissipated rapidly enough, and again overheating resulted. In some cases the process was regenerative, the coil form power factor becoming progressively worse as the temperature rose, producing still greater losses.

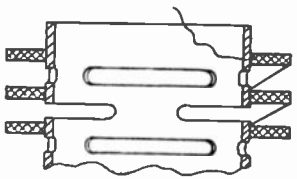

Fig. 6—Secondary coil form construction.

Consequently it is advisable to keep the coil form material in the field of the coil to a minimum and to provide as much air circulation around the pies as is practicable. Slotted thin wall impregnated paper bakelite tubing has been found to be one of the most satisfactory materials available, as well as one of the most economical. Figure 6 illustrates one satisfactory type of construction. For low voltage supplies horizontal coil mounting is preferable from the standpoint of air circulation (provided the coil is not placed too close to a metal surface). However, vertical mounting is generally used because of conveniences in wiring and greater adaptability to space requirements.

It will be noted that the calculated magnitudes of Q in Table II are quite high. For several reasons, it is not feasible to use the conventional Q-meter to measure these values. The frequency at which we are interested in the Q is close to the self resonant frequency of the coil so that in any series circuit such as used in a Q-meter the coil appears as a partially resonant circuit in series with the tuning capacitance rather than an inductance. Furthermore, the minimum value of capacity setting in the usual Q-meter is in the order of 30 micromicrofarads which is greater in most cases than the total second-

ary circuit capacity. Consequently the operating Q of the winding is most easily determined by adding sufficient high Q capacity to produce resonance at the desired frequency and then determining the frequency band required for the 70 per cent response points. Because of the very high impedances involved it is necessary to drive the secondary coil by means of a few very loosely coupled primary turns in order to prevent coupling an appreciable amount of generator impedance into the secondary. This will, of course, transfer a proportionately smaller amount of energy into the secondary and result in lower magnitude of detected voltage. A practical method of detecting the 70 per cent response points without the use of a vacuum tube voltmeter or other normally satisfactory "high impedance" device (which in this case would produce excessive loading and detuning) is through the use of a high gain oscilloscope and test probe. The input impedance of a typical

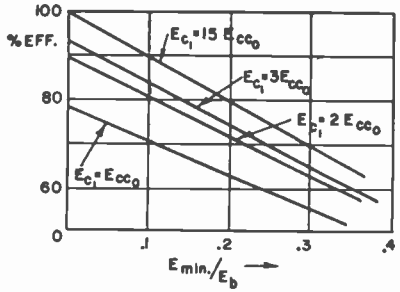

Fig. 7—Efficiency curves for class C operation.

probe may be equivalent to 5 or 10 micromicrofarads in shunt with 10 megohms. If this is placed about a half inch away from the secondary, negligible loading will result and a more accurate value of measured Q will be obtained. It is necessary that all other windings be removed from proximity to the secondary during this measurement or the loading effect of induced capacity currents in the coils coupled to it will result in incorrect readings of response points. When a tap at a small fraction of the total coil inductance is available it can be used with a high impedance oscilloscope probe to provide a further check of the Q value obtained from the first measurement. A signal generator with an incremental frequency dial graduated directly in small percentages of the output frequency has been found useful in permitting rapid and precise measurements to be obtained.

Oscillator Specifications and Operating Conditions

In order to obtain high efficiency and high power output, the oscillator tubes are operated under class C conditions. In Figure 7

curves are given indicating efficiencies obtainable for bias values up to several times cutoff. Figure 8 shows the ratio of peak to average plate current plotted against the ratio of actual bias to cutoff bias. Operation at high bias and high excitation results in small angles of flow, high efficiency and low power output. High grid driving power is required which in an oscillator must be supplied from the plate circuit. The ratio of peak to average currents at high efficiencies rises rapidly imposing greater emission requirements and increased tube drop. Optimum performance is obtained with angles of flow between 90 and 120 degrees and peak to average plate currents in the order of 6 to 1.

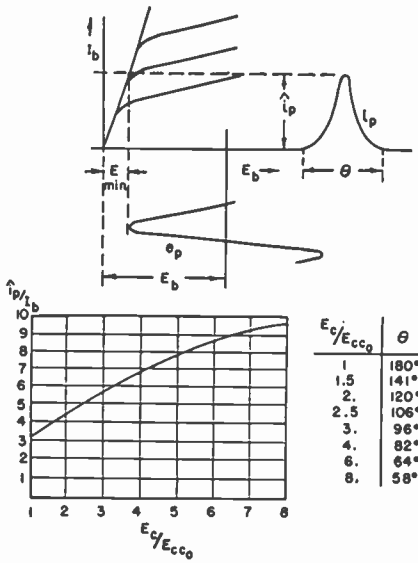

E_c/E_{cc_0}	θ	i_p/i_{dc}
1	180°	$\pi = 3.14$
1.5	141°	3.93
2.	120°	4.7
2.5	106°	5.35
3.	96°	5.9
4.	82°	6.9
6.	64°	8.8
8.	58°	9.7

Fig. 8—Ratio of peak to average currents for various angles of flow.

The computations involved in designing an oscillator circuit of the 90-kilovolt unit are typical of those used for all r-f supplies and are considered in detail.

On the basis of a 50 per cent overall efficiency (see Table I) the oscillator power input is 150 watts. For 80 per cent tube efficiency the power output is $P_o = 120$ watts and the tube loss 30 watts.

A circuit (Figure 9) using four 807's in parallel was chosen because of the low cost and low power supply voltage required by these tubes.

From an inspection of Figures 11 and 12 (see pages 64-65) it will be noted that operation at 80 per cent efficiency requires in general

a) $E_{c1} = 2\,E_{cc0}$; (12)

with $E_{min}/E_b = 0.1$ and $I_p/I_b = 4.5$

or

b) $E_{c_1} = 3\,E_{c_{co}}$;

with $E_{min}/E_b = 0.14$ and $I_p/I_b = 5.7$ (13)

As the peak power input is

$$\hat{P}_{in} = (I_p/I_b)\,P_{in} \tag{14}$$

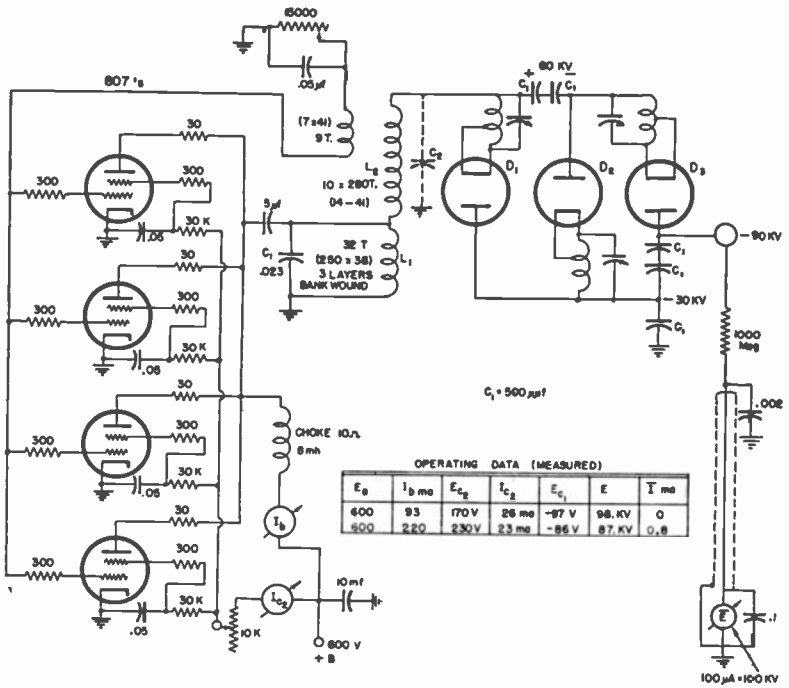

E_b	I_b ma	E_{c_2}	I_{c_2}	E_{c_1}	E	T ma
600	93	170 V	26 ma	-97 V	98. KV	0
600	220	230 V	23 ma	-86 V	87. KV	0.8

Fig. 9—Circuit of 90-kilovolt tripler.

The above equation gives

$$\hat{P}_{in} = 675 \text{ watts or } 870 \text{ watts} \tag{15}$$

with the peak plate current

$$I_p = \hat{P}_{in}/E_b \tag{16}$$

The four 807's operated at $E_b = 600$ volts must supply peak currents

a) $I_p = 4 \times 0.28a$ at $E_{min} = 60$ volts

or

b) $I_p = 4 \times 0.362a$ at $E_{min} = 84$ volts

Case (b) can just be realized as shown by the plate characteristics for 807's under the following operating conditions:

$E_b = 600$ volts $\qquad E_{c_1} \approx -90$ volts

$E_{c_2} = 250$ volts $\qquad +E_{g_1} = +15$ volts

(positive grid swing)

$I_p = 0.36$ ampere $\qquad I_{c_2} = 25$ milliamperes $\qquad I_{c_1} = 15$ milliamperes

The d-c plate current is

$I_b = I_p/5.7 = 63.2$ milliamperes (factor for $E_c = 3E_{co}$)

The d-c screen current:

$$I_{c_2} \sim I_{c_2}/5 = 5 \text{ milliamperes}$$

(see $I_{c_2} = f(E_b)$ from characteristic curves)

For four 807's the total B current I_B is therefore

$$I_{b(4)} \sim 250 \text{ milliamperes}$$

$$I_{c_{2(4)}} \sim 20 \text{ milliamperes}$$

$$I_B \sim 270 \text{ milliamperes}$$

The d-c grid current:

$I_{c_1} \sim I_{c_1}/8.8 = 1.7$ milliamperes (factor for $E_g/+E_g = 6$)

Each screen grid is fed by a series resistor $R_{sg} = \dfrac{600 - 250}{.005} = 70{,}000$ ohms. For the purpose of adjustment, it is practical to use 30,000 to 50,000 ohms per tube and a common 10,000-ohm adjustable resistor. The common grid resistor is

$$R_g = \frac{90}{4 \times 0.0017} \approx 13{,}200 \text{ ohms}$$

The power output of the tubes into the plate circuit is

$$P_o = (E_b \times I_b) \times \text{efficiency} = 120 \text{ watts} \tag{17}$$

and the plate load:

$$R_p = (E_b - E_{min})^2/2\,P_o \tag{18}$$

$$R_p = 516^2/240 = 1100 \text{ ohms}$$

These computations can be summarized for the 30-kilovolt tripler as follows:

From Table I average fixed losses are 16 watts. The power output is 10 watts and is the sum of the power dissipated in the bleeder load (2.5 watts) plus high voltage output (7.5 watts). If an oscillator efficiency of 73 per cent and an overall efficiency of 40 per cent is assumed, the power input will then be 25 watts.

$$\text{For } E_{c_1} = 3E_{c_{co}}; \text{ with } E_{min}/E_b = 0.22$$

$$\text{then } I_p/I_b = 5.7$$

and the peak power input is

$$\hat{P}_{in} = (I_p/I_b)\,P_{in} = 143 \text{ watts}$$

and

$$I_p = \hat{P}_{in}/E_b = 0.44 \text{ ampere}$$

Two 6Y6G's operated at 325 volts must supply peak currents of

$$I_p = 2 \times 0.22\,a \text{ at } E_{min} = 75 \text{ volts}$$

Summarizing and from inspection of 6Y6G characteristics:

$I_{c_2} = 25$ milliamperes	$I_{c_1} = 17$ milliamperes	$E_{c_{co}} = -20$ volts
$I_{c_2} = 7$ milliamperes	$I_{c_1} = 1.38$ milliamperes	$E_{c_1} = -60$ volts
		$+E_{g_1} = +12.5$

The grid power dissipated is 83 milliwatts.

The d-c plate current is

$$I_b = I_p/5.7 = 38 \text{ milliamperes (for } E_c = 3E_{c_{co}})$$

For two 6Y6G's the total B current is therefore

$$I_b \approx 76 \text{ milliamperes}$$

$$I_{c_2} \approx 14 \text{ milliamperes}$$

$$I_B = 90 \text{ milliamperes}$$

The series screen resistor is

$$R_{sg} = \frac{E_b - 100}{0.007} = 32{,}000 \text{ ohms}$$

The grid resistor is obtained from

$$R_g = E_{c1}/I_c = 44{,}000 \text{ ohms}$$

The power output to the plate circuit is

$$(E_b \times I_b) \times \text{efficiency} = 18.3 \text{ watts}$$

and the plate load

$$R_p = 254^2/36.6 = 1800 \text{ ohms}$$

Coupling, Plate Load, and Tuning

The transfer of energy between two coupled circuits depends on the existence of a common electro-magnetic field. As a percentage of the total flux, it is expressed as the coupling factor K. For purely inductive coupling

$$K = M/\sqrt{L_1 L_2} \tag{19}$$

where M is the mutual inductance. The uncoupled or leakage-inductances can be cancelled by the series capacitances C_1 and C_2, i.e., by tuning the circuits. The reaction of the secondary circuit on the primary circuit causes changes in its series impedance. Its series resistance changes to

$$r_{\mathrm{I}}' = r_{\mathrm{I}} + \mathcal{T}\, r_{\mathrm{II}} \tag{20a}$$

and its inductive reactance to

$$\omega L_I = \omega L_1 - \mathcal{T} x_{II} \tag{20b}$$

where r_{II} is the total series equivalent resistance, and x_{II} the series reactance of the secondary circuit. $\mathcal{T}$ is a transfer factor depending on coupling, frequency and series impedance z_{II} of the loaded secondary circuit. It is given by

$$\mathcal{T} = \omega^2 M^2 / z_{II}^2 = \omega^2 M^2 / [r_{II}^2 + (\omega L_2 - 1/\omega C_2)^2] \tag{21}$$

Resistance Transfer and Coupling

$\mathcal{T}$ has its largest value $\mathcal{T}_{(o)}$ when the secondary circuit is in resonance, as the denominator is then reduced to r_{II}^2.

$$\mathcal{T}_{(o)} = \omega^2 M_o^2 / r_{II}^2 \tag{22}$$

Resonant or near resonant conditions in the secondary circuit are obtainable by changing the frequency ω, that is by varying C_I of the primary tank circuit.

With Equation (19) and Equations (22) and (20a) one obtains an expression for the minimum coupling coefficient $K_{(o)}$ required to obtain a specified series resistance r_I' in the primary tank circuit tuned for resonance of the secondary circuit:

$$K_o = \sqrt{\frac{1}{Q_{II}'}\left(\frac{1}{Q_I'} - \frac{1}{Q_I}\right)} \tag{23}$$

where $Q_I = \dfrac{\omega L_I}{r_I}$ (Q value of primary tank circuit without load)

$Q_I' = \dfrac{\omega L_I}{r_I'}$ (Q value of loaded tank circuit; see Equation 20(a))

$Q_{II}' = \dfrac{(Z_{II} \text{ in parallel with } R')}{\omega L_2}$

(Q_{II}' is the Q value of secondary circuit with rectifier load R'; see Equation (1))

K_o is then the critical coupling necessary to reflect the proper shunt load to the oscillators under full power output conditions.

For the 90-kilovolt supply and selecting $F_o = 65$ kilocycles (see Table II): $Q_I \approx 400$ (A small loss in C_1 is to be expected.) The design will

be for: $Q_I' = 10$ and

$$Q_{II}' = \frac{\overbrace{(35 \text{ megacycles in parallel with } 150 \text{ megacycles})}^{Z_2} \text{ in parallel with } \overbrace{6 \text{ megacycles}}^{R'}}{.093 \text{ megacycles}} = 53$$

(This is the Q value for max. load)

where: 35 megohms is shunt coil loss at $F = 65$ kilocycles

150 megohms is shunt impregnant loss

6 megohms is effective load

The minimum coupling is with (23), therefore

$$K_{(o)} = 0.043$$

This coupling will transfer the power to the secondary circuit but will give very poor regulation. It is the condition where the desired energy transfer occurs, and the primary is tuned so that maximum voltage at full load is produced across the secondary. Under these conditions the reactance x_{II} is tuned out and Equation (20a) reduces to

$$r_I' = r_I + \omega^2 M^2 / r_{II} \tag{24}$$

Any reduction of the load (decrease of r_{II}) results in an increase in r_I', a lower shunt primary impedance, and higher oscillator power output. This results from the tendency of the oscillator to maintain a constant voltage amplitude across the primary tank circuit for moderate variations in load. The increased power supplied results in a rapid rise in secondary voltage.

Good regulation requires that

$$K \geqq 5K_o \tag{25}$$

By adjustment of ω, i.e., by tuning the primary, the transfer factor $\mathcal{T}$ in Equation (21) can be made to equal $\mathcal{T}_{(o)}$ in Equation (22) so that proper energy transfer results.

For $K/K_o = 5$ we may write the requirement:

$$r_I' = r_I + [(5\omega Mo)^2/(r_{II}^2 + x_{11}^2)]\ r_{II} \tag{26}$$

In order to maintain the same magnitude of coupled resistance to the primary under full load conditions, the term $(r_{II}^2 + x_{II}^2)$ must increase so that $r_{II}^2 + x_{II}^2 = 25 r_{II}^2$ max. This necessitates an operating condition where the magnitude of the coupling factor is determined by the residual reactance left in the secondary circuit at oscillator frequency, rather than by its resistance r_{II} max. Operation under such conditions, i.e., off resonance as far as the secondary self-resonant frequency is concerned, introduces a coupled reactance to the primary which is given by

$$x_{II} \approx 5 r_{II} \text{ max} \tag{27}$$

which follows from the fact that r_{II} is in quadrature and has little effect on amplitude of the transfer factor when Equation (27) is true. The denominator in Equation (21) varies less than 4 per cent for all values of secondary resistance between no load and full load.

Equation (26) can then be replaced by:

$$r_I' = r_I + \left[\frac{(5\omega M_o)^2}{x_{II}^2} \right] r_{II} \approx r_I + \left[\frac{\omega M_o}{r_{II\ max}} \right]^2 r_{II} \tag{28}$$

where the bracketed term is constant. A reduction of the load r_{II} now causes a reduction of r_I'. The oscillator power is thus transferred to the secondary in a manner similar to that occurring when a 100 per cent coupled transformer is used.

The required coupling $K \approx 5K_o$ may be computed with the aid of Equation (23). Should this coupling be unobtainable, the value Q_1' may be increased by reducing L_I. This will result in better regulation but at the expense of additional primary power loss.

The coupling can be increased by connecting L_2 in series with L_1 as shown in Figure 9, which gave $K = 0.235$. A slight decrease in spacing increases K considerably ($K = .25$ for S decreased by 12 per cent), and serves as a practical coupling adjustment. The coupling of a finished transformer is checked by measuring the frequency difference ΔF between the peaks of the two resonant responses, as $K \approx \Delta F/F_o$. This check must be made with the primary tuned to the frequency ω_o. This is the frequency of the secondary circuit measured with $C_1 = 0$. The primary circuit is then tuned to ω_o as indicated by equal frequency deviations $\Delta F/2$ of both peaks. Figure 10 shows this case (curve 4) as well as the operating condition (curve 7). The test circuit is indicated. The response curves of Figures 10 and 11 do not give

direct information on the voltage output under oscillating conditions, for which the primary voltage (not the current) is maintained nearly constant.

Reactance Transfer and Primary Constants

The reactance of the primary circuit is increased by the transferred series reactance x_{11} when the reactance of the secondary is capacitive.

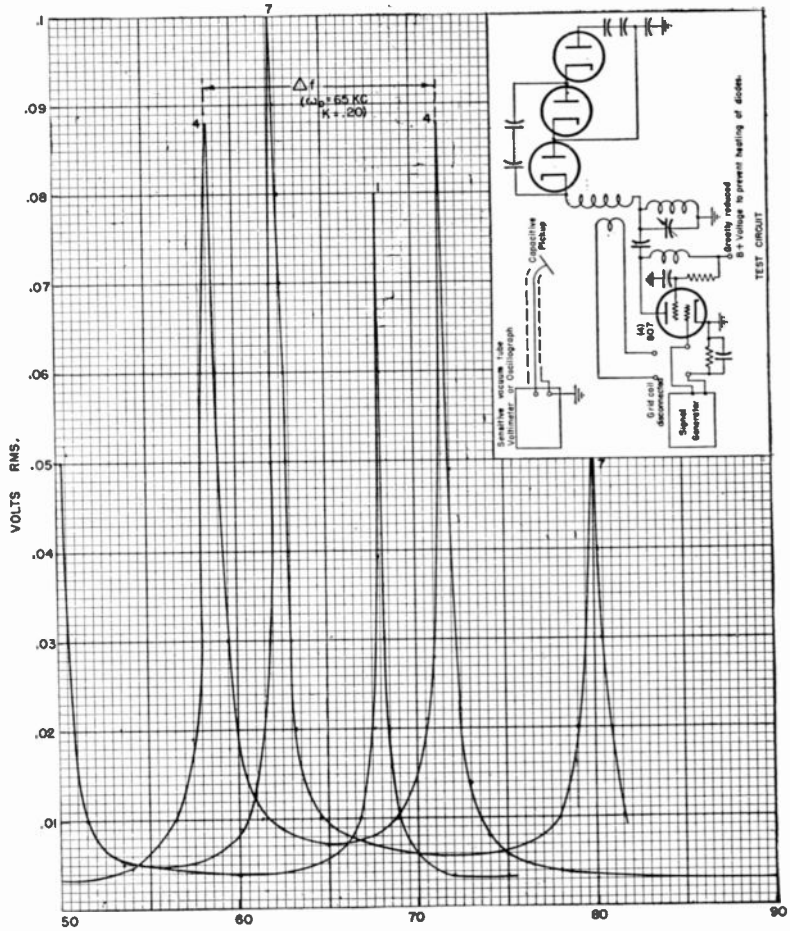

Fig. 10—Frequency characteristics of 90-kilovolt circuit (rectifiers not heated) for primary tuning conditions 1, 4, and 7 shown in Figure 11.

This is the desired operating condition, the circuit oscillating at the lower coupling frequency ω_1, with the secondary operating at a somewhat higher frequency than that obtained when equal primary and secondary tuning is used, but still below its self-resonant frequency ω_0.

For this operation, and $K \geqq 5K_o$ the inductive primary circuit reactance is given by

$$\omega L_I = \omega_1 L_1 + KK_o\omega_1^2 L_1 L_2 / r_{II}\,\text{max} \tag{29}$$

which can be derived from (20b) with

$$T = [\omega_1 M_o / r_{II\,max}]^2 x_{II}$$

by substituting

$$x_{II} = 5r_{II\,max},\ \omega_1^2 M_o^2 = K_o^2 \omega_1^2 L_1 L_2, \text{ and } K = 5K_o.$$

Factoring L_1 results in $L_1 = L_I/(1 + KK_oQ_{II}')$ (30)

It is now necessary, to determine ω_1 in terms of ω_o, K, K_o and Q_{II} so that a value of L_1 can be computed from L_I (effective primary inductance including effect of coupled secondary reactance).

The oscillator frequency ω_1 is given by

$$\omega_1/\omega_o = 1 - (K/2K_oQ_{II}') \tag{31}$$

which can be computed with the aid of Equations (25) and (27) by substituting

$$r_{II}' = \frac{\omega_o L_2}{Q_{II}'_o}$$

and setting $\Delta x = x_{II}/2.$

For the specific example $F_o = 65$ kilocycles, $K = 0.21$, $2K_o = 0.086$ and $Q_{II}'_o = 53$

$$\omega_1/\omega_o = 1 - (0.21/.086 \times 53) = 0.954$$

$$F_1 = 62 \text{ kilocycles}$$

and $$L_1 = 0.675\ L_I$$

The tank circuit is to be designed for a full load value $Q_I' = 10$. Then

$$\omega L_I = R_p/Q_I' \tag{32}$$

Substituting $R_p = 1100$ from (18), and $F = 62$ kilocycles, a value of $\omega_1 L_1 = 110$ is obtained and $\omega_1 L_1 = 74.5$ ohms. L_1 is then 190 microhenries. The necessary tuning capacitance is

$$C_1 = 1/\omega_1^2 L_1 = 0.0233 \text{ microfarads.} \qquad (33)$$

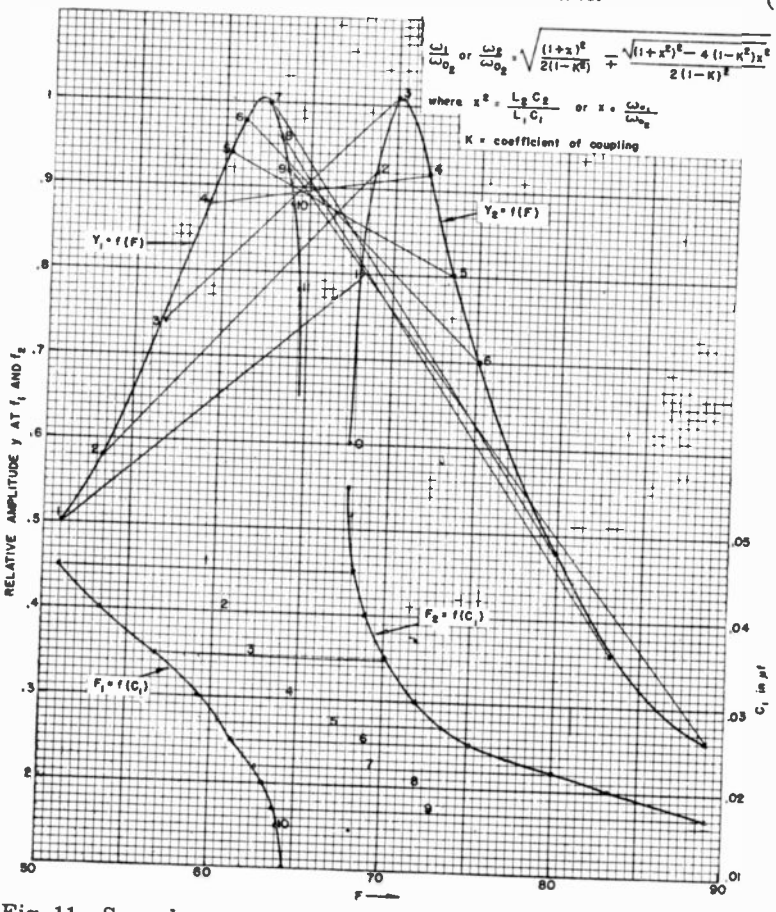

Fig. 11—Secondary output curves for various operating frequencies.

Figure 11 shows the envelope curves and relative amplitudes of corresponding coupling frequencies F_1 and F_2 obtained with constant grid excitation of the oscillator tubes (from a separate source) as a function of the primary tank tuning capacitance C_1. For the case where $C_1 = 0.04$ microfarad (points 2) the lower peak F_1 (53.5 kilocycles) produces a relative output of $Y_1 = 0.58$ and the upper peak F_2 (69 kilocycles) produces an amplitude $Y_2 = 0.92$. Operation at the lower frequency, near the peak of the curve (points 7 or 8) requires a smaller

tuning capacitance C_1 than operation at the higher frequency peak (points 2 to 3). Self-excitation by feedback from the secondary winding causes stable oscillations at the preferred frequency F_1 with normal feedback coil polarity (as if the secondary circuit did not exist). Operation at F_2 obtains upon reversal of the feedback coil polarity but causes lower tank circuit efficiency and somewhat poorer regulation. These relations are shown in vector form in Figure 12. The voltage induced in the secondary lags i_1 by 90 degrees, and that induced in

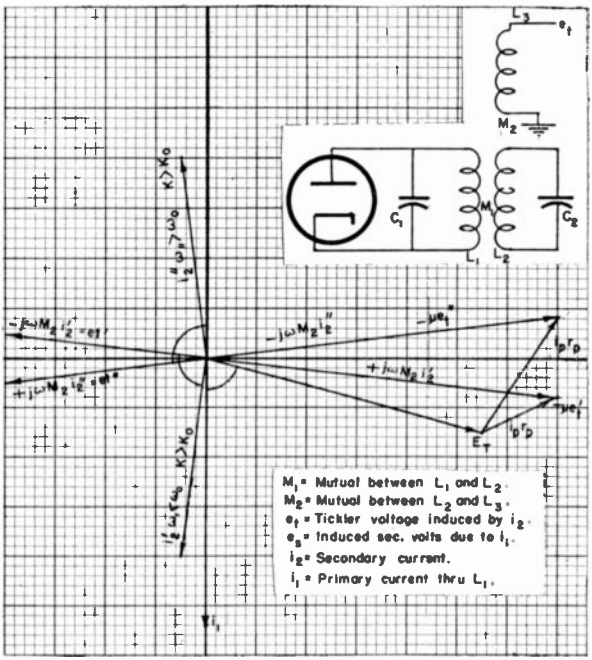

Fig. 12—Vector diagram of oscillator phase relations.

the tickler will either lead or lag i_2, the secondary current, by an additional 90 degrees. When $K > K_o$ and the tickler is inductively coupled to the secondary, oscillation can occur at either of the two peaks depending on the sign of the mutual inductance between tickler and primary. When $\omega_1 < \omega_o$ (the preferred condition), i_2' will lead the induced secondary voltage e_s. Inasmuch as the voltage vector e_t must lie in the third or fourth quadrant for oscillations to occur, the tickler voltage $e_t' = -j\omega M_2 i_2'$ is the effective vector for producing oscillations. Reversing the tickler with $\omega_1 < \omega_o$ results in the vector $+j\omega M_2 i_2'$ which has no component in the direction necessary for oscillation. Operation

at $\omega_2 > \omega_o$ will occur when the tickler is reversed. Reversing the direction of winding of the secondary has no effect as the signs of the mutual inductances between primary and secondary and between secondary and tickler are changed simultaneously.

Another phenomenon, not normally encountered under the usual conditions of oscillator operation, has resulted in a particular method of obtaining feedback. In the conventional oscillator circuit, the tickler winding is coupled to the primary and is so connected that the mutual inductance of the proper sign for oscillation is obtained. If a loaded tuned circuit of approximately the same frequency as that of the primary circuit is now tightly coupled to the primary there will be two new frequencies at which the primary tank circuit is substantially resistive. It is now assumed that the oscillator is operating at a frequency ω_1 which is below the self-resonant frequency ω_o of the secondary, and the primary self-resonant frequency is above ω_o. As the primary is tuned still higher in frequency the frequency of oscillation will approach ω_o, the output voltage will rise, and the loading on the primary will increase. A point will finally be reached at which the reflected load resistance is so high that insufficient primary tank impedance for continued oscillation will remain. At this point the oscillator frequency will "jump" to a higher frequency at which the primary tank is again sufficiently high to again permit oscillation. However the coupled secondary resistance will now be smaller and the resultant oscillator loading considerably less. If the primary is now tuned lower in frequency, the coupled resistance will again increase until a point is reached where the same condition of instability results. The oscillator will then readjust its frequency as described.

Thus, it can be seen that if the oscillator is tuned past a stable operating point and then turned off, it may start in its second mode of oscillation, where it possesses greater stability but does not provide the desired output voltage. This is obviously an undesirable operating condition. Ollendorf[2] has shown that this instability results from an abrupt increase in oscillator loading and has quantitatively analyzed the effect for various magnitudes of coupling and tuning directions.

Coupling the tickler to the secondary avoids such instability as the grid excitation increases with higher secondary voltages. While a jump in frequency will not be experienced with this arrangement, oscillator loading will increase with detuning in the normal manner. The smaller power supplies described including the 30-kilovolt tripler use this method of obtaining excitation. The 90-kilovolt unit obtains most of

[2] Ollendorf, S., DIE GRUNDLAGEN DER HOCHFREQUENZ-TECHNIK, J. Springer, Berlin, Germany, 1926 (pp. 393-411).

its excitation in this manner, a smaller part being supplied by the primary to tickler coupling.

Proper tuning with operation at ω_1 results in a decreasing high voltage with increasing values of C_1 and vice versa. Variation of C_1 causes a variation of the transfer constant and provides thereby an adjustment of the reflected oscillator plate load, and the high voltage output.

Calculation of the 90-kv Primary Coil

A power loss of n per cent requires the ratio of the tuned impedance of the fully loaded primary to the unloaded primary to equal n. Thus:

$$n = R_L/Q_I\omega L_1 \qquad \text{and} \qquad Q_I = Q_I'/n \tag{34}$$

For $n = 3$ per cent (see Table I), Q for the primary circuit with Equation (34) is:

$$Q_I \geqq 10/0.33 = 333 \tag{35}$$

The magnitude of ωL_1 can be obtained from (29) and (30), and the desired value of Q_I from (35), giving a value of r. The direct-current resistance r_o (see Equation 7) can then be estimated, substituting a value of 1 for k^2. The safe value of 1000 circular mils/ampere (Equation 10) is assumed to be satisfactory for a first trial to estimate the wire size from the circulating tank current. The peak voltage $E_1 = (E_b - E_{min}) = 516$ volts causes the root-mean-square tank current $I_2 = 516/\omega L_I \sqrt{2} = 3.3$ amps, and results in a wire size of $1000 \times 3.3 = 3300$ circular mils.

If #38 litz (15.7 circular mils) is chosen, the wire should have $3300/15.7 = 200$ strands for a first approximation. The litz wire diameter is roughly 50 per cent larger than that of the equivalent bare solid wire (#15), i.e., $D_{200} \approx 0.085$ inches. This wire will wind with 12 turns per inch.

For good coupling to the secondary, the tank circuit coil should not be too long and its diameter only as large as required by spark over distances to the high voltage winding.

A table can now be constructed with values for these coils with different strand numbers (see Table III), computed for $F_1 = 63$ kilo-

Table III—Primary Coil Data

#	N	Layers	l	a	n	$L\omega h$	k^2	r_o	r_1	ωL_1	$\frac{\omega L_1}{r_1}$	$\frac{\omega L_1}{r_1}$	I_I	$I_I^2 r_1$	KVA (1)
1	32	3	0.9"	0.2 "	200	180	1.1	0.13	0.27	71	260	410	3.3a	3.00a	1.2
2	32	3	1.1"	0.24"	250	175	1.16	0.11	0.24	69	290	460	3.3a	2.65a	1.2
3	33	3	1.3"	0.3 "	330	180	1.5	0.09	0.22	71	320	500	3.3a	2.42a	1.2

cycles (Equation (30) and (31) gave $L_1 = 190$ microhenries and $F_1 = 62$ kilocycles. For the purposes of the table exact values are not essential.) In order to determine the errors involved in the previous substitutions, Coil #2 is a good choice, having a power loss of only 2.65 watts. Coil #3 was calculated and built since litz wire with 330 strands was available for tests.

The plate feed choke should carry only a small percentage of the tank current, as it is not coupled to the secondary circuit. For a 5 per cent current it should have an inductance

$$L_{(CH)} \geqq 20L_I.$$

For the previous example $L_{(CH)} \geqq 20x.28 \geqq 5.6$ millihenries.

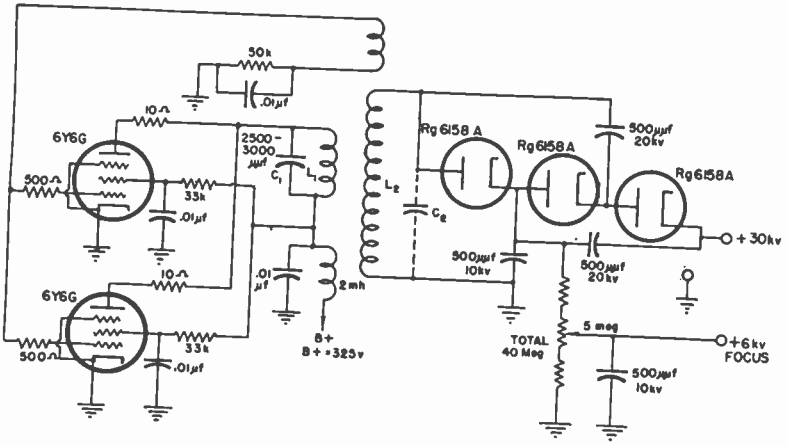

Fig. 13—Circuit of 30-kilovolt tripler.

While it is desirable to use shunt feed for convenience in tuning, added losses and expense are incurred, and series feed has been resorted to in the smaller units. *Note that the primary tank current does not flow over the bypass condenser* (Figure 13).

Filament Transformer Design

The energizing current for the filaments of the diode rectifiers can be conveniently obtained by either the use of a one- or two-turn loop inductively coupled to the primary of the transformer, or by resonating the capacity current through the diode in the primary of a step-down transformer. The former method is preferable for low voltage supplies using one rectifier. Where a number of rectifiers are used the physical

layout would result in long filament leads with added insulation problems and capacitance. In this case the latter system is preferable.

When a one- or two-turn loop is used, the size of the loop and its position in the energizing field can be adjusted until inspection of the rectifier filament indicates proper operation. Accurate adjustment is facilitated by comparison with a similar rectifier tube fed from a 60-cycle source.

A typical filament transformer assembly is shown in Figure 14 (90 kilovolts). The computations involved in calculating filament trans-

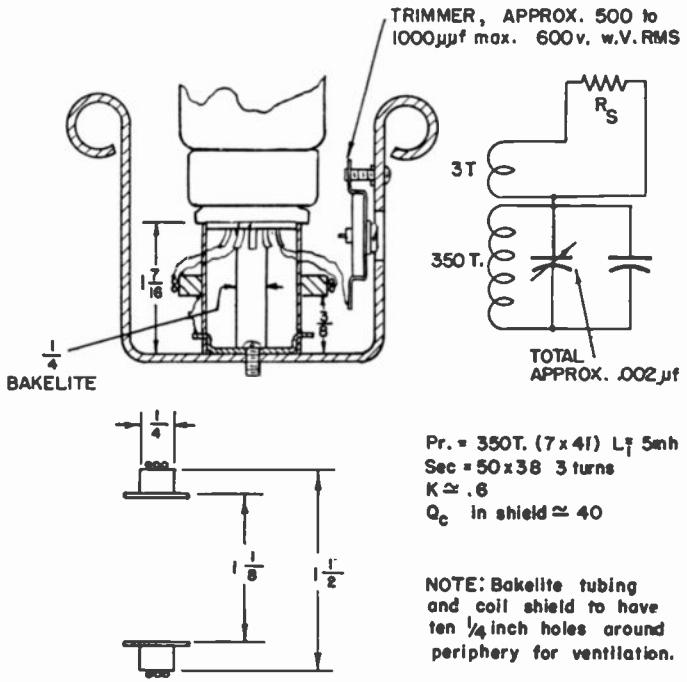

Fig. 14—Typical filament transformer assembly.

former performance are best illustrated by the following examples. For all cases the equivalent circuit is that represented by Figure 15. The line current (i_1) is given by

$$i_1 = \frac{E_{rms}}{X_c} \tag{37}$$

Where X_c is the diode capacitance (plate-to-cathode) and E_{rms} the r-f voltage across the diode. The transformer efficiency of η specifies the

power and resistance ratio for parallel circuits

$$\frac{R_1}{R_L} = \frac{\eta}{(1-\eta)} \qquad (38a)$$

where R_1 is the equivalent coil loss resistance and R_L the equivalent or reflected useful load resistance in shunt with the parallel-tuned circuit resistance. The ratio of the circuit Q with a load to that without load is given by:

$$Q_o'/Q_o = 1-\eta \qquad (38b)$$

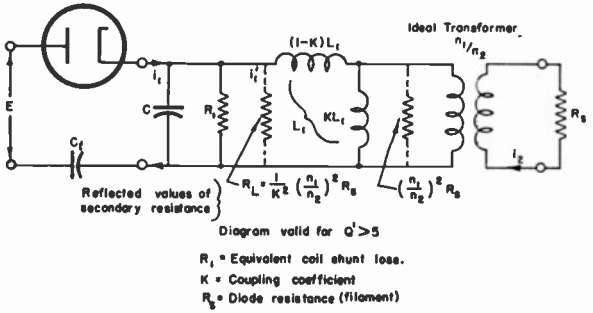

Fig. 15—Equivalent circuit of filament transformer.

It should be stated that the following expressions for the transformer design are based on the requirement that the loaded Q value (Q_o') of the primary circuit must be

$$Q_o' > 5. \qquad (38c)$$

Inasmuch as the reactive currents cancel out there is a division of the constant current i, between R_L and R_o. The fraction of current producing useful power output is therefore given by $i_1' = i_1\eta$. Hence

$$R_L = P_o/i_1^2\eta^2 \qquad (39)$$

and with Equation (38)

$$R_1 = \frac{P_o}{\eta(1-\eta)i_1^2} \qquad (40)$$

provided the LC circuit is in resonance with the driving frequency ω, i.e.

$$C = 1/\omega^2 L \qquad (41)$$

In the equivalent transformer circuit Figure 15 the reflected load resistance $(n_1/n_2)^2 R_s$ is shown in shunt with the coupled inductance $(K L_1)$. For Q values > 5 it is reflected across the tank circuit as the equivalent load resistance

$$R_L = \left(\frac{1}{K} \times \frac{n_1}{n_2}\right)^2 R_S \tag{42a}$$

the bracketed term being the effective transformer ratio. Substituting Equation (39) and $P_o = i_2^2 R_S$, it follows from (42a) that

$$\left(\frac{1}{K} \times \frac{n_1}{n_2}\right)^2 R_S = \frac{P_o}{i_1^2 \eta^2} = \frac{i_2^2 R_S}{i_1^2 \eta^2} \tag{42b}$$

The turns ratio for a given coupling is thus

$$\frac{n_1}{n_2} = \frac{K i_2}{\eta i_1} \tag{43a}$$

This equation shows that higher values of coupling indicate a greater required turns ratio. In general it will be found that there are two values of K which will give the same secondary current. In one case the reflected shunt load will be considerably less than the tuned tank impedance, the efficiency will be high, and the voltage drop across the tuned primary slightly higher than that obtained for a condition of perfect match with a loss-free transformer. In the second case the reflected shunt load will be higher than the unloaded tuned tank impedance and more power will be wasted in the transformer than is developed in the load. This, of course, will result in poor efficiency and an excessive voltage drop across the tuned circuit. The rectifier peak charging current will be unnecessarily limited and poorer regulation will result.

The inductance value can be obtained from the following expression

$$L = \frac{P_o}{\eta(1-\eta) Q_o \omega i_2^2} \tag{43b}$$

which can be derived from the previous equations.

A typical transformer calculation will be illustrated for the 90-kilovolt case where the following data are given or assumed:

$K = 0.6$ $\quad P_o = 2$ watts $\quad Q_c = 40$ (assumed)
$\omega = 390{,}000$ $\quad i_2 = 1.25$ amperes $\quad i_1 = 10$-12 milliamperes

Calculations should be made for the lower i_1 to provide a safety factor.

The turns ratio, inductance, and loaded Q can be computed from Equations 43a, 43b, and 38b respectively. These results are shown in Table IV.

Table IV—Filament Transformer Data

	10 ma		12 ma	
η%	Lmh	$\frac{N_1}{N_2}$	Lmh	$\frac{N_1}{N_2}$
85	10.1	88	7.	73
75	6.9	100	4.8	84
65	5.65	115	3.94	96
55	5.1	136	3.56	114

	η = 0.75			η = 0.65		
Q	Q'	Lmh	$\frac{N_1}{N_2}$	Q'	Lmh	$\frac{N_1}{N_2}$
40	10	6.9	100	14	5.65	115
50	12.5	5.5	100	17.5	4.54	115
60	15	4.6	100	21	3.77	115
70	17.5	3.9	100	24.5	3.23	115

The inductance value used is arbitrarily chosen to be about 5 millihenries as this will result in a coil which is not so large that its Q is adversely affected when it is placed in the corona shield. Powdered iron cores permit higher values of Q and inductance to be obtained. Higher efficiencies, smaller coils, and better couplings result.

The turns ratio, inductance, and other data for the 30-kilovolt tripler filament transformer follows:

$Q_c = 50$ $\quad L_1 = 5.6$ millihenries

Coupling $= 0.4$ $\quad$ Diameter of form $= \frac{3}{8}''$

Tuning capacitance $= 22$ micromicrofarads (for partial resonance)

Primary turns $= 500$ #10/41 Litz

Secondary turns $= 20$ #15/38 Litz

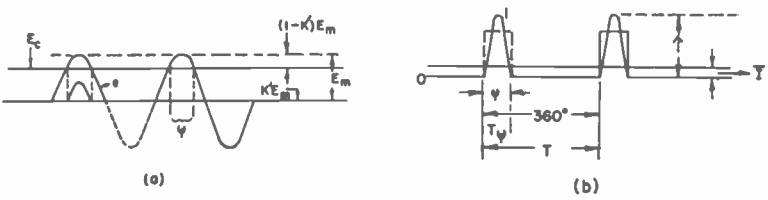

Fig. 16—Diode conduction.

Diode Currents and Regulation of the Rectifier Circuit

The relatively high frequency used in an r-f supply permits the use of a simple economical filter circuit. This circuit generally consists of a pi section resistance-capacitance (R-C) combination with the output capacity being formed from the shield to center conductor capacitance of the second anode supply lead. Inasmuch as the time constant of the filter condenser-load resistance combination is long compared with the discharge period between successive r-f pulses, the output voltage can be considered constant, and will have the value $K'E_m$, (where K' is a percentage of the peak voltage E_m) for a given load. This is shown graphically in Figure 16. The diode conduction angle can be derived from the equation

$$\psi^\circ = 2\cos^{-1} K' \qquad (44)$$

The magnitude of ψ for various values of K' has been computed and listed in Table V.

Figures 16(a) and 16(b) show the relation between the conduction time and the diode peak to average currents. The equivalent average diode current is determined by the ratio of the total time to conduction

Table V—Rectifier Data

K'	$\psi/2$	ψ	$\frac{360}{\psi}$	$\frac{2k'}{(1-k')}$	$\frac{R_L}{Z_s} \cdot \frac{2k'}{(1-k')} \frac{360}{\psi}$	$\frac{\hat{I}}{I} \cdot \frac{360\pi}{2\psi}$
.995	5.75	11.50	31.3	398.	12420.	49.
.99	8.1	16.2	22.2	207.	4400.	35.
.98	11.5	23.0	15.65	100.	1560.	24.6
.97	14.1	28.2	12.75	65.9	827.	20.
.96	16.25	32.5	11.1	48.3	522.	17.5
.95	18.2	36.4	9.9	37.9	378.	15.6
.94	20.	40.	9.	30.4	283.	14.2
.92	23.1	46.2	7.8	22.9	178.	12.3
.90	25.9	51.8	6.95	18.	124.	10.9
.88	28.4	56.8	6.35	14.5	92.7	10.
.86	30.7	61.4	5.87	12.3	84.5	9.25
.84	32.9	65.8	5.5	10.5	57.6	8.65
.82	34.9	69.8	5.16	9.1	47.0	8.1
.80	36.9	73.8	4.88	8.0	39.2	7.65
.78	38.79	77.5	4.65	7.05	32 8	7.3
.76	40.9	81.	4.45	6.32	27.8	7.

time for a cycle, $(T/T\psi)$. If this factor is multiplied by $\pi/2$, a ratio of peak to average current is obtained which, for sinusoidal diode currents, is a sufficiently close approximation for all practical purposes. Hence: $$i/I = \pi T/2T\psi \tag{45}$$

where $T/T\psi = 360$ degrees$/\psi$ degrees (for sine waves) or $T/T\psi = T_H/T\psi = T_H \times 180$ degrees$/T_R \times \psi$ degrees (for surge pulse voltages) T_H/T_R is the ratio of the total time of one cycle to the time duration of the surge pulse.

The energy delivered by the source during $T\psi$ must equal that dissipated during T. Thus equating the direct-current to alternating-current power $$TE^2/R_L = T\psi\ (K'E_m)^2/2R' \tag{46}$$

The equivalent alternating-current load R' during $T\psi$ is therefore

$$R' = T\psi R_L/2T \tag{47}$$

Replacing the diode load in Figure 17 by R' it is obvious that the voltage ratio $(1-K')\ E_m/K'E_m = Z_s/R'$, and $R' = K'/(1-K')\ Z_s$. With Equation (47) this furnishes $$R_L/Z_s = 2K'T/(1-K')\ T\psi \tag{48}$$

which is the ratio of the direct-current load resistance R_L to the effective series impedance Z_s. Computed values for this equation are given in Table V. Rectification efficiency $E/K'E_m$ and the peak-to-average diode current ratio i_d/I can thus be plotted as a function of the resistance ratio R_L/Z_s, as shown in Figure 17.

The impedance Z_s of the tuned circuit source is its surge impedance $Z_s = \sqrt{L/C} = \omega L = \dfrac{1}{\omega C}$. The energy delivered by the tuned circuit occurs at a time when no energy is being supplied to the tank circuit by the oscillator, as shown in Figure 18. During the diode conduction time a series combination of the diode resistance and the input filter capacitance is shunted across the tank circuit. The relatively large power supplied during this short interval has the effect of "braking" the normal flywheel characteristic of the tank circuit, slowing the frequency of oscillation, and producing phase delay of the tank current. During the next half cycle the oscillator will deliver sufficient energy to compensate the tank for the power delivered to the rectifier circuit, plus the normal tank circuit losses, resulting in a gain in phase.

The curves in Figure 17 are based on the relation $\omega CR \geqq 500$, which should still hold when the last stage of a voltage multiplier circuit is

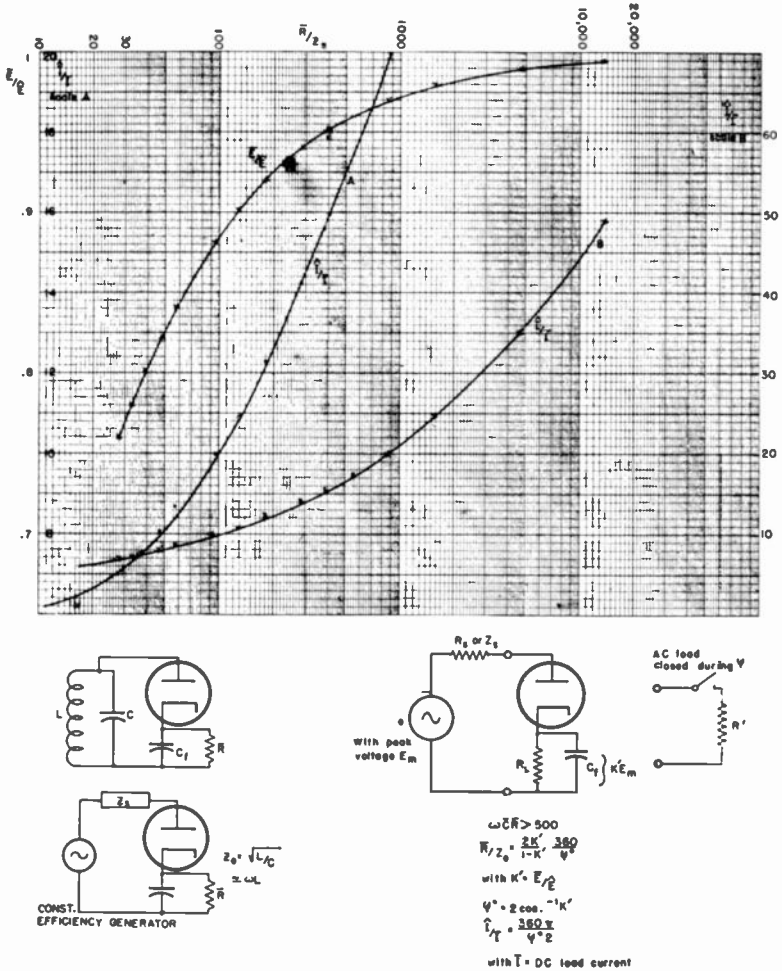

Fig. 17—Rectifier conduction curves.

connected over a number of series filter condensers.

In r-f supplies the effective filter capacitance C_f forms a voltage divider with the diode capacity, the ripple voltage being largely determined by the ratio of these capacitances. To prevent this voltage from causing excessive power loss in the output filter condenser, its capacitance should be large compared to the diode capacitance.

The effective series impedance Z_s of the 90-kilovolt circuit is given by $\sqrt{L/C} = 95{,}000$ ohms. The 110-megohm direct-current load of the tripler circuit can be reduced to parallel diode circuits with equivalent direct-current loads carrying the normal direct current for the same

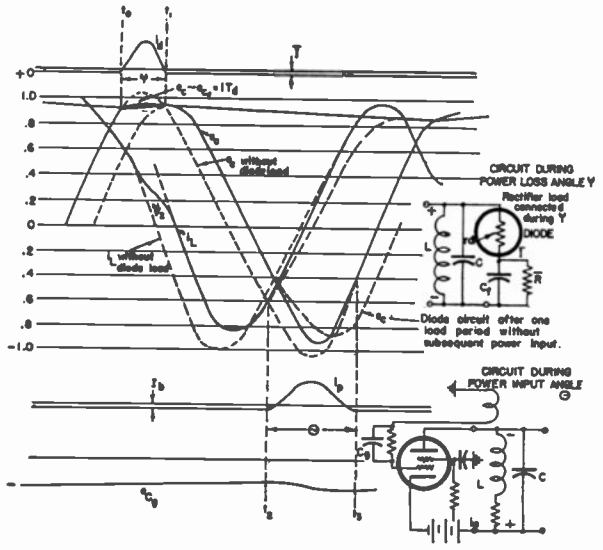

Fig. 18—Oscillator-rectifier circuit power relations.

total power dissipation, as shown in Figure 19. For the diode D_1 operating singly on one half cycle $R_r/Z_s = 378$ and from Figure 17 $\hat{\imath}/I = 15.6$. The rectifier efficiency for D_1 is $E/\hat{E} = 0.95$. Thus a regulation of about 5 per cent of 30 kilovolts or 1.5 kilovolts may be expected from the diode D_1 which conducts during one portion of the positive half cycle. During a portion of the negative half cycle diodes D_2 and D_3 conduct reducing the effective direct-current load to 18.3 megohms., R_L/Z_s will be 193 indicating a regulation of approximately 7.5 per cent from these diodes. This is equivalent to a 2.25-kilovolt drop for the 30 kilovolts from each diode. Adding these three output voltages, a loss of 6.0 kilovolts (or 6.7 per cent of 90 kilovolts) is obtained. In the previous derivations the diode resistance has been neglected. However,

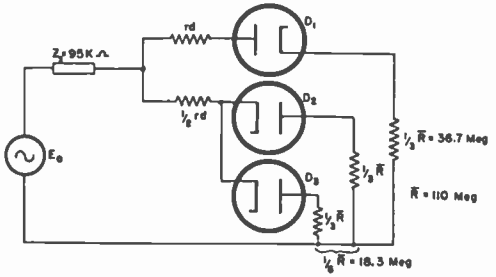

Fig. 19—Equivalent rectifier load circuit.

if this is large it should be added to the series generator impedance.

The oscillator tank circuit voltage is reduced during the time that it delivers power to the rectifier circuit, and is restored to its original value during the time that energy is supplied to the tank from the oscillator. The data in Figure 17 are based on constant oscillator efficiency. Actually the oscillator efficiency changes as a function of the load. The difference in oscillator efficiency between no load and full load is easily calculated. It is approximately 8 per cent for the 90-kilovolt circuit and this difference represents the power diverted from the tank circuit to tube loss. The corresponding primary voltage change is equal to the square root of the efficiency change. Therefore the oscillator regulation for this particular case is approximately 4 per cent.

The overall total regulation will then be in the order of 10 per cent at 800 microamperes.

Miscellaneous Operating Data

After constructing a supply in which the oscillator tubes are operated close to their maximum ratings, it may be desirable to check plate dissipation more accurately than is possible by estimating many circuit losses. In this case the operating data should be taken and the oscillator then disconnected and operated as a driven class C amplifier under the identical voltage and driving conditions. A plate load consisting of a single tuned circuit of known *Q* plus an added shunt resistance adjusted for the same plate current should replace the step-up transformer and associated circuit. A determination of actual power normally delivered to load plus all other dissipative elements is thus readily made, and actual tube dissipation easily calculated.

Excessive power input for the desired output can result from losses which are not readily apparent. The point at which these losses occur is most readily determined in the higher voltage supplies as heating progresses more rapidly due to greater energy dissipation. It is advisable to keep as much material as possible out of the field of the high voltage secondary even though such material is normally considered a good low loss insulator. A number of the plastics show rapidly increasing power factors with rising temperatures, resulting in a cumulative tendency toward breakdown. The importance of the impregnant used for the high voltage winding has been previously considered.

Several of the supplies have been built on plastic bases in order to simplify insulation problems, and reduce capacity and eddy current losses. The spacing used for the outer shield is determined by spark over, and secondary capacity loading. Close shielding of the secondary

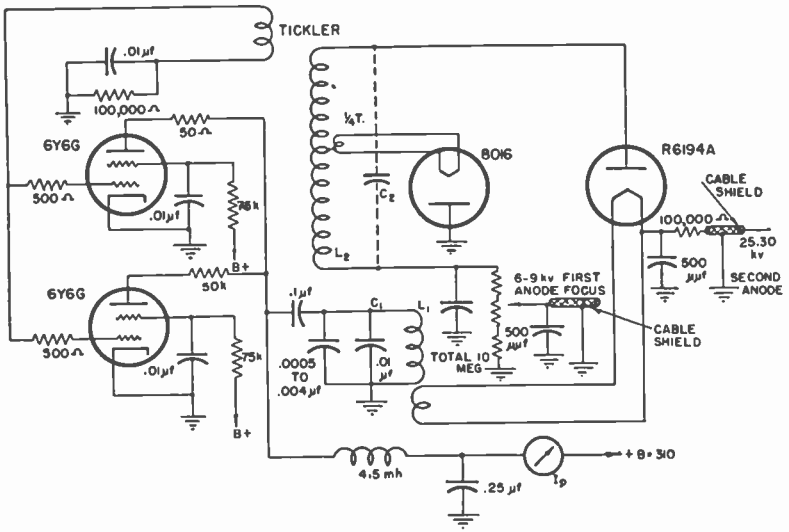

Fig. 20—Circuit of 30-kilovolt unbalanced doubler supply.

lowers its impedance, requiring greater oscillator current, and may cause increased corona difficulties.

The lead to the first diode from the top pie of the secondary should be large in diameter to avoid corona. It is advisable to start this lead at the center of a plane drawn through this pie. Any considerable mass in the field of the coil will become excessively hot after short

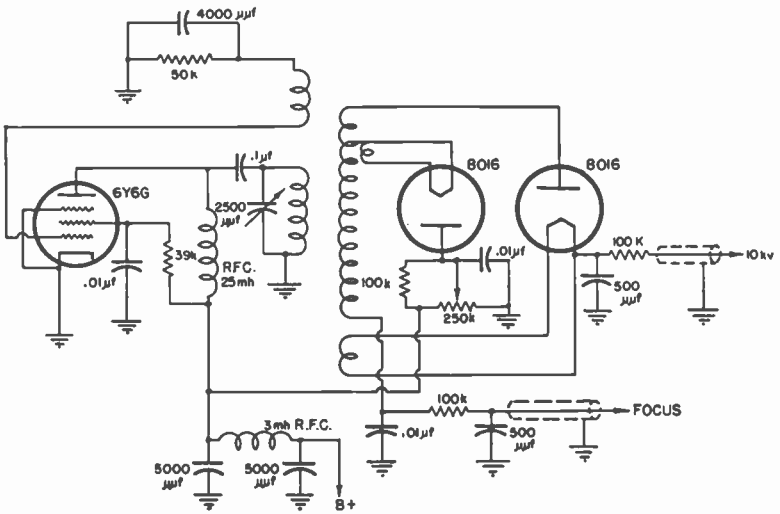

Fig. 21—Circuit of 10-kilovolt supply.

periods of operation, indicating the desirability of *very thin walled* tubing or preferably a closely wound spring. The latter arrangement is convenient for making connections and has worked satisfactorily.

Another cause of excessive oscillator current is the rectifier shunt loss occurring as a result of glass bombardment by cold emission on the inverse cycle. The 1B3GT tube will provide proper operation in the 30-kilovolt tripler, and the R-6194 in the 90-kilovolt supply.

Radiation from a supply can be largely reduced by proper filtering of the power leads, and by the use of full shielding. Ventilation must be supplied for the oscillator tubes and has been provided in most of the models illustrated by the use of holes punched in the shield near

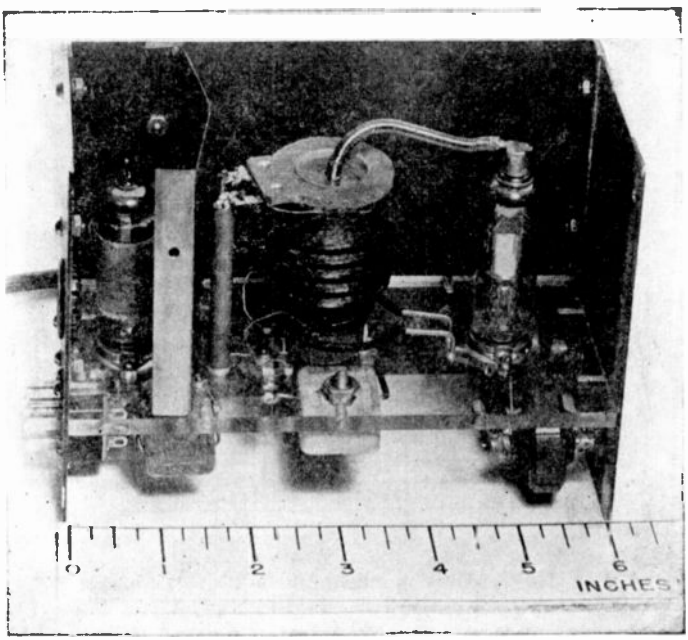

Fig. 22—Side view of 4-kilovolt supply.

bases and tops of the oscillator tubes. A close mesh screen is used over these holes, and an internal baffle placed between the tubes and the r-f transformer to minimize stray fields.

It has been found that the temperature rise can be considerably reduced by painting the inside and outside of the coil housing black, permitting better heat radiation.

Filament and high voltage output leads use polyethylene insulated wire. In order to minimize excessive voltage stress at the junction of the wire insulation and its shield, rounded corona-free fittings are

sweated to the shield at these points. These fittings also serve to anchor the wire shield tightly to the housing.

The type of resistor used for a bleeder must be carefully selected and particular attention given to its voltage rating per unit. In general more resistors will be required than indicated by their normal dissipation rating. This is caused by a change in resistance under high voltage stress and is another cause of excessive oscillator current under "no load" conditions. This may occur under actual operating conditions even though measurement of the bleeder with the usual low-voltage ohmmeter shows a normal value of resistance.

The circuits of the various supplies are given in Figures 1, 9, 13, 20, and 21. Photographs indicating the general layout and construction are

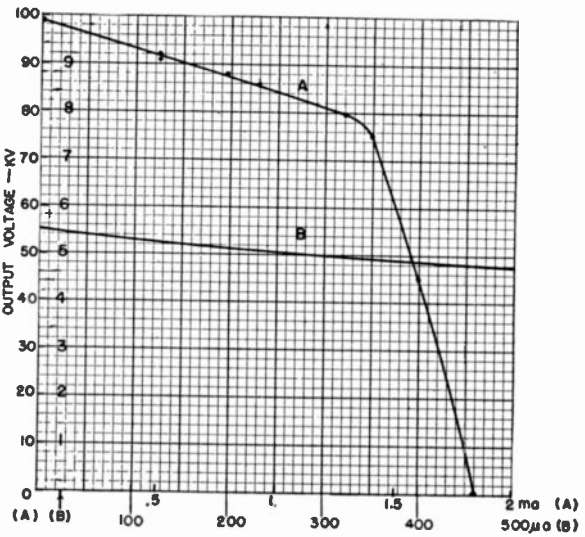

Fig. 23—Regulation curve for 90-kilovolt supply.

shown in Figures 3, 4 and 22. Regulation curves are shown in Figure 23.

A summary of coil data for several practical coils is given in Figure 5.

TABLE OF SYMBOLS

R'	effective shunt alternating current load on the secondary
$\overline{R}$	direct current load resistance
R_p	total effective plate load resistance
r_I'	total effective series resistance of loaded primary circuit
r_I	series loss resistance of primary circuit
r_{II}	total effective resistance of secondary circuit with any load

$r_{II\ max}$	total effective resistance of secondary circuit with maximum load
R_i	equivalent shunt loss of primary circuit
R_L	equivalent shunt load resistance on primary circuit
R_s	filament load on secondary of filament transformer
P_1	power dissipated in primary coil
P_2	power dissipated in secondary coil
$\hat{P}_{in}$	peak power input
P_{in}	average power input
P_{II}	power dissipated in secondary circuit
$\omega = 2\pi F$	operating frequency
$\omega_0 = 2\pi F_0$	self resonant frequency of secondary circuit
$\omega_1 = 2\pi F_1$	lower coupling frequency
$\omega_2 = 2\pi F_2$	upper coupling frequency
Q_I	value of primary tank circuit Q without load
Q_{II}	value of secondary tank circuit Q without load
Q_I', Q_{II}'	are respective Q values of loaded circuits
T	transformer transfer factor
$T_{(0)}$	transformer transfer factor at resonance
K'	rectification efficiency
K	coupling factor
K_c	minimum or critical coupling of coupled circuits
k	eddy current factor
ωL_1	reactance of primary coil
ωL_I	*effective* inductive reactance (series) of primary circuit
L_1	primary coil inductance
L_2	secondary coil inductance
$\hat{E}_2$	peak secondary voltage
E_{min}	minimum plate voltage
Z_{II}	parallel resonant impedance of secondary circuit
z_{II}	series impedance of secondary circuit
C_1	primary tuning capacitance
C_2	secondary tuning capacitance
n	number of cascaded rectifier stages
ϵ	dielectric constant
x_{II}	total effective series secondary reactance at the operating frequency
i_2	rectifier filament current
η	transformer efficiency

NOTE—In general, capital letters indicate shunt values, as R, R_p and lower case letters, series values, as r_I.
Peak values are indicated by a circumflex: $\hat{P}_{in}$, $\hat{E}_2$.
Average values are indicated by a horizontal bar: $\bar{E}$, $\bar{R}$.

TELEVISION RADIO-FREQUENCY TUNERS*†

By

Robert F. Romero

Industry Service Laboratory, RCA Laboratories Division,
New York, N. Y.

Summary—The assignment of seven television channels in the 200-megacycle region in addition to the lower-frequency pre-war channels introduced new problems in the design of television radio-frequency (r-f) tuners. The purposes of this paper are to discuss in general the requirements of r-f tuners, some possible ways of meeting these requirements, and to describe r-f tuners developed at the Industry Service Laboratory.

In a high-frequency channel-switching circuit, the switch used is an important part of the device. The residual capacitances and inductances of the switch and the complexity of the switch structure determine to a large extent the circuit used. Because of its availability, a standard twelve-position wave-change switch was used. This allows the selection of any eleven of the thirteen television channels. Only standard tube types and components available in quantity were considered in the design of the r-f tuners herein described.

General Requirements

A TELEVISION radio-frequency (r-f) tuner should have essentially the same electrical properties as a tuner for any other type of receiver. The more important of these characteristics are:

(a) Low local oscillator radiation,

(b) Good spurious-signal rejection (image and intermediate frequency (i-f)),

(c) High signal-to-noise ratio,

(d) Gain,

(e) Low oscillator drift,

(f) Good match to antenna transmission line and balance to ground.

Oscillator Radiation

Oscillator radiation from one receiver can cause severe interference with neighboring receivers. Interference possibilities from this source with an i-f frequency of 21-28 megacycles are shown in Table I.

At the present time in the New York City area there are in use a

* Decimal Classification: R583.5.
† Written in March 1947.

number of low intermediate frequency, pre-war television receivers without an r-f stage. Because of this, these receivers are in some cases causing interference on channel 4 when tuned to channel 2 and on channel 5 when tuned to channel 4.

In the absence of a suitable multi-grid television mixer, it is necessary to use common grid injection. It is apparent, therefore, that it is mandatory to provide isolation between antenna and mixer to shield the antenna from the injected oscillator energy.

Pentode R-F Amplifier Buffer

A suitable tube type for an r-f amplifier is the pentode, operated with grounded-suppressor and screen. A typical pentode has approximately 0.01 micromicrofarad capacitance between plate and grid, so that with three volts of oscillator energy on the plate and 300 ohms in the grid circuit there should appear 11 millivolts on the grid at 200 megacycles.

Triode R-F Amplifier Buffer

A cross-neutralized double-triode, such as the 6J6 or the 7F8, may be used as a push-pull r-f amplifier. To be as effective a buffer as a pentode, the neutralizing condensers must be adjusted to approximately 0.01 micromicrofarad, or for the 6J6 to about 0.75 per cent. Another complicating factor is that the degree of neutralization is a function of signal frequency due to residual inductances in the tube and in the capacitors themselves.

Neutralization of a triode reduces the coupling only for push-pull or balanced voltages. It will increase the coupling for unbalanced components of oscillator energy. It is therefore important that circuits using a neutralized triode r-f amplifier be very accurately balanced if oscillator radiation is to be reduced to a low value.

In addition to the oscillator energy fed back directly through the r-f tube, there is radiation from the oscillator tank and from the chassis. By shielding the entire r-f tuner unit, it is possible to reduce the radiation directly from the oscillator tank to a negligible quantity. It is much more difficult to reduce the radiation from the chassis. This radiation is caused by oscillator ground currents flowing in the chassis. The ground currents arise from three sources: (a) part or all of the return path for the oscillator current being in the chassis, (b) oscillator current return from the mixer grid to the oscillator, (c) current induced in the chassis by the oscillator magnetic field. The first source of chassis current can be eliminated by single-point grounding of the oscillator. There is no practical way of eliminating the latter source other than double shielding of the r-f unit.

Table I

A. I-F Interference (21.5-27.5 megacycles)[1]

i-f megacycles	Sources of Interference
21.5-21.7	International Broadcasting
25-27.2, 27.5-28	Fixed, Mobile, Government
21.7-25	Fixed, Aeronautical
25	Standard Frequency Transmission
27.2-27.5	Industrial, Scientific, Medical

B. Image Interference[1]

Channel No.	Image Frequency megacycles	Sources of Interference
1, 2	93-109	FM Broadcasting, Television and FM Receivers[2]
3	109-115	Ranges, Localizers, Television and FM Receivers[2]
4	115-121	Ranges, Localizers, FM Receivers[2], Airport Control
5	125-131	Aeronautical Mobile
6	131-137	Aeronautical Mobile, Government
7	223-229	Amateur, Government
8-13	229-265	Government

C. Direct Interference from Local Oscillators of Television Receivers (i-f 21.5-27.5 megacycles)

Channel Receiving Interference	Interfering Channel
4	1
5	2
6	3
11	7
12	8
13	9

[1] Data taken from Frequency Allocation Chart dated July 1945, prepared by RCA.
[2] Refers to local oscillator radiation from these receivers.

Oscillator

With an intermediate frequency of 21.25 to 21.75 megacycles for television sound, the local oscillator frequency varies from 71.5 megacycles for channel 1 to 109.5 megacycles for channel 6, and from 201.5 megacycles for channel 7 to 237.5 megacycles for channel 13.

If the television receiver has a sound channel 200 kilocycles wide, there is a margin of 75 kilocycles on either side of the center frequency of the sound with 25-kilocycle deviation. Obviously for this case it is desirable that the drift be less than 75 kilocycles. This is a reasonable

requirement for the lower six channels but is more of a problem at the higher frequencies.

Rejection Of Spurious Signals Induced In The Antenna

Both i-f and image-frequency signals are potential sources of interference, although any signal strong enough to produce cross-modulation also can be a source of trouble. Table I lists i-f and image-signal sources of interference for each television channel.

A general working rule is that an interfering signal ten times down (in voltage) is the threshold level for a usable picture, while 100 times down is just discernible interference. It follows that on an equal field-strength basis, the selective network should discriminate against unwanted signals by a factor of at least 100.

In general, it is not possible to attain 100:1 image rejection with two tuned circuits using simple magnetic or capacitive coupling, or stagger tuning. But by the use of increasingly complex coupling networks, it is possible to attain more spot frequencies of high rejection. Two such points of high rejection (i-f and image) require four coupling elements (e.g., two condensers and two coils, or their equivalents). The required rejections can be achieved by this method or by the use of at least three tuned circuits between the antenna and the mixer.

It should be noted that the rejection requirement for frequencies other than i-f and image is in general not as severe, since these frequencies can enter only as cross-modulation and as beat notes with harmonics of the local oscillator.

Match To Antenna Transmission Line And Balance To Ground

If the impedance looking into the antenna terminals of the r-f tuner is not equal to the surge impedance of the antenna transmission line, part of the antenna energy will be reflected back towards the antenna, and if the antenna is a poor termination, as it may be at most frequencies, the energy will again be reflected back towards the r-f tuner. If the transmission line delay is comparable to or greater than a picture element, the result is a loss of detail or a multiple image. The reduction of picture quality depends on the degree of mismatch and attenuation of the transmission line.

On the basis of the working rule mentioned above, that interference should be down 100 to 1, the maximum allowable mismatch at the r-f tuner, assuming 100 per cent mismatch at the antenna and negligible line loss, is one per cent for a just-discernible echo. An empirical study was made at video frequency, using a high-definition monoscope pattern

as a signal. With normal kinescope contrast, about ten per cent mismatch could be tolerated before the reflection became objectionable. The test was made with a 150-foot length of 72-ohm polyethylene coaxial cable, over 90 per cent mismatched at the sending end. Preliminary field tests indicate that somewhat higher reflection coefficients may be tolerated at radio frequencies, where line loss is appreciable and the antenna serves as a partial termination.

If the antenna input circuit is not balanced to ground, any voltages picked up on the transmission line are amplified in the r-f tuner, and may cause interference. For example, noise generated by a vacuum cleaner operated in close proximity to the line but relatively far from the antenna will get into the receiver if the input is not balanced. Obviously, balance does not reduce interference picked up by the antenna.

Noise Level And Gain

With the gains realizable in the r-f stage, the r-f amplifier stage determines the noise level. The noise contributed by the mixer is a small percentage of the total.

The 6J6 or 7F8 triodes provide lower noise levels than the 6AG5, 6AK5, 6AU6, and 6BA6 pentodes which are inferior by a factor of about two to one.

R-F Gain

The gain of the r-f stage, from r-f grid to mixer grid, can be expressed with sufficient accuracy for the following discussion either as

$$\text{Gain} = k\frac{g_m}{2\pi C\Delta f}, \tag{1}$$

or

$$\text{Gain} = kg_mR. \tag{2}$$

G_m is the r-f tube transconductance, C is the total shunt capacity, Δf is the bandwidth in cycles per second (usually six megacycles), k is a factor depending on the type of band-pass filter used, and R is the resonant impedance of the filter from mixer-grid to ground.

If the input conductance g of the mixer tube is less than $C\Delta\omega$, Equation (1) determines the gain. For the 6J6, 7F8, 6AK5, 6AU6, or 6BA6 tubes, Equation (1) determines the gain for channels 1 through 6. However, if g is greater than $C\Delta\omega$, Equation (2) determines the gain, where R is the reciprocal of g. Equation (2) may be written as

$$\text{Gain} = k\frac{g_m}{g}. \tag{3}$$

This equation determines the gain for channels 7 through 13 for most tubes except possibly for the 6J6 or 7F8 operated as a push-pull mixer, where the g is less than $C\Delta\omega$ even at channel 13.

Mixer Gain

The mixer gain is determined by the product of the conversion transconductance g_c and the plate load impedance. For a given tube the g_c is a function of the amplitude of the injected oscillator voltage.

Description Of An Eleven Channel R-F Tuner

A schematic diagram of an eleven channel r-f tuner is shown in Figure 1. All switch sections have two sets of contacts and two rotors connected in parallel to improve contact. Any decrease in switch inductance from the parallel connection is apparently offset by the increase in capacitance so the net size of the external inductance which can be used is substantially unchanged. The wafers are bakelite, except for the oscillator section, which is ceramic, to improve frequency stability.

Single-ended or unbalanced construction was used to minimize the number of wafers required, and otherwise simplify construction. Also with single-ended construction compound coupling is easily applied to improve the image ratio. The entire r-f tuner was built as a sub-assembly in a shielded box.

The Antenna Circuit

Single-ended construction necessitated the use of an unconventional antenna-input circuit to achieve some degree of balance. A tuned antenna transformer was not used, despite its advantage of improved signal-to-noise ratio, because of its increased complexity. The circuit used involves feeding the line to both grid and cathode of the r-f pentode. Neither the grid nor the cathode is grounded to r-f.

Figure 2 shows the input circuit with a longitudinal induced voltage e being fed through the line radiation resistance r. Impedance Z_1 and Z_2 represent all impedances between grid-and-ground and cathode-and-ground, respectively (but not impedance caused by cathode feed-back current) and Z_{12} is the coupling between Z_1 and Z_2. The cathode current I_k flows as a result of a voltage between grid and cathode and is given by

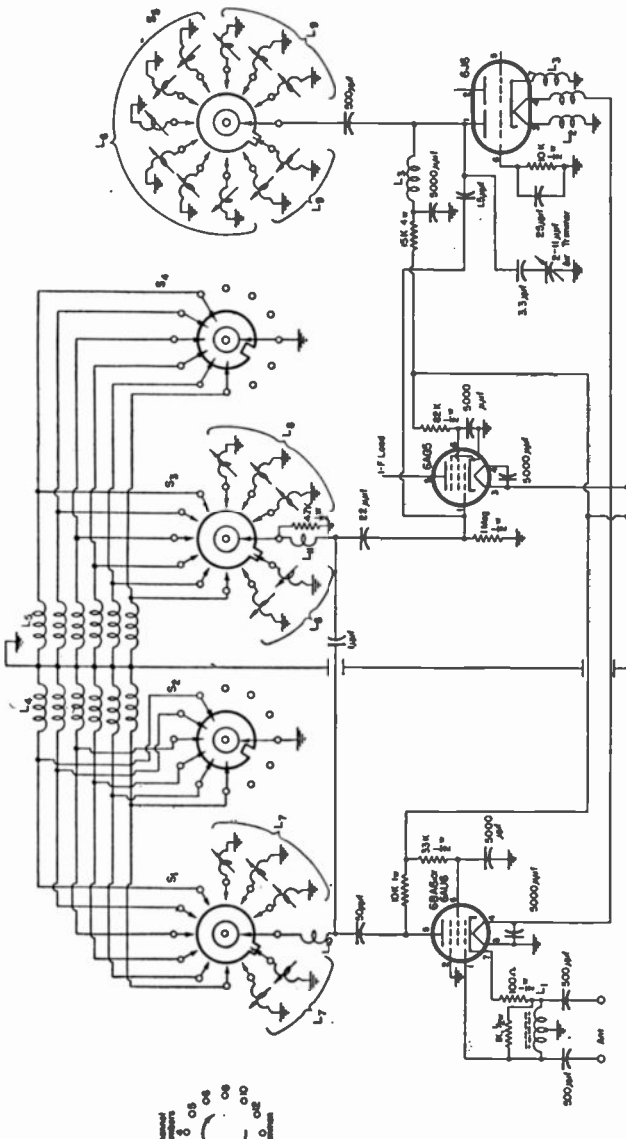

Fig. 1—Eleven channel r-f tuner.

$$I_k = e_{g\text{-}k} g_k,$$

where g_k is the cathode transconductance of the tube. A solution of the mesh equations for I_k as a function of induced voltage e yields

$$I_k = e \frac{r(Z_2 - Z_1)}{\Delta}, \tag{4}$$

where Δ is a fourth-order determinant involving r, Z_1, Z_2, Z_{12}, and g_k. The condition for balance is that $I_k = 0$, which from Equation (4) is satisfied if $Z_1 = Z_2$, provided Δ is not zero. It can be shown by substitution that Δ is not zero when $Z_1 = Z_2$.

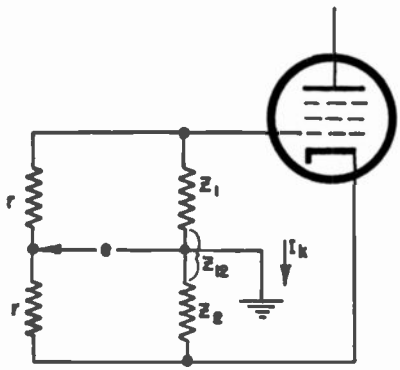

Fig. 2—Grid-cathode fed tube with longitudinal induced voltage.

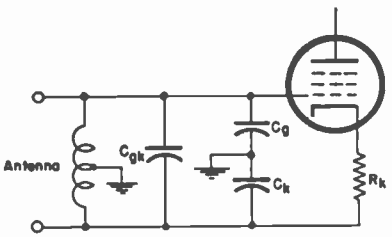

Fig. 3—Distributed capacities of grid-cathode fed tube.

The measured impedance between grid and ground will be quite different from that between cathode and ground, since the latter measured impedance would be affected by the cathode feed-back current. But when $Z_1 = Z_2$ longitudinal voltages cause no cathode current to flow.

Figure 3 shows grid-to-ground and cathode-to-ground capacities which in general are not equal and hence will not result in complete cancellation of longitudinal currents. The measured in-circuit capacities at the antenna terminals for a 6BA6 tube with grounded heater are (1) total grid-to-cathode, 6.23 micromicrofarads, (2) grid-to-ground, 6 micromicrofarads, (3) cathode-to-ground, 7 micromicrofarads.

It is necessary to use a 6BA6 or 6AU6 tube with this circuit since the 6AG5 and 6AK5 tubes have the suppressor connected internally to the cathode, which results in oscillator energy feed-back to the antenna via the large plate-suppressor capacity. In order to minimize the effect

of input loading due to transit time on the termination, 100 ohms degeneration is used in the cathode.

A center-tapped coil, wound with small wire on an iron core in order to attain high coupling, is connected to the antenna terminals. Its purpose is to tune out the input capacity for channels 1 to 6, to reject longitudinal currents by presenting a low impedance to ground to such currents, and to provide a direct-current return for the cathode current. The coil resonates with the input capacity at 62 megacycles, the geometric mean frequency between channels 1 and 6.

As shown in the Appendix, it is necessary to provide more loading than that caused by the cathode current to terminate a 300-ohm line. It was found empirically that 1000 ohms is more nearly correct than the calculated 690 ohms.

Reflection coefficients were calculated from standing-wave measurements. These measurements were made with a current pick-up loop arranged to slide along a 300-ohm line connected between the r-f tuner and a signal generator. The per cent reflection coefficient is given by

$$K_R = 100 \times \frac{SWR - 1}{\text{SWR} + 1}$$

where SWR is the magnitude of the standing-wave ratio.

As seen from Figure 4, the reflection coefficient at the higher frequencies can be improved greatly by shunting in a 0.18-microhenry coil to tune out the capacity. Either an additional wafer on the switch or a mechanical cam arrangement might be used to connect the additional coil on channels 7 to 13. If signal strength permits, an attenuation pad may be used to reduce the reflection coefficient considerably, as shown in Figure 4.

It should be noted that grid-cathode feed has the objectionable feature that termination depends on the tube transconductance, which can vary considerably in production tubes. This objection is partially overcome by the use of cathode degeneration, which tends to stabilize the transconductance.

Because of its effect on the input impedance of the tuner, control bias probably should not be applied to the r-f tube, except when termination of the system is not determined by the tuner.

Frequency Selective Network

The number of tuned r-f circuits was limited to two for economy and simplicity. Tuning capacity was restricted to tube, wiring, and switch capacities. It was found experimentally that one value of con-

denser used as high-side coupling provided substantially uniform bandwidth from channel 7 to channel 13.

The calculated coefficient of coupling with this one-micromicrofarad condenser is approximately 0.1, assuming the primary and secondary circuits each have a shunt capacity of 10 micromicrofarads, whereas a coefficient of coupling of only about 0.03 is theoretically required for 6 megacycle bandwidth at 200 megacycles. Probably such a large coupling condenser is required because it is actually tapped down on the high-frequency coils, which include the inductance of the tube leads. For this same reason, the coefficient of coupling tends to decrease progressively from channels 7 to 13, since the coupling condenser is tapped further down on the coils as the frequency increases. Thus the bandwidth tends to remain constant from channels 7 through 13.

A combination of magnetic coupling and capacity coupling was used for the lower six channels to avoid switching out the condenser used for coupling at the upper channels, and to provide improved image rejection.

By the T — π transformation, the last circuit in Figure 5 is equivalent to the first, provided

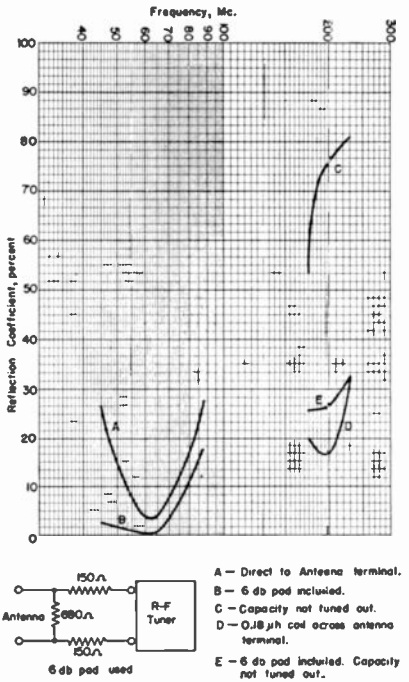

Fig. 4—Reflection coefficient of r-f tuner.

$$M' = \frac{(L + M)(L - M)}{M}, \tag{5}$$

$$L' = L + M. \tag{6}$$

It is evident that at the frequency f_∞, where

$$f_\infty = \frac{1}{2\pi\sqrt{M'C_c}}, \tag{7}$$

the rejection is infinite, since there is no coupling between primary and secondary. If $1/\omega C_c >> \omega M'$ in the pass band (that is, predominantly

magnetic coupling), then for constant C, C_c, and constant bandwidth,

$$M' \propto \frac{1}{\omega_0}, \tag{8}$$

and

$$f_\infty \propto \sqrt{\omega_0}. \tag{9}$$

It is evident from Equation (9) that f_∞ cannot be made to correspond exactly with the image frequency for all six of the lower channels. To make f_∞ correspond with the image frequency, it would be necessary to adjust both C_c and M for each channel. In this application, only M was adjusted, and only for correct bandwidth.

Although no attempt was made to adjust both C_c and M for optimum image rejection, it is seen that image rejection ratios of well over a hundred were obtained in channels 1 to 6, as contrasted to rejection ratios of 50 to 100 obtainable with simple magnetic or capacity coupling.

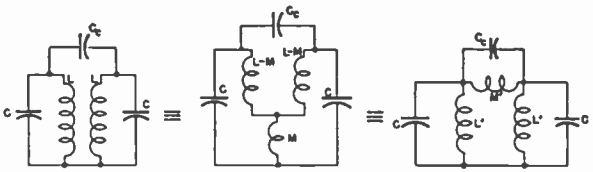

Fig. 5—Equivalent circuits of compound coupled network.

The i-f and image rejections for each channel are given in Table II.

It was necessary to ground the switch shaft at both ends because otherwise the shaft acts like a resonant trap and absorbs energy at one of the high channels. For the same reason, it is necessary to short the low-frequency coils when the high-frequency channels are in use. Alternatively, the resonant frequency of the offending low-frequency coils could be lowered by shunting them with a small capacity (say 1 micromicrofarad).

For the upper channels, the adjustable inductances consist of hairpin loops of phosphor-bronze wire with a movable brass shorting bar as shown in Figure 6. The coils for the lower channels consist of #31 enameled wire, close wound on one-quarter inch bakelite tubing with brass slug tuning. (Iron tuning can be used if desired and will provide increased tuning range.) Coil data are not given, since they would be correct only for the particular mechanical layout used.

At channel 13, if the secondary of the transformer is connected directly to the 6AG5 grid, the circuit is over-damped by the tube loading. Therefore, a capacity step-down, consisting of a 24-micromicrofarad coupling condenser was inserted. This provides critical

damping. The result is that channels 7 to 11 are somewhat overcoupled since the tube loading is less. To avoid excessive peak-to-valley ratios at the lower six channels, a 4700-ohm damping resistor is included from the switch rotor contact to ground. The resistor is placed here rather than at the mixer grid so that its damping effect at the upper channels will be minimized. In Figure 7 is shown the equivalent circuit of the mixer input at high frequency. The damping resistor R is tapped down by an amount depending on the ratio of the circuit and grid lead inductances to the total inductance.

Since grid-leak biasing is used, the mixer grid is returned to ground through a high resistance.

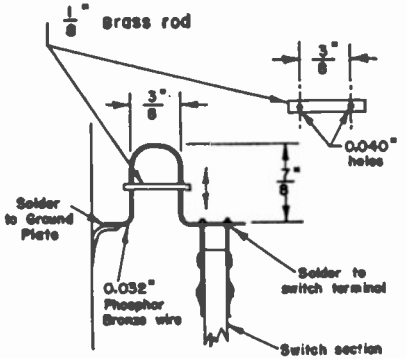

Fig. 6—Adjustable hairpin loops.

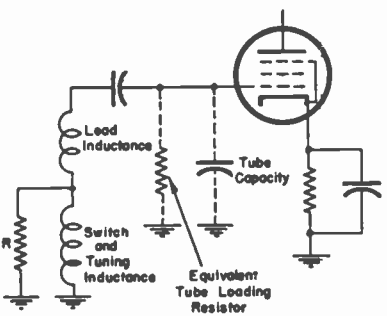

Fig. 7—High-frequency equivalent circuit of the mixer input.

MIXER

Grid-leak biasing and a series dropping resistor for the screen are used because of the self-regulating characteristics which result in the g_c being less critical to the amplitude of the injected oscillator voltage.

The cathode is returned to ground through a by-passed resistor, rather than being directly grounded to protect the tube in the event of failure of the local oscillator. If the cathode resistor is not by-passed, the overall gain is reduced about 40 per cent because of the degenerative effect of the resistor on the i-f signal and the lowered g_c caused by reduction in peak g_m obtainable at the positive peak of the local oscillator injected voltage.

LOCAL OSCILLATOR

For economy, it may be desirable to use an oscillator requiring only one switching point. A simple circuit which will extend over the required frequency range is the Colpitts, shown in Figure 8, using a triode, with the grid grounded and the cathode isolated by a choke.

One section of a 6J6 tube was used. It was necessary to isolate not only the cathode but also the heater with a separate r-f choke to maintain strength of oscillation at the upper channels. A grounded heater introduces more circuit capacity, that component between cathode and heater being low *Q*. On the other hand, it would be desirable to use a grounded heater to eliminate a choke and because the warm-up characteristics of the cathode-heater capacity tend to offset the drift caused by the other circuit capacities.

Oscillator energy is coupled to the mixer-grid circuit by a small condenser from the oscillator plate. Each channel has a separate adjustable oscillator inductance. For the lower six channels, the inductances consist of enameled wire close wound on one-quarter inch forms with brass slug tuning; (iron tuning can be used if desired). For the upper seven channels the adjustable inductances consist of hairpin loops of phosphor-bronze wire with movable brass shorting bars, as shown in Figure 6. Vernier tuning is accomplished with a 3-11 micromicrofarad variable air condenser. Vernier adjustment limits and the direct-current voltage developed at the mixer grid are shown in Table II.

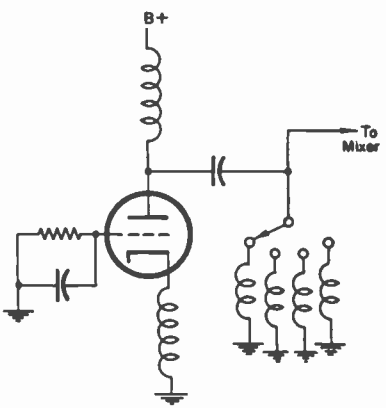

Fig. 8—Single-ended Colpitts oscillator.

Frequency drift of the local oscillator may be divided into two components, a short-term and a long-term drift. The short-term drift is due to heating of the oscillator tube, which causes the interelectrode capacities to change.

In Figure 9, the set of curves to the left of the dotted line shows the frequency drift caused by heating of the oscillator tube as a function of time after the set is turned on.

The long-term drift is caused by an increase in the temperature of the other oscillator circuit components. In general, drift caused by an increase in ambient temperature occurs over a long period of time, ceasing only when the complete receiver chassis has reached its final operating temperature. The set of curves to the right of the dotted line in Figure 9 show the long-term drift as a function of chassis temperature rise above room temperature.

To obtain the overall frequency drift, it is only necessary to add the short-term and long-term drifts shown in Figure 9.

Frequency Drift Caused by Tube Heating

The frequency drift caused by heating of the oscillator tube is influenced by the total circuit capacity. For this reason, it is desirable to use as much circuit capacity as possible. The plate voltage on the local-oscillator has a marked effect on the tube warm-up drift, as shown in Figure 10. In general, as low a plate voltage as possible should be used.

The plate voltage-dropping resistor should be of sufficient wattage so that its resistance will not change appreciably during operation. If this resistance increases during operation, the plate voltage will drop, and the negative-frequency drift will be increased.

About 130 volts on the plate appears to be a satisfactory compromise between stability and adequate oscillator strength.

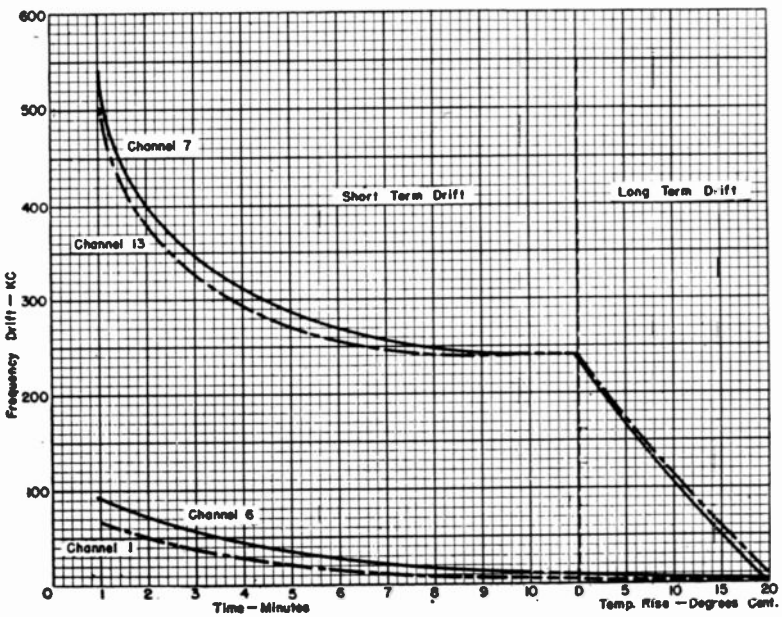

Fig. 9—Frequency drift of local oscillator.

Frequency Drift Caused by Increase in Ambient Temperature

The wave-change switch has a positive temperature coefficient of both capacitance and inductance. It is therefore necessary to compensate by the use of negative-coefficient condensers. The various condensers associated with the oscillator circuit each has a negative temperature coefficient of 750 parts per million per degree centigrade.

The oscillator inductors for the low-frequency channels can be made with either a positive or negative-temperature coefficient. As

is evident from Figure 11, if the coil form has a high thermal expansion coefficient relative to the brass slug mounting screw, the coil moves into the brass slug during heating, tending to reduce the coil inductance. A plastic coil form with a high coefficient of thermal expansion, and a steel screw to support the brass lug was used, as shown in Figure 11.

The wire size and distance of the coil from the mounting plate were chosen empirically so that approximately full compensation was achieved for a chassis temperature rise of 20 degrees centigrade, as shown in Figure 9.

Only partial compensation was possible for the upper seven channels. At these higher frequencies, a major portion of the oscillator

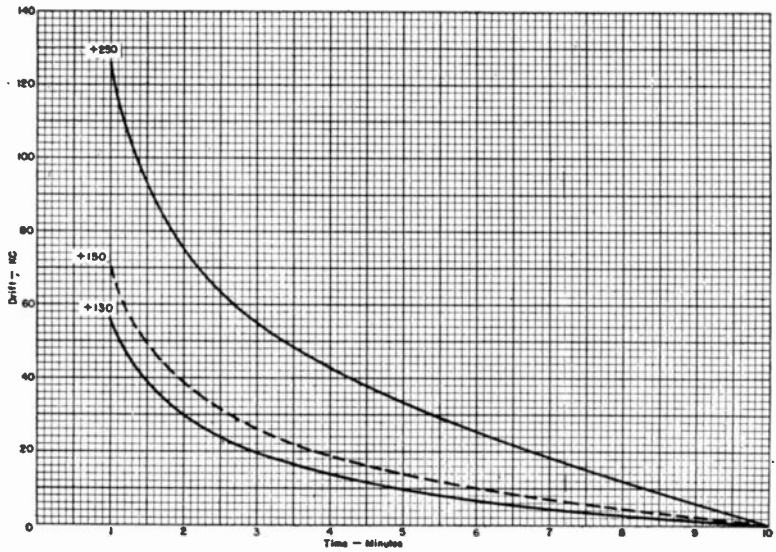

Fig. 10—Effect of plate voltage on oscillator tube warm-up drift.

inductance is in the wave-change switch, so that it is very difficult to compensate with the remaining adjustable inductance. Thus any compensation must be made by the use of small condensers with very high negative temperature-coefficients. The drift curves shown to the right of the dotted line in Figure 9 were taken with negative 750 parts per million per degree centigrade feedback and coupling condensers. As may be seen, only partial compensation was attained for channels Seven and Thirteen. Probably condensers with temperature-coefficients of at least negative 1500 parts per million per degree centigrade would be required for full compensation.

Switch Reset Errors

Because of imperfections in the switch detent mechanism, the oscillator frequency will in general be different each time a particular channel is switched in. The table shows maximum and arithmetical average errors observed for each of four channels for a typical switch.

Channel No.	Max. Error-kc	Average Error-kc
1	19	12
6	82	40
7	67	47
13	117	47

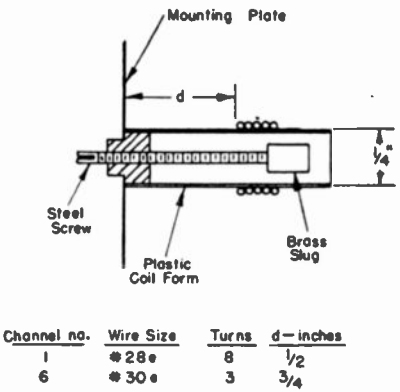

Channel no.	Wire Size	Turns	d—inches
1	#28e	8	1/2
6	#30e	3	3/4

Fig. 11—Temperature compensated oscillator coil.

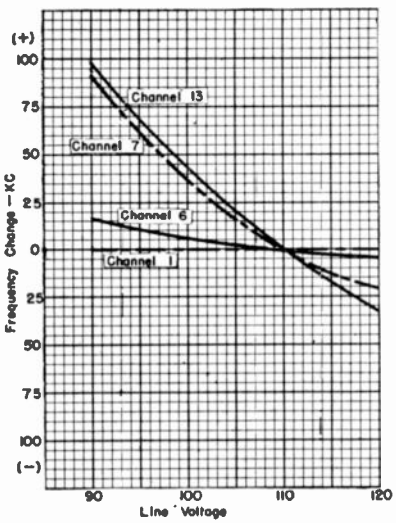

Fig. 12—Effect of line voltage on local oscillator frequency.

Effect of Line Voltage Variation

If the line voltage varies, the local-oscillator frequency will be affected principally by the change in temperature of the tube heater and by the change in plate voltage. Figure 12 shows the effect of variation of line voltage for each of four channels.

Several other arrangements using the Colpitts oscillator were tried which included additional tank capacity at the lower frequencies for improved stability. None were entirely satisfactory, however. One circuit used a coil directly at the oscillator plate. Variable condensers were shunted in with the switch for the lower channels and variable

inductances were shunted in for the upper channels. At channels 1 and 2, where the L-C ratio was lowest, the oscillator tended to oscillate at a high frequency determined by the switch inductance and tube capacity.

A 6C4 tube was tried, but the oscillator strength was low at the upper channels.

Oscillator Radiation

Two measurements were made of oscillator radiation. The first measurement was oscillator energy at the antenna terminals, while the second was overall radiation.

Oscillator Energy at Antenna Terminals

This component of radiation was measured with a shielded calibrated receiver connected to the antenna terminals with a short piece of transmission line. This component of radiation is lower than predicted on the basis of grid-plate capacity. The reason probably is that the cathode-plate capacity forms a bridge which tends to balance out the feed-back energy.

Overall Radiation

The overall radiation, including that from the chassis and the transmission line, was measured by connecting the r-f tuner to a calibrated 40-megacycle dipole and reflector with a 300-ohm transmission line about ten feet long, beamed directly at a similar antenna some 30 feet away which was connected to a receiver. The radiation, expressed in microvolts to the calibrated antenna, is given in Table II.

Gain

The gain from antenna terminals to the mixer plate was measured with a 100-ohm mixer plate load. The data as recorded in Table II are given as gain per 1000 ohms of mixer plate load.

The gain from induced antenna voltage to the mixer plate when the antenna is matched to the line will be one-half that given in Table II, because of the voltage drop in the antenna.

Noise

The noise was measured by cascading the r-f tuner to a high-gain 4-megacycle i-f amplifier. The procedure described in the 1938 bulletin "Standards on Radio Receivers" published by I.R.E., was followed, except that root-mean-square (r-m-s) noise measurements were made

by estimating the r-m-s value on a wide-band oscilloscope. The equivalent-noise-signal-input (ENSI) noise is given in Table II.

It was found that most of the total noise was generated by the r-f tube. This fact was determined by noting that shorting the antenna terminals had no appreciable effect on total noise, and removing the r-f tube from its socket reduced the noise several fold.

Alternate Switching Arrangements

It may be desirable in certain applications to provide for only eight channels, with provision for tuning to cover adjacent channels. The tuner schematic shown in Figure 13 differs from that shown in Figure 1 only in the switching arrangement and in the local oscillator. The rotor contact of each r-f switch section is the r-f return to ground. Coils L_6 and L_7 are used to tune channel 13. Inductances L_8 through L_{13} can consist of stampings of appropriate width between adjacent switch contacts, so that the inductances added to those of L_6 and L_7, respectively, tune to progressively lower odd-numbered high-frequency channels. In order to tune to the even-numbered high-frequency channels it is necessary to increase only the inductances of coils L_6 and L_7 with iron cores. Thus the inductances of L_8 through L_{12} need not be adjustable. The coil sets L_3 and L_4 are core tuned and magnetically coupled for six megacycles bandwidth. Except for certain combinations, these are tunable to adjacent channels, but must be adjusted individually. For some combinations, it may be necessary to add capacity across one or more coils. For this reason, it may be desirable to put in all six of the lower channels. This still leaves a blank switch position.

This type of switching has the advantage that all the unused coils are shorted so that there is no possibility of their acting as resonant traps to the signal or oscillator frequency.

Local Oscillator

The local oscillator shown in Figure 13 may be used with the circuit shown in Figure 1 as well. It is a balanced push-pull oscillator using a 6J6 tube. Tuning is done with iron-core inductances for all thirteen channels. A grade of iron core advertised as 100-megacycle iron is satisfactory.

This type of oscillator has marked advantages over the single-terminal switching circuit shown in Figure 1 in that (1) no isolating chokes are required, (2) the circuit capacity is less so that ordinary coil forms and cores may be used to tune the high channels (on a one-

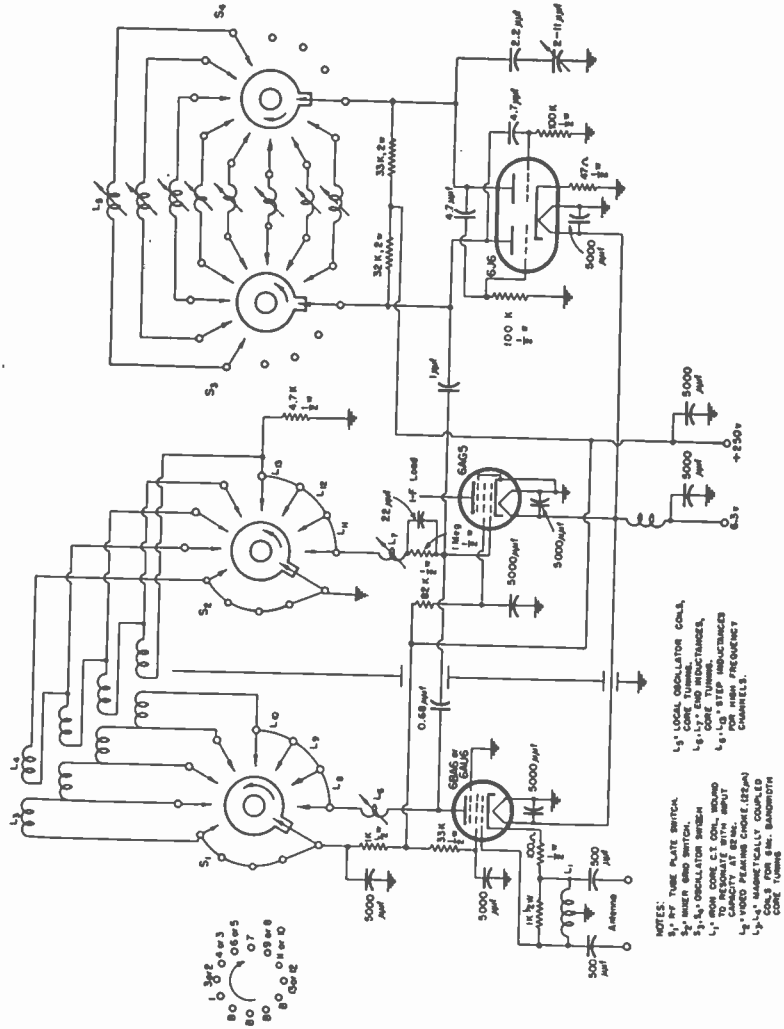

Fig. 13—Eight channel r-f tuner.

Table II—Performance of r-f tuner.

Channel #	Image Rejection Ratio	I-F Rejection Ratio	Gain[1] per 1000 ohms Mixer Plate Load	Overall Oscillator[2] Radiation Microvolts	Radiation at Antenna Terminals μv across 300 ohms	Balance to Unbalance Ratio	Noise μv (ENSI)	Limits of Frequency Trimmer megacycles	Band Width to 70 per cent Points	Developed Direct-Current Volts at Mixer Grid
1	715	71	6.9	1100	810	12	28	± .6	6	7.5
2	555	82	5.7	450	1500	14	28	± .6	6	6.2
3	2900	100	5.7	1000	1500	15	28	± .75	6	6.0
4	625	143	4.2	1200	440	15	22	±1.0	6	5.0
5	1660	200	4.2	1400	76	16	34	± .75	6	6.8
6	4500	200	6.2	380	410	18	30	±1.0	6	5.6
7	72	500	3.9	↑	2700	31	29	±1.5	5.5	4.5
8	83	350	4.2	↑	2000	21	23	±1.5	6.3	5.1
9	80	600	4.1	↑	2000	15	21	±1.7	6.0	4.9
10	67	1000	3.7	(3)	1500	11	16	±1.8	5.2	4.8
11	50	800	3.3	↓	1300	11	18	±1.9	5.1	4.6
12	25	550	2.9	↓	1000	10	17	±2	5.0	4.5
13	25	1000	3.9	↓	3000	6	13	±2	5.5	4.6

[1] Gain is from antenna terminals to mixer plate.
[2] Equivalent microvolts to a 40-megacycle dipole and reflector.
[3] Excessively high noise level made measurement impossible.

quarter inch form, the coil consists approximately of two turns of #20 wire, spaced a wire diameter for the high-frequency channels), (3) chassis currents are reduced since the main tank current return is through the switches.

It should be noted that the oscillator is not perfectly balanced. The injected voltage is taken from one plate, while the trimmer is connected to ground from the other plate. The only apparent effect is to increase the chassis currents.

Appendix

Input Impedance of Grid-Cathode Fed Tube

The mesh equations of the circuit are:

$$I_k = e_{g-k} g_k,$$

or

$$I_k = (e - I_k R_k)\, g_k, \tag{10}$$

and

$$e = I_o Z_1 - (I_k - I_o)\, Z_2 - (I_k - I_o)\, Z_{12} + I_o Z_{12}. \tag{11}$$

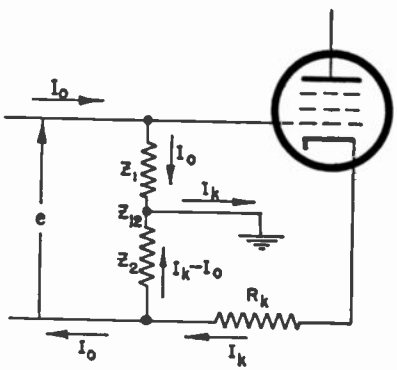

Fig. 14—Grid-cathode fed tube.

Solving Equation (10) for I_k gives

$$I_k = e \frac{g_k}{1 + R_k g_k}.$$

Let $$g'_k = \frac{g_k}{1 + g_k R_k}. \tag{12}$$

Substituting,

$$I_k = eg'_k. \tag{13}$$

Substituting for I_k in Equation (11), and solving for e yields

$$e = I_o \frac{Z_1 + Z_2 + 2Z_{12}}{1 + g'_k (Z_2 + Z_{12})}.$$

The input impedance is the ratio of e to I_o, or

$$Z_{\text{input}} = \frac{e}{I_o},$$

$$= \frac{Z_1 + Z_2 + 2Z_{12}}{1 + g'_k (Z_2 + Z_{12})}. \tag{14}$$

Let $Z_1 = Z_2 = Z$. From Equation (14),

$$Z_{\text{input}} = 2 \frac{Z + Z_{12}}{1 + g'_k (Z + Z_{12})}. \tag{15}$$

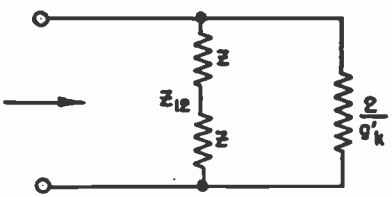

Fig. 15—Equivalent input circuit of grid-cathode fed tube.

Multiplying numerator and denominator of Equation (6) by $2/g'_k$ yields

$$Z_{\text{input}} = \frac{\frac{2}{g'_k}(2Z + 2Z_{12})}{\frac{2}{g'_k} + (2Z + 2Z_{12})}. \tag{16}$$

From Equation (16) it is evident that Figure 15 is the equivalent circuit when $Z_1 = Z_2 = Z$. The equivalent resistance $2/g'_k$ may be considered the loading introduced by the cathode feed-back current. Let $Z_1 = 0$, $Z_{12} = 0$ (grounded grid operation). From Equation (14)

$$Z_{\text{input}} = \frac{Z_2}{1 + g'_k Z_2}. \tag{17}$$

It is evident that for this case, the loading introduced by the cathode feed-back current can be represented by a resistance $1/g'_k$. Let $Z_2 = 0$, $Z_{12} = 0$ (grounded cathode operation). From Equation (14),

$$Z_{\text{input}} = Z_1. \tag{18}$$

For a 6BA6 tube with $R_k = 100$ ohms, $g_k = 6000$ micromhos, substitution in Equation (12) gives $g'_k = 3750$ micromhos. If Z_1 and Z_2 are equal, and if Z_1, Z_2, and Z_{12} are reactances, the input resistance is

$$R_{\text{input}} = \frac{2}{g'_k},$$

$$= 530 \text{ ohms.}$$

If it is desired to match to a 300-ohm line, an additional damping resistor, R, must be included.

$$R = \frac{530 \times 300}{530 - 300}, \tag{19}$$

$$= 690 \text{ ohms.}$$

For a 300-ohm input resistance, it is possible to use a g'_k as large as 2/300 millimhos or 6667 micromhos. A larger g'_k results in an input resistance less than 300 ohms.

Equation (10) assumes that the tube is a constant-current generator. This is true provided the total cathode impedance to ground is small compared to the cathode-screen dynamic tube resistance.

MAGNETIC-DEFLECTION CIRCUITS FOR CATHODE-RAY TUBES*†

By

OTTO H. SCHADE

Tube Department, RCA Victor Division,
Harrison, N. J.

Summary—An analysis of the operating cycle in fundamental sawtooth current generating circuits establishes the general requirements for obtaining linear magnetic deflection of cathode-ray beams.

The graphic representation of the circuit resistance as a load line in the plate characteristics of electron tubes functioning as an electronic switch, furnishes an accurate means of obtaining operating conditions and specifications for the design of practical tubes and circuits.

It is shown that a substantial fraction of the circulating power in certain deflection systems can be recovered as d-c power output from the circuit and, by the use of specific transformation ratios, may be recirculated through the system. Function and design of practical power feedback circuits are analyzed as well as the design requirements for efficient circuit elements, power- and booster-tubes.

INTRODUCTION

THE trend in the design of magnetically deflected cathode-ray tubes for television uses has greatly increased the magnitude of the field energies required to deflect the electron beam and has made the design of efficient deflecting circuits a major receiver problem. For example, a modern short kinescope having a 50-degree deflection angle and operating at 10 kilovolts would require over 50 watts of direct-current power for full deflection of the beam if circuits such as were used in prewar television receivers should be employed. From the economic viewpoint, this large power requirement would present a rather intolerable condition.

It has long been known that, in principle, an ideal cyclic system for deflecting an electron beam requires only wattless power, and that, in practice, the deflection circuit should function as a power control system and should dissipate only a fraction of the circulated power. The operation of such a control cycle can be illustrated by means of the simple circuit shown in Figure 1(a).[1] In this circuit, closing

---

* Decimal Classification: R138.312 × R583.
† Reprinted from *RCA Review*, September, 1947.

[1] Deflection circuits with diode (non-linear)—
(a) A. D. Blumlein, (Britain) U. S. Pat. 2,063,025 (Dec. 8, 1936);
(b) Andrieu, U. S. Pat. 2,139,432 (Dec. 6, 1938).

switch S allows the battery voltage E to drive an exponentially rising current i_1 through the inductance L. A high percentage of the delivered power is stored in the form of increasing magnetic energy in the deflection-coil field. When the current $(+i_1)$ and field strength which give the desired deflection of the cathode-ray beam from the center position have been attained, the switch is opened—Figure 1(b) and (c). The magnetic field must be quickly reversed to give a similar negative deflection (Figure 1(b)). This field reversal takes place without external control because a tuned circuit (LRC) is always formed by L and the inherent capacitance C of the system.

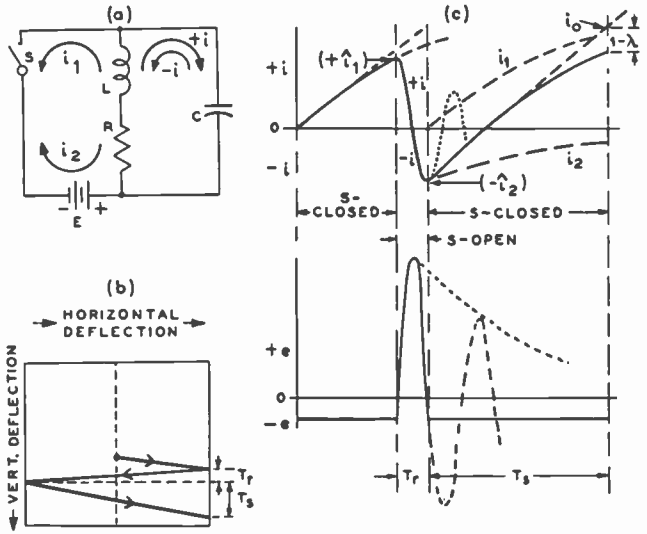

Fig. 1—Fundamental cyclic power-control system for deflecting an electron beam.

Thus, the magnetic energy is converted into potential energy in the electric field of the capacitance by current flow $+i$ from L to C and back again into magnetic energy by reversed current flow $-i$ in substantially one-half cycle of oscillation. The phase relation of voltage and current in low-Q circuits is shown by the vector projections in Figure 2. For values $Q > 3$, the assumption that $\beta = 0$ and $\psi = \pi/2$ is permissible. The retrace time of the beam is, therefore, determined by the constants L and C of the system and can be expressed as

$$T_r \simeq \pi \sqrt{LC} \tag{1}$$

The Q value of the tuned circuit determines the completeness of field reversal; i.e., the peak current ratio which can be written as

$$\hat{i}_2/\hat{i}_1 \simeq \epsilon^{-\pi/2Q} \tag{2}$$

The switch voltage e_s rises to a high value during T_r as shown by the following equation: $\hat{e}_s = E + \hat{e}_c \simeq E + \hat{i}_1 \sqrt{L/C}\, \epsilon^{-\pi/4Q}$ (3)

After reversal of the current flow, the magnetic energy is released for power feedback into the d-c source by closing the switch. The current in the subsequent deflection period T_s may be considered as the sum of two exponential currents $i = i_1 + i_2$ (see Figure 1(c)). The negative current section of the total current i recharges the battery while the beam deflects back to the center position.

Proper functioning of this circuit requires a high L/RT ratio; i.e., incomplete decay of the transient currents. If $R = 0$, the ideal linear current is indicated by i_0, in Figure 1(c). The linearity of the sawtooth current is expressed by $\lambda = (1 - \epsilon^{-RT_s/L})/RT_s/L$ (4) This linearity is not sufficient for television purposes with practical

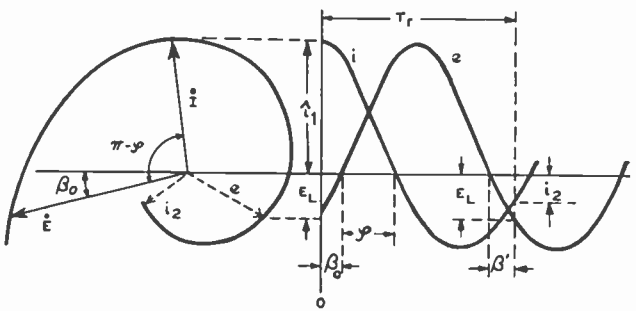

Fig. 2—Phase relations of voltage and current in low-Q circuits during retrace time. ($\tan \phi = 2Q$; $\sin \beta_0 = E_L/\hat{i}_1 \sqrt{L/C}$; $\sin \beta' = E_L/i_2' \sqrt{L/C}$).

coil constants since a deviation of $1 - \lambda = 0.05$ must be considered the upper permissible limit. The necessity for high-speed switching requires the use of electronic switches. The efficiency attainable from such methods has been poor in the past because of the large power losses in the circuit elements and in the switch circuit.

The development of suitable electron tubes for the switch circuit requires that the switching operation be performed at voltages and currents within the range of practical tube characteristics. To provide maximum performance, circuit and tubes must satisfy certain requirements as follows:

1. the deflection current should change linearly with time in circuits operating with present and future television scanning speeds; the circuit Figure 1(a) must, therefore, be modified;

2. the power consumption of the circuit should be minimized by reduction of current or power losses; large energy requirements indi-

cate, therefore, a return of power in a form suitable for feedback or other useful purposes; and

3. the circuit and system must be stable in operation, avoid critical adjustments, and have a moderate cost.

The cyclic transition from oscillatory to aperiodic circuit operation results in unusual operating conditions for the switch tubes. These tubes must control large currents with low voltage drop in the aperiodic phase (T_a), and withstand four to five kilovolts in the oscillatory phase (T_r) of the operating cycle.

The use of a voltage-step-down transformer provides a desirable reduction of the surge voltage on the elements in the secondary circuit and, besides, allows the use of larger capacitances in the secondary circuit, but it increases the current values. Since part of the electronic switching operation can be transferred to the secondary side of such a transformer, its transformation ratio and capacitance effects must be considered in conjunction with tube characteristics.

An analysis will show that linearity of the deflection current cannot be obtained unless the circuit resistance is cancelled during the aperiodic phase of operation. This cancellation requires that the electronic switch act as a negative resistance.

The concept of a negative resistance is very useful in problems of switch and circuit design. It establishes a direct link to general graphic solutions with actual tube characteristics which, in turn, furnish exact numerical values for all operating conditions of circuit and switch. A general analysis will show that certain circuits can be eliminated because of inefficient tube operation and that others can be ignored because of divergent requirements between current control in the tube and linearity in the circuit. The final choice of circuits and of tube types will depend as much on constructional requirements involving high-voltage insulation, low-capacitance mounting of circuit elements, and control of critical tolerances, as it will on operating efficiency and on power requirements.

Deflection Circuits With Controlled Negative Resistance

Linear deflection of the cathode-ray beam requires a deflection current with a constant rate of change with time. A deflection current i with constant rate of change induces a constant inductive voltage

$$e_L = L\, di/dt = \text{constant} \tag{5}$$

This relationship is obviously not true of the circuit of Figure 1, where

$$e_L = E - iR \tag{6}$$

To obtain linear deflection, therefore, it is necessary to eliminate the iR drop in the circuit. Although the deflection-coil resistance R cannot be made zero, a generator modulated in synchronism with the current i can be employed as shown in the circuit of Figure 3, to supply compensation for the iR drop in the aperiodic phase of circuit operation. Such compensation requires that the characteristic of the generator obey the law $\Delta e/\Delta i = -R$

a condition which can be met by utilizing the control characteristic of an electron tube. At first thought, it may appear that this control should be a direct function of the current i, but such control will cause instability in the form of relaxation oscillations because the circuit would then have no time constant of its own within the controllable current range of the tube. The control, therefore, must be effected by a voltage having an independent time constant, i.e.,

$$\Delta ep/\Delta ip = -R = f(e_g), f(t) \qquad (7)$$

The quantity $-R$ is a negative resistance and is shown graphically in Figure 4. With the operating path $-R$ given, it is now relatively simple to find the control voltage $e_g = f(t_s)$ required during the trace time T_s as a dependent variable from the electron-tube plate characteristic. It will be shown that circuit modifications are required by the fact that an electron tube can conduct only a positive current. The operating conditions during retrace time (T_r) place additional requirements on the switch circuit and determine the corresponding control voltage $e_g = f(t_r)$.

The complete control voltage wave $e_g = f(t)$ must also remain within certain limits of waveform and amplitude which can be generated in auxiliary circuits with the voltages available.

Electronic Switches With Negative Resistance

Switch with one electron tube

The function of an electron tube in generating a negative resistance is explained by the graphic construction of Figure 5. Stability of operation is obtained by varying the control-grid voltage of the tube as a function of time as required by Equation (7). Figure 5 shows that the operating path $-R$, constructed from current and voltage waves, is the familiar load line in the tube characteristic. The negative control signal voltage $e_g = f(t_s)$ is obtained by plotting the intersections of the grid voltage curves with $-R$ against Δt_s. Current range and control signal obviously depend on where $-R$ lies in the plate characteristics of the tube.

The bidirectional current $\pm i$ in the deflection circuits of Figure 1 or Figure 3 requires an operating path $-R$ passing through the zero

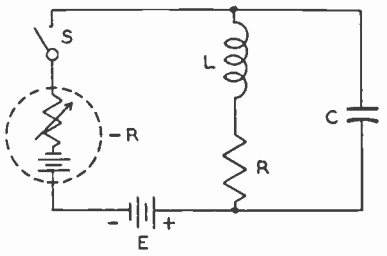

Fig. 3—Control system employing a generator to compensate for iR drop in deflection-coil resistance for linear deflection of an electron beam.

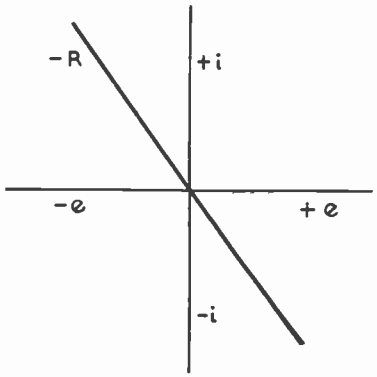

Fig. 4—Graphical representation of equivalent negative resistance generated in circuit of Figure 3.

current value. A single tube with one current-carrying electrode can, therefore, function only when the negative return current $-i$ is eliminated. The tuned circuit must then be made aperiodic by using a shunt resistance to dissipate all of the stored energy. This solution is satisfactory for low-frequency (vertical) deflection circuits where a short retrace time is obtainable with deflection coils of large turn-number and inductance. Equation (5) shows that the inductive volt-

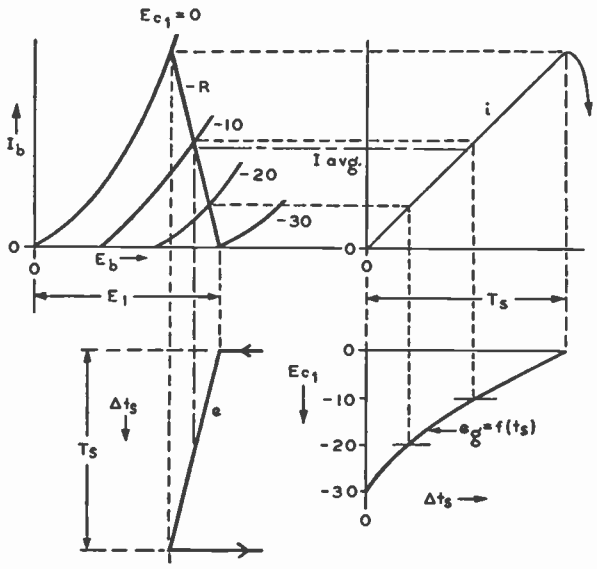

Fig. 5—Graphic construction indicating function of a single electron tube in generating a negative resistance.

age component is small and, therefore, the deflection coil acts predominantly as a resistive load R which can be matched by suitable transformer ratios to the tube characteristics.

This method, however, is too inefficient to be considered for high-frequency (horizontal) kinescope deflection, where dissipation of the stored energy in a damping resistor will double the required input power and lengthen the retrace time. It is, therefore, essential in this case to design the switch circuit for conduction of bidirectional currents.

A bidirectional current can be conducted by two electron tubes

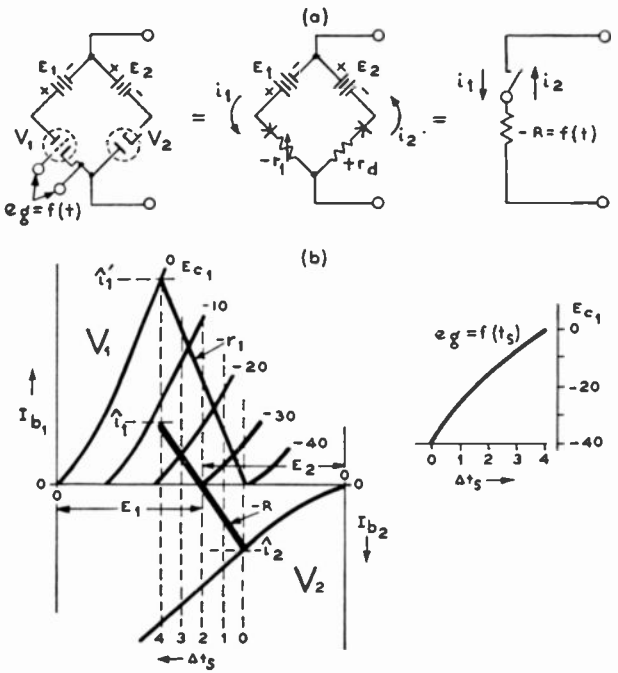

Fig. 6—Bridge and equivalent circuits for obtaining bidirectional currents; and, characteristic curves showing tube operating conditions for balance of steady current component.

forming a bridge circuit. The steady current component required by tube operation in the positive current region can thus be balanced out. It follows that to accomplish this, one of the tubes must have a controllable voltage drop.

Switch with triode and diode

A bridge circuit containing one triode V_1 and one diode V_2 is shown in Figure 6(a). Tube operating conditions for balance of the

steady current component are obtained from the joined characteristics shown in Figure 6(b). The load-line slope $-R$ is equal to the known positive resistance R of the deflection coils, ending at i_1 and i_2 in the respective quadrants of V_1 and V_2. The diode characteristic is drawn

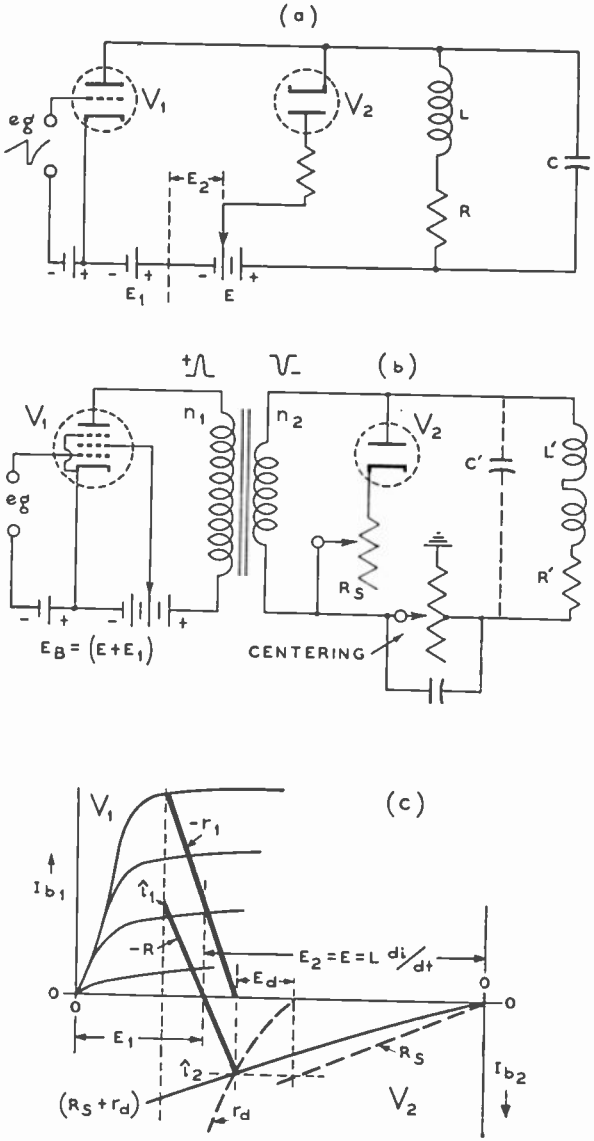

Fig. 7—Rearrangement of bridge circuit; circuit with addition of transformer; and, characteristic curves showing effect of increasing diode resistance by adding R_s.

so that i_2 lies on the diode line. This determines the plate battery voltage E_2. The negative resistance $-r_1$ which must be generated by V_1 is constructed point by point by the addition of the diode current and the current required by $-R$ at respective plate voltages (parallel to the current axis). The characteristic of V_1 is now shifted until i_1 lies at or below the zero grid-voltage line of V_1, thus determining E_1. The control grid voltage $e_g = f(t_s)$ is readily obtainable from the intersections of $-r_1$ with the grid voltage curves E_{c_1} of V_1.

It is apparent from the construction that V_1 must furnish a peak current in excess of the peak-to-peak deflection current. A higher

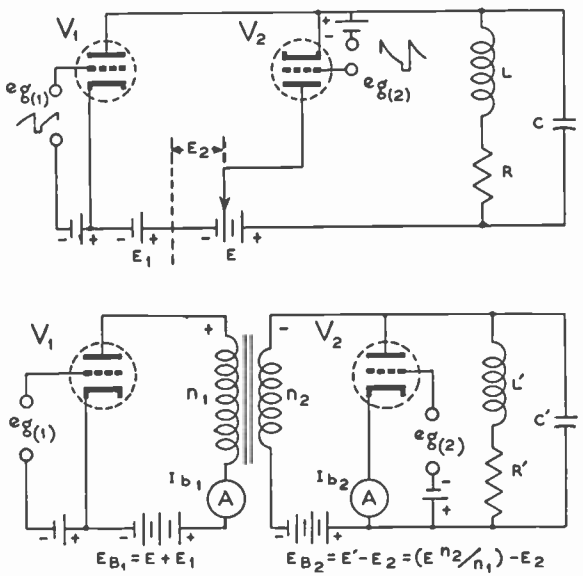

Fig. 8—Practical circuits with two controlled electron tubes.

diode resistance will reduce the peak current but will require a larger voltage E_2. Rearrangement of batteries results in the circuit Figure 7(a) where E_2 can be raised to equal E without additional voltage. With the addition of a transformer, this circuit (Figure 7(b)) will be recognized as a prewar deflection circuit. The diode resistance is adjusted by adding a variable series resistance R_s; linearity occurs when

$$R_s = [E - (i_1 R + E_d)]/i_2 \qquad (8)$$

and when the grid-voltage wave of correct shape is applied to V_1 (see Figure 7(c)). The transformation ratio from V_2 to V_1 is taken into account by multiplying current and voltage scales of V_1 with the turns ratios n_2/n_1 and n_1/n_2, respectively. Although giving linearity, the circuit has a low deflection-current efficiency, similar to that of an

aperiodic circuit, because of the large circulating bridge-current. It has, however, a shorter retrace period.

Switches with two controlled electron tubes

Considerably better performance is obtained with bridge circuits containing two controlled electron tubes.[2] Each tube contributes to the

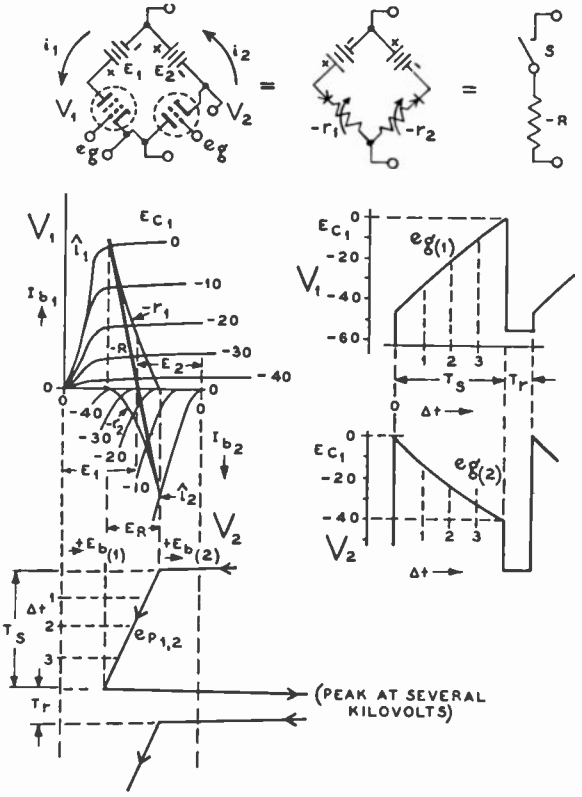

Fig. 9—Equivalent bridge circuits for Figure 8 and characteristic curves for the two tubes.

negative resistance $-R$ and circulating bridge-currents can be reduced to small values. The rearranged circuits are shown in Figure 8.

Switch circuit and combined characteristic of two controlled tubes V_1 and V_2 are illustrated in Figure 9, and may be treated like the

[2] Circuits with negative resistance—
(a) Max Geiger, U. S. Pat. 2,225,300 (Dec. 17, 1940); filed 6/9/38.
(b) R. C. More, U. S. Pat. 2,251,851 (Aug. 5, 1940); filed 6/16/39.
(c) W. A. Tolson, U. S. Pat. 2,280,733 (April 21, 1942); filed 6/30/39.
(d) H. A. Wheeler, U. S. Pat. 2,235,131 (March 18, 1941); filed 10/25/39.
(e) Otto H. Schade, U. S. Pat. 2,382,822 (Aug. 14, 1945), filed 6/30/42.

familiar push-pull amplifier characteristic with respect to graphic addition of currents. It is, however, important to keep in mind that voltages and currents are non-sinusoidal and asymetric and that the current change di/dt along the load line $-R$ must be constant.

The starting point for the graphical construction of Figure 9 is again the line $-R$ with end-points at i_1 and i_2 given by the required deflection and the Q value of the tuned circuit LCR. The characteristic of V_2 is drawn so that i_2 is located on the zero-bias curve, determining, therefore, the plate voltage E_2. The plate voltage E_1 for V_1 is obtained in a similar manner. Good efficiency and uncritical matching indicate grid-voltage amplitudes which cause cutoff on one tube when the other tube carries peak current.

The constant summation load characteristic $-R$ can be obtained with many different pairs of individual load characteristics $-r_1$ and $-r_2$ (see Figure 10). Each pair requires a specific pair of grid voltages $e_{g(1)}$ and $e_{g(2)}$. Given one grid voltage wave $e_{g(1)}$, the other voltage $e_{g(2)}$ is determined as follows:

Divide the plate-voltage change E_R into equal increments, ΔE, occurring at equally-spaced time increments, Δt. Locate the corresponding grid voltages on $e_{g(1)}$ (Figure 9) by using the same number of time increments, Δt. The intersections of these grid-voltage curves in the V_1 characteristic with corresponding ΔE values furnish, therefore, the desired currents i_1 and the load path $-r_1$. Obtain the load path $-r_2$ by subtracting the current values i_1 from the total current in $-R$. Plot the waveform $e_{g(2)}$ against time from the intersections of plate voltage, grid voltage and load path $-r_2$.

The waveform and amplitude of the grid voltage determine the magnitude of the matching current (in the bridge circuit), which contributes nothing to the deflection current. Figure 10 shows various degrees of current efficiency. Figure 10(a) indicates ideal but very critical class B operation for zero matching current and for an ideal tuned circuit having $R = 0$. For this arrangement, i_1 equals i_2. This condition represents ideal current utilization and has the significant relation $i_1 + i_2 = 8\, I_{b1}$, where I_{b1} is the average current value in V_1. For this condition, the current utilization factor or current efficiency becomes

$$\eta i = (i_1 + i_2)/8\, I_{b1} \tag{9}$$

A maximum current efficiency of ηi equal to unity does not indicate that the power loss in the electron-tube bridge circuit is zero; instead, it indicates that the power loss in the circuit LRC is zero and that there is a minimum current drain from the supply voltage source.

A good stable operating condition obtainable with practical grid-voltage waveforms and $\eta i = 0.63$ is shown by Figure 10(b). Figures 10(c) and 10(d) show conditions arising from poor adjustments and low-Q circuits. Figure 10(e) shows the comparatively low current-efficiency $\eta i = 0.25$ of the circuit Figure 7 when an uncontrolled diode is used to obtain a linear sawtooth current, while Figure 10(f) illustrates the gain in deflection obtainable with the same circuit by allowing a non-linear current i. This circuit requires a *positive* load line slope in the construction Figure 7(c) in order to effect diode cutoff.

Switch with pentode and plate-voltage-controlled diode

The characteristic of the pentode-triode switch (Figure 9) can be

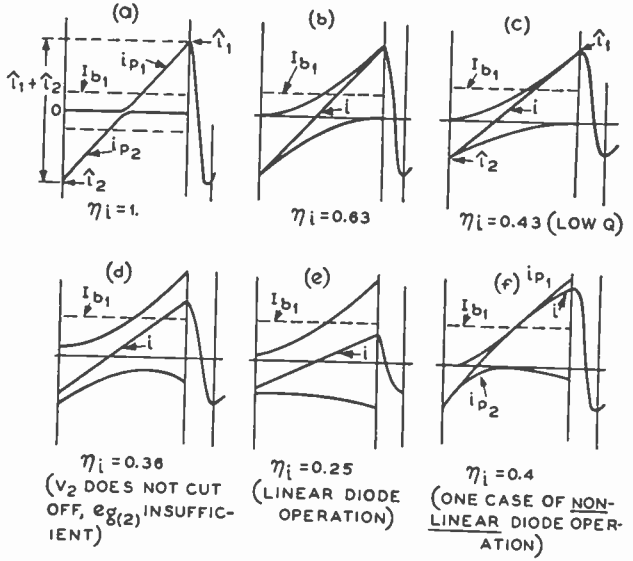

Fig. 10—Degrees of current efficiency with varying grid voltages, circuit adjustments, and tubes. $(i = (\hat{\imath}_1 + \hat{\imath}_2)/8\, I_{b_1})$.

duplicated with pentode and diode by displacing the diode line in the composite characteristic (compare Figure 6(b)) towards the left as a function of time, thus forming in effect a triode characteristic. This displacement is accomplished, in principle, by the insertion of an auxiliary synchronous generator (E_z) in series with the diode as illustrated in Figure 11. Efficient operation requires diode current cutoff by a decreasing diode plate voltage e_d, while linearity of deflection current requires an increasing voltage $E_L + iR$ across the deflection coil system. The auxiliary generator voltage is, therefore, specified by

$$e_z = f(t_s) = -(e_d + e_R) \qquad (10)$$

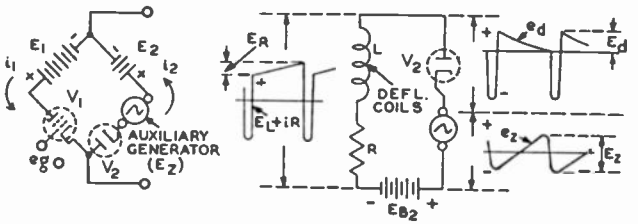

Fig. 11—Diode control circuit and equivalent switch current.

with the peak-to-peak value $$E_s = -(E_d + E_R) \qquad (10a)$$

To duplicate the triode action, the waveform of e_s should approximate a sawtooth. Insertion of e_s into the diode circuit can be effected by means of an auxiliary transformer T_2, having one of its windings in series with the plate or cathode connection of the diode. The control voltage can be supplied by an auxiliary small power tube V_3 or by the power tube V_1 as indicated in the fundamental switch circuits given in Figure 12. In the circuit of Figure 12(b), the transformer T_2 is given a small step-down ratio because the current i_1 must not only supply shunt losses but must also counteract and exceed the diode current i_2 in the secondary current $i_s = (n_p/n_d)\, i_1 + i_2$. The voltage e_s is developed across an impedance Z representing the internal impedance of the auxiliary generator and may be connected across either or both of the closely coupled primary or secondary windings of T_2. Proper phasing of e_s in these and in most practical circuits requires phase reversal of the secondary voltage.

For best circuit efficiency Z should be purely reactive. In order to obtain a good sawtooth waveform, Z should act as an impedance to at least several harmonic components contained in the sawtooth wave.

Although the simplest impedance of this type is a pure resistance, its use, however, results in some power loss. It is, therefore, of

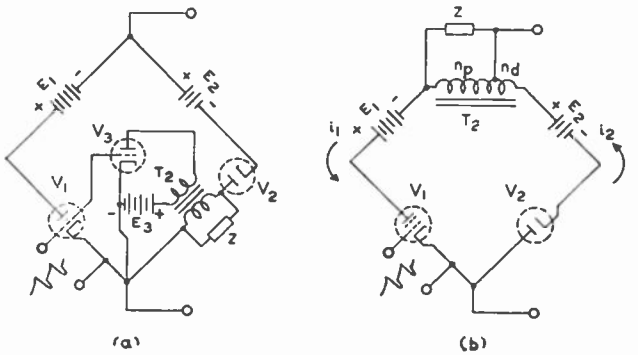

Fig. 12—Diode switch circuits with negative resistance $(-R)$.

interest to determine the limits within which amplitude, waveform, and phase of e_s may be varied for practical operating conditions of the electron-tube switch and linear deflection current. The waveform will indicate the requirements for the impedance Z with respect to higher-order harmonic components.

The graphic solution for the control voltage e_s is shown in Figure

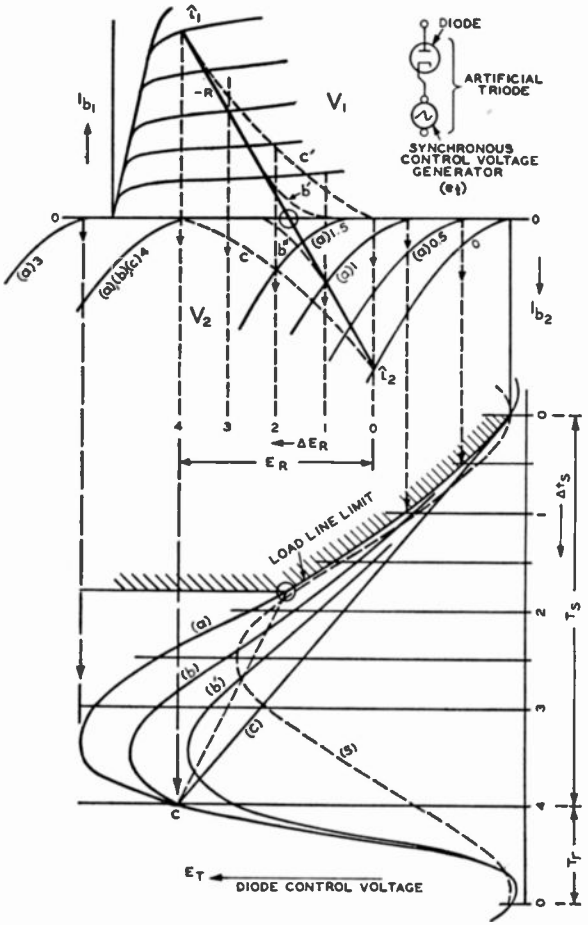

Fig. 13—Characteristics and control voltages for linear deflection with controlled diodes.

13. The limiting class B case (see Figure 10(a)) requires that the individual load path of V_2 should follow the load line $-R$ to the cut-off point 0 at $i = 0$ where it turns sharply to the left and remains at $i = 0$ for the second half of the load cycle. The current of V_1 is zero in the first half of the load cycle, its load path turning sharply at point 0 to follow the load line $-R$ to $\hat{\imath}_1$.

The diode* characteristic is drawn through the initial current i_2. The cutoff point places the value of the control voltage at $T_s = 0$. The voltage E_R changes linearly and is divided into equal increments ΔE_R, which correspond to equal time increments Δt_s on the control-voltage time base. The instantaneous value of e_T at a time $\Delta t_s = 1$ is found as the voltage increment by which the diode line must be shifted to the left to intersect $-R$ at the corresponding plate-voltage change $\Delta E_R = 1$. In this manner the control-voltage wave (a) is obtained, indicating the load-line limit as far as point 0 ($\Delta T_s = 1.8$). The cutoff point moves, then, along the broken line to point C. The waveform of e_z in the range $\Delta t_s = 1.8$ to $\Delta t_s = 4$ (points 0 to C) is unimportant so long as it remains to the left of the broken line. It may thus have the practical form indicated by curve (a) which, for the example, represents the closest approach to a sine wave giving efficient linear deflection. It is obvious that waveform, phase, and amplitude are critical.

It is not difficult to prove that practical operating conditions require the control-voltage wave to remain to the right of the shaded area marked by the load-line limit up to the crossover point 0 and that once having crossed the cutoff line (dashed) it should remain on its left side for the remaining portion of T_s. Waveforms (b) and (c) fill this requirement while the sine wave (s) crosses the cutoff limit again at $\Delta t_s = 2.7$ thus causing a premature return of the diode current and requiring, in turn, an enormous rise in power-tube plate current i, if deflection linearity is to be maintained.

Curve (b′) shows that an amplitude reduction of (b) causes a second crossover indicating that the magnitude of Z as well as the phase of e_z must be carefully adjusted. Voltages approaching the sawtooth shape (c) are less critical and more readily controlled as the impedance of Z approaches a pure resistance.

A practical form of the impedance Z which permits adjustment of phase and waveform is shown in the rearranged circuit of Figure 14.

The inductance L_2 of the transformer T_2 forms a damped resonant circuit with C and the adjustable resistance R_2. Variation of C (or L_2) provides a phase adjustment for E_z, while R_2 controls waveform and amplitude. Because of this interaction, the constants L_2 and C as well as the stepdown ratio must be properly selected. Higher impedance LC circuits and larger step-down ratios permit the use of larger values of resistance resulting in more flexibility than is obtainable with low-impedance circuits and transformers with smaller step-down ratios which require a higher value of Q to build up sufficient control voltage.

* Diode can be gas or vacuum type.

It is apparent that the plate supply voltage E_{B_1} must be increased to include the voltage drop across Z. This increase is given by $\triangle E_{B_1} = E_{Z(x)}/2$ when Z is purely reactive and increasing towards $\triangle E_{B_1} = E_Z = \hat{\imath}_{p_1} R_2$ when Z is a pure resistance.

The reactive voltage-drop and the corresponding power are substantially regained by the booster tube V_2 in the form of increased dc power output into the battery $E_{B_2} = (E' - E_2) + (E_{Z(x)}/2)$ (See section discussing power-feedback circuits — page 524.)

Although similar in deflection efficiency, the controlled diode circuit has more interacting parameters than a triode booster circuit which by its natural triode plate characteristic facilitates accurate matching of the V_1 and V_2 characteristics.

Switch-Circuit Properties Required by the Oscillatory Phase

Since the electron tube bridge must be an open circuit during retrace time T_r, a rapid plate-current cutoff in V_1 and V_2 is required

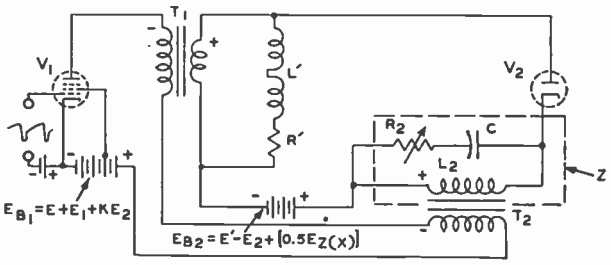

Fig. 14—Rearranged deflection circuit with controlled diode (as Figure 12 (b)) combining good efficiency and linear deflection.

to prevent damping of the tuned circuit. The switch voltage e_s in Figure 1 is obviously the sum of the battery voltage E and the voltages developed by the current i flowing through R and L. Thus,

$$e_s = E_B + (iR + L\, di/dt) \qquad (11)$$

The second term in Equation (11) is the plate load voltage of the tubes V_1 and V_2. It varies with time as shown in Figure 9. In the oscillatory time, T_r, the voltage $L\, di/dt$ has a sine-wave shape and rises to a high peak value, thus, $\hat{e}_L \simeq \hat{\imath}_1 \sqrt{L/C}\, \epsilon^{-\pi/4Q}$ (11a)

In the aperiodic time T_s, the voltage $L\, di/dt$ has the substantially constant value $E_L = -L\,(\hat{\imath}_1 - \hat{\imath}_2)/T_s = -L\,\hat{\imath}_1\,(1 + \epsilon^{-\pi/2Q})/T_s$ (12)

since the exponential terms approach unity in high-Q circuits. When $Q \simeq 6$, $\hat{\imath}_2 \simeq 0.85\,\hat{\imath}_1$, and the Equations (1), (11), and (12) furnish the approximate relation $\hat{e}_L \approx 1.7\, E_L\, T_s/T_r$ (13)

The maximum switch voltage $\hat{e}_s$ is thus inversely proportional to the retrace time. Current cutoff in a triode in the V_1 position requires,

therefore, a highly negative grid voltage pulse during T_r because, as Equation (13) indicates, positive peak voltages of several kilovolts may occur in practical circuits (see Table IV — page 535). A pentode or beam power tube is, therefore, most suitable as power tube V_1 since screen-grid tubes can be cut off with a small negative grid voltage which is substantially independent of the value of the plate voltage.

The "booster" scanning tube V_2 receives a negative plate voltage during the major part of T_r except during the short time angles β_0 and β' (see Figure 2). It can, therefore, be a diode, triode or pentode if its switch function only is considered. The grid voltage should, however, contain a negative pulse of sufficient magnitude to effect rapid

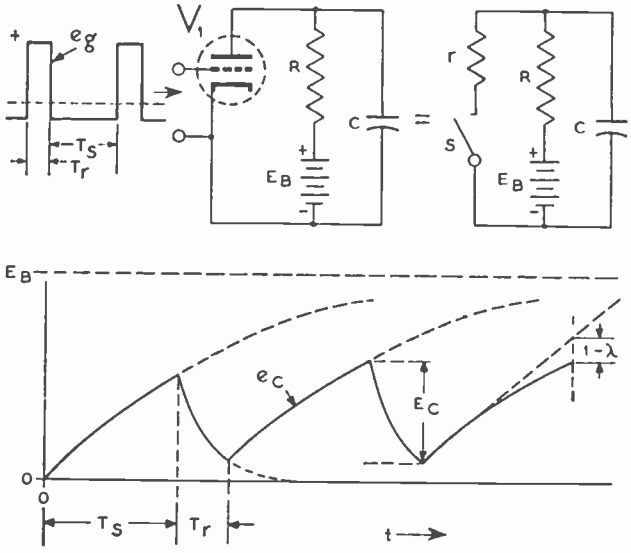

Fig. 15—Generation of control voltage for power tube, V_1.

cutoff within the angles β (Figure 2) where the plate voltage (e_p) is positive (see Figure 9).

Generation of the negative resistance $-R$ during T_s can be accomplished equally well with diodes, triodes or pentodes. However, proper functioning of the deflection circuit also requires that the tuned circuit become aperiodic at the beginning of T_s to prevent further current oscillations. The electron tube switch must, therefore, be a short-circuit or a low value of positive resistance (r_p) to damp out all parasitic voltage or current fluctuation while acting as a controlled negative resistance $-R$ only for the desired deflection current i.

It is thus essential that at least one of the tubes V_1 or V_2 have a low plate resistance (r_p). If V_1 is a high-impedance screen-grid tube,

the booster scanning tube V_2 must also act as a damping resistance requiring the low plate resistance obtainable with a low-μ triode or diode.

It is possible to obtain low effective r_p values with high-μ tubes by inverse feedback but difficulties in obtaining properly phase feedback voltages limit the usefulness of this method for practical circuits.

Generation of Control Voltages (e_g)

The control-grid voltage for the power tube V_1 is usually generated in an RC circuit by means of an electron-tube discharge switch. (Figure 15). In this circuit, the capacitor voltage rises exponentially during the charging period T_s. The linearity λ of the voltage rise is expressed by

$$\lambda = (1 - \epsilon^{-T_s/RC})\ RC/T_s \tag{14}$$

The following approximations may be used for values $\lambda > 0.75$ or values of peak-to-peak sawtooth voltage $E_c < 0.5\,E_b$, by assuming substantially complete discharge of C during T_r; i.e., for $r << R$,

$$E_c \approx 2E_b\ (1 - \lambda) \tag{15}$$

and

$$T_s/RC \approx (2/\lambda) - 2 \tag{16}$$

A negative pulse to cut off the power-tube plate current is obtained by addition of a resistance load in series with C. The pulse width should correspond to T_r of the deflection circuit. When shorter, as in case of a blocking-oscillator drive, the cutoff pulse can be obtained by feedback from the transformer secondary (see Figure 17).

The control-grid voltage for the booster triode V_2 can be obtained from the pulse voltage without the use of additional tubes.[3] The circuit function is illustrated by the equivalent of circuit Figure 16 which is a special case of the discharge circuit.

$$\text{With } \epsilon^{-T_r/RC} = K_1 \qquad \text{and } \epsilon^{-T_s/RC} = K_2 \tag{17}$$

the peak-to-peak capacitor voltage is given by

$$E_c = (E_1 + E_2)\,(1 - K_1)/[K_1 + (1 - K_1)\,(1 - K_2)\,] \tag{18}$$

The integrated voltage, e_c, is relatively small because of the short charging time. The differentiated voltage, e_r, is the pulse voltage minus the capacitor voltage as shown in Figure 16(b). The sawtooth section has the same amplitude as e_c, but opposite polarity; the negative pulse during T_r is more than sufficient for cutoff of V_2. The circuit constants are again given by Equation (16) with λ ranging from 0.3 to 0.8 according to grid-voltage wave shape. The voltage E_2 in Equation (18) is approximated by the average value of the sinusoidal pulse voltage $E_2 \cong 0.63\ e_2$. A practical control-voltage-generating circuit is shown in Figure 17. The impedance of the circuit $R_2\,C_2$ is limited by

the tube electrode capacitances to certain maximum values.

It should also be noted that the voltage pulse of practical transformers is not a smooth half-sine-wave pulse. It contains harmonic frequencies due to leakage reactance tuning with varying coupling and phase relations between windings. These ripples are degenerative in V_2 when the negative secondary pulse is used for generation of e_g of V_2.

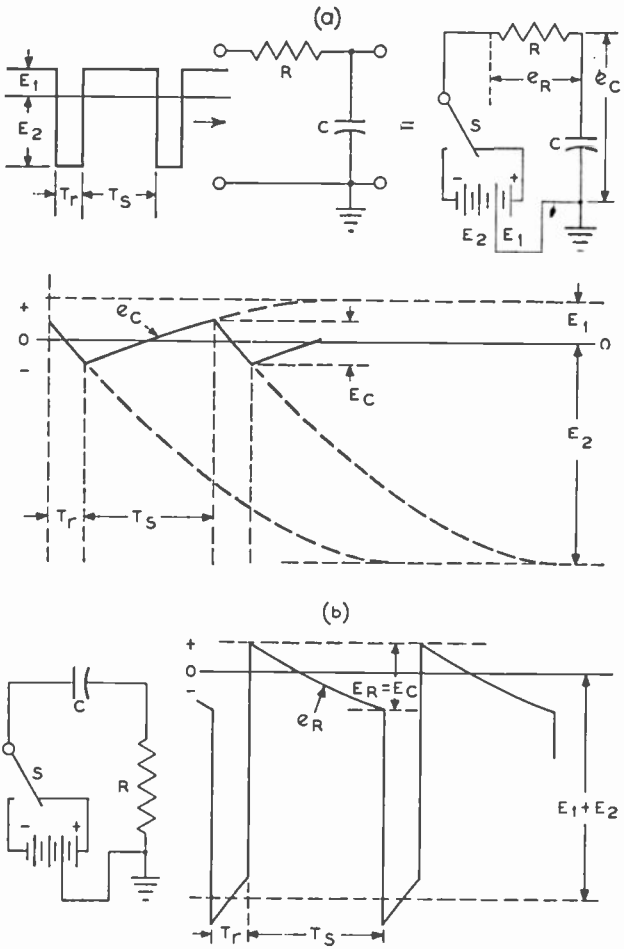

Fig. 16—Generation of control voltage for booster triode, V_2.

Efficiency and Power Feedback

The efficiency and power output of deflection circuits are relatively low. The overall efficiency can at best equal the square of the normal

oscillator efficiencies since the a-c power output of tube V_1 must again be controlled and rectified by a second tube V_2. The booster tube V_2 is thus in principle a rectifier. An operating efficiency of 80 per cent per tube and a similar circuit efficiency for the deflection coils and transformer would give an overall efficiency of 50 per cent.

The efficiency of circuits in actual practice may be considerably lower than this value and, in fact, equals zero when the d-c power output, $E_{B_2} \times I_{b_2}$, is dissipated in a bypassed resistor (Figure 17), which replaces the battery $E_{B_2} = E' - E_2$ in Figure 8(b).

It is possible, however, to feed the rectified power back into the power source or power tube by use of circuits employing proper trans-

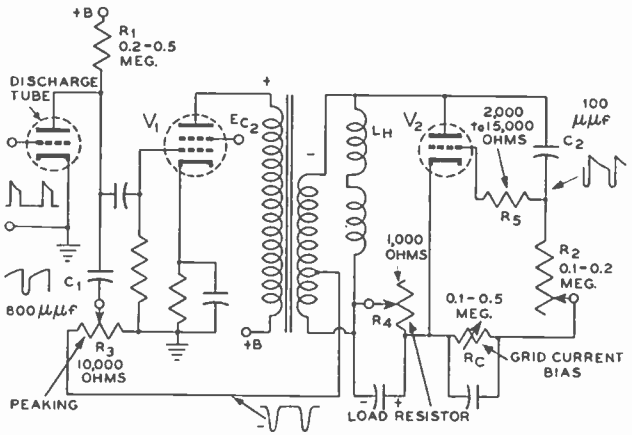

Fig. 17—Practical circuit for generating control voltage for booster triode, V_2.

former ratios. The use of such a circuit is justified, even for small power gains, if important operating advantages are secured. Various developments prior to and during the war indicated that as the definition of television systems is increased, the kinescope and pick-up tubes used require increasingly larger deflection energies. Such tubes would be impractical without some method of energy conservation. Based on investigations of power feedback, the author successfully demonstrated in 1944 a high-definition color television system utilizing series power feedback.

Parallel Power Feedback

Feedback of secondary d-c power into the power supply source requires the matching of voltages by means of a transformer with the proper step-up ratio. The transformer is given a step-up ratio $n_2/n_1 > 1$ which is adjusted to give $E_{B_2} = E_{B_1}$ with linear deflection current.

This ratio is: $$n_2/n_1 \simeq 1 + (E_1 + E_2)/E_L \qquad (19)$$

The parallel connection is shown in Figure 18.

The 3/2-power relation of current and voltage in electron tubes causes a change in the voltage ratio $(E_1 + E_2)/E_L$ for changes in current amplitude requiring adjustment of the transformer ratio. This is also true for frequency changes. The parallel feedback circuit, therefore, is of little practical interest.

Series Power Feedback (Booster Circuit)

Power feedback in series with the power source requires matching

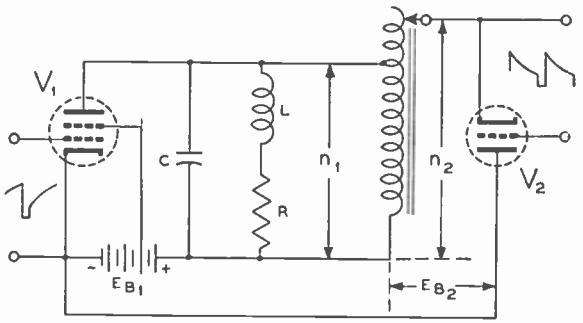

Fig. 18—Circuit with parallel connection for power feedback.

of average currents by adjustment of the transformer ratio. The transformer is given a step-down ratio, $n_1/n_2 < 1$, which is adjusted to give equal plate currents $I_{b_2} = I_{b_1}$ with linear operation. (Figure 19 (a)). After series connection of the secondary load terminals (i.e. the storage capacitance C_B) with the power source, the voltage E_{B_1} of the power source can be reduced to $E_{B_1}' = E_{B_1} - E_{B_2}$ (Figure 19(b)). The transformer ratio is: $$n_1/n_2 = I_{b_1}/I_{b_2}' \qquad (20)$$

where I_{b_2}' is the current obtained with $n_1/n_2 = 1$.

The ratio is independent of current amplitude and frequency as the circuit Q and wave shapes are substantially constant. Stability of operation at all amplitudes is obtained by an essentially independent screen-grid voltage. The circuit with series power feedback is, therefore, a practical step toward the ideal wattless deflection circuit and, thus, deserves further discussion.

Adjustment of the transformer ratio is, in effect, a linearity control. A smaller step-down ratio giving $I_{b_2} < I_{b_1}$ with linearity before series connection will cause overdamped operation after series connec-

tion (Figure 19(c)) because I_{b_2} is forced to equal the pentode-controlled current I_{b_1} (equivalent to a decrease of R in Figure 19(a)).

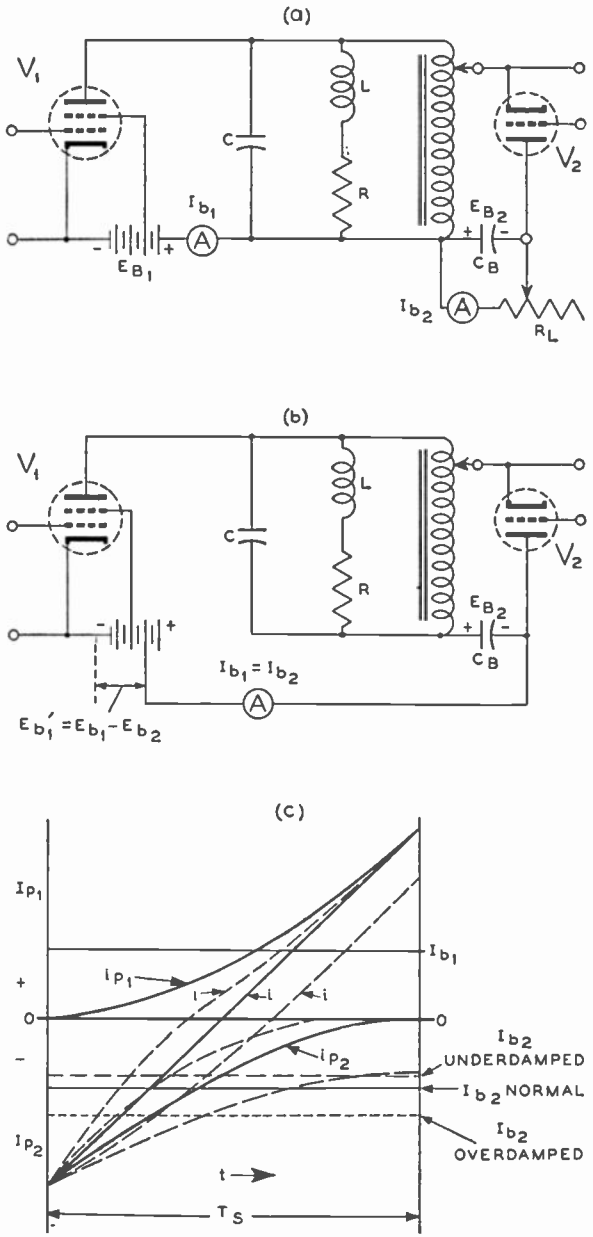

Fig. 19—Circuit with series connection for power feedback; and, effect of adjusting transformer ratio on linearity of current (i).

A larger step-down ratio causes $I_{b_2} > I_{b_1}$ with linearity before series connection, and after series connection, will give the underdamped condition indicated in Figure 19(c).

Small errors in linearity in a circuit with fixed transformer ratio can be corrected by adjustment of the grid-voltage amplitude or grid bias on V_2.

The transformer should have slightly less step-down for this purpose. As the current ratio is determined by the Q of the circuit, a

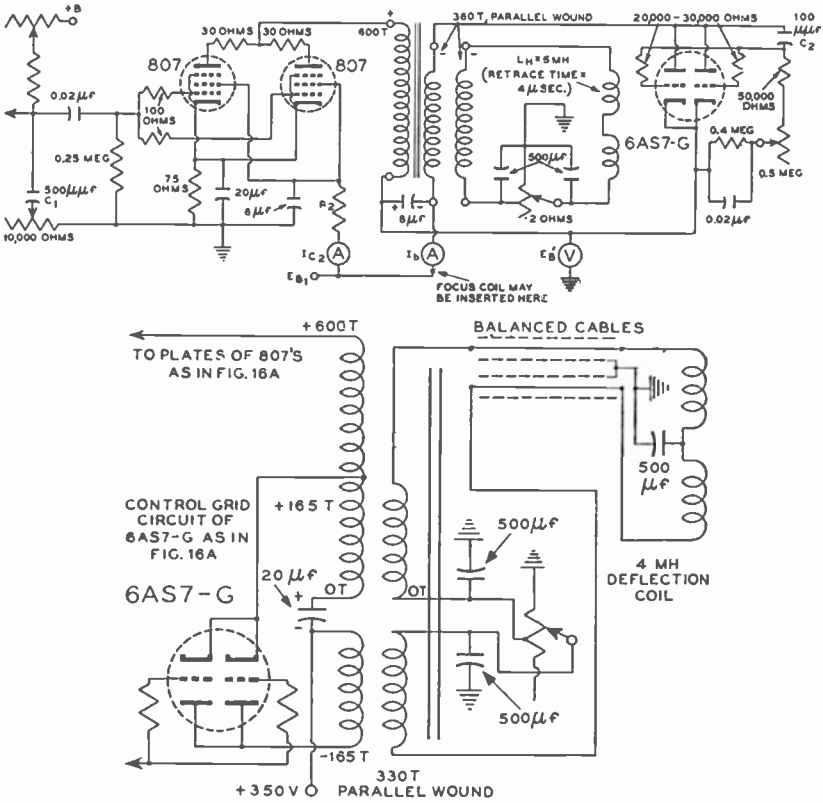

Fig. 20—Practical circuits with power feedback for balanced and urbalanced deflection-coil connections with 6AS7-G triode.

change in linearity will be observed when the power tube V_1 is made to load the circuit during T_r by reduction of its negative cutoff or peaking voltage. It must be kept in mind that only a change of the peak-to-peak to average current ratio will effect the linearity and when plate-current cutoff is maintained during T_r, bias or amplitude adjustments on V_1 will, therefore, be ineffective in changing the linearity of circuit operation.

Table I—Operation characteristics for the circuit of Figure 20(a).

Horizontal Deflection Frequency	15.75 KC		31.5 KC		Remarks
E_{B_1} (volts)	315	350	315	350	The maximum deflection amplitude at 15.75 kilocycles is approximately 30 per cent larger than at 31.5 kilocycles.
E_B' (volts)	350	382	490	520	
I_b (amperes)	0.175	0.195	0.135	0.14	
I_{c_2} (amperes)	0.025	0.022	0.029	0.026	
R_2 (ohms)	625	1650	625	1650	
Total Plate Power Input (watts)	61	75	66	73	$I_B \times E_B'$
Power Gain (watts)	6.1	6.2	23.6	23.8	$I_b (E_B' - E_{B_1})$
Plate Power Efficiency (per cent)	10	8.4	36	33	$(E_B' - E_{B_1})/E_B'$

This circuit property results in remarkable stability of deflection linearity. The circuit is further unique in being capable of linear operation at low and high frequencies; a large frequency change in circuits with booster triode requires only proportional changes of capacitance in the grid-voltage generating circuits (C_1 and C_2 in Figure 20(a)) to maintain normal grid-voltage wave shapes.

At low frequencies or small amplitudes, the booster rectifier tube V_2 consumes power from the supply E_{B_1} because the inductive voltage E_L is smaller than the tube drop E_2, thus causing E_{B_2} to be negative.

At high frequencies or large amplitudes, the inductive voltage becomes large; E_{B_2} is, therefore, positive, automatically meeting the requirement for increased plate supply voltage on V_1. This action protects the power tube V_1 against excessive plate dissipation when the grid signal is removed since the voltage E_{B_1} has a moderate value.

The step-down ratio of practical circuits varies between 1.4 and 1.7 according to the Q value. It is further increased in circuits where part of the boosted power is utilized for light external shunt loads, such as discharge circuits. The value of the inductive load has little effect (none for zero leakage reactance) on the transformer ratio and is determined by retrace-time considerations as in normal circuits. The voltage boost $E_{B_2} = E_L - E_2$, however, increases with load inductance, deflection frequency, and deflection current (see Equation (12)).

Examples of practical high power circuits for balanced and unbalanced deflection-coil connections are shown in Figures 20 and 21. Operation characteristics for the circuit of Figure 20(a) are given in Table I. Grounded deflection coils require impedance coupling or an

isolated winding parallel with the V_2 winding (2 wires at the same time) to eliminate leakage reactance.

Excitation of a focus coil (for kinescopes) can be obtained by a series connection, as indicated in Figure 20(a). Adjustment of excitation by a shunt resistor will not disturb the operation of this circuit.

The efficiency of practical circuits depends on the availability of electron tubes with low plate-voltage loss (E_1 and E_2) and the construction of efficient transformers and deflection coils. The table in Figure 20 shows that efficiencies up to 33 per cent have been obtained

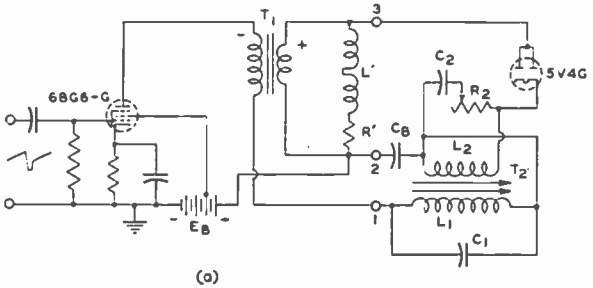

(a)

Circuit (a)
L' = 5 millihenries (deflection coil winding); $T_2 = L_1$ and L_2 wound parallel (#29 Formex) series-connected as shown to obtain tight coupling with permeability tuning.
L_1 = 2 to 7 millihenries
Turns ratio of $L_1/L_2 = 1.6$
L_2 = 0.9 to 2.7 millihenries
C_2 = 0.05 microfarads; R_2 = 500 ohms variable
C_1 = 0.015 microfarads;
C_B = 1 to 4 microfarads.

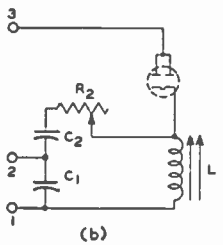

(b)

Circuit (b) combines C_B and C_2, but is restricted by capacitive tap to higher Q-values and more critical operating conditions (Class B) than circuit (a). Ratio C_2/C_1 adjusts stepdown.

Fig. 21—Circuit with power feedback and controlled triode.

with 6AS7-G booster triodes and conventional transformer designs. The efficiency of the diode circuits (Figures 21(a) and (b)) is similar, as the power dissipation in R_2 is compensated by the somewhat lower power dissipation in the diode. The measured plate voltage boost $E_B' - E_{B_1}$ is higher; the effective boost, however, is reduced by the voltage drop across Z which varies from 1/2 peak-to-peak voltage ($ET/2$) for $R_2 = 0$ to nearly peak-to-peak voltage E for large R_2 values.

Switch Circuits with Positive Resistance

The generation of linear sawtooth currents requires the closed-switch circuit to have the characteristic of a negative resistance $-R$. It has been shown that circuits with a diode (Figure 7) can function as $-R$ by inefficient operation with a large circulating current, or

with good efficiency by plate voltage control with auxiliary transformer (Figure 14). Switch circuits with decreasing diode current *and* plate voltage (V_2) or with increasing plate voltage on V_1 have a positive resistance. Linearity is, therefore, not obtainable with many circuits although good current efficiency (ηi) is possible.

One type of circuit utilizes the grid and cathode of a triode power tube V_1 as a diode (V_2) by means of transformer coupling in a self-excited circuit.[3] Plate and grid currents are controllable by varying the space potential in the control-grid plane. The desired change in current distribution, i.e., a rising plate current and decreasing grid current, however, requires a rising plate voltage and, hence, a positive resistance characteristic of the switch circuit. Since the inductive voltage E_L must decrease during T_s, current linearity is not obtainable in the particular circuit without auxiliary potentials.

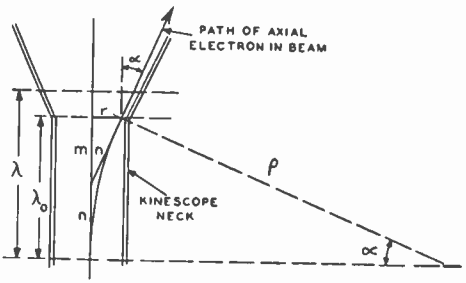

Fig. 22—Path of electron beam through transverse deflection-coil field of kinescope. ($m = n \cos \alpha$; $n = r/\sin \alpha$; $\lambda_o = m + n = r\ (1 + \cos \alpha)/\sin \alpha$).

Because of difficulties in maintaining stable grid characteristics, it is, in general, undesirable to operate small electron tubes having oxide-coated cathodes with heavy grid currents.

Design Constants for Kinescope Deflection Systems with Matching Transformers

Transformer ratios other than those given for the circuit with power feedback may be desirable because of preferred tube or circuit operating conditions. The evaluation of numerical constants is necessary to indicate the range of currents and voltages in practical circuits and to indicate desirable constants for the electron tubes.

---

[3] Sawtooth current oscillations (non-linear)—
(a) T. H. Mulert and H. Baehring; Transformator-Kippgeraete Hansmitteilungen der Fernseh AG; Vol. 1, No. 3, pp. 82-88, April, 1939.
(b) L. R. Malling; Triode linear sawtooth-current oscillator *Proc. I.R.E.*, Vol. 32, No. 12, December, 1944.

Deflection coil constants

The electron beam in a kinescope passes through the transverse deflection-coil field of intensity H (see Figure 22) with the volt velocity E (anode potential). $H = 0.4\,\pi\,NI/l_o$ (21)

In a magnetic field of constant intensity, the electrons follow a circular path with the radius $\rho = 3.33\,\sqrt{E}/H$ (22)

The transverse field must be limited to a depth λ_o to obtain an electron path leaving the field at a distance r from the axis at an angle α. The field depth λ_o below the neck junction is limited to

$$\lambda_o = r\,(1 + \cos\alpha)/\sin\alpha \tag{23}$$

The radius r (Figure 22) must provide clearance for beam thickness and glass neck tolerances.

With $\rho = \lambda/\sin\alpha$ from Figure 22, Equations (21) and (22) yield an expression for the ampere turns required for beam deflection over the angle as follows: $NI_{(\alpha)} = 2.65\,l_o \sin\alpha\,\sqrt{E}/\lambda$ (24)

The inductance of this winding is $L = 4\pi\,N^2A/l_o\,10^9$ (Henry) (25)

Equivalent dimensions for use of Equations (24) and (25) with practical coil designs are shown in Figure 23 where

l_o = air-gap length or inside diameter of iron shell in centimeters
λ = equivalent coil length in centimeters
$A = d \times \lambda$ = average cross section of flux in square centimeters

The coil winding is given approximately a constant number of turns per unit of projected length (l'). Modifications in field strength over the neck center or at the coil ends may be required for obtaining a rectangular trace on the kinescope screen depending on its radius of curvature and on the coil leakage field. (A large screen radius requires an increased effective length $\lambda \cong 1.2\,\lambda_o$ for 55-degree angle kinescopes

The equivalent coil field length changes inappreciably when the coil ends are folded up (Figure 23). Folding at the front end, however, permits an increase of winding length and pole-face length in the direction of the kinescope screen for a given value λ_o, and results in an increased effective length $\lambda \simeq 1.2\,\lambda_o$ for 55-degree angle kinescopes ($\alpha = 27.5$ degrees). The following calculations for a 55° deflection angle were made before the current 50° deflection angle was adopted, but they serve equally well to illustrate the method.

Folding of the back end does not permit a further change of length; it only shortens the coil physically. The leakage-field shape obtained with folded coil fronts reduces defocusing of the beam at large angles α and is, therefore, highly desirable.

When the design constants for wide-angle kinescopes are $\alpha = 27.5$ degrees, $r = 1.27$ centimeters, Equation (23) furnishes $\lambda_o = 5.18$ centimeters and with folded coils $\lambda = 6.2$ centimeters. The practical coil assembly (Figure 23) furnishes $l_o = 6$ centimeters and employing Equation (24) the required ampere-turns for the half-angle are determined as follows: $NI_{(27.5°)} = 1.18\,E$ (24a)

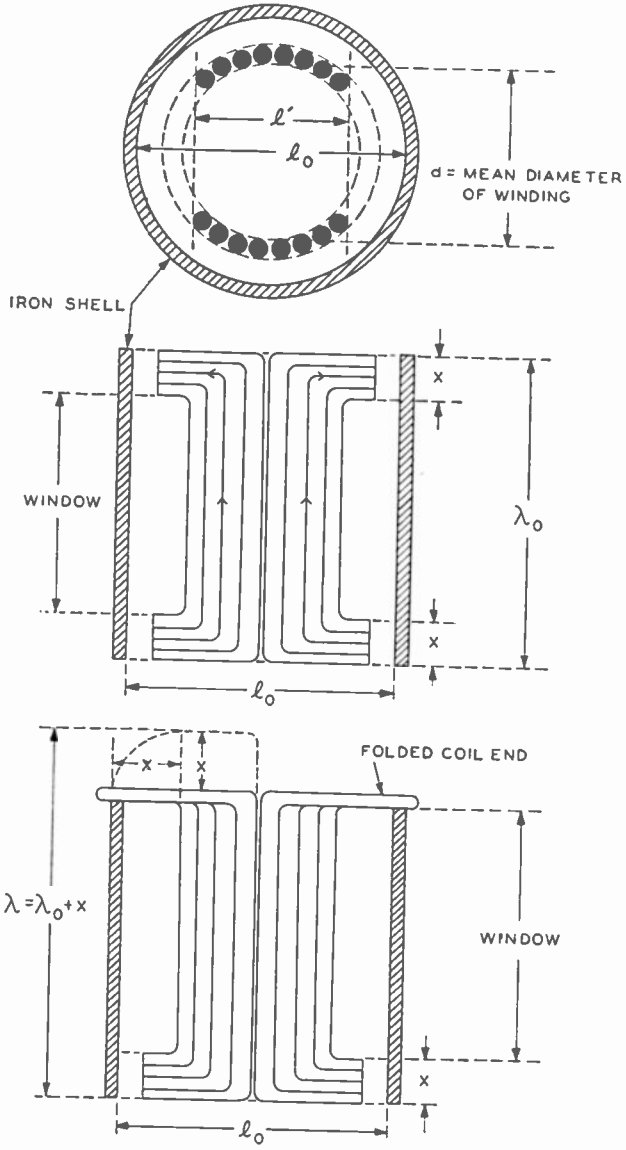

Fig. 23—Cross-sectional views of practical coil for magnetic deflection.

The value obtained by Equation (24a) must be multiplied by two for the peak-to-peak deflection over the full angle 2α.

The line length on the kinescope screen is approximately 83 per cent of the nominal tube diameter for present curved-face tubes. A picture size with a diagonal equal to the nominal tube diameter D, requires the deflection length $H = 0.8D$ and $V = 0.6D$ for a 4:3 aspect ratio. This furnishes

$$NI_{(H\,=\,0.8D)} \simeq 2.28\,E^{\frac{1}{3}} \qquad (24b)$$

and similarly $NI_{(V\,=\,0.6D)} \simeq 1.95\,E^{\frac{1}{3}}$ (λ_o is shorter for vertical coils.)

For obtaining good Q values at the retrace frequency $f_o = 1/2\,T_r$, the reduction of eddy-current losses in copper and iron requires small wire diameters in both windings and the iron shell as shown by Table II.

Table II—Q-Measurements on Horizontal Deflection Winding at 87 kilocycles.

Test No.	Wire Size	L(mh)	Q	Condition of Test
1	#29 SSE	4.42	50	H-winding by itself, no iron.
2	"	5.2	8	H-winding inserted in heavy wire vertical coils with iron wire shell.
3	"	5.2	10.7	H-winding in fine wire vertical coil (#29) with iron wire shell.
4	"	4.8	5.8	Same as (3) but connected to transformer secondary.

Transformer Ratio and Electron-Tube Characteristics

The capacitance C_o of the deflection system is the sum of the circuit element capacitances or their reflected values. It determines the

Table III—Estimated value of circuit element capacitances.

Circuit Element	C (micromicrofarads)	Remarks
Deflection coil	60-80	with short leads
Plate of V_1 (C_p)	10	with top cap connector (807)
Plate of V_2 (C_p)	20-40	with associated grid circuit
V_2 filament transformer....	25	used only for direct coupling
Transformer or choke	20-50	depending on winding method

Circuit constants for $Q = 6$, E(kinescope) = 10 kilovolts, $NI = 228$ ampere turns, and transformer constants as shown in Figure 24.

	$N_T = n_1/n_2$	C_o ($\mu\mu f$)	L_o (mh)	L_H (mh)	N_H	$I = \hat{i}_1 + \hat{i}_2$ (amp)	$\hat{i}_2$ (amp)	I_{b_2} (amp)	E_{L_2} ($volt$)	$\hat{e}_2$ (kv)	$\hat{i}_1'$ (amp)	I_{b_1} (amp)	E_{L_1} ($volt$)	$\hat{e}_1$ (kv)	807 E_{bb} min ($volts$)
Low C_o	1.	135	24.4	24.4	700	0.326	0.16	0.063	137	2.3	0.20	0.090	137	2.3	240
	1.5 ...	70	47.	18.8	615	0.370	0.18	0.072	120	2.	0.154	0.070	190	3.2	290
	2.	50	66.	14.8	546	0.417	0.20	0.080	106	1.8	0.130	0.060	224	3.8	320
	2.5 ...	43	76.5	11.	470	0.485	0.225	0.092	92	1.6	0.120	0.054	243	4.1	340
	3.	39	84.5	9.4	435	0.525	0.25	0.100	85	1.5	0.110	0.050	270	4.6	370
High C_o	1.	200	16.5	16.5	576	0.395	0.19	0.076	112	1.9	0.245	0.110	112	1.9	...
	1.5 ...	115	28.5	11.4	480	0.475	0.23	0.092	94	1.6	0.197	0.090	150	2.5	250
	2.	90	36.5	8.	402	0.567	0.27	0.008	78	1.3	0.175	0.079	165	2.8	265
	2.5 ...	79	41.5	5.9	345	0.662	0.32	0.128	68	1.2	0.165	0.074	178	3.	275
	3.	73	45.	4.45	300	0.760	0.36	0.144	58	1.	0.157	0.071	185	3.2	285
		retrace constants		deflection coil constants			V_2 load constants				V_1 load constants				

Table IV—The characteristic requirements for circuit elements in power tubes (V_1 and V_2) as a function of transformer ratio.

permissible inductance L_o of the system for a given retrace time (Equation 1). The circuit capacitances vary considerably with manufacturing and assembly methods. Estimated values are given in Table III.

The resultant effective capacitance C_o for the two extremes of capacitance in Table III and the inductance L_o have been computed for various transformer ratios between V_1 and V_2 for a normal television retrace time $T_r \simeq 6$ microseconds and scansion $T_s \simeq 58$ microseconds. Maximum and minimum values of C_o are given in Table IV.

The deflection coil current $(\hat{\imath}_1 + \hat{\imath}_2)$ is computed for $NI = 228$ as given by Equation (24b) for $E = 10$ kilovolts. The load constants for the tubes V_1 and V_2 are computed for the transformer network given in Figure 24, and include, therefore, a 10 per cent exciting current

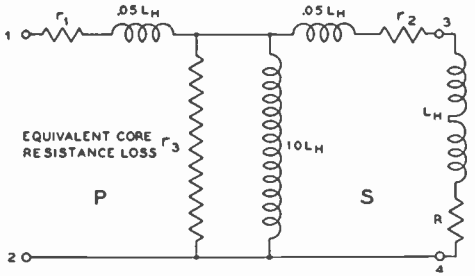

Fig. 24—Transformer network with representative load constants for V_1 and V_2.

and the effects of a 5 per cent leakage reactance per winding. The average plate currents are approximately $I_{b_1} \simeq 0.45\,\hat{\imath}_1$ and $I_{b_2} \simeq 0.4\,\hat{\imath}_2$.

Power Tube Characteristics and Supply Voltage

Table IV establishes the characteristic requirements for circuit elements and power tubes (V_1 and V_2) as a function of transformer ratio. Pulse voltage ($\hat{e}_2$), plate current ($\hat{\imath}_1'$), and effects of yoke capacitance decrease with increasing step-down ratio. The pulse voltage $\hat{e}_1$, however, increases and in practical circuits it is often 25 per cent higher than given because of sectional resonances. The power tube requires, therefore, a top cap plate connection. Practical designs without power feedback may correspond to the higher capacitance values (2nd half of Table IV) which require higher currents and lower voltages. Designs with power feedback require a small step-down ratio to the tube V_2. The supply voltage E_{bb} min in the last column

Table V—Characteristics of low-mu twin power triode 6AS7-G.

Electrical Characteristics:

Heater, for unipotential Cathode:

Voltage (a-c or d-c)	6.3	....	Volts
Current	2.5	....	Amperes

Mechanical Characteristics:

Mounting Position	Any
Maximum Overall Length	5-5/16 inches
Maximum Seated Length	4¾ inches
Maximum Diameter	2-1/16 inches
Bulb	ST-16
Base	Medium Shell Octal 8-Pin

D-C Amplifier

Values are for each unit

Maximum Ratings, Design-Center Values:

Plate Voltage	250 max.	....	Volts
Plate Current	125 max.	....	Milliamps
Plate Dissipation	13 max.	....	Watts
Peak Heater-Cathode Voltage:			
Heater negative with respect to cathode	300 max.	....	Volts
Heater positive with respect to cathode	300 max.	....	Volts

Characteristics:

Plate-Supply Voltage	135	....	Volts
Cathode-Bias Resistor	250	....	Ohms
Amplification Factor	2.0	.....	
Plate Resistance	280	....	Ohms
Transconductance	7000	....	Micromhos
Plate Current	125	....	Milliamps

Maximum Circuit Values (for maximum rated conditions):

Grid-Circuit Resistance:

For Cathode-Bias operation†	1.0 max.	....	Megohm

Booster Scanning Service

Values are for each unit

Maximum Ratings, Design-Center Values:

Peak Inverse Plate Voltage*	1700 max.	....	Volts
Plate Current	125 max.	....	Milliamps
Plate Dissipation	13 max.	....	Watts
Peak Heater-Cathode Voltage:			
Heater negative with respect to cathode	300 max.	....	Volts
Heater positive with respect to cathode	300 max.	....	Volts

Maximum Circuit Values (for maximum rated conditions):

Grid-Circuit Resistance:

For Cathode-Bias operation†	1.0 max.	....	Megohm

* The duty cycle of the peak inverse voltage pulse must not exceed 15% of one scanning cycle and its duration must be limited to 10 microseconds.

† Operation with fixed bias is not recommended.

is approximated for normal transformer and coil resistances by

$$E_{bb}\ \text{min} \simeq E_1 + 1.15\, E_{L_1} \tag{26}$$

E_1 is the peak-current tube-drop in an 807 power tube. Experience has shown that further allowances in voltage must be made for blanking margins, for variation in tubes to reduce screen-grid dissipation, and for a self-bias voltage which raise E_{bb} min by approximately 20 per cent.

Booster Triode Characteristics

To meet the characteristics and requirements outlined here for a booster tube, the 6AS7-G was developed. This tube was designed by the author and produced during the war for use in military television and radar equipment. It is now available and has been successfully utilized in the type of circuits suggested for magnetic deflection in this paper. Its characteristics are given in Table V (see preceding page.)

INTERCARRIER SOUND SYSTEM FOR TELEVISION*†

A Report

BY

INDUSTRY SERVICE LABORATORY, RCA LABORATORIES DIVISION,
NEW YORK, N. Y.

Summary—This paper describes a television sound receiving system known as the intercarrier sound system. Broadly it differs from conventional practice in two respects. The heterodyning frequency which determines the sound intermediate frequency is the video carrier. The frequency-modulated beat between the sound carrier and the video carrier is not separated from the video signal until just before the video signal is impressed on the grid of the picture tube.

The intercarrier sound system appears to have advantages over the method now used. However, there are certain disadvantages, the effects of which have not as yet been completely resolved.

The performance of intercarrier receivers field tested in the New York City area on channels 2, 4, and 5 has been satisfactory.

The intercarrier sound receiver is relatively immune to local oscillator instability. Although its signal-to-noise ratio is theoretically lower than that of the conventional receiver, in practice the signal-to-noise ratio of the new circuit may be equal to, or better than, that of the conventional circuit. The theoretical ratio of signal to noise is not always realized in the conventional system due to inherent local oscillator instability.

A simplified intermediate-frequency amplifier may be employed in the intercarrier receiver which is easier to build and align and which permits a more economical receiver design at the expense of some resolution and adjacent-channel rejection.

However, before the intercarrier sound system could be used commercially in home television receivers it would be necessary to amend the standards for television transmitters to insure that the carrier amplitude during transmission of a white picture not fall below ten per cent of the value of the unmodulated picture carrier during the synchronizing time. It is also necessary that, at the transmitter, the degree of spurious phase modulation of the video carrier due to amplitude modulation by picture information be held to a sufficiently low level to avoid spurious audio output at the receiver. The degree of phase modulation present on the picture carrier of the transmitters now operating on the lower channels in New York City is sufficiently low. However, it is possible that when transmitters are operated on the higher channels, difficulties may arise from this source due mainly to transit-time effects in the power amplifier stages.

THE CONVENTIONAL SYSTEM

FIGURE 1 shows in block form the conventional television receiver. The individual high-frequency signals comprised of the video carrier, amplitude modulated by the video signal, and the audio

* Decimal Classification: R583.5.
† Written in September, 1947.

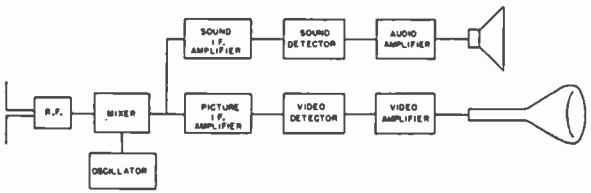

Fig. 1—Conventional television receiver.

carrier, frequency modulated by the sound signal, are heterodyned with the high-frequency local oscillator in the mixer. The difference frequency between the local oscillator and the video carrier is impressed upon the video intermediate-frequency (i-f) amplifier. It is next demodulated by the video detector, further amplified by the video amplifier, and then impressed upon the kinescope grid.

The difference frequency between the local oscillator and the frequency-modulated sound carrier is impressed upon the sound i-f amplifier. After amplication, the frequency-modulated i-f sound carrier is applied to a frequency-modulation (FM) detector. The audio output of the detector is amplified and fed to the loud speaker.

THE INTERCARRIER SYSTEM

The intercarrier sound system is shown in block form in Figure 2. In the mixer stage the picture and sound carriers are heterodyned by the local oscillator. Both i-f carriers and their side bands are simultaneously amplified in the single i-f amplifier, and are demodulated by the video detector. The output of the video detector is further amplified by the video amplifier. The video signal is then separated from the frequency-modulated intercarrier beat, and is fed to the kinescope grid. The frequency-modulated beat is further amplified and applied to a ratio detector. For all but the lowest contrast levels the amplifier operates in overload so the audio output is essentially independent of the setting of the contrast control. The output of the detector is amplified and fed to the loud speaker.

It may be seen that in the conventional system the high-frequency signal that beats with the FM audio carrier to produce the sound i-f is generated locally in the receiver whereas in the intercarrier system the high-frequency signal that beats with the FM audio carrier to

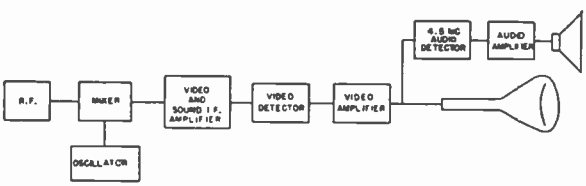

Fig. 2—Intercarrier receiver.

produce the sound i-f is the picture carrier which is generated at the transmitter.

In order to evaluate the theoretical merits of the two systems it is necessary to examine the effects of changes in frequency and amplitude of the high-frequency heterodyning oscillator on the operation of a conventional FM receiver.

Conventional Receiver Considerations

Frequency drift of the high-frequency oscillator in an FM receiver causes a departure of the frequency of the unmodulated i-f carrier from the center of the discriminator characteristic. If the frequency drift of the high-frequency oscillator, combined with the instantaneous frequency deviation of the FM carrier due to modulation, causes operation over a nonlinear portion of the discriminator characteristic, audio distortion results. If the drift of the high-frequency oscillator is in excess of one half the peak separation of the discriminator, the sound will either be lost or will be badly distorted.

Spurious phase and frequency modulation of the high-frequency oscillator in an FM receiver is passed through the i-f amplifier as additional phase or frequency modulation of the carrier, and is demodulated as such by the discriminator, giving rise to spurious audio components in the loud speaker. Hum modulation of the high-frequency oscillator and frequency modulation produced by microphonics and acoustic feedback (from the speaker to various frequency-determining elements in the oscillator) are examples of this.

Thus, in the case of the conventional television FM receiving system the lack of frequency stability of the local high-frequency oscillator results in deterioration of the sound.

The degree of frequency instability in the high-frequency oscillator of the home television receiver is known, being primarily governed by economic considerations. If cost were no consideration, frequency instability could be reduced to an inconsequential degree by the use, for example, of quartz crystals. The amplitude of the local high-frequency oscillator is usually sufficiently constant to contribute no degradation to the sound channel.

Intercarrier Receiver Considerations

If the amplitude of the local oscillator is very large compared to that of the signal, the amplitude of the beat frequency is nearly independent of the amplitude of the local oscillator. However, if the ampli-

tudes of the signal sources that produce the beat are commensurable, the amplitude of the beat frequency is a function of the amplitude of each signal. An FM receiver is insensitive to amplitude variations of the i-f FM carrier provided these variations are not in excess (chiefly in the negative direction) of any limiting action that may be obtained or of the capabilities of the ratio detector. However, amplitude variations of the i-f FM carrier may be converted into spurious phase modulation in an FM receiver, and as such will be demodulated by the FM detector, producing spurious audio components not present in the originally transmitted sound.

In the case of the intercarrier sound system, deterioration of the sound signal may be caused by changes in amplitude of the heterodyning oscillator (the video carrier which is amplitude modulated by the picture information). The power ratio of the sound to unmodulated video carriers of television transmitters is fixed by the Federal Communications Commission (FCC) at between 0.5 and 1.5. Moreover, the frequencies of the video and sound carriers of a particular channel are sufficiently different to be subject to different degrees of attenuation over the propagation path due to multipath, sporadic E, troposphere, temperature inversions, reflection, and F_2 on the lowest channel. This indicates that even if a fixed ratio between the unmodulated levels of the sound and picture carriers were standardized at the transmitter, substantial variation from station to station at a particular receiving antenna would be experienced. Variations in this ratio from receiving site to receiving site on a single channel likewise would be present. Therefore, it is necessary that the sound carrier be attenuated substantially below the picture carrier in the i-f amplifier in order to insure that the residual amplitude modulation on the sound i-f carrier due to picture modulation will be sufficiently low to be removed by the detector circuit and will not produce spurious phase modulation of the sound i-f.

In the sound channel of the intercarrier sound receiver the equivalent sound intermediate frequency is the beat between two carrier frequencies which are accurately controlled at the transmitter and therefore is unaffected by frequency variations of the local oscillator of the receiver. However, amplitude modulation of the video carrier by the picture information can give rise to spurious phase modulation of the video carrier at the transmitter. This, of course, will introduce spurious phase modulation into the sound i-f and cause spurious audio components in the loud speaker.

The degree of amplitude variation of the sound i-f that would be experienced in an intercarrier sound system is a function of many

variables. If the depth of modulation of the video carrier when transmitting maximum white is never to fall below, say ten per cent; if the phase shift of the video carrier at the transmitter due to picture amplitude modulation is held to a sufficiently small degree; if by proper design in the receiver the degree of amplitude modulation of the frequency-modulated sound i-f carrier is kept low enough to be ignored by the detector circuits; and if the spurious phase modulation of the i-f carrier due to these amplitude variations is sufficiently below the normal sound level; then the intercarrier system has considerable merit.

With these considerations in mind, an investigation of the intercarrier system was begun at this laboratory some time ago.

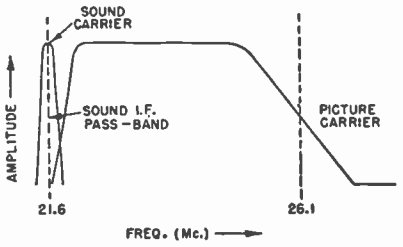

Fig. 3—I-f characteristic of conventional receiver.

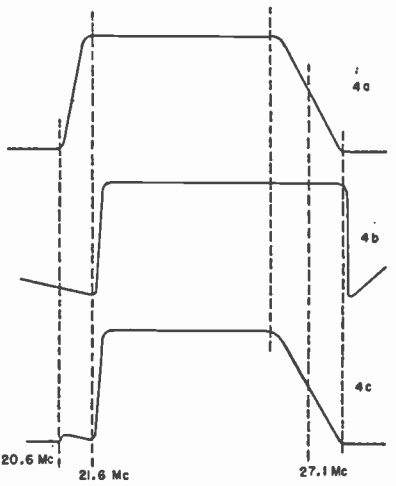

Fig. 4—Realignment of *m*-derived amplifier for intercarrier operation.

Experimental Investigation of the Intercarrier Sound Receiver

Initial Investigation

The frequency response of the i-f amplifier of an intercarrier sound receiver must differ from that of a conventional receiver. In Figure 3 is shown the familiar i-f characteristic of the conventional receiver. A receiver, using *m*-derived i-f transformers was modified for the initial investigation. The sound i-f amplifier was removed from the receiver, and the lower frequency parallel resonant "trap" in each of the first four i-f transformers was tuned one megacycle lower (to 20.6 megacycles). This provided the *overall* i-f band pass at the output of the fourth i-f transformer shown in Figure 4a. The tuning of the fifth i-f transformer was not changed; its frequency characteristic is shown in Figure 4b. The overall frequency of the modified i-f amplifier is shown in Figure 4c. A one-megacycle-wide plateau for the sound, down

in amplitude some 20 decibels below the maximum is obtained. This shape was felt to be desirable in order to insure that the level of the sound carrier would not change as the receiver tuning was varied over the range that would provide a picture of good definition.

The primary of a 4.5-megacycle double-tuned i-f transformer was inserted between the plate of the last video-amplifier stage and its load impedance. The primary was designed so that in conjunction with the high-frequency peaking employed in the plate-load impedance of the last video stage it provided almost flat response at the kinescope grid out to the sharp dip at 4.5 megacycles. The secondary of this transformer fed a 4.5-megacycle amplifier stage operating in overload. The amplifier drove a ratio detector.

Further investigation disclosed that while this arrangement is entirely suitable for use with the intercarrier sound system it is unnecessarily complex.

Simplified Receiver Design

An i-f amplifier having a frequency characteristic as shown in Figure 5, and a video amplifier having a series-resonant trap connected between the plate of the video-amplifier tube and ground was found to provide equally good results except for a somewhat narrower video pass band. The i-f characteristic of Figure 5 was obtained from an amplifier employing four stages using 6BA6 tubes and five stagger-tuned circuits, no i-f traps being employed. The 4.5-megacycle sound i-f takeoff is a tap on the trap. This combination 4.5-megacycle trap and sound takeoff circuit is shown in Figure 6. C_1 is of the order of one micromicrofarad and L_1 is designed to be series resonant with C_1 and the stray capacities to 4.5 megacycles.

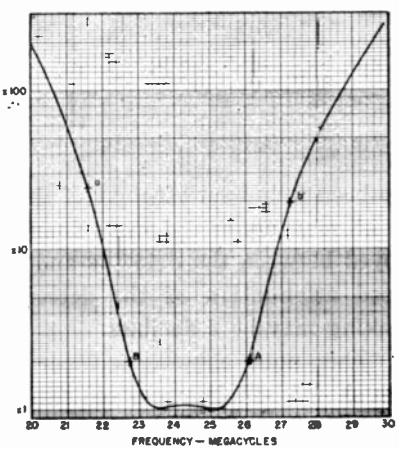

Fig. 5—Symmetrical i-f amplifier.

The pass band of the i-f amplifier of the intercarrier sound receiver shown in Figure 5 is seen to be essentially symmetrical. Hence the picture carrier may be placed on either side of the pass band, at either *A* or *B* (Figure 5), which places the sound carrier at either *a* or *b*. This permits placing the local high-frequency oscillator on either the high- or low-frequency side of the incoming signal. On certain of the

television channels this may reduce image or oscillator radiation interference. By operating the local oscillator on the low side on the higher television band (channels 7-13) a reduction in oscillator drift on this band is obtained. Since the sound channel of the intercarrier sound receiver is relatively immune to oscillator instability, the requirements on local oscillator stability are determined by a consideration of the characteristic of the video channel. The less rigid requirements of the video channel, coupled with the reduction in oscillator drift on the higher channels effected by operating the local oscillator on the low-frequency side of the incoming signal, may make it possible to dispense with the usual manually operated oscillator trimmer.

The Video Amplifier

The video compensation between the second detector and the grid of the video amplifier must be designed to pass the 4.5-megacycle beat energy. As a practical compromise between gain and bandwidth it

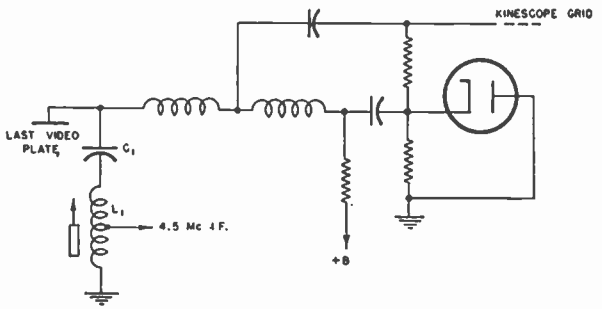

Fig. 6—Combination 4.5-megacycle trap and sound take-off.

has been found satisfactory if the attenuation is as much as 6 decibels at 4.5 megacycles. If more than a single video-amplifier stage is employed between the detector and the second i-f takeoff point, the combined attenuation of the detector compensation and the interstage peaking may be 6 decibels.

When noise clipping is incorporated in the video amplifier, precaution should be taken to avoid clipping of the video synchronizing pulses for the maximum setting of the contrast control that provides a usable picture. If the amplitude of the synchronizing pulses is sufficiently high to swing the control grid of the video-amplifier tube beyond plate-current cut-off, severe 60-cycle buzz output from the sound channel results. This condition may be avoided by taking off the 4.5-megacycle beat at the second detector.

The Sound I-F and Detector

The circuit of the sound i-f, detector and first audio stage is shown

in Figure 7. C_1 is of the order of one micromicrofarad in order not to affect the gain of the video amplifier below 4.5 megacycles. L_1 is resonant at 4.5 megacycles with its distributed capacity, the capacity of C_1 and the stray capacities. The grid of the 6BA6 is tapped down on L_1 to lower the impedance in the grid circuit of the 6BA6 below the point at which the tube will self-oscillate due to grid-plate feedback. The impedance in the plate circuit is made as high as possible so that the 6BA6 will be operating under conditions of plate voltage overload with as small a signal as possible applied to its grid. Then for all signals at the grid above this level the 4.5-megacycle output does not change.

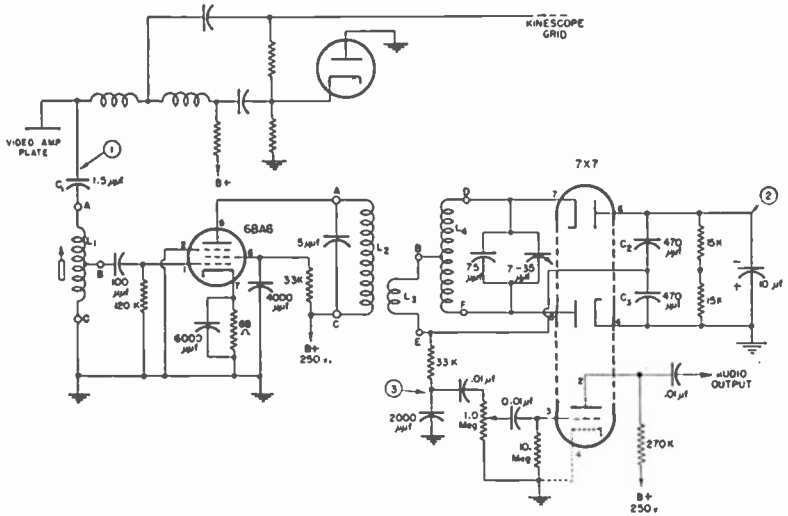

PERFORMANCE

① RMS INPUT	② DC VOLTS	③ AUDIO -25 KC DEVIATION	PEAK SEPARATION
100 mv	15.0 v.	1.4 v RMS	140 KC
10 v.	39.0 v.	2.5 v RMS	160 KC

Fig. 7—Circuit diagram of 4.5-megacycle amplifier and detector.

The detector is a ratio detector.[1] Since the audio output is approximately 2.5 volts root-mean-square for 25-kilocycle deviation, a voltage amplifier must be used between the detector and the output stage. To afford tube economy a 7X7 combination ratio detector and first audio amplifier is used.

Construction of the ratio detector transformer is shown in Figure 8. In the design of the transformer the coupling between L_3 and L_4 and the values of C_2 and C_3 were adjusted for minimum amplitude modulation (AM) response to a signal which was deviated 25 kilocycles

[1] S. W. Seeley and J. Avins, "The Ratio Detector," *RCA Review*, Vol. XIII, No. 2, pp. 201-236, June, 1947.

with FM and simultaneously modulated 30 to 40 per cent with AM. For this test, the system was operated below the level at which the driver overloaded. If the transformer is not duplicated exactly these values may require adjustment. If a tube type other than 7X7 is employed the design of the detector stage must be modified. The full voltage gain of the triode section of the 7X7 is not required and the excess gain may profitably be used for negative feedback.

General Considerations

The level of the sound carrier at the video detector must be maintained considerably below that of the picture carrier. If the levels are of substantially equal amplitude the picture is unusable. In addition to the 4.5-megacycle intercarrier beat there are present numerous heterodynes caused by beats between the picture side bands and the sound carrier. Under certain conditions there may even be an apparent reversal in modulation polarity. Furthermore, the amplitude of the 4.5-megacycle beats is comparable to the video information and produces a cross-hatch effect. Field experience, using the currently operating New York Stations, has indicated that the above described effects on the video channel do not materially degrade the picture if the sound carrier at the video detector is 14 decibels below the picture carrier or 20 decibels below the maximum gain of the i-f amplifier.

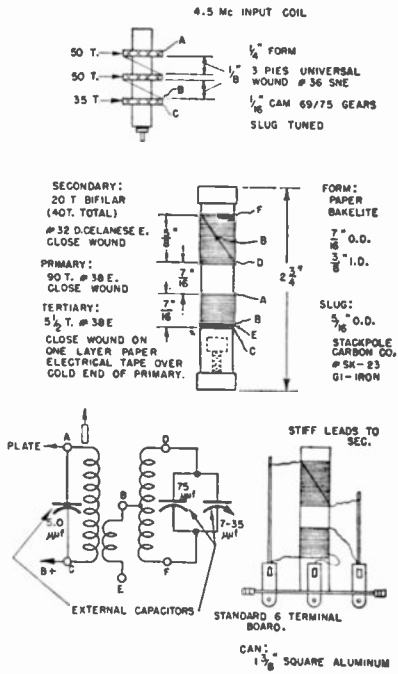

Fig. 8—Construction of 4.5-megacycle trap inductance and ratio detector transformer.

From a consideration of the requirements of the sound channel a somewhat lower ratio of sound to picture carrier is advantageous. The desirability of adjusting the audio-carrier amplitude to a substantially lower level than the video carrier, as indicated by an analysis of the effects of changes in their amplitudes on the amplitude of the resultant beat frequency has been discussed previously. The resultant (4.5 megacycle) heterodyne will be amplitude modulated by the video

to a much less degree than the depth of the video modulation if the amplitude of the sound carrier is of the order of one half or less of the minimum amplitude of the video carrier during downward modulation. The present FCC requirement regarding modulation capabilities of television picture transmitters is that the amplitude of the picture carrier when transmitting maximum white may not be more than 15 per cent of the picture-carrier amplitude when transmitting synchronizing pulses. If this were amended to include "nor less than 10 per cent of the picture carrier amplitude when transmitting synchronizing pulses", the amplitude of the sound carrier then should be attenuated in the intercarrier sound receiver to between 7.5 and 5 per cent of, or 23 to 26 decibels below, the maximum picture carrier amplitude. While the FCC requires that the power of the sound carrier be 50 to 150 per cent of the power of the picture carrier when transmitting peak synchronizing pulses, it appears that the various television stations are employing unity ratio between sound and maximum amplitude picture carrier.

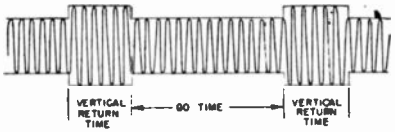

Fig. 9—Effect on audio output resulting from transmission of a white picture 100 per cent downward modulation of the picture carrier.

In typical installations variations in relative level of sound and unmodulated picture carriers of the order of 10 decibels have been encountered. The intercarrier sound receivers field tested by this laboratory having the sound carrier attenuated 26 decibels below the picture carrier (sound carrier 32 decibels below maximum gain of i-f) provided satisfactory sound reproduction with this variation in field strength.

For proper operation of the intercarrier sound system, it is necessary that a white picture not result in zero carrier output from the picture transmitter. If the depth of modulation during the transmission of white is 100 per cent, the intercarrier sound system becomes a pulsed FM system with a duty cycle of 15/100 during the vertical go time and an FM system with a unity duty cycle during the vertical return time. A sizable 60-cycle component in the audio output results. The audio output when this condition was produced in the laboratory is shown in Figure 9. This condition has never been experienced on any of the field tests. However, the newer transmitters may be more nearly capable of 100 per cent modulation, so that unless the minimum carrier level is controlled, the performance of intercarrier receivers may be unsatisfactory.

Spurious Phase and Amplitude Modulation

The sound and picture carriers are located on the skirts of the i-f amplifier characteristic. Since the sound carrier is frequency modulated, this gives rise to spurious amplitude modulation of the sound carrier at audio frequencies. However, the slope (Figure 5) is not great, being always less than 10:1 for a frequency range of one megacycle, and the ±25-kilocycle maximum deviation frequency modulation produces less than 2.5 per cent amplitude modulation. This spurious modulation is removed by the ratio detector.

Placement of the picture carrier on a slope gives rise to spurious phase modulation when the video carrier is amplitude modulated by the picture information. It may be shown that the maximum resulting spurious phase modulation due to 90 per cent negative video modulation of the picture carrier is of the order of 0.03 radians for the case of the highest audio frequency (15 kilocycles). One hundred per cent modulation of the sound carrier at 15 kilocycles produces an equivalent phase modulation of 1.67 radians. The spurious wave then will be 0.01795 of maximum audio. Since 75 microseconds deemphasis is employed in the audio section of the receiver the spurious output is multiplied by a factor of 0.1415. At the loud speaker the spurious level is 0.00254 or 52 decibels below 100 per cent modulation.

Performance of the Intercarrier Sound Receiver

Intercarrier sound receivers embodying these design considerations have been field tested for a period in excess of one year in New York City and on Long Island. Reception has been limited to channels 2, 4, and 5 since there have been no stations operating in this area on the higher channels. Results have been quite satisfactory.

In tests of one intercarrier sound receiver the consensus of a critical audience was that the user would not bother retuning the receiver despite overall variations in the local oscillator frequency of 1.4 megacycles. In a typical receiver employing the conventional sound system, audio deterioration is usually experienced when the local oscillator is shifted 75 or 100 kilocycles.

While the symmetrical i-f amplifier has a reduced bandwidth that is discernible when viewing a test pattern, the reduction in resolution is compensated by the simplicity that results.

The intercarrier sound receivers have been free from microphonics and hum modulation, and manual adjustment of the oscillator trimmer has not been required.

AUTOMATIC GAIN CONTROLS FOR TELEVISION RECEIVERS*†

By

K. R. Wendt and A. C. Schroeder

Research Department, RCA Laboratories Division, Princeton, N. Y.

Part I

GENERAL CONSIDERATIONS

By

K. R. Wendt and A. C. Schroeder

Summary—The general theory of automatic gain controls for television receivers is discussed. Several specific circuits are described in detail with the advantages and disadvantages of each.

Introduction

AUTOMATIC gain control (AGC) is as important in television receivers as in sound receivers, and actually serves more useful purposes in television than in sound. Manual gain adjustments in a television receiver are annoying, and a non-technical person experiences difficulty in learning to set the control properly, since the optimum level for limiting and sync separation is not easily judged from the picture contrast. Also, television signals may suffer from violent fading due to passing airplanes. This can be reduced or eliminated only by a fast AGC circuit. The use of an AGC not only provides easier adjustment, but also may allow the simplification of portions of the receiver, such as the sync separator, which would not be required to operate over wide ranges of amplitude. A properly designed and operating AGC makes the setting of the contrast and background controls simple and infrequent. AGC has, however, been little used because its design has not been sufficiently understood, and the early circuits have not performed satisfactorily.

In a sound receiver for amplitude modulation, the signal which is measured and which is held constant by the AGC, or AVC as it is called,

* Decimal Classification: R583.5
† Reprinted from *RCA Review*, September, 1948.

is the average carrier level. This is easily measured because the dc output of the detector is proportional to the average carrier level. In a television receiver it is the peak carrier level which must be held constant by the AGC. This peak carrier level may be obtained by measuring the voltage of the peaks of the synchronizing pulses at the output of the detector, provided that the load of the detector has the same dc as video-frequency impedance. The output of the measuring device is then fed back to the intermediate-frequency amplifier in such a way as to decrease the gain as the signal increases. Amplification of the AGC signal may be obtained by amplifying the signal before peak measurement or amplifying the dc output of the peak measuring device, or both. In either case, the amplification must be dc, and in the former case it must also amplify video frequency. The AGC measuring device consists of some detector, such as a diode feeding a capacitor. Since this circuit receives information only during the sync pulse, which is 8 per cent of the time, the capacitor must hold its charge between pulses.

Noise Considerations

A simple peak detector, when used for television AGC, is quite susceptible to peaks of impulse noise. The noise is predominantly in the black or increasing signal direction, and may be quite high as compared with the signal. The peak detector then measures the noise height rather than the signal height, and may reduce the gain of the receiver to a small value, giving very unsatisfactory performance under noise conditions which may be encountered quite often in outlying areas. A poor AGC circuit may render unsatisfactory a picture which, with a good AGC or manual control, would contain nothing more than nearly unnoticeable short black streaks. Many devices, such as automobiles, buzzers, electric shavers, etc., produce such interference. It is therefore important that AGC circuits be designed with noise immunity as a primary consideration.

AGC Speed

After a simple peak detector has responded to a noise peak, it can return to normal only as fast as the capacitor may be discharged through its associated resistor. The capacitor may be charged much more quickly than it is discharged, since it is charged through the low impedance video circuit and diode. The AGC thus normally is quicker in responding to than in recovering from a noise peak, the effect of noise peaks being thereby greatly extended.

It is desirable to have the AGC quite fast in order to have it follow

fast fading, and to minimize the effect of noise. However, the vertical sync signal interferes with fast operation. If the AGC is made fast, it removes a considerable portion of the vertical sync signal and produces a transient following the vertical signal. The mechanism, briefly, is as follows: The detector is not a true peak device. It must operate with a certain area (voltage $\times$ time) of the sync extending into the conduction region of the diode. The horizontal pulses are 8 per cent of a line interval in width. The vertical pulses, however, are 84 per cent of a line interval in width, and for the same height pulses approximately ten times as much current will be drawn during the vertical pulse. To the AGC circuit this appears as an increased signal. In a fast circuit the intermediate-frequency gain is therefore reduced during the vertical until the average diode current approximates that drawn during the horizontals. The vertical signal is thus reduced, or "pushed into a hole" by an amount approximately equal to the height that the horizontal pulses extended into the conduction region. It might appear advisable to reduce this conduction area by increasing the diode resistor so that it would require less power. Such operation is impractical, however, due to noise. A small amount of noise power is then able to take the control away from the signal. Nor is a limiter of much help with such a peak-operated detector. If the limited noise extends beyond the sync—and it must, in order to keep the limiter from destroying the information as to the height of the signal—the gain of the receiver will be reduced until the noise no longer fills the limiter. If the received noise-to-signal ratio were 10 to 1, and this can easily be, the signal would be reduced to approximately 1/10 the desired value by the AGC. For noise immunity, therefore, the simple AGC detector must be of relatively low impedance, and be energy operated, thereby using large areas of the sync signal. This also means that the circuit can not be made fast, due to the consequent loss of the vertical sync signal.

Early AGC Circuits

The receivers used in the field tests conducted in the early 1930's contained a picture AGC circuit. It consisted of a diode peak detector coupled directly to the video output of the second detector. The output of this peak detector was amplified by a triode amplifier and applied to the intermediate-frequency amplifier grids. The proper dc voltages were obtained by operating the detector and the cathode of the dc amplifier at about —50 volts and the plate of the amplifier at —3 volts.

Figure 1 shows the AGC circuit in the field test sets. T_1 is the detector, T_2 is the peak detector, and T_3 is the dc amplifier.

The first TRK-12 had a similar AGC except that the peak detector

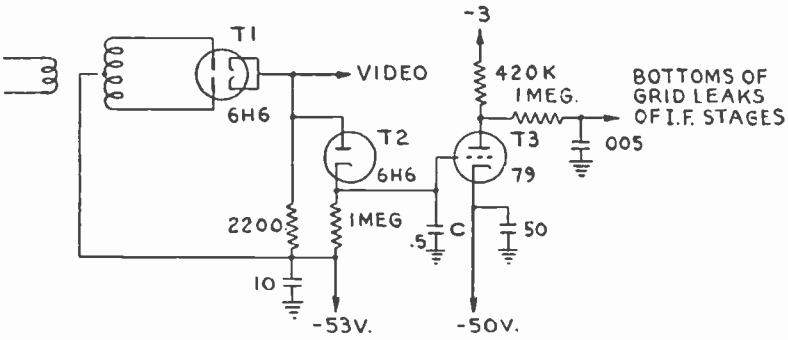

Fig. 1—Field test AGC (early 1930's).

was a triode in a cathode follower type circuit. Figure 2 shows the AGC circuit in the TRK-12 where T_1 is the detector, T_2 is the peak detector, and T_3 is the dc amplifier. It was found necessary to remove this AGC from these sets, partly to make room for a limiter which, under noisy conditions, was more necessary than an AGC, and partly because high peak noise caused the AGC to operate unsatisfactorily, as explained previously. A peak of noise would cause the gain to go down, and due to the long time constants in the circuits, appreciable time was required for the receiver to return to normal operation. This caused the picture to flash very badly in the presence of high peak noise, which would otherwise have been almost unnoticeable.

In both the field test set and the TRK-12 a high peak of noise charged C from a low impedance to nearly the height of the pulse; C then had to discharge through the high impedance of the cathode circuit of the peak detector.

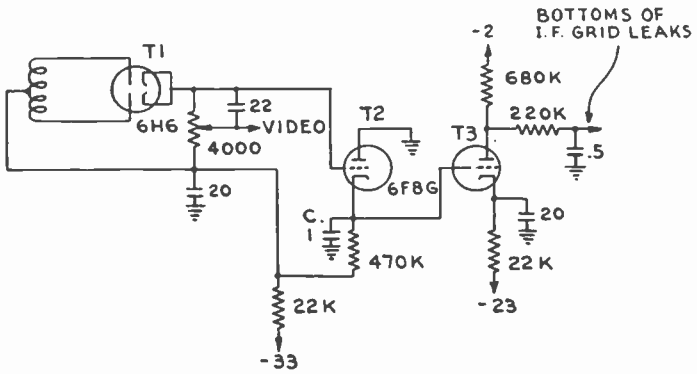

Fig. 2—TRK-12 AGC.

Circuits with Improved Noise Immunity

A satisfactory AGC must be immune to high peak noise. A limiter is of considerable help in this respect, if used with an energy-operated AGC detector. If the limiter cuts the noise down nearly to the level of sync and the noise is narrower than the sync, which it nearly always is, a detector which works on the energy in the sync peaks will be quite immune to the noise. It must be emphasized here that such a detector much be energy operated and use an appreciable area of the sync pulses.

Figure 3 shows a simple AGC circuit which has a limiter before the AGC detector and which operates quite satisfactorily. T_1 is the detector, T_2 is the limiter, T_3 is the AGC detector, and T_4 is a glow tube which brings the dc voltage down to the proper value to operate the intermediate-frequency grids. In operation, the limiter T_2 prevents

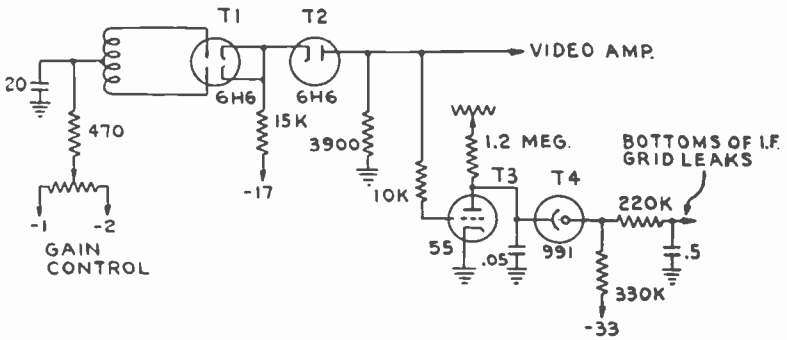

Fig. 3—Simple AGC with limiter.

currents flowing through the 3900-ohm load resistor of the detector if the detected voltage is higher than ground. If the AGC holds the peaks of sync at approximately ground, the gain can be varied if desired by changing the output voltage of the detector for zero carrier. This is accomplished by varying the potentiometer marked gain control. The signal after limiting is applied to the grid of T_3, which is cut off except when the signal approaches ground. In other words, T_3 conducts only if the peaks of sync are near ground potential. The peaks of sync then cause pulses of plate current to flow, which causes the dc voltage at the plate of T_3 to decrease. The voltage at the supply end of the plate resistor is adjusted so that with no plate current and just the current through the series combination of the 1.2-megohm plate resistor, the 991 glow tube, and the 330,000-ohm biasing resistor, the voltage at the low end of the glow tube (the voltage applied to the grids of the intermediate-frequency tubes) is zero. Then, when plate

current flows through T_3, causing the plate voltage to decrease, the voltage fed to the intermediate-frequency grids is also decreased by the same amount, decreasing the intermediate-frequency gain. The glow tube need not be of the selected, voltage regulator type, such as the 991, but can be of the type ordinarily used for illumination.

Another means of improving the noise immunity is by means of a double time constant arrangement.

As may be seen from Figure 4, this circuit uses one diode fed from the last intermediate-frequency transformer. Bias is applied to its cathode to delay the application of AGC bias until the video output is sufficient for full contrast. Two time constants are used and account for the improved performance obtained with this circuit over that obtained from a long-time-constant peak detector as has sometimes been used. R_1C_1 form the first time constant which is relatively fast—of the order of one picture line. R_2C_2 forms the second time constant and is much longer. It should not be less than 1/20 second. Because of the short input time constant a relatively small amount of energy is

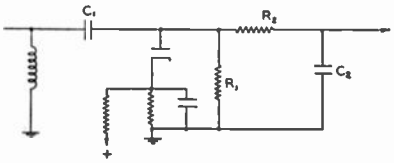

Fig. 4—Double time constant integration.

stored in C_1 and by the end of each line the voltage across it has dropped to approximately the black level at which time C_1 is again charged. R_2 and C_2 filter out both this ac component and the 60-cycle component caused by the vertical synchronizing pulses. In the presence of noise pulses C_1 is charged to approximately the peak amplitude of the pulses, but because its capacitance is low the energy stored is small. The ac component of this energy is removed by the subsequent filter, and the dc component is so small that it affects the AGC output only slightly. To operate in this ideal manner the R_1C_1 time constant should be of the order of four or five lines. However, it has been determined empirically that the AGC voltage is not greatly affected by the picture content if the R_1C_1 time constant is made as short as one line. Because the noise susceptibility of the system decreases as the input time constant is decreased, the shorter time constant is more desirable. This principle can be applied to advantage in many AGC systems.

Simplified Fast Circuit

Due to the desirability of a fast-acting AGC for the elimination of airplane fading, considerable work has been done in this direction. In the foregoing discussion of fast circuits, in which it was shown that the vertical sync signal was removed from the video, no mention was made of the fact that in such a case the vertical sync signal appears on the AGC control voltage. Attempts have been made to use this as the vertical sync signal. Such a vertical is unsatisfactory, however, since its amplitude varies radically with the incoming signal. For instance, a strong signal may provide very little vertical sync, since the intermediate-frequency tubes operate near cutoff, and require very little signal to change their gain appreciably. Also, the AGC voltage

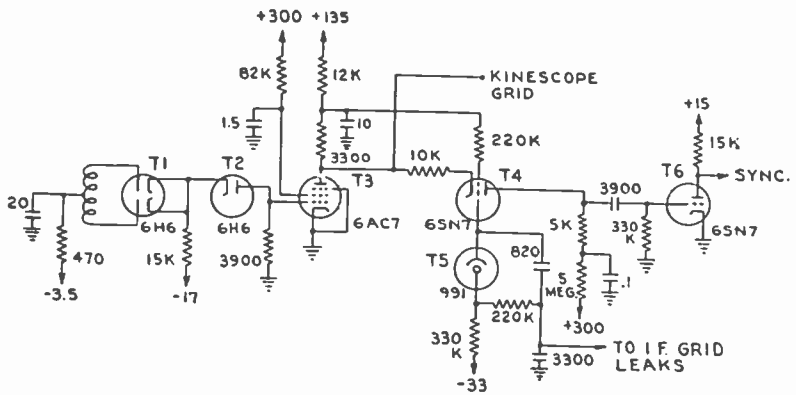

Fig. 5—Combined AGC and sync separator.

contains all the low frequency variations in the signal, such as that from fading caused by airplanes, which makes proper use of the AGC voltage as a vertical sync signal quite difficult.

It has been found possible to combine the operation of the AGC detector and the sync separator in such a manner that a satisfactory sync signal may be obtained with a fast circuit. The video signal still has the vertical "in a hole". However, the separated signal has in effect the AGC signal added to it, as far as vertical sync is concerned, and that which is lost from the video and appears on the AGC is added to the separated signal to produce a normal separated signal.

Figure 5 shows a circuit of this type. Up to the grid of the video amplifier the circuit is identical with the one previously described in Figure 3. In Figure 5, however, T_3 is the video amplifier which feeds the grid of the kinescope. Since the grid of T_3 is dc-connected to the detector, the correct second detector dc information is available from

T_3 by making its plate circuit flat to dc. This is done by simply choosing the ratio of the plate filter resistance to the screen filter resistance such that the ac amplification is equal to the dc amplification, and making the two time constants of the filters equal. The plate of T_3 is dc-connected to the grid of the kinescope so that if the AGC holds the peaks of sync at a given level it will hold not only the gain constant but also the black level on the kinescope constant so that there is no need for an additional dc setter. The AGC which is connected to the plate of T_3 is also the sync separator. The grid and cathode of T_4 act as a peak detector and the detected voltage is dropped to the proper level by the glow tube T_5 in a similar manner to the previous circuit. However, here the time constants are very much faster; in fact the glow tube and series resistance to the intermediate-frequency grids is by-passed for high frequencies by the 820-micromicrofarad condenser. The plate of T_4 is kept low with respect to its cathode by the large series resistance to +300 volts (5 megohms) so that it acts as an effective clipper. This allows only sync pulses to appear across the plate resistor and after further clipping by T_6 the sync is fed to the automatic-frequency control (AFC) sync circuits. The sync appearing at the plate of T_6 has full amplitude vertical even though the picture signal on the grid of the kinescope has its vertical "in a hole". This is because the grid of T_4, which is the AGC output, has the signal on it which puts the vertical "in the hole". Therefore the grid to cathode signal of T_4 has not lost the vertical sync.

This circuit, then, is a fast AGC circuit in which the disadvantage of losing vertical sync is overcome. Another incidental advantage is that, since there is no coupling condenser to the grid of the kinescope, capacity to ground on this lead is reduced, allowing greater gain or bandwidth in the amplifier. Also the three functions of sync separation, dc restoration, and AGC, are all obtained with a tube which usually only serves as sync separator.

Keyed AGC Circuits

Another method of obtaining improved AGC performance is by means of the keying principle. A keyed AGC system is one which is turned on, or made sensitive, for only small intervals of time, usually less than 8 per cent. A narrow pulse, occurring at horizontal frequency, is used to key the AGC. The pulse is usually obtained from the local horizontal oscillator, in which case synchronism must be established for proper operation. The pulse may also be obtained from separated sync, although this method is much inferior with respect to noise, since noise peaks become keying signals which measure themselves.

Keyed systems have several fundamental advantages. First, if the pulse is 5 per cent, a theoretical advantage of 20 times in noise immunity is obtained, since for 95 per cent of the time noise can not affect the AGC. Although this full gain is not obtained, since small noise pulses on a white signal do not affect a simple AGC, nevertheless a considerable gain is realized. Second, the vertical sync information is completely eliminated from the AGC, allowing it to be made as fast as desired without impairing vertical synchronization, and, third, since the speed of response may be made fast, the effects of rapid fading are not only reduced, but the receiver quickly recovers from any residual effects due to noise.

The basic balanced type of keyed AGC is shown in Figure 6.[1] Many arrangements are possible, but the simplest, providing proper

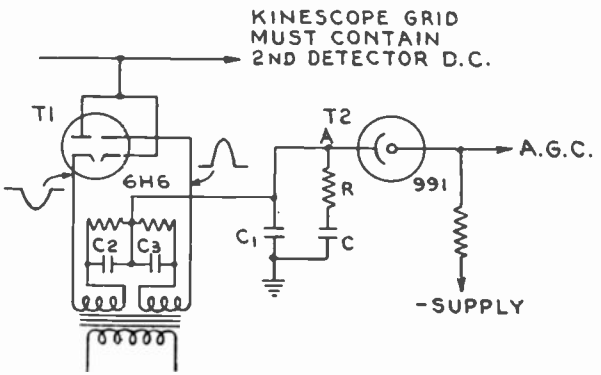

Fig. 6—Balanced keyed AGC detector.

2nd detector picture dc can be maintained to the kinescope, is the arrangement shown, in which the AGC detector operates from the maximum video signal. The keying pulses are supplied by the transformer shown, which may be driven by a tube, supplied with a pulse from the horizontal blocking oscillator, or the horizontal output stage. Alternatively, the two output windings shown may actually be wound on either the horizontal blocking, or output transformer, with the windings connected, of course, such that the pulses are of proper polarity to drive the diodes into conduction. As the pulses drive the diodes into conduction, capacitor C_1 is charged or discharged until point A is brought to the potential of the video circuit during the time of the pulse. The resistance-capacitance circuit across C_1 supplies damping and prevents overall oscillation. The dc voltage at A is positive with respect to ground, and must be reduced by means of one or

[1] K. R. Wendt, "Television DC Component", *RCA Review*, Vol. IX, No. 1, pp. 85-111, March, 1948.

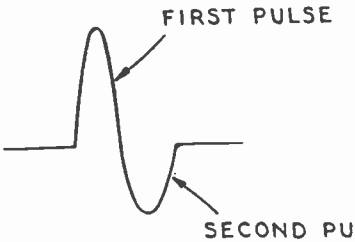

Fig. 7—Oscillator transformer wave form.

more glow tubes, to a negative potential suitable for the AGC control voltage. This AGC can be improved by following capacitor C_1 with a dc amplifier, or a cathode follower, in which case there is no dc load on C_1.

This keying circuit is independent of the height of the keying pulses, as long as they are sufficiently high to maintain the diodes open between pulses for all conditions of video signal.

The keying pulses should be appreciably narrower than the 8 per cent sync pulse in order to allow some variation in the phasing of synchronization. Also, for the same reason, the pulse should occur in the middle of the sync pulse when the synchronizing circuits are operating normally. For a triggered synchronizing system, this may be accomplished by using the first of the two oscillator pulses, as shown in Figure 7. For AFC synchronization, the second pulse may be used. The location of the pulse, with respect to the synchronizing pulse, may be varied in the AFC circuit by changing the delay in the sawtooth signal fed into the AFC, or by changing the total width of the pulse of Figure 7 by adding capacity across the oscillation transformer, or by altering the inductance of the transformer.

This balanced circuit can not be used to key on the "back porch," in order to improve the dc restoration on the kinescope. This is due to the fact that the vertical sync pulse occurs during the time normally occupied by the "back porch." Hence, wrong information would be supplied to the AGC, and the vertical sync pulse would be practically removed, with a severe transient occurring after it. This effect could be made small by making the circuit very slow, but thereby losing, at the same time, one of the advantages of keyed AGC.

Simplified Unbalanced Keyed AGC

In this arrangement a pulse in the black direction is added to the signal, and a normal AGC peak detector is used, or the detector is pulsed so that it "reaches down" to the sync signal only during the pulse. If the pulse is added to the video, the sync separation must be ahead of the AGC since the pulse would interfere with the separator. Such a system has the following advantages:

1. It has considerably increased noise immunity over a plain AGC, especially if a limiter is used on the signal, and the pulse is made large enough to maintain the AGC detector above the clipped noise peaks;

2. It may be made quite fast; and

3. It is somewhat simpler than the balanced type.

It also has these disadvantages:

1. It is very critical to pulse amplitude changes (any change in the pulse amplitude is interpreted the same as a signal amplitude change); and

2. It is faster in one direction than the other—that is, it is faster in the increased signal direction, as is a simple AGC. (This limits its noise immunity, since the effect of a noise pulse is prolonged, and, in order to make it fast enough in the decreased signal direction, it must be made very fast in the increased signal direction, and hence sensitive to noise pulses of very small energy or area that may occur during the keying pulse.)

Effect of Loss of Synchronism

The keyed AGC can not operate satisfactorily when synchronism has been lost. Depending upon the speed of the AGC, the pattern becomes darker or entirely black. This is due to the keying pulse attempting to hold at black the various portions of the picture upon which it falls. However, either sync or the limited edges of blanking are present to act as sync pulses. These tend to synchronize the oscillator frequency in the normal manner, and when the oscillator approaches synchronism or passes through the correct phase, normal conditions are restored by the AGC, and the oscillator can lock in properly. Although the pull-in range may be reduced somewhat by the AGC, synchronizing systems have in practice operated normally and satisfactorily in conjunction with keyed AGC systems.

Some General Considerations

The Video DC Amplifier. Any AGC system for television must maintain the 2nd detector dc information to the AGC detector point. The most economical point for the AGC detector is at the kinescope where the level is the highest. The easiest method of getting the 2nd detector dc to the kinescope is a dc amplifier. Usually, the video tube is a pentode, and some dc is unavoidably lost by the screen grid. As explained previously, it is possible to introduce into the plate circuit a low boost filter which can exactly make up this loss. The two filter time constants should match. However, if the by-pass capacitors are

reasonably large, and the screen does not have too high a resistor, compensation becomes quite non-critical. Figure 8 shows such a circuit. A limiter may be installed before the video tube, but care must be taken to insure that the dc signal is really maintained through the limiter. A two-stage video amplifier may also be used, in which the first tube acts as a limiter by being driven beyond cutoff. Such a limiter is not as sharp as a diode, but is satisfactory for operation with AFC and keyed AGC.

Kinescope Operation with Second Detector dc. Operation in this manner is quite different from operation with a dc restorer. First, the screen, in the absence of a signal, is white, with noise showing,

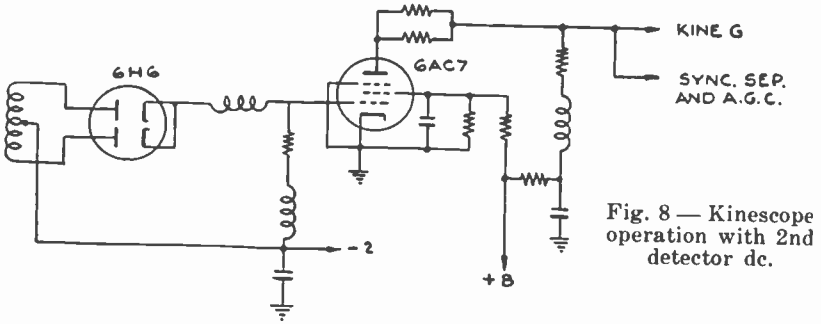

Fig. 8 — Kinescope operation with 2nd detector dc.

which is a definite indication that the station is not on. There is thus little danger of forgetting that the set is turned on after the station has signed off. If an unmodulated carrier is on, the screen is black, which is again a definite indication not obtainable with a separate dc restorer. This information is very helpful, especially if the contrast and brightness controls need not be operated. Its chief advantage is that the dc restoration for the kinescope can be made exceedingly accurate, yet no tube or equipment is required other than the AGC.

Gain and Filtering in AGC Circuits

In a sense, all television AGC circuits are keyed. In other words, information as to the output voltage is received only during short intervals of time. The control, of course, must be made to apply continuously.

The control voltage must therefore be integrated, or stored. This involves filtering and delay. If the ac gain of the system is too high it will oscillate. That is, the control voltage may be larger than needed, which will not be measured until the next pulse, at which time an opposite correcting voltage will be received, and the system will therefore oscillate. The gain of the system must be as low as possible for frequencies higher than approximately ⅓ the keying rate, or line

frequency. The gain below this frequency may be allowed to rise as rapidly as possible; delays should be avoided.

The dc gain may be quite high. The flatness of the AGC is determined by the dc gain. If the dc gain is too high, however, any low frequency delay, such as power supply filtering, may cause low frequency oscillation or motor boating.

In general, for maximum AGC speed, as in all feedback circuits, the filtering should all be in one place, which should be the capacitor receiving the charge from the detecting device. This capacitor should be by-passed by another larger capacitor, in series with a resistor, called the damping resistor, which should be adjusted for maximum stability. All other by-passing should be in the nature of intermediate- or radio-frequency grounding, and should not cause appreciable delay. The dc gain should be adjusted in accordance with the flatness or economy considerations desired.

Part II

A NEW FAST NOISE-IMMUNE TELEVISION AGC CIRCUIT

By

K. R. Wendt

Summary—A new inverted keyed AGC circuit has been developed, which is fast enough to remove airplane interference, possesses very high noise immunity, and is simple and non-critical. It requires 1 or 1½ tubes, and in addition restores the dc for the kinescope. The dc is automatically restored with the blanking level as the reference. The sync height thus becomes non-critical, and the noise limiter may actually remove a portion of sync without an undesirable result.

Introduction

AS EXPLAINED in Part I, television AGC rectifiers must be of the peak type, and since they operate on such a small area signal, they become excessively sensitive to noise. Usual peak rectifiers have two speeds: the response speed and the recovery speed. The response is the fast speed, and the recovery the slower. The response is caused by an increased signal drawing more rectifier current, and, of course, the larger the increase in the signal, the more the response. The slow speed of the circuit is its own recovery speed, and applies whenever the circuit is not drawing current. A sudden decrease in the signal will be followed only according to a resistance-capacitance time constant and not at the speed of decrease of the signal. Since the noise is usually in the increased signal direction, and the circuit is fast to respond to an increase in signal, the circuit is therefore

fast to respond to noise and slow to recover from the effect of noise. Keyed circuits are an improvement in this respect in that they are completely inactive between keying pulses. Therefore noise pulses between the keying pulses have no effect upon the operation of the keyed circuit. Furthermore, keyed circuits are fast in both directions, so that although they may respond quickly to a noise pulse they also recover quickly, thus reducing the effect of noise.

The circuit described herein has been called the "inverted keyed circuit" because the response to signal is inverted over the previous rectifier circuits in that it *responds* to a *decreased* signal rather than

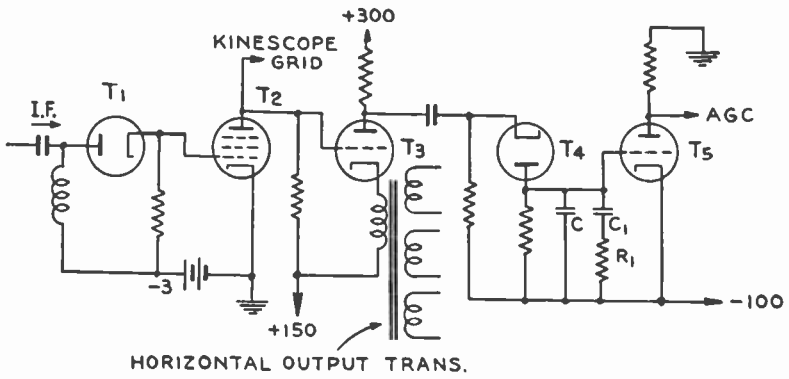

Fig. 9—Simplified schematic of inverted keyed AGC.

an *increased* signal. Furthermore, since it is keyed, no record remains of noise pulses occurring between keying pulses. A noise pulse which occurs during the time of the keying pulse usually appears as a sudden increase of signal. The circuit completely ignores such a sudden increase, and follows only in its slow speed. When the circuit returns to normal, that is, when a normal synchronizing pulse arrives, the circuit responds quickly in this decrease direction and promptly returns to normal operating conditions. The circuit therefore responds slowly to noise and recovers quickly from the effect of noise.

The New Circuit

The circuit which accomplishes this inverted keyed action is shown in Figure 9, in which T_1 and T_2 are respectively the second detector and the video amplifier. Two stages of video could be used, but, in any case, as explained in Part I, it is necessary for the amplifier to be dc-connected from the second detector to the AGC tube. For simplicity, no peaking coils are shown in this diagram. The video signal is connected directly to the grid of T_3. The signal has its sync pulse negative,

and is on the order of 50 volts. A negative pulse obtained from a few turns on the horizontal output transformer is applied to the cathode of T_3. This pulse must be of greater amplitude than the video signal, and may be approximately 75 volts. The pulse causes current to flow in T_3, depending upon the actual amplitude of the video signal. A large video signal will be more negative during sync and blanking time, and will cut off T_3 and very little pulse will be produced. A smaller video signal will hold the grid of T_3 more positive and a larger pulse will be produced. This pulse is connected by way of a capacitor through an ac connection only, to T_4, which is a diode for rectifying and obtaining a dc corresponding to the amplitude of the pulse. On the grid of T_5, therefore, a dc exists which is negative for small video signals and positive for large video signals. T_5 inverts the polarity and supplies an appropriate signal for an AGC voltage. The dc levels require that a negative supply be used, or at least that the intermediate-frequency tubes have their cathodes at some point more positive than the cathode of tube T_5. The voltage for the grid of T_5 is, of course, obtained by the way of an ac connection, and the rectifier T_4. The noise immunity of this circuit is seen, therefore, to come from two causes. First, the circuit is keyed and is completely immune to noise between keying pulses. Since the noise always extends negative on the grid of T_3, the noise pulses merely cut this tube off further than it has been cut off by the absence of the keying pulse and therefore no current can flow in its plate circuit. Second, due to the inverse action of this circuit, noise which produces a suddenly smaller pulse from T_3 does not cause current to flow in the diode T_4, and, hence, the noise is ignored by the circuit. Therefore, regardless of the amplitude of the noise, it is not measured by the circuit, which merely considers the noise as an increase in the signal which is followed slowly and from which it can recover quickly. If there is any noise in the white direction, however, the circuit is sensitive to it. Normally, however, the noise which occurs in this direction is a result of very infrequently encountered phase and amplitude conditions of the interfering carrier. In order for the detector output to be *reduced* by noise, and thus to give a white signal, the noise must be of approximately the same frequency and amplitude as the signal, and must remain in a phase opposite to that of the signal for an appreciable time. An appreciable area of noise which extends toward white is very seldom encountered. White noise may also be caused by intermediate-frequency overload. However, intermediate-frequency overload is minimized by the low impedance of the AGC driving circuit of tube T_5. This tube may be made to conduct very large currents necessary for a low impedance, since its current opposes the change in current in the intermediate-frequency and hence serves

to stabilize the overall load of the receiver. Also, the circuit opposes excessive white noise generation due to overload in any tube which has AGC applied to its grid; i.e., the white noise is a result of bias produced by grid current drawn by the noise pulses. The AGC immediately responds to the reduced signal applied to it and *reduces* the bias, thus opposing the bias produced by the grid current.

The pulse for operating this AGC circuit, which is applied to the cathode of T_3, is, as has been explained, obtained from the horizontal output transformer. This gives a low impedance pulse, and since the load of T_3 is small, it has no adverse effect upon the horizontal output circuit. The pulse should be reasonably wide. It may occur during the synchronizing pulse, but it must occur during at least a portion of the "back porch," or blanking level, following the synchronizing pulse. The pulse must end before the end of this blanking level, or very wrong information will be obtained. As receivers are normally operated, this condition obtains because it is necessary for the return line to occur and be completed during the blanking time of the signal. Therefore this horizontal output pulse is admirably suited for operating this type of AGC.

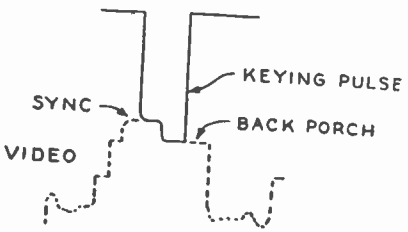

Fig. 10—The inverse modulated pulse.

Blanking Level Reference

This AGC actually operates by means of the blanking level, and not the synchronizing peak level. Therefore the actual sync height is unimportant, and the dc which is used on the kinescope is obtained from the blanking or true black level. This may be understood by noting that the signal on the grid of T_3 is at two levels during the keying pulse: first, at the synchronizing level, which is the more negative; and then at the blanking level, the more positive of the two levels. Therefore the larger pulse on the plate of T_3 is produced by the blanking level. The pulse obtained from the blanking level, therefore, is the pulse which actually operates the diode, T_4, and from which the AGC dc voltage is derived. Figure 10 shows in dotted form, the signal that would exist on the plate of T_3 from the video, and in solid form, the signal that does exist as the result of the video *and* the keying pulse. The maximum height of the pulse is seen to occur as a result of the blanking level of the video signal.

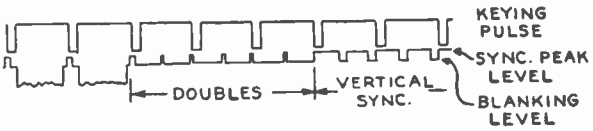

Fig. 11—Absence of blanking level during vertical sync and keying pulse.

THE VERTICAL SIGNAL

During the vertical sync signal there is no blanking level during the time of the keying pulse. This can be seen by referring to Figure 11. The AGC detector is therefore not operated during the vertical sync signal and it interprets the vertical as a sudden increase. Therefore the gain of the amplifier, and the vertical sync signal are reduced according to the time constant speed of the detector. This fact limits the speed for this arrangement of the inverted keying system. It would be impossible to operate on the blanking level, or "back porch," except by virtue of the inverted system, wherein an increased signal is followed slowly, and a decreased signal quickly. The circuit speed is therefore limited by the response desired during the vertical. If the vertical signal is treated too severely, the speed must be decreased somewhat. However, when the vertical signal is reasonably unaffected, the AGC is still fast enough to remove most airplane interference.

A SIMPLER ARRANGEMENT

In Figure 12 is shown a simpler arrangement of the circuit of Figure 9. T_3 itself is made the detector. The plate resistor is made quite large, and is bypassed by a capacitor which then makes T_3 a peak plate rectifier. The dc is generated on the plate and is conducted to the grid of the AGC output tube, T_5, by means of glow tubes such as the 991. It is not necessary in this application, however, to use the more carefully selected variety of glow tube, such as the 991. The commercial ¼-watt neon lamp without the ballast resistor may be used. These tubes act essentially as batteries in series with the circuit from the plate of T_3 to the grid of T_5 and dc changes appearing on the plate

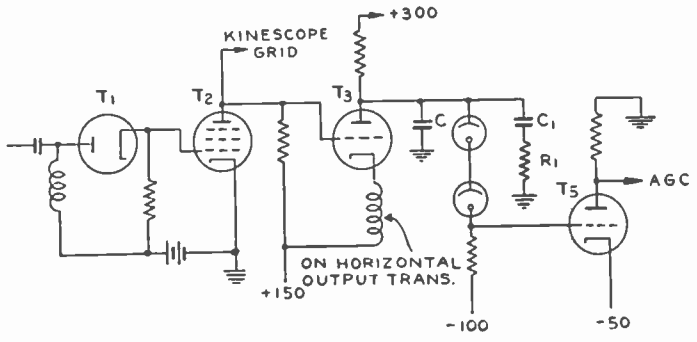

Fig. 12—T_3 operated as rectifier.

are therefore transmitted to the grid of T_5 except at a more negative dc level. This circuit eliminates one-half of a tube, but uses in its place the glow lamps. The operation of the circuit is relatively the same as the operation for the circuit using the diode, except that the gain of T_3 is reduced somewhat when used as a detector over the application in which it is used as an amplifier.

Filtering and Damping

Information for television AGC circuits, whether they be keyed or not, is obtained only over a small interval of time during the sync or blanking pulse. This information must therefore be integrated to control the signal until the next pulse is received. Such filtering is apt to introduce delays which may cause overswing and oscillation. If the filtering is accomplished entirely by one circuit, this tendency may be eliminated. The filtering in Figure 9 is accomplished by the capacitor C. Some bypass is necessary at each intermediate-frequency grid, but this filtering should be in the nature only of bypass for intermediate frequencies and should in no way affect the frequencies necessary for the AGC control. Since these frequencies are widely different it is possible to introduce sufficient intermediate-frequency bypass without introducing adverse delay for the AGC voltage. However, it is usually necessary to add some sort of damping. This damping should be introduced across the filter capacitor C. It is shown in Figure 9 as the circuit C_1R_1. C_1 is approximately 10 times C. R_1 is adjusted to give the minimum oscillation conditions. Providing there are no delays in other portions of the circuit, R_1 will be found to be non-critical. When R_1 is very small, oscillation may occur at a low frequency corresponding to the frequency of filtering of C_1. When R_1 is very large, oscillation may occur at the frequency caused by the filter capacity C. A point midway between these two values gives quite stable performance.

Circuit Adjustments

Figure 13 is Figure 9 redrawn with the required adjustments, screen supplies, etc. The most essential adjustment is that labeled "black level control". This control is not for the purpose of adjusting the black level on the kinescope, which should be accomplished in the normal manner, but is for setting the black level near the video noise clipping level. Clipping may be accomplished by plate current saturation on the video output tube, or by using a two-stage amplifier, and cutoff clipping in the first tube. In either case, the AGC equilibrium point must be adjusted by means of the black level control, until the sync pulses are held just inside the clipping level. The control may be

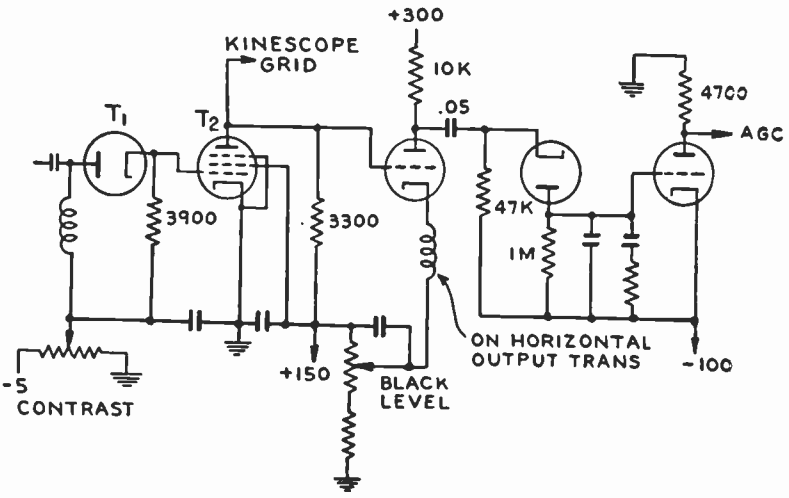

Fig. 13—Modified inverted keyed AGC circuit, showing screen supplies and controls.

a factory adjustment and need not appear on the front of the receiver. This control operates by varying the dc voltage on the cathode of T_3 and hence essentially adjusting the absolute level at which the peak of the measuring pulse occurs. Since it is the difference between this measuring pulse and the video which produces the AGC voltage, the video black level may be made to occur at any desired level by varying the dc in the pulse circuit as shown.

The other control shown is the video contrast control. This control adjusts the highlights of the picture without affecting the black level. As explained above, the black level is held at a fixed plate current level in T_2. If the bias on T_2 is changed by the dc control, the AGC circuit will bring the black level to the same value with reference to the cathode of T_2 as previously, and the difference between the zero output of T_1, which is the white level, and the black level, will have been changed, thus effecting a change in the overall signal swing or the white level on the plate of T_2 and the kinescope grid. This control may be included on the front panel, although the only important control of this nature is the background control for the kinescope, which, even so, should need adjusting only occasionally. A properly operating AGC will maintain the maximum whites at as near as possible the blooming level for the kinescope under all conditions except those of low modulation.

If the circuit of Figure 12 has been used, the black level control shown in Figure 13 is also able to correct for variation in the glow tubes, and is a satisfactory adjustment for tolerance in these tubes.

A Circuit for Maximum Speed

In cases where it is desired to increase the speed of operation of the inverted keyed AGC, a pulse must be used which occurs during the synchronizing pulse time. The keying pulse must be narrow and occur only during the synchronizing pulse time, which means that for correct operation, the keying pulse should occur wholly within the double frequency pulses, which are half as wide as the regular horizontal pulses. If the keying pulse should last over into the "back porch" time following the doubles, their height will be increased by the AGC, and difficulty will be experienced in properly separating the vertical pulse. Likewise, if the keying pulse lasts over into "back porch" time following the *regular* horizontal pulses, the AGC will operate as described previously,

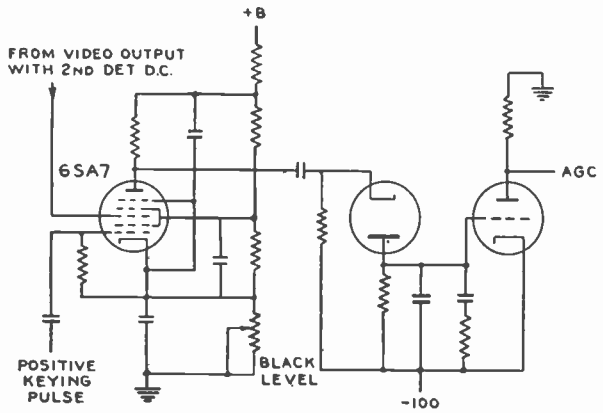

Fig. 14 — Circuit for high impedance or variable amplitude pulse.

and if too fast, will remove the vertical pulse. When a suitably narrow pulse is used, and it is made to occur on the sync pulse, extremely fast operation can be obtained without any errors being introduced.

A satisfactory keying pulse may be obtained from the blocking oscillator. However, difficulty will be encountered in properly applying such a pulse in the circuit of Figure 13. Figure 14 shows a circuit which is quite satisfactory. A 6SA7 has been substituted for the triode T_3 of Figure 13. The video is applied to the second control grid, and the keying pulse to the first grid. Black level control is effected by varying the dc potential of the cathode. The circuit otherwise operates essentially the same as the triode circuit of Figure 13, and is to be preferred over that circuit except for reasons of economy.

Use of Keying Pulse Which May Vary in Amplitude

In receivers which obtain the second anode voltage from the kick-back pulse in the horizontal output stage, the pulse varies in ampli-

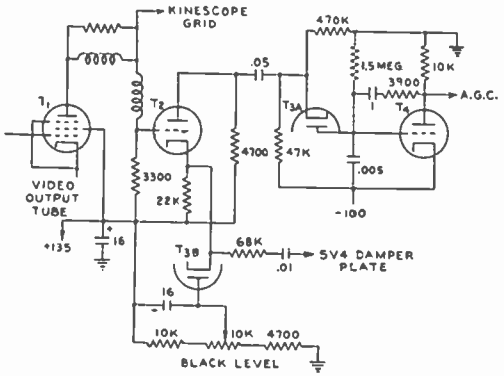

Fig. 15—Additional circuit for variable amplitude pulse.

tude with changes in kinescope current. The use of such a pulse for the AGC keying pulse results in an apparent loss of the dc component in the kinescope, and a limiting level which varies with the picture dc component, unless steps are taken to reference the pulse at its peak. This is accomplished satisfactorily by the circuit of Figure 14 which automatically references the pulse by means of grid current in the 6SA7. Another circuit for accomplishing this is shown in Figure 15. Actual values are given here for installing the AGC in a receiver of the 630TS type. It is necessary to dc connect the video amplifier, T_1 being the output stage. The video which appears across the 3300-ohm plate load is fed directly coupled to the grid of the AGC tube T_2. The cathode of this tube is driven negative by the pulse from the 5V4 damper tube plate. The pulse is reduced in amplitude by the 68K, 22K divider, and its peak referenced by the diode T_{3B} at a voltage determined by the setting of the 10K black level control. The resistance divider also serves as a series impedance between the pulse source and the diode T_{3B}, so that the loading of the diode widens the pulse to the desired width.

The modulated pulse from T_2, which appears across the 4700-ohm resistor, is applied through an .05 capacitor to T_{3A} with the bias resistor arranged as a divider which essentially applies a positive bias to the T_{3A} cathode. The pulse then need not become very small (with T_2 working near cut-off), when a small amount of rectified dc is required from the diode. The discharge resistor for the diode plate is returned to ground, which is positive, in order to make the discharge, or AGC speed, constant regardless of the signal level. The damping can be improved by connecting it as degenerative from the plate to the grid of T_4, as shown.

TELEVISION DEFLECTION CIRCUITS*†

Part I
MOLDED IRON DUST CORES FOR USE IN HORIZONTAL DEFLECTION CIRCUITS

By

A. W. Friend

Home Instrument Department, RCA Victor Division,
Camden, N. J.

Summary

The horizontal deflection of electron beams in television systems has required excessive dissipation of energy and expensive circuit components. For deflection by magnetic means, the deflection transformer and yoke have presented serious problems in the economical design of television receivers.

Transformer and yoke cores have been molded from powdered iron materials especially prepared for these applications. Very low cost materials have been developed to produce useful effective alternating-current permeabilities between 40 and 230. The precise value depends upon the peak amplitude of the alternating-current flux density.

Small particle thicknesses available, at low cost, in powdered iron materials make high-Q systems possible. Increased efficiency eliminates the necessity for dissipating large amounts of energy from the transformer and deflecting yoke structures. Molded core structures, in comparison with laminated core structures, produce negligible acoustic radiation.

Low-loss systems have been constructed with energy recovery arrangements. Such systems, requiring no additional electrical energy, provide large increases in deflection capability. Simultaneously, there are reductions in costs of transformer cores to less than one fourth those of equivalent laminated sheet or strip metal types.

A low-cost system has been constructed to provide full deflection and 27 kilovolts second anode potential for a fifty-degree kinescope driven by two type 807 or 6BG6G beam-tetrodes. The present pulse voltage ratings of available tubes limit the second anode voltage to approximately 17 kilovolts for a kinescope which is to be scanned from a circuit driven by a single 6BG6G tube. This second anode voltage may be derived from windings on the same deflection transformer via a voltage doubling rectifier.

(17 pages, 21 figures)

PART II
THEORY AND DESIGN OF COMBINED LOW-LOSS HORIZONTAL DEFLECTING AND HIGH VOLTAGE POWER SUPPLY SYSTEMS

Summary

When the special, low-cost, low-loss, molded iron powder cores described in Part I of this paper are used in the construction of television horizontal deflecting transformers and yokes, the energy losses are reduced sufficiently

* Decimal Classification: R583.13.
† *RCA Review*, March, 1947.

to permit the employment of certain simplified equivalent circuits and equations in the design procedure. The theory of low-loss horizontal scanning systems has progressed so that now the resultant transformer designs may be relied upon to produce the expected results, within approximately the tolerance limits which apply in the design of most of the other component parts. Design equations and charts are provided for application in the development of horizontal deflecting and high-voltage second-anode power supply systems.

(23 pages, 7 figures)

RADIO-FREQUENCY PERFORMANCE OF SOME RECEIVING TUBES IN TELEVISION CIRCUITS*†

By

ROBERT M. COHEN

Tube Department, RCA Victor Division,
Harrison, N. J.

Summary

Several types of receiving tubes may be used to advantage in television receivers designed to tune all thirteen channels. This paper discusses the performance of these tube types in radio-frequency amplifier, mixer, and local oscillator applications. Both push-pull "balanced" circuits and single-ended "unbalanced" circuits are discussed. Data are presented for over-all gain, noise, image rejection, and, to a lesser extent, on oscillator frequency stability. These data are taken at two representative channels in the television band: Channel No. 4 (66 to 72 megacycles) and Channel No. 11 (198 to 204 megacycles).

(13 pages, 4 figures, 5 tables)

* Decimal Classification: R262 × R593.6.
† *RCA Review*, March, 1948.

TELEVISION DC COMPONENT*†

By

K. R. WENDT

Research Department, RCA Laboratories Division,
Princeton, N. J.

Summary

Although important, and one of the oldest of the television techniques, the dc component is still one of the least understood. It is here explained in general, and with reference to transmitter and receiver applications. The various restorer circuits are described, with their advantages and disadvantages. Design considerations are given for equipment which handles the signal with the dc component present.

(27 pages, 20 figures)

* Decimal Classification: R583.1.
† *RCA Review*, March, 1948.

PROJECTION SCREENS FOR HOME TELEVISION RECEIVERS*†

BY

R. R. LAW[1] AND I. G. MALOFF[2]

Summary

One of the major problems of television development has been that of obtaining adequate brightness in the reproduced picture, particularly in the case of the projection receiver where large pictures are desired. Directional projection screens which concentrate the available light into the desired viewing field are an important aid in overcoming this difficulty. Although various directional screens have been proposed, the primary question always has been: How could a high quality screen be made at a cost that would permit its use in home projection receivers? This paper presents a study of the factors governing the design of projection screens for home television receivers and describes an improved laminated-plastic screen which provides a brightness gain of 7.5 without perceptible "hot-spot." If the viewing field is defined as that zone in which the brightness exceeds half the maximum value, it provides a vertical field of ±10 degrees and a horizontal field of ±25 degrees. In combination with large aperture, reflective optics it gives at 15- by 20-inch picture having highlights with a brightness of more than 75 footlamberts. This compares favorably with the highlight brightness obtained with direct-viewing kinescopes and more than satisfies the recommendations for good motion picture theater practice.

(6 pages; 9 figures)

* Decimal Classification: R583.5.

† *Jour. Opt. Soc. Amer.*, June, 1948.

[1] RCA Laboratories Division, Princeton, N. J.

[2] RCA Victor Division, Camden, N. J.

DESIGN FACTORS FOR INTERCARRIER TELEVISION SOUND*†

BY

S. W. SEELEY

Radio Corporation of America,
New York, N. Y.

Summary

Large scale production of television receivers employing intercarrier sound has focussed attention on the advantages and disadvantages of the system. This review emphasizes problems facing transmitter and receiver designers.

(4 pages; 5 figures)

* Decimal Classification: R583.5.

† *Electronics*, July, 1948.

TELEVISION RECEIVERS*†

BY

ANTONY WRIGHT

Home Instrument Department, RCA Victor Division,
Camden, N. J.

Summary

The promise of a postwar public television service can be realized only by quantity production and merchandising of receiving instruments. The styling and performance of television receivers has been a subject for conjecture for many years. Artists conceptions of the possible appearance of the home television receiver have appeared in material ranging from the cartoon to the constructive magazine article. In parallel, engineering opinion has been expressed in technical journals and incorporated in the many experimental receivers which have been built and which have included new circuits and other arrangements in an attempt to evaluate commercial acceptance. The receivers discussed in this paper represent up-to-date developments in both electrical and appearance engineering. No doubt the current thinking as expressed in these designs will be modified by public acceptance, competition and by the engineering experience gained in their design and manufacture. These receivers are important because they will serve, along with others, as a basis for the future expansion of television service. Several models are described, followed by a statement of design policy and a detailed discussion of various components.

(24 pages, 27 figures)

* Decimal Classification: R583.5.

† *RCA Review*, March, 1947.

TELEVISION ANTENNA INSTALLATION GIVING MULTIPLE RECEIVER OUTLETS*†

BY

R. J. EHRET

RCA Service Company,
Camden, N. J.

Summary

With the increasing realization of commercial television broadcasting, consideration is being given to the installation of television in hotels. This article deals with some of the general considerations and problems involved in engineering and making a hotel installation, and their application to the specific installation at the Hotel Pennsylvania.

(6 pages; 3 figures)

* Decimal Classification: R326.6.

† *Tele-Tech*, June, 1947.

APPLICATION OF I.C.I. COLOR SYSTEM TO DEVELOPMENT OF ALL-SULFIDE WHITE TELEVISION SCREEN*†

BY

AUSTIN E. HARDY

Tube Department, RCA Victor Division,
Lancaster, Pa.

Summary

Increased emphasis on the whiteness of the postwar television tube screen has demanded the use of an objective color-specification system in the development of new phosphors and in the control of the finished tube.

The I.C.I. color system adopted by the International Commission on Illumination in 1931 has been applied to this problem. In addition to providing accurate control of color, it has made possible the determination of desirable and undesirable color areas and has facilitated the obtaining of the greatest luminosity for any desired white.

Measurements of the relative efficiencies and spectral energy distribution of individual phosphors and phosphor mixtures have been made in a demountable cathode-ray tube with an automatic recording spectroradiometer. Particular emphasis has been placed on the factors that are peculiar to zinc-sulfide and zinc-cadmium-sulfide phosphors.

(10 pages, 8 figures)

* Decimal Classification: R138.313 × R200.

† *RCA Review*, September, 1947.

PULSED RECTIFIERS FOR TELEVISION RECEIVERS*†

BY

I. G. MALOFF

RCA Victor Division,
Camden, N. J.

Summary

Brief analysis of pulsed cascade rectifiers used in television receivers indicates that no component is subjected to potentials substantially higher than those encountered per section. In a doubler, this voltage is about half the output voltage from the rectifier.

(2 pages; 3 figures)

* Decimal Classification: R366.3XR583.

† *Electronics*, July, 1947.

COMPARATIVE PROPAGATION MEASUREMENTS; TELEVISION TRANSMITTERS AT 67.25, 288, 510 AND 910 MEGACYCLES*†

By

GEORGE H. BROWN, JESS EPSTEIN AND DONALD W. PETERSON

Research Department, RCA Laboratories Division,
Princeton, N. J.

Summary—In order to study propagation and multipath effects over a wide range of frequencies under typical broadcast conditions, comparative propagation measurements have been made using television transmitters at 67.25, 288, 510 and 910 megacycles. These measurements were taken along two radials from New York City. One radial extended slightly north of west over extremely hilly country with a number of suburban towns, large homes, many trees and elevations ranging from sea level to 1200 feet. The second line ran southwest over fairly level terrain with very few hills, the highest of which was 230 feet. Regular television broadcasts were used on 67.25 megacycles. A special laboratory transmitter and Turnstile antenna were used for measurements on 288 megacycles. Experimental low-power laboratory transmitters were used with directional antenna arrays for making the measurements on 510 and 910 megacycles.

The influence of hilly terrain on propagation is clearly illustrated by comparison of the data along the two radials. The best agreement with theoretical values at all frequencies was obtained along the comparatively smooth southwest line. There was closer agreement with the theoretical curves at 67.25 megacycles than at 288 megacycles, while the measured values at 510 and 910 megacycles were usually far below the theoretical. The data has been analyzed to assist in forming an overall picture of the situation.

Shadowing from hills and other obstructions increases steadily as the frequency increases, thus requiring higher power at the higher frequencies. A basis for estimating power requirements as a function of frequency is offered.

Multipath effects are present at both 67.25 megacycles and 288 megacycles, but are usually too slight to be serious. In obstructed or hilly areas, multipath at 510 and 910 megacycles is severe. However, in most places, a clean picture can be obtained by orienting the receiving antenna. It was generally possible to find several responses which gave a good picture. This was true when the receiving antenna was a large array having a narrow beam and a large front-to-back ratio or a single dipole and reflector with a low front-to-back ratio and a broad pattern.

INTRODUCTION

IN THE PAST, surveys have been made of the coverage of individual transmitters operating in the high frequency region. With the advent of black-and-white television on frequencies lying between

* Decimal Classification: R583.16.
† Reprinted from *RCA Review*, June, 1948.

50 and 216 megacycles and with growing interest in the possibilities of color television in the region between 500 and 900 megacycles, the need for comparative measurements over a wide range of frequencies became apparent. Accordingly, plans were made early in 1946 to carry out a series of experiments using the Empire State Building in New York City as the location for the transmitters. Field measurements and observations were planned to show attenuation as a function of distance over rough terrain and comparatively smooth terrain and to show the

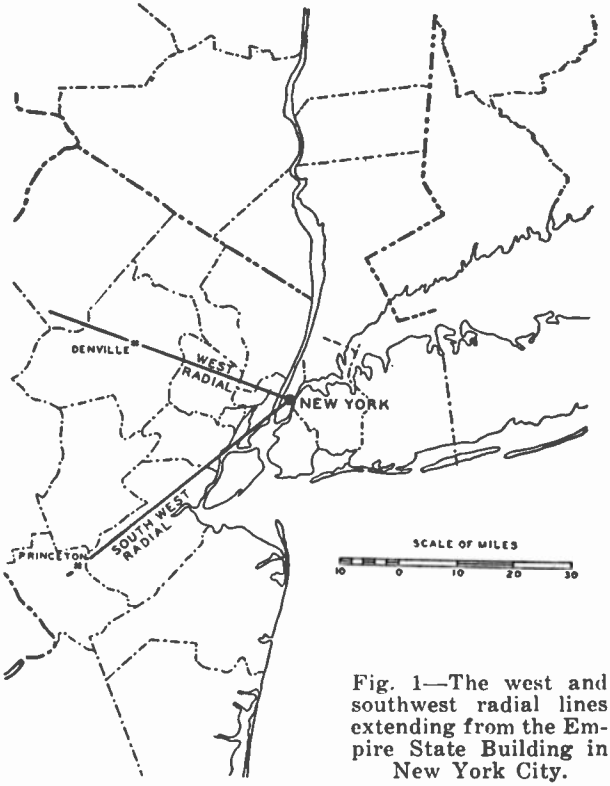

Fig. 1—The west and southwest radial lines extending from the Empire State Building in New York City.

magnitude and differences of multipath effects at the various frequencies.

Since it was evident that it would not be possible to make extensive measurements over the entire service area, two radial lines were selected which could be conveniently reached by the field truck and which presented a variety of terrain. One radial extended slightly north of west from the Empire State Building and will be referred to as the "west radial." This line extended over extremely hilly country, with many suburban towns generously supplied with large homes and multi-

tudes of trees. Elevations ranged from sea level to 1200 feet. The second line was southwest with very few hills, the highest of which was 230 feet.

The locations of these radial lines are shown in Figure 1, while Figure 2 gives the profiles along the radials.

Description of the Transmitting Facilities and the Field Measuring Equipment

Early in 1946, the WNBT transmitter began operating to furnish television broadcasting service with a picture carrier frequency of

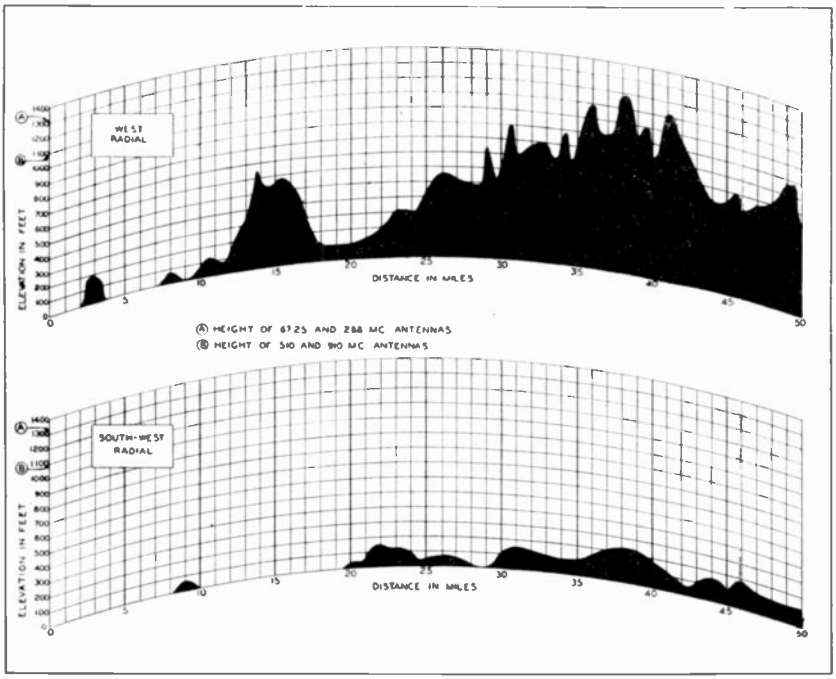

Fig. 2—The profiles along the west and southwest radials.

67.25 megacycles. The transmitter was available with test pattern during most of the daylight hours. This transmitter was located on the eighty-fifth floor of the Empire State Building. Another transmitter, especially constructed at the Laboratories for these propagation tests and operating at a frequency of 288 megacycles, became available and was moved to the eighty-fifth floor of the Empire State Building.

Separate Turnstile antennas for each transmitter were mounted on a single pole on the top of the building. Here, for the first time, an

excellent opportunity was afforded for making comparative tests of propagation at widely-separated frequencies with comparable radiated power and with the transmitting antennas at the same location and height.

The entire antenna system was erected at the Laboratories for purposes of measurement and test before erection on the Empire State Building. Figure 3 shows this antenna system. Closest to the roof may be seen the four-layer Turnstile antenna used to transmit the picture signal with a carrier frequency of 67.25 megacycles and the sound signal at 71.75 megacycles. Directly above this Turnstile antenna is a two-layer loop antenna system for transmission of a

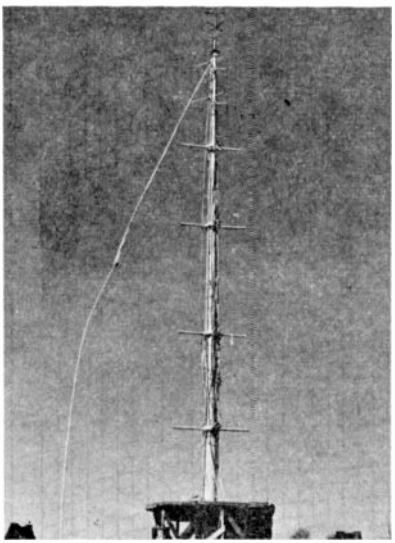

Fig. 3—The multiple antenna system erected at the Laboratories.

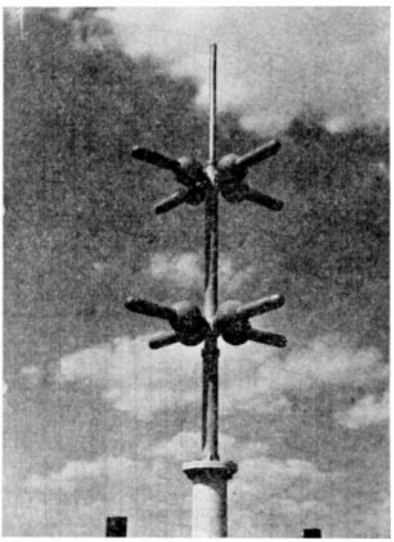

Fig. 4—The 288-megacycle Turnstile antenna.

frequency-modulated signal at 97.3 megacycles. This transmission constituted a broadcasting service which was not utilized in this survey. The 288-megacycle Turnstile antenna is located at the top, above the FM antenna, and may be seen in greater detail in Figure 4.

Power gain measurements were made for both Turnstile antennas when located as shown in Figure 3. In addition, the horizontal radiation patterns of both antennas were obtained by rotating the pole about its vertical axis while reading a field intensity meter located a few thousand feet distant. The vertical pattern of the 288-megacycle Turnstile was obtained by mounting this antenna in a horizontal position on a turntable. The 67.25-megacycle antenna was much too

large to handle in this fashion. However, the vertical pattern was obtained during the development stage by using the ground-plane setup shown in Figure 5. Here the vertical pattern of the final antenna was obtained by measuring the horizontal pattern of the arrangement shown.

During the course of the field measurements at the two frequencies mentioned, the effective radiated power of the 67.25-megacycle transmission was maintained at 3.63 kilowatts, while the effective radiated power at 288 megacycles was 2.6 kilowatts.

The field measuring equipment used a modified TRK-9 receiver. A single stage preamplifier preceded the receiver for 67.25-megacycle

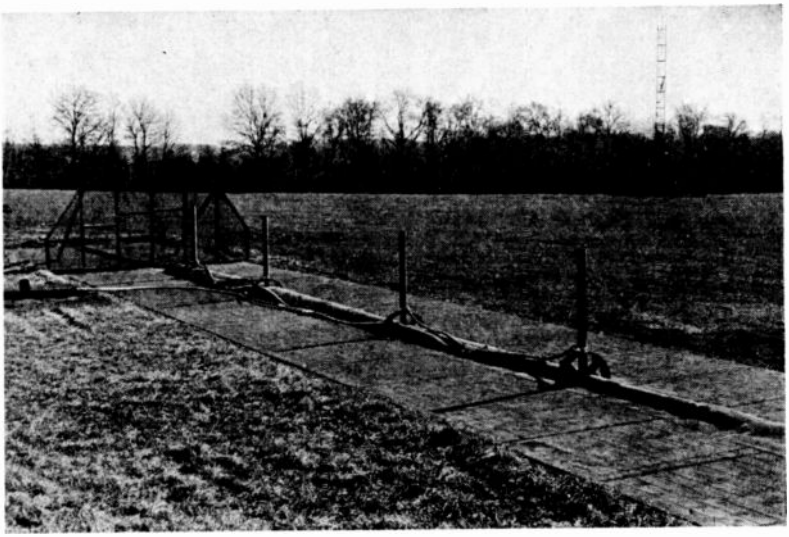

Fig. 5—Ground-plane for the 67.25-megacycle Turnstile.

reception. A 288-to-67.25 megacycle converter was used ahead of the preamplifier for 288-megacycle reception. The TRK-9 automatic-gain-control voltage was measured for field intensity information. All measurements were made with the same test pattern impressed on the transmitters at all times so that a known relation existed between the observed voltage and the value of peak signals. Voltage calibration of the receiver was obtained from a Model 80 Signal Generator.* The apparatus was installed in a panel truck with a portable power supply. A mast mounted on the truck roof was raised to place the two receiving dipole antennas 30 feet above the earth. Both receiving antennas were rotatable.

Measurements were made at approximately two-mile intervals along

* Manufactured by Measurements, Inc.

the two radials shown in Figure 1. Receiving sites were chosen in a variety of surroundings: in open fields, in wooded areas, along highways, atop hills, and in valleys. An effort was made to stay away from electric lines and large buildings. Whenever possible, the antenna was moved a wavelength or more toward the Empire State Building while observing test pattern and gain-control voltage. All data were taken between 10 a.m. and 4 p.m. in clear weather so that even at distances of forty miles or more the measurements may be expected to yield normal values.

The observations at 67.25 and 288 megacycles were carried out between late July and the end of October, 1946. At this time, an

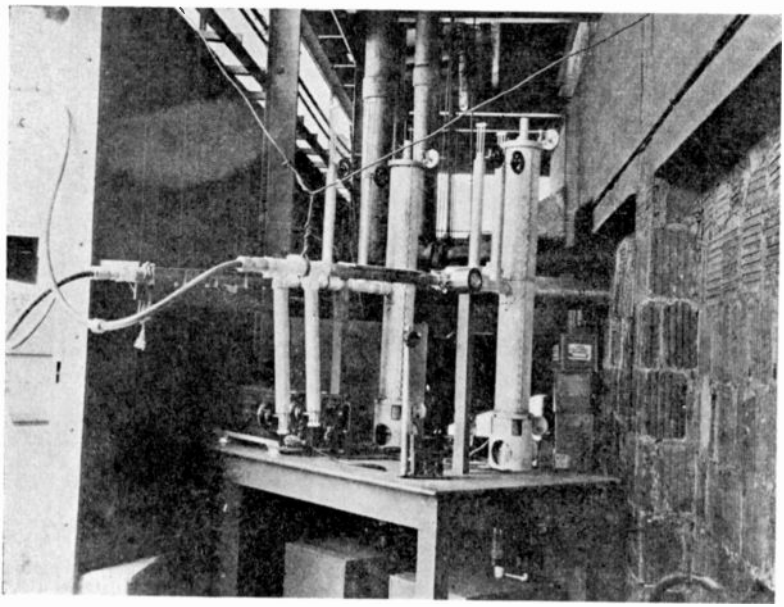

Fig. 6—The self-excited oscillators used in the 510- and 910-megacycle tests.

experimental tube capable of delivering a few hundred watts at frequencies as high as 900 megacycles became available. The measurements just completed indicated that a few hundred watts radiated in a broadcast fashion at 500 and 900 megacycles would yield field intensities too weak to measure easily and certainly too weak to observe multipath effects. Hence directional arrays were constructed and so mounted that the beams could be pointed along either radial. A beam antenna and a self-excited oscillator were provided for operation on a frequency of 510 megacycles, and a similar set of equipment was constructed for operation on 910 megacycles. There was not room to mount the equipment on the roof of the Empire State Building so the

oscillators were placed in a room on the eighty-seventh floor, with the antennas on a balcony at the same level. The antenna elevation was then 1061 feet above ground and 1109 feet above sea level.

The two oscillators are shown in Figure 6. The two directional antenna systems may be seen in Figure 7. Each array consisted of two cophased frames stacked one above the other. The radiation pattern of each system was then 35 degrees wide at the one-half voltage points in the horizontal plane, while the corresponding width in the

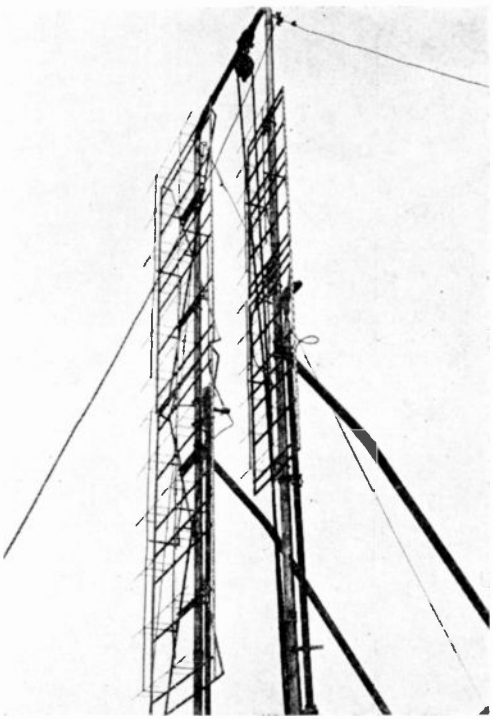

Fig. 7—The directional arrays used in the 510- and 910-megacycle tests.

vertical plane was 8.5 degrees. Another view of the antennas, looking down from above, is given in Figure 8 (page 184).

A modified AN/APR-4 receiver was used for the field intensity measurements. Two specially-constructed signal generators were used for calibration purposes. The receiving antenna for 510 megacycles was a single dipole in front of a flat metal reflector. For 910 megacycles, a similar antenna was provided. In addition a directional antenna was used which consisted of a single frame identical in construction to the two frames used for transmission. The three antennas mounted on the field truck are shown in Figure 9 (page 184).

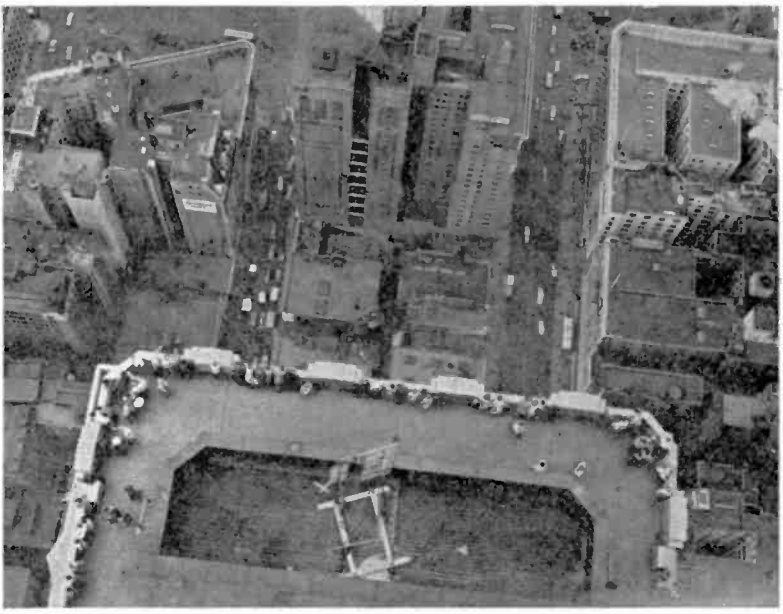

Fig. 8—The 510- and 910-megacycle antennas on the eighty-seventh floor balcony.

Fig. 9—The field truck with the 510- and 910-megacycle receiving antennas in place.

The two transmitters were operated simultaneously so that a measurement could be made at each frequency by a single visit to a measuring point. Measurements were made on each radial at exactly the same locations used in the previous survey at 67.25 and 288 megacycles. Measurements were also made at many additional locations.

These field intensity measurements were made during the summer of 1947. When the measurements were completed, the oscillators were modulated with a test pattern. A television receiver, Model 630TS, with an appropriate converter, was then used in the field truck to observe the effects of multipath propagation and the measuring points were again visited. For these latter observations, a frame similar to the directional array shown in Figure 9 was also used at 510 megacycles.

Measured Field Intensity Data

The principal factors involved in establishing the field intensity at high frequencies are the effective radiated power, the distance between the transmitting and receiving antennas, the heights of the transmitting and receiving antennas, the earth's curvature, the conductivity and dielectric constant of the earth, refraction resulting from changing dielectric constant of the air with height, and irregularities of the terrain. The last-named factor is not accounted for in theoretical treatments. If the earth is assumed to be a smooth sphere having uniform electrical properties and if the dielectric constant of the air is assumed to be a linear function of height, the field intensity calculation may be carried out by the methods described by K. A. Norton[1]. In order to review the effects of frequency where the ideal or theoretical conditions exist, Figure 10 was prepared. In these calculations, the following factors were used:

Height of transmitting antenna = 1250 feet
Height of receiving antenna = 30 feet
Conductivity of the earth = 50×10^{-15} electromagnetic units
Dielectric constant of the earth = 15
Effective radiated power = 100 kilowatts.

An inspection of Figure 10 reveals the increase in field intensity that accompanies an increase in frequency when the distance is less than

[1] A Report Prepared by K. A. Norton on the Calculation of Ground Wave Field Intensity over a Finitely Conducting Spherical Earth, and presented at the Hearing before the FCC in the Matter of Aural Broadcasting on Frequencies above 25,000 Kilocycles, March 18, 1940.

60 miles. At distances greater than 70 miles, the fields for the high frequencies fall far below those for the low frequencies. A line showing twice the free space field is also included on this figure. This line shows the limiting value above which the field intensity never rises, even when the direct wave and the ground reflected wave are in phase.

Figure 11 shows the measured field intensity of the 67.25-megacycle signal along the west and southwest radials as a function of distance. The calculated field intensity is shown in each case by the solid curve. The measurements along the southwest radial show close correlation

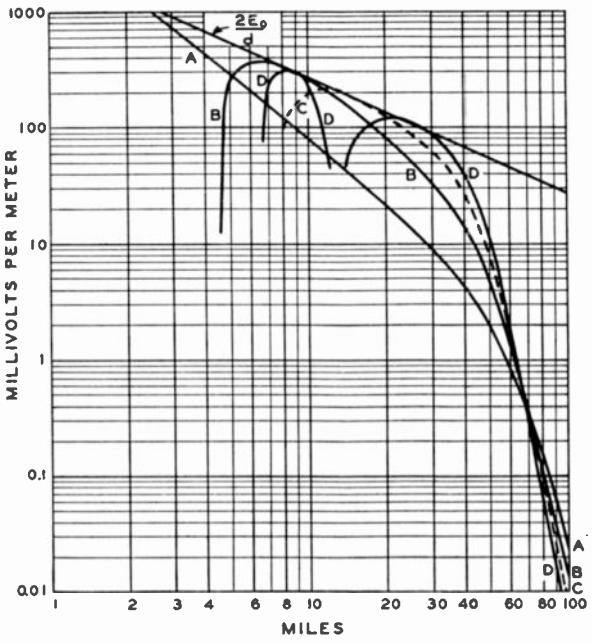

Fig. 10—Theoretical field intensities over a smooth spherical earth.
A. 67.25 megacycles. C. 510 megacycles.
B. 288 megacycles. D. 910 megacycles.

with theory. The comparatively smooth terrain is responsible. Data taken along the west radial shows much more scattering. An idea of the difference in terrain may be obtained by inspecting Figure 2.

The measured data taken at 288 megacycles along the same radials is displayed in Figure 12. The theoretical curve is again shown here. The scattering is pronounced. Several points on the charts are connected by vertical lines. This is to indicate that the two values thus

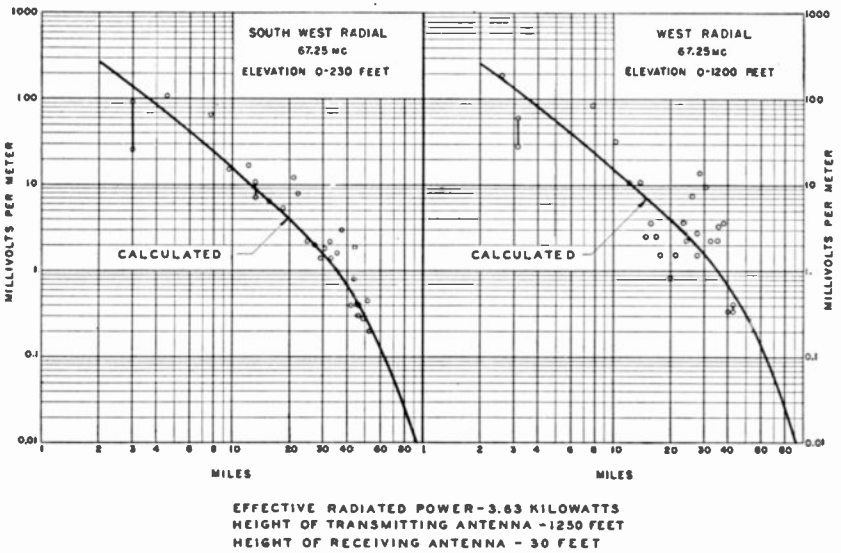

Fig. 11—Measured field intensity at 67.25 megacycles.

linked represent the maximum and minimum signals encountered in the vicinity of the measuring point. The asterisks on the figure indicate the location of points where the field intensity was below 0.1 millivolt per meter and was not measurable because of the noise level of the receiver.

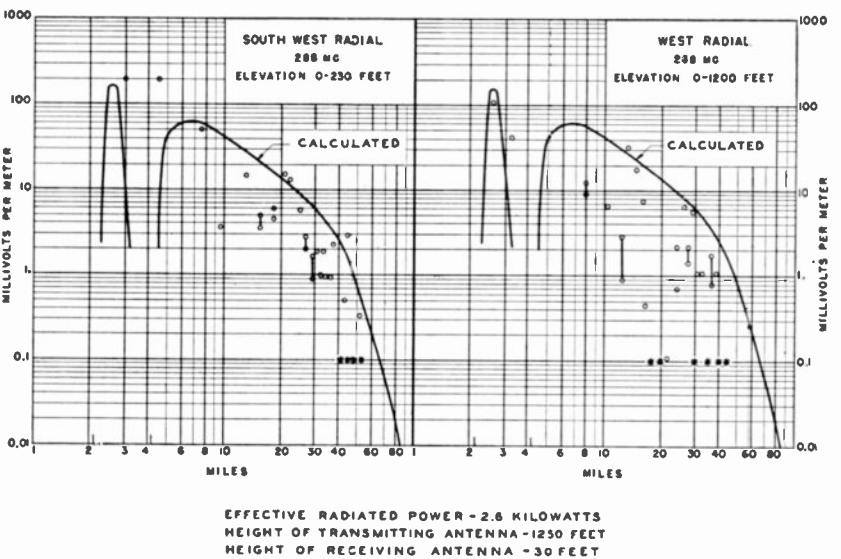

Fig. 12—Measured field intensity at 288 megacycles.

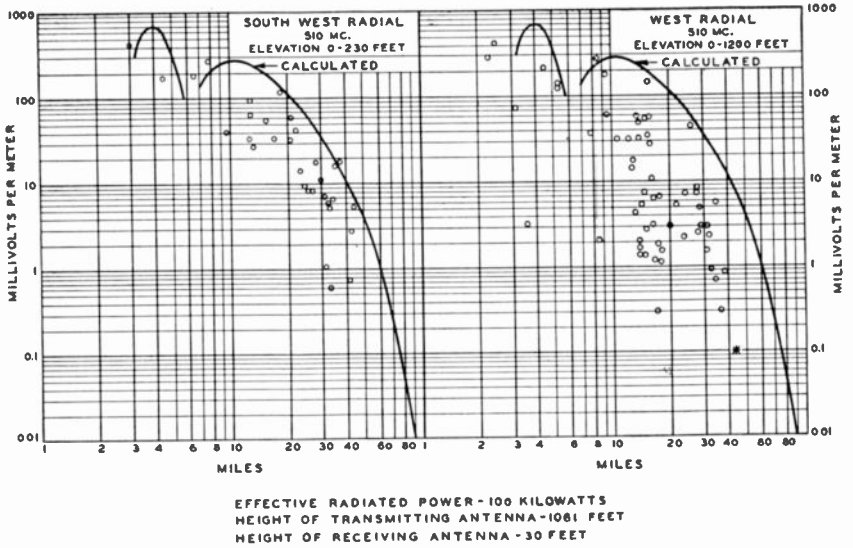

Fig. 13—Measured field intensity at 510 megacycles.

The measured field intensity along the southwest and the west radial at a frequency of 510 megacycles is shown in Figure 13. Before plotting in this figure, the measured values were corrected to an effective radiated power of 100 kilowatts. It should be noted that in this figure, the theoretical graph is based on a transmitting antenna height of

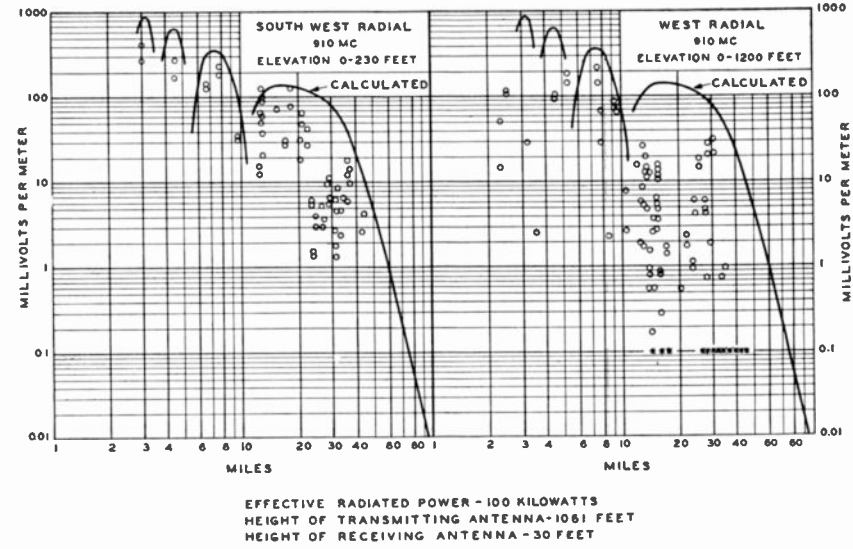

Fig. 14—Measured field intensity at 910 megacycles.

1061 feet, since for this transmission the antenna was on the eighty-seventh floor balcony. The effect of the roughness of the terrain on the west radial is becoming apparent at this frequency.

Figure 14 shows the measured values obtained at a frequency of 910 megacycles, again with the measured values corrected to an effective radiated power of 100 kilowatts. The calculated curve is based on a transmitting antenna height of 1061 feet. On the west radial, many locations are indicated where the field intensity was too low to be measured.

When measuring at 510 megacycles, the receiving antenna was a single dipole placed in front of a flat metal sheet. At many measuring points, when the receiving antenna was rotated the receiver voltage varied in such a way that it was evident that multipath signals were present. The same effect was noted to be more pronounced at 910 megacycles. At this higher frequency, measurements were made with a dipole in front of a plane reflector and with an array. The receiving array was 26 inches wide and 56 inches high. This array may be seen

Table I—Percentage Distribution of the Ratio V_A/V_D in Terms of Locations (Frequency = 910 Megacycles)

The ratio V_A/V_D lies between:	Percentage of locations where the ratio lies between the indicated limits.		
	Southwest radial	West radial	Both radials
0-1	0	18.	10.1
1-1.5	0	0	0
1.5-2	0	0	0
2-2.5	0	7.7	4.4
2.5-3	3.33	15.5	10.1
3-3.5	20.	12.9	15.9
3.5-4	10.	20.5	15.9
4-4.5	23.3	12.9	17.4
4.5-5	16.6	2.5	8.7
5-5.5	16.6	5.	10.1
5.5-6	3.33	0	1.5
6-6.5	0	0	0
6.5-7	6.66	0	2.9
7-7.5	0	2.5	1.5
7.5-8	0	0	0
8-8.5	0	2.5	1.5

Average V_A/V_D

On west radial — 3.3

On southwest radial— 4.38

On both radials — 3.75

in Figure 9. In many shadowed locations, it was possible to rotate the array and observe strong signals from many directions. This was accepted as evidence of strong multipath signals.

An additional disturbing effect was found at 910 megacycles. A coaxial switch was used to switch the receiver rapidly from the dipole to the array. In open locations, particularly on the southwest radial, the voltage on the receiver terminals was substantially greater when the array was used. However, in shadowed regions on the west radial, it was often found that the receiver voltage was lower with the array than the dipole. This was probably due to the fact that the field was badly

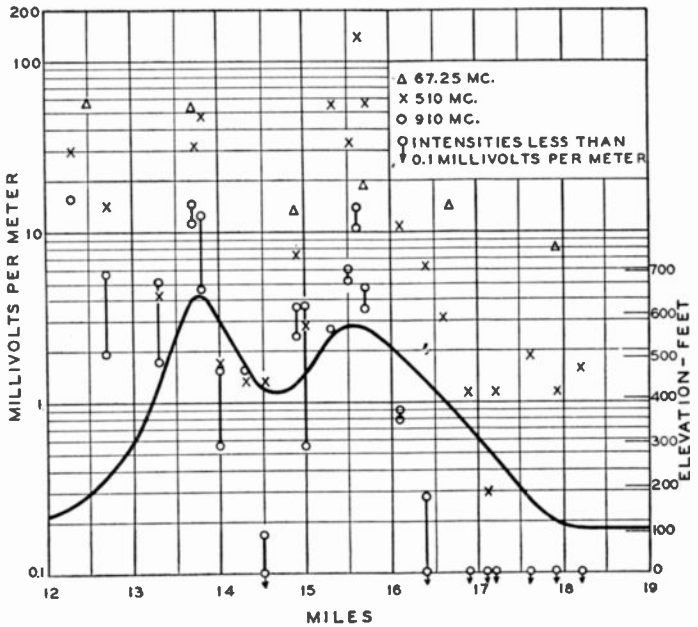

Fig. 15—The effect of a ridge of hills demonstrated at three widely-separated frequencies. (The measured field intensities have all been corrected to an effective radiated power of 100 kilowatts. The connected circles for the 910-megacycle signal indicate the two values of field intensity obtained at each location, one with the dipole antenna, the other with the array.)

distorted with large phase changes across the aperture of the array. Unfortunately, this effect was found only in the shadowed regions where the signal was weak and a boost in signal such as one might expect with an array was badly needed. Table I shows the number of places, expressed percentagewise, where the ratio V_A/V_D lies between the indicated limits. (V_A is the voltage on the receiver terminals when the array is used, while V_D is the corresponding voltage when the dipole is connected.) It is interesting to note that on the southwest

radial, no values less than 2.5 were obtained for V_A/V_D, while on the west radial 18 per cent of the observations show the ratio to be less than unity.

The manner in which the shadows due to large hills change with frequency is shown in Figure 15. Here the measured field intensities for 67.25, 510 and 910 megacycles have all been corrected to an effective radiated power of 100 kilowatts. The 67.25-megacycle signal is lowered somewhat by the ridge of hills, while the 510-megacycle signal fluctuates at a great rate. The shadows cast by the two peaks are quite apparent. However, even this large fluctuation does not compare with the effect at 910 megacycles. Behind the second peak, a region over three miles in extent was found where it was not possible to measure the weak signal of the 910-megacycle transmitter.

Analysis of the Field Intensity Data

While an inspection of Figures 11 to 14 inclusive shows the general trend of attenuation as the frequency is increased, it seems appropriate to attempt a more quantitative analysis of the data. With this in mind, Figures 16 and 17 were prepared. Figure 16 was constructed directly from the measured values and the theoretical curves shown in Figures 11 to 14. Thus, in Figure 16, a curve for a given frequency relates the measured field intensities at that frequency to the theoretical curve for the same frequency. However, a glance at Figure 10 reveals that the theoretical values for widely-divergent frequencies are not related by a simple law. To compare the results measured at four frequencies, it is necessary to establish a base. This has been done in preparing Figure 17. First, the curve for 67.25 megacycles on Figure 16 was transferred directly to Figure 17. Then on a copy of Figure 12 which shows the measured field intensities for 288 megacycles, a theoretical curve was plotted for the field intensity at 67.25 megacycles, using transmitting and receiving antenna heights of 1250 feet and 30 feet, respectively. The effective radiated power was assumed to be 2.6 kilowatts, the same value used in the 288-megacycle measurements. Then the measured 288-megacycle field intensities were compared to the theoretical curve for 67.25 megacycles. The result of this operation is shown by the 288-megacycle curve of Figure 17. Next, on Figure 13 was plotted a theoretical field intensity curve for a frequency of 67.25 megacycles, a receiving antenna height of 30 feet, and an effective radiated power of 100 kilowatts. The transmitting antenna height was taken as 1061 feet, to correspond to the height of the antenna used for 510 megacycle transmission. The measured field intensities at 510 megacycles were then compared to this new 67.25 megacycle theoretical

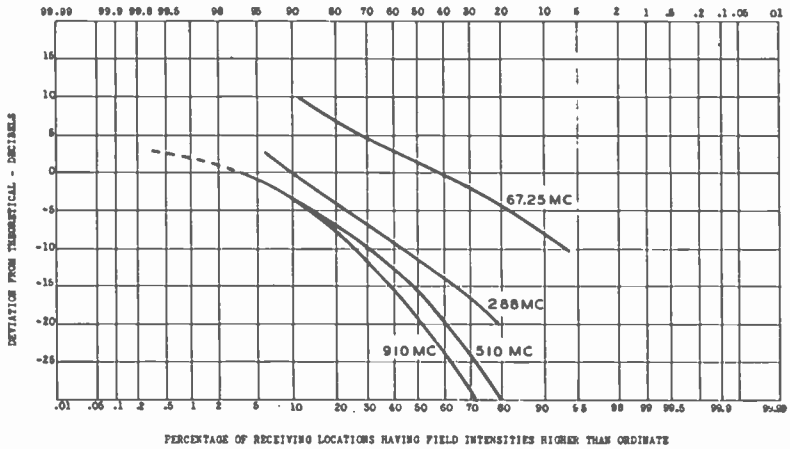

Fig. 16—An analysis of the data shown in Figures 11 to 14. (A curve for a given frequency relates the measured field intensities at that frequency to the theoretical curve for the same frequency.)

curve to form the 510-megacycle curve on Figure 17. The 910-megacycle curve on Figure 17 was constructed in the same manner.

The following interesting tabulation may immediately be made from Figure 17:

Frequency (megacycles)	Percentage of receiving locations having intensities greater than the 67.25-megacycle theoretical values	Percentage of receiving locations having intensities less than the 67.25-megacycle theoretical values
67.25	58.	42.
288.	52.	48.
510.	35.	65.
910.	22.	78.

Figures 16 and 17 have been replotted in a more demonstrative manner in Figures 18 and 19, respectively. A glance at Figure 19 shows that the whole group of distribution curves is reasonably flat from 67.25 megacycles to 288 megacycles. Thus, it may be concluded that for practical reception conditions such as were encountered in this survey, essentially the same field intensity in millivolts per meter may be expected to result for any frequency between 67.25 megacycles and 288 megacycles, for a given transmitting antenna height and transmitter power. As the frequency is increased still further, expectations of a given field intensity are notably decreased.

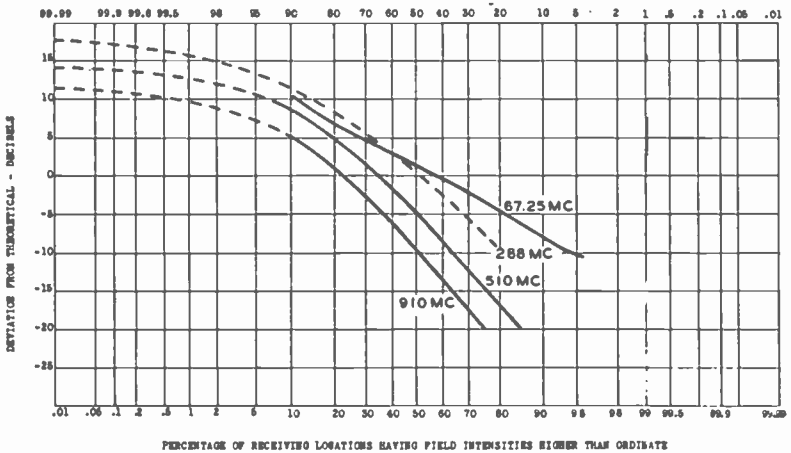

Fig. 17—A second analysis of the data shown in Figures 11 to 14. (The theoretical curve referred to on the ordinate scale is the theoretical curve for 67.25 megacycles. A curve for a given frequency relates the measured field intensities at that frequency to the theoretical curve for 67.25 megacycles at a corresponding antenna height.)

Figure 19 now affords a means of drawing some conclusions concerning the power requirements at the frequencies suggested for color television, namely the region between 500 and 900 megacycles. Assume that a signal is being received on a half-wave dipole and this dipole

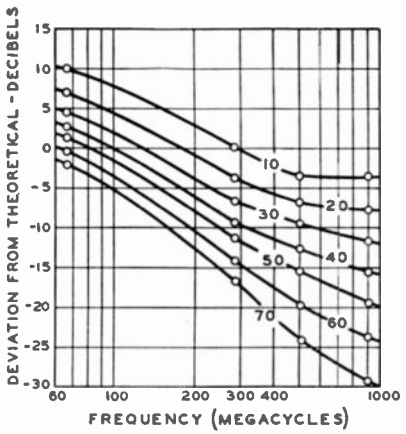

Fig. 18—Figure 16 replotted to demonstrate the phenomena more clearly. (The numbers on the individual curves indicate the percentage of the receiving locations having field intensities higher than the ordinate values shown on the left-hand scale.)

Fig. 19—A replot of Figure 17. (The measured field intensities are compared to the theoretical values at 67.25 megacycles.)

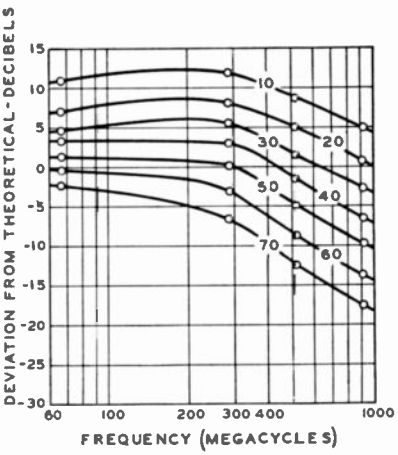

in turn feeds the signal to a transmission line through a suitable matching section. Then if it is also assumed that the receiver input impedance is the same as the characteristic impedance of the transmission line, the voltage on the transmission line (essentially the same as the voltage on the receiver terminals for a low-loss line) is

$$V_{TL} = \frac{\lambda E}{2\pi} \cdot \sqrt{\frac{Z_c}{R_r}}$$

where Z_c = the characteristic impedance of the transmission line,

R_r = the radiation resistance of the half-wave dipole,

λ = the wavelength, in meters,

E = the field intensity in millivolts per meter,

V_{TL} = voltage on the transmission line, in millivolts.

Since it is assumed that the antenna is cut to be one-half wave in length at the frequency in question, the voltage on the transmission line will decrease accordingly as the wavelength is decreased. If the frequency is multiplied by a factor n, the field intensity E must be also multiplied by the same factor to keep the voltage on the transmission line constant. That is, if the frequency is n times 67.25 megacycles, the power used at 67.25 megacycles must be multiplied by a factor n^2 to offset the effect of the shorter antenna at the new and higher frequency. A second multiplying factor is then necessary to account for the difference in propagation characteristics at the two frequencies in question. Suppose that at 510 megacycles, one wishes to insure that in at least 50 per cent of the receiver locations the signal on the transmission line will be at least as great as the signal enjoyed by 50 per cent of the receiver locations when the frequency is 67.25 megacycles. On Figure 19, the curve indicated for 50 per cent is examined and a difference in signal level of 6.5 decibels is found for the two frequencies. The power must be multiplied by a factor of 4.46 to take care of the difference in propagation. For this example, n^2 is 57.3, so the total factor on the power is 255. In other words, to insure that the receiver input voltage at 50 per cent of the receiving locations using a frequency of 510 megacycles will exceed the value exceeded by 50 per cent of the receiver locations using 67.25 megacycles, the power used at 510 megacycles must be 255 times the power used at 67.25 megacycles.

The two upper curves of Figure 20, constructed in the manner just outlined, apply to 70 and 50 per cent of the locations when it is assumed that half-wave dipoles are used.

If instead of half-wave dipoles as receiving antennas directional arrays are used with power gains of n^2, the power multiplying factor consists only of the factor obtained from Figure 19. The two lower curves on Figure 20 result.

It seems appropriate at this point to discuss the matter of power gain as applied to the receiving antenna. In the case of a directional or beam antenna in which the aperture or mouth opening has a given area, one may quickly estimate the maximum possible power gain by

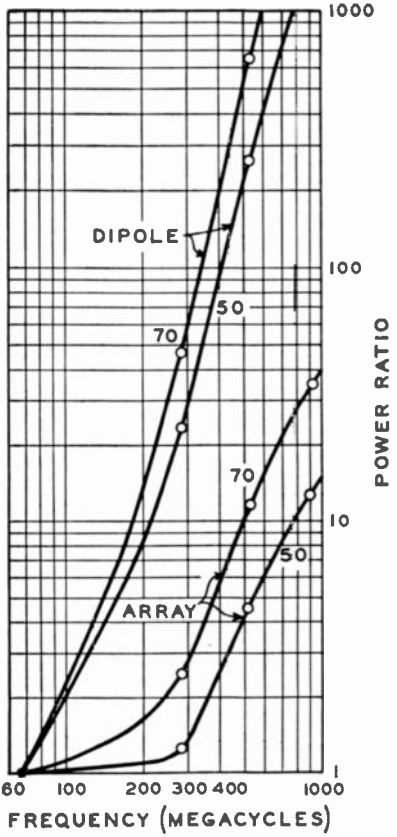

Fig. 20—An estimate of the power requirements for television broadcasting versus frequency. (The ordinate scale is the factor by which the power used at 67.25 megacycles must be multiplied, when moving to a new frequency, in order to obtain the same voltage on the receiver transmission line. The upper two curves assume the use of a half-wave dipole at each frequency, while the lower two curves postulate the use of an array with a power gain sufficient to overcome the loss due to the shortening of a half wave dipole as the frequency is increased. The numbers on each curve refer to the percentage of receiving locations considered.)

expressing the area in terms of the wavelength. Then the power gain is 7.65 times the area measured in square wavelengths. As the frequency increases and the wavelength decreases, the power gain increases proportionally as the square of the frequency, since for a fixed area the number of square wavelengths included in the area increases in the same manner. However, this power gain is expressed in terms of the power received by a half-wave dipole at the particular frequency under consideration. But as the frequency increases the reference half-wave

dipole becomes shorter. The practical result is that to obtain a given voltage on the terminals of the transmission line, where the field intensity remains constant in millivolts per meter as the frequency increases, use must be made of an antenna of constant physical aperture. The effective aperture or capture area of a half-wave dipole at 67.25 megacycles is approximately 28 square feet. Hence to obtain the same voltage on the transmission line at 510 megacycles, one must use the same area for the directive antenna, and at 910 megacycles one must again use an antenna with an aperture which is over 5 feet on a side. This hypothetical antenna with a mouth opening of 28 square feet will have a power gain of 57.5 at 510 megacycles and a power gain of about 180 at 910 megacycles.

The fact demonstrated in Table I, namely that on the extremely hilly radial the directional receiving array failed to improve the signal in 18 per cent of the locations has already been indicated. These were at locations where the signal was weak and the gain was badly needed. Hence the true picture of the needed power ratio versus frequency lies somewhere between the two groups of curves shown in Figure 20.

Multipath Observations

Multipath observations on the 67.25- and 288-megacycle channels were carried out during the summer of 1946 at the same time that the field intensity measurements were made. The observations were all made outside of Manhattan, so that extreme conditions of multipath effects were not observed. Multipath effects were usually different at the two frequencies. Where usable field intensities were obtained on both frequencies, it was generally possible to orient the receiving antennas and receive good pictures on either frequency, with multipath effects entirely absent or of such low magnitude as to be quite unimportant. At two sites approximately 2.5 miles from the transmitter on the west radial, the picture received on 67.25 megacycles with a receiving antenna height of 30 feet showed both positive and negative ghosts. When the receiving antenna was lowered to 6 feet, the picture was materially improved. Only two sites, at about 30 miles on the west radial, were found where the 67.25-megacycle picture obtained with the dipole antenna was not usable due to multipath. At both sites, no 288-megacycle signal could be found.

On the comparatively smooth southwest radial, very little evidence of multipath was noted on either frequency except in a few locations in the vicinity of large fields of oil storage tanks.

In the early fall of 1947, the 510 and 910 megacycle oscillators were modulated with the test pattern. On the southwest radial, the pictures

were clean and free from multipath. When the directional arrays were used, a strong clean picture was obtained when the receiving antenna was pointed in the direction of the Empire State Building. When the antenna was rotated to point in other directions, weak reflected signals were sometimes noted but these reflected signals were usually too weak to use. In the vicinity of the oil storage tanks mentioned above, the reflected signals compared in intensity to the main signal but there was no real difficulty in obtaining a clean picture on either frequency, using either an array or a dipole in front of a screen.

On the west radial, particularly in the shadowed areas but also in many open spaces flanked by hills or buildings, signals arriving by many paths were numerous. As the directional arrays were rotated, it was generally possible to find several positions where strong signals were received. Surprisingly, many of these reflected signals were as strong as the main signal and produced as clean a picture. The difference between multipath effects at 510 megacycles and 910 megacycles is simply that the multipath signals are more profuse at the higher frequency, and, of course, in shadowed areas it was harder to receive a signal strong enough to give a satisfactory picture at the higher frequency. At many points where an acceptable picture was obtained at 510 megacycles, the signal was too weak to give a good picture at 910 megacycles.

While multipath propagation is very much in evidence at both frequencies, it appears to be a simple matter in most instances to orient the receiving antenna to obtain a clean picture free of multiple images. This conclusion should be qualified because of two factors which may play an important part in successful television broadcasting at these higher frequencies. First, while it seems generally possible to find a receiving antenna position which will produce a clean picture, it is quite possible that this will not be the best position for another transmission at some other frequency in the band between 500 and 900 megacycles. Hence the receiving antenna installation problem might be complex for a television service established in this band of frequencies. Secondly, in the tests at 510 megacycles and 910 megacycles, directional transmitting antennas were used in order to obtain adequate signals. This directivity at the transmitting antenna prevents multipath signals which arise from reflections from buildings on Manhattan Island. For example, if a signal were truly broadcast from the Empire State Building, a receiver on the west radial might be subject to multipath signals originating by reflections from buildings lying to the north or south or even east of the Empire State Building, while these signals could not be present when directive transmitting antennas are used.

Hence the conclusions drawn from the tests concerning multipath effects in the 500- to 900-megacycle band may be somewhat optimistic when applied to a broadcast service.

Conclusion

The influence of hilly terrain on propagation is clearly illustrated by comparison of the data along the west and southwest radials. The best agreement with theoretical values at all frequencies was obtained along the comparatively smooth southwest line. There was closer agreement with the theoretical curves at 67.25 megacycles than at 288 megacycles, while the measured values at 510 and 910 megacycles were usually far below the theoretical. The data has been analyzed and presented in Figures 16 to 19 to assist in forming an overall picture of the situation.

Shadowing from hills and other obstructions increases steadily as the frequency increases, thus requiring higher power at the higher frequencies. Figure 20 offers a basis for estimating power requirements as a function of frequency. In general, the service area depicted by a series of contours of constant field intensities will be about the same size for the high frequencies as for the lower frequencies, but the service area for the high frequencies will be spotted with local areas where the signal is low or nonexistent. To insure signals of usable strength in some of these local shadow areas, at frequencies between 500 and 900 megacycles, it would be necessary to increase the radiated power by a fantastic ratio. On the other hand if the entire service area of a 900-megacycle transmitter consisted of terrain similar to that encountered on the southwest radial, one might expect to provide a very substantial service with a radiated power of the order of 100 kilowatts.

The effect displayed in Table I, namely the failure of high-gain directive receiving antennas to function properly in shadowed areas where the field is badly distorted, cannot be over-emphasized since this makes it impossible to employ a simple means of making use of weak signals.

Multipath effects are present at both 67.25 megacycles and 288 megacycles, but are usually too slight to be serious. In obstructed or hilly areas, multipath at 510 and 910 megacycles is severe. However, in most places, a clean picture could be obtained by orienting the receiving antenna. It was generally possible to find several responses which gave a good picture. This was true when the receiving antenna was a large array having a narrow beam and a large front-to-back ratio or a single dipole and reflector with low front-to-back ratio and

a broad pattern. It is quite likely that the best position and orientation of the receiving antenna for one station operating in the frequency band between 500 and 900 megacycles will not prove to be best or even suitable for one or more other stations operating on other channels in the band. Indeed, receiving antennas may be required which are rotatable and even this added luxury may prove to be insufficient. At least, it seems evident that the receiving antenna problem will be of primary importance in establishing a successful television broadcasting service at these higher frequencies.

ACKNOWLEDGEMENT

The assistance rendered by others in bringing this extended investigation to a successful conclusion is gratefully acknowledged. In particular, mention should be made of the operating staff of Television Station WNBT who operated the test transmitters and kept detailed records of operation while carrying out their normal duties, as well as the several groups of engineers at RCA Laboratories who constructed the 288-megacycle transmitter, developed the tubes and designed the oscillators for the 510 and 910 megacycle transmissions, and produced the converters to use with the 630TS receivers.

APPENDIX

System Calibration for Determining Field Intensities

In the process of measuring the field intensities at 510 and 910 megacycles, it was necessary to determine a number of physical quantities at the transmitting end. The effective radiated power was found by estimating the power gain of the directive array, reducing this figure slightly to allow for power loss in the transmission line, and finally multiplying these factors by the actual power output of the oscillator. The power output was determined by replacing the antenna by a water-cooled load resistor arranged so that water flow and temperature rise of the cooling water through the resistor could be measured. A thermal type milliammeter with a square-law scale was loosely coupled to the transmission line and its deflection was proportional to power; the proportionality constant was determined by the test with the water-cooled resistor. The power-indicating meters may be seen on the two transmission lines shown in Figure 8.

On the receiving end, the effective length and gain of the receiving antenna was measured. These figures, together with transmission line loss and signal generator calibration, related the signal generator reading to the field intensity.

When the field measurements were completed, the entire set of transmitting equipment used at 510 and 910 megacycles was moved to the Laboratories in Princeton, where the directive transmitting antennas were erected on the roof of a one-story building. The field intensity measuring equipment in the field truck with the receiving antenna 30 feet above ground was used to measure the signal in the beam of the transmitting antenna at a number of points a few hundred feet from the transmitting antenna. The vertical beam width of the transmitting antenna was narrow enough so that for a distance of over 400 feet the receiving antenna was subjected to only the direct wave, with no ground-reflected signal. Only two quantities were necessary in this determination. The first was the deflection of the power-indicating meter on the transmission line feeding to the transmitting antenna. This meter reading may be referred to as D. Then in the field truck, the receiver was tuned to the operating frequency and the deflection of the output meter noted. The antenna was then replaced by the signal generator and the signal generator output adjusted until the output meter on the receiver showed the same deflection as before. The signal generator output voltage was then recorded. This latter quantity is designated as V_{sg}.

The free-space field for P kilowatts of radiated power is

$$E \text{ (millivolts per meter)} = \frac{137\sqrt{P}}{d_{\text{miles}}} = \frac{724{,}000\sqrt{P}}{d_{ft}} \tag{1}$$

But

$$\mathrm{E} = V_{sg}K_1 = \frac{724{,}000\sqrt{K_2 D}}{d_{ft}} \tag{2}$$

where K_1 = the product of receiving-antenna gain, effective length, and the loss factor for the transmission line; and

K_2 = factor on the power-indicating meter to convert to kilowatts, lumped with the power gain of the transmitting antenna, including transmission line loss.

It should be remarked that it is not even necessary that the signal generator be calibrated in absolute value, but only necessary that the linearity be established and an unknown coefficient of linearity be assumed. This latter coefficient may then be lumped in K_1.

The solution of Equation (2), gives

$$\frac{K_1}{\sqrt{K_2}} = \frac{724{,}000\sqrt{D}}{V_{sg} \cdot d_{ft}} \tag{3}$$

Following this procedure, the ratio $K_1/\sqrt{K_2}$ was determined at both 510 and 910 megacycles, using a dipole in front of a flat reflector and a directional array for receiving at each frequency. Thus there were obtained four values of this ratio for reference use in determining actual values from the field data obtained along the west and southwest radials.

The field intensity at some point along a radial is proportional to the square root of the effective radiated power. This field, called E′, is

$$E' \text{ (millivolts per meter)} = F \cdot \sqrt{K_2 D'} \tag{4}$$

where D' is the reading of the power meter at the transmitter, shown by the log book to be the value existing at the approximate time of measurement of field intensity. K_2 is the same as the coefficient used in Equation (2) because the same transmitting equipment was used in both cases. The quantity, F, is a function of the transmitting and receiving antenna heights, the frequency, and a number of other variables, including the effect of hills and trees on the propagation. F could be determined analytically only by possessing unlimited mathematical ability. In any event, it is seen that F is field intensity in millivolts per meter for one kilowatt of radiated power, the quantity that was the object of the survey.

With the receiving equipment, the signal generator reading is determined that corresponds in strength to the signal found on the receiver terminals. This reading is V'_{sg}. Then the field intensity is

$$E' = V'_{sg} K_1 \tag{5}$$

Equating (4) and (5), the quantity F is found to be given by the relation

$$\mathrm{F} = \frac{V'_{sg}}{\sqrt{D'}} \times \frac{K_1}{\sqrt{K_2}} \text{ (millivolts per meter for one kilowatt)} \tag{6}$$

Thus to obtain the quantity F, one needs simply the measured signal generator output, V'_{sg}, the power output meter deflection D', and the appropriate ratio determined in Equation (3). The experimental values shown in Figures 13 and 14 were derived from the field observations in this manner.

It is interesting to see that the method outlined in this Appendix yields the desired field intensity data, namely millivolts per meter for one kilowatt of effective radiated power, without it becoming necessary actually to measure the power or to calibrate the receiving equipment or signal generator.

FIELD TEST OF ULTRA-HIGH-FREQUENCY TELEVISION IN THE WASHINGTON AREA*†

By

George H. Brown

Research Department, RCA Laboratories Division,
Princeton, N. J.

Summary—A field test of ultra-high-frequency television was conducted by RCA and NBC in the Washington area during the fall of 1948. A picture transmitter and a sound transmitter, together with a high-gain transmitting antenna, were installed at the Wardman Park Hotel.

Two types of converters were designed and constructed for these field tests. More than fifty converters and appropriate receiving antennas were installed in homes having conventional receivers.

A field intensity survey was conducted and the results are analyzed in terms of coverage.

At each of the home locations, voltages corresponding to the ultra-high-frequency transmission and to the transmission of WNBW on Channel 4 were measured. An analysis of this data is included, with respect to power requirements for satisfactory picture reception and with respect to comparative coverage at the low and high frequencies. The results of the field intensity survey are compared to the results obtained at home locations.

Observations concerning the effectiveness of directional receiving antennas as well as conclusions concerning multipath effects are included.

Introduction

MEASUREMENTS and observations have already been published[1] which afford a direct comparison of the propagation characteristics of radio waves at the frequencies 67.25, 288, 510 and 910 megacycles. The major portion of this work consisted of field intensity measurements taken with mobile equipment, so it seemed logical to follow this project with a program which would look toward reception in home locations under typical operating conditions. In the spring of 1948, the work of RCA Laboratories on color television was aimed in the direction of a field test involving transmissions on frequencies in the region of 500 megacycles; four transmitters were being built. Three of these transmitters were needed for the simultaneous color system of transmission, while the fourth was the accompanying sound transmitter. It was planned to install the sound transmitter and one of the picture transmitters at the Empire State Building in

* Decimal Classification: R583.16.

† *RCA Review*, December, 1948.

[1] George H. Brown, Jess Epstein, and Donald W. Peterson, "Comparative Propagation Measurements; Television Transmitters at 67.25, 288, 510 and 910 Megacycles", *RCA Review*, Vol. IX, No. 2, pp. 177-201; June, 1948.

New York prior to the completion of the entire system. This was to hasten the gathering of data typical to a broadcast operation and to gain experience with the installation of converters in home receiving locations.

With the announcement by the Federal Communications Commission of a public hearing in the matter of utilization of frequencies in the band 475 to 890 megacycles for television broadcasting, plans were altered and a decision was made to carry out the initial phase of the experiment in Washington. Hence, one picture transmitter and the sound transmitter were moved to Washington and installed in the transmitter room of Television Station WNBW at the Wardman Park Hotel.

The Washington experiment was intended to provide typical broadcast coverage with receivers installed in home conditions. The results of the transmissions could then be observed by many interested parties while field intensity measurements and other pertinent data were being accumulated.

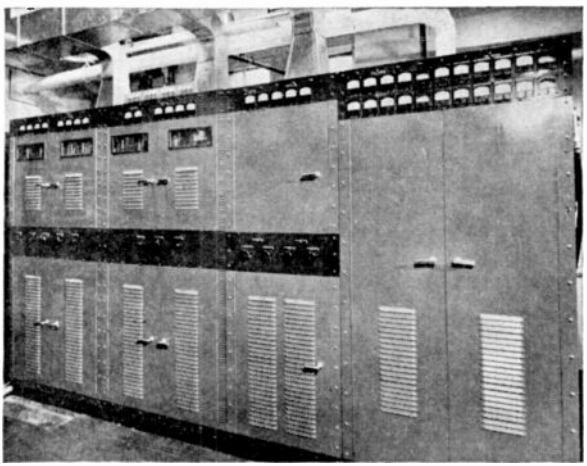

Fig. 1—The ultra-high-frequency transmitter installed in the transmitter room of WNBW.

Description of the Washington Installation

The Transmitters

The transmitters installed at the Wardman Park Hotel operated in the band of frequencies between 504 and 510 megacycles. The picture carrier frequency was 505.25 megacycles, while the sound carrier frequency was 509.75 megacycles. Figure 1 shows these two transmitters in their location at the Wardman Park Hotel.

A monochrome transmission was provided using the same standards

that apply in the 12 channels now used for commercial television broadcasting. The power amplifier tube in each transmitter was a modified Type 8D21. The 8D21 is a production type tube used in commercial five-kilowatt television transmitters. However, for the high-frequency experiments, it has been necessary to modify the construction slightly to reduce high-frequency power losses. This tube is capable of operation at only the low-frequency end of the 475 to 890 megacycle band and then at considerably reduced power.

The picture transmitter operated with a peak power of 1000 watts, while the sound transmitter delivered 1000 watts of average power.

The Transmitting Antenna and Transmission Line

In anticipation of field tests of color television in the vicinity of 500 megacycles, a broadcast antenna with a power gain of 10 was developed. This antenna uses the Turnstile principle, which provides a well-matched antenna over a broad band of frequencies and permits the use of a simple diplexer for feeding the sound and picture signals into a single antenna. The antenna structure consists of a seamless steel tube six inches in diameter and over twenty feet in length. When the Washington experiment was proposed, it seemed logical to place the high-frequency antenna on top of the Channel 4 antenna used by WNBW. A study of the mechanical problem revealed that it would be desirable to design and construct an antenna of smaller dimensions in order that the supporting pole not be stressed unduly. Hence an antenna ten feet in length and six inches in diameter was constructed especially for the Washington installation. Sixteen slots were cut in the tube and each slot was energized from a transmission line inside the tube.

The power gain of this antenna used in the Washington field tests was 5, with a single half-wave dipole used as the unit of reference.

Figure 2 shows the high-band antenna mounted above the WNBW Superturnstile, with the center of the high-band antenna 357 feet above ground and 563 feet above sea level.

As in the case of the larger antenna with a power gain of 10, a simple diplexer may be used to feed the picture signal and the sound signal into the same antenna. It was intended to use the diplexer in this manner, with the diplexer mounted in the base of the antenna and with two separate transmission lines, one running from the picture transmitter to the diplexer and the other running from the sound transmitter to the diplexer. However, because of the short time available to construct a very special transmission line as well as the installation problem on the tower, it was decided to use only one line from

the transmitter room to the antenna and to couple the two transmitters to this transmission line through an isolating filter.

A diplexer was nevertheless mounted in the base of the antenna, but not for the usual purpose. At the point where the sound line is connected in conventional operation, a resistance of fifty ohms was inserted. The inclusion of this resistor was brought about through a theoretical study carried out at these laboratories which revealed that a resistance of the proper value placed at this point on the diplexer, when the diplexer is used in conjunction with a Turnstile antenna, will provide a perfect termination for the other end of the diplexer and will insure a circular radiation pattern in the horizontal plane. The term chosen for this approach is "resistance stabilization."

Fig. 2 — The high-band antenna mounted above the WNBW Super-turnstile.

While the antenna used in Washington had a power gain of 5, it should be recalled that the power gain was limited to this figure by the mechanical strength of the supporting pole and that an antenna with a power gain of 10 has already been constructed and tested. In an installation where one had complete control of the design of the supporting structure, it would be quite feasible to realize this higher power gain.

It was originally intended to use commercially available transmission lines to carry power from the transmitters to the antenna. A critical examination soon revealed that none of the familiar commercial lines would be suitable for use in the range of frequencies between 475 and 890 megacycles. The unsuitability was caused by electrical discontinuities on the line due to the insulator effect. A transmission line which is electrically smooth throughout this range of frequencies was developed and it was this new type of construction which was used in the Washington field tests. The outer conductor of the line was over three inches in diameter. Even with this large line, the attenuation was 0.31 decibels per 100 feet, so that with a line 450 feet in length, only 72.5 per cent of the transmitter power arrived at the antenna.

While the power gain of the antenna itself was 5, one must consider the transmission line, with a "power gain" factor of 0.725, to be part of the antenna system. Hence, the power gain of the antenna system was 3.625. Then the effective radiated peak power for the picture transmission was 3625 watts, with 3625 watts average power for the sound transmission.

The Vestigial Sideband Filter

New circuit developments were applied to the problem of designing a vestigial sideband filter for use in the ultra-high-frequency range which resulted in a compact filter that had the same electrical characteristics as those used with present commercial television transmitters. This filter was installed with the ultra-high-frequency transmitter in Washington and has been used throughout the tests. This successful operation means that as far as the transmission standards are determined by the vestigial sideband characteristics they may be the same as the present commercial standards.

Converters and Receiving Antennas

Two television converters were developed at the laboratories for experimental use in the Washington field tests. The converters were intended for operation in conjunction with any standard television receiver having a push-pull input connection of 300 ohms impedance.

The Model A converter had a tuning range from 480 to 800 megacycles, while the Model B converter had a tuning range from 480 to 600 megacycles. Both models had self-contained power supplies and both models converted ultra-high-frequency television signals down to Channel 3 on a standard television receiver.

The noise factor for the Model A converter, using a crystal mixer, was 10 decibels above thermal noise, and the corresponding factor for the Model B converter was 22 decibels above thermal noise.

In Table I, the results of a number of calculations concerning the noise limitations of these converters are shown. In the case of the theoretical noise voltage for the 300-ohm resistor, the band width was taken as 4 megacycles. The noise voltages for the two converters are shown in the same column. The right-hand column shows the peak radio-frequency signal required to give a signal-to-noise ratio (i.e., the ratio of peak radio-frequency signal to root-mean-square noise voltage) of 30 decibels. A radio-frequency signal-to-noise ratio of 30 decibels gives a useful peak-to-peak signal to root-mean-square noise at the kinescope of 28.6 decibels, assuming standard synchronizing pulse and black level, with white level at 15 per cent. This is a value

which is considered to be a nominal value for acceptable service, and possibly may be considered a minimum acceptable signal.

Table I

Source of Noise	Root-Mean-Square Noise Voltage (Microvolts)	Peak Radio-Frequency Signal Required to Give Signal/Noise Ratio of 30 Decibels (Microvolts)
300-ohm resistor	2.19	69.0
Model A converter (Noise factor 10 db.)	6.9	219.0
Model B converter (Noise factor 22 db.)	27.1	860.0
Commercial television receiver in average adjustment (Noise factor 14.5 db.)	11.5	365.0

By using the equation on page 194 of Reference 1, the field intensity required to produce 219 microvolts on the 300-ohm input terminals of the Model A converter can be computed. In deriving this equation, it was assumed that the signal was being received on a half-wave dipole and that this dipole in turn fed the signal to a 300-ohm transmission line through a suitable matching section. It is found that at a frequency of 505.25 megacycles, the microvolts on the receiver terminals should be multiplied by a factor of 5.3 to obtain the field intensity in microvolts per meter. Then, a field intensity of 1160 microvolts per meter would be required to produce, under these circumstances, a voltage of 219 microvolts on the terminals of the Model A converter.

Lower field intensities could be used if circumstances permit the use of a directional receiving antenna. However, in many locations, the field is so distorted that little or no benefit is derived from a directional receiving antenna.

In designing television receiving antennas, one is concerned with the problems of obtaining a desirable radiation pattern over a wide band of frequencies and of obtaining a reasonable impedance match between the antenna and transmission line. If the receiver is well matched to the transmission line, the efficiency of signal transfer from the antenna to the transmission line may be expressed in terms of the antenna impedance. However, a more convenient method makes use of the measurement of the voltage standing-wave-ratio on the transmission line when the antenna is used in the transmitting condition. If we call this ratio of minimum voltage to maximum voltage R,

$$E'/E'' = \frac{2\sqrt{R}}{1+R}$$

where E'' is the voltage received on the receiver terminals when the antenna is perfectly matched to the line and E' is the voltage received on the receiver terminals when the actual antenna which is not perfectly matched is used. Table II gives a number of values for this ratio of voltages.

Table II

Standing-Wave-Ratio, R	$(E'/E'') \times 100$
1.0	100.
0.7	98.5
0.6	96.7
0.5	94.2
0.4	90.2
0.3	84.2
0.2	74.3
0.1	57.4
0.05	42.5

Thus it can be seen that if the standing-wave-ratio R is not less than 0.5, less than 6 per cent of the maximum possible voltage is lost.

In preparation for the Washington experiment, several simple antenna types were designed and constructed. Since it was planned to install converters in a large number of homes under a variety of conditions, it seemed appropriate to concentrate on relatively inexpensive constructions that would not in general be objectionable when installed on the average home.

A broad-band receiving dipole is shown in Figure 3. This antenna retains its characteristics as an effective dipole over the entire band of frequencies from 475 to 890 megacycles. The impedance match expressed in terms of transmitting standing-wave-ratio is better than 0.6, so Table II shows that less than 4 per cent of the received voltage is sacrificed by mismatching losses over the entire band. In the neighborhood of 500 megacycles, the radiation pattern is very similar to that of a conventional dipole, while at the upper end of the band the pattern is somewhat narrower with a slightly higher antenna gain factor.

A rather simple directional receiving antenna is the rhombic shown in Figure 4. This antenna is a little over six feet in length and less than four feet in width. The impedance match is excellent over the entire band.

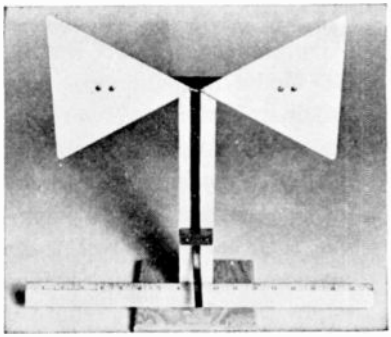

Fig. 3—A fan dipole useful in the ultra-high-frequency band.

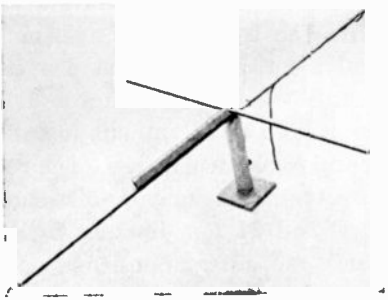

Fig. 4—A rhombic receiving antenna used in the Washington field tests.

A simple directional antenna using a dipole and a parasitic director is shown in Figure 5. This antenna is limited in use to the 504 to 510 megacycle channel by its impedance characteristic and by its changing directional pattern. Through this limited band, the standing-wave-ratio under transmitting conditions is greater than 0.5 and the antenna thus operates at good efficiency.

A compact broad-band unidirectional antenna using four dipoles connected by a transmission line network has been developed and is shown in Figure 6. The pattern does not change materially in the band between 475 to 890 megacycles, and the impedance match is also very good throughout this same band.

The simplicity of installation with the relatively unobtrusive fan dipole is illustrated by the photograph of a typical home installation shown in Figure 7.

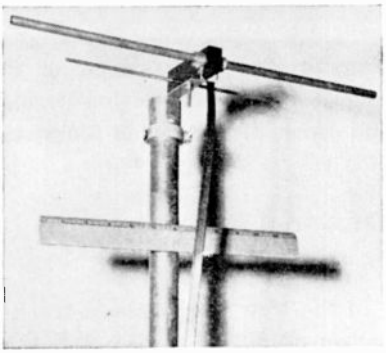

Fig. 5—A dipole-director array for the band from 504 to 510 megacycles.

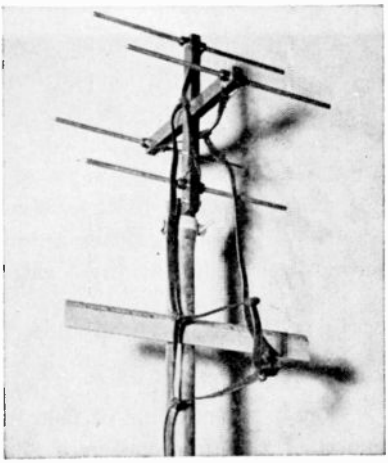

Fig. 6 — A broad-band unidirectional array developed for use in the ultra-high-frequency channels.

Installation of converters and receiving antennas started shortly after the beginning of transmissions on September 1, 1948. During that month, 35 Model A converters and 16 Model B converters were installed in the Washington area. Of these installations, 47 were accompanied by an antenna installation which appeared to be appropriate for the particular set of circumstances. These included 3 dipole-director arrangements, 5 broad-band unidirectional arrays, 15 rhombics, and 24 fan dipoles. In each case, the installation crew tried a variety of antenna positions as well as the various antenna types. The predominance of the fan dipoles was due to two factors. Where a satisfactory picture could be obtained with the fan dipole, it was selected because of its simplicity. In many other instances, particularly in the shadowed areas, it was often found that the fan dipole gave at least as strong a signal as the directional antennas. The rhombic antenna often gave results superior to any other type and was used

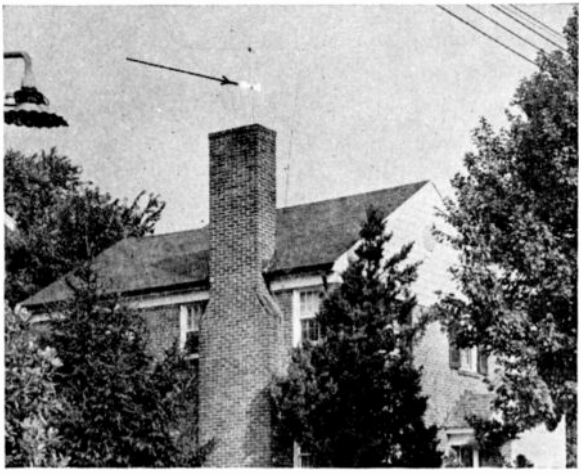

Fig. 7—A fan dipole installed in a typical home location.

in those instances. In some of the shadowed areas it was inferior to the fan dipole, but in at least one extremely obstructed position it was far better than the other antennas. The dipole-director was found to be of little value in any location.

Data Obtained from the Washington Experiment

The Field Intensity Survey

For measurements of field intensity in the New York area, a truck-mounted receiving antenna at an elevation of 30 feet was used, the truck was moved around a local area, where possible, and the receiving antenna was rotated at the same time. In this way, a search was made

for maximum signal with the most usable picture. Since maximum signal did not always correspond to the most usable picture, the field intensity corresponding to best picture was recorded. Receiving sites were chosen in a variety of surroundings: in open fields, in wooded areas, along highways, atop hills, and in valleys. An effort was made to stay away from electric lines and large buildings. The same procedure was followed in the Washington area.

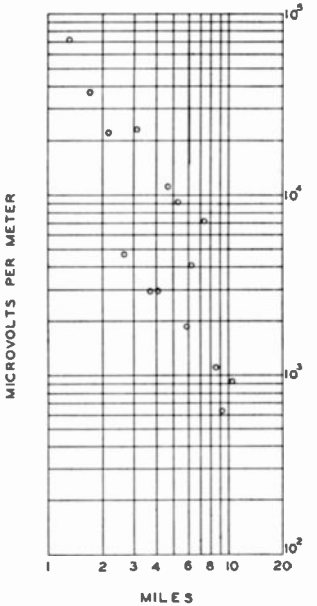

Fig. 8 — Field intensity measured along the north radial. The receiving antenna was 30 feet above ground. The effective radiated power at 505.25 megacycles was 3.6 kilowatts.

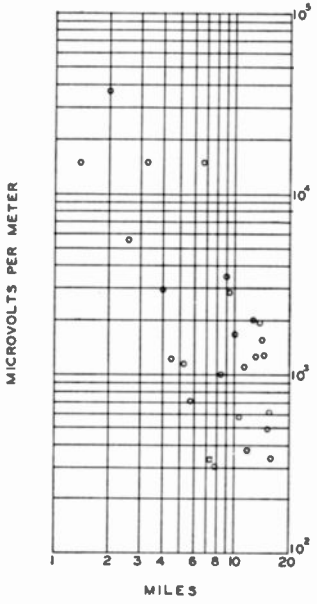

Fig. 9—Field intensity along the northeast radial.

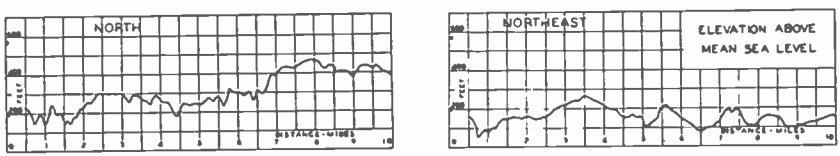

For reference in connection with this survey and to show the type of terrain in the Washington area, profiles have been plotted for eight radial lines with the WNBW tower as the point of origin. These profiles are shown at the bottom of Figures 8 to 15, inclusive. Only part of the story is indicated by these figures, since Washington has a great number of large trees, large homes, and many apartment buildings. The profile of the southeast radial looks very flat in the first

five miles, but actually this is the region of large hotels and office buildings.

The field intensity measured along these eight radial lines is shown in Figures 8 to 15, inclusive. The exception should be noted that in Figure 15 the profile is along the northwest radial while the field intensity measurements are taken along the northnorthwest radial. This change was necessary in order to use available roads. During the course of these measurements, the effective radiated power referred to peak of synchronizing signal was 3.6 kilowatts. The field intensity recorded in these figures refers to peak of synchronizing pulse.

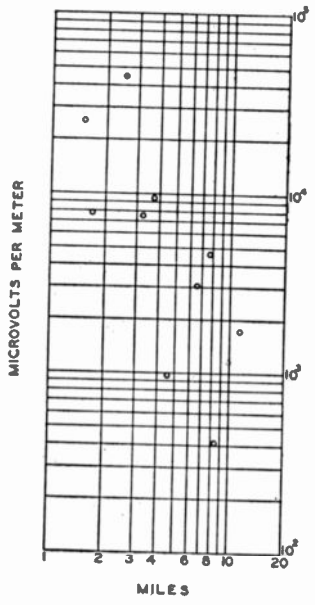

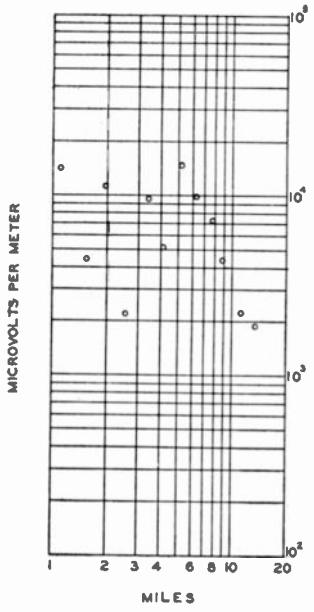

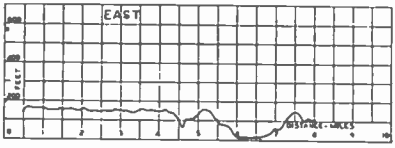

Fig. 10—Field intensity along the east radial.

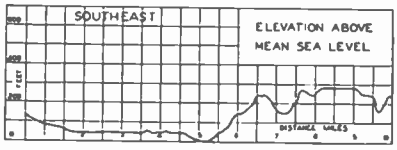

Fig. 11—Field intensity along the southeast radial.

A comparison of Figures 8 to 15 with the corresponding profile reveals a distinct correlation between the profile and the measured field intensity, with some departure due to local effects such as trees and buildings.

In making a comparison of the measured field intensity with theoretical values, the profiles on each of the eight radials shown in Figures

8 to 15 were averaged. The average elevation for each profile was then used in a calculation of the theoretical field intensity curve for the particular radial. Then the measurements of Figures 8 to 15 were analyzed on a statistical basis, with the results shown in Figure 16. Curve A relates the measured values to the theoretical curve at 505.25 megacycles. Curve B was constructed by comparing the measured values at 505.25 megacycles with the theoretical field intensity curve at 67.25 megacycles, with the same effective radiated power in each case.

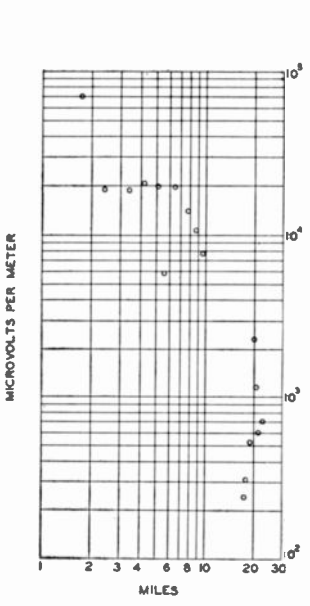

Fig. 12—Field intensity along the south radial.

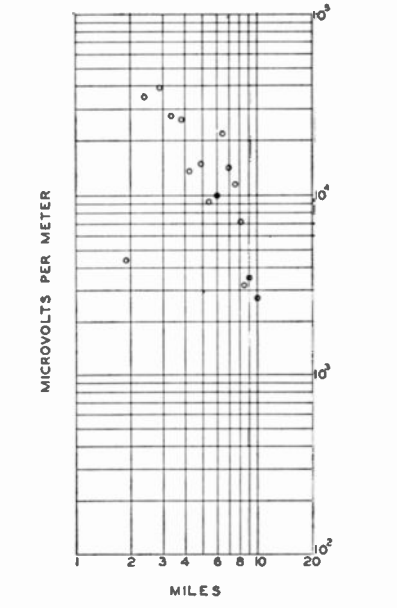

Fig. 13—Field intensity along the southwest radial.

Signal Strength on Receiver Terminals in Home Locations

The locations of 44 converter installations in the Washington area are shown in Figure 17. At these locations, the 505.25-megacycle voltage on the terminals of the converter was measured. At the same time, the voltage on the receiver terminals of the low-band antenna was measured for the WNBW Channel 4 transmission. At the time of these measurements, the effective radiated power for the 505.25-mega-

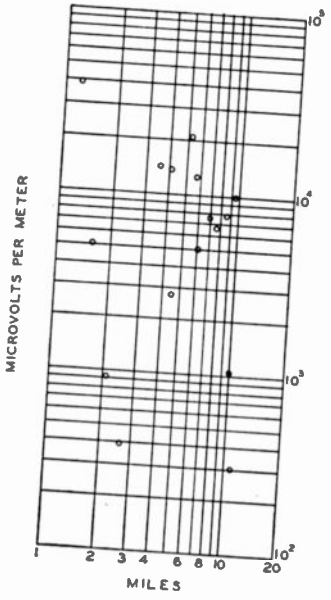

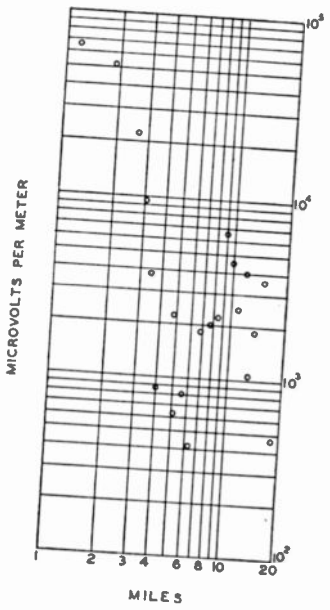

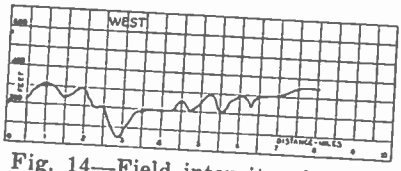

Fig. 14—Field intensity along the west radial.

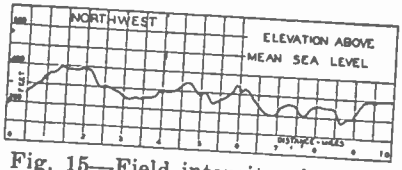

Fig. 15—Field intensity along the northnorthwest radial.

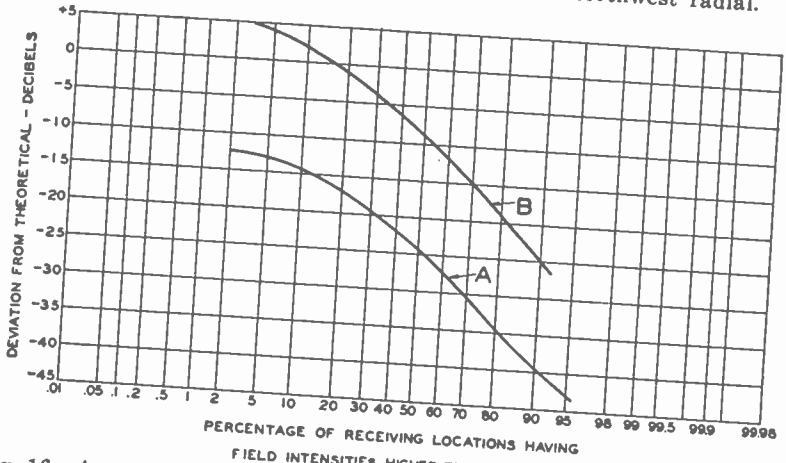

Fig. 16—An analysis of the data shown in Figures 8 to 15. Curve A relates the measured field intensities at 505.25 megacycles to the theoretical curve for the same frequency. Curve B relates the measured field intensities at 505.25 megacycles to the theoretical curve at 67.25 megacycles.

cycle transmission was 3.6 kilowatts, while the effective radiated power for WNBW was 20.5 kilowatts.

Table III lists the map location and distance from WNBW for the converter installations shown on Figure 17, as well as the 505.25 megacycle and 67.25 megacycle voltages measured on the receiver terminals.

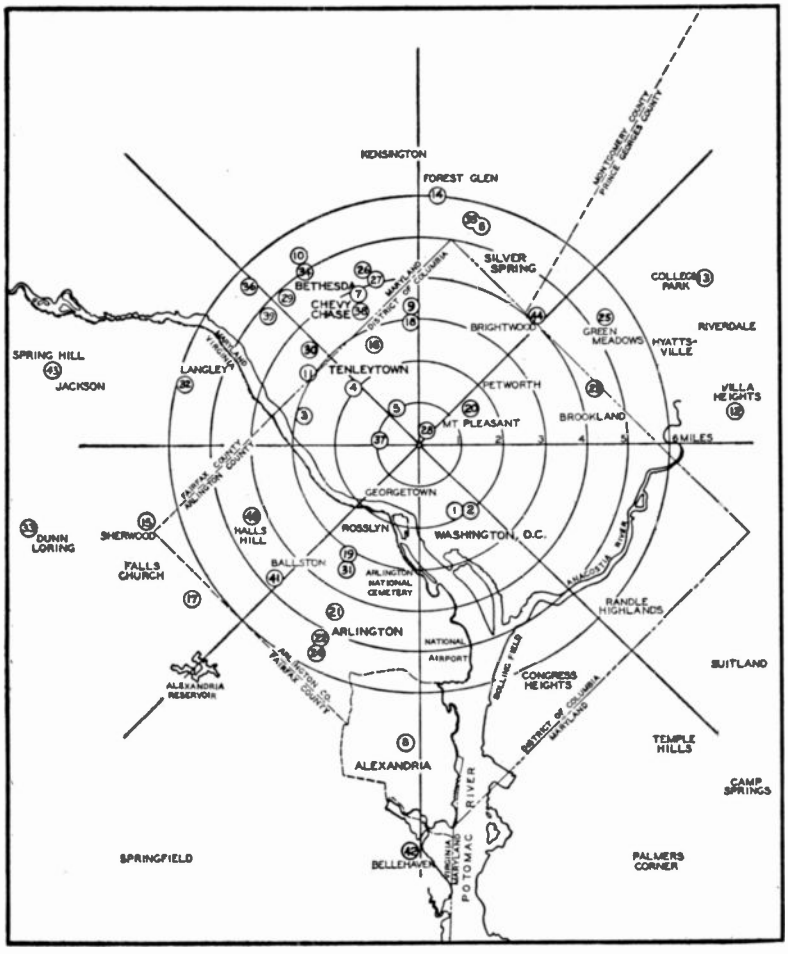

Fig. 17—A map of the Washington area showing the locations of converters and receiving antennas listed in Table III.

From a comparison of the measured voltages on the receiver terminals at 505.25 megacycles and at 67.25 megacycles, the probability curve shown in Figure 18 has been constructed. From this curve one can find the power needed at 505.25 megacycles in order that the receiver voltages at a given percentage of the receiver locations shall

TABLE III

Location Number	Distance (miles)	Receiving antenna	Receiving antenna height (ft.)	Converter	Receiver voltage (microvolts) 505.25 Mc	67.25 Mc
1	2	Dipole-director	Roof of 12-story bldg.	A	2,250.	188,000.
2	2	Fan	Roof of 12-story bldg.	A	4,750.	137,000.
3	3	Rhombic	50	A	338.	950.
4	2	Fan	40	A	565.	9,250.
5	1	Broad-band array	47	A	485.	18,800.
6	5.3	Rhombic	45	A	550.	3,500.
7	4	Broad-band array	75	A	1,950.	25,000.
8	7.2	Fan	Indoor, attic of apartment bldg.	A	580.	7,000.
9	3.3	Rhombic	45	A	1,010.	10,000.
10	5.3	Rhombic	—	A	127.	11,000.
11	3.2	Fan	55	A	338.	8,250.
12	7.2	Rhombic	40	A	466.	8,000.
13	7.7	Rhombic	42	A	Below 50	325.
14	5.8	Dipole-director	42	A	1,650.	1,375.
15	7	Rhombic	35	B	1,430.	32,500.
16	2.5	Fan	40	B	8,000.	82,500.
17	6.6	Rhombic	40	A	Below 50	8,500.
18	2.9	Fan	50	A	775.	50,000.
19	3.3	Fan	42	B	503.	25,000.
20	1.4	Fan	30	A	233.	23,800.
21	4.6	Fan	33	B	2,760.	2,250.
22	5.5	Broad-band array	Attic	A	Below 50	3,750.
23	4.1	Fan	40	A	Below 50	8,250.
24	5.6	Fan	Attic	B	Below 50	3,660.
25	5	Dipole-director	38	A	565.	6,750.
26	4.4	Rhombic	32	A	142.	4,500.
27	5	Rhombic	38	A	474.	16,250.
28	0.2	Fan	50	A	19,800.	32,500.
29	4.7	Fan	38	A	263.	4,000.
30	3.5	Fan	50	A	417.	9,500.
31	3.4	Fan	40	B	3,080.	21,300.
32	6	Fan	28	A	475.	4,000.
33	9.6	Broad-band array	50	A	256.	11,000.
34	5	Fan	40	A	396.	3,750.
35	5.4	Rhombic	35	B	550.	10,500.
36	5.6	Fan	28	A	680.	10,750.
37	1.1	Rhombic	8 fl. bldg.	B	19,800.	250,000.
38	3.5	Fan	45	B	110.	7,500.
39	4.8	Rhombic	40	A	900.	4,000.
40	4.3	Fan	40	B	1,350.	10,250.
41	5	Fan	35	A	1,320.	18,800.
42	9.7	Fan	35	B	1,140.	4,250.
43	9	Rhombic	40	A	210.	5,000.
44	4	Fan	25	A	450.	5,750.

be as great as the receiver voltages obtained with 20.5 kilowatts of effective radiated power on Channel 4. It may be seen that with the present radiated power of 3.6 kilowatts at 505.25 megacycles, only 4 per cent of the locations achieve a signal strength as great as that obtained on Channel 4. In order that 50 per cent of the locations realize this goal, the power requirements at 505.25 megacycles would be 1200 kilowatts. To obtain the same result for 70 per cent of the locations, a radiated power of 5000 kilowatts would be required.

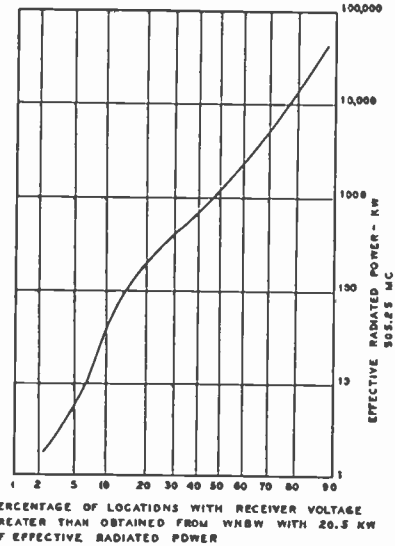

Fig. 18—A statistical analysis of the voltages on receiver terminals in home locations, expressed in terms of power requirements at 505.25 megacycles in order that a given percentage of locations shall have as great a signal as obtained from WNBW with 20.5 kilowatts of effective radiated power.

It may be of interest to return for a moment to the survey in the New York area. Using Figure 20 of the Reference 1, and assuming that a half-wave dipole was used for the receiving antenna, it was estimated that the power required at 505.25 megacycles should be 210 times the power of the Channel 4 station WNBT to obtain equality of receiver voltages for the two frequencies at 50 per cent of the locations. Multiplying 210 by the effective radiated power of WNBW, 20.5 kilowatts gives 4300 kilowatts. Again using the results of Reference 1, it is found that the power required to achieve the same result at 70 per cent of the locations would be 10,660 kilowatts. The following comparison of the Washington tests and the New York survey can then be made.

Percentage of receiving locations with receiver voltage equal to the Channel 4 signal.	Power requirements estimated from the Washington tests. (kilowatts)	Power requirements estimated from the New York tests. (kilowatts)
50	1,200	4,300
70	5,000	10,660

The agreement between the power estimates obtained from these experiments in two different areas of somewhat different topography is well within the limits of experimental accuracy for this type of data.

In addition, it should be remembered that in many installations in the Washington area directive receiving antennas were used effectively while the estimates from the New York data were based on the use of a dipole.

Since at most of the receiver locations in the Washington tests the Channel 4 signal is far in excess of the value required to give a completely noise-free picture, it may be more appropriate to examine the power requirements at 505.25 megacycles to obtain a noise-free picture or at least a marginal picture. With this objective in mind, Figure 19 was constructed from the data in Table III. The lower curve in this figure shows the power requirements to obtain 219 microvolts on the receiver terminals at a given number of locations. This is the value of voltage which was estimated earlier in this paper as being necessary to give the minimum acceptable signal-to-noise ratio on the Model A converter. Examination of the lower curve reveals the following power requirements when the Model A converter is used.

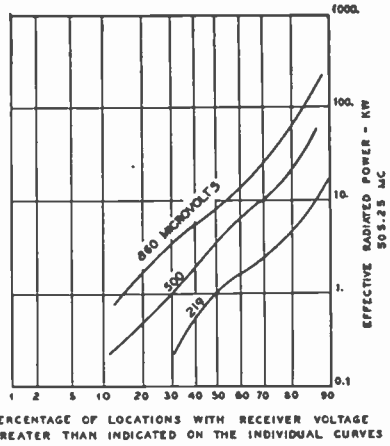

Fig. 19 — Power requirements at 505.25 megacycles in order that a given percentage of the receiving locations shall have a receiver terminal voltage as great as the values indicated on the individual curves.

Percentage of receiving locations with a receiver voltage of at least 219 microvolts	Power estimate (kilowatts)
50	1
70	2.4
78	3.6
80	4.7

The middle curve on Figure 19 holds for a receiver voltage of 500 microvolts. This would give a noticeably better picture than the minimum acceptable value of 219 microvolts. From this middle curve, the following power requirements are found to yield at least 500 microvolts on the receiver terminals.

Percentage of receiving locations with a receiver voltage of at least 500 microvolts	Power estimate (kilowatts)
51	3.6
70	10.2
80	22.0

The upper curve in Figure 19 is an attempt to estimate the power requirements to obtain a minimum usable signal on the Model B converter, that is, with 860 microvolts on the receiver terminals. Examination of this curve shows the following power requirements.

Percentage of receiving locations with a receiver voltage of at least 860 microvolts	Power estimate (kilowatts)
32	3.6
50	8.2
70	26.0
80	66.0

In an attempt to correlate the voltage measurements made in home receiving locations with the field intensity measurements, the field intensity data for the northnorthwest radial of Figure 19 has been transferred to Figure 20 where it is shown by the circles. A study of Figure 17 shows that the home locations numbered 4, 5, 7, 10, 11, 16, 29, 30, 34, 36, 38, and 39 are within reasonable distance of the northnorthwest radial. At two-thirds of these home locations, fan dipoles were used. It has been shown earlier that to convert receiver voltage to field intensity, for a dipole receiving antenna, a factor of 5.3 should be used. Hence the receiver voltage for the above twelve locations was converted in this manner, with the results shown by the crosses on Figure 20. A reasonable correlation may be seen with the limited data.

Conclusion

Contrary to experience in the New York area, multipath interference was found to be of little consequence in the Washington installations. Multipath signals were in evidence and it was necessary to move the receiving antenna to eliminate it. However, the major problem in many installations was to find a spot where the main signal was strong enough. The difference may be due to two factors. The signals observed on the west radial in the New York tests were radiated from the Empire State Building, with many tall buildings surrounding the source, but

at lower level. However, it was felt that the use of a directional transmitting antenna in the New York tests had minimized the multipath effects. The second factor may be due to the relative powers used in the two tests. In New York, high values of radiated power were used so that both the main signal and the reflected signals were well above the noise. In many cases in Washington, the main signal was only marginal and it may well be that the multipath signals were obscured because they were below noise level.

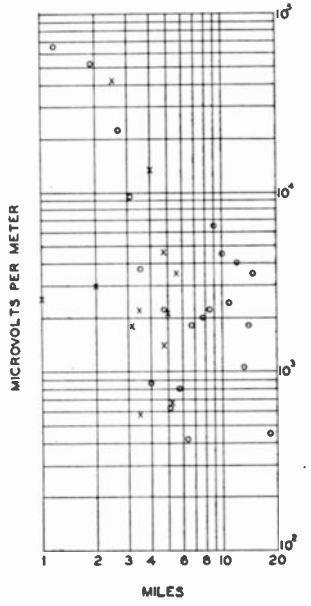

Fig. 20—A comparison of field intensity data with voltage on receiver terminals. The circles are the measured field intensities along the northnorthwest radial. The crosses are the apparent field intensity obtained from the receiver terminal voltages at home locations divided by the effective height of a dipole antenna.

A literal interpretation of Figure 18 shows that enormous amounts of power are required at 500 megacycles to give the same coverage as obtained on the Channel 4 station. It should be remembered, however, that in the area of the measurements, the Channel 4 station furnishes practically blanket coverage. Hence, not too extravagant amounts of power at 500 megacycles will furnish a reasonable coverage over a limited area, without providing the large area coverage of the low channels. When studying Figure 19 which indicates moderate power levels for reasonable coverage of a large percentage of the home locations, one should, nevertheless, not fail to consult Figure 17 and take note of the fact that the majority of the home locations used in this analysis were grouped in areas rather close to the transmitter.

The analysis of data shown in Figure 16 indicates a greater departure from theoretical values in the Washington area than was found in the New York tests. Two factors may account for the difference. In New York, the transmitting antenna was over 1000 feet above ground, while in Washington the transmitting antenna was only about 350 feet above the immediately surrounding terrain. In addition, the probability curve for the New York tests was formed by averaging the results from the hilly west radial which passed through residential districts with the results from the southwest radial which passed over

relatively barren territory. The terrain on all eight radials in Washington was not unlike the west radial of the New York tests.

ACKNOWLEDGMENT

Under usual circumstances of publication of scientific results, recognition of creative contributions to a project is established by joint authorship and assistance of a valuable but more routine nature is acknowledged by a formal statement incorporated as part of the paper, with individual names cited. In a project of the scope and magnitude of the Washington field test, neither procedure seemed practical since various phases of the work were carried out by several groups in the RCA organization. The author appears solely in the role of correlator and narrator and he wishes to emphasize the importance of the enthusiastic cooperation of the numerous engineers of RCA Laboratories Division who developed and designed the transmission equipment, the receiving antennas, and converters and who made all the measurements displayed in this paper; the engineers of the National Broadcasting Company, Inc., who contributed greatly to the installation and operation of the transmission equipment; the staff of RCA Victor Division which cooperated in the manufacture of the converters and transmitting tubes; and the RCA Service Company, Inc., which carried out the task of installing converters and receiving antennas in the Washington area.

DEVELOPMENTAL TELEVISION TRANSMITTER FOR 500-900 MEGACYCLES*†

By

R. R. Law, W. B. Whalley and R. P. Stone

Research Department, RCA Laboratories Division,
Princeton, N. J.

Summary—Tubes and circuits have been developed which make possible a one-kilowatt-peak-power wide-band television transmitter for the 500-900-Mc band. A detailed account of these developments is presented.

The ultra-high-frequency tube employed in this transmitter is a modified form of the 600-Mc oxide-coated-cathode pulse-triode developed during the war[1]. In a push-pull amplifier a pair of these tubes gives a continuous-wave output of more than one Kw at 800 Mc, and in wide-band service such as would accommodate a color television picture of the highest quality, a peak power of more than one Kw is readily obtained. A novel feature of the new tube is the tungsten-wire grid which leads to an unusually rugged tube. Because of excellent grid cooling there is no trace of grid emission; this fact undoubtedly contributes to the stability of the system.

Wide-band operation imposes severe requirements on circuit design. In the rf amplifier, precaution is taken to keep the stored energy low. In the video amplifier, operation at high power level is accomplished by employing the above mentioned pulse triode to cathode-modulate the rf amplifier. This combination of a large-area-cathode "Class-A" modulator tube and an intermediate-area-cathode "Class-B" rf tube is advantageous for wide-band service.

Introduction

DURING the course of the development of a 600-Mc oxide-coated-cathode pulse triode during the war[1], it became apparent that a modified version of this tube would be advantageous for continuous-wave applications. Consideration of the fundamental electronics of ultra-high-frequency transmitting tubes[2-7] indicated that

---

* Decimal Classification: R583.4 × R583.6

† Reprinted from *RCA Review*, December, 1948.

[1] R. R. Law, D. G. Burnside, R. P. Stone, W. B. Whalley, "Development of Pulse Triodes and Circuit to Give One Megawatt at 600 Megacycles" *RCA Review*, Vol. VII, No. 2, pp. 253-264, June, 1946.

[2] D. C. Prince, "Vacuum Tubes as Power Oscillators", *Proc. I.R.E.*, Vol. II, p. 275, June; p. 405, August; and p. 527, October, 1923.

[3] W. G. Wagener, "The Developmental Problems and Operating Characteristics of Two New Ultra-High-Frequency Triodes", *Proc. I.R.E.*, Vol. 26, pp. 401-414, April, 1938.

[4] A. V. Haeff, "Effect of Electron Transit Time on Efficiency of a Power Amplifier", *RCA Review*, Vol. IV, No. 1, pp. 114-122, July, 1939.

[5] C. C. Wang, "Large-Signal High-Frequency Electronics of Thermionic Vacuum Tubes", *Proc. I.R.E.*, Vol. 29, pp. 200-214, April, 1941.

[6,7] See following page.

such a tube might perform satisfactorily in the 500- to 900-Mc band, particularly if the interelectrode spacing could be kept small.

On the basis of this theory and as a result of preliminary tests it appeared that a push-pull rf power amplifier employing a pair of these tubes should give one-Kw continuous-wave at 800 Mc. Furthermore, from an estimate of the ratio of stored-to-active energy, it seemed that such an amplifier should have a bandwidth of between 15 and 20 Mc. In the light of the thinking at that time, development of wide-band transmitters to explore the possibilities of television at higher frequencies was very desirable. Also, there were a number of basic questions to be answered. Are oxide-coated-cathodes suitable for use in moderate power ultra-high-frequency transmitting tubes? What is the best way to modulate the triode? And finally, is neutralization necessary in grounded-grid circuits? This paper outlines the results of a study to answer these and other questions.

Tube Development

The essential features of the tube developed for these tests may be seen in Figure 1. Starting at the lower left and proceeding clockwise around the photograph may be seen: 1) the stem assembly; 2) the cathode-support assembly; 3) the heater; 4) the cathode; 5) the cathode-heater assembly; 6) the cathode-stem assembly; 7) the grid assembly; 8) the grid-stem assembly; 9) the final assembly; and in conclusion, in the center of the photograph, the complete tube including air-cooled radiator.

The cathode is approximately one and one-half inches in diameter and has a coated area of about 7.5 square centimeters. The heater, a single helical coil of 0.010 inch diameter insulated tungsten wire, requires about 3 amperes at 18 volts to bring the cathode to operating temperature in the absence of back bombardment.

The grid consists of 180 pieces of 0.007 inch diameter tungsten wire silver-soldered to the oxygen-free-high-conductivity copper cap and support cone. The ends of the tungsten wires are lightly nickel-plated to facilitate "wetting" by the solder. In order that none of the wires shall inadvertently bow inward, they are sprung outward by a stainless-steel jig which holds them as they are soldered in a hydrogen-atmosphere furnace. The slots in the base of the grid cone provide flexibility to mitigate ill effects from differential expansion between

[6] G. J. Lehmann and A. R. Vallarino, "Study of Ultra-High-Frequency Tubes by Dimensional Analysis", *Proc. I.R.E.*, Vol. 33, No. 10, p. 663, October, 1945.

[7] R. R. Law, "Electronics of Ultra-High-Frequency Triodes", accepted for publication in *Proc. I.R.E.*

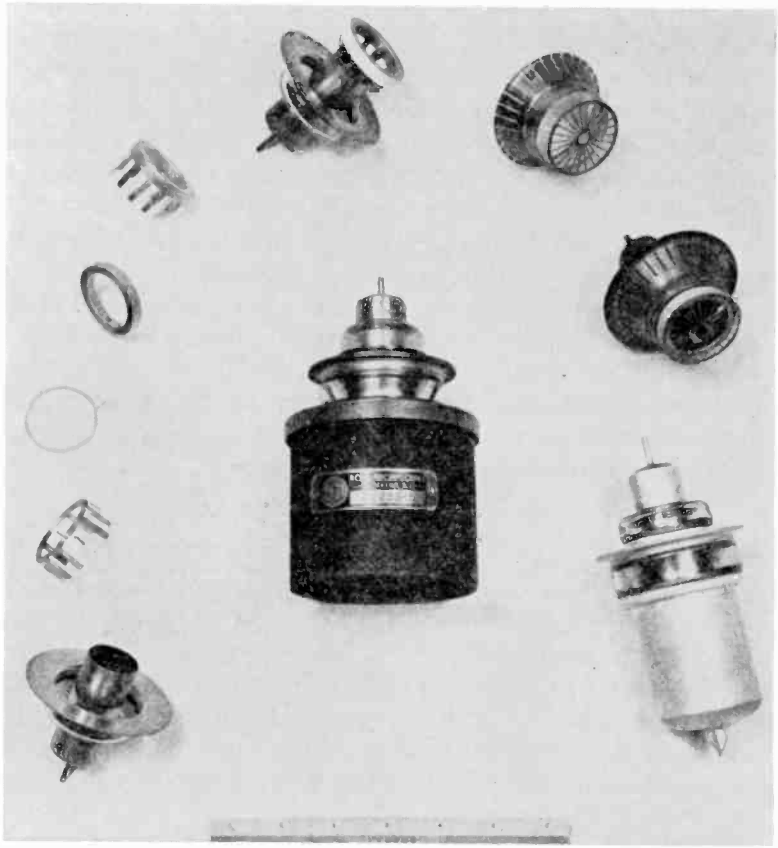

Fig. 1—Details of ultra-high-frequency continuous-wave triode.

the grid cone and the Kovar grid flange. The grid cone is spot welded directly to the grid flange. An electroplated layer of nickel on the base of the cone facilitates making this weld. Because of the excellent grid cooling there is no trace of grid emission. This construction makes possible an unusually rugged tube, and the wires are so refractory that the grid is almost indestructible.

One of the perennial problems in making vacuum tubes is how to seal in the mount or assembled tube without damaging critical parts. Although use of a nitrogen atmosphere to prevent oxidation[8] will suffice for thoriated-tungsten filament tubes, oxide-coated-cathode tubes are more susceptible to damage by overheating and contamination. "Cold-sealing" has been accomplished by radio-frequency-heating tech-

[8] S. Frankel, J. J. Glauber, J. P. Wallenstein, "Medium-Power Triode for 600-Megacycles", *Proc. I.R.E.*, Vol. 34, pp. 986-991, December, 1946.

niques[9], but for experimental tubes the equipment required for this process cannot be justified. In view of the attractiveness of the gold-diffusion seal[10], development of a technique for joining Kovar-to-Kovar by this method was undertaken. It was found that such a seal could be made by the following procedure: 1) copper-plate the Kovar parts, approximately 0.001 inch thick; 2) fire in hydrogen atmosphere for 20 minutes at 1030°C to bond the copper to the Kovar; 3) perform glassing operation in the conventional manner; 4) remove oxide and again copper-plate, the copper layer so applied adheres firmly to the Kovar and provides a vacuum-tight copper-Kovar bond; and finally, 5) a gold ring compressed between the two copper-plated Kovar parts serves to unite the parts during baking by the familiar gold-diffusion process.

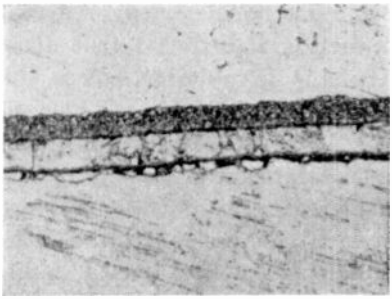

Fig. 2—Diffusion seal for bonding Kovar-to-Kovar.

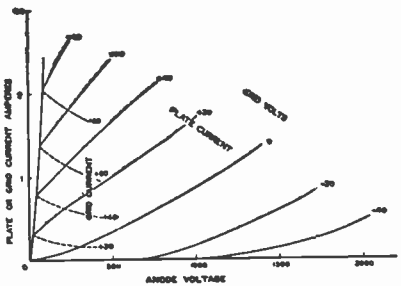

Fig. 3—Static characteristics of ultra-high-frequency continuous-wave triode.

Figure 2 is a photomicrograph of one side of such a composite seal. The Kovar is below, the gold above. The lighter layer between the gold and Kovar is the copper-plate that was fired at 1030°C. The dark layer is unfired copper. There is no visible evidence that the gold has penetrated the copper during the 450°C bake, but when the parts are forcibly pulled apart a layer of gold adheres to the copper. This sealing technique permits assembly of the tube parts without contamination and in the present case does away with the all too familiar problem of poisoning of the oxide-coated-cathodes. Furthermore, the better vacuum obtainable with cleaner parts undoubtedly improves life.

The static characteristics of this tube are shown in Figure 3. For purposes of comparison, its continuous-wave performance as an oscil-

[9] W. P. Bennett, E. A. Eshbach, C. E. Haller, W. R. Keye, "A New 100-Watt Triode for 1000 Megacycles", *Proc. I.R.E.*, Vol. 36, No. 10, pp. 1296-1302, October, 1948.

[10] J. B. Fiske, H. D. Hagstrum, L. P. Hartman, "The Magnetron as a Generator of Centimeter Waves", *The Bell System Technical Journal*, Vol. XXV, No. 2, April, 1946.

lator at 800 Mc is shown in Figure 4. On the basis of this performance the empirical relation for efficiency[7] indicates that its equivalent cathode-grid spacing is 0.015 inch. This checks with the dimensions of the parts when allowance is made for the fact that the hot spacing is approximately 60 per cent of the cold spacing.

Preliminary life tests were made at power levels corresponding to 300, 400, and 500 watts continuous-wave output in rf amplifier service. With the limited data available there is no correlation between life and power level. Inasmuch as the 300-watt-continuous-wave level with a single tube corresponds to transmitting one-kw-peak-power with a "black" picture in the two-tube television transmitter, the remainder of the tests were run at the 300-watt-continuous-wave level.

The primary factor affecting life is cathode temperature. Because of back bombardment resulting from transit-time effects, the heater input must be materially reduced. In practice, it is found that after the tube is up to normal power, the heater power should be reduced about 50 per cent. An additional point of interest came out of the life test data in view of the fact that early samples employed a cathode coating of less than 3 milligrams per square centimeter, whereas 7 to 12 milligrams per square centimeter is recommended. This compromise was introduced in the early tests to minimize cathode peeling during manufacture which frequently occurs during humid weather. These samples gave 400 to 600 hours life. Later samples employing the recommended coating gave more than 1,000 hours life. Evidently life is proportional to cathode thickness.

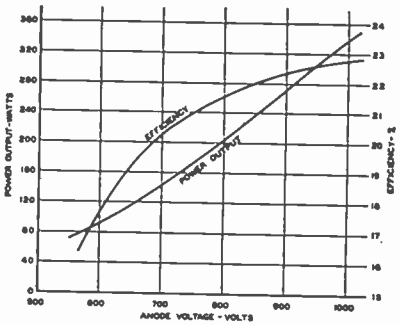

Fig. 4—Performance of continuous-wave triode as oscillator at 800 Mc.

Circuit Development

From the static characteristics of Figure 3 and the experimentally determined optimum operating point it may be deduced that the rf anode voltage swing is about 1,000 volts peak-to-peak under conditions corresponding to one kilowatt power output from the two-tube transmitter. In view of the 0.080 inch grid-anode spacing, the energy stored at the tube electrodes is about 1.0 micro-joule or less than 0.06 micro-joule per square centimeter. The active energy, or energy supplied by the tubes on the other hand is 1.2 micro-joules or approximately 0.08 micro-joule per cycle per square centimeter at 800 Mc. Inasmuch as

$$Q = (2\pi)\ \text{(Stored Energy)}/\text{(Active Energy per Cycle)}$$

and bandwidth or frequency separation between half-power points Δf is[11]

$$\Delta f = \text{(Operating Frequency)}/(Q \text{ of System}),$$

the bandwidth resulting from the capacitance of the tube elements themselves would be greater than 180 Mc. This bandwidth is so large as to be of little practical significance other than to emphasize the fact that the circuit will be the determining factor.

In the case of the cathode-modulated rf amplifier the energy stored in the cathode-grid circuit has no adverse effect on bandwidth. In fact, it may be desirable to store energy in this circuit to stabilize the driver during peak power pulses. In contrast, energy stored in the anode circuit is very detrimental. Unfortunately the present tube cannot be operated in fundamental-mode circuits at these frequencies, and harmonic-mode operation materially increases the stored energy. For push-pull operation the anode line must be three-halves wavelength long. Connections for dc are made at the midpoint. Furthermore, if the circuit is to be tunable over an appreciable frequency range, the electrical position of the discontinuity between tube and circuit will shift. In view of this, it is desirable to keep the characteristic impedance of the circuit so low that special means of transformation will not be required. This is possible in the present case. The four-inch-diameter-internal-conductor one-quarter-inch-radial-separation line even with the most unfavorable match gives rise to a maximum voltage of less than 600 volts peak-to-peak. On this basis the maximum energy stored in the circuit at 800 Mc would be about 5 micro-joules.

To complete the estimate of bandwidth, allowance must be made for the energy stored in the unmatched portion of the output system. Because it is difficult to adjust the load coupling loop size, matching stubs are desirable. With a voltage-standing-wave ratio of $\sqrt{2}$, the energy stored in the stubs and unmatched portion of the output system is about 3.0 micro-joules. To sum up, at 800 Mc the energy distribution would be:

Energy stored in tubes	1.0 micro-joules
Energy stored in circuit	5.0 micro-joules
Energy stored in matching stubs	3.0 micro-joules
Total energy stored	9.0 micro-joules
Active energy per cycle	1.2 micro-joules

[11] F. E. Terman, RADIO ENGINEERING HANDBOOK, McGraw-Hill Book Co., Inc., New York, N. Y., 1943, pp. 429-430.

whereupon the estimated bandwidth is

$$f = \frac{(800)\,(1.2 \times 10^{-6})}{2\pi\,(9.0 \times 10^{-6})} = 17 \text{ megacycles.}$$

In practice the bandwidth may be somewhat greater than this if the load-coupling-loop match or the tube-to-circuit match are more favorable.

The physical layout of the circuits developed for this transmitter may be seen in Figures 5 and 6. In Figure 5, the unit on the left is the driver and the unit on the right is the cathode-modulated rf amplifier. The coaxial line serving to transmit power from the anode cavity of the driver to the cathode cavity of the amplifier with its

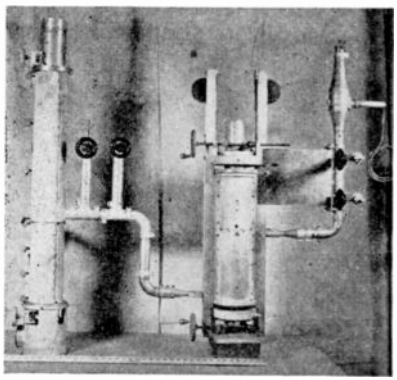

Fig. 5—500-900 Mc driver and rf power amplifier.

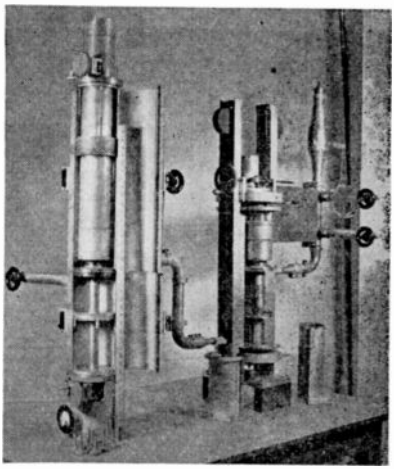

Fig. 6—Rf circuit details.

matching stubs may be seen in the center of the picture. The coaxial line serving to transmit power from the amplifier to the water-cooled resistance load with its matching stubs may be seen in the right of the picture. In Figure 6, the covers of the units have been swung open or partially removed to reveal circuit details.

To take advantage of the bandwidth capabilities of this amplifier, the wide-band modulator shown in Figure 7 was developed. This modulator employs a pair of the aforementioned pulse triodes[1] to cathode-modulate the rf amplifier. These modulator tubes make possible a current change of more than two amperes at an equivalent transconductance of 0.15 amperes per volt. Such a combination of a large-area-cathode "Class-A" modulator tube and an intermediate-area-cathode "Class-B" radio frequency tube is advantageous in wide-band service. The cathode-coupled stage ahead of the pulse triodes serves

to lower the effective input capacitance presented to the video amplifier.

Bias to the cathodes of the amplifier and final modulator stage is supplied through the special choke "L" which is split into sections of progressively increasing size to provide relatively high impedance over the video band. So long as this impedance is large compared to $R_p/(1+\mu)$, the gain is substantially constant and equal[11] to $\mu/(1+\mu)$. In operation, the dc current to the anodes of the amplifier and modulator is substantially constant; modulation at video frequencies serves to switch the current from the amplifier to the modulator and vice versa.

Performance of System

The overall performance of the rf power amplifier and composite system is indicated in Figures 8, 9, and 10.

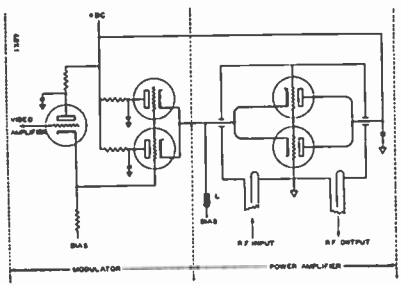

Fig. 7—Wide-band modulator circuit.

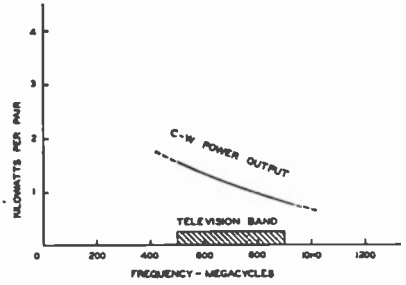

Fig. 8 — Variation of rf power amplifier output with frequency.

Figure 8 shows the variation of continuous-wave power output with frequency at a fixed anode voltage of 900 volts. It will be observed that the anode efficiency of the amplifier is appreciably higher than that shown for the oscillator in Figure 4. The difference arises from the fact that the oscillator must supply its own exciting power whereas the amplifier does not. Inasmuch as the power gain of this tube as an amplifier under typical operating conditions is approximately three, the amplifier output and efficiency may be expected to be about 50 per cent greater than that of the oscillator

Figure 9 indicates the broadband potentialities of the amplifier. Here is plotted the relative voltage in the sidebands as a function of sideband frequency relative to the 800 Mc carrier. The circled points joined by the solid line were taken by direct measurement of sideband voltage in a calibrated spectrum analyzer. Conjugate points were measured with the same circuit adjustment; in each case adjustments were made so that both sidebands would have equal amplitude. The ease with which these adjustments could be accomplished suggests that

the response is nearly symmetrical. Due to the finite bandwidth of the spectrum analyzer it was not possible to measure the response immediately adjacent to the carrier. The intermediate region was checked by direct observation of percentage modulation on the oscilloscope[12]. To increase the accuracy of readings the data were taken at high percentage modulation. Thus, the amplitude of the modulating voltage was adjusted to give 90 per cent modulation at low frequency, whereupon its amplitude was held constant as its frequency was varied. Because of this choice, the ordinate scale of Figure 9 corresponds to percentage modulation as well as relative sideband voltage.

As may be seen from this response curve, the —3-db points are approximately 19 Mc apart. If vestigial sideband operation were employed, such an amplifier would accommodate a color television picture of the highest quality.

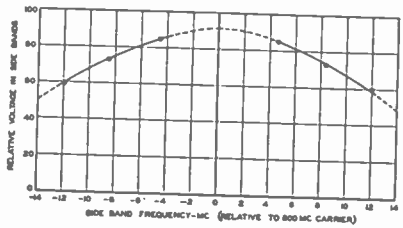

Fig. 9—Wide-band response of rf power amplifier.

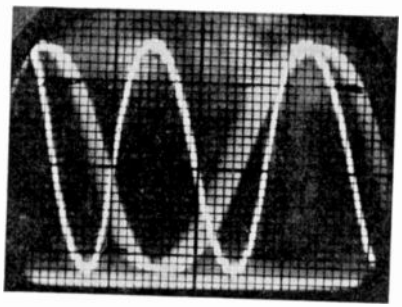

Fig. 10—Rectified rf output with sine wave modulation.

The linearity of modulation is indicated in Figure 10. This photograph shows the rf load-diode-voltage as a function of time with 1.6 Mc sine wave modulation. Zero power level as established by the vibroswitch[12] is indicated by the horizontal line at the bottom of the picture. Under the conditions portrayed the peaks correspond to 1.4 Kw and the modulation is very nearly 100 per cent.

Contrary to the experience of previous workers[8,13,14] there has been no indication of a need for neutralization. This difference arises from the low impedance of the present tubes as compared to those previously available. Although it is possible to adjust the present amplifier so that it will oscillate, this adjustment is far from the normal operating

[12] T. J. Buzalski, "A Method of Measuring the Degree of Modulation of a Television Signal", *RCA Review*, Vol. VII, No. 2, pp. 265-271, June, 1946.

[13] E. Labin, "Design of the Output Stage of a High Power Television Transmitter", *Electrical Communications*, Vol. 20, No. 3, p. 193, 1942.

[14] C. E. Strong, "The Inverted Amplifier", *Electronics*, Vol. 13, pp. 14-16, July, 1940.

point. Because of the relatively high mu, the cathode-anode capacitance is low and the undesired cathode excitation is small in comparison to the driver excitation required for the low impedance system throughout the 500-900 Mc frequency range. Oscillation is possible only when the amplifier is unloaded and when the anode and cathode cavities are detuned to give the appropriate grid-anode-voltage phase relationship[15].

CONCLUSIONS

Tests in a developmental 500-900 Mc television transmitter indicate that oxide-coated cathode triodes may be used for moderate power ultra-high-frequency transmitter applications. Although modulation of the triode presents a serious problem, for wide-band service this difficulty is in part overcome by employing a large-area-cathode "Class-A" modulator tube to cathode-modulate an intermediate-area-cathode "Class-B" rf tube. With tubes and circuits of proper design operating under wide-band conditions there is no need for neutralization in this frequency range.

ACKNOWLEDGMENTS

The writers wish to express their appreciation for the stimulating discussions and practical assistance given by many members of the RCA Laboratories Technical Staff and Service Groups.

[15] E. E. Spitzer, "Grounded-Grid Power Amplifiers", *Electronics*, Vol. 19, pp. 136-141, April, 1946.

AN EXPERIMENTAL SIMULTANEOUS COLOR-TELEVISION SYSTEM*†

By

R. D. Kell, G. C. Sziklai, R. C. Ballard, A. C. Schroeder, K. R. Wendt and G. L. Fredendall

Research Department, RCA Laboratories Division, Princeton, N. J

Part I — Introduction

R. D. Kell

Summary—During 1945 and 1946 a complete sequential television system was constructed and tested. This was followed by the development of a simultaneous system, compatible with the present commercial monochrome television. This paper is the introduction to a group of two papers which describe the transmitting and receiving apparatus used in the simultaneous system.

WITH the resumption of peacetime research and development, color television became a major item in the research program of RCA Laboratories.

A color-television receiver of the simultaneous type had been constructed in 1939. The circuit and tube limitations at that time were such that satisfactory registration of the three-color images could not be obtained.

In 1941 a sequential color system had been used by the National Broadcasting Company to broadcast television pictures. With this work as a background, the first step of our new research program consisted of building, and putting into operation, a complete sequential type of color-television system.[1] The camera made use of the new image orthicon for direct studio pickup. The associated sound was carried by variable-width pulses occurring during the horizontal-return-line time.[2] The result of this work was demonstrated on December 13, 1945. In some of the tests, the radio transmitter operated on 288 megacycles,

* Decimal Classification: R583.

† Reprinted from *Proc. I.R.E.*, September, 1947.

[1] R. D. Kell, G. L. Fredendall, A. C. Schroeder, and R. C. Webb, "An Experimental Color Television System," *RCA Review*, Vol. 7, pp. 141-154, June, 1946.

[2] G. L. Fredendall, K. Schlesinger, and A. C. Schroeder, "Transmission of Television Sound on the Picture Carrier," *Proc. I.R.E.*, Vol. 34, pp. 49-61, February, 1946.

with a power output of approximately 5 kilowatts. In other tests, radio-relay-type equipment was used, operating on approximately 9000 megacycles. With this work as a background it was possible to evaluate more accurately the technical difficulties more or less inherent in such a system.

In parallel with this work, a study was being made of the possibilities of a simultaneous color system. The important fact that the simultaneous color system could be made an integral part of the expanding black-and-white television service made such a system extremely attractive. Because the three primary pictures are transmitted at the same time in the simultaneous system, each of the three primary color pictures can have the same number of lines per picture, the same number of fields per second, and the same other standards as the present monochrome system. If they are so chosen, the present monochrome and the simultaneous color systems are identical in all basic respects, except that the color system transmits three independent monochrome signals at one time. This condition results in the enormously important fact that, with only the addition of a radio-frequency converter, and without any alterations, a present monochrome receiver will receive the programs transmitted by the simultaneous color method (reproducing them in monochrome). The radio-frequency signal, corresponding to the green picture, contains information as to picture detail and values of light and shade which, when translated into black and white in the monochrome receiver, is capable of producing an excellent picture. By associating the frequency-modulated sound channel with the green picture, at the same spacing as in the present monochrome standards, the tuning of the converter to the green-picture radio-frequency channel not only makes possible the reception of a black-and-white image from the color transmission, but also makes possible the reception of the associated sound. The red- and blue-picture signals may be transmitted on separate radio-frequency carriers and vestigial sidebands located adjacent to the green signal. Without regard for compatibility, visual observations alone indicate that the properties of flicker and resolution of images containing red and green components are sufficiently similar to monochrome images that the same standards should also apply. With reference to the blue component, observations have indicated that an appreciable reduction in the bandwidth of the blue video is possible without degradation of the color image. This is due to the eye having lower acuity for blue light than for red and green light at brightnesses which are considered desirable and at the relative brightnesses which produce subjective white. A

simple confirmation of the lower acuity may be made by observation of the blue component of a black-and-white test pattern of satisfactory brightness at the normal viewing distance. It is found that the apparent resolution in the blue image is definitely inferior to the resolutions of red, green, or black-and-white images. From the point of view of economy of bandwidth in channel allocation for color television, this is a fortunate condition. A satisfactory blue video bandwidth for the experimental system was 1.3 megacycles.

The transmission standards used are the flolowing:

525 scanning lines
Odd-line interlacing } green, red, and blue components
60 fields

Standard synchronizing wave form on the green video signal
4.5-megacycle bandwidth for green and red signals
1.3-megacycle bandwidth for the blue signal.

In the color receiver, the three signals are separated by means of intermediate-frequency circuits and used to control the brightness of the three color images, which are optically superimposed.

Preliminary attempts at producing pictures using the simultaneous method involved the use of a single cathode-ray tube having three electron guns with a single deflecting yoke. The three scanning rasters were at different positions on the face of the cathode-ray tube. Preliminary results with this tube were sufficiently promising to justify the design and construction of a color-slide scanner capable of generating the three color signals of the simultaneous system.[3] The limitations in a system in which different areas of a single cathode-ray tube are scanned soon became evident. Work was then concentrated on the construction of a projection-type receiver having a 15- by 20-inch screen where three small cathode-ray tubes simultaneously projected the three color images on the viewing screen.[4] The reproduction of a picture by this receiver using signals transmitted by coaxial cables was demonstrated to the press and others on October 30, 1946.[5]

At a later demonstration, on January 29, 1947, receivers of this type were operated over a radio-frequency circuit. At this time a simple radio-frequency converter connected in the antenna circuit of a standard black-and-white receiver made possible the reception of the green

[3] G. C. Sziklai, R. C. Ballard, and A. C. Schroeder, Part II, "Pickup Equipment," *Proc. I.R.E.*, this issue, pp. 862-871.
[4] K. R. Wendt, G. L. Fredendall, and A. C. Schroeder, Part III, "Radio-Frequency and Reproducing Equipment," *Proc. I.R.E.*, this issue, pp. 871-875.
[5] A progress report, "Simultaneous All-Electronic Color Television," *RCA Review*, Vol. 7, pp. 459-468; December, 1946.

component of the simultaneous color picture, along with the associated sound. To illustrate the optical efficiency of a simultaneous color system, the next step in the development program was the construction of a projection-type receiver capable of producing a picture 7½ by 10 feet. This picture had a brightness of approximately 10 foot lamberts. The receiver was demonstrated at the Franklin Institute on April 30, 1947, using color slides and 16-millimeter motion-picture film as subject material.

Several major technical items remain before color television can be considered for a commercial service. Among these items may be included studio and outdoor cameras. One of the major remaining problems is the field testing of the complete system. This will involve the construction and installation of high-power television transmitters with the associated terminal facilities for film and studio transmission. Propagation measurements must be made to determine the broadcast coverage possible in the new range of ultra-high frequencies required for color. The preliminary indications are that much higher effective radiated powers will be required for color transmissions in the 500- to 900-megacycle region than are at present required in the commercial television channels. Tests on various types of receivers under actual operating conditions must be made to determine the practicability of the receiver design when placed in the hands of the layman. The tests of the simultaneous color system have been sufficiently complete to indicate that there are no serious fundamental technical difficulties. The work with the system has indicated, directly or as a result of analysis, the objectives of further research and development.

It is the purpose of this group of papers to describe the system, the experimental apparatus, and the tests that have been made. The description is divided into two parts: "Pickup Equipment," and "Radio-Frequency and Reproducing Equipment."

ACKNOWLEDGMENT

The authors of this group of papers wish to acknowledge the interest and encouragement of E. W. Engstrom and V. K. Zworykin. The flying-spot tubes and color kinescopes used were developed by D. W. Epstein and his associates, with phosphors supplied by H. W. Leverenz. The dichroic mirrors were made by M. E. Widdop. Credit should also go to all the other members of the RCA Laboratories organization who participated in the work.

Part II — Pickup Equipment

G. C. SZIKLAI, R. C. BALLARD AND A. C. SCHROEDER

Summary—The technical development of the present flying-spot-type color-television pickup equipment is described. The use of a high-voltage kinescope with a short persistence phosphor, of the multiplier-type phototubes and dichroic filters, permit the construction of apparatus for flying-spot scanning of color slides and color motion picture film providing excellent color video signals. The circuit equalization for the phosphor persistence is described in detail. The use of the simple flying-spot scanner for studio pickup is described.

I. INTRODUCTION

ONCE a careful study of the technical aspects of color-television systems reached a point where a systematic development of a particular system could be scheduled, the first part of the program was to develop terminal equipment with the greatest flexibility and reliability. For the initial adjustments of the first simultaneous-color-television image reproducers, a monoscope signal was divided by three parallel-input amplifiers, and thus the three grids of the reproducer were controlled by the same signal. This type of signal was perfectly adequate to check resolution, registration, and proper balance of control voltages to produce a good black-and-white picture. By adjusting the balance of the picture signals, a monochrome picture in a choice of colors could be obtained. The registry obtained with three identical simple signals was sufficiently encouraging to justify undertaking the development of a signal source providing a complete color picture.

The use of the monoscope as a source set the standards high, since it could be relied on for good resolution, perfect registration, high signal-to-noise ratio, freedom from spurious signals, etc. In order to obtain a similarly high-quality color signal, a special slide scanner was developed, to be used with Kodachrome transparencies to provide the desired high-quality color video signals from a wide variety of subjects.[1]

II. THE SLIDE PROJECTOR

A signal-generation method using a cathode-ray-tube flying-spot scanner, with beam splitters and multiplier phototubes, was chosen because of the inherent registry and natural freedom from spurious signals of such a system. The concept of cathode-ray-tube flying-spot

[1] The slide and motion picture scanners, as well as the color receivers, have been described briefly in a progress report; see "Simultaneous All-Electronic Color Television," *RCA Review*, Vol. 7, pp. 459-468, December, 1946.

scanning is old. It was attempted both in this country and abroad several years ago, but due to the lack of satisfactory components for the system, several times it was tried and abandoned.

A re-examination of the problem in the course of the development revealed that improved and new tools were available which made the flying-spot scanning not only practical, but, from many respects, superior to other known methods of picture-signal generation, even for black-and-white transmission.

With the use of very-short-persistence phosphors in the flying-spot cathode-ray tube, the problem of equalization has been considerably simplified. The use of multiplier phototubes provides high video input to the amplifiers, thus minimizing the usual difficulties in shielding to eliminate spurious signals. In spite of the equalizaton for the phosphor characteristic, the amplifier is very simple and the amplifier noise is negligible.

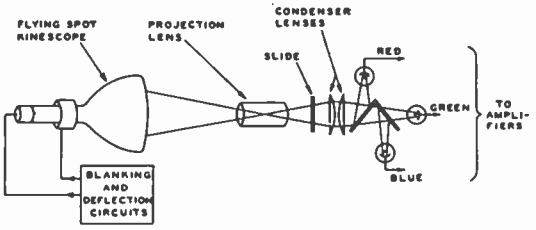

Fig. 1—Diagram of the color-slide scanner.

The schematic diagram of the color-slide scanner is shown in Figure 1. As shown, the optics of a conventional slide projector are used in reverse. The screen of a short-persistence-phosphor kinescope replaces the projection screen, and the projection lamp of the slide projector is replaced by the light-dividing assembly and the phototubes. The scanning raster is imaged by the projection lens onto the slide. The transmitted light is then collected by the condensing-lens system and then divided by dichroic mirrors which reflect one color of light and pass the other colors. The divided light beams are further filtered by color-absorption filters, then collected by multiplier phototubes which convert the varying light intensity of the spot as transmitted by the slide into video signals corresponding to the three primary colors of the slide.

A photograph of the complete flying-spot color video signal generator is shown in Figure 2. The synchronizing, blanking, and deflecting circuits for the flying-spot kinescope are at the bottom of the rack. The anode supply is in the center and the video amplifiers are at the top. The location of the cathode-ray tube and light paths are shown by the dotted lines.

The flying-spot kinescope utilizes a zinc-oxide phosphor[2] which decays to less than 5 per cent of its original intensity in 1 microsecond. The kinescope is operated at 30 kilovolts and 400 microamperes. The first-anode focusing potential is variable around 7 kilovolts. The raster has a brightness of approximately 200 foot lamberts. In order to have a definite black-level reference, the return lines of the scanning raster are blanked out by applying blanking pulses to the kinescope grid.

The objective lens is an $f/1.9$ high-quality color-corrected lens in a focusing mount. Lenses with a lesser degree of color correction were tried and were found to provide satisfactory signals, but the change of lenses is definitely noticeable; and since the slide scanner is relied upon as a standard signal generator, the lens with the best color correction was chosen. The whole optical assembly is mounted on the same chassis with the three video amplifiers.

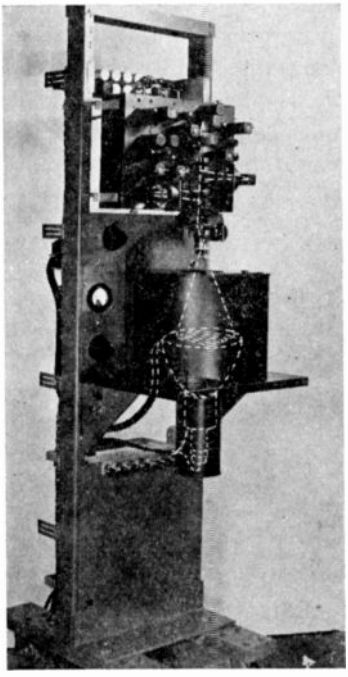

Fig. 2—The color-slide scanner.

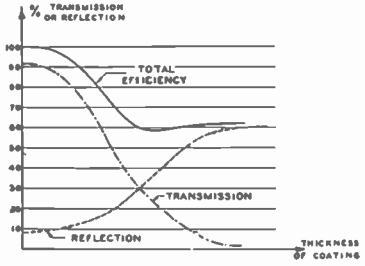

Fig. 3—Transmission and reflection of chromium mirrors.

III. The Dichroic Mirrors

The use of dichroic mirrors for a light-splitter, instead of half-silvered mirrors and color filters, reduces the light losses and therefore provides a signal with a higher signal-to-noise ratio. If semitransparent mirrors were used in the arrangement, as shown in Figure 1, the light flux would be divided in three parts, and thus only 33 per cent of the red, blue, or green light of the total would reach the phototube even if the semitransparent mirrors were 100 per cent efficient. Actu-

[2] H. W. Leverenz, "Luminescence and Tenebrescence as Applied in Radar," *RCA Review*, Vol. 7, pp. 199-239, June, 1946.

ally, the efficiency of a chromium mirror drops rapidly when the transmission is reduced, as shown in Figure 3. Considering that the first mirror would reflect 17 per cent of the light to the red tubes, and transmit 58 per cent, and the second mirror would divide the transmitted light by providing 30 per cent of the 58 per cent, or 17.4 per cent, of the original light, the light flux would be divided equally, but the over-all efficiency would be reduced by a factor of approximately 6.

Dichroic mirrors which reflect one color light and transmit others have been known for some time, and were made with certain crystals, aniline dyes, or thin metallic films. A thin film of gold transmits green light and reflects the lights in the red spectral region. The dichroic mirrors used in the present color-television terminal equipment are the quarter-wave dielectric-film type.[3] This type of dichroic mirror is made by evaporating alternate layers of insulators with high and low index of refraction of predetermined thickness on glass. The mirrors have no appreciable absorption, and if both sides are properly coated to eliminate undesirable reflection, they may be considered 100 per cent efficient. Figure 4 shows the spectral characteristics of two dichroic mirrors, the ordinate representing the transmission at various frequencies within the visible range of the spectrum. The complementary percentage is reflection. By using a dichroic mirror with a characteristic as shown in curve *A* of Figure 4 as the first beam divider, practically all the red component of the light flux is reflected to the phototube of the red channel, while the remaining portion of the spectrum is transmitted to the second dichroic mirror, having a characteristic as shown in curve *B* of Figure 4, reflecting substantially the total blue portion of the light and transmitting the whole green component. Thus it may be readily seen that, by the use of dichroic mirrors, a light-flux input about six times higher is available than with the use of semi-transparent mirrors.

Another compact beam-splitting arrangement available with dichroic filters is shown in Figure 5. The light beam, after passing the transparency, falls upon the crossed dichroic mirrors. While both mirrors pass the green component, the combination will not pass the red and blue components of the light, which are reflected to their proper phototubes.

Due to the fact that the dichroic mirrors used did not have the ideal spectral response for the three chromatic separations of the picture, thin absorption filters were used in front of the phototubes to improve upon the spectral selectivity of the dichroic mirrors.

[3] G. L. Dimmick, "A New Dichroic Reflector," *Jour. Soc. Mot. Pic. Eng.*, Vol. 38, pp. 36-44, January, 1942.

IV. The Amplifier Circuits

In some of the literature on flying-spot scanning[4] it was assumed that a different frequency compensation would be needed for the transition from black to white than for the change from white to black. This was based on the known rise-and-decay characteristic of the phosphor. The assumption would be correct if a pulse corresponding to the video signal appeared on the grid of the flying-spot kinescope, since the phosphor excitation is practically instantaneous, while the decay is exponential. However, when a transition from black to white is scanned, the spot in time has an exponential shape and a changing position. Thus it delivers to the phototube through the front edge of the transition its maximum brightness; then, as it moves, it still provides the maximum instantaneous brightness *plus* the decaying brightness. The light input to the phototube is thus proportional to the integral of the original light-decay characteristic. Since the decay curve is an e^{-x} type of function, its integral is also of the e^{-x} form. As the scanning spot moves from white to black, the light falling on the phototube decreases according to $(1 - e^{-x})$, both the rise and fall signals following the same law. Figure 6 shows an oscillogram at line frequency of the voltage generated in the scanning of a vertical white bar. The shape is typical of the square-wave response of a circuit in which the high frequencies are deficient. The fact that the light decay characteristic of the phosphor is exponential simplifies the equalization. The equalization required is of the type supplied by simple resistance-capacitance combinations. Figure 7 shows the same signal after equalization. The sides of the wave are now square within the accuracy of the measurement.

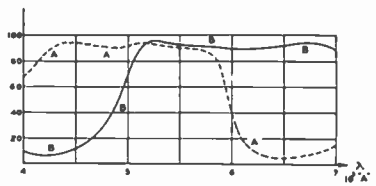

Fig. 4—Spectral characteristic of two dichroic mirrors.

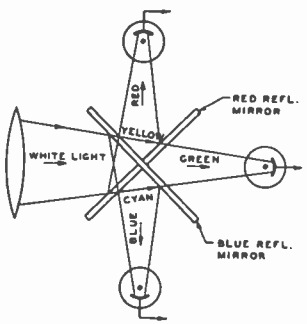

Fig. 5—Crossed dichroic beam-splitter.

The oscillogram is a composite of all the 525 lines of the scanning

[4] Kurt Bruckersteinkuhl, "The Persistence of Phosphors and its Meaning for Flying-Spot Scanning with Cathode-Ray Tubes," *Fernseh A.G.*, Vol. 1, pp. 179-186, August, 1939.

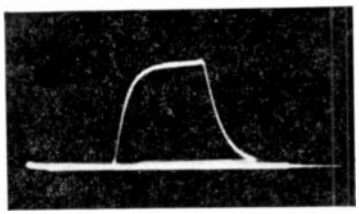

Fig. 6—Oscillogram of the signal from a white bar.

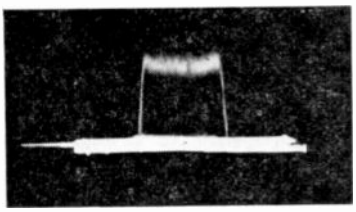

Fig. 7—Oscillogram of the corrected signal from a white bar.

raster. The irregularities across the top of the wave are due to the random grain structure of the phosphor.

The circuit constants used to correct for the phosphor are much the same as those used to correct for the capacitance across the input circuit of a conventional television-camera amplifier. However, it was found from observation of the square-wave response of the flying-spot scanner that the decay characteristic of the phosphor is only to the first approximation a simple exponential.

The square-wave response of the flying-spot scanner is shown again with time and amplitude co-ordinates as the bottom curve in Figure 8. The experimental determination of the required equalization time constant indicated that it was about 1.5 microseconds. With this correction applied, however, it was found that there was a large residual transient overswing response to the square wave, as shown in the top curve. An additional circuit having a time constant of 0.2 microsecond was experimentally determined as being required to make the response to the square wave come within the accuracy of measurement.

The circuit diagram of the equalized amplifier is shown in Figure 9. The 120,000-ohm resistor shunted by the 25-micromicrofarad variable

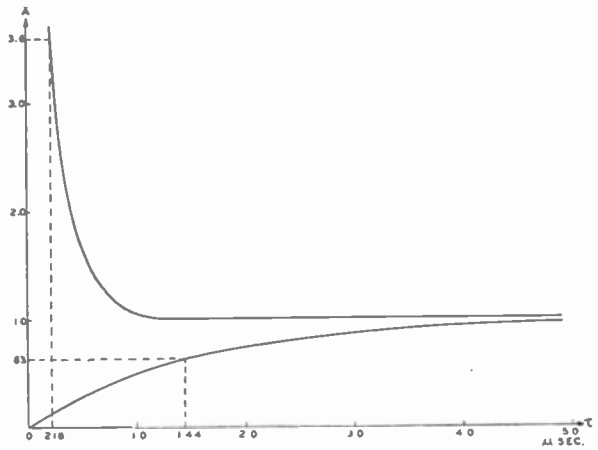

Fig. 8 — Unit-function responses of the flying-spot scanner.

capacitor in the plate circuit of the first stage is adjusted to the time constant of 1.5 microseconds. The 560 ohms in series with the 390-micromicrofarad capacitor across the output of the phototube is the other circuit having the time constant of 0.2 microsecond.

It may be interesting to note that some of the multiplier dynodes and the photocathode of all three phototubes are supplied by a grounded positive supply, while the last stages are connected to the regulated B supply of the amplifier. This circuit arrangement minimizes the high-voltage requirements with respect to the ground, as well as the feedback and cross talk due to the varying current drain of the last dynode stages. The voltage of the first seven dynodes of all three tubes may be controlled by the variable D (dynode) supply, and by this means the

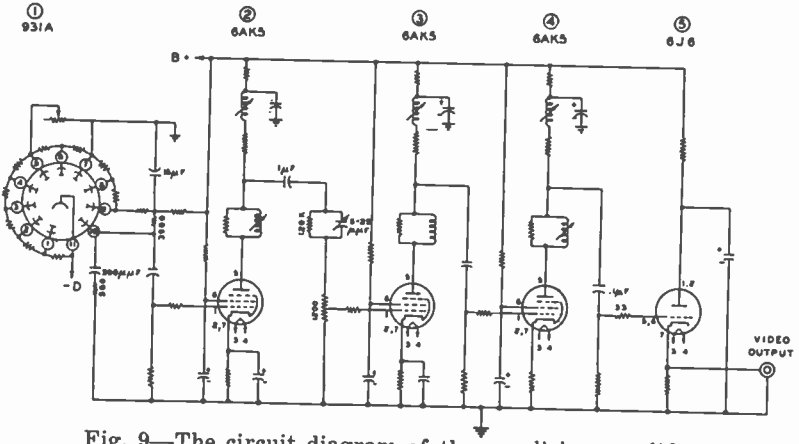

Fig. 9—The circuit diagram of the equalizing amplifier.

video levels of all three channels may be varied simultaneously to compensate for the different densities of the slides. Three variable shunt resistors between dynodes 5 and 7 of each phototube can also be used for adjusting the video level, and with control each channel may be varied individually to provide the desired color balance. Optionally, the potentiometer in the grid circuit of the second video amplifier may also be used for color balance. Due to the low impedance of the controls, the high-frequency response of the signal is not affected. The output of the four-stage video amplifiers at normal brightness level is in the order of 1 volt peak-to-peak.

V. Gamma-Correction Circuit

For maximum fidelity of color reproduction, the light output of the receiver should be directly proportional to the light input to the photo-

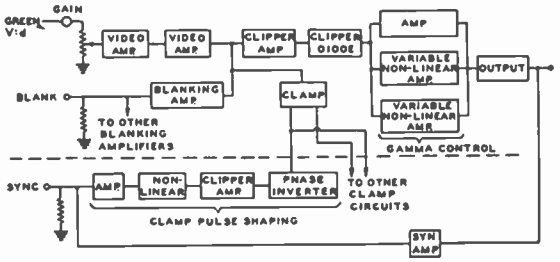

Fig. 10 — Block diagram of the green channel of the gamma-control amplifier.

sensitive device. In other words, the gamma of the system should be unity.

Since, in the flying-spot type of pickup, the voltage output is directly proportional to the light input, the video signal with linear amplifiers will have voltage proportional to light input.

However, the kinescope is not linear, since it takes more volts to give the same change in light output at low light than at high lights. A nonlinear amplifier must, therefore, be provided, with the reciprocal of the kinescope characteristic, in order to make the relation of the input to the output light linear. Since this amplifier attempts to make the over-all gamma unity, it is called the "gamma-correction amplifier." There are, of course, three separate amplifiers required, one for each color. In these amplifiers the kinescope blanking is added to all three signals and the RMA synchronizing signal is added to the green signal.

Figure 10 shows a block diagram of the green part of the amplifier. The other two are identical, except that the synchronizing amplifier is omitted.

The blanking and video signals are mixed in the common plate load of two 6AC7 tubes. Most of the blanking is clipped off by the clipping circuit to leave a small amount of setup. Since the black level in a color synchronizer must be accurately controlled, the clipper must be linear down to clipping level, and the clipping level must be accurately controlled. For this reason a special type of clipper is used, and a clamp circuit is used to set the direct current on the grid of the clipper. Figure 11 shows the clamp circuit in detail. Equal pulses of opposite polarity are applied to the plate and to the cathode of two diodes with the indicated polarity. During the time of these pulses, the

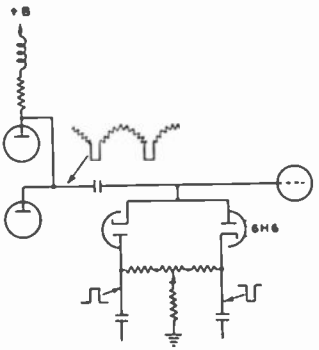

Fig. 11—Detail of the clamp circuit.

clamp circuit may be considered as a short circuit to a point halfway between the plate and cathode. The direct voltage of this point with respect to ground and cutoff voltage of the clipper is obtained by grounding the proper point of the resistor between the plate and cathode. Since the pulses are at horizontal frequency and occur during horizontal blanking, the black level in the picture is held at a constant direct voltage, which is so chosen that it is very close to the cutoff level of the clipper.

The pulses for the clamp circuit, which must occur immediately after each synchronizing pulse, are derived from the RMA synchronizing signal by a nonlinear differentiating circuit, as shown in Figure 12.

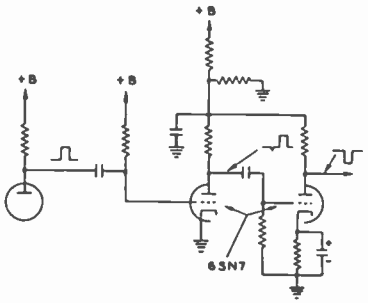

Fig. 12 — Detail of the nonlinear differentiating circuit for making clamping pulses of RMA synchronizing signals.

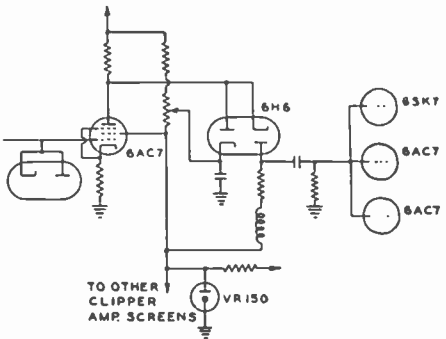

Fig. 13—Detail of the clipper circuit.

Due to the high positive bias on the grid resistor of the first half of the 6SN7, the tube draws considerable grid current and holds the grid at zero bias. When the output of the amplifier driving this tube attempts to swing the grid positive, the grid draws slightly more current, but holds the zero bias so that there is no change in the plate current. However, at the back edge of the input pulse there is nothing to stop the grid from swinging far below cutoff. Due to the very small coupling capacitor, the grid immediately starts to charge up to +300 volts at a rate determined by this capacitor and the grid resistor until it reaches zero bias again. By adjusting the time constant of this input circuit and the amplitude of the driving signal pulses, any desired width can be obtained, starting at the back edge of the synchronizing pulses. After some further clipping, these pulses are fed to the grid of a phase inverter with equal plate and cathode resistors. These push-pull pulses are then fed to the three clamp circuits.

Figure 13 shows the clipper circuit. The plate load resistor is fed through a diode so that, when the plate voltage is higher than a certain

value, no signal will pass. This, however, changes the plate load to a higher value, and the signal is then so high that some of the high frequencies get across the diode capacitance. To eliminate this, a second diode shorts out the high-frequency plate load soon after the first diode opens up.

The output of the clipper is fed to the three grids of the nonlinear gamma-correcting circuit shown in Figure 14. Black is positive on the grids and is held at zero bias by the grid current of the three tubes.

The screen voltages of two of the tubes are variable in steps by a five-position switch. When this switch is in the first position, both screen voltages are at 0 and these tubes are inoperative, only the 6SK7 passing the signal. On the second position one of the tubes has some screen voltage, but its cutoff is low so that only the blacks are amplified. Going to the third, fourth, and fifth positions, the blacks are amplified

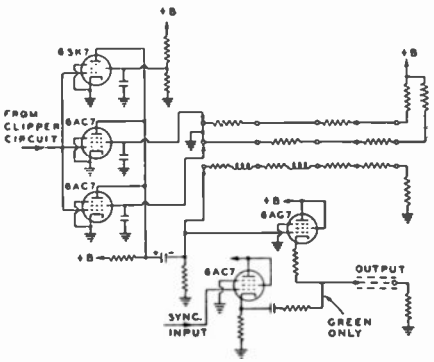

Fig. 14 — Detail of the gamma-control circuit.

more, and thus the gamma is further reduced. In order to keep the peak-to-peak signal constant, the plate load resistor is also switched, being lowered for each successive position. The signal is then fed to the cathode follower output of the amplifier, where the RMA synchronizing signal is added in the case of the green signal.

VI. Motion-Picture-Film Scanner

Essentially the same scheme was utilized in a motion-picture-film scanner with the film gate replacing the slide holder. Since a 30-frames-per-second reproduction of the film was both acceptable and expedient, the job at hand was a simple one. The film moving mechanism of a standard RCA 16-millimeter home sound-film projector was altered by substituting a synchronous-motor drive. The arrangement of the motion-picture scanner is shown in Figure 15. The flying-spot raster on the kinescope replaced the projection screen, and it is imaged by the $f/1.65$ lens on the film. The transmitted light is treated in the same

manner as described for the slide scanner. Under this condition each frame is scanned twice to give the required 60 fields per second. The pull-down mechanism may be speeded up considerably; otherwise, it is necessary to blank approximately 30 per cent of the field time to avoid showing the distorted picture produced during the film pull-down time. The proper 24-frames-per-second operation may be obtained by any of the schemes utilized in the past with nonstorage pickup devices.

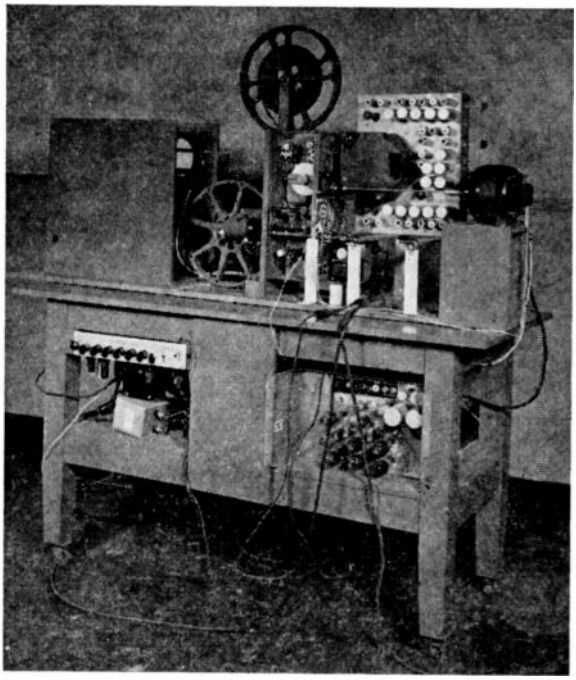

Fig. 15—The motion-picture scanner.

VII. The Flying-Spot "Live" Pickup

The equipment used for scanning of opaque objects, shown in Figure 16, is similar to that used for the slide scanning. The flying-spot kinescope is mounted horizontally to project the raster by means of a 5-inch focal-length projection lens of $f/1.5$ aperture to an area approximately 18 by 24 inches, about 12 inches behind the rectangular phototube assembly frame, and at a convenient height from the floor. Illumination from any source other than that from the kinescope contributes only a noise component to the picture signal and is, therefore, to be avoided. The meter beneath the kinescope indicates the beam current. Directly below is the video-amplifier chassis, the circuit of which is quite similar to that of the slide-scanner amplifier. Beneath this is the synchronizing, blanking, and deflection chassis, which is

identical to that of the slide scanner. At the bottom of the rack is the kinescope anode supply. This unit is a recently developed regulated radio-frequency direct-current supply which delivers approximately 1 milliampere beam current at 30 to 40 kilovolts.

The three similar uncovered units on the adjacent rack are regulated direct-current supplies. The panel with the control at the left is a 2000-volt phototube supply with grounded positive. Just below is a heater supply and the main control panel. The amplifier strips at the top were added for future development work.

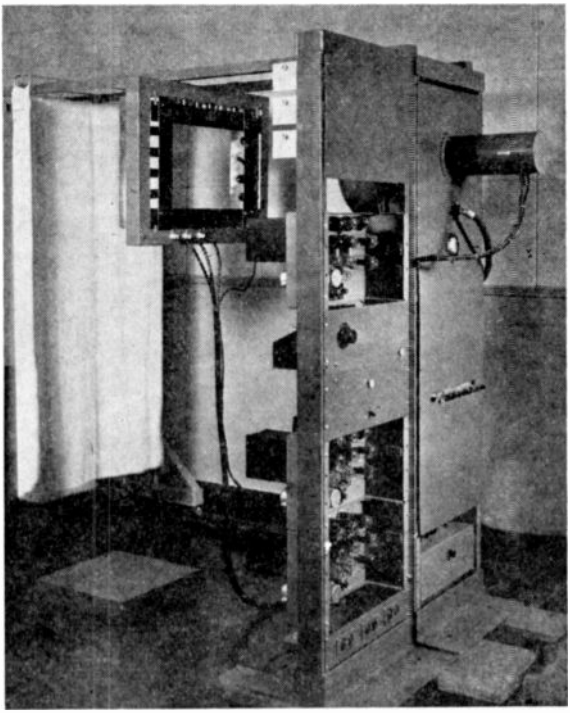

Fig. 16—The live-pickup scanner.

The phototube assembly used in the opaque pickup is shown in detail in Figure 17. It consists of a hollow metal frame on three inside edges of which are mounted a series of type 931A phototubes These are arranged so that along the frame there is a succession of red-, green-, and blue-filtered phototubes. Additional red tubes are used to compensate for lack of sensitivity in the long wavelengths. All phototubes of each color were paralleled to feed into common load resistors.

It may be pointed out that, with flying-spot scanning, each phototube picking up light reflected from the scanned area produces in the reproduced picture an effect the same as though a light source were at

that location. Since, with color-selective individual phototubes, the effect is as though the subject were illuminated by colored lights, to avoid separation of colors it is desirable to have the phototubes collect light of all three colors at the same point. An auxiliary spot pickup (providing an effect similar to a spotlight) was added to supplement the flat lighting effect of the phototube frame. This was conveniently accomplished by the use of three phototubes and the crossed dichroic mirror system. Figure 18 shows the essential parts. A condenser lens was used in front to increase the efficiency.

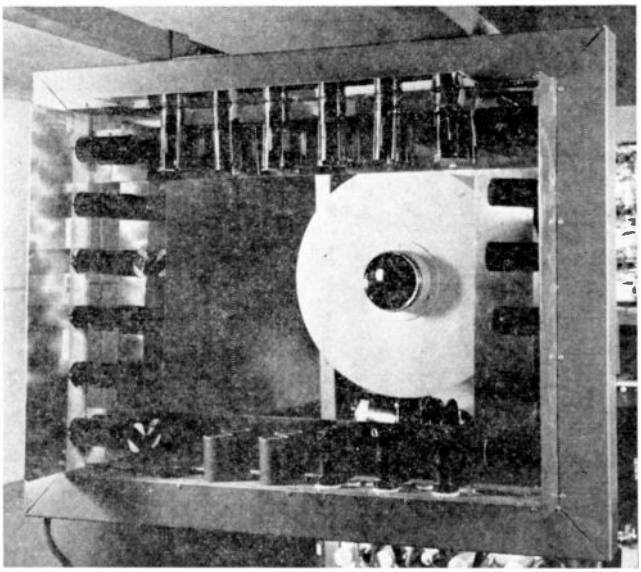

Fig. 17 — The phototube assembly.

Since the 931-A type of phototube does not lend itself readily to high-aperture optical systems, new experimental multiplier phototubes have been developed. Figure 19 compares these with the 931-A type. In the new phototubes the whole front end serves as the photocathode, which in the large tube shown is 5 inches in diameter. This tube has a stacked-ring dynode assembly of the turbine-blade type. Due to the large sensitive area, it greatly outperforms the 931-A type in signal-to-noise ratio at low light levels. For color it must be used at some distance from the subject, or be provided with a light-mixing system to avoid the color separation previously mentioned.

The smaller phototube is of similar construction. Its 1½-inch diameter makes it suitable either for close grouping or for use with a dichroic mirror system. In either case, a lens may be added to increase the pickup.

These new phototubes make it possible to exceed the performance of the human eye at low light levels. An observer standing beside the phototube is unable to distinguish details of the subject which are reproduced satisfactorily by the system.

VIII. Performance

The amplifiers have a flat response up to 5.5 megacycles, and a resolution of 400 lines or better can be obtained in both directions. The pictures are free from shading and other spurious signals and have excellent halftone gradations. The registration of the three signals is inherently correct.

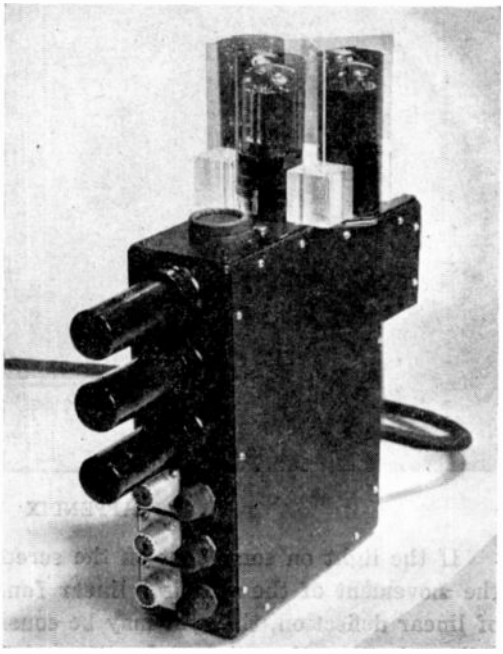

Fig. 18 — The phototube "spot" assembly.

With the electron-multiplier phototube operating at the light levels involved in the flying-spot-scanning arrangement, the noise output of the phototube is proportional to the light input. As a result, the noise is a constant percentage of the signal, giving the equivalent in appearance to grain in motion-picture film. This is a very desirable condition, as contrasted with the conventional camera tube where the noise is of constant amplitude, independent of the picture brightness.

By removing the light-splitter and using a single phototube and amplifier, an excellent black-and-white signal generator may be obtained. The freedom from noise, shading, and other spurious signals

provides a contrast range and picture quality not yet attained, even for black and white, by any other means than a monoscope. The simplicity and excellence of performance of the arrangement is such that it has much to recommend it as a source of television signals for general laboratory and factory test use. Its flexibility is such that it will find application in the television studio as a very convenient method for televising titles, special effects, and as a flexible substitute for the monoscope.

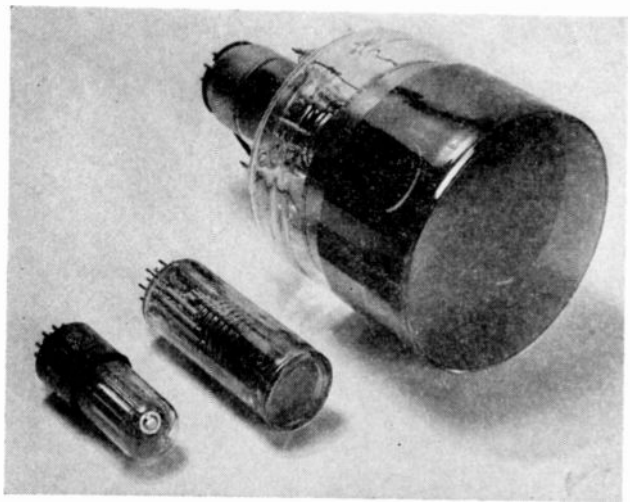

Fig. 19—Larger-aperture phototubes.

APPENDIX

If the light on some spot on the screen is a function of time, and the movement of the spot is a linear function of time, as in the case of linear deflection, the spot may be considered to have a shape along a line given by the original function of time.

When the spot moves from behind a mask into an opening, at first only the light from the spot being hit by electrons strikes the phototube. A little later, as the spot moves farther into the opening, the light from the spot being hit by the electrons has the light from the spots which had been hit a short time before added to it, since they are still emitting some light. In other words, the light output as a function of time as the spot moves into an opening is the integral of the light output with respect to time of the phosphor.

Assume that the light output as a function of time rises instantaneously and decays according to the function.

$$L(t) = a\epsilon^{-\lambda_1 t} + b\epsilon^{-\lambda_2 t}.$$

Then the signal will be

$$S = \int_0^t L(T)\,dT = \int_0^t (a\epsilon^{-\lambda_1 T} + b\epsilon^{-\lambda_2 T})\,dT$$

$$S = \frac{a}{\lambda_1} + \frac{b}{\lambda_2} - \frac{a}{\lambda_1}\epsilon^{-\lambda_1 t} - \frac{b}{\lambda_2}\epsilon^{-\lambda_2 t} \tag{1}$$

so that, when the spot is completely in the opening (at $t = \infty$),

$$S = \frac{a}{\lambda_1} + \frac{b}{\lambda_2}.$$

Starting from this level of signal, when the spot goes behind a mask,

$$S = \frac{a}{\lambda_1} + \frac{b}{\lambda_2} - \int_0^t L dt = \frac{a}{\lambda_1} + \frac{b}{\lambda_2} - \int_0^t (a\epsilon^{-\lambda_1 t} + b\epsilon^{-\lambda_2 t})\,dt$$

$$S = \frac{a}{\lambda_1}\epsilon^{-\lambda_1 t} + \frac{b}{\lambda_2}\epsilon^{-\lambda_2 t}.$$

The correcting networks for the $Z_n 0 - (Z_n)$ phosphor in the amplifier described are shown in Figure 20.

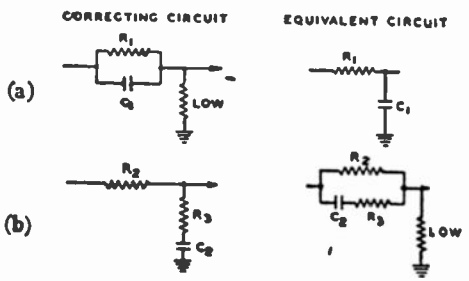

Fig. 20—Correcting networks.

The unit-function response of the network for which (a) is the correction is

$$f_1 = 1 - \epsilon^{-t/R_1 C_1},$$

and for which (b) is the correction,

$$f_2 = \frac{R_L}{R_2}\left[1 + \frac{R_2}{R_3}\epsilon^{-t/R_3C_2}\right].$$

Since only the shape of the function is of interest, it may be normalized by dividing by R_L/R_2, so that $f_2 = 1 + \frac{R_2}{R_3}\epsilon^{-t/R_3C_2}$. This means that the flying-spot in passing a boundary gives a signal as though a unit function had gone through two networks, one having the unit-function response f_1 and the other f_2. In order to find the unit-function response after going through both these networks, we use the superposition theorem, which states that

$$F(t) = f_1(0)f_2(t) + \int_0^t f_1'(t-T)f_2(T)\,dT.$$

Since $f_1(0) = 0$,

$$F(t) = \int_0^t \frac{1}{R_1C_1}\epsilon^{-\frac{t-T}{R_1C_1}}\left[1 + \frac{R_2}{R_3}\epsilon^{-\frac{T}{R_3C_2}}\right]dT,$$

$$= \frac{1}{R_1C_1}\epsilon^{\frac{-t}{R_1C_1}}\left[\int_0^t \epsilon^{\frac{T}{R_1C_1}}\,dT + \frac{R_2}{R_3}\int_0^t \epsilon^{\frac{T}{R_1C_1} - \frac{T}{R_3C_2}}\,dT\right],$$

$$= \frac{1}{R_1C_1}\epsilon^{\frac{-t}{R_1C_1}}\left[R_1C_1\,\epsilon^{\frac{t}{R_1C_1}} - R_1C_1 + \frac{R_2}{R_3}\left(\frac{R_1C_1R_3C_2}{R_3C_2 - R_1C_1}\epsilon^{\frac{t}{R_1C_1} - \frac{t}{R_3C_2}} - \frac{R_1C_1R_3C_2}{R_3C_2 - R_1C_1}\right)\right],$$

$$= 1 - \epsilon^{\frac{-t}{R_1C_1}} - \frac{R_2C_2}{R_1C_1 - R_3C_2}\epsilon^{\frac{-t}{R_3C_2}} + \frac{R_2C_2}{R_1C_1 - R_3C_2}\epsilon^{\frac{-t}{R_1C_1}},$$

$$F(t) = 1 + \left(\frac{R_2C_2}{R_1C_1 - R_3C_2} - 1\right)\epsilon^{\frac{-t}{R_1C_1}} - \frac{R_2C_2}{R_1C_1 - R_3C_2}\epsilon^{\frac{-t}{R_3C_2}},$$

which is the unit-function response of the flying-spot system without correction. The phosphor-decay characteristic is the derivative of the above:

$$D = \frac{dF(t)}{dt} = -\frac{1}{R_1C_1}\left(\frac{R_2C_2}{R_1C_1 - R_3C_2} - 1\right)\epsilon^{\frac{-t}{R_1C_1}} + \frac{R_2}{R_3(R_1C_1 - R_3C_2)}\epsilon^{\frac{-t}{R_3C_2}},$$

$$= \frac{R_2}{R_3(R_1C_1 - R_3C_2)}\epsilon^{-\frac{t}{R_3C_2}} - \frac{R_2C_2 - R_1C_1 + R_3C_2}{R_1C_1(R_1C_1 - R_3C_2)}\epsilon^{-\frac{t}{R_1C_1}}.$$

$$D = \frac{1}{R_1C_1 - R_3C_2}\left[\frac{R_2}{R_3}\epsilon^{-\frac{t}{R_3C_2}} - \frac{R_2C_2 - R_1C_1 + R_3C_2}{R_1C_1}\epsilon^{-\frac{t}{R_1C_1}}\right].$$

In the amplifier described it was found that, for best correction, $R_1 = 120{,}000$ ohms, $C_1 = 12$ micromicrofarads, $R_2 = 3900$ ohms, $R_3 = 560$ ohms, and $C_2 = 390$ micromicrofarads. Substituting, we find for the apparent square wave response*

$$F(t) = 1 + .243\epsilon^{-t/1.44} - 1.243\epsilon^{-t/.2184},$$

and for the phosphor decay* $D = 5.69\epsilon^{-t/.2184} - .1686\epsilon^{-t/1.44}$.

* The original paper gave the apparent square-wave response as $F = 1 + .247\epsilon^{-t/1.44} - 1.245\epsilon^{-t/0.218}$, and the phosphor decay as $D = 6.98\epsilon^{-t/0.218} - .21\epsilon^{-t/1.44}$. An error was discovered in the original calculations, and they have been reworked to give the values shown here. The revised coefficients do not materially alter the characteristics attributed to the system.

Part III — Radio-Frequency and Reproducing Equipment

BY

K. R. WENDT, G. L. FREDENDALL AND A. C. SCHROEDER

Summary—Two possible types of transmission, the three-carrier system and subcarrier system, are outlined. Radio-frequency and intermediate-frequency receiving equipment is discussed for both systems. Several reproducing devices and the associated deflecting and video equipment for the trinoscope are described. The solutions of some problems encountered in registration are set forth.

SIMULTANEOUS COLOR TRANSMITTERS

SINCE red, green, and blue video signals exist simultaneously, the transmission problem may be solved on the basis of frequency division. The subcarrier system and the three-carrier system are

possible choices. Since a subcarrier transmitter involved much less development work this system was used, but the choice was one of expediency. Figure 1(a) shows the essential components of the subcarrier transmitter in which the three color signals are multiplexed, as in the practice of carrier telephony. One subcarrier at a frequency of 8.25 megacycles is modulated by the red video signal and the lower sideband is partially suppressed. The frequency of the blue subcarrier is 6.25 megacycles and the blue upper sideband is partially suppressed. The term "mixer" indicates that a composite signal is formed, which is the direct addition of the green video signal and the two modulated subcarriers (Figure 1(b)). A substantially linear mixer is required if cross modulation of the color signals is to be avoided. Finally, the composite signal modulates the radio-frequency carrier. The lower

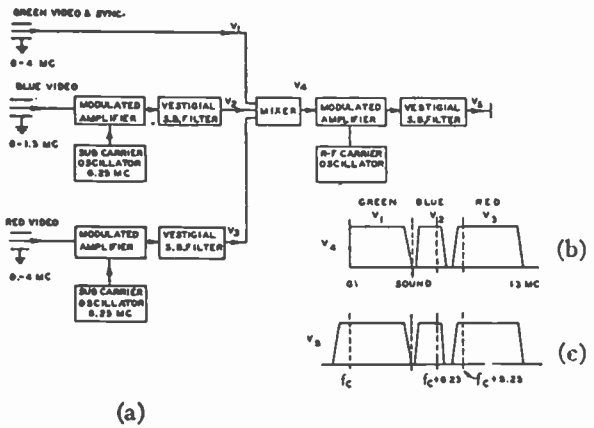

Fig. 1 — Simultaneous color transmitter of the subcarrier type.

sideband of carrier is partially suppressed, which results in the radiated spectrum in Figure 1(c). Thus, including guard bands, a total channel width of approximately 14.5 megacycles is called for. All radio-frequency circuits were designed for this bandwidth.

As in other multiplex arrangements, the maximum amplitude of the principal carrier must exceed the maximum amplitude of a subcarrier by an amount that depends upon the number of subcarriers. The ratio of amplitudes is 5 to 1 here.

The three-carrier system illustrated in Figure 2(a) embodies three substantially independent transmitters feeding through a suitable coupling device or "triplexer" into a common antenna. One sideband of each transmitter is partially suppressed by a vestigial-sideband filter, as in monochrome transmission. Figure 2(b) illustrates one of the many dispositions possible of the three carriers in the color channel. The arrangement in Figure 2(b) appears to be especially suitable for

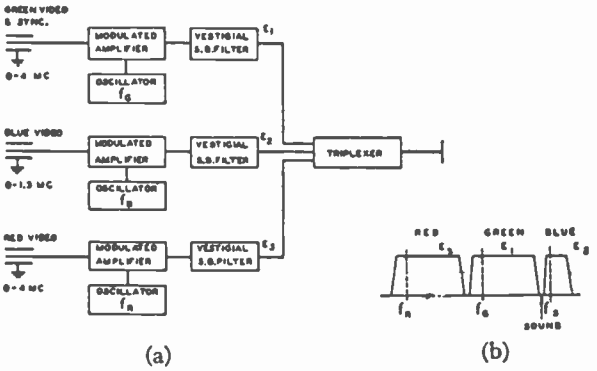

Fig. 2—Simultaneous color transmitter of the three-carrier type.

reception of the green signal by a monochrome receiver, because the red and blue signals act as guard bands against adjacent color channels.

Only the antenna must cover the full channel of approximately 14.5 megacycles. The red and green transmitters have a bandwidth approximately equal to 6 megacycles, the standard width for monochrome television, while the bandwidth of the blue transmitter may be restricted as dictated by the acuity of the eye for blue light.

Simultaneous Color Reception

The signal circuits of a subcarrier receiver for simultaneous color reception are shown in block form in Figure 3(a). Attenuation of the main radio-frequency carrier by 6 decibels as required for detection in a vestigial sideband system is provided in the broad-band radio-frequency and intermediate-frequency amplifiers. The composite video signal T_2 in Figure 3(a) is present in the output of the linear detector in the same form as the mixed signal in Figure 1(b). Attention must be given to assure linearity of detection, if cross-modulation of the color signals is reduced to an imperceptible amount. A low-pass filter

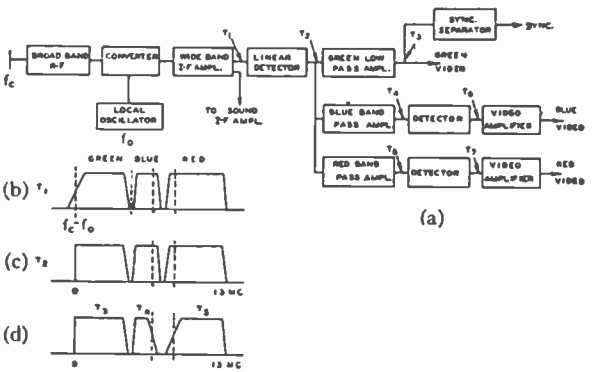

Fig. 3 — Simultaneous color receiver for subcarrier reception.

selects the green video signal, including the synchronizing signal, and rejects the red and blue subcarriers and sidebands. The red and blue subcarrier spectrums are isolated, as T_4 and T_5 in Figure 3(d), by band-pass amplifiers which also attenuate the subcarriers by 6 decibels. T_6 and T_7 indicate the desired video signals obtained by demodulation of T_4 and T_5.

Figure 4(a) is a block diagram showing the essential signal circuits of a simultaneous receiver which is operable on the signals of both types of transmission, subcarrier or three-carrier. The radio-frequency spectrum shown by S_1 in Figure 4(b) may represent both transmissions, since the distinction is only the difference between the relative amplitudes of the carriers. A bandwidth equal to the channel width must be covered by the radio-frequency and common intermediate-fre-

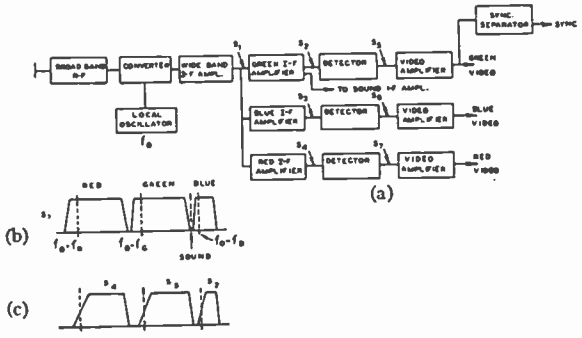

Fig. 4 — Simultaneous color receiver for three-carrier or subcarrier reception.

quency amplifiers, but subsequent amplifiers which isolate a particular color signal are 6 megacycles or less in width. Attenuation of the carriers by 6 decibels is accomplished in the individual amplifiers. Subsequent detection in each of the chains gives the required video signal.

Transmission of Sound

In the subcarrier system, television sound may be transmitted either as a subcarrier centered at a point 4.5 megacycles from the main carrier, or as a separate radio-frequency carrier at the same point. Such a spacing is required by the principle of compatibility. A radio-frequency sound carrier at the final frequency at a spacing of 4.5 megacycles from the green carrier would be used in the three-carrier color transmitter.

The Reproduction of the Color Image

The kinescope shown in Figure 5 is the three-gun single-neck tube mentioned in Part I. The photograph also shows the yoke and the

optical system used for registration of the three images. In this tube the three cathode-ray beams cross inside the yoke and thus are deflected by the same field. The three rasters then appear opposite the three guns on different areas of the tube face. The tube face has a curvature whose center is at the center of the yoke. The three images are filtered to produce the three colors, and are combined by a system of mirrors and the lens to form a registered color image. It is possible with this tube to register the three images quite satisfactorily, and experience gained with it indicated that registration might also be achieved with three separate tubes and lenses. Such an arrangement appears to be more straightforward, and at the same time leads to improved resolution and brighter images. This device has been denoted by the convenient term "trinoscope."

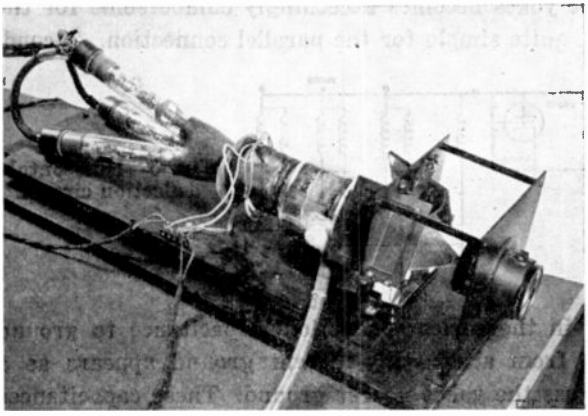

Fig. 5—Three-gun single-yoke tube.

THE TRINOSCOPE

The term "trinoscope" is a designation for an assembly of three kinescopes, three lenses, and three deflection yokes which are energized from a common sawtooth deflection generator.

An ideal trinoscope having identical yokes and tubes is probably not realizable in an experimental setup. Hence provision was made for adjusting each yoke separately. Equalization of the horizontal size was obtained by moving a yoke slightly along the axis of a tube, thus obviating a complicated size-control circuit containing a variable inductance with approximately the same Q and self-resonant frequency as the yoke. The vertical sizes are adjusted through a small range, or trimmed by variable resistors in series with each vertical winding, to produce three rasters of equal size. Each yoke could be rotated slightly by a mechanical adjustment for angular alignment of the scanning rasters.

On first thought, it would seem best that the same current flow through each yoke, a condition which should be insured by a series connection of yokes. However, identical fields are desired, rather than identical currents, and since there is a variation between individual yokes, different currents are required to produce identical fields. If the variation between yokes is caused by a variation in the number of turns, then parallel operation is particularly advantageous, since the yoke having the larger number of turns requires the smaller current, which is actually the case due to the higher impedance. At any rate, trimming is necessary, and a method of connection should not be chosen to minimize trimming if other difficulties are introduced. There are at least two serious difficulties in series operation which are not encountered with the parallel connection. First, individual centering and trimming of the three yokes becomes exceedingly cumbersome for the series connection, but quite simple for the parallel connection. Second,

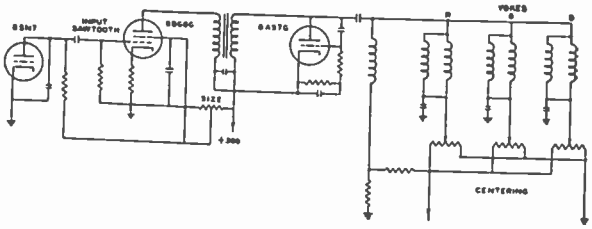

Fig. 6—Horizontal-deflection circuit.

and most important, in the series connection, capacitance to ground of the yokes remote from alternating-current ground appears as a shunt capacitance across the yokes nearer ground. These capacitances are of such magnitude in the horizontal deflection circuit that considerable current is by-passed around the yokes nearer ground. Also, high-Q series resonances occur in both the horizontal and vertical coils as a result of these capacitances. These circuits are shock-excited by the return-line pulse and cause objectionable transients on the left side of the picture that are different in the three yokes.

Figure 6 shows a simplified diagram of the horizontal-deflection system. It is a normal power-feedback circuit using the 6AS7G damper tube except that three yokes and centering circuits connected in parallel are substituted for the usual single yoke and centering circuit. Figure 7 shows the vertical circuit. In the absence of a suitable transformer, a direct-coupled circuit with feedback was used. Although this arrangement is wasteful of power, it gives ample and good deflection with a minimum of time spent on adjustment. The linearity control is unusual in that excellent linearity is achieved without either changing the size or bouncing the raster when the control is varied.

The yokes for the trinoscope must be carefully designed and built. They should have high efficiency and should be as nearly alike as possible. They should produce a rectangular raster with neither pincushion nor barrel distortion. Such distortion will produce misregistry at the edges or corners of the image, if the assembly is not mechanically correct. For example, pincushion distortion occurs commonly when tubes with flat faces, as in the trinoscope, are deflected. The amount of distortion at any one point depends upon the total deflection there, including that from both the sawtooth and the direct-current, or shifting, source. If, then, due to poor mechanical alignment in the trinoscope assembly, appreciable electrical shifting of one or two of the rasters is required to register them, additional distortion will be introduced. The important point is that the distortion will be different on the three rasters since the shifting in each must necessarily be in a different direction to bring them together.

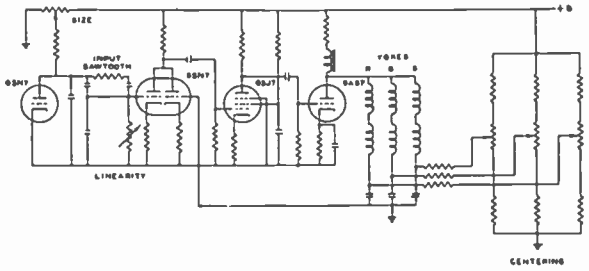

Fig. 7—Vertical-deflection circuit.

The inductance of the horizontal yoke winding is 8 millihenries, or approximately the same as a normal one-yoke deflection circuit, and the circuit is designed to supply three times normal current. Presumably, yokes having three times the normal inductance could be operated in parallel in order to give normal circuit impedance. Such an arrangement would reduce the current in the circuit, but raise the voltage. Experience, however, has shown that a yoke with an inductance above 3 millihenries requires voltages which occasionally may cause breakdown within the yoke. The two coils of a horizontal pair within a yoke are connected in parallel. However, the two vertical coils are connected in series in order to obtain an impedance as high as possible, since here the impedance is limited by a practical size of wire. With a given size of wire the impedance for the series connection is four times that for the parallel connection.

The kinescopes for the trinoscope assembly must be aluminized.[1]

[1] D. W. Epstein and L. Pensak, "Improved Cathode-Ray Tubes with Metal-Backed Luminescent Screens," *RCA Review*, Vol. 7, pp. 5-10, March, 1946.

A thin layer of aluminum completely covers the phosphor and those inside surfaces of the tube which are held at second-anode potential. This layer is transparent to the high-voltage electrons, but opaque to light. The coating also has high conductivity, which insures that the three phosphors will be at the same potential, thus obviating any difference in raster size due to different beam voltages in the three

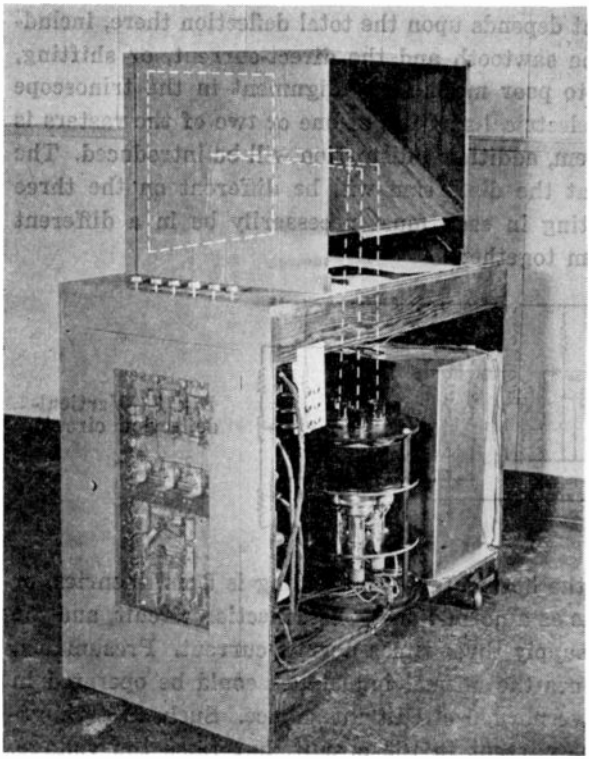

Fig. 8 — Receiver showing trinoscope assembly.

kinescopes. Furthermore, the entire volume inside the bulb beyond the second anode is equipotential, and no distortion can be caused by spurious wall charges or potential drops. The kinescope guns should be as well-centered and mechanically stable as possible, since any variation contributes to misregistry.

The choice of phosphors for the red, green, and blue kinescopes was guided by a consideration of the over-all light efficiencies of the phosphors in combination with any light filters required for color correction. Thus, an orange phosphor in combination with a red filter yielded more light than available red phosphors.

The trinoscope optical system included three separate lenses. The three tubes were assembled at the corners of a triangle, as shown in

Figure 8, with their faces in the same plane. The axis of each lens in front of a tube is perpendicular to the tube face, but is offset from the tube axis toward the center of the assembly by an amount sufficient to register the three images. If the lenses are rectilinear, no distortion will result from such a displacement. Figure 9 shows the principle of this registration with two tubes. The principle is the same as that used in photography where, by means of the rising front, tall buildings may be photographed from the ground without distortion. The image and object, or film and scene, are simply made parallel and the lens axis perpendicular to them, the center of the lens being on the line joining the center of the image and object to make the image distortionless, or rectilinear. This, of course, requires a larger field, or increased covering power from the lens. Any noticeable falling off of light towards the edge of the lens will result in color shading in the registered picture, since the shading will be different in the three colors. The lenses for the trinoscope need not be color-corrected, since each passes only one color.

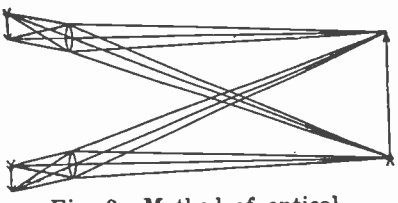

Fig. 9—Method of optical registration.

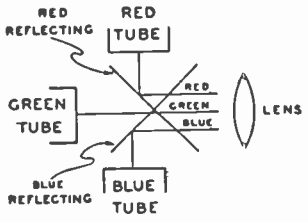

Fig. 10—Registration with three dichroic mirrors and one lens.

Another optical method of registry was tried in which ordinary mirrors were used to direct the light from the three tubes into one lens, but the arrangement was rejected as impracticable. Half-silvered mirrors, though feasible, waste much light. Dichroic mirrors,[2] however, provide an excellent solution to this problem. Figure 10 shows the arrangement of the three tubes and the two dichroic mirrors, which are cut in the middle and crossed. One mirror reflects red, and passes green and blue, and the other reflects blue, and passes red and green. While this arrangement is still in the experimental stage, it offers great promise for a simple and economical method of registration.

The Video System

The video system consists essentially of three identical video amplifiers of two stages each, with cathode follower outputs. Approximately 75 volts peak-to-peak is available. The frequency response is flat to 5

[2] See Part II of this series.

megacycles. Two controls, the gain and background, are provided in each channel. Eventually, of course, simpler arrangements would be used, and individual gain controls dispensed with. The gain controls here, however, are useful for demonstrating color balance, and in making experimental adjustments. The background controls must be set accurately. Controls would be necessary even in the simplest receivers, although, once set, they would require adjustment only if the cutoff of a kinescope changed due to aging. Accurate setting of the "blacks," or background, is extremely important in any additive color system. That is, the black portions of the reproduced image must correspond with the blacks of the original scene, and, even more important, the blacks of the three colors must agree with each other. If one of the colors were incorrect, such that zero light were produced when a low value were needed, all of the reproduced colors requiring low levels of that color would receive none, and wrong colors would be obtained.

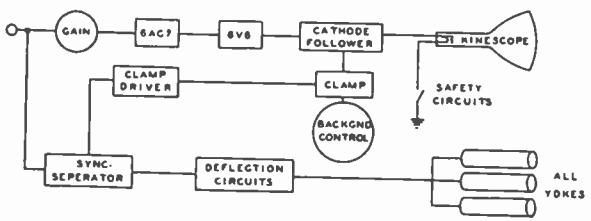

Fig. 11—Video block diagram of green channel.

Therefore, the picture direct current is reinserted by the double-diode clamp, one of the best restorers. The direct current is reinserted on the grid of the cathode follower. Delayed pulses, obtained from separated synchronizing signal, operate the clamp circuits during the back-porch interval. Such a circuit can restore the correct picture back level and maintain it regardless of picture content, incorrect or spurious low frequencies, or switching transients. Restoration is also independent of synchronizing-signal height, which means that the red and blue backgrounds remain correct when these channels are switched to the green signal, as when reproducing a black-and-white picture from a low-band station.

The synchronizing signal is separated from the green-channel signal. Figure 11 is a block diagram of the green video amplifier and the synchronizing-signal circuits.

Safety circuits are provided for protection of the kinescopes in the event of deflection or power failure. Protection against power failure, such as a blown fuse or disconnected cable, is necessary since the deflection would cease before the accelerating voltage, and an undeflected spot would remain long enough to damage the kinescope screen.

COLORIMETRY IN TELEVISION*†

By

WILLIAM H. CHERRY

Research Department, RCA Laboratories Division,
Princeton, N. J.

Summary

The colorimetrically exact reproduction of color in simultaneous television is now possible, through the congruence of the camera spectral sensitivities to definite characteristics specified by colorimetry and through the combination of the camera signals in both positive and negative amounts by suitable circuits and amplifiers. The negative sensitivities of the photo-pickups formerly required for certain spectral wavelength intervals are obviated by these signal mixing circuits, and simultaneous color television, both as to color range and accuracy of reproduction, is capable of the finest color reproduction available anywhere. The mixing circuits perform a function resembling that known in color photography as masking, but whereas the latter is always approximate and often a hit-or-miss procedure, the television system can approach perfection without undue complication.

The basic concepts and relations of trichromatic colorimetry are here developed. Many of these relationships are of immediate importance in color reproduction and are stated explicitly, with the aid of a concise notation. In addition, certain rather philosophic aspects of television as a means for the communication of sense perception are discussed and a plea is made for the extension and compilation for television purposes of knowledge about the properties of the eye.

(33 pages, 4 figures)

---

* Decimal Classification: R583 × R800 (535).

† *RCA Review*, September, 1947.

SIMPLIFIED TELEVISION FOR INDUSTRY*†

By

R. E. Barrett and M. M. Goodman

Tube Department, RCA Victor Division,
Lancaster, Pa.

Summary—A new iconoscope makes possible circuit simplification and permits reproduction on the receiving cathode-ray tube screen comparable to newspaper half tones. Complete circuit details are given for the 250-line 60-frame system.

THE use of a television system to view dangerous operations at Bikini without endangering human life effectively demonstrated that there exists an important use for television other than entertainment. Industry could use a simplified system advantageously, and so could schools and experimenters.

A major step toward reducing the cost of a television system has been made with the introduction of a new two-inch iconoscope, the RCA 5527. It is relatively inexpensive and has been designed so that the equipment associated with it can be compact, simple, and economical. For a satisfactory picture with this pickup tube, only about 1,000 foot-candles of incident illumination are required. This amount of light is roughly the same as that used in present television broadcasting studios and can be obtained with three 200-watt lamps placed four feet from the subject. An outdoor scene televised by the 5527 on a normal sunny day produces a picture, when viewed on a 7GP4 directly-viewed kinescope, comparable in quality to a newspaper reproduction of a photograph.

Although the tube is designed to operate with 800 volts on the accelerator electrode, it will perform satisfactorily at 600 volts with only a slight loss in picture definition. The small area of the mosaic permits the use of a low-cost lens such as the lens of a 35-mm camera having a speed of f:3.5 or greater.

Many of the new techniques learned during experimentation with military tubes were used to great advantage in the design of this tube, making it superior to the now obsolete forerunner, type 1847. A new method of mosaic treatment, for example, permits the transmission of a greater amount of light to the photosensitive surface and, conse-

---

* Decimal Classification: R583.

† Reprinted from *Electronics*, June, 1947.

quently, improved sensitivity is achieved. Greater signal output is obtained by the use of a high-capacitance mosaic which older-type tubes could not support. A direct contact to the mosaic signal plate, instead of the capacitive coupling used in type 1847, improves the low-frequency response.

Although the tube uses electrostatic deflection rather than the more expensive and cumbersome electromagnetic deflection system, good picture definition is obtained through the use of the wartime-developed fine-spot cathode-ray gun with balanced deflection. The resolution capabilities of the tube are exceptionally good, and as measured by television standards, (lines per picture height) are 250 lines. The difficulty from nonuniform background signals, or dark spots found in all iconoscopes, is ordinarily not troublesome in industrial applications and, therefore, very satisfactory pictures are obtained without the use of shading signals. In addition, the tube does not require keystone correction.

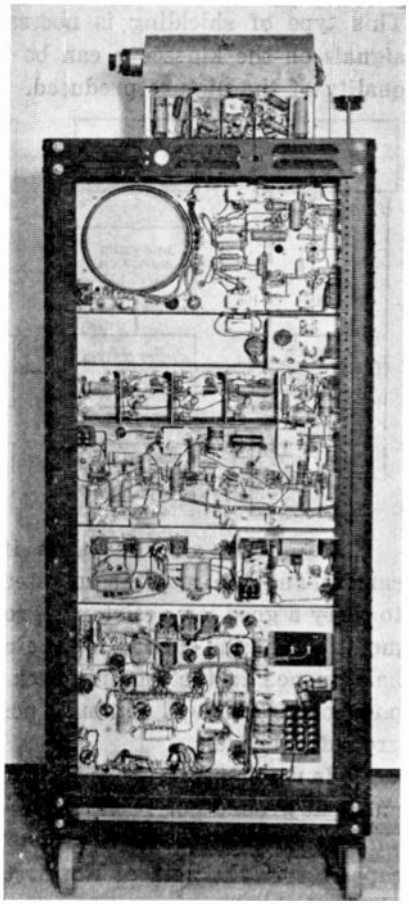

Fig. 1—Television camera and picture system chassis in a 4-foot rack.

The system illustrated in Figure 1 contains all of the components necessary to give a good television picture and can be adapted to a transmitting and receiving system. The sensitivity and resolution of the system, together with the modest cost of components, make it applicable to many uses in both the industrial and educational fields. The adaptability of the system and its excellent performance make the system extremely versatile and provide a wide range of possible applications.

The complete system includes the camera and monitor as illustrated in the block diagram of Figure 2. The scene to be televised is converted to an electrical signal by the pickup tube. This signal is then

amplified and reproduced on the screen of the kinescope. The necessary synchronizing circuits, blanking amplifiers, and power supplies are included.

Camera System

The components contained in the camera are the two-inch iconoscope, a four-stage video preamplifier, and the lens mounting. The entire camera housing is made of 1/16-inch copper and a partition of the same material separates the camera tube from the video preamplifier. This type of shielding is necessary, since the presence of spurious signals on the kinescope can be very annoying and detract from the quality of the picture produced.

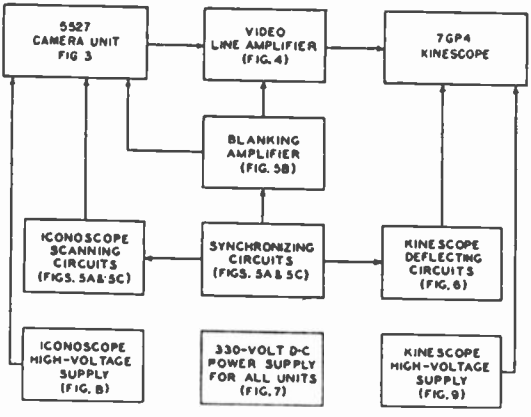

Fig. 2—Block diagram of television camera and complete picture system.

Care should also be taken if long cables are used between the camera and the monitor to filter all electrode voltages properly and to carry a good low-resistance ground between the two pieces of equipment. All of the shields for the cables and the camera housing should be returned to the monitor rack and a solid connection made at one point only. This will eliminate possible pickup loops due to nonuniform ground potentials.

It is recommended that the camera tube be operated with its second anode at ground potential and its cathode at a high negative potential. This method of operation eliminates the need for a high-voltage input capacitor to the grid of the first preamplifier stage, since the signal plate of the iconoscope operates at second-anode voltage. Operating the iconoscope in this manner also eliminates the possibility of coupling hum from the high-voltage power supply into the input of the video preamplifier.

The video preamplifier, diagrammed in Figure 3, consists of four stages using the miniature tube type 6AG5. Conventional shunt peaking is used to obtain a flat response over the range from 60 cycles per

second to 2.5 megacycles. Because of the shunt capacitance of the iconoscope signal electrode and the input stage of the first video preamplifier, it is necessary to compensate the video preamplifier for the loss of high frequencies. The loss of high-frequency picture intelligence may be observed on the kinescope as a black streak following a black bar on a white background. The action of the compensation stage is to reduce in amplitude the low-frequency response and to amplify the high frequencies, giving an overall linear response with reduced amplitude over the desired bandwidth. Over-compensation of the amplifier, that is, peaking the high frequencies too much, is evidenced by a white streak following a black bar on a white background. The output of the video preamplifier is fed over a 75-ohm coaxial cable, at a level of 0.6 volts peak-to-peak, to the gain control at the input to the video line amplifier.

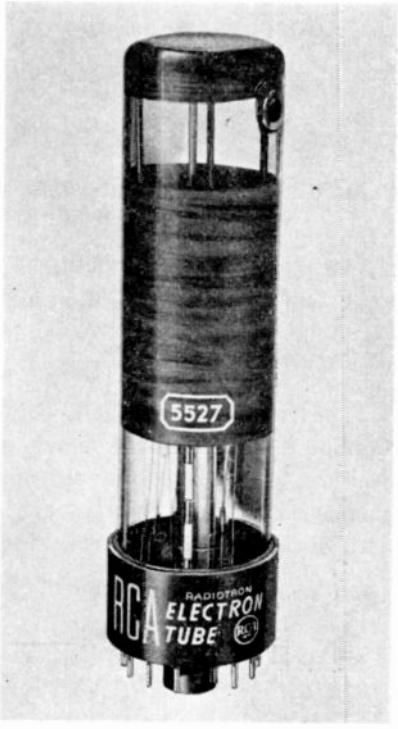

Two-inch iconoscope for the 250-line system.

Optical System

The lens mount and optical focusing system for the camera consist of two pieces of concentric tubing. The smaller tubing has the lens mounted on one end and the inside surface of this tubing is painted a matte black to reduce inside wall reflections. The larger tubing is solidly mounted on the front panel of the camera.

Optical focus is obtained by sliding the smaller tubing back and forth on its axis inside the larger tubing. The two pieces of tubing take the place of a bellows since they are light tight and give a wide range of focus. Because of the small mosaic in the two-inch iconoscope, a physically small lens with a large opening (f:2 or f:3.5) and a short focal length (2 to 3 inch) may be used. A short focal length lens of this type is inexpensive and easy to obtain.

It is also desirable to have an adjustable iris on the lens so that best light conditions can be obtained. With this simple optical system

Capabilities of the system are illustrated by this same-size reproduction of a photograph taken of the screen of the 7GP4 kinescope.

a good picture of about 250-lines resolution can be obtained with about 1,000 foot candles scene illumination.

Video Line Amplifier

The video line amplifier, Figure 4, uses three 6AC7 type tubes as amplifiers and, like the video preamplifier, uses conventional shunt peaking to obtain a flat response from 60 cycles per second to 2.5 megacycles. The output of the amplifier is a video signal complete with horizontal and vertical kinescope blanking pulses and is capable

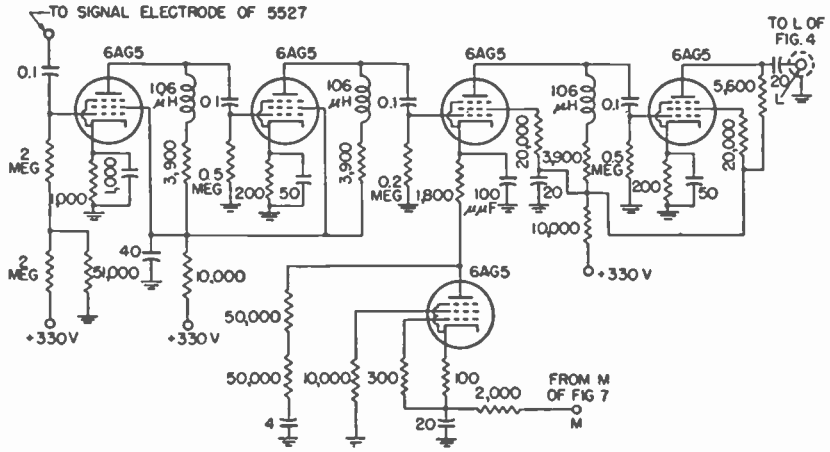

Fig. 3—Video preamplifier circuit.

of producing a 40-volt peak-to-peak signal to drive the grid of the 7GP4 kinescope.

Because this system was not designed for transmitting a video signal, the insertion of synchronizing pulses was eliminated. These synchronizing pulses could be inserted into the line amplifier after the blanking insertion stage. In this case, the output of the video line amplifier would be a composite video signal with the synchronizing pulse superimposed on the blanking pulses. This output could then be coupled into a video modulator for transmission of a televised picture.

Synchronizing and Blanking Circuits

The standard method of interlaced scanning for both the kinescope and the iconoscope was rejected in favor of a simpler method

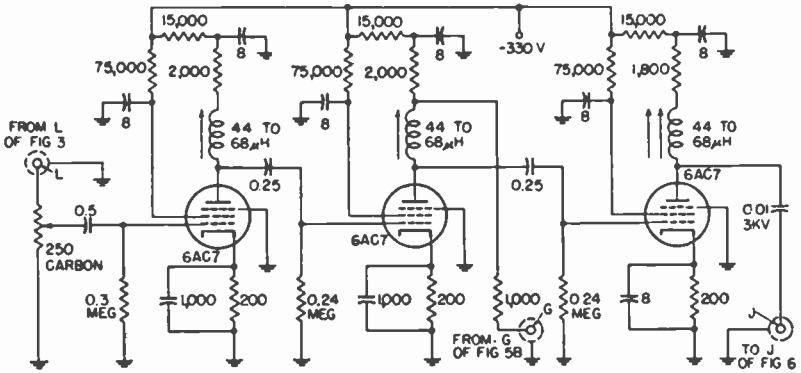

Fig. 4—Circuit of video line amplifier.

to keep the expense low and physical size of the equipment small. The 60-cycle-per-second relaxation oscillator synchronized to the 60-cycle-per-second power frequency supplies the vertical time base. This simple oscillator synchronized with the power frequency is stable enough to eliminate the need of a speed control. A free-running multivibrator operating at approximately 15,000 cycles per second supplies the horizontal time base. These frequencies give a 250-line, 60-frame noninterlaced scanning raster, which when properly blanked, gives a stable picture.

Vertical and Horizontal Oscillators

A 6AC7 tube is used for the vertical oscillator, as shown in Figure 5A. The frequency of oscillation is determined by the tube capacitance in conjunction with the RC constants in the screen-grid and suppressor-grid circuits. A 60-cycle saw-tooth voltage is developed in the

plate circuits of this oscillator and coupled into a 6SN7-GT phase inverter.

The output of the inverter stage is a push-pull saw-tooth voltage of sufficient amplitude to scan the iconoscope in the vertical direction. The screen circuit of the 6AC7 vertical oscillator produces a straight-sided pulse of approximately 20 volts peak-to-peak which is used as the driving pulse for the kinescope vertical scanning. With this method

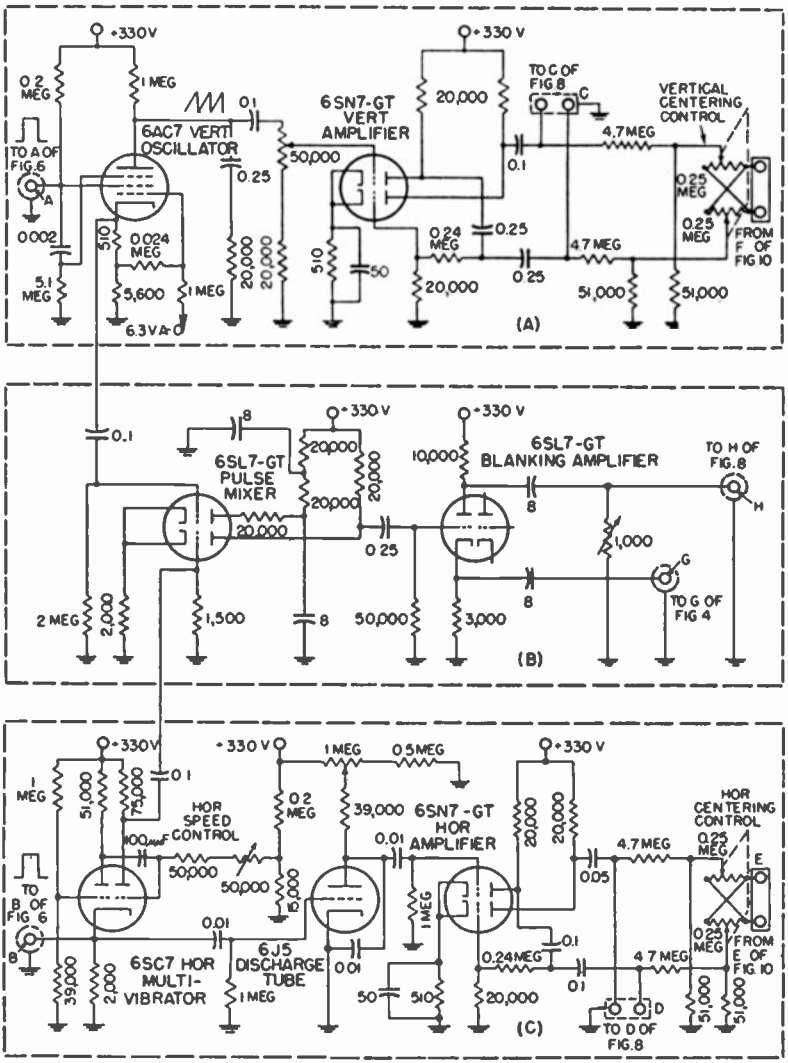

Fig. 5—(Top) Vertical oscillator and scanning circuit for the 5527. (Middle) Mixing and blanking circuits. (Bottom) Horizontal multivibrator and scanning circuit for 5527.

both the iconoscope and kinescope vertical scanning systems are in synchronization.

The horizontal synchronizing pulses and driving pulses are derived from a free-running cathode-coupled multivibrator utilizing a 6SC7, as shown in Figure 5C. The cathode of the horizontal multivibrator produces a positive straightsided pulse which is coupled to a 6J5 discharge tube; this cathode pulse is also used as the driving pulse for the horizontal kinescope scanning. The output of the horizontal discharge tube is coupled to a 6SN7-GT phase inverter and pushpull output tube which produces the horizontal deflection for the iconoscope.

Across the cathode resistor of the vertical oscillator, a straight-sided negative pulse of approximately eight volts peakt-to-peak is developed. In the plate circuit of the horizontal multivibrator, a similar straight-sided negative pulse is produced. These two pulses are combined in the 6SL7-GT pulse-mixer tube, Figure 5B, and then amplified in the 6SL7-GT blanking amplifier. The kinescope mixed blanking voltage is developed across the cathode resistor of the blanking amplifier and fed into the second stage of the video line amplifier. The iconoscope mixed blanking voltage is taken from the plate of the blanking amplifier and fed to grid 1 of the iconoscope. Since the vertical and horizontal blanking pulses are derived from the same oscillators that produce the driving pulses for the scanning circuits, the blanking time is not sufficient to eliminate the bright edges which appear on the sides of the scanned raster. This effect is not desirable but it does not detract too much from the quality of the picture produced.

Deflection Circuits for Kinescope

The electrostatic deflection for the 7GP4 kinescope is developed from the horizontal and vertical timing oscillators. These driving pulses are coupled into the grid circuits of a pair of 6J5 discharge tubes, Figure 6, which produces horizontal and vertical saw-tooth voltages. The horizontal and vertical saw-tooth voltages developed in the plate circuits of the 6J5 discharge tube are coupled to a pair of 6SN7GT phase inverter and push-pull output tubes. The width control is in the plate circuit of the horizontal discharge tube, and the height control is in the plate circuit of the vertical discharge tube.

Power Supplies

The direct-current power supplies for the complete television system consist of a 330-volt, 300-milliampere electronically regulated supply, two radio frequency operated high-voltage supplies, and two glow

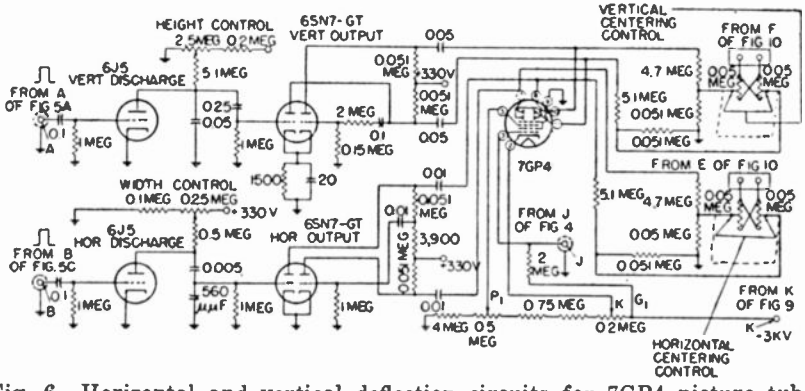

Fig. 6—Horizontal and vertical deflection circuits for 7GP4 picture tube.

tube regulated supplies. The 330-volt d-c supply, Figure 7, operates the deflection circuits, the video amplifiers, the blanking amplifier, and the oscillators for the high-voltage supply. One radio frequency high-voltage supply, Figure 8, operates at —1 kilovolt maximum and is capable of one milliampere current drain. This supplies the focus and P_3 voltage for the iconoscope. The second radio frequency high-voltage supply, Figure 9, operates at —three kilovolts and supplies focus and P_2 voltages for the 7GP4 kinescope. The two glow-tube regulated supplies, Figure 10, operate at —75 volts and produce electrostatic centering voltages for the iconoscope and kinescope.

All of the components in this simplified television system may easily be mounted on a standard rack measuring 22 × 47 × 17 inches. The camera unit, however, may be mounted separately in a small compartment 4 × 12 × 6 inches and cabled to the monitor rack. All of the components may be cabled together by means of Jones plugs or Amphenol connectors. In this way, any components may be removed from the rack for servicing or study without unsoldering any connections.

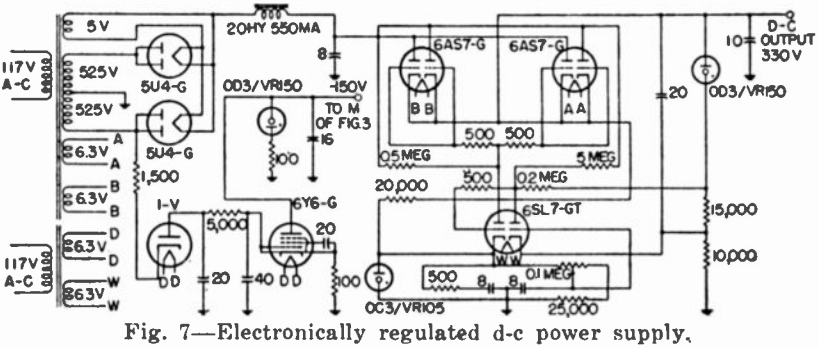

Fig. 7—Electronically regulated d-c power supply.

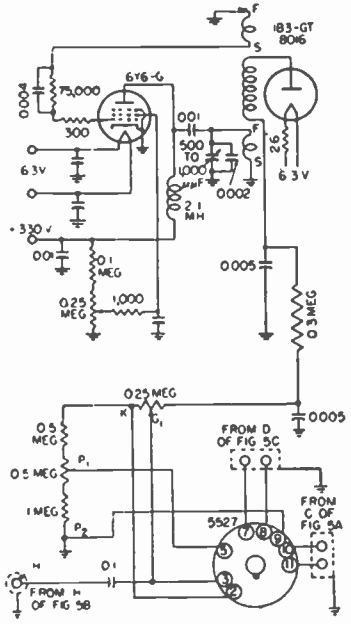

Fig. 8 — Circuit of r-f operated high-voltage supply for the 5527.

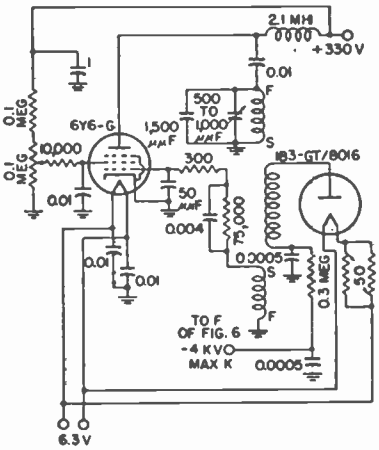

Fig. 9—R-f-operated high-voltage supply for the 7GP4.

Operating tests have proved that this television equipment is reliable and stable. Under proper lighting conditions, it is possible to obtain a good television picture with sufficient detail to meet the requirements of most industrial or educational needs. The equipment is small and compact and because of its simplicity, does not require highly trained personnel.

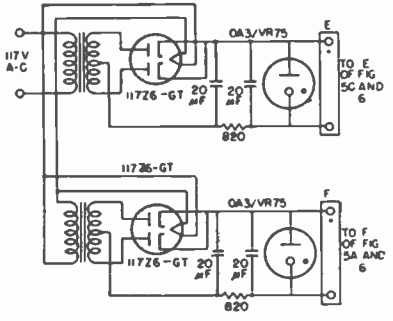

Fig. 10—Horizontal and vertical centering supplies.

THE SENSITIVITY PERFORMANCE OF THE HUMAN EYE ON AN ABSOLUTE SCALE*†

By

Albert Rose

RCA Laboratories Division,
Princeton, N. J.

Summary—An absolute scale of performance is set up in terms of the performance of an ideal picture pickup device, that is, one limited only by random fluctuations in the primary photo process. Only one parameter, the quantum efficiency of the primary photo process, locates position on this scale. The characteristic equation for the performance of an ideal device has the form

$$BC^2\alpha^2 = \text{constant}$$

where B is the luminance of the scene, and C and α are respectively the threshold contrast and angular size of a test object in the scene. This ideal type of performance is shown to be satisfied by a simple experimental television pickup arrangement. By means of the arrangement, two parameters, storage time of the eye and threshold signal-to-noise ratio are determined to be 0.2 second and five respectively. Published data on the performance of the eye are compared with ideal performance. In the ranges of B(10^{-6} to 10^{2} footlamberts), C(2 to 100 per cent) and α(2′ to 100′), the performance of the eye may be matched by an ideal device having a quantum efficiency of 5 per cent at low lights and 0.5 per cent at high lights. This is of considerable technical importance in simplifying the analysis of problems involving comparisons of the performance of the eye and man-made devices. To the extent that independent measurements of the quantum efficiency of the eye confirm the values (0.5 per cent to 5.0 per cent), the performance of the eye is limited by fluctuations in the primary photo process. To the same extent, other mechanisms for describing the eye that do not take these fluctuations into account are ruled out. It is argued that the phenomenon of dark adaptation can be ascribed only in small part to the primary photo-process and must be mainly controlled by a variable gain mechanism located between the primary photo-process and the nerve fibers carrying pulses to the brain.

Introduction

THE designer of picture pickup devices such as television pickup tubes, photographic film and electron image tubes is faced steadily with the problem of comparing the performance of these devices with the performance of the human eye. This is especially true for comparisons of sensitivity. Neither television pickup tubes nor photographic film match the ability of the eye to record pictures at

* Decimal Classification: R583.1.

† Reprinted from *Jour. Opt. Soc. Amer.*, February, 1948.

very low scene luminances. Film ceases to record at a scene luminance of a few footlamberts, and present television pickup tubes at a few tenths of a footlambert. (Lens diameters and exposure times are assumed equal to those of the eye.) The eye, however, still transmits a picture at 10^{-6} footlambert. This is a striking discrepancy, especially when it is known that eye, film and pickup tube each require about the same number of incident quanta to generate a visual act. By visual act is meant a threshold visual sensation for the eye, the rendering of a photographic grain developable in film or the release of a photo-electron in a television pickup tube. This number of incident quanta is in the neighborhood of 100. The sources of this discrepancy will be discussed later. For the present, the discrepancy is introduced and emphasized for the following reason. Since television pickup tubes and photographic film are already limited in their performance by more or less fundamental statistical fluctuations (noise currents in pickup tubes and graininess in film) and since the low light performance of the eye so far outstrips that of pickup tubes and film, it is not unreasonable to inquire whether the performance of the eye also is limited by statistical fluctuations.

The purpose of this paper is, in fact, to lay out clearly the absolute limitations to the visual process that are imposed by fluctuation theory and to compare the actual performance of the eye with these limitations. The gap, if there is one, between the performance to be expected from fluctuation theory and the actual performance of the eye is a measure of the "logical space" within which one may introduce special mechanisms, other than fluctuations, to determine its performance. These special mechanisms can only contract the limits already set by fluctuation theory. This point is especially important because it restricts the freedom with which one can introduce such assumptions as: (1) rods or cones with variable thresholds of excitation, (2) an absorption coefficient for the retina that varies with scene luminance or (3) photo-chemical reaction rate equations with arbitrary coefficients.

The following discussion begins with a description of ideal performance, that is, performance limited only by statistical fluctuations in the absorption of light quanta. Next an experimental realization of ideal performance is introduced in the form of a special television pickup arrangement. The performance data for the eye is then compared with ideal performance and finally some implications of this comparison are discussed.

It must be emphasized that this discussion is concerned primarily with the low light end of the light range over which the eye operates. It is here that fluctuation limitations would be expected to be the

dominant factor. At very high lights other limitations set in, as for example, the finite structure of the retinal mosaic, or the limited traffic carrying capacity of the optic nerve fibers. Important as these factors are for a complete understanding of the eye, they do not constitute, as do statistical fluctuations, an absolute limit to the possible performance of the visual process. They are the particular boundary conditions pertaining to the eye, which, in another device or in an "improved eye," might take on other values. The light range considered here is still the larger part of the total light range of the eye, namely, from 10^{-6} to 10^{2} footlamberts. The excluded range is 10^{2} to 10^{4} footlamberts.

Also the discussion is confined, except for a few remarks on color, to the sensitivity performance of the eye for white (as opposed to colored) test patterns.

Performance of An Ideal Picture Pickup Device

An ideal picture pickup device is defined to be one whose performance is limited by random fluctuations in the absorption of light quanta in the primary photo-process. Each absorbed quantum is assumed to be observable in the sense that it may be counted in the final picture. From well known statistical relations, an average absorption of N quanta will have associated with it deviations from the average whose root mean square value is $N^{\frac{1}{2}}$. These deviations are a measure of the accuracy with which the average number N may be determined. They also control the smallest change in N that may be detected. Thus if this smallest change is denoted by ΔN:

$$\Delta N \sim N^{\frac{1}{2}}, \tag{1}$$

or

$$\Delta N = kN^{\frac{1}{2}}, \tag{1a}$$

where k is a constant to be determined experimentally. k is called the threshold signal-to-noise ratio.

Let the average number of quanta, N, be absorbed in an element of area of side length h, and in the exposure time of the pickup device. Then N/h^2 is proportional to the luminance of the original scene and ΔN to the threshold change in luminance and we may write

$$\text{scene luminance} \equiv B \sim (N/h^2), \tag{2}$$

$$\text{threshold contrast} \equiv C = \Delta B/B \times 100\% = \Delta N/N \times 100\% \sim 1/N^{\frac{1}{2}}. \tag{3}$$

Combining Equations (2) and (3) we get:

$$B \sim 1/C^2h^2, \tag{4}$$

$$B \sim 1/C^2\alpha^2, \tag{4a}$$

or

$$B = \text{constant } (1/C^2\alpha^2), \tag{4b}$$

where α is the angle subtended by h at the lens. Equation (4b) is the characteristic equation for the performance of an ideal picture pickup device. It is based on the simplest and most general assumptions regarding the visual process. Since no special mechanism has been called upon, it applies equally well to chemical, electrical or biological processes of vision. The constant factor includes among other constants, the storage time, quantum efficiency and optical parameters of the particular device. When two ideal devices are compared for performance under equivalent conditions, the only distinguishing parameter is their respective quantum efficiencies.

Equation (4b) provides the threshold value of any one of the variables when the other two are arbitrarily specified. Thus Figure 1 shows a plot on a log — log scale of threshold contrast as a function of visual angle for various fixed values of the scene luminance. In Figure 2, threshold contrast is plotted as a function of $1/(B^{\frac{1}{2}}\alpha)$ and, as expected from Equation (4b), all of the performance data of Figure 1 collapse into a single straight line. The location of this line determines the constant in Equation (4b) and from this constant the quantum efficiency of the device may be computed (see Equation 5).

It should be clear that there is nothing in the fluctuation theory used to derive Equation (4b) that would prevent the lines in Figure 1 from being extended indefinitely to the right toward small angles or indefinitely downward toward low contrasts. It should also be clear, on the other hand, that any actual physical device will impose such limitations. The smallest angle that can be resolved may be limited either by structure in the surface on which the optical image is focused or eventually by diffraction effects in the optical focus itself. Also any actual physical device cannot generate artbitrarily high signals as would be required if the lines in Figure 1 were extended to arbitrarily small contrasts. Both these limitations have no necessary connection with fluctuation theory and serve merely to define the boundaries within which such a theory may be applied. Such boundaries may be shown, for example, as in Figure 1 by the two dash-dot lines. The lines

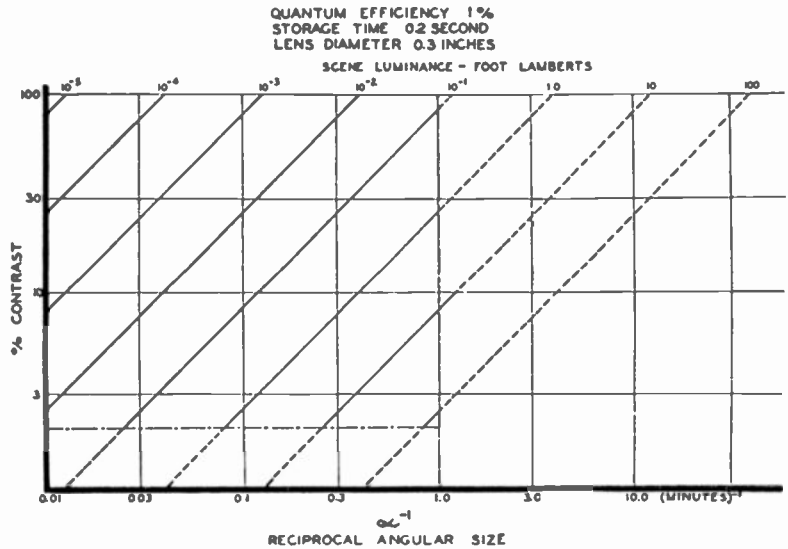

Fig. 1—Performance of ideal pickup device. The experimentally determined value, 5, of threshold signal-to-noise ratio was used to compute these curves.

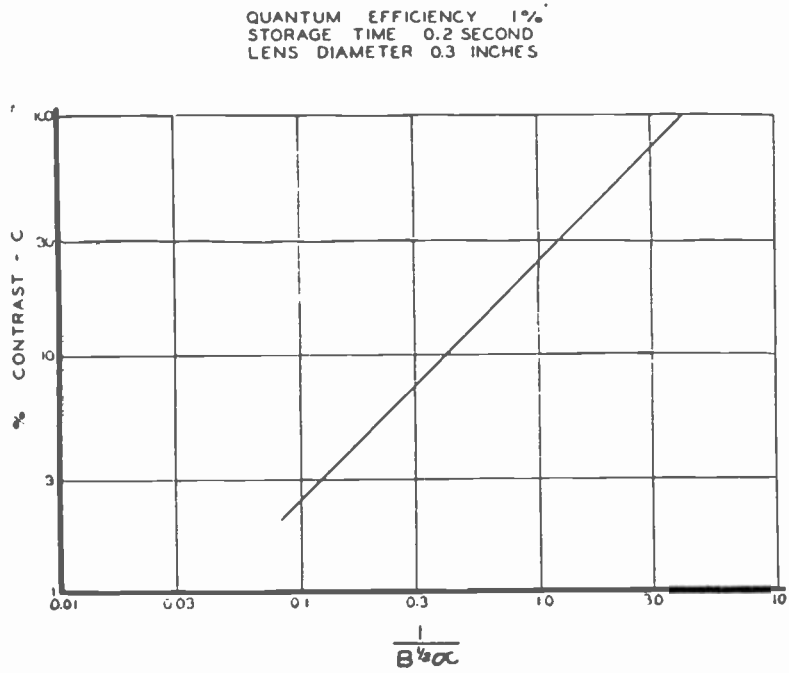

Fig. 2—Performance curve for ideal pickup device. A reduced plot of the curves in Figure 1.

represent asymptotic values approached by an actual device under high light conditions. For this reason, data plotted for an actual device would be expected to bend away from their theoretically straight lines as they approach the dash-dot boundaries.

The complete characteristic equation with the constant factor written out is

$$B = 5(k^2/D^2t\theta)\,(1/\alpha^2C^2) \times 10^{-3} \text{ footlambert}, \tag{5}$$

where the symbols have these meanings and units:

k—threshold signal-to-noise ratio [see Equation (1a)],

D—diameter of the lens (inches),

t—exposure time (seconds),

θ—quantum yield ($\theta = 1$ means 100 per cent quantum efficiency),

α—angular size of the test object in minutes of arc,

C—per cent contrast of the test object [i.e., $C = (\Delta B/B) \times 100$ per cent].

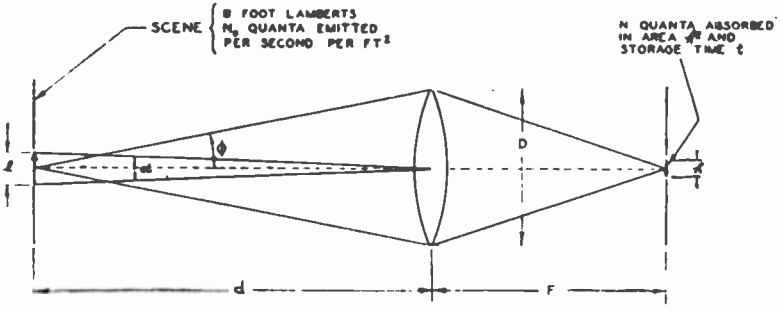

Fig. 3

The constant factor is derived as follows. In place of Equation (2) we write (see Figure 3):

$$N = \theta N_0 t l^2 \sin^2\phi, \tag{6}$$

where N_0 is the total number of quanta emitted per square foot of the scene per second according to a Lambert distribution. Now since

$$l \doteq (d/F)\,h, \qquad \text{and} \qquad \sin\phi \doteq D/2d,$$

we can write

$$N = \tfrac{1}{4}\theta N_0 t D^2 (h^2/F^2) = 1.4\theta N_0 t D^2 \alpha^2 \times 10^{-10}, \tag{7}$$

where α is expressed in minutes of arc and D in inches. Using the equivalence, one lumen of white light $= 1.3 \times 10^{16}$ quanta per second,

$$N_0/1.3 \times 10^{16} = B \text{ footlamberts},$$

$$N = 2\theta B t D^2 \alpha^2 \times 10^6,$$

and

$$B = 5(N/D^2 t\theta\alpha^2) \times 10^{-7} \text{ footlamberts}. \tag{8}$$

From Equations (3) and (1a) we get:

$$C = 100k/N^{\frac{1}{2}}. \tag{9}$$

Combining Equations (8) and (9) we get:

$$B = 5(k^2/D^2 t\theta)\,(1/\alpha^2 C^2) \times 10^{-3} \text{ footlamberts}. \tag{10}$$

The factor k in Equation (5) is of special interest because its value has frequently been assumed to be unity. That is, the statement is made that a threshold signal is one that is just equal to the root-mean-square noise.* Some estimates made recently by the writer[3] and based on observations on photographic film and on television pictures lay in the range of 3 to 7. Additional and more direct evidence is given in the next section that the value of k is not unity but is in the neighborhood of 5.

An Experimental Approach to An Ideal Picture Pickup Device

One of the oldest means of generating television pictures is the so-called light spot scanning arrangement in which the subject to be transmitted is scanned by a small sharply focused spot of light. The

---

* Such an assumption, for example, was made by the writer (reference 1) and also by H. DeVries (reference 2).

[1] A. Rose, "The Relative Sensitivities of Television Pickup Tubes, Photographic Film and the Human Eye," *Proc. I.R.E.*, Vol. 30, No. 6, p. 295, June, 1942.

[2] H. DeVries, "The Quantum Character of Light and its Bearing upon Threshold of Vision, the Differential Sensitivity and Visual Acuity of the Eye," *Physica*, Vol. 10, p. 553, 1943.

[3] A. Rose, "A Unified Approach to the Performance of Photographic Film, Television Pickup Tubes and the Human Eye," *Jour. Soc. Mot. Pic. Eng.*, Vol. 47, p. 273, October, 1946.

variable amount of light reflected from the subject is picked up by a photocell and these variations translated into beam current variations in a kinescope whose beam scans a fluorescent screen in synchronism with the first light spot. The arrangement is shown in Figure 4. Recent developments in luminescent materials and photo multipliers have brought renewed interest in the arrangement for certain types of pickups.[4] On the one hand, it is especially simple and free from the spurious signals usually found in pickup tubes. On the other hand, it is limited in application to those scenes that may be conveniently illuminated by a scanning light spot. Its particular virtue for the present discussion is that it offers a close approximation to the performance to be expected from an ideal picture pickup device. The photo-cathode of the electron multiplier represents at once both the lens opening and primary photo surface of the usual pickup device. The gain in the multiplier section is sufficient to make each photo electron, liberated

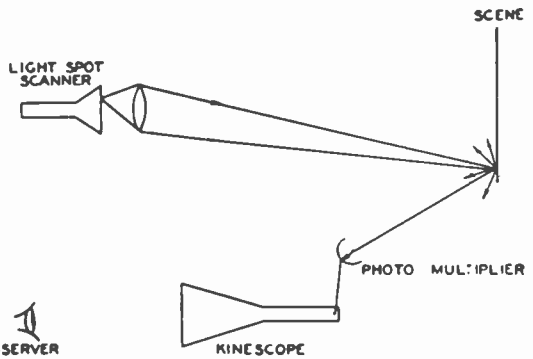

Fig. 4 — Television pickup arrangement using a light spot scanner.

from the photo-cathode, visible on the kinescope screen as a discrete speck of light. That is, each quantum usefully absorbed at the primary photo-surface can be counted in the final picture. The exposure time of the system is the exposure time of the final observer (human or instrumental) that looks at the reproduced picture on the kinescope.

The special test pattern used as subject or scene for the light spot scanner is shown in Figure 5. This test pattern is in fact a materialization of the theoretical curves in Figure 1. The disks along any row decrease in diameter by a factor of two for each step. The disks in any column have the same diameter but vary in contrast stepwise by a factor of two. If this pattern is reproduced by a pickup device performing in accordance with Figure 1, all of the disks to the upper left of some 45-degree diagonal should be visible and all of those to the

[4] G. C. Sziklai, R. C. Ballard and A. C. Schroeder, "An Experimental Simultaneous Color Television System, Part II: Pickup Equipment," *Proc. I.R.E.*, Vol. 35, No. 9, p. 862, September, 1947.

lower right should not. As the illumination is increased, the diagonal demarcation between visibility and invisibility should move to the right and in particular should move from one diagonal of disks to the next for a factor of four increase in illumination.

The series of pictures shown in Figure 6 is a series of timed exposures of the picture reproduced on the kinescope as the light spot from another cathode ray tube scanned the test pattern. For experimental convenience, the exposure time, rather than the scene luminance, was increased, since, according to Equation (5), it is only the product Bt that is significant. The first pictures in the series show what is transmitted at exceedingly low scene luminance. In fact the number of "quanta" per unit area may easily be counted. As the scene luminance is increased, more and more of the pattern becomes visible.

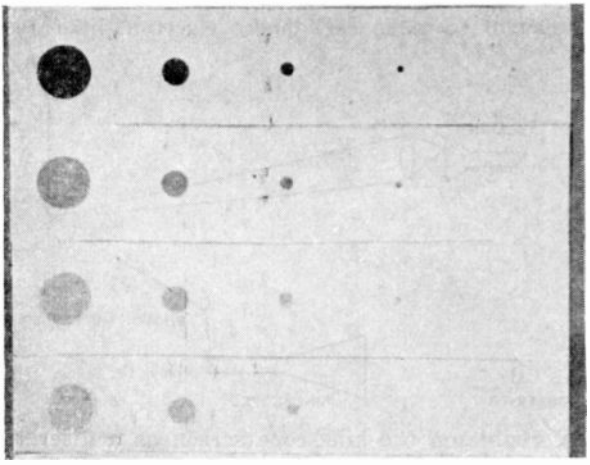

Fig. 5—Photograph of test pattern used as subject for the light spot scanner.

Equation (5) and Figure 1 are quantitatively borne out by these pictures in two important respects. First, the demarcation between visibility and invisibility is, with good approximation, a diagonal. That is, the threshold contrast varies as the reciprocal angle of the test object. Second, the demarcation shifts by one diagonal for a factor of four change in scene luminance. That is, the threshold scene luminance varies as the square of the reciprocal contrast or as the square of the reciprocal angle. While the precision of the separate pictures is not high, the precision of the series is, since there are no significant cumulative or progressive departures in the large range of scene luminance covered.

The series of pictures in Figure 6 also establishes the values of two of the parameters in Equation (5), namely the threshold signal-to-noise ratio (k) and the exposure or storage time (t) of the eye. The

threshold signal-to-noise ratio has this meaning. Take the smallest black (not grey) disk that may be seen in any one of the pictures. Transpose the outline of the disk to the neighboring white background. Count the average number of "quanta" (specks of light) within this outline. The average number of "quanta" is the signal associated with the black disk; the square root of the average number is the root mean square fluctuation,* and the ratio of signal to root-mean-square fluctuation, also the square root of the average number, is the threshold

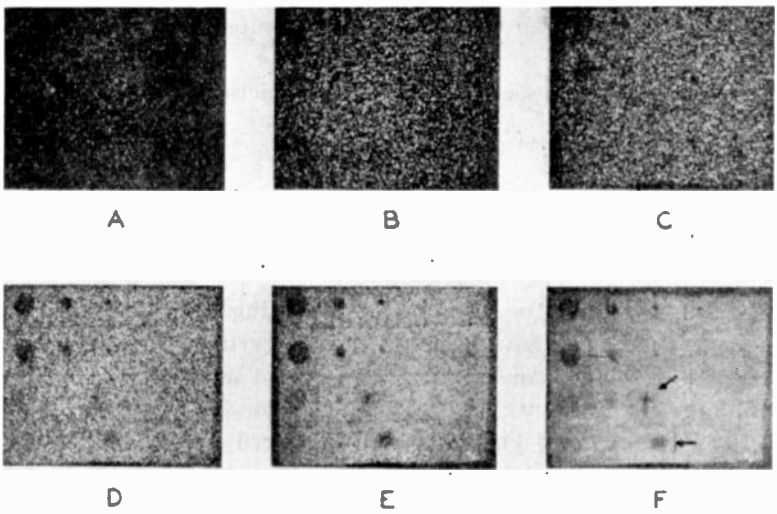

Fig. 6—Series of timed exposures of the test pattern shown in Figure 5 as transmitter by the television pickup arrangement shown in Figure 4. The exposure times, starting with Figure 6a, are 1/16, 1/4, 1, 4, 16 and 64 seconds respectively. These exposures were chosen so that the diagonal demarcation between visibility and invisibility fell to the right of rather than on a particular diagonal of discs. Thus the smallest visible black dots are somewhat above threshold visibility. To get a short decay time, the ultraviolet emission from a special zinc-oxide phosphor scanner was used.† Two obvious blemishes that were not apparent under visible light, and have no connection with the test, are indicated by arrows in Figure 6f.

signal-to-noise ratio. A similar operation can be carried out for any of the grey dots to obtain the same value of k. The results of this operation are that k lies in the neighborhood of 5. A more precise value of k depends on a more precise operation for determining the threshold visibility of any one of the black disks. A more precise value for k would, however, not depart significantly from the one given here.

* This has been roughly verified by actual counts taken on Figure 6a.

† This was suggested to the writer by O. H. Schade of the RCA Victor Division, Harrison, N. J. See also R. E. Shrader and H. W. Leverenz, "Cathodoluminescence Emission Spectra of Zinc-Oxide Phosphors," to be published in an early issue of the Journal of the Optical Society of America.

This is based on the fact that the range from substantial certainty of not seeing to substantial certainty of seeing is covered by a factor of four in scene luminance. This corresponds to a factor of two in the range of k values that might be selected. The interesting fact is that the threshold signal-to-noise ratio is not unity as is usually assumed but more nearly five.

The storage time of the eye is usually taken to be about 0.2 seconds. The series of photographs in Figure 6 confirmed that choice if confirmation were needed. The visual impression of the kinescope picture matched within a factor of two the photographic exposure for 0.25 second.

To summarize this section, the series of pictures in Figure 6 form a simple, quantitative representation of the operation of an ideal picture pickup device.

Comparison of the Performance of the Human Eye With Ideal Performance

Experimental data for the human eye relating scene luminance, contrast and visual angle have been scarce. The writer[3] has already made use of the data of Connor and Ganoung[5] and of Cobb and Moss[6] to cover the range from 10^{-4} to 10^{2} footlamberts. These data are reproduced in Figures 7 and 8 and are to be compared with Figures 1 and 2. As in the previous use of the data, values of α less than two minutes of arc and values of contrast less than two per cent were omitted. These points are close to the absolute cut-offs of ½ minute of arc and ½ per cent contrast set by other than fluctuation limitations and would be expected to depart from the theoretical curves of Figure 1.

Recently a more complete and thorough investigation of visual performance has appeared by Blackwell.[7] The points in Figures 9 and 10 were computed from Blackwell's data for grey disks on a white background. In order to plot both Figures 8 and 10, Reeves'[8] data on pupil diameter versus scene luminance were used.

In Figure 7, the data have been approximated by lines of 45-degree slope in accordance with Equation (4b). The fit is close enough to be significant. The same degree of fit is not, however, present in Black-

[5] J. P. Connor and R. E. Ganoung, "An Experimental Determination of Visual Thresholds at Low Values of Illumination," *Jour. Opt. Soc. Amer.*, Vol. 25, No. 9, p. 287, Sept., 1935.

[6] P. W. Cobb and F. K. Moss, "The Four Variables of Visual Threshold," *Jour. Frank. Inst.*, Vol. 205, No. 6, p. 831, December, 1928.

[7] H. R. Blackwell, "Contrast Thresholds of the Human Eye," *Jour. Opt. Soc. Amer.*, Vol. 36, No. 11, p. 624, November, 1946.

[8] P. Reeves, "The Response of the Average Pupil to Various Intensities of Light," *Jour. Opt. Soc. Amer.*, Vol. 4, No. 2, p. 35, March, 1920.

well's data in Figure 9. Here the 45-degree lines are drawn tangent to the best performance at each value of scene luminance. The data in each case curve away from the straight lines. The degree of fit is still, however, sufficiently good for many engineering purposes. It is also sufficiently good to draw significant conclusions regarding the mechanism of the eye, as will be discussed below. In comparing Figures 7 and 9 with Figure 1 it is to be noted that the correction for the variation in pupil diameter has not yet been introduced. Such correction is introduced in Figures 8 and 10.

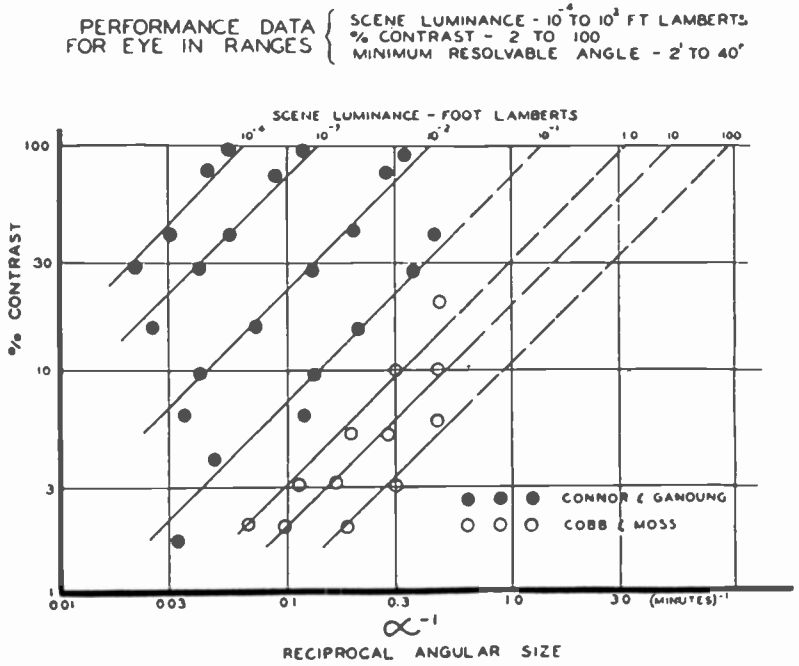

Fig. 7—The solid lines with 45-degree slope are approximations to the experimental data by ideal performance curves.

In Figures 8 and 10 the data are re-plotted as in Figure 2. If the quantum efficiency, exposure time and threshold signal-to-noise ratio of the eye were invariant with scene luminance, and if the performance of the eye were limited by fluctuations in the absorption of light quanta, the data in Figures 8 and 10 should all lie along a single straight line. The fact that the data do not lie along a single straight line but have some spread is a measure of the departure from one or more of the above conditions. Before discussing these departures it is well to note that Blackwell's data are substantially contained between the same two straight lines as are the data of Connor and Ganoung and Cobb and Moss.

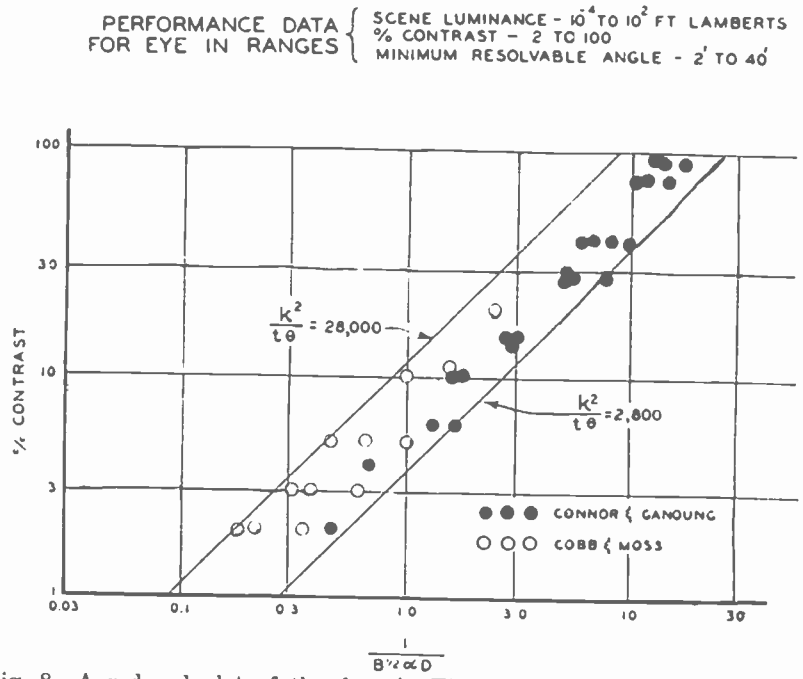

Fig. 8—A reduced plot of the data in Figure 7. The two solid lines are computed from Equation 5 for an ideal device.

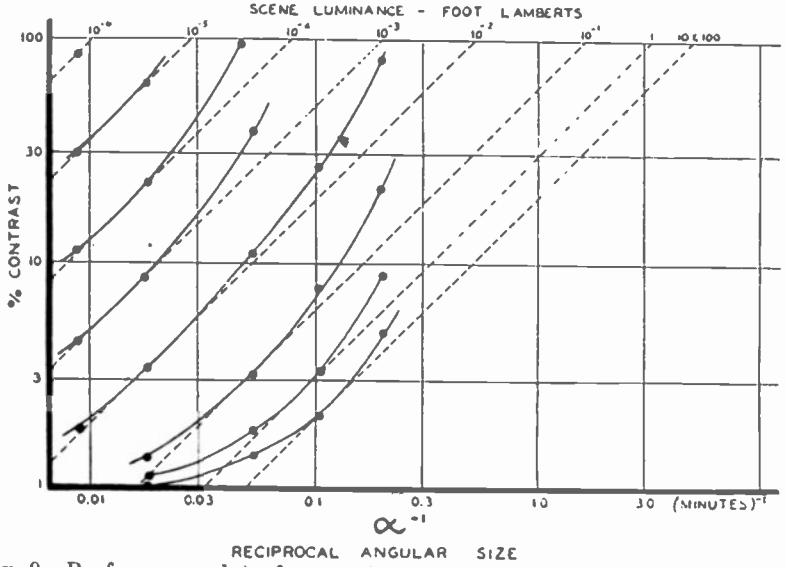

Fig. 9—Performance data for eye (computed from Blackwell). The dotted lines with 45-degree slope are ideal performance curves drawn tangent to the best observed performance at each value of scene luminance.

The two straight lines that bracket the data both in Figure 8 and in Figure 10 are labelled $k^2/t\theta = 2800$ and $k^2/t\theta = 28{,}000$. Equation (5) was used to compute these values. The significance of these lines may be indicated as follows. If one arbitrarily assumed that k and t were invariant with scene luminance and that the performance of the eye were limited by fluctuations and took for k and t the values of 5 and 0.20 respectively, then one would conclude that all of the data contained within these lines could be represented by an ideal picture pickup device having a quantum efficiency between 0.5 and 5 per cent. On the one hand, this is a large spread in quantum efficiency; on the other

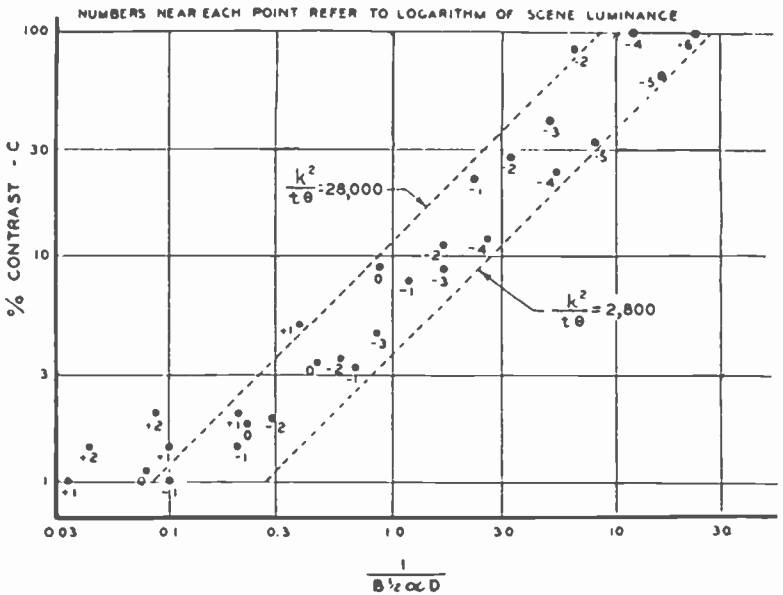

Fig. 10—A reduced plot of the data in Figure 9. The two dotted lines are the same as the two solid lines in Figure 8.

hand, even this large spread severely limits the choice of mechanisms used to explain the phenomenon of dark adaptation, the latter covering a range of "apparent sensitivities" of over a thousand to one.

If, now, k and t instead of being assumed constant, were allowed to vary with scene luminance, their most reasonable direction of variation would be such as to reduce the range of variation of θ, the quantum efficiency. So also, if mechanisms other than fluctuations in the absorption of light quanta are used to describe the performance of the eye, these mechanisms, because they would be introduced at the high light end, would tend to reduce the range of variation of θ. In brief, a factor of ten represents the maximum variation that the quantum efficiency of the eye undergoes in the range of 10^{-6} to 10^{2} footlamberts.

General Discussion

A. Problems of Engineering Importance

The fact that the bulk of the performance data of the eye can be simply summarized by the performance of an ideal picture pickup device operating with a quantum efficiency of 5 per cent at low lights and 0.5 per cent at high lights is of considerable technical convenience. The ranges of the three parameter are:

scene luminance	10^{-6} to 10^{+2} footlamberts
per cent contrast	2 to 100
visual angle	2′ to 100′

The types of problems that are clarified by this approach are: specification of the performance of television pickup tubes that are designed to replace the human eye; estimate of the factor by which pickup tubes should exceed the eye in performance when the reproduced picture is viewed at a higher luminance than the original scene; estimate of the maximum gain in intelligence that may be obtained by any picture pickup device interposed between the eye and the scene; the setting up of criteria for the visibility of noise in a television picture or of graininess in photographic film; and finally, the ordering of the performance of present television pickup tubes and film relative to that of the eye. Two of these problems will be discussed briefly.

If the eye may be treated as an ideal pickup device, the criterion of threshold noise visibility is simple. It is that the signal-to-noise ratio associated with an element of area of the retina be approximately equal to the signal-to-noise ratio associated with the same element of area in the original scene in which noise is to be observed. Thus, in a series of tests in which pictures similar to those in Figure 6 were directly viewed on a kinescope, it was found that the noise in these pictures could be reduced to threshold visibility by interposing a neutral filter between the eye and the kinescope. The transmission of the neutral filter was such that, at threshold, the number of white specks per unit area per unit time on the kinescope face was approximately equal to the number of light quanta absorbed by the retina from the same area per unit time. A quantum efficiency of 0.5 per cent was used for this computation. It is probably more significant to apply the same type of analysis to data already published, as for example, in the paper by Jones and Higgins[9] on the graininess of photographic film. Table I, column 1 shows the values of signal-to-noise ratio measured by Jones and Hig-

[9] L. A. Jones and G. C. Higgins, "Photographic Granularity and Graininess," *Jour. Opt. Soc. Amer.*, Vol. 36, No. 4, p. 203, April, 1946.

gins for several widely different types of film and for a test area 40 microns in diameter on the film. In column 2 are given the computed values of signal-to-noise ratio for the same test area at the retina under what they call threshold conditions for seeing graininess. To compute column 2, a quantum efficiency of 0.5 per cent was assumed for the eye as well as a pupil diameter of 4 millimeters and a storage time of 0.2 second.

The large discrepancy between the low light performance of the eye and that of present television pickup tubes and photographic film was referred to at the beginning of this paper. Its origin is this. The eye appears to act like an ideal device over a large range of scene luminances. That is, as the scene luminance is decreased the signal received by the retina falls linearly while the noise associated with the signal falls as the square root of the scene luminance. And these relations hold even down to 10^{-6} footlambert. The same relations hold for pickup tubes and film but usually only over the relatively narrow light ranges in which they are normally used. In these ranges, they act like ideal devices with a quantum efficiency about the same as that of the eye. As the scene luminance is lowered, however, various sources of fixed noise (invariant with scene luminance) dominate and obscure the picture. These sources of noise include the noise in a television amplifier, the shot noise in a scanning beam, and the fog in photographic film. None of these sources represent absolute limits to the performance of pickup tubes or film since designs are conceivable in which these sources of noise are absent and only the intrinsic noise in the primary photo process is present. They do, however, represent present and, it is hoped, transient limitations. A further handicap to the performance of film at low illuminations is the fact that more than one absorbed quantum is needed to make a grain developable. When the incident concentration of quanta falls below the concentration of grains, the picture disappears as if by a "clipping" action. In brief, photographic film would satisfy ideal performance even, or especially, at arbitrarily low scene luminances if (a) fog were absent and (b) a single absorbed quantum were sufficient to make a grain developable. Film could then *count* each absorbed quantum.

B. Dark Adaptation and Related Phenomena

The outstanding feature of dark adaptation is well known. Immediately after exposure to a luminance of about 100 footlamberts, the lowest luminance the eye can detect is over 1000 times larger than the luminance it can detect after extended dark adaptation. The significant question here, that bears on the mechanism of the eye, is, "Is the

Table I.

Film	Signal-to-noise ratio of 40-micron-diameter disk on film. (From Jones and Higgins.[9]) Density of film $\doteq 0.4$	Signal-to-noise-ratio of image of 40-micron-diameter disk at retina. Computed for 0.5 per cent quantum efficiency and 0.2 seconds storage time.
Tri-X	11	13
Super XX	23	22
Pan X	36	39
Fine grain	77	58

sensitivity, that is, quantum efficiency, of the dark adapted eye over a thousand times greater than that of the light adapted eye?* The answer, from Figures 8 and 10, is definitely in the negative and with a large factor of safety. From these figures, at most a factor of ten can be ascribed to change in quantum efficiency. The rest, except for some contribution of pupil opening, must come from another mechanism. And a reasonable mechanism to postulate is a gain control mechanism located between the primary photo process at the retina and the nerve fibers that carry the impulses to the brain. A gain mechanism, minus the idea of control or variability, is not at all *ad hoc*. It is needed to raise the energy level of the absorbed quanta to the energy level of their corresponding nerve pulses. To add variability to the gain mechanism is indeed a minor assumption and one that can readily account for the large range of dark adaptation.† From necessarily subjective evidence, the gain control appears to be automatically set so that noise is near the threshold of visibility. At very low lights, around 10^{-4} footlambert, "noise" appears to be more easily visible than at moderate lights around one footlambert. The writer has been most impressed by the appearance of noise in dimly lit scenes after the thorough dark accommodation that comes from several hours of sleep-

* If one takes, for example, Hecht's (reference 10) assumption that threshold visibility corresponds to a fixed amount of sensitive material decomposed by the incident threshold light, then since the threshold light intensity changes by a factor of 10^4 (see Figure 3 of Hecht's paper, "Rod portion of the 'blue' curve"), from low to high adaptation light intensities, the quantum efficiency must also change by this factor.

[10] S. Hecht, "The Instantaneous Visual Thresholds After Light Adaptation," *Proc. Nat. Acad. Sci.*, Vol. 23, p. 227, 1937.

† Parallels to the idea of a variable gain element are common in electron tubes. In the image orthicon (reference 11), for example, an electron multiplier acts as the variable gain element that raises the level of signal and noise coming out of the tube above the noise level of the amplifier to which the tube is connected.

[11] A. Rose, P. K. Weimer, and H. B. Law, "The Image Orthicon, a Sensitive Television Pickup Tube," *Proc. I.R.E.*, Vol. 34, No. 7, p. 424, July, 1946.

ing in a dark room. Since these conditions are not the normal ones for making reliable observations, the reference must be regarded as one of interest but not of evidence.

At the risk of being repetitive, the conclusions of this section may be stated in another way. Photo-chemical mechanisms that are confined to the primary photo-process at the retina cannot account for more than a few per cent of the total range of dark adaptation. By primary photo process is meant the process in which the incident light quanta are absorbed. The *products* of the primary photo process may however be transmitted to the nerve fibers with variable efficiency consistent with the variable gain mechanism already discussed. Thus the assumption of a variable concentration of active material whose absorption of incident light quanta is correspondingly variable, or the assumption of rods and cones with a variable threshold of excitation can be expected at most to play only a minor role in dark adaptation.

It is interesting to record here a possible but less certain application of the gain control mechanism. At high lights, luminosity, visual acuity[12] and contrast discrimination are substantially the same for red and blue illumination having the same luminance. At very low lights, less than 10^{-3} footlambert, luminosity, visual acuity[12] and contrast discrimination under red light rapidly approach zero while under blue light, significantly finite values are maintained. In the intermediate range of 10^{-3} to 1 footlambert, the range of present interest, the luminosity of red light drops below that of blue light while acuity[12] and contrast discrimination[13] remain substantially the same for the two colors. A formal explanation of the observations in the intermediate light range follows immediately if one allows fluctuations in the primary photo process to determine visual acuity and contrast discrimination. Then, if the gain control is set high enough so that these fluctuations are apparent to the brain, all possible intelligence is thereby transmitted to the brain and variations of the gain setting vary luminosity but not acuity or discrimination. According to this argument, the gain for red light is less than that for blue light in the intermediate light range.

C. Other Mechanisms

It was stated earlier in this paper that the departure of the actual performance of the eye from that to be expected from an ideal device

[12] S. Shlaer, E. L. Smith and A. M. Chase, "Visual Acuity and Illumination in Different Spectral Regions," *Jour. Gen. Physiol.*, Vol. 25, p. 553, 1942.

[13] M. Luckiesh and A. H. Taylor, "Tungsten, Mercury and Sodium Illuminants at Low Brightness Levels," *Jour. Opt. Soc. Amer.*, Vol. 28, p. 553, 1942.

was a measure of the "logical space" within which one could introduce mechanisms, other than fluctuations in the primary photo process, to determine the performance of the eye. Such other mechanisms would, of course, lead to lower performance than would fluctuations in the primary photo process alone. What is important, then, is to get an estimate of the extent of this "logical space."

To clarify the problem, reference is made to Figures 8 or 10. If independent measurements of k, t, and θ verify that $k^2/t\theta$ is 2,800 at low lights and 28,000 at high lights as shown in these figures, then, except for minor departures, the actual performance of the eye matches the performance expected from an ideal device and the "logical space" is substantially absent. The inquiry then leads to what is known of k, t, and θ separately.

The threshold signal-to-noise ratio, k, was taken from Figure 6. Its value, 5, is primarily a low light value in that it applies to the condition that noise is easily visible. If noise is not easily visible, as at higher lights, an increase in k can be invoked. But such an increase is in the direction already noted in Figures 8 and 10 and would only relieve the quantum efficiency (θ) of the necessity of varying from low to high lights.

The storage time (t) was also observed from Figure 6 and the original kinescope pictures to be about 0.25 second. This value applies to the intermediate light range. At very low lights, if one takes the constant in the often quoted law of Blondel and Rey, the storage time is still about 0.2 second. Finally, the data of Cobb and Moss in the range of 1 to 100 footlamberts were taken for an exposure time of 0.18 second and match the data of Connor and Ganoung fairly well, the latter having been taken for an observation time of one second. All of this points to a storage time of 0.2 second independent of scene luminance. Langmuir and Westendorp[14] confirm this constancy except for a suggestion of a longer storage time near absolute threshold.

In spite of all of these independent sources of evidence pointing to a storage time of 0.2 second, there is still some uncertainty. The uncertainty comes from not having good data on how well the memory process can extend the physical storage time to times longer than 0.2 second. Such extension would of course vary with the observer and improve with training. Some remarks and data in Blackwell's paper suggest that memory may extend the effective storage time up to seconds. The most that may be said for the data quoted in the present paper, with the exception of the Cobb and Moss data, is that the

[14] I. Langmuir and W. F. Westendorp, "A Study of Light Signals in Aviation and Navigation," *Physics*, Vol. 1, No. 5, November, 1931.

effective storage time may be anywhere between the physical storage time of 0.2 second and the actual observation time of one second.

Independent measurements of quantum efficiency at low lights bracket the value of 5 per cent used in this paper. Hecht,[15] by a statistical analysis of threshold measurements, consistently arrives at about 5 per cent. Brumberg, Vavilov and Sverdlov,[16] by a similar experiment, arrive at values from about 5 to 25 per cent. Both Hecht and Brumberg's measurements are for blue light in the neighborhood of maximum visual response. They should be divided by a factor of about three to reduce them to white light for comparison with the value of 5 per cent already noted in this paper. At high lights, the writer knows of no independent measurements of quantum efficiency.

To summarize the discussion thus far, independent measurements of k, t, and θ agree well with the low light value of $k^2/t\theta$ in Figures 8 and 10. At high lights there is uncertainty both about k and θ. If k increases or θ decreases, the high light value of $k^2/t\theta$ in Figures 8 and 10 might be independently verified. In that event, little room is left for mechanisms other than fluctuations in the primary photo process to determine the acuity and contrast discrimination of the eye. If, however, k and θ are independent of scene luminance, as much as a factor of ten in performance can be ascribed to the limitations imposed by other mechanisms.

There remains the departures from straight lines noted in Figure 9. Since, at a fixed scene luminance, k, θ, and t should remain constant these could not account for such departures. It is rather more likely that the departures represent optical defects in the sense that, as the scene luminance is lowered, the eye combines signals from neighboring rods and cones to form larger picture elements. These larger picture elements, if they are of the same order as the smallest resolvable black disks, would limit acuity in the same way that the separate cones set a final limit to acuity. That the eye combines signals from neighboring rods and cones is a consequence of the fact that more than one absorbed quantum is needed to generate a visual sensation (see also Hecht[15]). Objective measurements by Hartline[17] on the frog's eye also point to such a combining process.

---

[15] S. Hecht, "The Quantum Relations of Vision," *Jour. Opt. Soc. Amer.*, Vol. 32, No. 1, p. 42, January, 1942.

[16] E. M. Brumberg, S. I. Vavilov and Z. M. Sverdlov, "Visual Measurements of Quantum Fluctuations," *Jour. Phys. U.S.S.R.*, Vol. 7, p. 1, 1943.

[17] H. K. Hartline, "Nerve Messages in the Fibers of the Visual Pathway," *Jour. Opt. Soc. Amer.*, Vol. 30, No. 6, p. 239, June, 1940.

SUMMARY

The performance of the eye over the bulk of its operating range may be matched by an ideal picture pickup device having a storage time of 0.2 second and a quantum efficiency of 5 per cent at low lights decreasing to 0.5 per cent at high lights. For many engineering problems in which the performance of the eye must be quantitatively compared with the performance of man-made pickup systems, the substitution of an equivalent ideal device for the eye considerably simplifies the analysis. The match between the eye and an ideal device also provides at minimum a good first approximation to an understanding of the performance of the eye in terms of fluctuations in the primary photo process. Depending mostly on how well further independent measurements of the quantum efficiency of the eye agree with the quantum efficiencies deduced in this paper, the analysis of performance in terms of fluctuations may be appreciably better than a first approximation.

ACKNOWLEDGMENTS

The writer has profited from many discussions of the subject of this paper with Dr. D. O. North of these laboratories.

ELECTRO-OPTICAL CHARACTERISTICS OF TELEVISION SYSTEMS*†#

By

Otto H. Schade

Tube Department, RCA Victor Division,
Harrison, N. J.

Summary—The optical and electro-optical conversion processes in television systems are examined as intermediate stages of a multi-stage process by which optical information at the real object is "transduced" into sensory "response" at the brain. The characteristics of the human eye and vision in the final stage of this process determine the requirements and standards for preceding stages. When expressed on a unified basis by "transfer" and "aperture response" characteristics, the properties of the process of vision can be correlated with those of external imaging and transducing processes. It is shown that image definition, or the corresponding information from optical or electrical image-transducing stages, can be specified by the characteristics of an equivalent "resolving aperture." These characteristics may be computed and measured for all components of the system.

Quantitative data from measurements permit definite quality ratings of optical and electrical components with respect to theoretical values. A subjective rating of the resolution in an imaging process external to the eye such as a television system is derived by establishing a characteristic curve for the relative "sharpness" of vision as affected by the "aperture response" of the external imaging process.

A general review of the material and the broad methods of analysis employed are given in the Introduction. Following this, Part I treats characteristics of vision and visual systems. In this part, viewing angle, sensation characteristics, color response, persistence of vision, flicker, resolving power, response characteristics, and steady and fluctuating brightness distortions are discussed and related to the characteristics of external imaging systems and the television process.

Introduction

THE function of a television system is to generate optical images which create in the mind of the observer the illusion of seeing real objects and action scenes. The degree of technical perfection in the optical image required to create this illusion depends to a considerable extent on the televised subject matter and the skill exhibited in capturing and directing the interest of the observer.

---

* Decimal Classification: R138.3 × R583.11.

† This paper consists of an Introduction and four parts: Part I—Characteristics of Vision and Visual Systems; Part II—Electro-Optical Specifications for Television Systems; Part III—Electro-Optical Characteristics of Camera Systems; Part IV—Correlation and Evaluation of Electro-Optical Characteristics of Imaging Systems.

Reprinted from *RCA Review*, March, 1948.

The process of "tele-vision," illustrated by Figure 1, requires a complex electro-optical system to extend the optical imaging process in the eye to the lens of the television camera which sees the real object. The system components ((1) to (4), Figure 1) should not limit the capabilities of the eye; but on the other hand, they should not be required to pass information the eye cannot see. It is neither essential nor desirable for easy vision to reproduce stationary images with minute detail requiring inspection at closer than normal viewing distances, because magnification and "close-ups" of interesting detail are functions performed with greater reality and better perspective by the television camera at the real object.

Contrast, gradation, color, sharpness, and brightness distortions in the reproduced image are judged by the eye. The capabilities and optical characteristics of the eye determine, therefore, the optical standards for the reproduced image. It would be rather hasty to con-

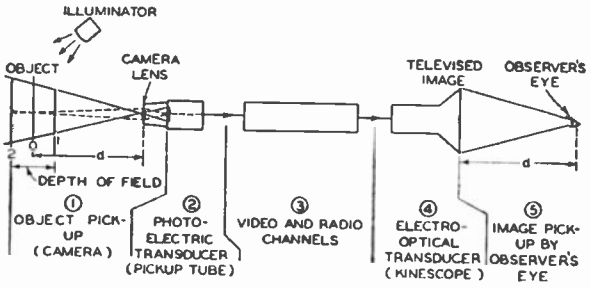

Fig. 1—Optical and electrical components of television process.

clude that the same optical standards of quality apply as well to the optical image formed by the camera lens, even in a purely photographic process. This assumption would require that the quality of the entire conversion process between the optical and reproduced images in the system exceed the quality of both images by a substantial factor leaving but a very small margin for degradation in each individual process. Losses and degradations, however, occur in every stage of a practical process, and it is by no means obvious what degree of perfection should be attained in optical or electrical components where an unbalance of performance is economically or technically sound, and where a correction may best be introduced to compensate for a deliberate unbalance or a limitation. The answers to these questions can hardly be given in a usable form unless a carefully planned examination of all processes in the system, including the process of vision is made.

It might appear logical to analyze the system in an order beginning with the camera and progressing through the various stages of con-

version to the final optical image. This course, however, would lead to a very specific or an unnecessarily broad treatment of processes which can be avoided by first establishing the guiding standards for optical images which are based on the characteristics of the visual process. After the transfer characteristics of the kinescope are determined, these optical standards can be translated into electrical specifications for the television process and the "video" signal. The generation of signals can then be treated in a normal sequence. Beginning with a discussion of the photoelectric conversion process, the properties of lenses, camera tubes, and video signals can be reviewed on a unified basis permitting coordination in a final evaluation of the television process.

All components of a television system are fundamentally converters or "transducers" of energy. In the simplest case a transducing process can be specified by a single number, which will be termed the "transfer factor." The transfer factor (g) is the ratio of the output "signal" to the input "signal" in appropriate units and often implies the efficiency of the process. In most cases, however, the transfer factor is a variable dependent on one or many parameters such as the average signal level, the input signal intensity, the output "load", the frequency and form of the signal, and others. The transfer properties of a transducer are, therefore, more accurately described by one or several characteristic curves; i.e., the "transfer characteristics". Examples of well-established transducer characteristics are the static characteristics of electron tubes and of photographic film, and the transfer characteristics of electrical coupling networks and filters.

The methods of determining or measuring transfer characteristics and their use in the graphic determination of signal distortion and dynamic operating conditions are fundamentally similar in all of these cases. Moreover, the same methods can be applied to all transducing processes in a television system. When the transducing system of the eye and vision is discussed later on, the similarity of the treatment to that of electrical transducers will be apparent and useful, although the treatment may seem at first glance to be a rather unorthodox method of covering a much discussed and somewhat controversial subject. In this and other instances, the derived characteristics are based on data and observations reported in the literature by specialists in the particular field, although the form of presentation may, at times, be different.

Aperture Considerations and Detail Visibility

One property of particular interest in the analysis of image-trans-

ducing systems, discussed in detail in Parts II and IV but referred to throughout this paper, is the loss of resolution and quality which occurs in each process of optical or electrical conversion. In a broad sense each conversion process has a "frequency response characteristic" which shows a decrease of "signal output" in response to "input signals" of increasing spatial or electrical frequency when analyzed by scanning.

In electrical terms, transducers act as low-pass filters. When the signal is of electrical origin (as in the case of fluctuation "noise" signals) the entire transducing system is advantageously treated as an electrical filter system.

In most cases, however, it is of advantage to retain the physical concepts of scanning when treating resolution and the response of transducers to detail signals. According to these concepts the "resolving element" of optical and electrical devices can be regarded as a small "aperture". This "aperture" may be a real scanning aperture as in a Nipkow scanning disc or in an image-dissector tube; it may be a multiplicity of reduced optical images of one larger aperture simultaneously forming countless figures of confusion as in the case of a defocussed lens; or again it may just be a fictitious or equivalent aperture, moving or stationary, which determines the cross section of elemental beams of light or electrons.

If the size and flux distribution of this "aperture" is known, the response characteristics or "aperture effects" can be computed by analysis with the scanning process and vice versa. Mathematical evaluations of the aperture response based on a Fourier analysis of a step function or pulse wave can be found in the literature[1-4], but the results do not apply directly to practical aperture shapes or test patterns.

A more practical approach requires a method of expressing the aperture response in a form which can be checked by measurements of the response to signals generated with normal test objects producing repetitive square-wave flux patterns (optically such as the standard bar or line pattern). The detail area in these test objects is defined with respect to the picture area or a unit area. When the resolving aperture is symmetric, the resolved area can be specified by its length

[1] H. A. Wheeler and A. V. Loughren, "The Fine Structure of Television Images", *Proc. I.R.E.*, Vol. 26, pp. 540-576, May, 1938.

[2] Pierre Mertz, "Television—The Scanning Process", *Proc. I.R.E.*, Vol. 29, pp. 529-537, October, 1941.

[3] M. Cawein, "Television Resolution as a Function of Line Structures", *Proc. I.R.E.*, Vol. 33, pp. 855-864, December, 1945.

[4] R. E. Graham and F. W. Reynolds, "A Simple Optical Method for the Synthesis and Evaluation of Television Images", *Proc. I.R.E.*, Vol. 34, pp. 18W-30W, January, 1946.

in one direction (horizontal or vertical), but most commonly the length is expressed by the reciprocal value: the line number per unit length (N/mm) or the line number per picture frame height (N).

When the resolving aperture is asymmetric, a square having an equivalent detail area can be specified by a balanced line number $\overline{N} = \sqrt{N_H \times N_V}$. It is well known that the balanced line number $\overline{N}$ indicates for a television system the minimum electrical frequency channel Δf required for its reproduction. For a given frame time T_f, a balanced line number N_{co} at channel cut-off, and normal blanking percentages, the frequency channel is given by the relation

$$\Delta f = 0.85\, N_{co}^2/T_f \qquad (1)$$

This equation establishes a connection between optical and electrical picture information.

Response characteristics have been computed for various aperture types as a function of the line number in square-wave flux patterns in order to compare them with the measured characteristics of optical and electrical processes. A series of photographs illustrating the response of optical apertures give quantitative proof of the theory.

Any point on a response curve is expressed by a response factor, which is the ratio of the aperture signal output at a line number N to the normal signal output at $N = 0$. Absolute signal values, such as the optical detail contrast, are easily derived, but should not be confused with the response factor which only indicates such values on a percentage basis. It is important to remember, especially in the treatment of the eye, that a small response factor may represent signal intensities well above threshold values when the "signal" to the aperture is sufficiently large provided it does not cause overload or saturation of the "indicating device."

With these principles in mind it appears logical to review the characteristics of the eye and vision as a transducing system and to develop, if possible, some of its transfer and aperture response characteristics as a guide in determining desirable optical specifications for the final image of a reproducing system. Comparison of these standards of quality with those of the graphic arts will be made on various occasions for reference to the performance level of accepted practices.

The subject of brightness distortion, especially the visibility of undesired optical detail signals resulting in graininess of the image, is treated in greater detail. The visibility of these "random brightness fluctuations" is observed by experiment and evaluated by taking into account the "filtering effect" due to the response characteristics of eye

and kinescope. The results of this analysis are expressed by grain-visibility constants which are optical "signal-to-noise" ratios.

With this background a number of characteristics and parameters of the television process can be examined more specifically in relation to optical performance standards. Translation of these standards into specifications for the electrical or video signal is based on the electro-optical transducing process: the transfer and aperture characteristics of the "kinescope".

Electrical signal-to-noise ratios for high-quality images and various optical effects arising from scanning-line structures and response characteristics of limited electrical channels can then be evaluated.

The relative sharpness of images, reproduced by a television process with certain characteristics and by photographic processes with limited resolving power can be compared by subjective methods as described by Baldwin[5].

The results are of considerable importance because they indicate certain television system specifications necessary to achieve equality with accepted motion picture performance. Because of differences arising from the use of small scanning apertures, sharply defined electrical channels, and the influence of grain or "noise" in practical images, a re-evaluation of the relative sharpness by a subjective method is of interest.

Video Signal Generation and Factors Determining the Over-all Performance of the Television System

As will be discussed in Parts III and IV, present methods of generating video signals for transmission over a single electrical channel are based on the scanning process. Fundamentally, a projected area of the field of view is inspected through a small "aperture" moving with uniform speed along adjacent parallel paths. The spatial distribution of light along these paths, placed end to end, is thus converted into an order of time distribution and the light fluctuations "observed" through the scanning aperture can readily be transduced into electrical signals.

An early application of this principle is the light-spot scanning system which has again become of interest for certain uses. In modern applications, the mechanical aperture of the old Nipkow scanning disc is replaced by an equivalent aperture defining the size of the light-exciting electron beam in a high-voltage kinescope. The intense electrically-deflected light spot is focused onto opaque or transparent

[5] M. W. Baldwin, Jr., "The Subjective Sharpness of Simulated Television Images", *Bell Sys. Tech. Jour.*, Vol. 19, pp. 563-587, October, 1940.

objects. The light reflected or transmitted from the elemental object area under the scanning light spot is picked up by a phototube which transduces the received light-flux variations into electrical signals. To overcome various limitations imposed by this special method of object illumination, later efforts have been directed toward solutions permitting the use of a normal continuous illumination.

The principle of electrical charge storage as first applied by V. K. Zworykin in his iconoscope[6,7] overcame the serious lack of efficiency which occurs when continuously illuminated objects are "observed" with an instantaneous photoelectric transducer through a scanning aperture. Because only the small fraction of light energy under the scanning aperture is converted into signals at any one instant, the conversion efficiency of instantaneous transducers (with respect to the total light flux) decreases in direct proportion to the size of the scanning aperture.

Because of the energy storage between repetitive periods of signal development, the signal current and efficiency of storage-type transducers under continuous exposure conditions are basically independent of the size of the scanning aperture. The iconoscope thus made possible the first direct pickup of scenes with good resolution under natural lighting conditions.

The need for still higher sensitivity remained, and it is largely due to the work of Rose, Iams, Weimer, and Law[8-11] that the efficiency of all three stages of the transducing process has been increased to the present high level obtained in the image orthicon.

Although further increases of sensitivity are possible and desirable, the factors controlling the quality of television signals and images have become more important. Of particular interest are the relations of scene illumination, sharpness, and signal-to-noise ratio which depend on the combined characteristics of optical and photoelectric processes in the television camera.

---

[6] V. K. Zworykin, "The Iconoscope—A Modern Version of the Electric Eye", *Proc. I.R.E.*, Vol. 22, pp. 16-32, January, 1934.

[7] V. K. Zworykin, G. A. Morton, and L. E. Flory, "The Theory and Performance of the Iconoscope", *Proc. I.R.E.*, Vol. 25, pp. 1071-1092, August, 1937.

[8] H. A. Iams, G. A. Morton, and V. K. Zworykin, "The Image Iconoscope", *Proc. I.R.E.*, Vol. 27, pp. 541-547, September, 1939.

[9] A. Rose and H. A. Iams, "The Orthicon", *RCA REVIEW*, Vol. 4, No. 2, pp. 186-199, October, 1939.

[10] A. Rose, "The Relative Sensitivities of Television Pickup Tubes, Photographic Film, and the Human Eye", *Proc. I.R.E.*, Vol. 29, pp. 293-300, June, 1942.

[11] A. Rose, P. K. Weimer and H. B. Law, "The Image Orthicon—A Sensitive Television Pickup Tube", *Proc. I.R.E.*, Vol. 34, pp. 424-432, July, 1946.

The efficiency of the optical imaging process performed by the camera lens is not only a function of the field depth which is to be imaged sharply, but it is also a function of detail size. The properties of camera lenses as transducers of light can be expressed in terms of optical transfer factors, transfer characteristics, and aperture response characteristics. Because the conversion of light energy into physical information on film is not exactly comparable to the purely photoelectric process in television camera tubes, the principles and limitations of optical imaging deserve reviewing. Variation of optical parameters causes in some respects dissimilar effects which must be considered in the use and selection of lenses and pickup tubes for the television camera.

The optical transfer factor of the television camera, for example, is independent of image size and is determined by the lens diameter (not the f: number) which has a fixed value for a specified viewing angle and sharpness in depth. The minimum "plate" size for practical cameras, however, is limited by optical and electrical difficulties in obtaining adequate resolving power.

Observations on television signals and difficulties experienced in making accurate test patterns for television purposes have indicated that the aperture response of camera lenses may depart considerably from the theoretical curve expected from their limiting resolution. As data on the aperture response of lenses are practically non-existent, a series of optical tests were made with a variety of lenses to indicate the order of the deviations and the type of equipment best suited for direct measurements.

A "television micro-photometer" was developed which, in principle, is an optical lens-bench arrangement except that observation and measurements are made through a television system. The lens under test is set up to form a greatly reduced image of an intensely illuminated line test pattern taxing its resolving power. The optical image from the lens is inspected through a high-powered microscope over a television camera chain and is seen as a highly magnified image on the television screen. One cross section through this image is made visible on an oscilloscope by means of a "line selector". The waveform represents the transduced light-flux variations in the lens image and is a photometric trace of its aperture response.

The response characteristics obtained in this manner furnish exact numerical values for expressing the sharpness of the optical camera image and permit correlation with the performance of other system components.

Given the aperture characteristics of the components, the over-all

aperture response of the process can be computed and approximated by the response of one equivalent aperture having an effect similar to the combined effect of all aperture processes in the system including that of the eye. The conditions for equivalence are debatable in some processes, requiring verification by other methods, but the aperture effect of single components can be judged by its influence on the over-all response of the system. It will be apparent that much can be gained by improving the response of nearly all system components.

For a better understanding of both its strong points and limitations, the transducing process in television pickup devices will be examined in somewhat greater detail. In storage types, the storage capacity and efficiency of the signal-developing process determine latitude and obtainable signal-to-noise ratios which, in turn, determine gradation and range of light values in the final image. The shape of the over-all transfer characteristics showing light output as a function of light input is not fixed by individual characteristics because it can be controlled in the electrical channel. Modifications are limited, however, by the character and magnitude of the fluctuation noise signals.

The question of whether or not the television process should have a transfer curve like a photographic process cannot be answered with a definite yes or no, because both processes have strong and weak points and both will give optimum performance only when properly used within their limitations.

* * *

PART I—CHARACTERISTICS OF VISION AND VISUAL SYSTEMS

(A) Some Characteristics of Vision and Visual Systems

It is impossible to simulate accurately the process of normal vision by an equivalent device or to formulate the operational characteristics of the process of vision except for relatively simple and properly defined viewing conditions and test objects.

The viewing conditions for television images have no exact precedent in the visual arts, although they are quite similar to the conditions prevailing when small motion pictures are viewed in the home. A formulation of the viewing conditions is attempted but they are based on the characteristics of the eye and not necessarily on present standards of related visual arts.

1. *Viewing Angle and Viewing Ratio*

The normal field of vision covers an angle (2α) of 30 to 40 degrees (see Figure 2). A considerably larger field (approximately 90 degrees

for color vision) is imaged on the retina but it is rather poorly resolved by the eye. It is well known that only the central area (fovea centralis) extending over hardly more than 2 degrees is capable of high resolution. The resolving power decreases rapidly, away from the optical axis for the remaining area which acts primarily as a view finder.

For sharp vision the eyeballs are, therefore, moved continuously to enclose and follow sections of interest in the viewing field within this small angle. Comfortable vision over extended periods should not require movement of the head and the field under observation should, therefore, not exceed a certain angle. The length of one line in a book of normal size indicates this angle to be of the order of 25 degrees. Pictorial objects are usually viewed under a smaller angle such as 15 to 20 degrees in order to obtain a more simultaneous impression of the entire object. Standard television images have the dimensional ratios V:H:D = 3:4:5 (Figure 2). It is convenient to express the diagonal

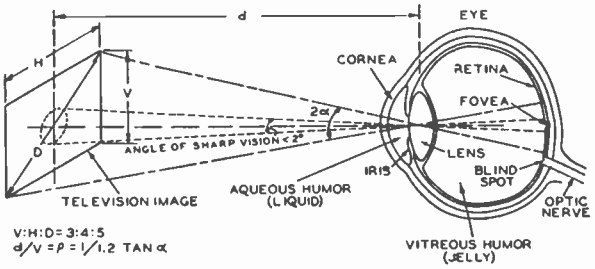

Fig. 2—Pickup of television image by the eye.

viewing angle 2α by the ratio ρ of viewing distance d to picture height V; hence

$$\rho = d/V = 1/1.2 \tan \alpha \qquad (2)$$

Comfortable vision requires a viewing ratio $\rho \geqq 4$. The values generally found in motion picture theaters range from $\rho = 1$ for the front seats to $\rho \simeq 7$ for the rear seats. The ratio $\rho = 4$ will thus be considered as the *minimum* standard viewing ratio at the receiver.

2. *"Static" Transfer Characteristics of the Signal Conversion Process in the Eye.*

Light entering through the lens system of the eye is transduced into stimulating signals perhaps by the photoreceptors of the retina (cones and rods). The signals are transmitted over nerve channels to the visual center of the brain for analysis and interpretation. The sensation of brightness (S) may be regarded as one of the "output

signals" of this process and is a function of the retinal illumination (E_r). The curve of S as a function of E_r is a "static transfer characteristic" of this transducing process. Its shape, range, and slope, even though approximate, are of considerable interest in evaluating requirements for external imaging processes. The characteristic curves $S = f(E_r)$ cannot be measured directly but they can be generated by the integration of incremental slope values which are known for specified viewing conditions. The reciprocal of these slope values is the "minimum perceptible brightness difference" $\triangle B_{min}/B$ which has been measured[12] as a function of field brightness B. One such characteristic for adjacent areas is shown in Figure 3a. Characteristics with larger values for the unit S will be obtained for separated areas; further variations occur when the brightness of the background surrounding the viewing field is changed.

Figure 3a is a general type of transfer characteristic, but the value of the sensation unit ($S = 1$) should not be considered as absolute. The unit of equivalent retinal illumination E_r corresponding to an external field brightness B is the "troland" (Td.)[13] The ratio of E_r to the viewing field brightness B is determined by the optical constants of the eye lens system and is proportional to the effective area (A) of

---

[12] John W. T. Walsh, PHOTOMETRY, Constable & Co., Ltd., London, Eng., 1926. (Page 53, Figure 26—The "Troland" supersedes the "photon"; both have the same definition.)

[13] L. T. Troland, "Absence of the Purkinje Phenomenon in the Fovea", *Jour. Frank. Inst.*, Vol. 182, pp. 111-112, July, 1916.

There is a good deal of laxity in the presentation of characteristics of the eye and use of the "troland" (formerly photon) unit. It is often impossible to correlate various data because of omission of information. Some authors use the troland unit, assuming a fixed pupil area, which is called "normal" and may be anything between 1 to 10 millimeters. Data on flicker, color sensitivity acuity, and, in general, all information on eye characteristics are of little use unless viewing angle, average field brightness, and/or the iris opening are specified because these values determine light flux density and internal eye illumination. Without definite specification, the data are as useless as film measurements made with great care with a camera having an f:2 lens but which neglects the fact that the camera has an automatic iris varying the aperture from f:2 to f:10 according to an unspecified law which may be a function of intensity, total light flux, flux distribution, color, and exposure time, or all combined. It is only to be expected that the results obtained for the film lack correlation and that curves of film characteristics show peculiar variations from normal steady functions.

Conversely, it must be expected that curves of film (or eye) performance versus external field brightness will exhibit the variations caused by the action of the automatic iris.

In this paper the conversion into troland units is based on the iris area as a function of the average field brightness regardless of color as given in Figure 4 which may be a reasonable assumption for a viewing ratio (ρ) of 4. In view of this, the author does not claim a high degree of accuracy for the general characteristics of the eye which may represent but a rough approach to accurate facts.

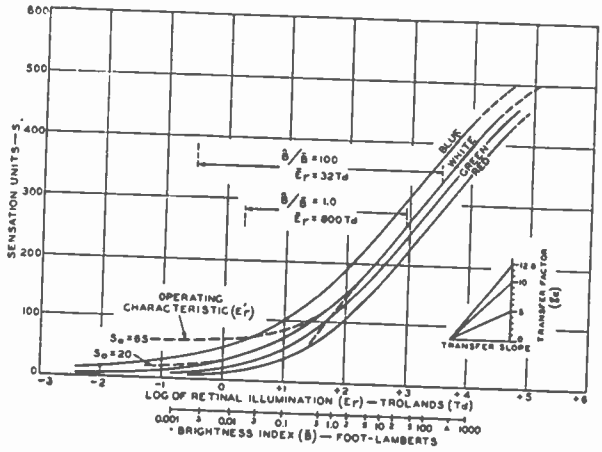

Fig. 3a—Static characteristics of the eye.

the lens of the eye. By definition

$$E_r/B = 3.43A \tag{3}$$

where A is in square millimeters, B in foot-lamberts, and E_r in trolands. Lens diameter and area A are controlled automatically by the iris of the eye in response to field brightness and follow the relation shown by Figure 4.[12] The triangles in Figure 4 indicate check points obtained

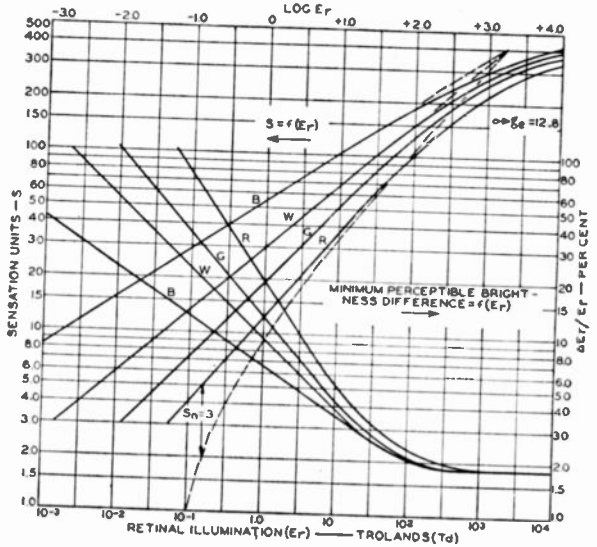

Fig. 3b—Static characteristics of the eye and threshold response to light increments.

with a viewing ratio (ρ) of 4 on an 8×10-inch kinescope raster of uniform brightness in a dark room. The action of the iris causes the brightness ratio (Equation (3)) to shift at most by a factor of two (see Figure 4) for a 10:1 change in the brightness of the object field. Because the shift is small, it is justifiable to make the simplifying assumption that it is the average value $\overline{B}$ of the field brightness which determines aperture and brightness ratio E_r/B.

The transfer curves (Figure 3a) obtained by integration of incremental slope values permit many graphic solutions and their use is in many respects similar to that of electron tube characteristics or sensitometric curves for photographic film. The transfer characteristics of the eye cover the enormous "input signal" range of 10 million to 1 (approx.). This range cannot be seen in one image because of various

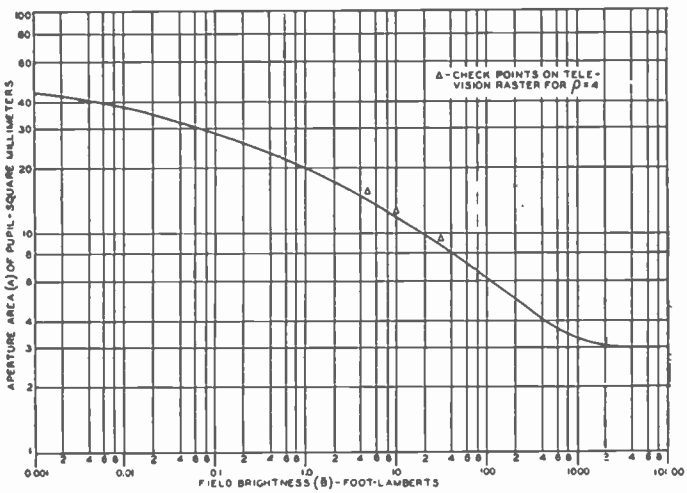

Fig. 4—Variations of aperture area of pupil with field brightness.

effects in the optical system and "development" process such as the optical scattering of light and the interaction between strongly and weakly exposed sections of the image surface which is similar to the electron redistribution in iconoscopes and image orthicons or to film development in limited solutions.

When the incremental slope values are integrated for the particular characteristic, in Figure 3a, the integration constants, i.e., the values of the curves for $S = 0$ are uncertain, although the unit $S = 1$ is defined as the minimum perceptible brightness difference. By replotting $S = f(E_r)$ on a logarithmic scale (Figure 3b) it was found that the toe sections follow a power law because the curves become straight lines upon addition (or subtraction) of certain constant values (Δ'S)

to S. This addition represents merely a vertical shift of the curves of Figure 3a without deformation.

The process of determining the integration constant is analogous to the process of determining the contact potential (E_o) of electron tubes. Their characteristics are known to follow the power law $I = K(E)^{1.5}$ which is a straight line with a slope of 1.5 on log-log coordinates. In this case, the measured curve $I = K(E + E_o)^{1.5}$ differs by an additive constant E_o, the contact potential.

One may speculate that the true additive constant for the straight line section of the eye characteristic in Figure 3b should express the fluctuation "noise" level which determines the threshold excitation of visual sensation. The constant is determined as the value at which the minimum perceptible brightness difference $\Delta E_r/E_r$ becomes unity and, according to Figure 3b, has the value of $S_n \simeq 3$. Subtraction of $S_n = 3$ furnishes then the actual transfer curve (indicated for red light by the broken line in Figure 3b) with $S \leqq 0$ when $\Delta E_r/E_r = 1$.

This correction has not been made on the curves because no absolute validity is claimed for the particular characteristic, although both the value $S_n = 3$ as well as the corresponding threshold level E_{r_o} for color vision are of the correct order of magnitude. The relative position of the characteristics for light of different color in Figure 3a is thus obtained by a replot of the corrected auxiliary curves of Figure 3b.

The center sections of the curves of Figure 3a have a substantially constant slope $\Delta S/\Delta E_r = 1/0.018E_r$. If the sensation unit itself is considered a log unit, the slope or "transfer factor" (g_e) of the logarithmic characteristic may be defined as

$$g_e = \Delta S/10 \ (\log E_r - \log \ (E_r + \Delta E_r)) \tag{4}$$

The value of g_e decreases for Figure 3a slowly from 12.8 to zero in the long "toe" of the curves.

3. *Operating Characteristics*

The brightness range which can be seen in one object field is a function of the ratio of the peak to average brightness $\hat{B}/\overline{B}$. This ratio approaches unity for small objects in a large white field. As a test object, a logarithmic step tablet (10×2 centimeters approximately) may be placed over a white 8×10-inch field (kinescope raster) for viewing at a distance of 32 inches ($\rho = 4$). When the field surrounding the tablet is covered with black paper, the other extreme $\hat{B}/\overline{B} \simeq 100$ is obtained.

If an internal eye-reflection factor of 1 percent is assumed and

other effects neglected, the zero-sensation level S_o will occur at $E_o = 0.01\bar{E}_r$ and the operating curve (E'_r) may be constructed from the static curve by subtracting E_o from E_r $(E'_r = E_r - 0.01\bar{E}_r)$. See Figure 3a. A 10:1 decrease in transfer factor, i.e., when $g_e \simeq 1.3$, at the dark end of the light range may be considered as a *practical* contrast visibility limit corresponding to a black level raised above S_o by approximately 6 sensation units.

For a peak brightness of $\hat{B}$ equal to 30 foot-lamberts, the limits $\hat{B}/\bar{B}$ equal to either 1 or 100 give $\bar{B}_1$ equal to 30 foot-lamberts $(\bar{E}_r = 880$ Td) and $\bar{B}_2$ equal to 0.3 foot lamberts $(\bar{E}_r = 32$ Td), respectively. The corresponding operating curves are shown in Figure 3a and cover the ranges 350:1 for the test with white background and 10,000:1 for the test with dark background.

These ranges agree substantially with those observed in a dark room with the step-tablet test. The compression of tone values in the lower third of the ranges below $g_e \simeq 1.3$ is quite evident and observation indicates that this section may be combined into one level. The essential contrast range varies from 100 to 1000 depending upon the size and distribution of the light and dark areas.

It is difficult to satisfy this remarkable capability of the eye. Fortunately, there are few really black objects (deep cavities) in normal scenes. White snow with nearly 100 percent reflection factor and black velvet with 1 percent reflection represent, in general, the extremes in range, excluding specular reflections. It must, however, be considered that even larger differences in object brightness can occur when the illumination differs greatly in parts of the scene (light and shadows), although each part may have a range considerably less than 100 to 1. An image brightness range of *100* to 1 can probably be considered for most cases as an adequate standard.

4. *The Over-all Transfer Characteristic of Television Systems*

Because the operating characteristic of the eye is identical when viewing object or image, any imaging process capable of reproducing an object with natural brightness must have a linear transfer characteristic for *truthful* reproduction of tone values. The transfer characteristic will be linear also for an image of reduced brightness so long as both object and image cause the eye to operate with similar characteristics. It is evident from Figure 3a that an object-contrast range of 100 to 1 with $B/\bar{B} = 5$ and a peak illumination $\hat{E}_r$ at 1000 Td up to 10,000 Td will meet these conditions. Objects can thus be reproduced by a linear system for all values of object or image peak brightness in the corresponding ranges of $\hat{B} \simeq 20$ to 1000 foot-lamberts. It is to

be understood that this statement applies only to a *true* reproduction of light ratios over a 100 to 1 range. Specular reflections or highlights exceeding this range have to be compressed for optical or electrical reasons. *It may, however, be very desirable to expand or contract the transfer characteristic in sections of the operating range to create artistic effects* in the image which may give a more pleasing illusion than a true reproduction of object tone values would give.

The peak brightness of modern kinescopes permits operating with $\hat{B} \geqq 20$ foot-lamberts. Studio monitors should, therefore, be operated at similar brightness levels or correction of their transfer curve is necessary because uncorrected low-level operation in a dark monitor room with $\hat{B} \simeq 5$ foot-lamberts is not exactly comparable due to the increased black compression by the eye at the lower brightness value. This effect, however, may be considered small when compared to changes in the transfer characteristic of the over-all system which may be introduced by a non-linear characteristic of one or several system components such as the expansion of brightness values in normal kinescopes or a dark-range compression in black-level setters or amplifiers. These deviations should be compensated for by an inverse transfer characteristic in the (electrical) system *if* a substantially linear over-all relation between object and image brightness is desired. The degree and ratio of the precompression of signal amplitudes at the transmitter are largely dependent on the over-all expansion in the transfer characteristic of the electro-optical receiver and a factor governed by receiver "noise" conditions. They are not entirely dependent on gradation requirements. However, it should again be stated that additional compression or expansion (not necessarily logarithmic) of the over-all system response may be desired for intentional changes of the brightness scale.[14,15]

5. *Color Response*

Reproduction of colored objects as black-and-white images with a natural brightness scale requires that the spectral response of the photo-sensitive surface in pickup cameras be similar to that of the eye (Figure 5). Larger deviations from the eye curve (often in the blue, red, and infrared regions) must be corrected by filters or by adjustment of color temperature in illumination. For natural appearance of tone values in artificially illuminated scenes, the product of the spectral characteristics of light source, photosensitive surface, and matching

[14] D. G. Fink, "Brightness Distortion in Television", *Proc. I.R.E.*, Vol. 29, pp. 310-321, June, 1941.

[15] W. Mortensen, ON THE NEGATIVE, Simon & Schuster, Inc., New York, N. Y., 1940.

filter (if required) should equal the product of the luminous sensation curve of the eye (Figure 5) and light of normal color temperatures, i.e., the temperature of light which would be used on the object for direct viewing by the eye. (A point-by-point match of the frequency characteristic is required to determine normal color temperature.)

The reproduction of objects by an image in natural colors requires information on the frequency of light within the range of visible energy covered by the luminosity curve. According to the trichromatic theory, the eye analyzes the colors of the spectrum by a triple receiving mechanism, each covering widely overlapping sections of the frequency range with a different frequency response. The frequencies of maximum color stimulation are red, green, and blue light. The brain weighs these response curves; equal energy stimulation of each of the primary sensations is analyzed as white light. The corresponding stimulation or mixture curves are shown in Figure 5. The eye does not discriminate between a monochromatic color and one resulting from a com-

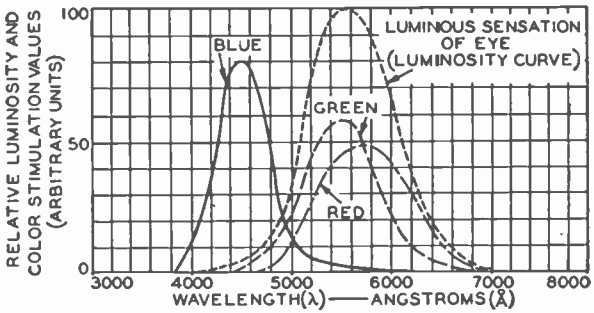

Fig. 5—Mixture curves.

bination of frequencies or frequency bands causing the same relative stimulation of the three primary color sensations. For this reason all colors can be synthesized, theoretically, by mixing suitable amounts (including negative amounts) of light from the three principal regions of the spectrum (monochrome or bands).

Color-reproduction processes based on only three primary colors are not perfect because they require the existence of hypothetical negative values. The values required decrease rapidly toward zero as the number of saturated primary color bands is increased. Much theoretical and experimental work has been done in color printing and photographic processes to determine the best practical trichromatic set of color filters for analysis and synthesis. One of these sets is the Wratten tricolor filter series A#25 red, B#58 green, and C5#47 blue for use with daylight and panchromatic (Type B) film. Deviations in the

spectral characteristics of light sources or photosensitive surfaces require amplitude and/or frequency-response correction to obtain a similar over-all color response. At the camera, it is generally desirable that white light should cause signals of equal amplitude from each primary color band; at the reproducer, equal signals should again produce color intensities combining to white light. The over-all brightness response for each component should again be linear with modifications as stated for black-and-white image reproduction.

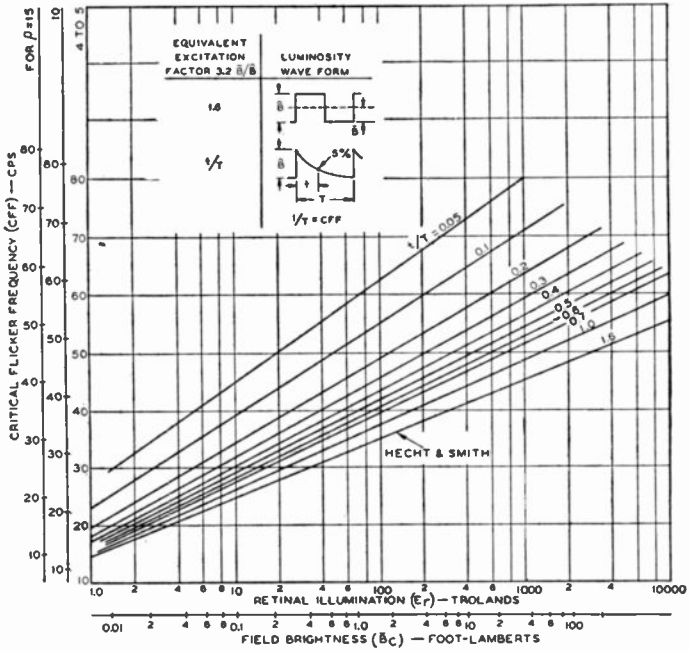

Fig. 6—Threshold flicker values for intermittent illumination.

6. *Persistence of Vision and Flicker*

The response of the eye to light, though rapid, is not instantaneous. Cyclic fluctuations in light intensity cause the sensations of flicker. This sensation disappears at low light intensities (low g_e) and when the fluctuation frequency is increased beyond certain values.

The critical frequency (C.F.F.) at which flicker is just noticeable in large areas depends on viewing ratio (ρ), luminosity, amplitude, and wave shape of the brightness fluctuation. The curve family given in Figure 6 has been constructed for exponentially decaying impulse waves of white light from the known curve for a square-wave brightness fluctuation. Assuming that the critical peak brightness $\hat{B}_c$ at any

particular frequency is substantially constant for waveforms with $\hat{B}_c/\overline{B}_c > 3$, it follows that the critical average brightness $\overline{B}_c$ in an area may be expected to decrease in proportion to the excitation time of the eye (decay time of kinescope phosphor) during one cycle.

This proportionality is modified by the decrease in g_e toward low light values which require intersection of the curves near $S = 0$. Convergence and spacing of the curves are somewhat uncertain according to different investigators. The general distribution was taken from Engstrom.[16] The slope of the square-wave fluctuation curve, however, seems to be well established. For a 10-to-1 change of B_c, the change in C.F.F. is 10 cycles.

The impulse excitation caused by a rapidly moving light spot of high intensity scanning a television screen is a rather special case of integration. It may be expected to follow the same general trend and will be discussed in Part II.

The flicker sensitivity of the eye to intermittent white and colored light from a steady source is constant for a given luminosity[12] at normal brightness levels. This statement does not apply to light sources in which the impulse wave shape and duration are functions of color or wave length. Evaluation of B_c by direct measurement is thus indicated for kinescopes in general and especially when composite screen materials are used because simulated conditions with optical projectors are not equivalent.

7. *The Resolving Power of the Eye*

The interference of light waves sets a limit to the resolving power of an optical system, because *two* points cannot be resolved when forming an angle (α_o) with the eye smaller than given by

$$\sin \alpha_o = 1.22\, \lambda/\delta \qquad (5)$$

For a pupil diameter (δ) of 0.3 centimeters and the wave length (λ) of 0.000055 centimeters, this angle is 0.77 minutes.

At a focal distance (F) of 15 millimeters, the two points are imaged 0.0033 millimeters apart on the retina which corresponds approximately to the diameter of one photoreceptor at the fovea centrals (cone diameter $\simeq$ 0.003 millimeter). For viewing ratio, p, of 4, this diameter limits eye resolution N_e to 2200 television lines for the optical system of the eye alone and to 1500 lines approximately if the cone structure is considered also. Effects of aberration, diffusion, and

[16] E. W. Engstrom, "A Study of Television Image Characteristics", *Proc. I.R.E.*, Vol. 23, pp. 295-310, April, 1935.

fluctuation phenomena (noise) in the visual process, however, are neglected.

The over-all "frequency response characteristic" of the visual process for small optical signals, i.e., its ability to translate optical detail into sensory response as a function of detail area or line number (N), remains to be determined by subjective measurements. At very low light levels this function is expected to be controlled by fluctuation phenomena in the process of transducing signals to the brain; at normal light levels and for small angles it should follow the law of optical "aperture effects."

8. *Detail Response Factor (r_e) and Response Characteristics of the Eye*

The "aperture" response* for the optical system of the eye cannot be determined separately from its transfer effects because response measurements include the transducing process which culminates at the brain in a light sensation. Various occurrences in this process alter the over-all detail response characteristic as in sensitive television pickup transducer systems in which saturation effects, leakage, and interactions between mosaic areas may outweigh the optical "aperture" response.

A representative response characteristic $r_e = f(N)$ of the "eye" for television conditions can be obtained by measuring the brightness difference and contrast required for threshold visibility of detail. This method is analogous to the variable-input/constant-output method employed for determining the frequency characteristics of electrical networks. The operating point (light bias) on the transfer characteristic (Figure 3a) should remain substantially constant. This requirement calls for a constant** average brightness $\overline{B}$ of representative value ($\overline{B} \simeq 7$ foot-lamberts), a fixed viewing ratio and field size, and a test object with calibrated detail size (line wedge) and adjustable contrast. A simple optical test setup includes a white screen with a 4:3 aspect ratio illuminated by a fixed source of light to an average brightness $\overline{B}$. A vertical line wedge covering about 15 per cent of the picture area on a transparent slide is "faded" in optically by projection. The projector brightness at which the first outlines appear has a value ΔB_o; finer detail, i.e., higher line numbers (N) become successively distinguishable at increased brightness values ΔB_N. The measurement should be made with white lines on a dark slide and dark lines on a white slide. The latter test requires correction of $\overline{B}$ at high values of projector

* See INTRODUCTION and also its specific treatment in Part II.
** Not very critical as long as g_* remains constant.

brightness. (Care must be taken to obtain uniform field illumination from either light source). The increments ΔB_N are found to be small signals with values $\Delta B_N < 0.1\,\bar{B}$ up to $N \simeq 400$. The absolute value is determined at a higher line number at which $\Delta B = B_2 - \bar{B}_1$ is easily measured.

The measurement has also been made under actual television conditions by viewing a white kinescope screen ($\bar{B} = 7$ foot-lamberts) and electrically fading in the test-wedge image by video signal control. The system used 525-line interlaced scanning, a 20-megacycle video channel with signal correction adjusted to give a substantially constant wedge sharpness (horizontally) on a 12-inch high-definition kinescope

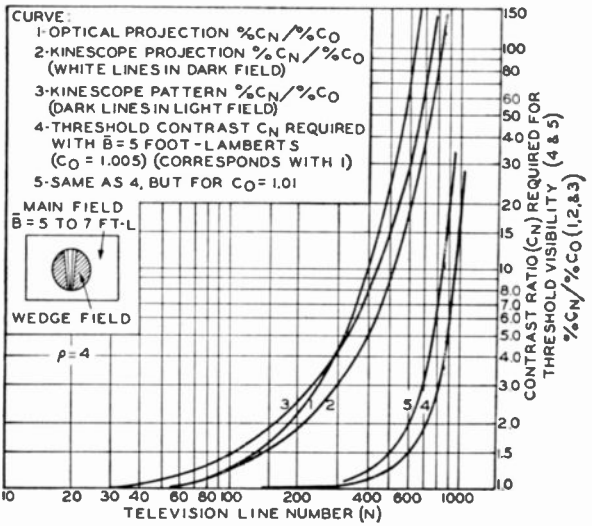

Fig. 7—Object contrast and ratio required for threshold vision.

up to approximately 800 lines. In this case the small signal ratio $\Delta B_N/\Delta B_o$ is measured by the video signal ratio. Positive and negative wedge images are easily obtained by reversing the signal polarity.

The results of a number of measurements are plotted in Figure 7 in terms of the per cent contrast ratio $\%C_N/\%C_o$ which shows the required optical input signal ratio for a constant minimum sensation output as a function of the television line number N. The object contrast ratio C_N required for threshold visibility of N is shown also.

The pickup response factor of the eye (r_e) as a function of N is expressed by

$$r_e = \Delta S_N/\Delta S_o \qquad (6)$$

Because of the logarithmetic transfer characteristic (Equation (4))

$$r_e = g_{e(o)} [\log (\overline{B} + \Delta B_o) - \log \overline{B}] / g_{e(N)} [\log (\overline{B} + \Delta B_N) - \log \overline{B}] \quad (7)$$

which is equivalent to $r_e = g_{e(o)} \log C_o / g_{e(N)} \log C_N$ (7a)

For moderate signals and constant average brightness, the transfer factor is constant. With $g_{e(o)} = g_{e(N)}$ and for particular values $\overline{B}$

$$\left.\begin{aligned} r_e &= \log C_o / \log C_N \\ r_e &= (\log (\overline{B} + \Delta B_o) - \log \overline{B}) / (\log (\overline{B} + \Delta B_N) - \log \overline{B}) \end{aligned}\right\} \quad (8)$$

For small signals $\Delta B < 0.1\,\overline{B}$ the small section of the transfer characteristic approaches linearity. It can be shown that the following ap-

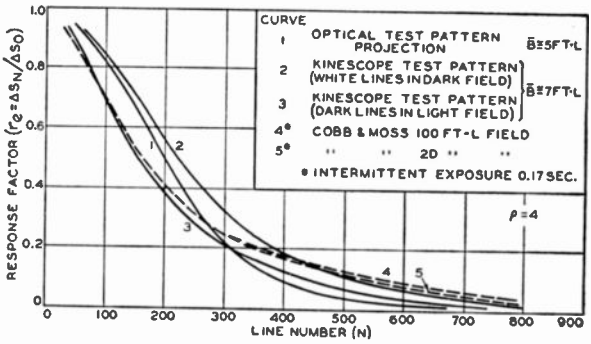

Fig. 8—Detail response factor of the eye.

proximations hold with a maximum error of less than 10 per cent.

$$\text{For } \Delta B < 0.1\,\overline{B} \left\{\begin{aligned} & C \simeq 1 + (\Delta B/\overline{B}) \text{ and } \%C \simeq 100\,\Delta B/\overline{B} \\ & \log C_o / \log C_N \simeq \Delta B_o / \Delta B_N \\ & \text{hence:} \quad r_e \simeq \Delta B_o / \Delta B_N \end{aligned}\right. \quad (9)$$

The simple relation Equation (9) is, therefore, useful for $N < 400$ in determining the pickup response factor r_e; higher line numbers require computations of r_e with Equation (8).

The sharper cutoff obtained with the optical method (See Figure 8) is probably caused by limited detail contrast of the 35-millimeter film and projector used in the test.

The curves 1 and 2 in Figure 8 indicate an "effective" resolving aperture in the over-all pickup system of the eye equivalent to $N \simeq 200$

lines at $\rho = 4$ with a limiting resolution (1 per cent contrast) near 900 television lines. ($\alpha_o \simeq 1$ minute for $\rho = 4$ and $\overline{B} \simeq 7$ foot-lamberts).

Curves 4 and 5 in Figure 8 have been plotted from data given in a paper by Cobb and Moss.[17] These curves show the same general position even though they were measured with a short subject exposure of 0.17 second and a different test object. At very high values of brightness, the response characteristic r_e is displaced toward the cutoff limit of the optical system ($N_{co} \simeq 1500$). As brightness decreases, r_e shifts towards lower line numbers and at low values of brightness it becomes very poor because of fluctuation noise. It is further affected by superposition of reflected light from other parts of the viewing field. All these effects have their counterparts in photography and in television pickup tubes in which a small light bias may improve detail signals, but a strong light bias (glare) may cause saturation effects in the signal development process and the reduction of detail signals.

The significance of the response characteristic r_e may be illustrated by a representative operating condition on the transfer characteristic of the eye, Figure 3a. If an average brightness $\overline{B}$ of 4 foot-lamberts and a peak brightness $\hat{B}$ of 20 foot-lamberts is assumed, the operating section in Figure 3a extends from $\hat{E}_r = 1000$ Td downwards. Subtracting 1 per cent (2 Td) of the average level for reflected light inside the eye, we obtain a total of approximately 200 sensation units in a 100-to-1 brightness range from 10 to 1000 Td. The size of the sensation unit decreases as a function of line number as indicated by the response factor and is

$$S_N = S_o r_e \qquad (10)$$

For 500-line detail, the sensation scale comprises only $200 \times r_e = 18$ steps and shrinks to 6 units at $N = 700$, 4 units at $N = 800$, and 2 units at $N = 900$ lines. If the original unit size for $N = 0$ is correct, a difference of one single unit $S_o r_e$ should be perceptible upon careful observation at the average level (200 Td). The number of simultaneously observable gradation steps over the entire range, however, is probably smaller and the essential and easily visible number of steps is even considerably smaller.

Brightness ranges of 100 to 1 are rather exceptional in optical reproductions. Prints and theatre motion pictures seldom exceed a large area contrast ratio of 30 to 1. The contrast of *fine detail* areas is further substantially reduced by "aperture" and diffusion effects.

It may be concluded that an imaging system having a substantially flat over-all response up to $N = 500$ will furnish an image of excellent sharpness for a viewing ratio $\rho = 4$ because it cuts off only a small

[17] P. W. Cobb and F. K. Moss, "The Four Variables of the Visual Threshold", *Jour. Frank. Inst.*, Vol. 205, pp. 831-847, June. 1928.

percentage of object detail which is visible to the eye only at stationary contours of high contrast.*

Equation (1) indicates an electrical channel ($\triangle f$) of 6.35 megacycles for a frame time (T_f) of 1/30 of a second and a balanced line number ($\overline{N}_{co}$) of 500.

Tests were conducted with many observers who viewed both live-pickup and still pictures over a high-quality variable-channel television system with a maximum band width of 20 megacycles. These tests show that up to $\overline{N} = 800$ lines slight increases in sharpness can be detected by the eye at a ρ of 4 on fine detailed stationary subjects of high contrast such as small type, *but little preference was indicated for increases beyond* $\overline{N} = 500$ *when viewing motion scenes, persons, and other normal television subjects.**

It is of interest to note that satisfactory half-tone prints in magazines employ rasters producing 85 to 133 points per inch. Gradations from black to white are obtained by variation of the point size from small white points in a black field (dark) to alternate black-and-white squares for 50 percent white, and small black dots for near white. If both black-and-white points in a 50 percent tone are counted, the prints have 170 to 266 television lines per inch and for a ρ of 4 at the normal viewing distance of 12 inches, they correspond to a 3×4-inch television raster with 510 to 800 lines. The points in the 800-line print cannot be resolved with the naked eye while a 600-line print shows a barely visible structure.

Color prints employ, side by side or superimposed, the same number of points for each of the printing colors (3 and higher) which results in 3 or more times as many picture elements as used for black and white.

The television line process gives continuous tone variations in the horizontal direction without structure, while in the vertical direction a fine spot size** with a diameter of ½ the line width is desirable for high resolving power and will give a 1000-line structure (counting again spaces and lines) with 500 scanning lines. The present television raster with 525 scanning lines is, therefore, in comparison with good-quality printing standards quite satisfactory.

(B) Brightness Distortions (Steady and Fluctuating)

When optical images are viewed, brightness values are compared

* The subject of image sharpness with respect to line number and resolving power in different processes will be treated on various occasions as it can be approached in many ways. A more precise evaluation will be given in the last part of this paper when the over-all "aperture response" of cascaded transducing systems is treated.

** See Part II.

with mental pictures of real objects. Eye and mind detect rather quickly an error in brightness if it is of sufficient magnitude and is inconsistent with the illusion caused by the image. Transfer factor (g_e) and field brightness fluctuations (flicker) have been discussed. This section deals with steady and fluctuating brightness distortions in limited areas.

1. *Steady Deviations*

The steady deviation ($\triangle S$) permissible from normal sensation values, as readily seen from Figures 3a and 8, is a function of area, the brightness distribution or "shape" of the variation ($\triangle B$), its color, and the average brightness level $\bar{B}$. That the eye will tolerate a sinusoidal or other variation with a gradual gradient change ($\triangle S$) of 10 to 15 sensation units ($\triangle B = 20$ to 30 per cent at $g_e = 12.8$) when extending over the entire viewing field, especially when some detail is present is exemplified by the variations of field brightness found in commercial projectors. For smaller areas in the order of $N = 10$ to 50, the deviation should not exceed 1 to 2.5 sensation units ($\triangle B \simeq 2$ to 5 per cent at $g_e = 12.8$) with gradual distribution.

Areas with fine detail such as spots and scratches are of lower visibility because of attenuation due to the low-pass filter characteristics (Figure 8) of the eye. The deviation caused by such areas should remain below $1/r_e$, where r_e is the detail response factor. For the eye transfer factor (g_e) of 12.8, this brightness deviation is

$$\triangle B \simeq 0.018\, B/r_e \tag{11}$$

The above values apply to black-and-white images or white light. Images in natural colors have substantially the same tolerances for non-uniformity of color brightness, but are affected, in addition, by non-uniform color response. The eye is equally sensitive to deviations in color saturation or mixture, but they are seldom detectable in black-and-white images.

2. *Random Fluctuations and Visibility Factors (Grain and "Noise")*

A statistical amplitude-distribution sample of random occurrences or impulses is shown in Figure 9. Electrical fluctuations of this type[18] are caused by current fluctuations termed "noise" in elements of the electrical channel, especially in the pickup tube and in first amplifier stages. It is well known that the frequency components and power of the complex fluctuation wave are uniformly distributed in pass bands with constant amplitude response. Fluctuation peaks occur when all

components are in phase and the peak duration is determination by the highest-frequency component in the pass band. These random impulses cause, therefore, brightness fluctuations on the viewing screen appearing as a moving grain structure of picture element size.

Picture element and apparent grain area are inversely proportional to the balanced line number $(\overline{N}_{co})^2$ in a television channel. The "grain", however, is seen through low-pass filters, i.e., the eye and kinescope, which attenuate the high-frequency components in the visible fluctuation wave. It is generally accepted[18] that fluctuations within any one small section $\Delta f'$ of a very wide frequency band occur at a rate proportional to the frequency and within the same amplitude limits. Oscillograms of fluctuations in any one section of the frequency spectrum are identical when taken with a writing speed proportional to the section frequency.

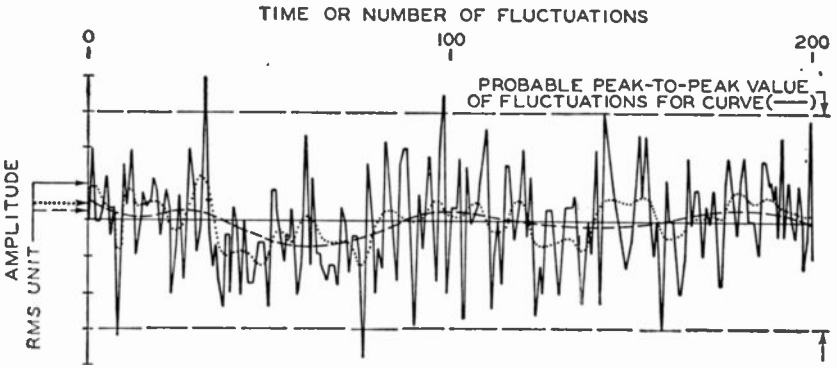

Fig. 9—Sample plot of random fluctuations.

Power and voltage developed by a fluctuating current in a constant impedance have, therefore, constant values for a given increment $\Delta f'$, independent of the value f. The incremental power ΔP can be written

$$\Delta P = K \Delta f' Y^2 = \bar{a}^2 P_o \qquad (12)$$

[18] a. B. J. Thompson, D. C. North and W. A. Harris, "Fluctuations in Space-Charge-Limited Currents at Moderately High Frequencies", *RCA REVIEW*, Vol. IV, No. 3, pp. 269-285, January, 1940.

b. D. O. North, "Diodes and Negative Grid Triodes", *RCA REVIEW*, Vol. IV, No. 4, pp. 441-472, April, 1940.
Vol. V, No. 1, pp. 106-124, July, 1940.

c. D. O. North, "Multi-Collectors", *RCA REVIEW*, Vol. V, No. 2, pp. 244-260, October, 1940.

d. B. J. Thompson and D. O. North, "Fluctuation Caused by Collision Ionization", *RCA REVIEW*, Vol. V, No. 3, pp. 371-388, January, 1941.

e. W. A. Harris, "Fluctuations in Vacuum Tube Amplifiers", *RCA REVIEW*, Vol. V, No. 4, pp. 505-524, April, 1941.
Vol. VI, No. 9, pp. 114-124, July, 1941.

where K is a constant, Y a significant amplitude or a root-mean-square value of the fluctuation wave in the frequency limits $\Delta f'$, and P_o the normal power value. The factor $\bar{a}$ in the second form is an amplitude or gain coefficient specifying the mean deviation from a normal value Y when the frequency is varied. The factor $\bar{a}$ applies only to the frequency characteristic of system components located between the point of fluctuation insertion and the point of observation.

The total fluctuation power (P_N) in a band width extending from f_o to f_c is then:

$$P_N = \int_{f_o}^{f_c} P_o \bar{a}^2 df \tag{13}$$

which may be evaluated as the sum of incremental powers:

$$P_N = \sum P_1 \bar{a}_1^2 + P_2 \bar{a}_2^2 + \cdots + P_n \bar{a}_n^2 \tag{13a}$$

(a) System components with flat frequency response have a constant amplitude or attenuation factor a. It follows from (13) that

$$P_N = K(f_c - f_o) = K\,\Delta f \tag{14}$$

The fluctuation wave amplitude is, therefore, $Y_N = K' \Delta f^{1/2}$ (15)

(b) System components with a frequency response proportional to frequency have amplitude factors $\bar{a}_1$, $\bar{a}_2$, $\bar{a}_n$ which increase in proportion to frequency. Equation (13) furnishes the relations

$$P'_N = K\,\Delta f^3 \tag{16}$$

and

$$Y'_N = K' \Delta f^{3/2} \tag{17}$$

(c) System components with non-uniform frequency response will change the power distribution from the "normal" values P_N or P'_N given in Equations (14 and 16). The modified power distribution is obtained by subdividing the frequency band into equal increments $\Delta f'$ and multiplying the normal power increments ($P_n = \Delta P_N$) by the corresponding mean deviation factors squared ($\bar{a}_n^2$) (See Figure 10). Summation of the products $P_n \bar{a}_n^2$ (Equation 13a) furnishes the total power, the square root of which is the fluctuation voltage for comparison with the normal voltage.

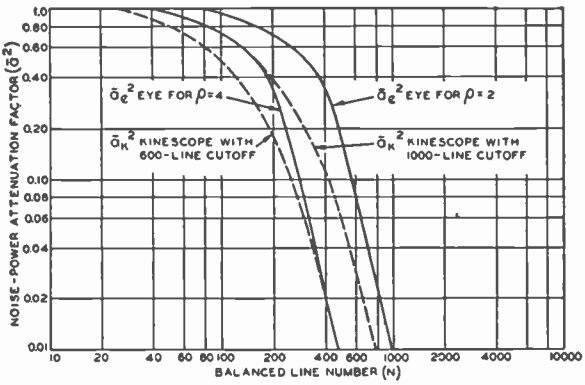

Fig. 10—Noise attenuation due to filter effect of eye or kinescope.

"*Fluctuation filter factors*" (m) may be determined by which normal small fluctuation values (brightness, voltage, or current) are multiplied to specify the effect of electrical or optical low-pass filters such as kinescope and eye. The filter factor (m) is defined as the square root of the ratio of the modified noise power to the normal noise power.

Filter factors have been computed as a function of the balanced resolution number for various combinations of kinescope and eye with the attenuation factors $\bar{a}^2$ as shown in Figure 11. Equivalent electrical channel widths are given by Equation (1). A reasonable unbalance[5] of horizontal and vertical resolution does not materially affect the result.

The relative filter effects of eye and kinescope on fluctuations of small amplitude from "flat" and "peaked" channels are shown by Figure 12. Curve 1 in the lower group shows the normal proportion of the fluctuation or "noise" amplitude to the balanced-resolution line

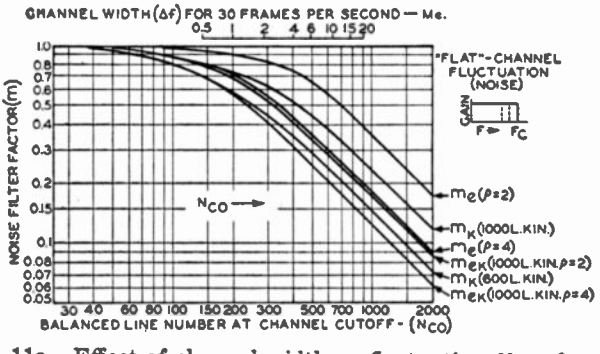

Fig. 11a—Effect of channel width on fluctuation filter factors for a flat channel.

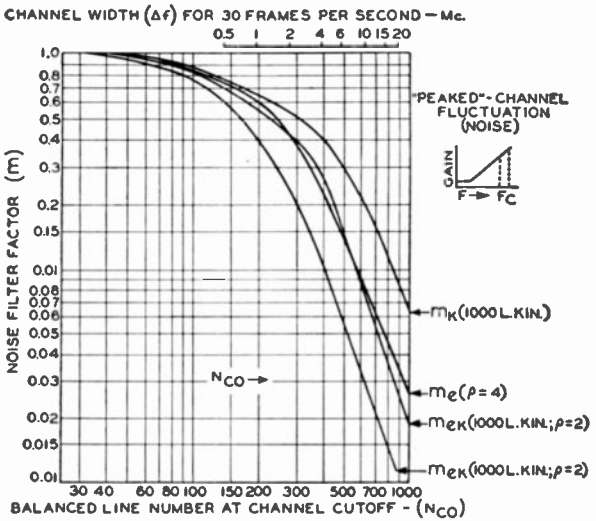

Fig. 11b—Effect of channel width on fluctuation filter factors for a peaked channel.

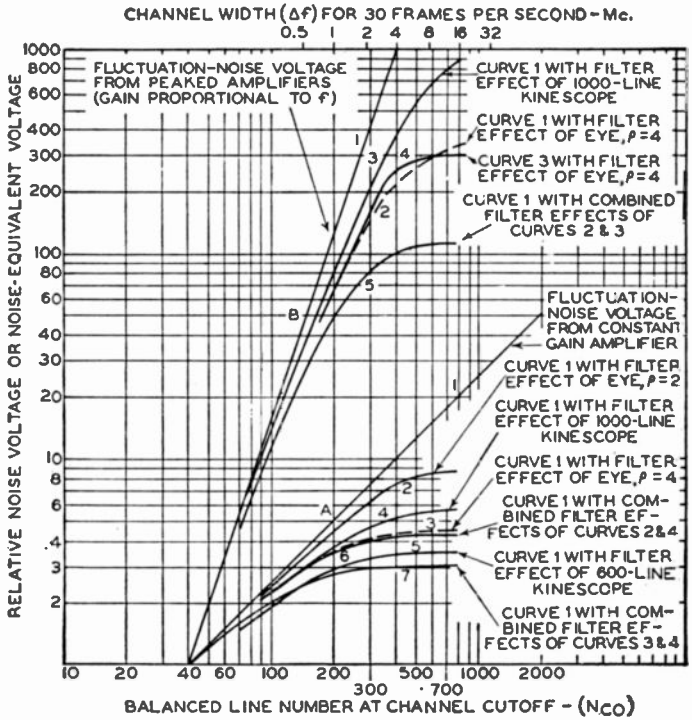

Fig. 12—Integrated filter effects of eye and kinescope on fluctuations of small amplitude.

number at cutoff for constant gain channels; curves 2 to 7 show the equivalent noise amplitude after attenuation of high-frequency components by the low-pass filter action of the eye, kinescope, or kinescope and eye.

The upper group has been computed similarly for fluctuation noise which has previously passed through electrical channels with an amplitude response proportional to frequency, such as used in camera amplifiers with capacitive input impedance. This "peaked" noise increases in proportion to the 3rd power of the balanced resolution ($\overline{N}_{co}$) in the channel (curve 1) and is attenuated by eye, or by eye and kinescope, as shown by curves 2 and 5, respectively.

Figure 12 shows that the filtered fluctuation amplitude, i.e., the visibility of small fluctuations for a viewing ratio of 4, approaches a constant value for channels passing more than 400 lines. This condition is confirmed by observations of noise visibility in television channels over 400 lines, indicating again that higher resolution contributes little to image detail. It is further seen (Figure 11) that the relative attenuation and *visibility of noise in peaked and flat channels differ by a factor of three for the present channel width of 4.25 megacycles.*

The ratio of peak values to root-mean-square values is expected to remain constant for any section of a wide frequency band. This ratio has been checked for flat-channel fluctuations by measurement of root-mean-square voltage and the (representative) peak-to-peak deflection voltage on an oscillograph (20-megacycle flat response) with bandwidths up to 20 megacycles. The peak-to-peak voltage measured normally is fairly well defined because theory and observation indicate a rapid decrease in the occurrence of peaks exceeding a certain level.

The ratio of peak-to-peak values to root-mean-square values is 6 to 1 for practical measurements as observed for channels with a band width of 4 to 20 megacycles. This value is indicated on the statistical amplitude distribution sample (Figure 9).

3. *Grain-Visibility Constant and Signal-to-Noise Ratios*

Observations indicate that the threshold sensitivity of the eye to low-frequency components in random brightness fluctuations is equivalent to approximately one sensation unit or a 2 per cent brightness change (peak value) at normal field brightness values ($g_e = 12.8$ in Figure 3a).

The visibility of complex brightness fluctuations such as caused by motion-picture-film grain or electrical fluctuations seen through a linear transducer (ideal kinescope) should be obtainable by multiplication with appropriate filter factors (m) because effective area and ampli-

tude of the fluctuation peaks depend on the combined effect of *all* components. The optical signal-to-noise ratio *at the source of the image light flux* for threshold visibility of grain or noise fluctuation at normal operating points on the eye characteristic ($g_e = 12.8$, $\overline{B} > 2$ foot-lamberts) is therefore:

a) with respect to the peak-to-peak fluctuation value

$$\hat{R}\phi = \overline{B}/\Delta B_{N(p\text{-}p)} = m/0.04 = 25m \tag{18}$$

b) with respect to the root-mean-square fluctuation value

$$|R|\phi = 6\hat{R}\phi = 150m \tag{19}$$

The significance of Equations 18 and 19 will be illustrated by practical cases.

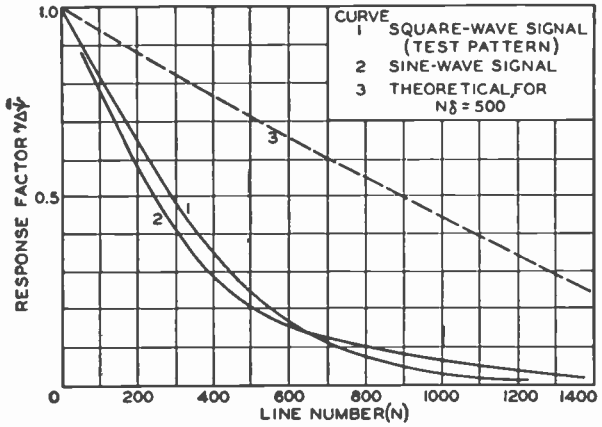

Fig. 13—Equivalent square-wave aperture response of "1000-line" kinescope.

The over-all resolution of an optical motion picture projection* is represented sufficiently well by a kinescope characteristic with 1000-line cutoff (Figure 13) for which filter factors m_K have been computed. Threshold ratios for reproduction over an ideal linear transducer (kinescope) and various flat channels are obtained from Equations 18 and 19 and Figure 11 and are listed in Table I. The threshold ratios of the 1000-line channel indicate values which may be considered representative for a purely optical transmission of the motion picture image. All conditions apply also to television systems with ideal linear transducers. The third column applies to film noise measurements and

* This includes deterioration in camera, printing, and projecting processes on normal 35-millimeter film; not on special test reels.

appears to be in substantial agreement with values observed on high-quality 35-mm film.

The ratio of signal to peak-to-peak noise $\hat{R}_\phi = \frac{1}{2}$ may well be considered as indicating the grain size of the film itself. If the ratio of signal to peak-to-peak noise is equal to 4.3 (See Table I) in a 1000-line channel, it will decrease to ½ when the channel is increased to $N_c = 8600$ lines. At this bandwidth the vertical frame dimension of 15.7 millimeters can accommodate $N_c = 8600$ television lines or 548 television lines per millimeter. This line number corresponds to 274 elemental light pulses spaced by 274 grains in one millimeter with an

Table I

Channel Resolution N_{ce}	Kinescope (representing 35-millimeter film)			Eye and Kinescope			Eye		
	Filter factor of system m_k (1000)	$\hat{R}_\phi$	$\lvert R\rvert_\phi$	Filter factor of system m_{ek}	$\hat{R}_\phi$	$\lvert R\rvert_\phi$	Filter factor m_e	$\hat{R}_\phi$	$\lvert R\rvert_\phi$
410	0.5	12.5	75	0.29	7.3	44	0.41	10.3	62
500	0.45	11.2	68	0.24	6	36	0.35	8.8	53
800	0.29	7.3	44	0.15	3.8	23	0.25	6.3	38
1000	0.23	5.8	35	0.12	3	18	0.17	4.3	26
	For $\rho < 1$, $m_e = 1$			For $\rho = 4$			For $\rho = 4$		
	Optical ratio on film in motion						Optical ratio on screen or electrical ratio at grid of linear ideal transducer.		

average intensity B (See Equation (18)) equal to ½ the peak-to-peak noise fluctuations ($\Delta B_{N(p\text{-}p)}$). The resolving power of the random grain structure of film is approximately 6 grain diameters or 90 lines per millimeter. (See Part III)

It is significant that grain size and resolving power of 35-millimeter motion picture film are in this order. It is stated further by film manufacturers that a resolving power of 50 lines per millimeter permits enlargement to 10 or more diameters "without objectionable graininess". This resolving power corresponds to 760 or less television lines in 3 inches for which $\rho = 4$ at close viewing distance (12 inches). This figure again agrees with the limiting resolution of the eye.

It should be pointed out that the relation between limiting resolution and grain diameter stated above is not necessarily general.

When sharp signals are superimposed on a fluctuating grain pattern from a separate source as in many television images, recognition of elemental signal pulses is possible with $\hat{R}_\phi \simeq 0.5$ ($|R| = 3$); line patterns with elemental line width $1/N_c$ are visible with even much lower signal-to-noise ratios as the eye integrates along the line. It is also observed that motion of the ground-glass view plate in the focal plane of a camera allows observation of much finer detail (with a magnifying glass) than when stationary.

The values given by Equations 18 and 19 refer to signal-to-noise ratios at particular brightness levels B_o. They refer to the entire gradation range only (for $g_c = 12.8$) when signal and noise remain proportional.

The noise decreases with signal in film and phototubes, although not in proportion. The random noise currents, however, generated in video amplifiers or by the scanning beam of present storage-type pickup tubes have constant values for a given operating condition. The threshold ratio R_ϕ at a brightness level B_o requires, thus, for a constant noise source and linear transducers the relationship

$$R_{\phi\max} = R_\phi \hat{B}/B_o \tag{20}$$

Threshold signal-to-noise ratios in the video signal channel require specification of the function $B = f(E)$ and the electro-optical transfer factor g_k (usually a variable) between observation points, such as kinescope grid signal and screen brightness.

Therefore: $$\hat{R}_{\max} = \hat{R}_\phi g_{k(o)} \hat{\mathcal{E}}/B_o \tag{21}$$

and with (18) $$\hat{R}_{\max} = 25m\, g_{k(o)} \hat{\mathcal{E}}/B_o \tag{22}$$

where $\hat{\mathcal{E}}$ = peak signal voltage required for $\hat{B}$ (i.e. $\hat{B} = f(\hat{E})$), and $g_{k(o)}$ = transfer factor (foot-lamberts/volt) at the brightness B_o for which threshold visibility of noise is desired.

Numerical values for the signal-to-noise ratio of high-quality television signals will be given in Part II in which general specifications for television systems and components are discussed.

ELECTRO-OPTICAL CHARACTERISTICS OF TELEVISION SYSTEMS*†

By

Otto H. Schade

Tube Department, RCA Victor Division,
Harrison, N. J.

NOTE: This paper consists of an Introduction and four parts: Part I — Characteristics of Vision and Visual Systems; Part II — Electro-Optical Specifications for Television Systems; Part III — Electro-Optical Characteristics of Camera Systems; Part IV — Correlation and Evaluation of Electro-Optical Characteristics of Imaging Systems. The Introduction and Part I appeared in the March 1948 issue of *RCA REVIEW;* a summary is reprinted herewith for reference purposes. (A limited number of copies of the March 1948 issue is still available for those who desire a complete file on this paper.) Part II is included in this issue. The remaining parts are scheduled for publication in the September and December issues of Volume IX of *RCA REVIEW* during 1948.

INTRODUCTION; PART I — CHARACTERISTICS OF VISION AND VISUAL SYSTEMS

(Reprinted from RCA REVIEW, March 1948)

Summary—The optical and electro-optical conversion processes in television systems are examined as intermediate stages of a multi-stage process by which optical information at the real object is "transduced" into sensory "response" at the brain. The characteristics of the human eye and vision in the final stage of the process determine the requirements and standards for preceding stages. When expressed on a unified basis by "transfer" and "aperture response" characteristics, the properties of the process of vision can be correlated with those of external imaging and transducing processes. It is shown that image definition, or the corresponding information from optical or electrical image-transducing stages, can be specified by the characteristics of an equivalent "resolving aperture." These characteristics may be computed and measured for all components of the system.

Quantitative data from measurements permit definite quality ratings of optical and electrical components with respect to theoretical values. A subjective rating of the resolution in an imaging process external to the eye such as a television system is derived by establishing a characteristic curve for the relative "sharpness" of vision as affected by the "aperture response" of the external imaging process.

A general review of the material and the broad methods of analysis employed are given in the Introduction. Following this, Part I treats characteristics of vision and visual systems. In this part, viewing angle, sensation characteristics, color response, persistence of vision, flicker, resolving power, response characteristics, and steady and fluctuating bright-

* Decimal Classification: R138.3 × R583.11.
† Reprinted from *RCA Review*, June, 1948.

ness distortions are discussed and related to the characteristics of external imaging systems and the television process.

* * * * * * * * * * * * *

There follows the second paper in this series: Part II—Electro-Optical Specifications for Television Systems.

The Manager, RCA REVIEW

PART II — ELECTRO-OPTICAL SPECIFICATIONS FOR TELEVISION SYSTEMS

Summary—*The ability of an image-forming device to reproduce fine detail can be specified basically by the size and flux distribution of the small light spot formed as the image of a point source of light. It is shown that the defining ability of practical image transducers is specified more accurately by response characteristics obtained by scanning a test object with the elemental point image which represents the "resolving aperture" of the imaging device. Methods of computing and measuring the "aperture flux response" of practical image transducers are developed for correlation of optical and electrical system components.*

The television raster is treated as a sampling process and its effect on the system resolution is evaluated as an aperture process. Brightness, repetition rate, and flicker in television images are treated in relation to the screen materials and performance of practical kinescopes.

A. The Analysis of Image Definition and Structure and Their Specification by the Flux Response Characteristics of Equivalent Resolving Apertures

The ability of an imaging device or process to form a clear image of fine detail is specified basically by the size of the small light spot formed by the device when imaging a point source of light. The elemental point image (known as a "figure of confusion", a "diffraction disc", a "picture element", or, less specifically, as an "elemental area") depends in size on certain characteristics of the particular transducing process. Optical images contain a very large number of elemental areas which can be formed simultaneously or in rapid sequence by one or many beams of light or electrons. The element controlling the cross section of these beams is usually a physical aperture. The specific action of a transducer in defining or changing the size of an elemental area (even without a physical aperture) has, therefore, been termed an "*aperture process*". The action of defining the elemental area in any transducing process can be assigned, in a transferring sense, to an equivalent resolving aperture. This equivalent "aperture" is equal in size, shape, and flux distribution (or transmission) to the elemental area itself when a "point" signal is transduced.

The effect of the "aperture" on the definition of images can be evaluated by the process of scanning in the form of a "frequency response" characteristic or "aperture response" characteristic because the scanning motion identifies spatial variations in image flux as different frequencies according to the detail size in the image. It will be confirmed by optical experiments that the "aperture response" of simultaneous figures of confusion in optical images is identical with the aperture response obtained by scanning the image with one aperture equal to one figure of confusion.

It is quite adequate to specify the definition in an image by the size and flux distribution of its resolving aperture rather than by the aperture effect. The accuracy in measuring small "spot" sizes and their flux distribution is limited, however, in practical cases by fluctuation phenomena (noise) which usually do not permit intensity measurements to be made with a precision better than one to two per cent. It will be shown in the section on complex apertures that errors of this order can cause a 50 per cent change in the response factor of practical apertures.

Aperture response characteristics computed by scanning "square-wave" line patterns are, therefore, especially suitable for rating the performance of practical imaging devices because they permit a direct comparison of theoretical and measured data. The combined aperture response of several aperture processes in cascade can be established from individual aperture characteristics by repeating the scanning process.

1. *Aperture Response Characteristics*

The aperture effect on definition is determined by the simple geometric process of moving the aperture over a "flux pattern" and plotting the integrated flux passing through the aperture as a function of displacement. A unit-function flux change which is optically a sharp boundary between two brightness levels B_1 and B_2, a single rectangular pulse or a series of pulses forming a square flux wave are useful test patterns.

To pass over a unit-function flux change, the aperture must progress one aperture diameter, δ. (Figure 14). The form of the "transition curve" depends, obviously, on the shape and flux distribution within the aperture. A square aperture with uniform density gives a straight-line transition; a round aperture with uniform or cosine-square density has an S-shaped transition. The transition curve has symmetric halves and is given for several apertures in Table I of the Appendix.

The most useful pattern (for obtaining a standard detail test signal) is, for many reasons, the square-wave flux pattern, which, optically, is the standard line or bar test pattern. Groups of lines or a tapered

wedge are used to vary line width or line number with respect to the aperture diameter δ. (See Introduction, and Part I).

For computation of aperture response curves, the aperture may be considered as a three-dimensional body such as a cube, cylinder, cone, etc. The base of this body represents the aperture size and shape; the height represents the flux density; and a vertical central cross section represents the density distribution. Finding a point on the response curve or flux wave generated by passing the aperture over a flux boundary or a number of boundaries is, hence, the problem of determining the total volume within the vertical sections of the aperture body located between boundaries containing signal flux. The aperture flux

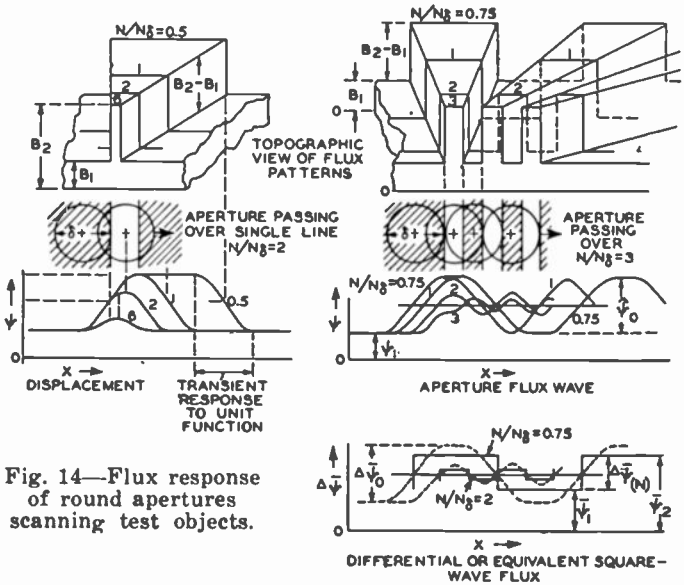

Fig. 14—Flux response of round apertures scanning test objects.

waves are the plot of the active flux volume as a function of aperture displacement. The flux wave generated by passage of the aperture over square-wave flux patterns is characterized by its amplitude and its wave form. (See Figure 14).

The amplitude response factor $r\Delta\hat{\psi}$* is defined as the ratio of the flux amplitude $\hat{\psi}_N$ at a line number N to the amplitude $\hat{\psi}_o$ at $N = 0$.

$$r\Delta\hat{\psi} = \hat{\psi}_N/\hat{\psi}_o \qquad (23)$$

The response factor $r\Delta\hat{\psi}$ as defined by Equation (23) is single valued

* It should be pointed out that the response factors derived in this paper differ by definition from those obtained by a two dimensional Fourier analysis; see References 1, 2 and 3 of Part I.

and independent of the contrast of the test object. It is unity in the range from $N = 0$ to the line number $N\delta$ at which the aperture diameter (δ) is equal to one line width. (The line number N in this paper is expressed in television lines; both dark and light lines are counted).

The waveform of the flux wave changes in this range from a square at $N = 0$ to a trapesoid for $N > 0$, the top of the trapezoid shrinking to a point at $N = N\delta$. At $N = N\delta$, the wave becomes a triangle (square aperture) or a sine wave (round aperture). Beyond $N\delta$ it decreases in amplitude towards zero which occurs at a particular value $N = N_c$. (The wave changes again towards a square at $N = N_c$ for the square aperture).

The computed response characteristics, Figure 15, show that sharply

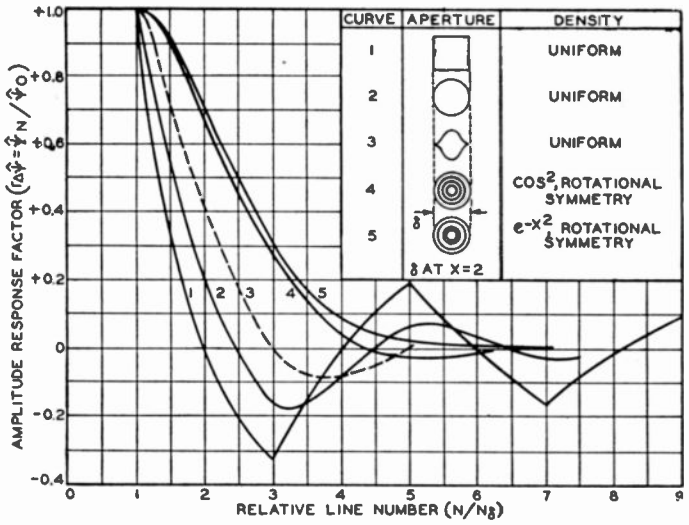

Fig. 15—Amplitude response of various apertures to square-wave flux pattern.

defined apertures have multiple zero points. These curves are analogous to the transient response of electrical networks with sharp cutoff. The response beyond the first zero is a spurious signal having one line in the pattern missing after each zero. The negative sign refers to the polarity of the flux with respect to its a-c axis and indicates a sudden phase reversal; black lines continue as white lines and vice versa. The "overshoot" is a maximum for a square aperture with uniform flux density and zero for a round aperture with exponential flux distribution.

The Differential Flux Response Factor (Equivalent Square Wave)

The detail contrast in the optical signal from the aperture is a maximum when $r\Delta\check{\psi} = 1$ and when the flux wave is rectangular. The

average flux change obtained by intergration of half waves specifies the degree of equivalent contrast. The ratio of $\Delta\bar{\psi}_N$ at the line number N to the flux change $\Delta\bar{\psi}_o$ of the perfect square wave at $N = 0$ is the differential flux response factor

$$r\Delta\bar{\psi} = \Delta\bar{\psi}_N/\Delta\bar{\psi}_o \tag{24}$$

This response factor is also single valued and independent of the test object contrast. The detail contrast itself is easily derived from $r\Delta\bar{\psi}$ but depends on absolute values (See below). The differential flux response is by definition the *equivalent square-wave amplitude response.* It is unity only at $N = 0$, decreasing linearly past the 70-per cent value

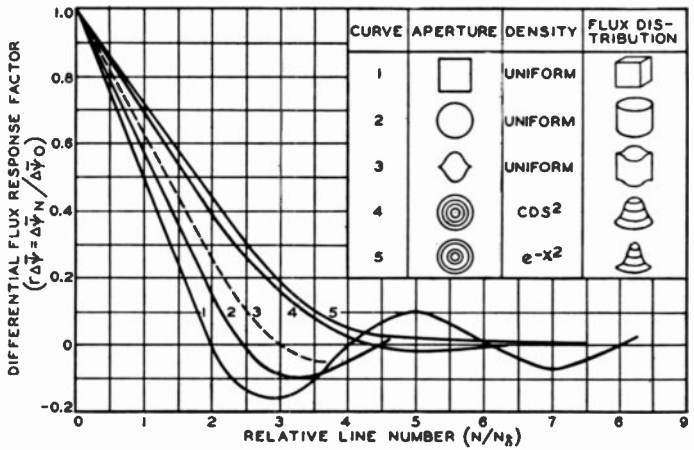

Fig. 16—Equivalent square-wave response of various apertures to square-wave flux pattern.

at $N \simeq N\delta$* and reaches its first zero at $N = N_C$. Round apertures with a cosine-square or exponential flux distribution with rotational symmetry (lenses and electron beams) generate flux waves substantially sinusoidal in shape in the range from $N\delta$ *to* N_C permitting the useful approximation:

$$\text{for } N > N\delta; \qquad r\Delta\bar{\psi} \simeq 2r\Delta\hat{\psi}/\pi$$

The flux response factors $r\Delta\bar{\psi}$ computed for various aperture types are shown in Figure 16. (See Table II in Appendix).

In certain cases, the aperture characteristic may be described by the *energy response factor* which is the response to absolute signal

* The square aperture is an exception.

values. For optical objects the energy response is expressed by the contrast ratio

$$C = \bar{\psi}\ (\text{white})/\bar{\psi}\ (\text{black}) = \bar{B}_2/\bar{B}_1 = (\bar{\psi}_1 + \Delta\bar{\psi})/\bar{\psi}_1 \qquad (25)$$

or the "per cent contrast" $$\%C = 100\ (1 - 1/C) \qquad (26)$$

The energy response factor is expressed by

$$rC\delta = \%C_N/\%C_o. \qquad (27)$$

A test object with substantially 100 per cent contrast furnishes the value:

$$rC\delta = \%C_N = [\,(1 - (1 - r\Delta\bar{\psi}))/(1 + r\Delta\bar{\psi})\,]\ 100. \qquad (28)$$

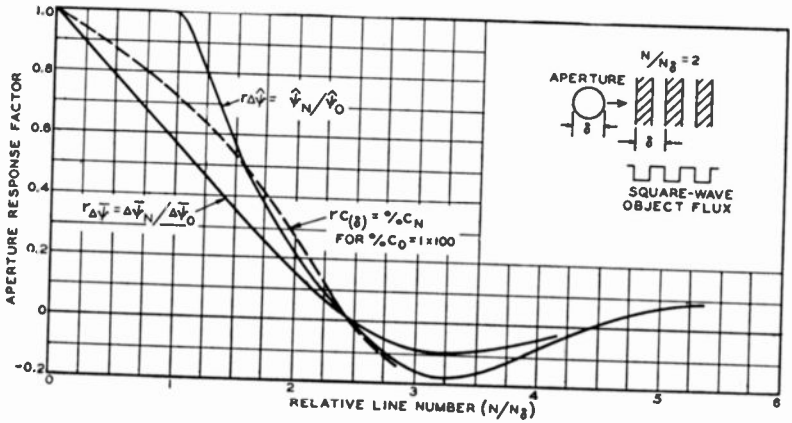

Fig. 17—Flux response of round aperture with uniform flux density or transmission.

The three response curves for a round aperture are shown in Figure 17.

2. Complex Apertures

Practical apertures have, in many cases, a flux distribution following a complex law. The complex aperture is considered as a superposition of a number of simple coaxial apertures and the complex aperture response is obtained as the arithmetic sum of the response curves of the component apertures each having a certain flux (ψ_n), density distribution, and diameter δ_n. In round apertures, the flux ψ_n in component apertures of equal shape is proportional to the product of their density (height) and base area (δ_n^2). Figure 18 illustrates the graphic construction of the response characteristic for a round aperture with cosine-square flux cross section as the sum of 5 coaxial round apertures

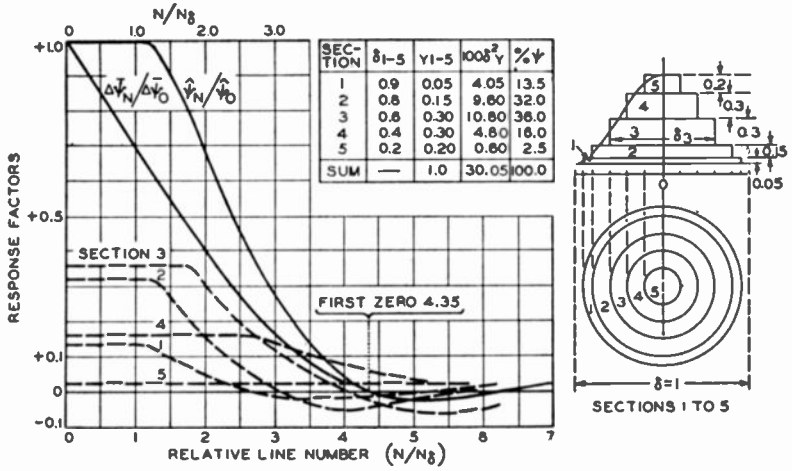

SECTION	δ_{1-5}	Y1-5	$100\delta^2_Y$	%Ψ
1	0.9	0.05	4.05	13.5
2	0.8	0.15	9.60	32.0
3	0.6	0.30	10.80	36.0
4	0.4	0.30	4.80	16.0
5	0.2	0.20	0.80	2.5
SUM	—	1.0	30.05	100.0

Fig. 18—Synthesis of flux response of a round aperture with cosine-squared flux density or transmission.

with different diameters and uniform flux density. It should be noted that the response curves of the larger sections are continued to the value N_c of the smallest section because their "spurious" response values beyond the first zero must be included when adding up individual response curves.

The aperture response of a fine light spot surrounded by a relatively low-intensity diffusion disc is illustrated by the constructions in Figure 19. The insert drawing shows the cross-sectional flux distribution resulting from two coaxial cosine-square apertures with the diameter ratio $\delta_2/\delta_1 = 5$ and the flux amplitude ratio $\hat{\psi}_2/\hat{\psi}_1 = 0.05$. The corresponding aperture response $r\Delta\bar{\psi}$ is that of Curve 1. Because of the large diameter (δ_2) the flux ψ_2 in the "diffusion" disc is 57 per cent of the total flux and causes a pronounced "kink" in the response curve, which

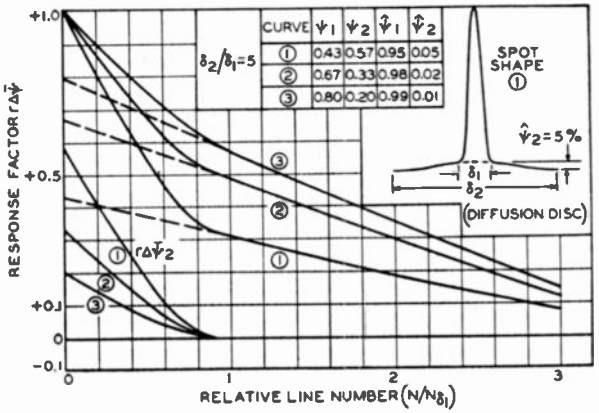

Fig. 19—Effect of aberrations (diffusion disc) on the aperture response.

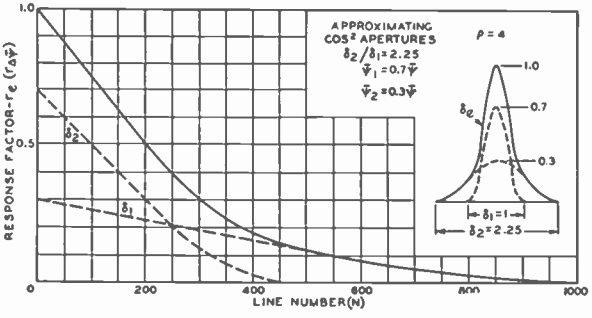

Fig. 20—Formalized aperture response characteristic of the eye for $\rho = 4$.

is still noticeable for a 1-per cent diffusion intensity (Curve 3). The similarity of the eye and kinescope response characteristics as shown in Figures 20 and 13*. These and other measured characteristics may thus be analyzed for aberrations by the reverse graphic procedure of subtracting the normal extrapolated fine-aperture response curve from the total curve. Table III in the Appendix is useful for curve extrapolation.

3. Simultaneous Imaging by Multiple Apertures

The waveforms, zero points, and spurious components computed for various aperture types are not a pecularity of the scanning process but occur in simultaneous imaging with multiple apertures or figures of confusion as well. The effects are, therefore, accurately duplicated by out-of-focus imaging with lenses. Figure 21 shows that a point of light focused on a screen at a distance d is produced by a light beam which has a cross section shaped by the lens aperture. When the screen is moved out of focus (d_1 or d_2), the light spot increases and assumes the cross section and flux distribution of the lens aperture. The spot image is the "figure of confusion". The upper right-hand corner of

* Part I—page 35.

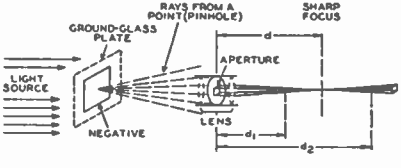

Fig. 21—Aperture effect on shape of point-imaging beam in out-of-focus imaging.

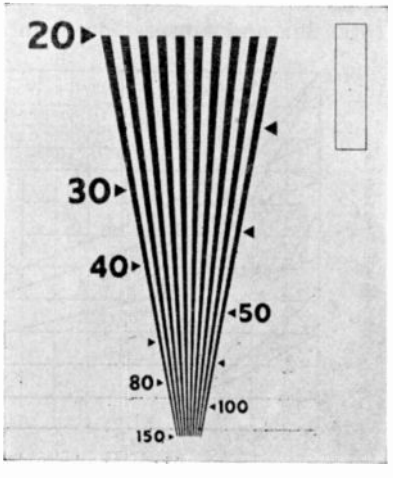

Fig. 22—Wedge test pattern and pinhole apertures in sharp focus.

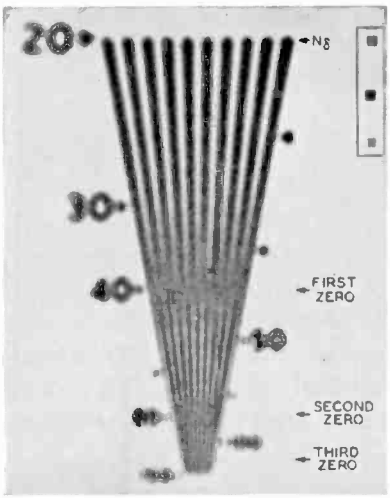

Fig. 23—Test pattern image formed by square aperture (defocused lens) as shown by pinhole images.

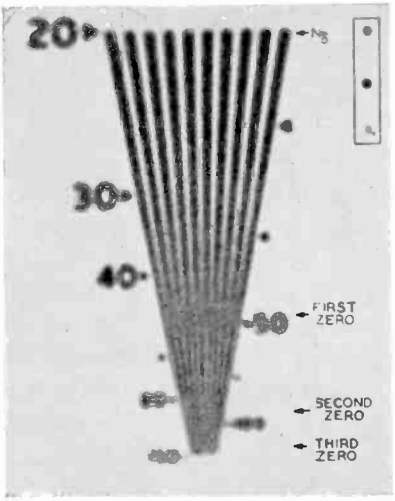

Fig. 24—Test pattern image formed by round aperture (defocused lens) as shown by pinhole images.

Figures 22 to 25 show the respective size and shape of the generating aperture or figure of confusion produced by three pinholes in the negative. In the wedge patterns of these photographs, the multiple zeros and spurious signals are plainly visible. Note the sharp crests (triangular wave) in Figure 23 at $N\delta$, the square shape near the zeros, and the phase shift and loss of one wedge line at every zero, all of which

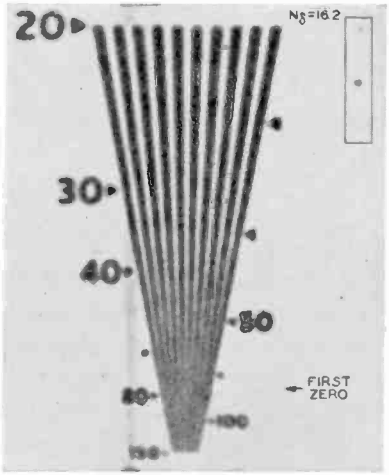

Fig. 25(a) — Test pattern image formed by round aperture with cosine-squared flux (defocused lens) as shown by pinhole images.

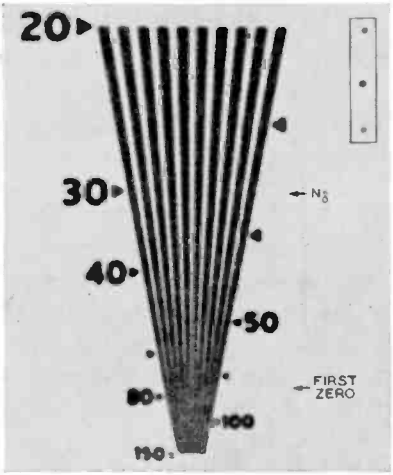

Fig. 25(b) — Test pattern image formed by round aperture with uniform flux computed to give a cutoff equal to that of Figure 25(a).

are in perfect agreement with computed values. The cosine-squared aperture with rotational symmetry (Figure 25(a)) was synthesized by multiple exposures with the following lens apertures.

$1/\delta \propto$ f:	5	6	6.8	8	9.6	12	14.4	19.2	32
exposure t (seconds)	0.5	1.	1.5	1.5	1.5	1.	1.	1.	1.

A 10-second exposure was made first at f/8.6 with a single round aperture ($N\delta = 30$) of equivalent flux, computed to have substantially the same cutoff point as the cosine-squared aperture with $N\delta = 16.2$ (Figure 25(b)). It served to set the out-of-focus lens adjustment which remained the same for the cosine-squared exposures. This cosine-squared distribution has rotational symmetry and applies to electrical

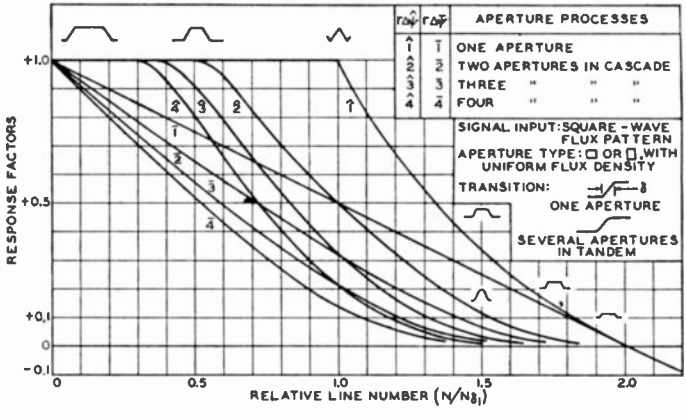

Fig. 26—Flux response of identical square apertures in cascade.

beams and lenses. It should not be confused with the shaped aperture shown in Figures 15 and 16 by Curve 3.

4. Aperture Processes in Cascade

The degradation of detail signals in multi-stage transducing processes is an effect caused by a progressive integration of the signal flux within aperture areas modified by their transmission or density characteristics. To obtain the over-all response characteristic of aperture processes in cascade, it is necessary to repeat the process of scanning with apertures. While the test pattern signal in the second operation is modified in waveform and amplitude by the first process, the signal to the third scanning operation is modified by the second process, and so forth. When starting with a square-wave flux pattern, each succeeding process rounds off the flux waveform and "stretches" the transition

curve produced by a unit function boundary in the original pattern. After several repetitions of the process, the response characteristics of all aperture types resemble each other closely as shown by the curve families Figure 26 and Figure 27 computed for two dissimilar aperture types (See Table IV in Appendix). The nature of the process and the substantially uniform contraction of the response characteristic occurring in each additional process, suggest a trial of the rule of squared sums for an approximation of progressive response characteristics. Cawein* observed that the scale contraction δ_p of (sine wave) response characteristics for a number of equal aperture processes in cascade follows this rule fairly well as expressed by

$$\delta_p^2 = \delta_1^2 + \delta_2^2 + \cdots \delta_n^2. \tag{29}$$

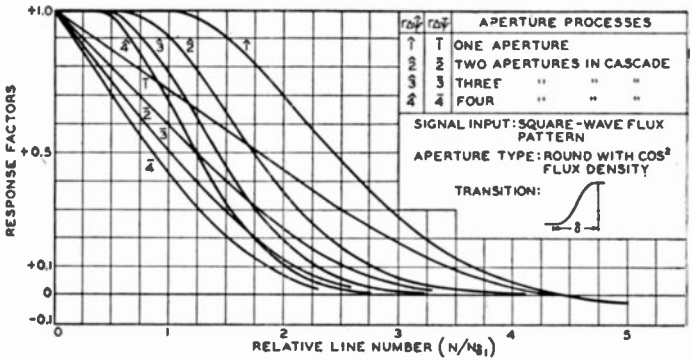

Fig. 27—Flux response of identical round apertures (cosine-square flux) in cascade.

In this expression δ_p is the "width index" or the equivalent aperture diameter of the over-all process and δ_1 to δ_n are the width indices or aperture diameters of the component aperture processes. The equivalent aperture of two identical processes in cascade, for example, is $\sqrt{2}$ times larger in diameter than the aperture of each single process. Examination of the true characteristics Figure 26 and Figure 27, discloses that this general rule does not apply accurately to strongly curved sections of the response characteristics $r\Delta\bar{\psi}$ or $r\Delta\hat{\psi}$, but holds well in the substantially linear part of the differential flux response curves $r\Delta\bar{\psi}$ even for widely different aperture types. The over-all aperture response of a number of aperture processes in cascade is obtained, therefore, with good accuracy from measured or computed characteristics $r\Delta\bar{\psi} = f(N)$ of individual processes by observing the following rules. An aperture response value $r\Delta\bar{\psi}$ is selected which

* Part I—Reference 3.

occurs in the substantially linear part of any one individual response characteristics. As characteristics of practical aperture processes have often a pronounced "knee" (See Figure 19) a point-by-point evaluation or an approximation of the characteristic by an equivalent linear characteristic with lower cutoff may be required if the "knee" occurs within the range of observation. Cutoff values (N_c) should never be used. The selected response $r\Delta\overline{\psi}$ (usually greater than 0.3) furnishes particular resolution line numbers $N_1, N_2, - - - N_n$ for the individual stages. The line number N_p at which the same response is obtained from the cascaded process is computed by the rule of squared sums:

$$N_p = 1/\sqrt{1/N_1^2 + 1/N_2^2 + - - - 1/N_n^2}. \tag{30}$$

5. The Aperture Response in Sampling Processes

a. The Sampling Principle

Practical imaging processes analyze and reproduce the continuous light-flux distribution in optical images by a sampling method. The spatial distribution of the light-flux samples may be random, as in photographic film (grain), or it may be arranged to follow a regular pattern termed a "raster" as in printing and television processes.

In principle, samples of the image flux are taken by the "analyzing" aperture of a photosensitive transducer at image points specified by the raster. The integrated aperture flux is transduced into signal "amplitudes" which are transduced again into flux samples by the "synthesizing" aperture of the image-reproducing device. Proper spatial location of the samples in the re-created image is obtained by matching or "synchronizing" the rasters in the two processes. The amplitude of the reproduced flux samples is controlled by the signal amplitudes, but the area occupied by the sample is determined by the size of the synthesizing aperture. (In some cases, it is also a function of signal amplitude.)

The accuracy of the process in sampling the flux amplitude at any raster point is expressed by the aperture response of the analyzing aperture, but information on the flux between raster points is inaccurate or missing. To restore the continuity of signals between sampling points in the recreated image and to avoid interference by the structure of the raster, the missing information is approximated by increasing the dimensions of the aperture "depositing" the flux samples at the raster points (or lines) in proportion to the raster pitch distance Δx. With respect to image definition, the lack of information due to sampling as well as the increase of aperture dimension in the reproducing aperture cause loss of detail and can be expressed by respective aperture response factors. (See below)

To be useful, all imaging processes are followed by the process of vision. The aperture process of the eye can therefore perform the required widening operation and restore continuity of the image field when the raster pitch distance ($\triangle x$) is decreased below certain values. Small apertures with high response factors ($r\triangle\bar{\psi}$) can then be used to advantage in both transducers. The flux response of the three basic apertures of the sampling process in television systems will be treated in a subsequent section.

b. Line Number and Threshold Visibility of Raster Fields

The "vertical" aperture displacement in the television line scanning process occurs in small discrete steps $\triangle V$ which are inversely proportional to the "active" scanning line number N_V in the image. The stepwise displacement of the aperture path causes an image structure termed a "line raster".

Visibility of the raster in the image field depends on the aperture size of the image-forming transducer as well as on the aperture sizes of all succeeding processes through which the (kinescope) image is observed.

Continuity of the image field termed a "flat" field* or the illusion of seeing a flat field is produced by spaced "samples" when the sampling point spacing coincides with a zero response value N_c of the transducing or observing aperture. The equivalent television line number of a raster is $N_R = 2n_x$, where $n_x = 1/\triangle x$ is the number of raster points or lines in the vertical picture dimension. A minimum flux variation occurs for the condition

$$N_R = N_c = 2n_x. \tag{31}$$

Complete null points or flat fields without residual flux "ripples" are obtained only with certain apertures*. The out-of-focus projections of a fine line structure in Figure 28 demonstrate flat-field conditions (center and right side) for three apertures with uniform density. Inaccuracies in aperture shape caused residual ripples and slight shifts of the theoretical null points of the square and diamond apertures. Apertures with sharp cutoff have several critical flat field conditions, while apertures with gradual cutoff, such as the eye, maintain a flat field for $2n_x \geqq N_c$. The line width or aperture diameter (δ) of the kinescope can therefore be given any value when the raster line number $N_V = n_x$ satisfies Equation (31) where N_c is the limiting resolution of the eye. For a viewing ratio $\rho = 4$, the eye response as given in Figure 20 (See also Figure 8‡) is limited to $N_c = 1000$ lines. *A televi-*

* Part I—Reference 1.

‡ Part I—page 26.

sion line raster field with an active line number $N_v = 500$ lines will therefore appear continuous at $\rho = 4$.

It is apparent that the number n_s in a raster should be increased (by $\sqrt{2}$ for a 45-degree angle) to maintain continuity or eliminate visible serrations at the edges of slanting contours*. A step structure will therefore be visible at certain image flux distributions when the raster is dimensioned according to Equation (31). (See next Section.)

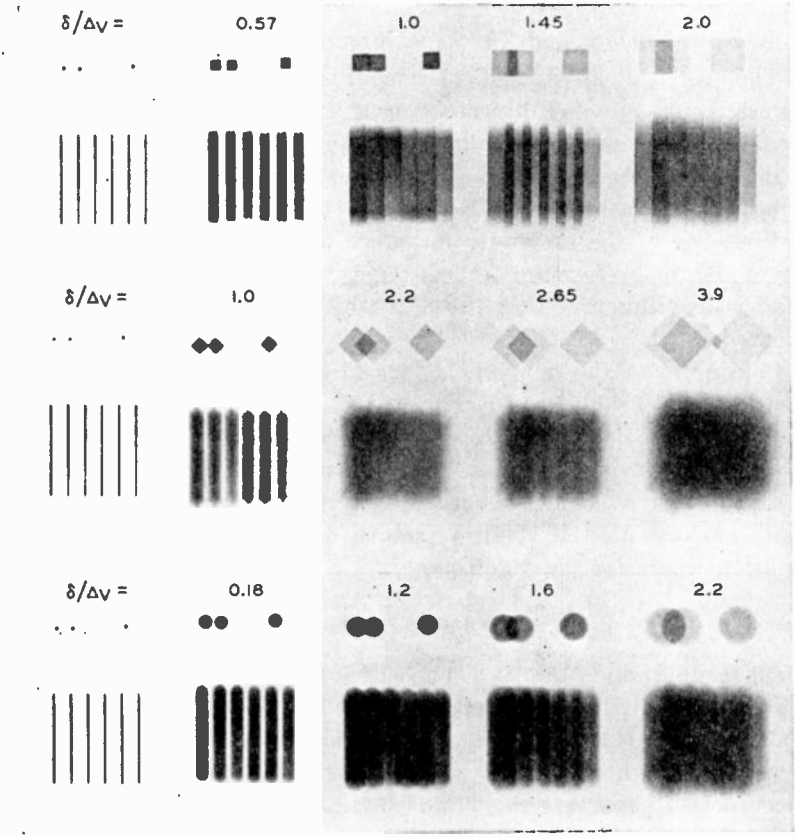

Fig. 28—Widening of raster samples by various aperture types and sizes.

c. *The Sampling Process and Aperture Response in Television Systems*

The signal amplitude from a photoelectric transducer with constant aperture size is proportional at any instant to the integrated light flux within the aperture area. When this "analyzing" aperture (A_1) is displaced in finite incremental steps Δx or ΔV, the generated signals

* Part I—Reference 1.

are exact "samples" of the aperture flux wave obtained by continuous displacement of the same aperture.

The "modulation envelope" of the sampling pulse wave is therefore specified by the normal aperture response factors $r\triangle\hat{\psi}$ and $r\triangle\bar{\psi}$. It may appear that the vertical aperture response of television scanning apertures is a special case because a continuous aperture displacement

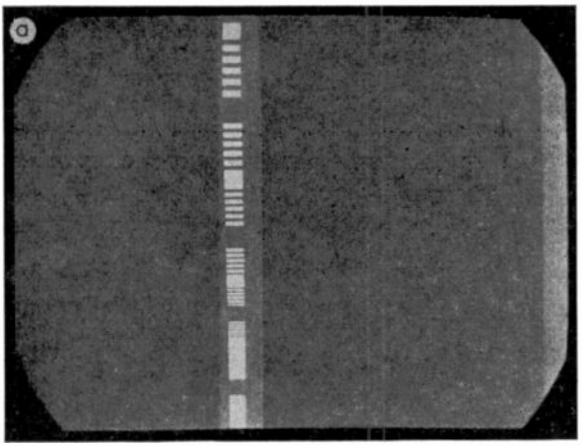

Fig. 29 — Kinescope images of "vertical" aperture-response samples.

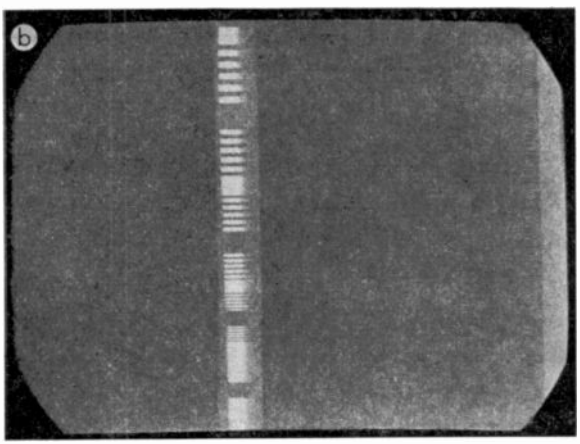

occurs simultaneously in the horizontal direction. A line element $\triangle H$ of a cosine-square aperture, for instance, has a rectangular base and the shape given in Table I of the Appendix. Calculation of the (vertical) aperture response of this line element however discloses no change from the horizontal flux response of the aperture.

Normal aperture response characteristics can, therefore, be measured by incremental (vertical) scanning of square-wave test patterns. Their equivalence with characteristics obtained by continuous scanning

is demonstrated as follows. The beam of a 5-inch projection kinescope with short decay phosphor is used as a scanning aperture for generating signals in a light-spot scanning system. The aperture signals of the light spot are transduced by a 931-A multiplier phototube into electrical waveforms which are observed on an oscilloscope with cross section selector. The test object is a transparency of parallel-line groups which can be inserted vertically or horizontally into the light-spot scanner. The image of this object can be seen on a monitor kine-

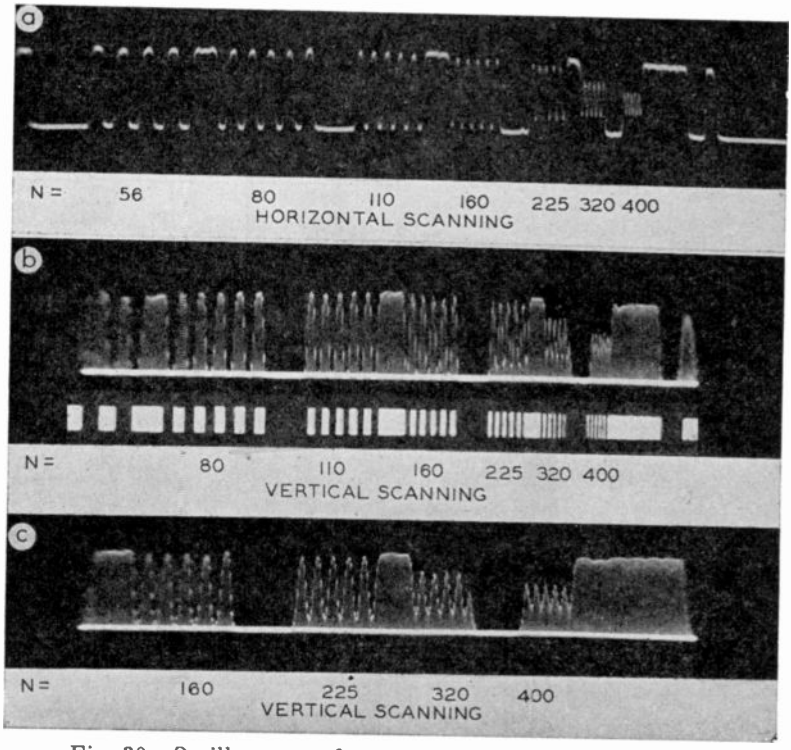

Fig. 30—Oscillograms of aperture response of a kinescope light spot ($N\delta \simeq 160$).

scope and appears for vertical scanning as shown in Figure 29. Trace (a) in Figure 30 is an oscillogram showing the light-spot aperture response as the modulation of the continuous (horizontal) line trace; while the traces (b) and (c) show the response of the same aperture in the vertical direction as the envelope of the scanning pulse wave generated by the step displacement ΔV of the scanning aperture. The ratio N_V/N of the active scanning line number to the test-object line number is the number of samples per test pattern line. In trace (c) Figure 30, the ratio N_V/N is considerably greater than unity for all

line groups, while in trace (b) it has been reduced to $N_V/N \simeq 1.25$ for the finest line group.

For better interpretation of waveforms, the number of samples can be increased by compressing the scanning raster in the light-spot scanner. This compression does not affect the aperture response or calibration which is set by the optical magnification of the lens system.

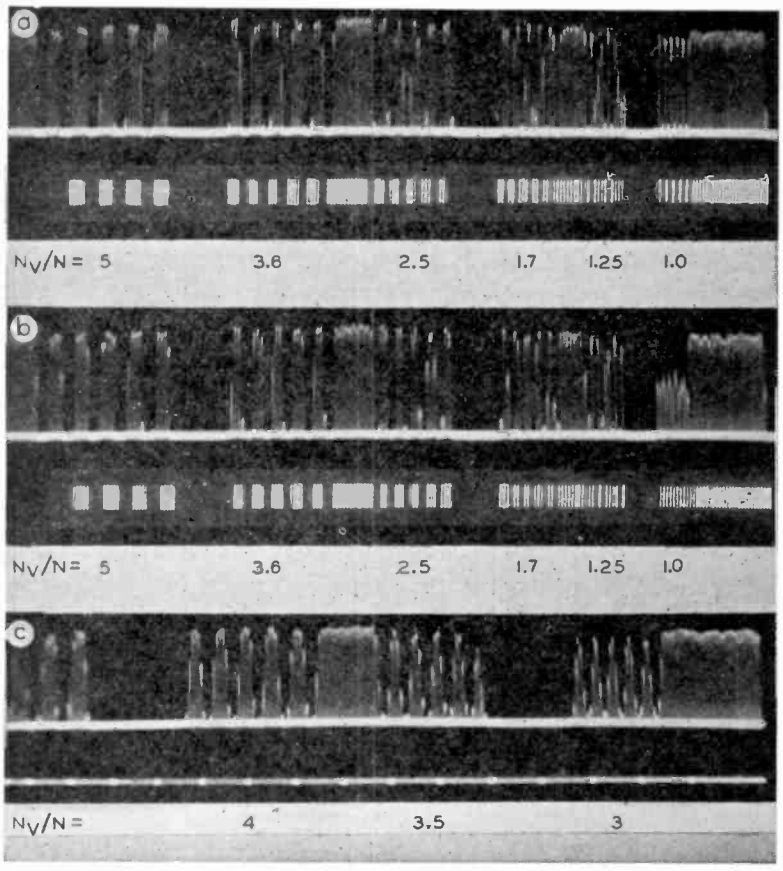

Fig. 31—Oscillograms of aperture response of a kinescope light spot ($N\delta \simeq N_v$).

The increased aperture response of a fine scanning aperture is shown in Figure 31. The traces (a) and (b) and the corresponding kinescope images also illustrate the effect of phase differences at $N = N_V$. Trace (b) shows the critical condition of sampling the null points of a square wave with a small aperture. Both figures show spurious signal components which are beat frequencies between N_V and N. Their pattern is most evident in the oscillograms because the pulse top is

recorded strongly by the oscilloscope, the fainter amplitude lines being the horizontal pulse sides. The amplitude lines which are invisible on the oscilloscope with sharp horizontal definition (Figure 29(a)) are made visible by decreasing the horizontal frequency response by a shunt capacitance (Figure 29(b)). The scanning tests verify that the normal aperture response of the scanning aperture can be determined accurately by the vertical sampling process.

The cascaded aperture effect of the principal apertures in a sampling system in which the eye serves as a "pulse lengthener" is illus-

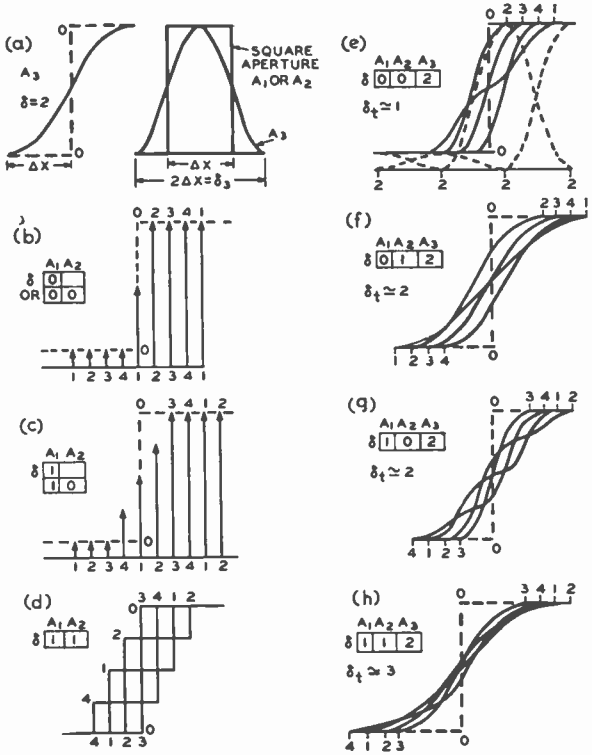

Fig. 32—Effect of sampling and aperture response on a unit function transition.

trated by a series of graphs in Figure 32. Aperture numbers and sizes are listed in the left corner of each graph. The symbols A_1 and A_2 indicate the apertures of the photoelectric (pickup) and electro-optical (kinescope) transducers. A_3 is an observing aperture simulating the eye. The aperture diameter δ of A_1 or A_2 is listed as zero for an aperture much smaller than the raster pitch and as unity when a square aperture $\delta = \Delta x$ is used. The aperture simulating the eye is shown as a line element with cosine-square cross section (See Figure 32(a)) to

produce a perfect flat field for samples of constant amplitude. Its diameter, therefore, is $\delta_3 = 2(\Delta x)$. The test object is a unit function flux change marked as $0 - - - 0$.[19]

The effects of changing the aperture size δ_1 from near zero to unity are shown in Figure 32(b) and (c) by the four phasing conditions (1 to 4). The small aperture produces only one intermediate signal amplitude (1) in the four positions shown. The amplitude is nearly always correct, but the phase may vary within one line pitch (Δx). This position error is the "raster effect" which may rate on the average an aperture value $\delta_r = 0.5$ (See later). The square aperture $\delta_1 = 1$ is correct in amplitude only once (3) and in error most of the time, the average transition length (envelope of amplitude points) rating one line pitch ($\Delta x = \delta_1 = 1$); it also has the same phase error ($\delta_r = 0.5$). Figure 32(d) is the effect of two square apertures $\delta_1 = 1$ and $\delta_2 = 1$ in cascade. It is correct in amplitude only once (3); it widens the transition to $\Delta x = 1$ on the average; and it has the phase error. The case of two small apertures is the same as (b).

More significant and readily interpreted differences are seen in the overall processes $A_1 + A_2 + A_3$ shown by the transitions (e) to (h) for which the respective transition length δ_t is indicated. The broken lines in (e) show the four sample points (2) from a small δ_2 widened to the aperture size δ_3. Their sum produces the curve 2. It is a curious fact that the transition δ_t is only one half as wide as that of A_3 alone ($\delta_3 = 2$); (the effect can be observed by experiments with real apertures and with different objects) but a position error within $\Delta x = 1$ is still in evidence. When one larger aperture is used, the transition is lengthened to $\delta_t \simeq 2$. Condition (g) may be rated as a little shorter transition, but it is more distorted than that shown by (f), where the sequence in sizes is reversed. Two larger apertures (Figure 32(h)) cause a further lengthening to $\delta_t = 3$. The phase- or position-error is progressively reduced. The reduction is a normal effect expected from the aperture addition in quadrature (Equation (29)). Computation of δ_t by Equation (29) furnishes the value

$$\delta_t = \sqrt{\delta_1^2 + \delta_2^2 + \delta_3^2 + \delta_r^2} = \sqrt{1 + 1 + 2^2 + 0.5^2} = 2.5$$

which represents the effective transition length quite well if the fact that the cutoff points are not accurately following Equation (29) in normal cascaded aperture processes (Figure 26) is considered. Similar

[19] The vertical brightness transition for a specified kinescope aperture and raster has been similarly evaluated: see R. D. Kell, A. V. Bedford and G. L. Fredendall, "A Determination of Optimum Number of Lines in a Television System", *RCA REVIEW*, Vol. V, No. 1, pp. 8-30, July, 1940.

answers have been obtained with other test objects (sloping transitions, irregular waves, and square waves). It may be concluded that, *on the average, the sampling process does not change the normal aperture response.*

d. The Aperture and Response Characteristics of the Raster

The phase or position error caused by the sampling process is better known as a "spurious" signal component or a "beat pattern". It is especially noticed in images having parallel slanting lines, circular line groups, wedges, etc. The position error disappears with larger apertures or line numbers when the aperture process preceding and including the first scanning aperture has a cutoff $N_c < n_x$ (See reduced phase error in central portion of Figure 32(h)). The effect of the phase error on sharpness may be rated as an aperture factor. In the directions of the raster pitch the phase uncertainty is, on the average, $\delta_r = 0.5\Delta x$. As the raster point- or line-distance Δx changes with angle, a 45-degree angle may be considered as an average value. The average phase error in the image is, therefore, 0.5 $\sqrt{2}$ times the raster pitch (Δx). If the eye rates a small position error as an equivalent decrease in sharpness, the phase error may be expressed by an equivalent "raster aperture". *The equivalent symmetric "raster aperture" of the sampling process is, hence, a square aperture with a tentative size*

$$\delta_r \text{ square} \simeq \Delta x/\sqrt{2}. \tag{32a}$$

The response factor $r\Delta\overline{\psi}$ of this aperture is 50 per cent at a line number N equal to $\sqrt{2}$ times the raster line number (n_x) and the aperture response curve (See Figure 16) is a straight line from $r\Delta\overline{\psi} = 1$ at $N = 0$ to

$$r\Delta\overline{\psi} = 0.65 \text{ at } N = n_x = N_V \tag{32b}$$

and has a limiting resolution $N_c = 2\sqrt{2}nx$. (32c)

The effect of the raster structure varies with picture content. It can be evaluated by subjective tests with normal image subjects on television systems without electrical channel limitation and known apertures. Such measurements have been made by Baldwin[5] with a television system employing two square apertures $\delta_1 = \delta_2 = \Delta x$. Equations (29) and (32a) furnish the value $\delta_p = \sqrt{1 + 1 + 1/2}\,\Delta x = 1.58$ for this process. Baldwin found by optical comparison that the equiva-

[5] See Part I.

lent optical square figure of confusion of his television images was $\sqrt{2.67}$ or $\delta_p = 1.63\ \Delta x$. His raster contained only 240 lines and in view of the difficulties of maintaining a flat field without visible structure with large square apertures, the agreement with the computed value can be considered as excellent.

The sampling process itself (with infinitesimal apertures) is a process with constant amplitude response from $N = 0$ to its nominal *sharp cutoff* at $N_{co} = n_x$. These characteristics are significant and outstanding, and cannot be duplicated by normal aperture processes. They are approached, however, quite closely by phase-corrected electrical filters with sharp cutoff. This and other similarities permit the deduction that an electrical channel can be replaced by an equivalent two-dimensional aperture.* The response characteristics of the electrical channel and its equivalent aperture are discussed in a subsequent section.

6. Random Fluctuations and the Aperture Effect of Grain Structures

Random fluctuations (noise) of the image signal have, in principle, no effect on the aperture response of an imaging system. For a given finite time of observation, a high fluctuation level will obscure detail signals to a greater extent than large area signals, but it does not change the *ratio* of detail to large area signals which is specified by an aperture response factor. A high fluctuation level may limit a response factor measurement by uncertainty of observation to relatively large values (for example to $r\Delta\overline{\psi} > 0.5$) while a low "noise" level permits accurate measurement of the cutoff resolution $r\Delta\overline{\psi} = 0$.

The elemental structure found in all signals (unit charge, electron, diffraction disc, grain), however, causes an aperture effect which can be observed with sufficient "magnification". The number of elemental samples or signal "units" occurring per unit area and time of the pass band is a measure of the fluctuations in the signal, i.e., it determines the signal-to-noise ratio. In the case of electrical signals the aperture effect of the elemental unit is so small that it is negligible within the limits of optical pass bands. Fluctuations, therefore, may be observed but there is no aperture effect due to electron size. When the elemental unit is of a size which can be resolved by the optical pass band (grain or particle sizes of photographic emulsions, pickup tube mosaics, kinescope screen materials) its aperture effect is noticeable and affects the aperture response of the imaging process. The existence of an aperture effect does not exclude the possibility of a low fluctuation level as it does not necessarily specify the number of grains per unit area or

* This treatment is permissible when the asymmetry of the aperture of the over-all process remains within certain limits; see Reference 5, Part I.

time, which determines the signal-to-noise ratio. The aperture response of a number of grain structures has been measured with a television microphotometer and will be discussed further in Part III of this paper.

B. General Specifications for Television Systems

1. *Line Raster and Aperture Size*

The analysis of the sampling process has shown that it is unnecessary to limit the diameter of the scanning apertures in television systems to one line width ($\triangle V$) when the eye can perform the required widening operation to obtain a "flat" field. For a viewing ratio $\rho = 4$, Equation (31) states that an active line number $N_V \geqq 500$ is satisfac-

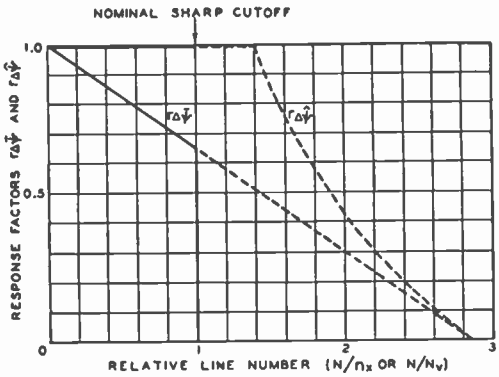

Fig. 33—Flux response characteristics of the equivalent two-dimensional square aperture of a raster process.

tory for use with small-diameter scanning apertures. The equivalent aperture of the raster itself has been evaluated in terms of a *two-dimensional square aperture* $\delta_r = 0.7/N_V$ (Equation (32)) with the aperture response shown in Figure 33. The increase in sharpness obtained with small apertures as compared to apertures covering a flat field in both transducers is illustrated by Figures 34 and 35 which should be viewed at a distance which gives threshold visibility of the line structure in Figure 34.

2. *The Equivalent Optical Aperture of the Frequency Channel and Theoretical Limits of Television Systems*

The definition of television systems is limited in the horizontal dimension by an electrical frequency channel ($\triangle f$). Electrical filters can be designed to have a considerably sharper cutoff than normal optical apertures. The square-wave response factors of the theoretical band pass filter with sharp cutoff can be derived from the Fourier components of a square wave, which contains only odd harmonics ($n = 1,3,5 - - -$) decreasing in amplitude according to order

Fig. 34—400-line television picture with small scanning apertures in camera and kinescope.

Fig. 35—400-line television picture with scanning apertures increased to give a "flat" field in camera and kinescope.

$$Y_n = 4/\pi n. \tag{33}$$

A finite frequency channel limits the frequency components in the square wave. A square line repetition occurring at one-fifth cutoff frequency can therefore generate a signal containing only the first, third and fifth harmonic. For repetition frequencies greater than one-third cutoff frequency, the channel will pass only the fundamental frequency.

The theoretical wave shapes for uniform phase delay up to cutoff frequency are shown in Figure 36(b). The square wave from a finite

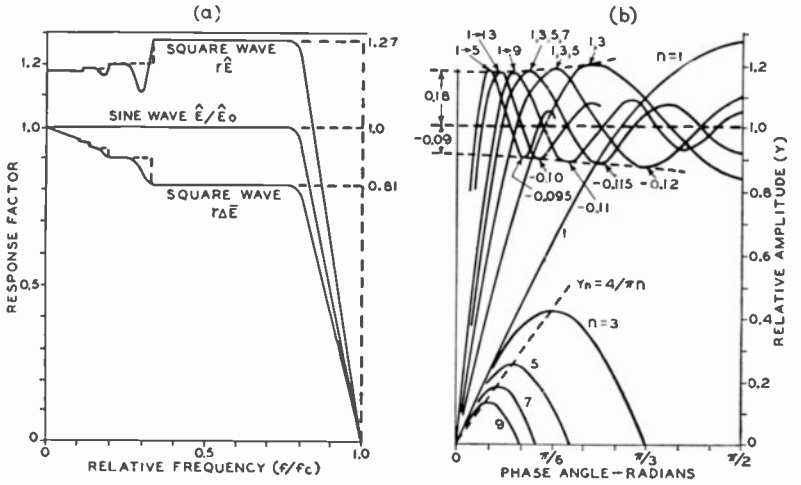

Fig. 36—Square-wave response characteristics of limited frequency channels.

frequency channel exhibits, therefore, "underswing" and "overshoot" preceding and following the rise or drop in current because of missing high-frequency components. These peaks change or disappear when the channel exhibits non-uniform phase delay or a gradual cutoff.

The amplitude response $r\hat{E}$ of the theoretical sharp-cutting channel is, therefore, greater than unity as shown by the dashed curve in Figure 36(a), exhibiting discontinuities where f_c/f is an odd number. The effect of a sloping cutoff (solid curve in Figure 36(a)) having no phase error and beginning at $f/f_c < 1$ results in dips in the amplitude response at the harmonic points. Because of phase shift errors, these dips usually do not occur with practical cutoff filters.

The equivalent square-wave response $r\Delta\bar{E}$ obtained by averaging the response per half cycle, remains at 81 per cent after an initial drop

in the first third of the frequency channel until the amplitude response begins to drop. The similarities of the electrical response characteristics and the vertical sampling process are apparent and it may be expected that the equivalent symmetric aperture of the electrical channel is in the same order as that of the sampling process.

The overshoot and following transient oscillations impose a restriction on the minimum horizontal line number N_H because the third and following odd number peaks cause multiple contours in the image and should be near threshold visibility at $\rho = 4$. Lower line numbers require reduction of the equivalent square-wave brightness step, $\triangle B$, between the second and third transient peaks by a more gradual cutoff in the electrical channel. Threshold visibility of a peak-to-peak brightness fluctuation, $\triangle B$, is obtained (Equation (11)*) when $\triangle B/B = 0.018/r_e$.

The value $\triangle B$ is proportional to the equivalent square-wave value $\triangle \hat{E}_{2,3} = (2/\pi)\ \hat{E}_{2,3}$ of the second and third transient peaks, which is 56 per cent[20] of the first and second peak-to-peak value $\hat{E}_{1,2}$ as expressed by

$$\triangle B \propto 1.12\ \hat{E}_{1,2}/\pi$$

A brightness value $B = \hat{B}/2 = E/2$ may be considered as an average value for unit function steps of various amplitudes and levels, when E is the signal voltage corresponding to a unit function from zero to $\hat{B}$. The threshold visibility requirement is hence expressed by

$$\triangle B/B \propto 2.24\ \hat{E}_{1,2}/\pi E = 0.018/r_e$$

$$\hat{E}_{1,2}/E \simeq 0.025/r_e. \qquad (34)$$

Equation (34) states the requirement for a television system with unity aperture response. When the response is limited by finite aperture sizes in the camera chain and kinescope, the frequency response of the channel can be corrected to compensate the decrease in horizontal signal components due to the aperture effect of the transducers. The correction requires a rising frequency response of the video amplifier (high-peaking circuits) and appropriate phase correction and is termed "aperture correction". The over-all response in the horizontal direction is then again determined by the requirements for unity aperture response (Equation (34)).

The degree of correction obtainable in practical systems depends on the signal-to-noise ratio. A high aperture response is of course still desirable as this aperture correction is not effective for vertical signal

* Part I—page 29.

[20] Jahnke, Emde, TABLES OF FUNCTIONS (Si (X) Function). Dover Publications, New York, N. Y., 1943.

components. (The effects of aperture asymmetry on the over-all response will be discussed in Part IV.)

The present standard television channel $\Delta f = 4.25$ megacycles accommodates the line numbers $N_V = 490$ and $N_H = 340$. The response factor of the eye is $r_e = 0.225$ (Figure 20) at 340 lines and Equation (34) furnishes the maximum transient ripple percentage $\hat{E}_{1,2}/E \simeq 11.0$ per cent.

The relation between sine-wave amplitude and transient response of electrical filters has been treated in detail by various authors[19,21,22]. Typical response curves and corresponding ripple percentages ($\hat{E}_{1,2}/E$) are shown in Figure 37. Curve 4 indicates the approximate channel response for a (standard) television channel with $N_H = 340$ lines giving a threshold transient ripple of 11.0 per cent.

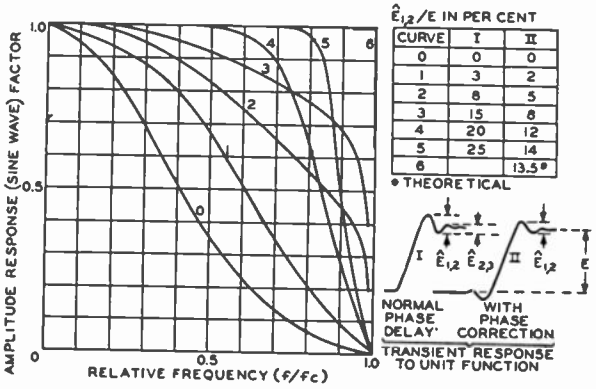

Fig. 37—Amplitude response and transient response of electrical channels.

An equivalent aperture size of the frequency channel is indicated by the length and shape of the transition curve obtained for a unit function signal. The S-shaped transition curve indicates a cosine-square aperture type (Table II, Appendix) with a diameter $\delta_H = 1/N_H$ for the square-cut frequency response curve. The aperture diameter increases with decreasing frequency response of the channel and has been plotted in Figure 38 as a function of transient ripple voltage (data from Kell et al. and Kallmann et al.[19,22]). The aperture diameter is indicated by the line number $N\delta_H$ at which the flux response factor $r\Delta\overline{\psi}$ is 71 per cent. *The equivalent two-dimensional aperture* δ_f *of the frequency channel* is specified by the horizontal component of a 45-degree

[21] A. V. Bedford and G. L. Fredendall, "Analysis, Synthesis, and Evaluation of the Transient Response of Television Apparatus", *Proc. I.R.E.*, Vol. 30, October, 1942.

[22] Kallmann, Spencer & Singer, "Transient Response", *Proc. I.R.E.*, Vol. 33, March, 1945.

line* $$\delta_f = \delta_H/\sqrt{2} \tag{35a}$$

with the equivalent line number $$N\delta_f = N\delta_H\sqrt{2} \tag{35b}$$

The equivalent optical aperture of a (standard) television channel with $N_H = 340$ lines is, hence, a cosine-square round aperture with $r\Delta\bar{\psi} = 0.71$ at $N\delta_f = 0.75 \times 340\ \sqrt{2} = 360$ lines. 50-per cent response (See Figure 16) occurs at $N_{(0.5)} = 630$ lines.

The equivalent optical aperture of a television system with ideal components is the *cascaded* value of the raster aperture δ_r and the channel aperture δ_f. For the line number $N_V = 490$ and $N_H = 340$ of the standard 525-line system, the line number at $r\Delta\bar{\psi} = 0.5$ computed with Equation (32) and Figure 33 is $N_r = 490\ \sqrt{2} = 690$ for the raster

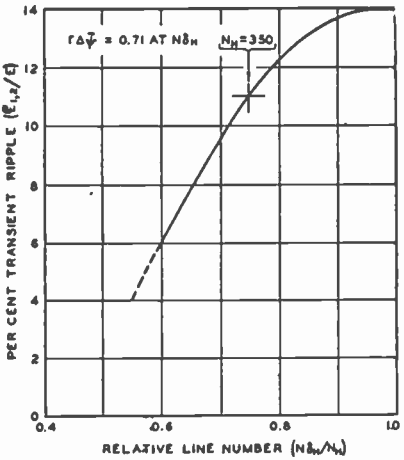

Fig. 38—Aperture size ($1/N\delta_H$) of of frequency channels as a function of transient ripple.

aperture. It is interesting that it is nearly equal to the channel response which was found to be 630 lines for this response factor.

The equivalent optical aperture of the standard 525-line television system and frequency channel ($\Delta f = 4.25$ megacycles) has, therefore, a response $r\Delta\bar{\psi} = 0.5$ at a line number $N = 465$ lines as a theoretical limit. (Computed with Equation (30).)

8. *Brightness, Repetition Rate, and Flicker in Television Images*

a. *Brightness and Flicker of the Image Field*

Adequate discrimination of detail is known to require a high-light image brightness equal to or greater than 15 foot-lamberts, because the average brightness $\overline{B}$ should be greater than 2 foot-lamberts for operation with a normal transfer factor g_e of 12 on the eye transfer characteristic (Figure 8‡).

* This choice is indicated by the addition of apertures in quadrature.
‡ Part I—page 16.

The illusion of seeing the cyclic light-spot synthesis of television image fields without brightness fluctuations depends on the persistence of vision and requires a certain minimum field repetition rate or "critical flicker frequency" (C.F.F.).

The C.F.F. for intermittent light flashes having a fixed exponential decay times (t) can be obtained by replotting Figure 6‡, as shown by Figure 39. The three frequency scales on the ordinate of Figure 6

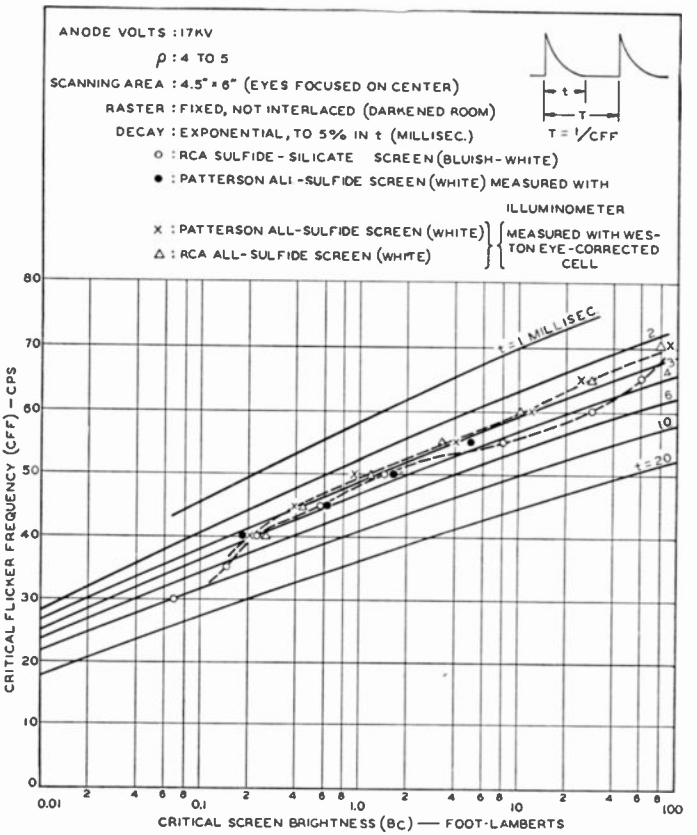

Fig. 39—Critical screen brightness of kinescope fields (white light) as a function of field frequency.

indicate the effect of a change in viewing ratio (ρ). A low ratio causes exposure of the rod-populated peripheral region of the retina which is more sensitive to flicker. These curves may be expected to indicate, in general, the slope of kinescope flicker curves, but it can hardly be expected that the impulse light wave produced by a single high-speed scanning spot is directly equivalent to a simultaneous impulse excita-

‡ Part I—page 22.

tion of the entire screen area. The peak brightness of the kinescope light spot is extremely high and saturation effects are likely to occur at high average values of brightness, $\overline{B}$, in the eye as well as in measuring devices. Furthermore, the decay of sulfides and mixtures of sulfides with silicates, deviates from an exponential law, and is also a function of current density and excitation time. *The time constants and C.F.F. of practical phosphors for the generation of white or colored light must, therefore, be determined by observation under actual operating conditions.*

The C.F.F. for unmodulated white light from various kinescopes (uniformly bright screen) has been measured and is indicated in Figure 39. This figure shows that all-sulfide screens permit a critical flicker brightness (B_c) of 10 to 13 foot-lamberts at 60 cycles, while sulfide-silicate mixtures permit a B_c of approximately 30 foot-lamberts.# These values increase by a factor of two for large viewing ratios (See ordinate scales of Figure 6). All measurements were made with a viewing ratio of 4 to 5 with eyes fixed at the center of the scanned area (4.5×6 inches) of actual television rasters. Care was taken to eliminate all spurious electrical fluctuations such as 60-cycle ripple, line fluctuations of the raster, and spurious interline flicker. The scanning raster was generated without interlacing but with interlocked frequencies in order to obtain a stationary line raster of 400 to 500 lines. Variation of spot size from 0.010 to 0.1 inch showed little effect on the C.F.F. in 500-line rasters. The screen brightness or rather "luminosity" B_c was measured directly with a Weston eye-corrected cell which follows closely the luminosity curve of the eye (Figure 5‡). These readings are somewhat lower than illuminometer readings on white light.* Sufficient time was allowed for adaptation of the eye and adjustment of pupil diameter. Repetition of measurement was advisable for consistency of observation, especially at higher field-repetition rates.

The critical flicker brightness of kinescope images is a function of the light distribution in the image. Modulation of the kinescope light-spot intensity breaks up the flickering area into smaller areas, for which viewing ratio (ρ) and critical brightness have higher values. The critical peak brightness $\hat{B}_c$ of the television image may, therefore, be considerably higher, especially when the high-light areas are small.

The indicated decay time is only an *equivalent* value and does not indicate that the light from the material has actually decreased to 5 per cent after t.

‡ Part I—page 21.

* The discrepancy is possibly an integration error of the cell due to its saturation characteristic. For the same reason, illuminometer readings made with a brightness reducing filter may give a higher value than the actual luminosity to the eye.

It has been observed on normal television pictures that the average brightness level of the image can be raised to a value equaling, roughly, that of the critical flicker brightness B_c for unmodulated light without obtaining objectionable flicker of the image. The average screen brightness $\overline{B} = B_c = 10$ to 30 ft-L for present phosphors and for a field frequency of 60 cycles per second can therefore, be considered as a satisfactory value which permits a high-light brightness ($\hat{B}$) in the order of 50 to 150 foot-lamberts in normal television images.

b. Color Flicker

It has been checked by observation on scanned rasters that B_c and the C.F.F. remain substantially constant for a fixed light-color and repetition period independent of the time of scansion (T_v) of the raster, as long as the decay time (t) is less than the repetition period (T). (See sketch in Figure 39.)

Image fields scanned within the time T_v equal to or smaller than T (say $T_v \leqq 1/60$ second) but repeating after the same time T (say $T = 1/60$ second), appear to have substantially the same values of B_c and C.F.F.‡ In a sequential color transmission system using three primary colors, one bright field is scanned in $T_v = T/3$. The critical color field brightness of the primary colors (red, blue, green) generated with composite sulfide screen materials has been checked on television rasters by viewing and measuring the luminosity of the kinescope light (white) through Wratten color filters.** (Figure 40). It should be emphasized that the luminosity differences in Figure 40 apply to the particular screen material and may be caused by differences in decay time of the components. Relative energy and luminosity (standard eye response) of the components for white light from fluorescent "daylite" lamps and kinescopes are given in Table II in round figures as obtained with a monochrometer and an eye-corrected cell, respectively.

The color filters reduce the energy from the kinescope to 12 per cent, i.e., their effective equalized filter factor is 8.3 (approximately). The energy passed by any one single color (say green) is thus 4 per cent of the kinescope output because transmission occurs only every third field in one color cycle.

The critical brightness for unmodulated light in a sequential color

‡ Observations were made with $T = 1/60$ second, $T_v = 1/60$ second and 1/180 second for white and green light by four observers. One required a 25 per cent reduction of B_c at $T_v = 1/180$ second, but all reported no change in the white to green ratio, which was found to be unity (See W/G in Figure 40).

** Measurements of B_c were made with the Weston eye-corrected cell because color-comparison readings by illuminometer vary widely with different observers.

Table II—Relative Energy and Luminosity of Color Primaries for Two Light Sources.

	Type of light	Transmission through Wratten Filters			
Wratten Filter		#47(B)	#58(G)	#25(R)	#26(R)
Relative Energy	Fluorescent "daylite"	11%	11%	22%	20%
Relative Luminosity	Fluorescent "daylite"	3.8	26	14.8	13

		Approximate values for obtaining white light from kinescope through rotating filters.		
Wratten Filter		#47(B)	#58(G)	#26(R)
Relative Energy	Kinescope light	12%	12%	12%
Relative Luminosity	Kinescope light	3.5	28	7

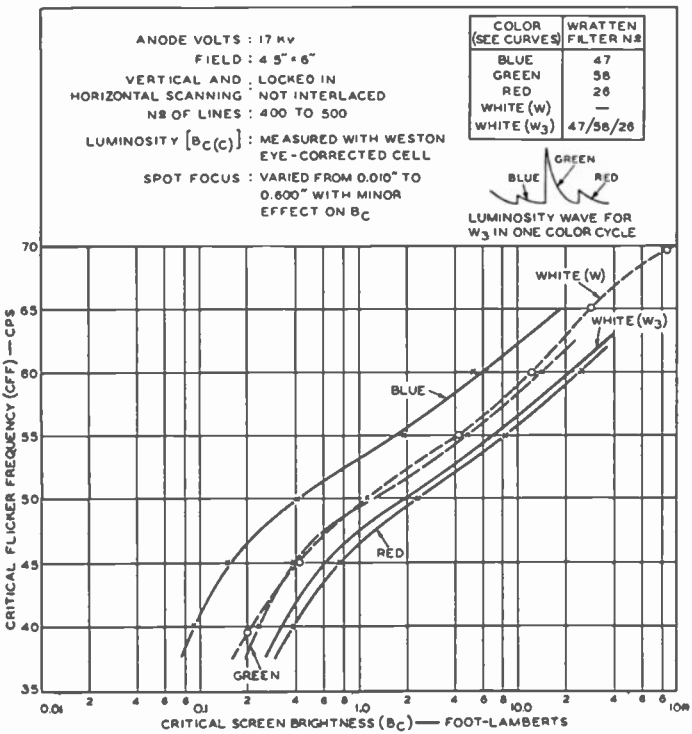

Fig. 40—Critical screen brightness of kinescope fields (colored and white light) as a function of field frequency.

transmission with a C.F.F. of 40 color cycles is restricted for a viewing ratio of 4 to the values $B_{c(G)}$ of 0.2 foot-lamberts and a synthetic white $B_{c(W3)}$ of 0.32 foot-lamberts which must be considered inadequate for easy vision. Normal values, $B_{c(G)} \geqq 6$ foot-lamberts and $B_{c(W3)} \geqq 9.6$ foot-lamberts, require a C.F.F. $\geqq 56$ color cycles (168 fields per second).

c. Interline Flicker

Interline flicker may occur due to sequential displacement of part rasters by one or several lines. In a raster interlaced 2 to 1, black-and-white lines interchange position in alternate fields at a frequency equal to one half the field repetition frequency. The critical brightness $B_{c(N)}$ per half raster is one half of the average screen brightness $B_{c(frame)}$ for unmodulated white light and is obtained by dividing the screen brightness (B_c) from Figure 39 or 40 by the resolution factors of eye and kinescope. The kinescope response factor is to be multiplied by $\sqrt{2}$ as it is effective only in one dimension.* The critical frame brightness is then given by

$$B_{c(frame)} = 2B_{c(N)}/\sqrt{2}\, r_e r_k \qquad (36)$$

For a black-and-white transmission with $1/T_f = 30$ cycles per second, $N = 500$ per half raster and Figure 39 and Equation 36 furnish B_c $(500) = 2 \times 0.1/0.04 = 5$ foot-lamberts for the kinescope resolution shown in Figure 13‡. This value increases with increases of viewing ratio when the kinescope light is modulated.

d. Detail Flicker

A detail flicker effect caused by the interlacing process occurs upon reproduction of high-contrast detail having a vertical dimension in the order of one scanning line or less. A narrow dark line in a white background, for example, located substantially parallel to a scanning line will be reproduced only in one interline field and, therefore, the white lines adjacent to the dark line appear with a flicker frequency equal to the frame frequency because the interline remains dark. A relatively short line is reproduced with full visibility, as $N = 75$ for 1/100 of the horizontal line length. Near the short line, therefore, the critical brightness is reduced to less than 1 foot-lambert without benefit of filter factors ($r_e = 1$ and $r_k = 1$).

For an interlace ratio of 2:1, the flicker will disappear when the line object is scanned in both interlaced fields: i.e., when the vertical resolution is decreased to one-half by defocussing the camera lens or the scanning beam of the pickup tube. It is not eliminated but actually

* The kinescope is here treated as an object.

‡ Part I—page 35.

increased in intensity by defocussing the kinescope scanning beam as the flickering detail area is enlarged. This type of flicker is often confused with inaccurate or unstable interlacing because it causes the effect of a vibrating contour or line structure. (observable in the horizontal line wedge of a test pattern.)

Elimination of the effect without loss of resolution requires reduction of B, a kinescope phosphor with longer persistence, or an increase in frame frequency.

4. Kinescope Characteristics

a. Kinescope Transfer Characteristics

The transfer characteristic ($B = f(E)$) of normal kinescopes follows approximately a 3rd-power law in its central section. Current distribution (masking) and/or saturation effects of screen materials may cause a decrease at higher brightness values as exemplified by Figure 41. In the low brightness range, the characteristic is normally exponential unless modified by "variable-μ" effects of the control element.

It is desirable to standardize a "normal" characteristic for the kinescope because its inverse determines the signal compression required at the transmitter for maintaining a specified over-all transfer characteristic for the system.

The brightness range in directly viewed or projected television images is greatly reduced by illumination of the screen by ambient front or rear light. The amount of such contrast losses depends on the reflection factor of the screen.[23,24] The ranges indicated in Figure 41 have been measured in a dark room on a kinescope with settled screen and a test pattern image containing roughly 60 per cent black areas. The larger range 70:1 is the contrast measured between the white background and a point ¼ inch inside a black rectangle (1 × 2 inches) in an 8 × 10 inch image. The smaller range 50:1 was obtained close to the edge of the rectangle.

This relatively good contrast range decreased to 13:1 when the image contained only 10 per cent black in a white background because of increased rear illumination by light reflected from the bulb walls.

Recently developed kinescopes with aluminum backing[25] eliminate the rear illumination completely and in a dark room maintain a constant

[23] R. R. Law, "Contrast in Kinescopes", *Proc. I.R.E.*, Vol. 27, pp. 511-524, August, 1939.

[24] V. K. Zworykin and G. A. Morton, TELEVISION, John Wiley and Sons, New York, N. Y., 1940.

[25] D. W. Epstein and L. Pensak, "Improved Cathode-Ray Tubes with Metal-Backed Luminescent Screens", *RCA REVIEW*, Vol. VII, No. 1, pp. 5-10, March, 1946.

large-area contrast range of over 100 to 1 which is independent of the ratio $B/\overline{B}$. For normal peak-to-average ratios $\hat{B}/\overline{B} = 4$ to 6, the ambient rear illumination is quite small in correctly designed kinescopes and aluminum-backed screens show, therefore, little, if any increase in general contrast for a given screen material.

Aluminizing of the screen rear surface has no effect on the contrast reduction caused by external "front" illumination of the viewing screen. The contrast loss due to front illumination (E_o) is controlled by the reflection factor (K) of the screen material and the optical transmission (τ) of materials (glass, filters) interposed between the screen and the source of ambient light. The effect of ambient room illumination (E_o)

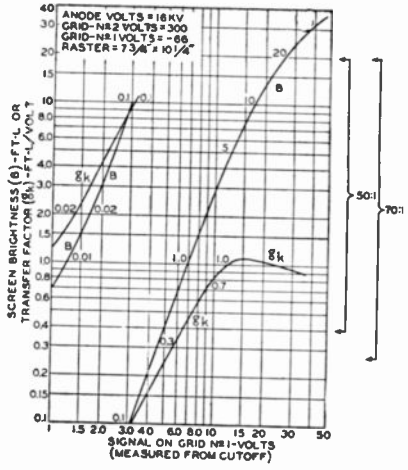

Fig. 41—Kinescope transfer characteristics.

on the contrast C obtained for $E_o = 0$ is given by

$$C' \simeq (\hat{B} + K\tau E_o)/(B_{\min} + K\tau E_o + 0.05E_o) \qquad (37)$$

with $\hat{B}/\overline{B}$ min = Contrast in dark room with $E_o = 0$

$\hat{B}$ = Peak brightness K = Reflection factor of screen material

τ = Transmission factor of filters placed over screen (neutral or color)

$0.05\,E_o$ = Reflection from filter or glass surfaces.

The factor K varies from $K = 0.6$ to 0.8 for present kinescope screens. A neutral filter or coating on the tube surface attenuates the ambient light by its transmission factor τ, but it also attenuates the kinescope light. Table III shows the effect of room illumination ($E_o = 1$ and 3 foot-candles) for a tube with a contrast C_o of 100 to 1, K of 0.7, and for various values of τ. The spectral qualities of kinescope

Table III—Effect of Ambient Room Illumination (E_a) and Filter Transmission (τ) on Brightness ($\hat{B}'$) and Image Contrast (C').

	$E_a = 1$		$E_a = 3$		$E_a = 1$		$E_a = 3$		$E_a = 1$		$E_a = 3$		$E_a = 1$		$E_a = 3$	
$\hat{B}$	C'	$\hat{B}'$	C'	$\hat{B}'$	C'	$\hat{B}'$	C'	$\hat{B}'$	C'	$\hat{B}'$	C'	$\hat{B}'$	C'	$\hat{B}'$	C'	$\hat{B}'$
20	22	21	10	22	34	10			47	5			60	2.5		
40	35	41	17	42	50	20	26	20	64	10	38	10	75	5		
80	52	81	28	82	67	40	40	40	78	20	54	20	86	10	67	10
120											64	30	90	15	75	15
	$\tau = 1$				$\tau = 0.5$				$\tau = 0.25$				$\tau = 0.125$			

and room light are assumed to be identical. The kinescope brightness is then reduced by the same factor τ to $\hat{B}' = \tau\hat{B}$.

The underlined values show the gain in contrast range (C') for a normal transmitted peak brightness ($\hat{B}'$) of 20 foot-lamberts when the (filter) transmission (τ) is decreased at the expense of kinescope power.

It is seen, however, that the image contrast, when $\hat{B}'$ is 20 foot-lamberts and τ is 0.25, differs little from that when $\hat{B}'$ is 40 foot-lamberts and τ is 0.5. The same kinescope power is required for both values ($\hat{B} = 80$ foot-lamberts), but the brightness is twice as great for $\tau = 0.5$ and the image contrast, therefore, will appear just as good or even better to the eye because of the higher transfer factor of the eye characteristic (Figure 3(a)*).

The last column in which τ is equal to 0.125, is representative of the conditions for sequential color transmission and indicates that the kinescope brightness $\hat{B}$ must be in the order of 100 foot-lamberts for a normal image brightness.

b. The Aperture Flux Response of Kinescopes

Detail contrast and aperture-response characteristic of the kinescope are a function of the electron-beam diameter, electron- and light-scattering effects in the screen material, and reflections on glass surfaces (halation). The aperture response factor r_k ($r\Delta\bar{\psi}$) can be measured by the threshold visibility method (See Part I for discussion of response characteristic of eye) by fading-in a test pattern or sine-wave signal. The eye is used as an indicator to detect a fixed value of thresh-

* Part I—page 16.

old contrast. The screen is, therefore, viewed at a close range and the viewing angle, including the signal lines or bars, is maintained substantially constant. A magnifying glass is used for higher line numbers to insure a fixed threshold-contrast value for the eye. The response characteristic of a kinescope measured by this method is shown in Figure 13.*

The curve shape can be analyzed as the sum of two cosine-square aperture characteristics (See Figure 19) from which the corresponding beam-current distribution, line cross section, and transition curves are easily computed. (See Section on Complex Apertures).

A second and more reliable method to measure kinescope aperture characteristics is by signal generation in a light spot scanning system. The general principle has been outlined in the section on aperture processes. Because normal kinescope screen materials have a relatively long decay, measurements are made at low frequencies by observing the vertical aperture response. (See Figures 29 to 31). The signal amplifier must be corrected for effects of the phosphor decay which is compensated to allow decay of the light output within one line length. Trailing should, in general, not exceed ½ scanning line length and the scanned bar length (slit width) should be constant for all values N. A vertical slit mask is placed over the kinescope or the test pattern bars for observation of their cross section (See Figure 29). The slit has a constant width of 1/10 to 1/30 line length. The optical magnification ratio between kinescope "spot" diameter and test bar width determines the line number calibration. If, for example, the slide has a bar pattern containing 10 lines per millimeter and the kinescope screen has a vertical size $V = 180$ millimeters, an aperture response test at $N = 500$ requires the optical reduction $\frac{1}{M} = \frac{180}{500} \times 10 = 3.6$ between kinescope and test pattern. With M properly adjusted, the actual scanning line number N_V and vertical deflection on the kinescope under test are relatively unimportant and the raster can be compressed for obtaining a sufficiently continuous "modulation envelope" on an oscillograph operating with a "vertical" deflection speed. The oscillograph beam is keyed on by a short "horizontal" pulse (double-frequency synchronizing pulse) occurring in the center of scanning lines to eliminate all oscilloscope traces except for a vertical strip through the center of the scanned area. (The combination of vertical slit mask and oscilloscope pulse is a vertical line selector). The signal response from kinescopes used for image reproduction should be confined to visible light. A light filter (Wratten #2A) eliminating ultraviolet

* Part I—page 35.

radiation may be required because the ultraviolet tends to give increased resolution from certain phosphors (not the case for standard sulfide screens).

Several high-voltage kinescope characteristics measured by this method are shown in Figure 42. Curve 1 shows the beneficial effect of high cathode "loading" (high E_{c_2} voltage) which causes a considerable increase of $r\Delta\bar{\psi}$ in this tube. This experimental tube operated at 17 kilovolts represents a close approach to the ideal kinescope for a 500-line picture although an increase in response can still be obtained if aberrations can be eliminated. Curves 2a, b, c, illustrate that the aperture size may increase as a function of beam current, a well-known fact which may cause "blooming" (overlapping of traces) at high intensities.

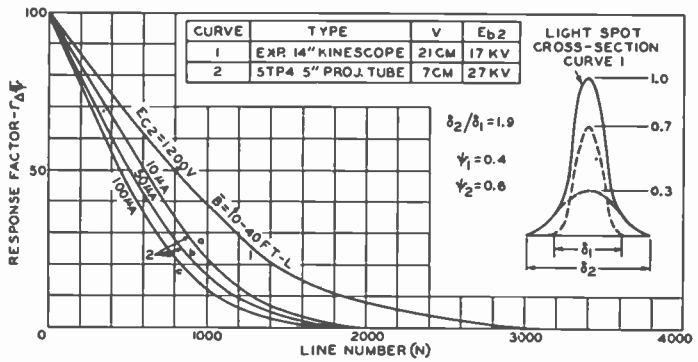

Fig. 42—Aperture flux response of two kinescopes.

5. Threshold Signal-to-Noise Ratios Required for High Quality

Threshold signal-to-noise ratios (R) at the control grid of the kinescope or at the transmitter (for a constant transfer factor to the kinescope grid) can be specified on the basis of a standard kinescope transfer characteristic. It is obvious from Equation (22)‡ that R maximum increases with kinescope brightness ($B = f(E)$) and also with kinescope resolution* because the noise filter factor m (See Part I) changes from m_{ek} to m_e for an ideally sharp kinescope which may be approached by pre-emphasis of high frequencies in the video channel. (In the horizontal direction).

Signal-to-noise ratios R_{max} for threshold visibility as a function of average field brightness level B_o (foot-lamberts) have been computed

‡ Part I—page 37.

* This relationship applies also to increases of motion picture brightness and resolution.

Table IV—Threshold Signal-to-Noise Ratio $\hat{R}_{max}$ at the Kinescope Grid (Fig. 41) for a Channel Resolution ($\bar{N}_{e_e}$) of 400 Lines, a Peak Brightness ($\hat{B}$) of 32 Foot-Lamberts, and Constant Noise

Average brightness level B foot-lamberts	g_k	m_e 0.22	m_{ek} 0.1	m_e 0.45	m_{ek} 0.3	computed $m_{ek} = 0.41$	observed with m_{ek} threshold	good
0.2*	0.15	60	27	121	81	111	100	67
3.	0.85	62	28	126	84	115	115	67
5.	1.0	44	20	90	60	82	80	57
10.	1.1	24	11	50	33	45	63	40
		peaked channel		flat channel			flat channel	
		$\rho = 4$				$\rho = 2$		

* The factor *25* in Equation (22) (Part I—page 37) is reduced at $B_e = 0.2$ by the reduced transfer factor (g_e) to $25 \times 1.8/3.2 = 19.5$ (See Figure 3a) (Part I—page 16).

from Equation (22*) on the basis of the kinescope transfer characteristics given in Figure 41 for a peak brightness ($\hat{B}$) of 32 foot-lamberts ($\hat{E} = 40v$) and a 400-line channel (See Figure 11‡) and are given in Table IV. The values for the eye and an ideal kinescope response are listed in the columns m_e. The columns m_{ek} are computed for the eye and kinescope response given in Figure 13.**

Signal-to-noise ratios observed for $\rho = 2$ are in excellent agreement with computed values. If 5 foot-lamperts is selected as a representative average value for B_o (for $\hat{B} = 32\ Ft\text{-}L$) it may be stated that good quality at $\rho = 4$ in a 400-line channel *with constant noise level* requires the following values:

Signal-to-noise ratio in:	$\hat{R}_{max}$	$\lvert R\rvert_{max}$
flat channels	50-90	300-500
peaked channels	17-40	100-250

These values are to be measured at a point in the system where the video signal is related to the kinescope grid voltage by a constant factor.

Signal-to-noise ratios at the television camera differ from the above

* Part I—page 37. ‡ Part I—pages 32-33. ** Part I—page 35.

values when the gradation scale of the system is changed in the electrical channel. The camera signal-to-noise ratio will be discussed in Part III of this paper. It is also pointed out that a kinescope screen material of much longer persistence or a storage-type reproducer will reduce the above values by increasing the number of simultaneously visible fluctuations or "flux samples". A reduction in the threshold signal-to-noise ratio would be indicated by a characteristic causing no flicker at frame repetition rate (30 cycles per second).

APPENDIX

Table I—Area and Volume of Aperture Sections

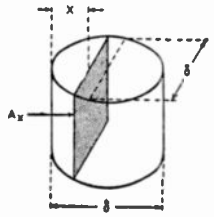

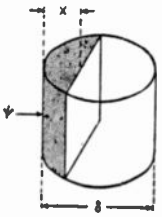

X/δ	Area Ax/A_{max} Cos²	Uniform	Transition curve (one half) Cos²	$\int_{x=o}^{x} \psi dx$ Uniform
0.	0.	0.	0.	0.
0.05	0.011	0.438	0.00054	0.019
0.1	0.0575	0.6	0.0043	0.0525
0.15	0.147	0.714	0.015	0.097
0.2	0.277	0.8	0.038	0.142
0.25	0.433	0.866	0.0775	0.195
0.3	0.60	0.915	0.132	0.252
0.35	0.756	0.954	0.205	0.312
0.4	0.885	0.98	0.294	0.375
0.45	0.97	0.995	0.393	0.405
0.5	1.0	1.0	0.50	0.50

(See page 285 for Table II)

Table III—Useful Aperture Flux Response Factors

Aperture	Density	$N_e/N\delta$	N_e/N for a response $r\Delta\overline{\psi} = 0.3$	0.5	0.7
Square	Uniform	2.	1.43	2.	3.34
Round	Uniform	2.47	1.48	2.08	3.5
Round	Cos²	4.35	1.74	2.46	4.15

Table II—Aperture Response Factors (Figures 15 and 16)

Aperture type	Square		Round			Round			Round		
Flux	Uniform		Uniform			Cos²			e^{-x^2}		
$N/N\delta$	$r\Delta\hat{\psi}$	$r\Delta\bar{\psi}$	$N/N\delta$	$r\Delta\hat{\psi}$	$r\Delta\bar{\psi}$	$N/N\delta$	$r\Delta\hat{\psi}$	$r\Delta\bar{\psi}$	$N/N\delta$	$r\Delta\hat{\psi}$	$r\Delta\bar{\psi}$
0	1.	1.0	0	1.	1.0	0	1.	1.0	0	1.	1.0
0.5	1.	0.75	0.5	1.	0.785	0.5	1.	0.855	0.5	1.	0.86
0.75	1.	0.625	0.75	1.	0.68	0.75	1.	0.78	0.75	1.	0.78
1.0	1.	0.50	1.0	1.	0.57	1.	1.	0.715	1.	1.	0.72
1.25	0.6	0.375	1.25	0.80	0.47	1.25	0.98	0.65	1.25	0.98	0.655
1.5	0.34	0.25	1.5	0.56	0.36	1.5	0.91	0.58	1.5	0.92	0.59
1.75	0.14	0.125	1.75	0.37	0.255	1.75	0.81	0.51	2.	0.72	0.46
2.	0.	0.	2.	0.215	0.155	2.	0.70	0.44	2.5	0.52	0.33
2.5	—0.2	—0.135	2.25	0.09	0.065	2.5	0.48	0.31	3.	0.31	0.20
3.	—0.33*	—0.165	2.47	0.	0.	3.	0.28	0.18	3.5	0.18	0.115
3.5	—0.14	—0.105	2.75	—0.095	—0.006	3.5	0.13	0.09	4.	0.09	0.057
4.	0.	0.	3.	—0.16	—0.09	4.	0.04	0.025	4.5	0.05	0.032
4.5	+0.11		3.25	—0.18	—0.10	4.35	0.	0.	5.	0.03	0.019
5.	+0.2*		3.5	—0.16	—0.09	5.	—0.28		6.	0.01	0.0064
5.5	+0.09		4.	—0.08	—0.05	5.5	—0.25				
6.	0		4.47	0.	0.	6.3	0.				
			5.	+0.07							
			5.5	+0.07							
* Sharp maxima			6.5	0.							

Table IV—Aperture Response Factors of Identical Apertures in Cascade (1 to 4)

a) Square apertures with uniform density (Fig. 26)

$r\Delta\overline{\psi}$	$N/N\delta_1$ for Aperture Number Indicated				$r\Delta\hat{\psi}$	$N/N\delta_1$ for Aperture Number Indicated			
	1	2	3	4		1	2	3	4
1.0	1.	1.	1.	1.	1.0	1.	0.5	0.36	0.3
0.8	0.4	0.28	0.23	0.2	0.9	1.05	0.64	0.51	0.42
0.7	0.6	0.42	0.35	0.3	0.8	1.11	0.72	0.59	0.5
0.6	0.8	0.56	0.47	0.41	0.7	1.18	0.80	0.67	0.575
0.5	1.0	0.71	0.59	0.515	0.6	1.26	0.90	0.74	0.65
0.4	1.2	0.87	0.72	0.63	0.5	1.34	1.0	0.83	0.72
0.3	1.4	1.03	0.86	0.76	0.4	1.43	1.1	0.92	0.80
0.2	1.6	1.21	1.02	0.89	0.3	1.54	1.22	1.025	0.90
0.1	1.8	1.42	1.22	1.08	0.2	1.67	1.36	1.15	1.02
0.05	1.9	1.56	1.36	1.23	0.1	1.82	1.53	1.32	1.18
					0.05	1.91	1.66	1.44	1.30

b) Round apertures with $\cos^2$ density (Fig. 27)

$r\Delta\overline{\psi}$	$N/N\delta_1$ for Aperture Number Indicated				$r\Delta\hat{\psi}$	$N/N\delta_1$ for Aperture Number Indicated			
	1	2	3	4		1	2	3	4
1.	1	1	1	1	1.0	1	0.6	0.45	0.35
0.8	0.70	0.50	0.41	0.35	0.9	1.52	1.0	0.77	0.66
0.7	1.07	0.75	0.62	0.52	0.8	1.77	1.25	0.97	0.83
0.6	1.42	1.0	0.80	0.70	0.7	2.0	1.42	1.15	0.96
0.5	1.78	1.25	1.03	0.85	0.6	2.2	1.6	1.3	1.12
0.4	2.14	2.52	1.25	1.06	0.5	2.45	1.76	1.45	1.25
0.3	2.52	1.8	1.5	1.27	0.4	2.67	1.94	1.6	1.4
0.2	2.82	2.12	1.76	1.53	0.3	2.93	2.15	1.75	1.55
0.1	3.42	2.60	2.15	1.88	0.2	3.25	2.4	2.0	1.75
0.05	3.8	2.9	2.4	2.1	0.1	3.7	2.77	2.3	2.02
					0.05	3.96	3.1	2.6	2.25

ELECTRO-OPTICAL CHARACTERISTICS OF TELEVISION SYSTEMS*†

BY

OTTO H. SCHADE

Tube Department, RCA Victor Division,
Harrison, N. J.

NOTE: This paper consists of an Introduction and four parts: Part I—Characteristics of Vision and Visual Systems; Part II—Electro-Optical Specifications for Television Systems; Part III—Electro-Optical Characteristics of Camera Systems; Part IV—Correlation and Evaluation of Electro-Optical Characteristics of Imaging Systems. The Introduction and Part I appeared in the March 1948 issue of *RCA Review* and Part II in the June 1948 issue; summaries of these parts are reprinted herewith for reference purposes. Part III is included in this issue. Part IV is scheduled for publication in the December issue.

INTRODUCTION; PART I—CHARACTERISTICS OF VISION AND VISUAL SYSTEMS

(Reprinted from RCA REVIEW, March, 1948)

Summary—The optical and electro-optical conversion processes in television systems are examined as intermediate stages of a multi-stage process by which optical information at the real object is "transduced" into sensory "response" at the brain. The characteristics of the human eye and vision in the final stage of the process determine the requirements and standards for preceding stages. When expressed on a unified basis by "transfer" and "aperture response" characteristics, the properties of the process of vision can be correlated with those of external imaging and transducing processes. It is shown that image definition, or the corresponding information from optical or electrical image-transducing stages, can be specified by the characteristics of an equivalent "resolving aperture". These characteristics may be computed and measured for all components of the system.

Quantitative data from measurements permit definite quality ratings of optical and electrical components with respect to theoretical values. A subjective rating of the resolution in an imaging process external to the eye such as a television system is derived by establishing a characteristic curve for the relative "sharpness" of vision as affected by the "aperture response" of the external imaging process.

A general review of the material and the broad methods of analysis employed are given in the Introduction. Following this, Part I treats characteristics of vision and visual systems. In this part, viewing angle, sensation characteristics, color response, persistence of vision, flicker, re-

---

* Decimal Classification: R138.3 × R583.12.
† Reprinted from *RCA Review*, September, 1948.

solving power, response characteristics, and steady and fluctuating brightness distortions are discussed and related to the characteristics of external imaging systems and the television process.

PART II—ELECTRO-OPTICAL SPECIFICATIONS FOR TELEVISION SYSTEMS

(Reprinted from RCA REVIEW, June, 1948)

Summary—The ability of an image-forming device to reproduce fine detail can be specified basically by the size and flux distribution of the small light spot formed as the image of a point source of light. It is shown that the defining ability of practical image transducers is specified more accurately by response characteristics obtained by scanning a test object with the elemental point image which represents the "resolving aperture" of the imaging device. Methods of computing and measuring the "aperture flux response" of practical image transducers are developed for correlation of optical and electrical system components.

The television raster is treated as a sampling process and its effect on the system resolution is evaluated as an aperture process. Brightness, repetition rate, and flicker in television images are treated in relation to the screen materials and performance of practical kinescopes.

* * *

There follows the third paper in the series: Part III—Electro-Optical Characteristics of Camera Systems.

The Manager, RCA Review

PART III—ELECTRO-OPTICAL CHARACTERISTICS OF CAMERA SYSTEMS

Summary—Fundamental relations between energy and signal quality are derived by the concepts of discrete energy "samples" to establish the principal parameters controlling the energy transfer in television camera systems. Signal-to-fluctuation ratios and the transfer and aperture-response characteristics of practical camera components are evaluated subsequently. The optical characteristics of camera elements are discussed with particular emphasis on the aperture response of lenses as measured by a television microphotometer.

A. Fundamental Relations Between Energy and Quality in Image Signals

The quality of an imaging process may be judged by three properties of the final image: graininess, sharpness, and tone scale. These

properties are measured and specified by the signal-to-"noise" ratio $|R|$, the aperture response $r\Delta\overline{\psi} = f(N)$, and the light-transfer characteristic (ψ image $= g\psi$ object) of the system, and are controlled, to a large extent if not entirely, by the characteristics of the transducing processes in the camera. The three characteristics are not independent of each other because the energy required by each one increases with the respective figure of merit.

An imaging process may be regarded fundamentally as a sampling process. (See Part II, A.5 (page 257 et seq.)) With a given number of energy "samples", such as a certain number of silver grains in photographic film, graininess can be decreased in exchange for resolution by integration of samples (defocusing) without effect on the tone scale in large areas. The transfer characteristic may be altered by contracting samples into one level by eliminating half tones to increase sharpness (as in line copying). The resolution may be increased in exchange for graininess by increasing the relative energy in small areas by an "aperture correction" process (masking).

The fundamental relations of signal properties can be readily established by the concepts of discrete energy samples which can be applied to all forms of energy or energy flux used in television and photographic processes.

1. Picture Element Number, Resolution, and Frequency Channel

The smallest detail area a which can be resolved by an imaging process is a small equivalent square the linear dimension of which is specified by the limiting resolution line number N_c or the balanced cutoff line number $\overline{N}_{co}$ in the image. This area will be defined as a "picture element". The number of picture elements is, therefore, given

by $$n = \overline{N}_{co}^2 \times (H/V) \tag{38}$$

where H/V is the aspect ratio of the image.

In a television channel, the total number of picture elements is the number of half-cycles at cutoff frequency Δf in the active scanning time for one frame. Because of "blanking" periods, the number of active picture elements, n_c, for the camera image or n_k for the kinescope image, are

$$n_c = 1.7\, T_f\, \Delta f \qquad \text{and} \qquad n_k = 1.58\, T_f\, \Delta f \tag{39}$$

where T_f = frame repetition time.

The relation between line number $\overline{N}_{co}$ and frequency channel Δf

given by Equation (1), (Part I, page 9) is obtained by combining Equation (38) and n_k from Equation (39). These equations furnish $\overline{N}_{co} = 410$ and $n_k = 224{,}000$ for a standard kinescope image ($\Delta f = 4.25$ megacycles, $T_f = 30$ cycles) and $n_c = 240{,}000$ for the camera image.

2. Sample Number and Signal-to-Fluctuation Ratio

A critical comparison of picture elements representing a constant level discloses deviations of intensity from a mean value. To find the cause of these deviations, the element is inspected with high magnification by removing electrical or optical channel limitations (at least theoretically). Each element is found to have a structure consisting of a certain number of "sub-elements" which are groups or aggregates of still smaller "quanta": atom groups forming the silver grains in photographic film, quanta of light in optical images, electron groups in television images. The size or density of the sub-element can be grown from extremely small aggregates or even single quantum units by multiplication or "development" processes, but the number of sub-elements or "samples" remains substantially constant. By counting the number of samples, the cause for the observed deviations from an average intensity value is found to be a variation in the number of energy samples within the picture-element dimension. When the distribution of samples is random (following the Gaussian error function), the average number of samples n' in the selected area (N_c) multiplied by the sample energy q is the signal energy $n'q$; the root-mean-square value $q\sqrt{n'}$ is the root-mean-square fluctuation or "noise" energy. The signal-to-"noise" ratio, or using the more adequate term the "*signal-to-fluctuation*" ratio $|R|$ is, therefore,

$$|R| = n'q/q\sqrt{n'} = \sqrt{n'}. \quad (40)$$

The total energy Q in an image representing a constant level is obviously the number of samples per element multiplied by the element number (n) of the image

$$Q = nn'q. \quad (41)$$

Combining Equation (41), (40), and (38) yields the relations

$$Q = |R|^2 nq \quad (42a) \qquad Q = |R|^2 \overline{N}_{co}^2 (H/V) q. \quad (42b)$$

The image or signal energy increases as the square of both signal-to-fluctuation ratio and resolution, and in proportion to the sample energy (q).

The physical size, i.e., the effective diameter δ_q of the sample, imposes a restriction on the maximum obtainable value of the balanced line number $\overline{N}_{co}$ because of the aperture effect of the sample (compare Part II, A.6). A picture element is not resolved by *random* samples

unless the spatial or time dimension of the sample is smaller than the picture element. The aperture effect of the samples in grain structures can be measured by the same methods used for normal defining apertures and will be discussed in Part IV.

The reader is cautioned that the picture element area, in which a subelement count is made without channel restrictions, *does not* represent a scanning or resolving aperture with uniform transmission; such apertures resolve elements (N_c) smaller than their diameter. Equation (42b) is valid only for the particular "aperture" represented by an electrical frequency channel of constant sine-wave-amplitude response and sharp cutoff, as specified by the symbol $\overline{N}_{co}$. Determination of the size of physical or optical "apertures" and response characteristics yielding the same root-mean-square (r-m-s) fluctuation value as a specified electrical channel ($\overline{N}_{co}$), requires evaluation of the "filter factor" m (see Part I, page 32) of the aperture. The equivalent scanning aperture size will be evaluated in Part IV in the discussion of motion picture film characteristics.

8. Frame Number, Storage Factor, and Energy Flux

The number of images which must be generated per unit time by a television or motion picture camera is determined by the property of the visual process to store impressions for a certain length of time. Incomplete storage causes flicker which has, therefore, determined the number of image fields per second in television and motion picture systems. An estimate of the storage time in the visual process may be obtained from the following observations.

A square-wave brightness change with 100 per cent amplitude (black-to-white) occurring at a rate of 24 cycles per second causes a just perceptible flicker (good storage) at a critical brightness $B_c = 0.1$ foot-lambert (Part I, Figure 6, page 22). The flicker amplitude, however, increases rapidly when the brightness is increased, indicating a likely decrease of storage.

At an average field brightness $\overline{B} = 1$ foot-lambert, the amplitude of the 24-cycle fluctuation must be decreased by a factor of 16 to reduce flicker again to a just perceptible value. The effective storage time, hence, has decreased to less than 1/24 second assuming 2 per cent as the minimum perceptible brightness difference. Observations made by the author on interlaced television fields repeating at 60 cycles per second have shown,* similarly, that flicker becomes noticeable at $\overline{B} = 10$ foot-lamberts when consecutive fields are made to differ only 8 per cent in intensity when a 30-cycle fluctuation of this small amplitude

* The measurements were made on (standard) sulfide screen materials.

is introduced. It may be concluded that motion picture or television images shown at a rate of 48 and 60 fields per second, respectively, are stored and blended by the eye at "normal" brightness levels of 1 and 10 foot-lamberts, respectively, over a period hardly exceeding two fields. The motion picture shows a complete image in every field, the image content, i.e., the sample distribution, being changed every two fields. The number of simultaneous sample impressions alternates, therefore, from Q when the same frame repeats to not more than $2\,Q$ when successive fields are different frames. The average number of sample impressions is, therefore, increased by a storage factor $s' \simeq 1.5$ at $\overline{B} = 1$ foot-lambert.

The situation is different in television. Because of the interlacing process, new samples are shown in the same image area only at a constant 30-cycle rate. The number of simultaneous impressions is not increased by storage beyond that of a single frame and the storage factor is unity ($s' = 1$ at $\overline{B} = 10$ foot-lamberts). Changes in the decay characteristics of kinescope screen materials or of the interruption periods in motion picture shutters may increase these storage factors somewhat. Increases in brightness levels above these (normal) values decreases s', while reductions of $\overline{B}$ can effect considerable increases of the effective storage factor of the visual process.

The energy flux ($\mathcal{F}$) which must be generated by a television or motion picture camera system is, therefore, $\mathcal{F} = Q/(T_f \times s')$ (43)

when $1/T_f =$ number of complete images or frames in one second and $s' =$ storage factor of the eye with the tentative values $s' = 1$ at $\overline{B} = 10$ foot-lamberts for 30-frame television and $s' = 1.5$ at $\overline{B} = 1$ foot-lambert for 24-frame motion pictures shown with twice the field number. Combining Equations (43) and (42a) expresses the signal flux in terms of the average number of samples per unit time

$$\mathcal{F} = |R|^2 nq/(s'T_f) \tag{44a}$$

or with Equation (42b) $$\mathcal{F} = |R|^2 \overline{N}_{co}{}^2 (H/V)\, q/(s'T_f). \tag{44b}$$

In optical units, the energy flux is the light flux $\mathcal{F} = \psi$ lumen; the smallest sample energy being one quantum of light. For white light, $q_o = 7.7 \times 10^{-17}$ lumen.

In electrical units, the energy flux is the current $\mathcal{F} = \mathrm{I}$ ampere; the smallest sample being the energy of one electron $q_e = 1.6 \times 10^{-19}$ ampere.

In motion picture film, the sample q represents one average or equivalent grain.

The signal current in a television channel is expressed by combining Equations (44a) and (39) $\mathcal{F} = |R|^2 1.7\Delta f q_e$;

$$I = 2.72\,|R|^2\Delta f \times 10^{-19} \text{ ampere} \qquad (45)$$

This current is, for example, the photocathode current in a light-spot scanner using a kinescope phosphor with negligible time delay. It is also the signal current of an image dissector tube divided by the gain of its electron multiplier. For a frequency channel $\Delta f = 4.25$ megacycles and $|R| = 100$, $I = 0.0116$ microamps.

It is apparent that the signal flux (or current) which is required for a given signal quality should be determined at a point where succeeding processes do not decrease the sample number. Processes which increase the sample energy (q) by (electron) multiplication or amplification do not affect the value $\mathcal{F}$ (or I) although they may change the balance between $|R|$ and N_c by an aperture effect which can be evaluated separately.

4. Additive Fluctuation Energies (Q_f)

Many conversion or amplifying processes introduce additional fluctuation energy which contributes nothing to the desired signal but increases the fluctuation level. The resulting change of the ratio $|R|$ can be determined as follows.

The normal signal-to-fluctuation ratio in a process is given by Equation (40).

Additional random samples representing the fluctuation energy $n_f q$ per element do not increase the desired signal n', but by being added to the total number increase the fluctuation value to $q(n' + n_f)^{1/2}$, with the result:

$$|R'| = n'/(n' + n_f)^{1/2} \quad (46) \qquad \text{or} \qquad |R'|^2 = |R|^2/(1 + n_f/n'). \quad (47)$$

By substituting this expression into Equation (42) or (44), it is readily seen that the flux $\mathcal{F}$ or the signal input energy Q to a process introducing additional fluctuation energy must be increased (to maintain a given ratio $|R|$) to the values

$$Q' = Q(1 + Q_f/Q) \text{ and } \mathcal{F}' = \mathcal{F}(1 + \mathcal{F}_f/\mathcal{F}) \qquad (48)$$

or the additional fluctuation energy will cause a decrease of $|R|$ to the lower value given by Equation (46).

Addition of a *constant* fluctuation energy alters the manner in which $|R'|$ varies as a function of signal energy.

The effect of inserting various constant amounts of fluctuation

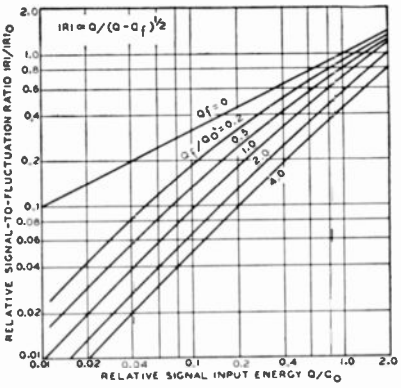

Fig. 43—Effect of introducing constant fluctuation energies on the normal signal-to-fluctuation ratios.

energy into a system is shown in Figure 43 where the ratio $|R|/|R|_o$ is plotted from Equation (46) as a function of the relative signal energy Q/Q_o with Q_f/Q_o as parameter. For $Q_f = 0$, the normal ratio $|R|$ decreases with the ½ power of the signal. The addition of a constant fluctuation energy may occur by introducing the shot "noise" of a beam or amplifier current in a television camera or the "fog" caused by a developing process, or stray illumination (haze, flare) in a photographic process. The addition causes a more rapid decrease of $|R|$ which decreases in proportion to the signal for the signal range where $Q_f \geqq Q$.

5. *Non-Linear Transfer of Signals and Fluctuations*

The relations between the signal-to-fluctuation ratio $|R|$ and the signal forms Q or $\mathcal{F}$ in Figure 43 are not disturbed by amplification in transducers having a linear transfer characteristic, i.e., a constant transfer factor (g) independent of signal amplitude and "operating point". The transfer of energy over a non-linear characteristic, however, alters $|R|$ because large and small signals are no longer affected in proportion.

The effects of signal distortion by non-linear transfer characteristics are well known in electron tube engineering. The transfer factor G for large unidirectional signals $\Delta\mathcal{F}$ measured from a zero point differs from the differential small-signal transfer factor g as illustrated by Figure 44. The large-signal transfer factor is the ratio of the increments $\Delta\mathcal{F}$ measured from the operating point 0,

$$G = \Delta\mathcal{F}_{out}/\Delta\mathcal{F}_{in} \quad (49a)$$

while the differential transfer factor is determined by the slope of the characteristic

$$g = d\mathcal{F}_{out}/d\mathcal{F}_{in}. \quad (49b)$$

It is apparent that G as well as g are functions of $\mathcal{F}$. The choice of the zero-signal point or operating point 0 has a considerable effect on the relative values of signals with superimposed fluctuations.

When the operation point 0 coincides with the value $\mathcal{F} = 0$, the

"transfer ratio" G/g has values smaller than unity when g is increasing steadily (Figure 44(a)) and values larger than unity when g is decreasing (Figure 44(b)). The signal-to-fluctuation ratio $|R|$ is then increased or decreased by the factor

$$|R|_{out} = G/g|R|_{in}. \qquad (50)$$

For power-law characteristics, the transfer ratio has a constant value. A square-law characteristic has the value $G/g = 0.5$, and for a cube-law characteristic (kinescope characteristic, see Figure 41, Part II, page 279), $G/g = \frac{1}{3}$. The relative fluctuation increase in these cases is accompanied by a gradual expansion of signals ($\Delta\mathcal{F}$) and a correspondingly larger expansion of differential signals at all levels. Characteristics with increasing slope (g) increase, therefore, the contrast in the highlights as well as the detail contrast* although they decrease

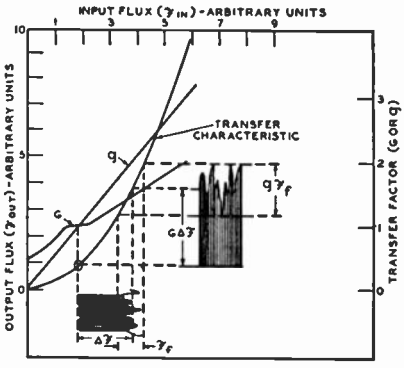

Fig. 44(a)—Decrease in signal-to-fluctuation ratio due to transfer characteristic with increasing slope.

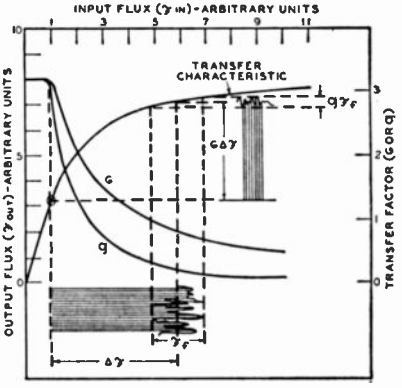

Fig. 44(b)—Increase in signal-to-fluctuation ratio due to transfer characteristic with decreasing slope.

the signal-to-fluctuation ratio $|R|$; an exchange which should be expected from Equation (42b). The opposite effect occurs with transfer characteristics of decreasing slope which cause a compression of signals. A ½-power characteristic, for example, has a constant transfer ratio $G/g = 2$. Fluctuations are reduced, i.e., $|R|$ increases by this factor, but the high-light contrast as well as the detail contrast at all levels is decreased by the same factor.

Practical transfer characteristics depart more or less from a true power law. Many processes also cause a reversal of signal polarity, i.e., "negative" image signals, where "black" represents a high flux value and "white" a low flux value. The reversal of polarity may then cause

* This detail contrast increase is not an "aperture" effect because the aperture response is a ratio measured at one given signal level.

the transfer ratio G/g to become inverted because G is a different function of $\Delta\mathcal{F}$.

When the operating point 0 is placed at a value $\mathcal{F} > 0$, which is the case in most amplifying processes as well as in the use of photographic negative film, the transfer ratio G/g is, in general, a function of the signal flux. Its initial value is always unity. With larger signals G/g increases or decreases depending on the curvature of the non-linear characteristic. Characteristics following a constant power law cause the transfer ratio to change from unity at small signals to the values obtained for $0 = 0$ when the signal amplitude has become sufficiently large. The range of signal amplitudes in which this change occurs is small when the operating "bias" is small, i.e., when 0 is only slightly above zero level. A more gradual change of G/g from unity to its final value is obtained with larger "bias" values. It follows, in general, that the signal-to-fluctuation ratio $|R|$ may vary as a function of signal in many different ways depending on the curvature of the transfer characteristics and the position of the operating point 0 on the characteristics. Expansion of a signal or tone range decreases $|R|$ and increases the detail contrast within the expanded section, and vice versa. Restoration of linearity in the over-all "amplifying" process results again in the original ratio $|R|$.

6. *The Transfer Characteristic, Storage Capacity, and Signal-to-Fluctuation Ratio in Primary Signal-Conversion Processes*

Of particular interest are the effects of a non-linear transfer characteristic on the properties of the primary signal-conversion process in the camera system, i.e., the process which determines the lowest energy level and sample number in the signal generating system. A signal-conversion process may be linear or have a transfer characteristic following a law of diminishing returns. In the latter case, sample number and energy (see Equations (40) to (42)) may increase according to the law $Q = Q_{max}\,(1 - e^{-kQ_{in}})$ which is usually modified by secondary effects: retarding forces which increase with the number of transduced or stored samples as shown by the characteristics in Figure 45. Typical examples of transducers with diminishing returns are the eye, photographic film, and television pickup tubes such as the iconoscope, and the image orthicon. It is evident that characteristics of this type can cover a large range of input energy with a relatively small change in the total number of transduced or stored samples. The small range of Q can be expanded again in later processes by transfer characteristics with increasing slope.

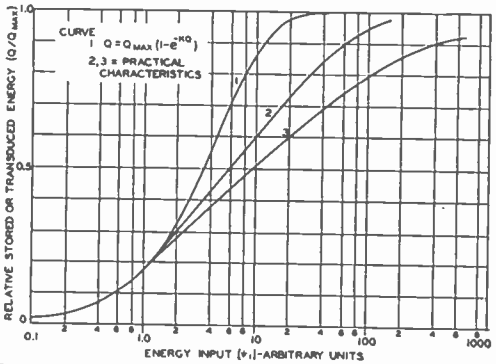

Fig. 45—Transfer characteristics with diminishing returns.

A primary signal-conversion process with a nonlinear transfer characteristic of the above type offers basically no advantage over a linear process with respect to sensitivity or the total input (light) energy. It does require, however, only a fraction of the energy-handling or *storage capacity* of the linear process. To cover an input range of 200 to 1, the "sample" capacity of the linear process (1) in Figure 46 must be 12.5 times larger than that of the "logarithmic" process (2); for a given limited "capacity," therefore, the linear process is restricted in range. The storage capacity of photographic film, for example, is determined by the number of developable grains per unit area. It increases with grain density and area. The energy storage in television transducers (camera tubes) occurs in form of electrical charge storage

$$Q = CE_c. \tag{51}$$

The total electrical capacitance C of the storage area and the potential E_c to which it may be charged increase, therefore, with signal quality and range. The required capacitance can be related to resolution ($\bar{N}_{co}$ or Δf) and $|R|$ by substituting Equations (42a) and (39) into (51) yielding

$$C = 2.72\,|R|^2 \Delta f\, T_f \times 10^{-19}/E_c.$$

Because the developing process may introduce additional fluctuations

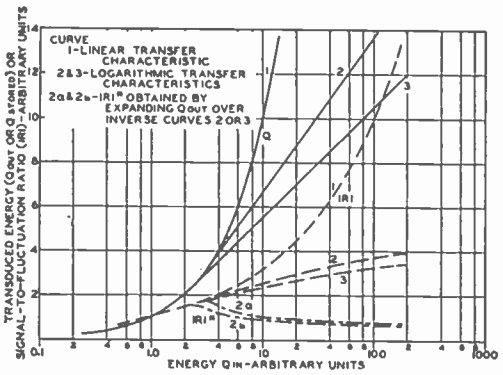

Fig. 46—Primary signal-to-fluctuation ratios $|R|$ and modified signal-to-fluctuation ratios $|R|^*$ for several transfer processes.

by an auxiliary current I_f, we obtain according to Equation (48) the more general equation $C = 2.72\,|R|^2(1 + I_f/I)\Delta f\, T_f \times 10^{-19}/E_c$ (52)

where C = capacitance in farad, I_f = auxiliary current (beam current) required for obtaining the particular signal current I at the ratio $|R|$, and E_c = maximum charge potential on C in volts. (The performance of practical camera tube types is discussed in Section B.2).

The signal-to-fluctuation ratio of both linear and logarithmic characteristics is plotted against input energy in Figure 46. It increases in proportion to the square root of the output energy (Q), but in the logarithmic process (Curve 2), $|R|$ is no longer proportional to the square root of the input energy (Q_{in}) and increases only by a factor of two from $Q_{in} = 4$ to $Q_{in} = 200$. The slow increase results from the "saving" in output energy but is not necessarily a disadvantage. When expanded in later transducing stages to give a *linear* over-all response, the ratio $|R|$ is decreased as shown by Curve (2a). The expansion can be made in several stages, as long as the product produces the inverse transfer characteristic of the primary process.

Transfer characteristics with lower slope (Curve (3) in Figure 46) will cause a larger decrease of $|R|$ as a function of signal when the over-all response is linearized (Curve 3a). A certain slope can, therefore, be found for which $|R|$ will remain fairly constant.* This condition permits a maximum in performance with a minimum output energy and storage capacity because the constant incremental sensitivity of the eye in the range above 1 foot-lambert indicates that a constant $|R|$ in this range is probably satisfactory. (Discussed further in Part IV.)

The logarithmic response of the visual process (Figure 3a, Part I, page 16) suggests that the sensation scale (S) may be related by a similar mechanism to the sample energy Q transduced by the light conversion process and that $|R|$ is constant for $B > 1$ foot-lambert. Threshold conditions imposed by the fluctuation ratio $|R|$ in the toe region of the transfer characteristic have been discussed recently by A. Rose in several papers[26,27].

The transfer characteristics, transfer efficiency, and aperture re-

---

* If a certain degree of compression is retained (as in motion pictures), the optimum slope of the primary characteristic has a lower value than required for a linear reproduction.

[26] A. Rose, "A Unified Approach to the Performance of Photographic Film, Television Pickup Tubes and the Human Eye", *Jour. Soc. Mot. Pic. Eng.*, Vol. 47, No. 4, p. 273, October, 1946.

[27] A. Rose, "The Sensitivity Performance of the Human Eye on an Absolute Scale", *Jour. Opt. Soc. Amer.*, Vol. 38, No. 2, pp. 196-208, February, 1948.

sponse characteristics of optical and electrical components in practical camera systems will be evaluated in subsequent sections.

B. Transfer Characteristics and Aperture Response of Camera Components.

1. Optical Characteristics

The camera lens performs two principal functions: the collection of light energy emitted or reflected from an object or scene; and, the transfer of this energy to a photosensitive surface on which it must form an accurate image of the energy distribution in the object. The energy level in the image is determined, therefore, by parameters controlling the collection and transfer efficiency of the lens, while the accuracy in reproducing the energy distribution is specified by the transfer and aperture-response characteristics of the lens.

a. Collection Factor and Transfer Factor ($g_{(o)}$)

The camera lens covers a field of view with the diagonal angle 2θ. The field is in sharp focus at a certain lens-to-object distance d (see Figure 47). For a standard television aspect ratio ($H/V = 4/3$), the

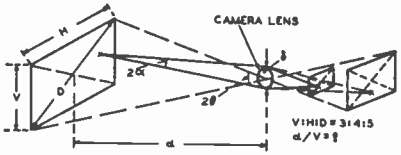

Fig. 47—Light flux pickup of camera lens.

projected dimensions of the object area (A_o) is $A_o = (4/3)\,V^2$. (53)

Expressed by the viewing ratio $\rho = d/V = 1/(1.2 \tan \theta)$ (54)

the object area is given by $A_o = (4/3)\,(d/\rho)^2$. (55)

The light flux reflected from A_o is determined by measuring the average flux density $\overline{B}_o$ (foot-lamberts) with an exposure or foot-candle meter. The object light flux is given by $\overline{\psi}_o = \overline{B}_o\, A_o/144$ lumen or with Equation (55)

$$\overline{\psi}_o = 0.92\, \overline{B}_o\, (d/\rho)^2\, 10^{-2} \text{ lumen } (d \text{ in inches}). \quad (56)$$

The camera lens admits to the camera a cone of light with the solid angle 2α from the hemispherical radiation of each elemental object point. Assuming a Lambert distribution of the object-point flux, the fraction K admitted by the lens diameter δ to the camera is given by $\psi_{2\alpha}/\psi_{2\pi} = K = \sin^2\alpha;\ K = 1/((2d/\delta)^2 + 1)$ (57)

The collection factor K decreases for points near the edges of the field especially for thick lenses and large angles of view (θ)*. With few exceptions the object distance is much larger than the lens aperture

($d >> \delta$) permitting the simplification $K = (\delta/2d)^2$ (58)

In passing through the lens, the light flux is reduced by reflections on glass-air surfaces and by absorption in cement layers. These losses are specified by the transmission factor. For normal angles, a good three-piece lens with six glass-air surfaces and two cement layers has a transmission factor $\tau \simeq 0.92$ (coated) and $\tau \simeq 0.75$ (uncoated) The product τK specifies the efficiency of the lens in collecting and transducing light flux to the image surface.

$$\overline{\psi}_i/\overline{\psi}_o = \tau\ (\delta/2d)^2 \tag{59}$$

Combining Equations (59) and (56) yields an expression for the light flux in practical units

$$\psi_i = 2.3\ \tau\ (\delta/\rho)^2\ B_o\ 10^{-8} \text{ lumen (Lens diameter } \delta \text{ in inches).} \tag{60}$$

The ratio $$g_o = \Delta\psi_i/\Delta B_o = 2.3\ \tau\ (\delta/\rho)^2\ 10^{-8} \tag{61}$$

is *the optical transfer factor of the television camera.* It is proportional to the lens-stop diameter squared but independent of f: number and focal length (F) of the lens.

The optical transfer factor for photographic film is more adeqnately expressed by an illumination-to-brightness ratio

$$g_{of} = \Delta E_i/\Delta B_o \tag{62}$$

because the film exposure depends on light flux density, the total flux ψ_i being, therefore, a function of image area. By dividing Equation (59) by the ratio of the areas which equals the linear magnification squared: $$A_i/A_o = M^2$$

and with the substitutions $\delta = F/f$: *and* $d = \left(\frac{1}{M} + 1\right) F$

The optical transfer factor for film is obtained in the familiar form:

$$g_{of} = \Delta E_i/\Delta B_o = \tau/(2f:(M+1))^2 \tag{63}$$

A specific photographic "signal" requires a given energy Q per

* (See Section B.1(c).)

unit of film area to effectively serve as an attenuator of light after development. The total energy increases, therefore, with film area, but the signal quality increases because of a corresponding increase in resolution.

The television signals from an f:2 lens with 2-inch focal length to an image "plate" with a 1.5-inch diagonal, or from an f:6 lens of 6-inch focal length to an image plate with a 4.5-inch image diagonal, however, are identical because the diameters (δ) of these lenses are equal and, also, the value of light flux ψ_t. (See Equation (60)). The difference is caused by the fixed resolution in a given frequency channel which specifies a constant energy flux (See Equation (45)) for a given signal quality.

The selection of a large or small television camera image depends, therefore, on factors such as the relative aperture response of lenses and pickup tubes of different size in the range below the cutoff resolution $\overline{N}_{co}$ of the system.

b. Optical Transfer Characteristics and Contrast Range in Camera Images

The light transfer characteristic of optical imaging systems departs from the ideal linear relationship $E_t/B_o = \text{constant}$ because of reflection and scattering of light in the camera.

Reflections and diffusion of light in the camera lens can be treated as an "aperture" effect caused by a large diffusion disc of very low intensity (See Part II, Figure 19, page 252) which reduces the flux response at low line numbers. This effect, termed "lens flare", is of a different order than the detail response factor at higher line numbers (See next Section). Lens flare is reduced considerably by "coating" the glass-air surfaces of the lens, but depends also on the general correction of the lens which determines its detail response. The large diameter of the diffusion disc (in the order of centimeters) causes the optical transfer characteristic to become a function of image content. This function is best illustrated by the transition curve from a unit function boundary which can be measured statically by projection in an enlarger (Figure 48). For a rough but useful approximation in evaluating the effects of lens flare the back of the lens surface may be considered as a source of diffused image light flux $\overline{\psi}_b$ which is a certain fraction

$$b = \overline{\psi}_b/\overline{\psi} \tag{64}$$

of the total light flux ($\overline{\psi}$) transmitted through the lens. The value of b is in the order of $b \simeq 0.05$ for uncoated lenses and $b \simeq 0.01$ for coated lenses.

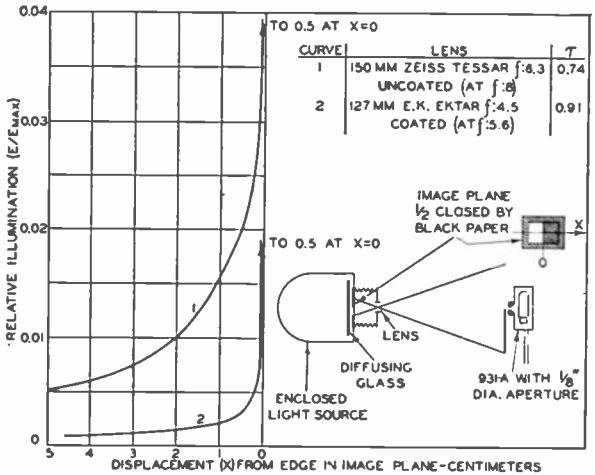

Fig. 48—Transition curves for coated and uncoated lens.

The light flux $\bar{\psi} b$ is superimposed as a more or less uniform "light bias" on the image flux, displacing the transfer characteristic by an additive constant $b\,\bar{E}$ as shown in Figure 49a. The value $b\,\bar{E}$ is, therefore, the minimum illumination in the transferred image which limits the maximum contrast in the image to

$$C_{max} = (\bar{E} + b\,\bar{E})/b\,\bar{E}. \quad (65)$$

The average illumination $\bar{E}$ of the image plane can be considerably higher than the average image illumination $\bar{E}_i$ *inside* the useful image frame when light sources are imaged by the lens outside the frame area. To illustrate this case, assume a normal ratio of peak-to-average illumination $\hat{E}_i/\bar{E}_i = 6$ in the image. A bright sky imaged outside the frame may, however, raise the total average to $\bar{E} = 10\,\bar{E}_i$. For an uncoated lens with $b = 0.05$, Equation (65) furnishes the maximum image contrast $C_{max} = 13$. A coated lens ($b = 0.01$) would give a maximum contrast $C_{max} = 61$.

The contrast range is increased considerably by restricting the light pickup of the lens to the useful image area by means of a rectangular shade of proper dimensions. The average values $\bar{E}$ and $\bar{E}_i$ are then identical which, for the above example, increases the image contrast to $C_{max} = 121$ and 601, respectively.

In television transducers, such as the image orthicon, a lens shade is particularly effective because the deterioration of the tone scale in the "blacks" is augmented by "electron reflection" from saturated high-light areas in the transmitted image, or imaged on unused por-

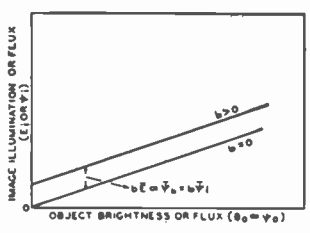

Fig. 49(a) — Transfer characteristics and "flare" light-bias of a lens.

tions of the photocathode. To prevent further loss of contrast, the camera walls should be treated to have a very low reflection coefficient. Surfaces should be rough, broken up into cavities by grooving, or coated with fluffy dead black material (velvet, etc.). Light baffles or masks must cover unused portions of the image surface, which itself should be made as non-reflecting as possible. When the image surface is transparent, as in modern transducers, all tube parts exposed to transmitted light should be treated similarly. Most important, however, is the use of lens shades to prevent excess light from passing through the lens and entering the camera.

Measured values of maximum image contrast ranges are shown in Figure 49(b) as a function of the peak-to-average ratio $\hat{B}/\bar{B}$ (illumi-

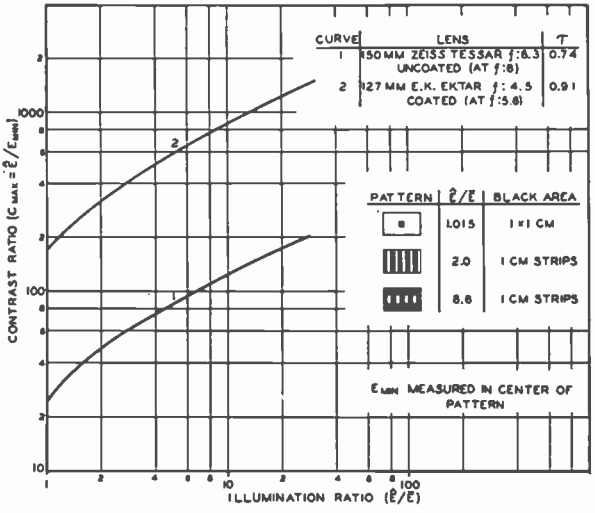

Fig. 49(b)—Large-area contrast in optical camera images.

nation ratio $\hat{E}/\bar{E}$ in Figure 49(b)) for simple test objects.

Correction of the transfer curve

It is electrically quite simple to subtract a light bias by adjusting the electrical black level (clipping level or shading), provided b is a constant or varies smoothly from top to bottom or side to side of the image. If the transducer has a linear transfer characteristic (in the blacks especially), the original linear tone scale can be restored in this manner.

In non-linear processes the correction is more difficult requiring a curved transfer characteristic. In both cases the "bias" light flux

contributes nothing to the useful signal and is, therefore, a fluctuation energy (Q_f or $\mathcal{F}_f$) decreasing the ratio $|R|$ as shown in Section A.4.

c. Resolving Power and "Aperture" Response of Camera Lenses

The resolving power of a perfect lens is limited by the finite wavelength (λ) of light. The optical elements filling the lens opening may be perfect for directing an undistorted wavefront from an object point to a point focus, but the finite boundaries of the lens give rise to phase differences and spreading of light at the edges of the limited wavefront section. This "diffraction" of light causes interference effects. The point image is spread out over a disc area and surrounded by dark and

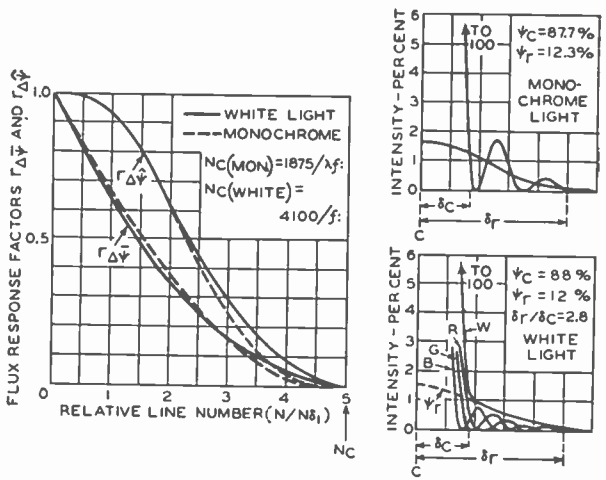

Fig. 50—Aperture flux distribution and response factors of theoretically perfect lens.

light rings of low intensity. (See Figure 50). The effect of diffraction decreases with distance and increasing ratios of lens area to boundary length. The diffraction disc diameter δ_c is, therefore, proportional to the focal length F and inversely proportional to the lens or stop diameter δ[28],[29]

$$\text{For } F/\delta > 1.5 \qquad \left.\begin{aligned} \delta_c &= 1.22\ (2\lambda/\delta)F \\ \delta_c &= 2.44\ \lambda\ f: \end{aligned}\right\} \qquad (66)$$

[28] M. Born, OPTIC, EIN LEHRBUCH DER ELECTROMAGNETISCHEN LICHTTHEORIE, Springer, Berlin, 1933 (p. 207).

[29] C. P. Shillaber, PHOTOMICROGRAPHY IN THEORY AND PRACTICE, John Wiley & Sons, Inc., New York, N. Y., 1944.

The perfect lens has a resolving power limited by the diffraction disc size, which is its circle of confusion and effective resolving "aperture". The light flux[28] within the central disc area can be approximated by a cosine-square distribution (Figure 50) with the equivalent diameter $\delta_o \simeq 2.2\,\lambda\, f{:}$. See (Part II). Because the limiting resolution is $N_o = 4.35\,N\delta$ the diffraction cutoff line number for monochromatic light in television lines per millimeter is

$$\text{For } f{:} > 1.5 \qquad N_o = 4.35 \times 10^3/\delta_c = 1875/\lambda\, f{:}$$

$$\text{and for } f{:} < 1.5 \qquad N_o = (4100 \times \text{numerical aperture})/\lambda \tag{67}$$

with λ expressed in microns (1 micron = 0.001 millimeter).

The aperture response characteristic of a perfect lens is a complex curve which can be approximated by the sum of two response characteristics. The flux rings are approximated by a coaxial diffusion disc $\delta_r = 2.8\delta_c$ with a flux amplitude $\hat{\psi}_r/\hat{\psi} = 0.016$ and a flux distribution

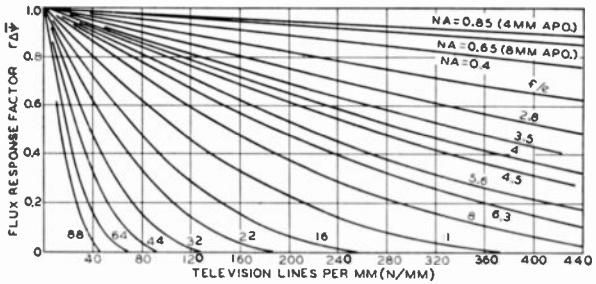

Fig. 51—Flux response characteristics of theoretically perfect lens as function of $f{:}$ number.

equal to that of the main "aperture" δ_o as shown in Figure 50. (See complex apertures, Part II). The theoretical aperture characteristics* of the perfect lens for monochromatic and white light obtained by this synthesis are shown in Figures 50 and 51, and Table V. The aperture response for white light has been computed by superposition of three coaxial monochromatic "apertures" with equal flux at $\lambda_1 = 0.45\ \mu$, $\lambda_2 = 0.55\ \mu$, and $\lambda_3 = 0.65\ \mu$. Figure 50 furnishes the relations $N_c/N\delta = 5$. For $f{:} > 1.5$, $N_{c(w)} = 4100/f{:}$ (Television lines per millimeter). (68a)

For microscope objectives with $f{:} < 1.5$

$$N_{c(w)} = 8400 \times \text{numerical aperture} \tag{68b}$$

* The resolving "aperture" should not be confused with the lens stop "opening" which is normally designated as the lens aperture.

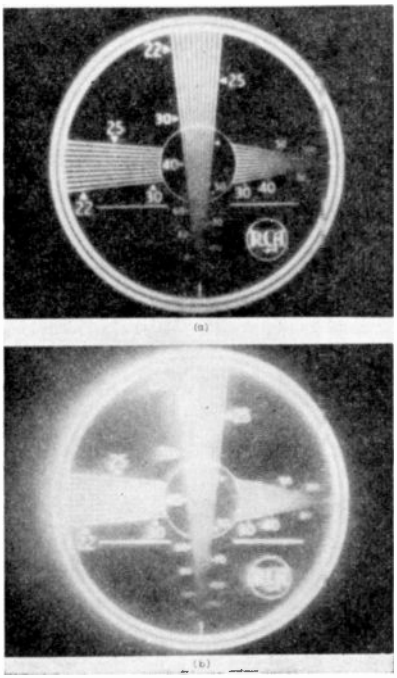

Fig. 52—Photomicrographs of test-pattern image (½ millimeter) taken at f:1.9 with white light.

a. On lens axis ($N_o \simeq 1000$)

b. 10 degrees off lens axis

Theoretical cutoff values N_c are obtained in the center of the field with good small-diameter lenses and with high-quality lenses of large diameter at two to three stops below maximum opening. The theoretical aperture response shown in Figure 51 is not attained with practical lenses and especially not with open large-diameter lenses because of distortions and phase delays which occur in portions of the light wavefront.

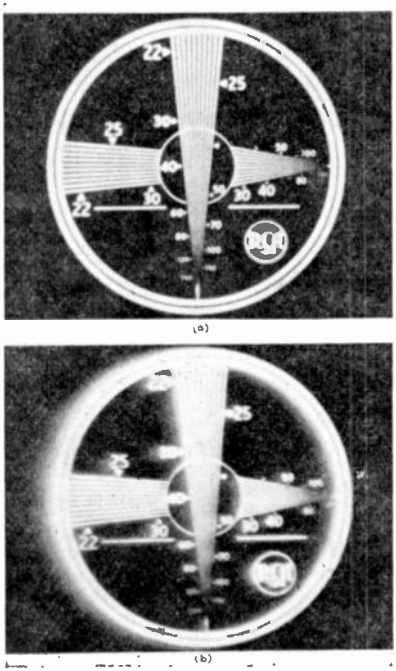

As a result, the effective resolving aperture diameters δ_c and particularly δ_r increase and the "aperture" flux response $r\Delta\bar{\psi}$ remains low, (exhibiting a pronounced "knee") far below the limit of resolving power which is often maintained by the density peak in the "aperture" flux. This point may be illustrated first by the photographic performance of a well-corrected coated lens.

The photomicrographs, Figures 52, 53, and 54 show the

Fig. 53—Photomicrographs of test-pattern image (½ millimeter) taken at f:4 with white light.

a. On lens axis ($N_o \simeq 900$)

b. 10 degrees off lens axis

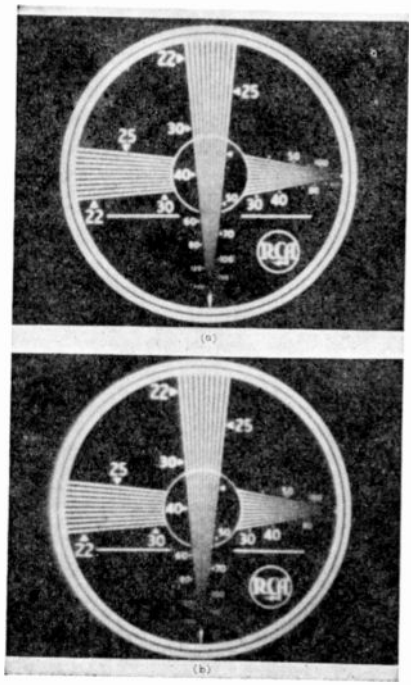

Fig. 54—Photomicrographs of test-pattern image (½ millimeter) taken at f:8 with white light.

a. On lens axis ($N_o \simeq 480$)

b. 10 degrees off lens axis

relative excellence of an f:1.9 50-millimeter lens, as diffraction cutoff is obtained up to f:4 for axial points.# Larger stops show less resolving power and contrast due to spherical aberration and flare. The degradation for angular rays is evident for $f: < f$:8.

These photographs were taken with a microscope focussed normal to incident rays on the image point. They do not show the effects of field curvature. The loss of resolution caused by angular rays and field curvature is illustrated by Figure 55, showing a test object photographed on an Eastman Kodak high-resolution plate.** The small test patterns in the center and the top right corner have again a diameter of 1/2 millimeter on the plate, an angular separation of approximately 19 degrees, and are shown highly magnified in Figures 56 and 57, respectively.

Because the eye and the photographic process have non-linear transfer characteristics, it is difficult to estimate the aperture response of the lens from optical images. A photometric trace of the light flux variations in a square-wave test-pattern image can be obtained by observing the image with high magnification through a television system. This "television microphotometer" transduces optical flux variations into electrical current variations permitting accurate measurement of the aperture response of lenses. A brief description of the apparatus is given in a subsequent section.

The pattern image is 0.5 millimeter in diameter; the numbers on the pattern multiplied by ten give television lines per millimeter. The diffraction cutoffs appear in the original photographs but have been lost in the illustrations.

** Type 649 GH Spectroscopic plate.

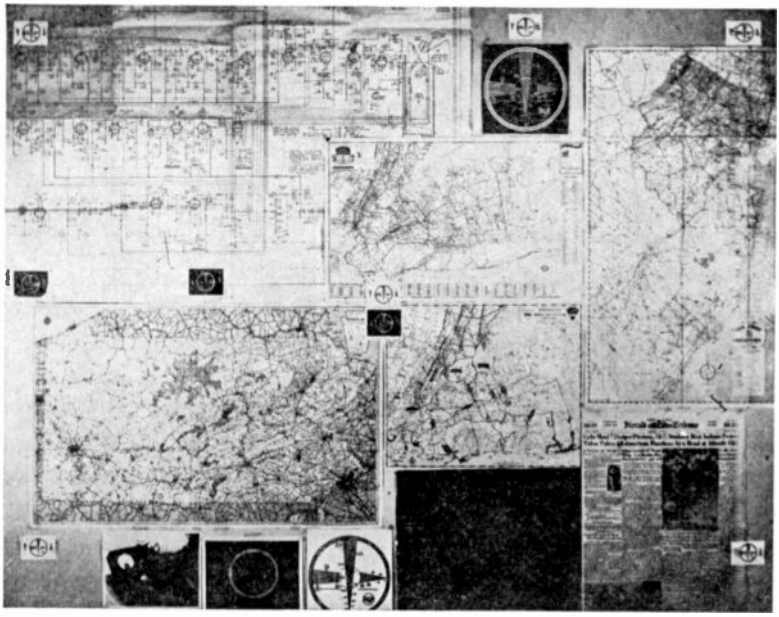

Fig. 55—Test object photographed on Eastman Kodak high-resolution plate with f:1.9, 50-millimeter lens at f:4.

Because of the variety of parameters and factors which control the performance of a lens, a number of curve families are required to describe its aperture response characteristics and to form an opinion on the lens quality. The effect of *chromatic aberration* on the aperture response is illustrated in Figure 58(a) and (b) on two similar high-quality camera lenses of different design at one (optimum) lens stop. The lenses are focused and measured with green light (Wratten filter #58). The measurement is repeated with different light colors (white, #47 blue, #26 red) without disturbing the focus adjustment. The lens in Figure 58(a) is not in focus for red light (zero point at $N = 140$ lines per millimeter) because of chromatic aberration. The chromatic error increases with lens stop diameter and causes a reduction of the white-light aperture response as shown. Both characteristics indicate a "diffusion" disc in the light flux distribution ("knee" in the curves). The relative performance of the same lenses *at different angles* from the optical axis is shown in Figure 59(a) and (b). The situation is now reversed. The lens with better chromatic correction is not as well in focus at the image plane at larger angles partly because of a larger "field curvature", but even when "focused in" there is little difference at 20 degrees between the two lenses. These errors increase normally with larger stops. The curves show also the decrease of the collection

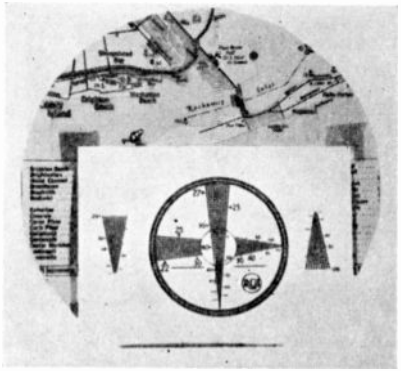

Fig. 56—Enlargement of ½-millimeter test-pattern circle in center of plate (Figure 55) ($N_e \simeq 760$).

Fig. 57—Enlargement of ½-millimeter test-pattern circle at corner of plate (Figure 55) at $0 = 19$ degrees.

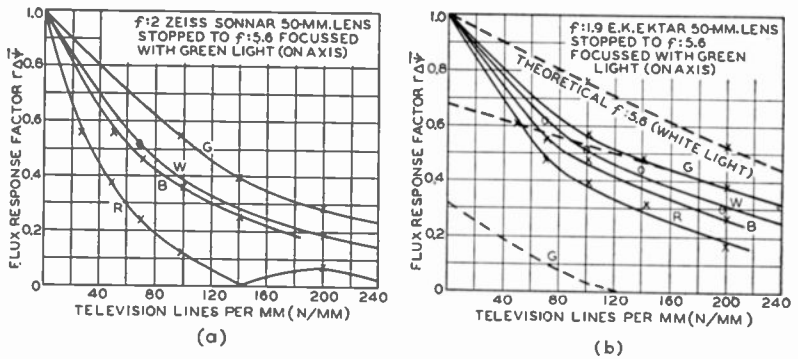

Fig. 58—Flux response characteristic of miniature-camera lenses illustrating chromatic aberration.

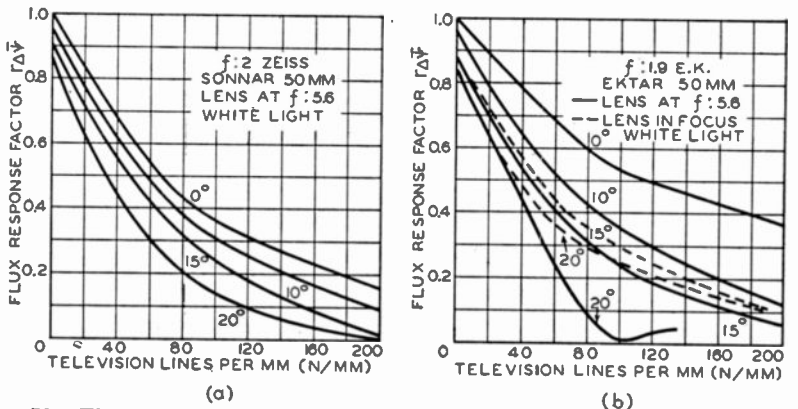

Fig. 59—Flux response characteristic of miniature-camera lenses for angles from 0 to 20 degrees off axis.

Table V—Theoretical Aperture Response Factors of Lenses (Figure 50)

Monochrome Light			White Light*		
$N/N\delta_1$	$r\Delta\psi$	$r\Delta\bar{\psi}$	$N/N\delta_2$	$r\Delta\psi$	$r\Delta\bar{\psi}$
0.5	0.99	0.83	0.5	0.99	0.815
0.75	0.97	0.74	0.75	0.965	0.725
1.	0.93	0.66	1.0	0.93	0.64
1.5	0.80	0.51	1.5	0.80	0.49
2.	0.615	0.39	2.	0.625	0.36
2.5	0.42	0.27	2.5	0.45	0.26
3.	0.25	0.16	3.	0.30	0.175
3.5	0.114	0.08	3.5	0.176	0.11
4.	0.035	0.022	4.	0.088	0.056
4.35	0.	0.	4.5	0.03	0.02
			5.	0.	0.

* Composite response of three coaxial spots.
** Millimicrons.

λ	450 $m\mu$**	550 $m\mu$	650 $m\mu$
δ	0.82	1.	1.18
$\hat{\psi}$	0.47	0.31	0.22
ψ	1/3	1/3	1/3

factor K with angle, because the response does not increase to unity at $N = 0$. The curve families in Figure 60 illustrate the change of aperture response as a *function of the f number*. The response increases at first when the lens is stopped down (increase of f number) because spherical and chromatic aberrations are decreased; for smaller stops it decreases as may be expected from theoretical considerations. (See Equation (68a) and Figure 51). A photograph of the aperture-response changes as seen on the oscilloscope of the television microphotometer is shown in Figure 61. This figure illustrates the progressive diffraction cutoff from $f/8$ to $f/11$. It should be noted that the response at lower line numbers ($N = 100$/millimeter) increases from $f/2$ to $f/8$.

Although most lenses have a much higher limiting resolution (N_c) than can be used with normal photographic film or a television channel, their aperture response departs considerably from theoretical values at low line numbers. For an image height $V = 25$ millimeters, which is the approximate size in miniature cameras and the present image orthicon (2P23 and 5655), the line number $N = 500$ represents 20 lines per millimeter. The response factors at this line number for a number

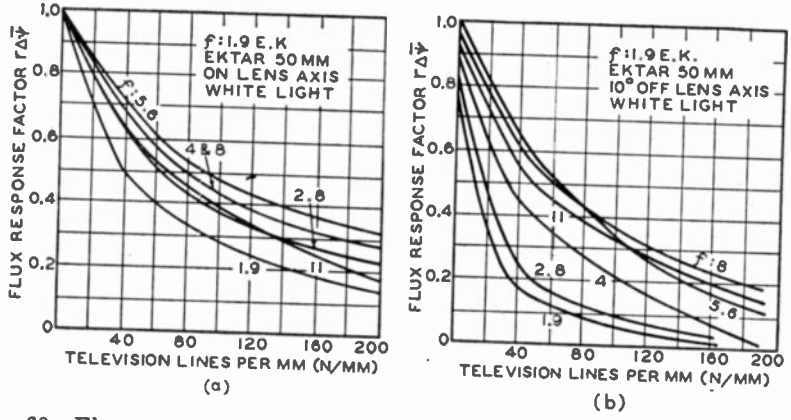

Fig. 60—Flux response characteristics of miniature-camera lens as function of *f:* number. (Compare Figures 52, 53, and 54).

of high-quality camera lenses are shown in Figures 62(a) and 62(b) as a function of lens diameter (δ/F) and f number. If a 10-degree angle is selected as an average value, it can be seen that the response $r\Delta\bar{\psi}$ at 20 lines per millimeter ($N = 500$ for $V = 25$ millimeters) averages $r\Delta\bar{\psi} = 0.7$ at small lens stops ($f: > 4$) and decreases below this value for "faster" lenses. For the purpose of computing the over-all aperture response of the system, the line number $N_{0.5}$ at which $r\Delta\bar{\psi} = 0.5$ has been plotted as a function of f number in Figure 63(a) and (b).

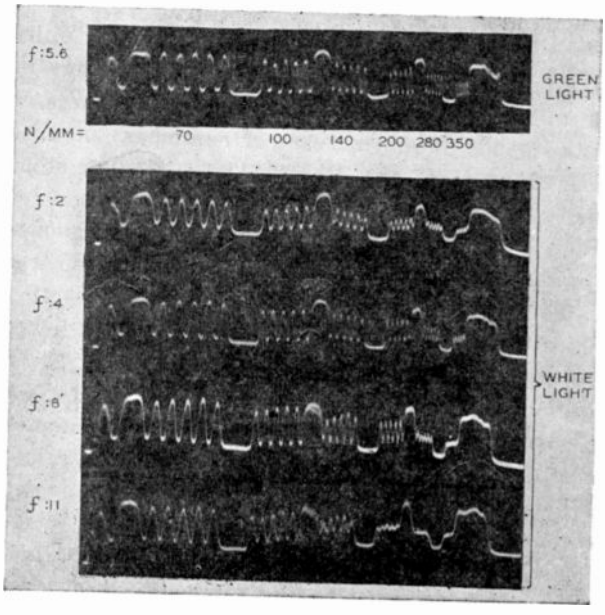

Fig. 61—Oscillograms of aperture response of *f:*1.9 miniature-camera lens (0 = 0 degrees) taken with television microphotometer (Figures 71 and 72).

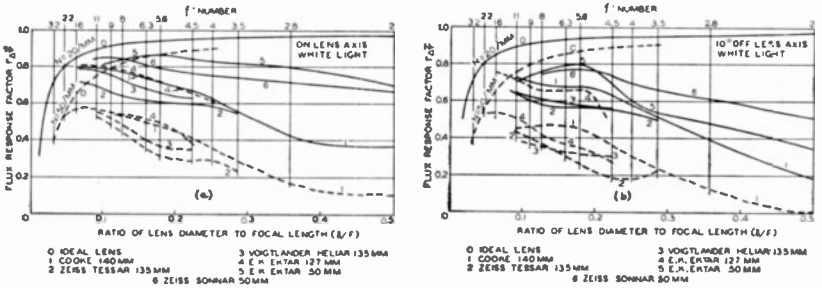

Fig. 62—Flux response characteristics of various high-quality camera lenses at specified detail size.

An examination of various lens characteristics indicates that aberrations decrease, in general, with the focal length F of the lens although not in proportion. A larger image size results, therefore, in a generally higher response factor for a given f number and line number N in the image dimension. Because the transfer efficiency of the television camera lens is constant for a given lens diameter δ, an increase of image dimensions corresponds to an increase in the f number of the lens ($f := F/\delta$) and a correspondingly rapid increase in the relative response factor of the lens. As the largest lens diameters and collection factors (See Equation (58)) are obtainable in lenses with a long focal length the sensitivity of the television camera increases with image size. The selection of practical image sizes is, therefore, governed by factors such as weight, availability of lenses, the required mechanical precision in tube and camera construction as well as certain electrical operating requirements which are a function of size.

Lens Diameter and Aperture Response for Deep Fields of View

When imaging three-dimensional fields, the camera image can be

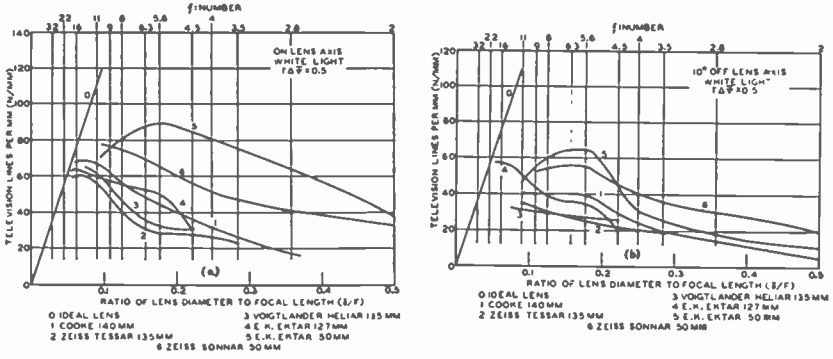

Fig. 63—Line number reproduced with 50 per cent response by various high-quality camera lenses.

Fig. 64 — Relations between lens diameter, circle of confusion, and depth of field for finite distances d_1 and d_2.

in focus at one distance only. The effective resolving "aperture", therefore, is enlarged for planes at the front and rear limits of deep fields to a "disc of confusion". The relations between lens diameter, "depth of field", and disc of confusion are easily established by geometrical optics from the ray diagram Figure 64.

The object plane O_m is assumed in sharp focus for an image plate placed at P_m. Points in all other planes between O_1 and O_2 are out of focus and are imaged as discs of varying diameter but not exceeding the diameter $\delta_i = M\,\delta_o$. This diameter is obviously determined by the out-of-focus distance and the lens stop diameter, and has a minimum value in a given "depth of field" when the lens is focused to the mean distance

$$d = 2d_1\,d_2/(d_1 + d_2). \tag{69}$$

The depth of field $(d_2 - d_1)$ is related to δ and δ_o by

$$d_2 - d_1 = (d_1 + d_2)\;\delta_o/\delta. \tag{70}$$

The theoretical disc of confusion (δ_o) is a round resolving "aperture" with cosine-square flux distribution (See Part II). To maintain an aperture response $r\Delta\bar{\psi} = 0.71$ within the field limits, its largest diameter should not exceed the value

$$\delta_o = V_o/\overline{N}_{co}. \tag{71}$$

(V_o = Vertical object field dimension)

By expressing the object depth by its ratio to the field height:

$$p = (d_2 - d_1)/V_o \tag{72}$$

and combining Equations 70, 71 and 72, the lens stop diameter required

$$\left.\begin{array}{l}\text{for } N\delta_o = \overline{N}_{co} \text{ is specified by } \delta_{max} = (d_1 + d_2)/(p\overline{N}_{co}) \\ \text{for the mean distance} \qquad d = \rho(d_2 - d_1)/p\end{array}\right\} \tag{73}$$

A representative depth of field may be obtained from the consideration that three-dimensional scenes or objects are frequently extending over a depth equal to their vertical dimension (i.e., $p = 1$). Table VI has been computed with Equation (73) for equal depth and height $(p = 1)$ of the "sharply" imaged field for a fixed distance $d = 18'$ and the sharpness limit $\overline{N}_{co} = 400$. (Camera equipped with lens turret and fixed position.) The lens stop diameter (δ_{max}) is practically constant

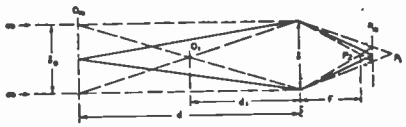

Fig. 65 — Relations between lens diameter, circle of confusion, and depth of field for hyperfocal conditions.

for all conditions. The lower section of the table lists focal length (F) and f: number for this stop diameter for four different image plate diagonals D; all give the same sharpness and, for a given viewing ratio ρ, equal television signals. *The optical transfer factor g_o (Equation (61)) is, therefore, a constant specified by the required sharpness in depth and the viewing angle.* This fact remains substantially unchanged for variations of camera distance. When the rear distance limit (d_2) is moved to infinity, a depth of field from d_1 to infinity requires focusing to the "hyperfocal" distance (See Figure 65) $d = 2d_1$. (74a)

Obviously $\delta_o = \delta$ and with (71) and (54) $\delta_{max} = d/(\rho \overline{N}_{co})$. (74b)

The above evaluation has assumed the hypothetical condition that the lens can produce a mathematical point image. Actually, the image is of finite size because of diffraction and aberrations. The disc of

Table VI — Camera and Lens Constants

(for $d = 18'$, $p = 1$, $N\delta_o = 400$)

Viewing Ratio	ρ	2.5	4.	8.
Mean distance	d	18	18	18 feet
Depth and height of field	$d_2 - d_1 = V_o$	7.2	4.5	2.25 feet
	$d_1 + d_2$	37.4	36.7	36.3 feet
Lens stop diameter (Equation 73)	δ_{max}	1.12	1.1	1.09 inches
Optical transfer factor (Equation 61)	$g_o = \Delta\psi_i/\Delta B_o$ ($\tau = 0.9$)	1/2400	1/6350	1/25800 Lumens/foot-lambert

Viewing Ratio 2.5					4			8		
D	V	M	F	f:	M	F	f:	M	F	f:
Inches		Inches			Inches			Inches		
1.5	0.9	1/96	2.22	2.	1/60	3.54	3.2	1/30	6.95	6.4
3.	1.8	1/48	4.4	3.9	1/30	6.95	6.3	1/15	13.5	12.4
6.	3.6	1/24	8.7	7.8	1/15	13.5	12.3	1/7.5	25.4	23.3

confusion is, therefore, somewhat larger in size and is decreased in first approximation by the cascaded value of the in-focus resolving aperture of the lens. A viewing ratio $\rho = 4$ for a 1.5-inch plate diagonal (Table VI, 2nd column) is obtained, for example, with an f:3.2, 3.54-inch lens, which has an (in focus) aperture response of 50 per cent at $N \simeq 20$ lines per millimeter (See Figure 63(b)) corresponding to $N = 500$ for this image size. The disc of confusion (δ_o) selected according to Equation (73) gives 71 per cent response at $N\delta_o = \overline{N}_{co} = 400$ and has a 50 per cent response at $N = 1.75\, N\delta = 700$ (See Part II, Appendix Table II, page 285). The line number $N_{0.5}$ for which $r\Delta\overline{\psi} = 0.5$ at the field limits is obtained with Equation (30) Part II

$$N_{0.5} = 1/\sqrt{1/700^2 + 1/500^2} = 406.$$

It may be concluded, therefore, that the aperture response of the optical system cannot be neglected in its effects on the television system quality and especially not when the image size is small.

2. *Photoelectric Transducers (Camera Tubes)*

The construction and operating principles of television camera tubes have been adequately described in the literature.* The following treatment will be limited to an evaluation of their characteristics as transducers of light into electrical signals.

a. Storage Capacitance and Transfer Characteristics

The quality of signals developed by photoelectric transducers such as the iconoscope, orthicon, and image orthicon, depends, in principle, on the total energy Q which can be stored and transduced into electrical signals. The storage capacity of transducers is determined by the electrical capacitance C and the maximum charge potential E_o of the storage surface as expressed by Equations (51) and (52). The mechanism effecting the transfer of charges into television signal currents, however, imposes limitations on the maximum energy value and is, therefore, a controlling factor in the design of practical camera tubes. To retain image definition it is essential that each incremental area Δa of the storage surface (target) in the transducer be associated with an individual storage capacitance ΔC. In iconoscopes and orthicons, this association is accomplished by breakup of the photosensitive image surface into a mosaic of minute silver islands. The "space" capacitance of these elements is increased by addition of a parallel grounded plate, termed "signal plate". Dependent on its position, the signal plate is a solid conductor (iconoscope), a conductor transparent to light (orthicon), or a conductor transparent to electrons (collector screen in image orthicons).

* See References (7), (8), (9), (11) in Part I.

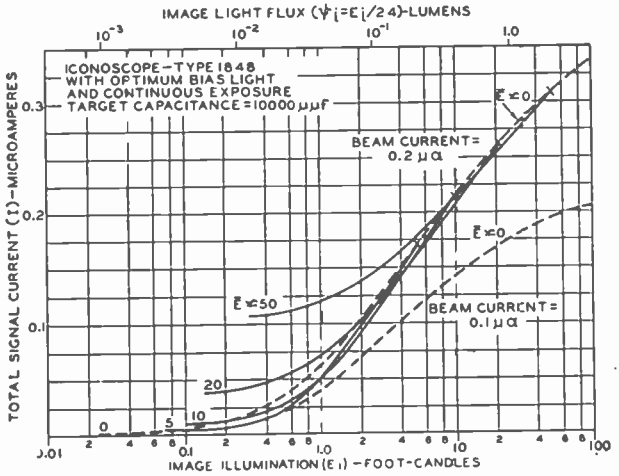

Fig. 66—Dynamic transfer characteristics of an iconoscope.

Orthicons operate with saturated photoemission. Element potential and charge increase in proportion to the image light flux (ψ_i), but are limited by insufficient beam current or secondary emission to certain maximum values. The transfer characteristic $I = f(\psi_i)$ is linear but breaks off when E_o is approximately 6 volts. Higher potentials cannot be neutralized by low-velocity beams because of excessive generation of secondary electrons.

In iconoscopes, the photoemission from elements takes place largely without strong collecting fields and E_o is limited by emission velocity distribution and partial discharge by secondary and photoelectrons to a maximum of approximately 2 volts. The function $E_o = f(\psi_i)$ and the transfer characteristics follow a curve of diminishing returns as shown by the characteristics in Figure 66. The gradual signal compression is a desirable characteristic for well-lighted subjects of good contrast and requires little electrical correction in the amplifier. High average levels of light flux (See $\bar{E}$ in Figure 66) cause an excess of photoelectrons which discharge small signal charges thereby reducing the signal range.

The image orthicon combines characteristics of the iconoscope and orthicon. Its saturated photoemission forms a photocurrent image focused on a thin glass target having the properties of a storage surface with incremental capacitances which are charged by secondary electrons from bombardment of high-velocity photoelectrons, but which can be discharged from the opposite side by a low-velocity scanning beam as in the orthicon. An electrically transparent signal plate (fine mesh screen) collects the secondaries from the image current. It per-

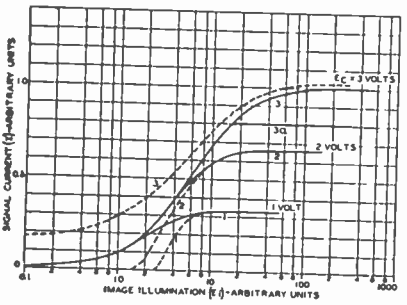

Fig. 67(a) — Dynamic transfer characteristics of image orthicon as function of target potential.

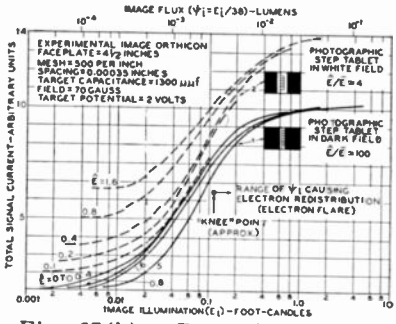

Fig. 67(b) — Dynamic transfer characteristics of an image orthicon at optimum target potential.

mits adjustment of the capacitance (by spacing) and limits the charge potential maximum of the storage surface (target) according to the applied potential. With the charge potential under control, the transfer characteristic does not end abruptly and can be changed from a linear function to one similar to that of an iconoscope.

Although a particular characteristic curve of signal-current output as a function of light input shows a definite saturation value (See published curve of Type 2P23), it is not necessarily describing the transfer characteristic of the tube. This signal curve represents the transfer characteristic only when the range of light values does not exceed the "knee" of the curve. At higher light-flux values, the actual dynamic transfer characteristic is determined by electron redistribution and becomes a function of image content and the peak-to-average ratio of the light flux values. The effects of electron redistribution on the useful contrast range are in some respects similar to "lens flare" as shown by the transfer characteristics in Figure 67(b) which have been measured on an experimental high-capacitance tube to be discussed later.

It is logical to conclude that increases in the target capacitance C of storage tubes will result in a larger range of the transfer characteristics and in higher signal-to-fluctuation ratios $|R|$, provided the stored charges can be transduced into signal currents. A camera tube with low element capacitance is more suitable for low light operation because it develops higher potentials with small photocurrents and low values of light flux which are easier to transduce than low-potential charges in a tube with large capacitance. The low-capacitance tube, however, cannot store large charges because of the voltage limit (E_{cmax}) and, thus, is limited to a lower image quality. High-capacitance elements cannot be discharged as completely as low-capacitance ele-

ments containing an equal charge. This condition is particularly true for orthicons and image orthicons because of the velocity distribution in electron beams. An incomplete discharge forces the element potential to build up in successive exposure periods until the scanning beam is capable of removing the number of electrons emitted during one exposure period. The consequence of this action is a delayed slow appearance of under-exposed objects and their delayed disappearance or "smearing" (following "ghosts") in motion. *The maximum useful capacitance* of storage-type tubes is limited by difficulties in generating electron beams (especially of the low-velocity type) having a small velocity distribution and sufficient current density to affect a substantially complete discharge of low-potential elements. This restriction limits the performance of present pickup tubes. Small storage surfaces require a higher beam-current density for a given light flux than larger surfaces. Larger tubes are thus capable of discharging higher capacitances and attaining higher resolution and signal-to-fluctuation ratios.

The transfer characteristics of the iconoscope (Figure 66) and the image orthicon (Figure 67) are plotted on semi-logarithmic coordinates to permit a direct comparison with the *primary transfer characteristic* of photographic film. The total signal current including "flare" or level currents from these camera tubes is a measure of the stored and transduced energy Q_e. The corresponding stored energy in the photographic process is the quantity of silver "specks" caused by photoelectric reactions and "amplified" chemically in the development process into a quantity of silver grains Q_s. This silver quantity is measured by the "density" of the film to which it is directly proportional[30]. Because the density D is plotted to a linear scale in sensitometric curves of film, the characteristics Figures 66 and 67 permit a direct comparison with photographic film.* (Discussed in Part IV of this paper).

The dynamic transfer characteristics of high-capacitance image orthicons depend on a number of parameters[11]. Two of these parameters, beam current, and collector-mesh potential, E_c, are controllable. Others,

---

[30] C. E. Kenneth Mees, THE THEORY OF THE PHOTOGRAPHIC PROCESS, The Macmillan Company, New York, N. Y., 1942.

* The film, however, is used as an attenuator in a second light transducing process (copying) in which the density effects light modulation by absorption. As an arithmetic increase of density causes a *geometric* increase of light absorption, the linear scale D is also a logarithmic scale $D = 1/\log$ transmission when both transducing processes are considered. The two processes are invariably connected together and the log/log slope of the film curves is defined as the *gamma* (γ) of the film. It is apparent that the slope of the electrical transfer characteristics, i.e., their *transfer factor g* is not a "gamma" and cannot be manipulated mathematically like the gamma of film, because the relation between Q_e and light output is dependent on the entirely different transfer characteristics of separate transducers (amplifiers and kinescopes).

such as the secondary-emission ratios of target (glass) and collector-mesh materials cannot be adjusted in a finished tube. The dynamic characteristics of the image orthicon depend on these parameters as illustrated qualitatively in Figure 67(a). The solid curves 1, 2, and 3, show the effect of varying the mesh potential E_c which controls the maximum charge potential of the storage capacitance (glass target). The beam current is increased in proportion to E_c. When the current is insufficient, the high-light region is compressed as indicated by curve 3a. These characteristics are obtained with "low key" lighting as represented by a small photographic step tablet in a dark field in which redistribution effects are small. When the field surrounding the step tablet is light, the transfer characteristics remain unchanged as long as the peak illumination $\hat{E}_i$ remains below the "shoulder" of the curves. When $\hat{E}_i$ is increased and approaches the flat portion of the shoulder, electron redistribution increases and modifies the low-light range as indicated by the dotted "high key" characteristics for the following reasons. Assume that the mean velocity of secondary electrons emitted by interception of high-velocity photoelectrons on the collector-mesh wires is two volts. A "white" background in the image causes a large number of such secondaries which can "land" on the glass storage surface when its potential E_c with respect to the mesh is equal to or smaller than two volts. The secondaries from the mesh discharge especially, therefore, the small charges in the low-light region for $E_c < 2$ volts and shorten the transferred light range by "black compression". At higher mesh potentials, $E_c > 2$ volts, this discharge action decreases and, as shown by the dotted curve 3, may be overcompensated by the effect of a "flare" light bias due to the optical system. It is apparent that the secondary emission velocity determines, in general, the optimum mesh bias E_c for a particular tube. (There are other parameters which have been neglected).

The transfer characteristics, Figure 67(b) of an image orthicon were obtained by measuring the signal from a small logarithmic step tablet in both a dark field (curves 1) and a light field (curves 2). The light field covers only a portion of the image area as indicated in Figure 67(b). These two conditions are representative of extremes in actual images. In this particuluar case both "black level" and "white level" are raised considerably with increasing exposure in "high key" images, (curves 2), the added exposure contributing nothing to the actual signal (ΔI) above $\hat{E}_i = 0.4$. Over-exposures cause the center of black areas to "wash out" due to "electron flare", their edges remaining dark which, of course, is undesirable for good quality. For similar reasons, higher exposures than $\hat{E}_i = 0.8$ for the case of dark (low key)

Images (See curves 1) must be considered as undesirable over-exposures. Over-exposure (curves 2) requires an increase of beam current to accommodate the black-level current. Because of the low modulation factor in present tubes, (See following section), the signal-to-fluctuation ratio $|R|$ at different signal levels in one image varies substantially in proportion to the signal level (ΔI). It can be shown that $|R|$ decreases, therefore, at all levels by the square root of the black-level current.

Image orthicons of the 5655 type have storage capacitances, and transfer characteristics similar to the experimental tube on which the transfer characteristics, Figure 67(b) were taken. The light range transduced by these camera tubes is in the order of 100 to 1 as in normal photographic processes. (Discussed in Part IV).

b. Transfer Efficiency and Transfer Factors

The generation of video signals in storage-type camera tubes occurs in two stages: the photoelectric conversion of image light into electrical charges and the development of signal current from the charges. The corresponding transfer equations have these forms:

$$Q_e = g_1 \psi_i T_{ex} \text{ (photoelectric process)} \tag{75}$$

and

$$I = g_2 Q_e / T_f \text{ (signal development process)} \tag{76}$$

where the symbols have the following meanings:

Q_e = stored electrical charge energy (coulombs)

ψ_i = image light flux (lumens)

T_{ex} = exposure time (seconds)

$g_1 = \tau s S$ = photoelectric transfer factor

τ = optical transmission factor of elements absorbing light

S = photosensitivity in microamperes per lumen

s = storage factor of camera tube

I = primary signal current (microamperes) before amplification

T_f = frame period (seconds)

g_2 = transfer efficiency of the signal developing process (excluding amplification).

For a continuous exposure (no shutter), the exposure time equals the frame time; $T_{ex} = T_f$ and Equations (75) and (76) combine to the simple expression

$$\psi_i = I / g_1 g_2 \text{ (lumen)}. \tag{77}$$

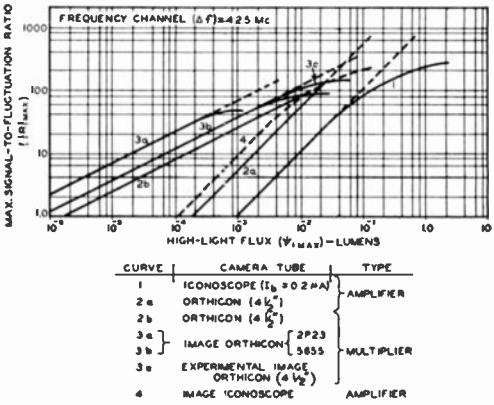

Fig. 68—Maximum signal-to-fluctuation ratios of television camera tubes.

By substituting Equations (45) and (48) the image light flux is expressed in terms of the signal quality, ($|R|$ and Δf determining $\overline{N}_{co}$).

$$\psi_{i(R)} = 2.72\,|R|^2\,\Delta f\,(1 + I_f/I) \times 10^{-13}/(g_1\,g_2)\ \text{(lumen)}. \qquad (78)$$

The factor $(1 + I_f/I)$ is required, because signal development by a beam current $I_b = I_f$ introduces additional current fluctuations. In camera tubes with electron multiplication (orthicon and image orthicon types), the reciprocal ratio $I/I_f = I/I_b$ is the modulation factor of the beam by the signal current I which seldom exceeds 25 per cent in practical tubes. Because the beam current must remain constant and have a value sufficient to discharge the maximum signal charge, the factor $(1 + I_f/I)$ equals 5 for the high-light flux $\hat{\psi}_i$ only. The flux values $\psi_{i(R)}$ computed by Equation (78) for a standard channel $\Delta f = 4.25$ megacycles and various values $|R|_{max}$ have been plotted in Figure 68. These curves do not represent the change of $|R|$ versus light flux changes in a given image because I_f is then a constant and $|R|$ varies as shown by the curve $Q_f/Q_o = 4$ in Figure 43.

Approximate values for the transfer factors $g_1\,g_2$ and contributing factors (See Equation (76)) are listed in Table VII for several camera tube types. Upper limits for $|R|_{max}$ computed from the capacitance of the storage surfaces by Equation (52) are indicated by the length of the solid line curves in Figure 68.

A certain percentage of charges may be lost for signal generation because of unsaturated photoemission or a partial discharge by secondary electrons. Both effects are small in the orthicon types. ($g_2 = 1$, $s = 1$) In iconoscopes, however, they decrease the effective storage (s) to 60 per cent (approx.) at moderate light levels and to less than 20 per cent at high light levels. Because of incomplete collection of the

Table VII—Transfer Factors ($g_1 g_2$) of Camera Tubes

	Camera Tube Type	Approx. C-$\mu\mu f$	S μa/lumen	τ	sg_2	Avg. Value $g_1 g_2$	Spectral Response	Signal Amplification
1	Iconoscope	10,000	7-10	1.	0.12*	1.	Normal	Amplifier
2	Orthicon	750	6-8	0.5-0.9	1.	5.	Normal	Amplifier or Multiplier
3a	Image Orthicon 2P29	250	20-30	1.	1.5**	35.	High red and infrared	Multiplier
b	5655	750	5-10	1.	1.5**	10.	Normal	Multiplier
4	Image Iconoscope	5000	7-10	1.	0.2×5**	8.	Normal	Amplifier

* Decreases above a certain light flux.

** Includes gain in image multiplication and decreases above a certain light flux.

signal current, the transfer efficiency of iconoscopes is further reduced as indicated in Table VII.

Incomplete storage and partial cancellation of charges by redistributed secondary electrons* occur also in image orthicons, especially at high-light conditions. (See Figure 67) The effective storage of this tube varies as a function of light and collector mesh potential from near 100 per cent at low light levels and normal collector potentials to 20 per cent and less under high-light conditions and low collector potentials as evident from the transfer characteristics shown in Figure 67. Representative photosensitivities (S) and utilization factors of practical transducer types suitable for direct pickup in television cameras are given in Table VII.

Signal amplification by amplifiers—In some camera tube types the video signal is developed across a resistance in the signal plate lead without the use of an electron multiplier. Because of the large number of electrons required as a "carrier" current for small signals in amplifier tubes, their modulation factor is extremely low and the signal-to-fluctuation ratio is dominated by the constant amplifier fluctuation current I_f and requires, therefore, large signal energies for good quality. The current I_f is a function of tube and circuit conductances and may be computed from the equivalent noise resistance of the amplifier tube.[186] For a minimum fluctuation current the input circuit capacitance C_1 of the amplifier (camera tube plus amplifier grid circuit capacitance) should be made the controlling factor of the circuit impedance.

* There are also other causes.

The amplifier is compensated to give constant voltage output with constant signal-current input and has, therefore, a gain proportional to frequency over most of its range Δf (See Part I). Assuming $C_1 = 25$ micromicrofarads as the dominating input impedance, the amplifier noise current in the type 6AC7 amplifier tube is expressed by

$$I_f = 3.7(\Delta f)^{1.5} \times 10^{-19} \text{ amperes.} \tag{79}$$

The character of the resultant "peaked" "noise" and its effect on visibility have been discussed in Part I and must be considered when comparing signal-to-fluctuation ratios of multipliers and amplifiers. For visual equivalence of the "peaked" noise from this amplifier with flat channel noise from multipliers, $|R|$ is to be multiplied by the ratio K of the fluctuation filter factors for the two types of noise

$$K = m_{ek} \text{ (peaked)} / m_{ek} \text{ (flat)} \tag{80}$$

shown in Part I, Figure 11, as a function of Δf. The signal current in terms of equivalent flat-channel noise exceeds the fluctuation current by the ratio $|R|$ and is, therefore, given by:

$$I' = 3.7\,|R|\,K(\Delta f)^{1.5} \times 10^{-19} \text{ amp.} \tag{81}$$

The required light flux is obtained with Equation (77) being reduced slightly by the camera blanking ratios to

$$\psi'(R) = 3.14\,|R|\,K(\Delta f)^{1.5} \times 10^{-13}/(g_1 g_2). \tag{82}$$

A comparison of camera tube performance and a table of the scene brightness or luminance (B_o) required for their operation will be given in Part IV.

c. The Aperture Response of Television Camera Tubes

Television camera tubes contain a number of elements in cascade which may restrict the resolving power. In storage types, the scanning beam and physical apertures in conductors (collector mesh in image orthicons) are, in general, the principal limiting apertures. Secondary aperture effects such as those caused by unstable focus of the electron image or by graininess of photoelectric and storage surfaces can be made negligible by proper design of tubes and equipment.

The over-all aperture response of the transducer is measured by observing amplitude and wave shape of the electrical signal. The optical signal source is a large (8 x 10-inch) square-wave test pattern picked up by a high-quality lens, with known aperture response. The electrical signal is observed on an oscilloscope with cross-section selector (horizontal or vertical).

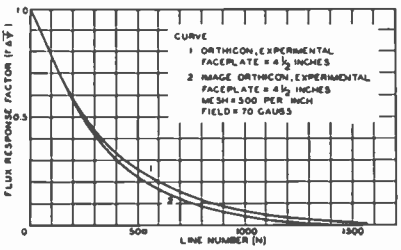

Fig. 69—Flux response characteristics of two camera-tube types.

The measurement in the horizontal direction gives the combined aperture response of transducer and electrical channel. To obtain the aperture response of the transducer directly, the electrical channel must be capable of reproducing the signal waveforms generated by the transducer. This requirement specifies a frequency band exceeding by at least a factor of five the frequency ($f\delta$) or line number ($N\delta$) at which the transducer response becomes sinusoidal, i.e., the point where its amplitude response begins to depart from unity.

The aperture response $r\Delta\overline{\psi}$ of two developmental storage transducers operating into a flat twenty-megacycle channel is shown in Figure 69. Although representing peak performance of present constructions their response decreases to approximately 22 per cent at 500 lines. The aperture response of transducers can be corrected by optical or electrical processes having a "negative" aperture characteristic as discussed in Part IV of this paper.

3. *A Television Microphotometer for Measuring the Aperture Response of Lenses and Grain Structures.*

Aperture response measurements require, in principle, a scanning process. An arrangement for scanning an optical image and transducing light-flux variations into electrical current variations for observation and measurement is a television system used as a photometer. Because of the relatively high resolving power of lenses, it is expedient to magnify the optical image considerably by a microscope before it is scanned in a television camera tube. With adequate optical magnification of the image the resolving power of the television system is removed as a limitation, and the response limit of the microphotometer depends only on the resolving power of the microscope objective.

A photograph and block diagram of the principal parts of the television microphotometer are shown in Figures 70 and 71.

A test pattern (2) (Figure 70) illuminated by a projection lamp and condenser system (1) is imaged by the lens under test (3) with a reduction equal to or greater than 20 to 1 to remain within the normal correction range of the lens. With this reduction the optical input signal from a good test pattern is sufficiently accurate at the lens cutoff (N_o).

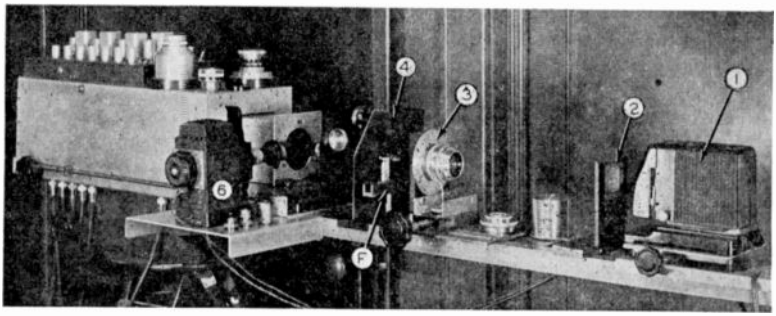

Fig. 70—Photograph of television microphotometer.

A small part of the image is observed with a television camera through a microscope (4) giving high optical magnification ($M = 100$ to 1000 as needed) and having a resolving power much higher than the lens under test (A 4-millimeter Apochromat, $NA = 0.95$, for use without cover glass resolves $N_c = 8000$ television lines per millimeter). The magnified image is scanned in the television pickup transducer (5) and translated into electrical aperture-response signals.

Amplitude response and wave form of these signals are observed and measured on an oscillograph with line selector, the microscope image being visible on the monitor kinescope for inspection and focussing. (Figure 72). To avoid errors by non-linear transfer characteristics of the camera tube or amplifying system, the amplitude of the light flux wave is measured optically at the input to the television camera. A fine light bar produced by a slit mask in a calibrating projector, (6) in Figure 70, is superimposed on a dark "line" of the test pattern image (See Figure 72), appearing as a pulse signal in

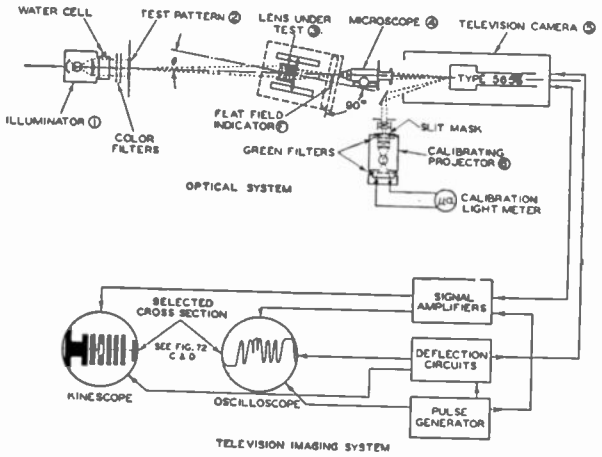

Fig. 71—Block diagrams of television microphotometer system.

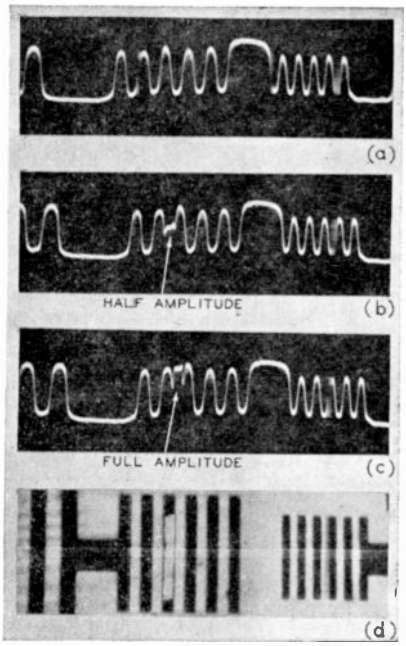

Fig. 72 — Oscillograms and kinescope image showing measurement of flux response with television microphotometer.

the oscilloscope trace. The calibrating light intensity is increased until the negative wave peak is raised to the level of the positive wave peaks. The difference ΔB introduced by the calibrating source is the peak-to-peak brightness difference in the flux wave which is thus measured by reading the relative light output of the calibrating source with photocell and meter (See Figure 71). By the use of sharp green filters in front of the cell and the slit mask, the calibrating light can be controlled by varying the lamp current.

All measurements are made on the same line of sight along the optical axis of the system to avoid errors due to variations in light distribution of the projector or the sensitivity of the camera tube. The line number, hence, is changed by moving the test pattern slide to bring different line sizes under the calibrating light slit which remains in a fixed position.

The base plate carrying the lens and focussing adjustment is equipped with a "flat field" indicator ((F) in Figure 70), a knife-edge slider which can be moved in a guide set perpendicular to the lens axis. The lens image is brought into focus coinciding with the knife edge for axial rays. This lens setting with respect to the slider guide is maintained throughout one measurement series. For angular measurements the entire mount base is rotated and the slider, moved to indicate the image plane at the selected angle, is brought into focus by moving the mount base with respect to the microscope objective. This operation requires several trials to line up calibration slit, slider, and the image section under observation. It solves automatically for the nodal point of the lens. The object-to-image distance is of course increased by $1/\cos\theta$ for the particular angle.

The aperture response of photographic film (test patterns) is measured in a similar manner by placing the film directly in front of the microscope objective. The aperture effect of translucent grain struc-

tures has been measured by projecting a sharp optical image on the grain structure which is placed in the focal plane of the microscope.

The number of bars in test-pattern line groups should be sufficient to allow the flux wave to build up to a steady value (See Part II, Figure 14, page 248). It is, therefore, recommended to use *at least* four black bars at line numbers between $N\delta$ and N_c; two bars being sufficient below $N = N\delta$. The line groups should be separated by alternate black and white spaces of sufficient length which serve to give "level" signals. (See Figures 61 and 72).

By definition, the aperture response factors are independent of the absolute image contrast. The contrast reduction by microscope objectives is, therefore, of no consequence. Measurements with test patterns of low contrast ($C = 1.5$) have shown in some cases a slight increase of $r\Delta\overline{\psi}$ in the high-resolution section of the response curve in comparison with high-contrast patterns ($C \simeq 1000$). Positive and negative patterns gave identical results. The reference calibration $r\Delta\overline{\psi}$ at $N = o$ and zero angle is obtained by measuring the white-to-black signals between the shadow cast by the knife edge slider in the image plane and the white background of the test pattern image. Lens flare has normally little effect on the measurement and should be determined separately. It should be mentioned that the color temperature of the light source should be adjusted by filters to result in a reasonably uniform response from the camera tube for red, green, and blue light of normal spectral energy to avoid misinterpretation of chromatic aberration effects in "white"-light-response measurements.

ELECTRO-OPTICAL CHARACTERISTICS OF TLEVISION SYSTEMS*†

By

Otto H. Schade

Tube Department, RCA Victor Division,
Harrison, N. J.

NOTE: This paper consists of an Introduction and four parts: Part I—Characteristics of Vision and Visual Systems; Part II—Electro-Optical Specifications for Television Systems; Part III—Electro-Optical Characteristics of Camera Systems; Part IV—Correlation and Evaluation of Electro-Optical Characteristics of Imaging Systems. The Introduction and Part I appeared in the March 1948 issue of RCA Review, Part II in the June 1948 issue, and Part III in the September 1948 issue. Part IV, the concluding part, follows.

PART IV — CORRELATION AND EVALUATION OF ELECTRO-OPTICAL CHARACTERISTICS OF IMAGING SYSTEMS

Summary—Principal characteristics of the motion picture process are evaluated and co-ordinated with the television process by determining the transfer characteristics, signal-to-fluctuation ratios, and the aperture flux response of photographic film. A quantitative analysis and comparison of the performance of specific imaging systems such as the standard television and motion picture system is undertaken. The transfer characteristics of the image orthicon and the gradation scale of television images are treated in greater detail, and the critical brightness for threshold grain visibility (noise) is determined from the optical signal-to-fluctuation ratio in the reproduced image.

Methods for increasing the image sharpness are shown to be processes adding a negative "aperture" characteristic to the system. A general curve for a subjective rating of image sharpness is established by combining the "aperture"-response characteristics of the eye and the external imaging process.

A. Characteristics of the Motion Picture Process

Photographic film is used extensively in television systems as a source of picture signals, particularly in the form of motion picture film. A brief analysis is made to co-ordinate the characteristics of the photographic process and the silver image on positive film with the television process.

1. *Signal-to-Fluctuation Ratios and Transfer Characteristics*

The principles of the photoelectric and energy-storing processes in

---

* Decimal Classification: R138.3×R583.12.
† Reprinted from *RCA Review*, December, 1948.

photographic and television cameras have been discussed in Part IIIA. It is known that, when photographic film is exposed to light, photoelectric action produces a certain number of submicroscopic silver "specks" which are subsequently developed into much larger silver grains. The number of grains per unit area is proportional to the photographic density D and increases with exposure E according to a law of diminishing returns. Because the grain distribution is substantially random and grain sizes are controlled to remain within certain limits for a particular film type, signal and fluctuations in the primary process (light to grain number) are determined fundamentally by the number n' of "equivalent" grains in a given picture element area a as outlined in Part IIIA, Equation (40).*

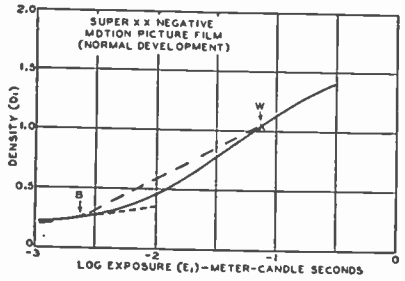

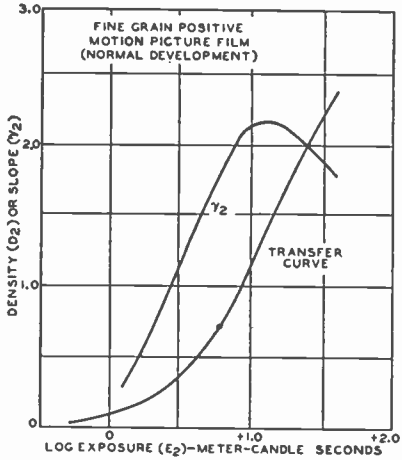

Fig. 73 — Transfer characteristics of motion picture film.

The normal sensitometric curves of film $D = f(\log E)$

shown in Figure 73 may, therefore, be regarded also as a graph of the relative silver grain density n'/a as a function of exposure E in semi-logarithmic coordinates and may thus be compared directly with the transfer characteristics of the camera tube shown in Part III, Figures 66 and 67. The signal-to-rms fluctuation ratio $|R|_D$ of the primary process can, therefore, be computed with Equation (40) and may be written

$$|R|_D = D/(D/n')^{\frac{1}{2}} \tag{83}$$

where n' is the number of equivalent grains at the density D of 1 in a selected elemental area a. In the secondary (copying) process of light modulation by the film, the new transfer characteristic $\tau = f(D)$ is introduced and the fluctuation ratio is altered because of the

* Deviations from the theory occur near the ends of the transfer range as in most practical processes.

reciprocal logarithmic relation between density and transmission τ, $D = 1/\log \tau$. The modified ratio $|R|_1$ in the light-signal transmitted by the negative film is inverted and increases with the transmission τ as computed from the rms density fluctuation or deviation

$$\Delta D_1 = (D_1/n')^{\frac{1}{2}} = \log \Delta\tau_1/\tau_1 \quad (84a) \qquad \text{and} \qquad |R|_1 = \tau_1/\Delta\tau_1. \quad (84b)$$

The ratios $|R|_D$ and $|R|_1$ are shown in Figure 74 as a function of negative film transmission τ_1 for a grain number n' of 100 per element at unit density D of 1. To represent a particular film type, the picture element a must be specified, or, for a specified elemental area (channel width), $|R|_1$ is to be determined by a grain count or by measurement (See page 657).

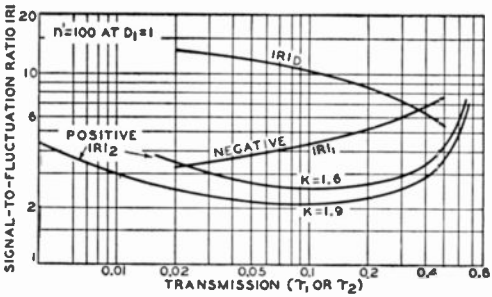

Fig. 74—Signal-to-fluctuation ratios in the motion picture process:
For $\overline{N}_{ee} = 410$ and Super XX negative film, multiply $|R|$ by 5.25
For $\overline{N}_{ee} = 410$ and Panatomic X negative film multiply $|R|$ by 7.8

The theoretical change of $|R|_1$ from $\tau = 0.06$ to $\tau = 0.44$ is confirmed by the oscillograms, Figure 75, taken with the television microphotometer on Super XX film. The ratio of signal (pulse at right hand side) to peak-to-peak fluctuation agrees in relative magnitude with the computed values in Figure 74.

Signal and fluctuations undergo further changes in the copying process from the low-gamma negative to a higher-gamma positive film which causes, in general, an expansion of the light signal. The ratio $|R|_1$ is, therefore, reduced to a lower value $|R|_2$ (See Part III, A5). Because of logarithmic transfer relations, the exposure E_2 of the positive film is given by

$$\log E_2 = K - D_1 \quad (85)$$

where K is a constant specifying the exposure level. Typical overall transfer characteristics, $\tau_2 = f(E_1)$, for a motion picture film process computed with the values $K = 1.6$ and 1.9 and the film characteristics, Figure 73, are shown in Figure 76. The modified fluctuation ratio $|R|_2 = \tau_2/\Delta\tau_2$ (See Figure 74) is computed with Equation (84) by multiplying the deviation ΔD_1 by the associated positive film gamma:

$$\Delta D_2 = \Delta D_1 \gamma_2 = \log \Delta\tau_2/\tau_2 \qquad \text{and} \qquad |R|_2 = \tau_2/\Delta\tau_2. \tag{86}$$

This value $|R|_2$ does not contain fluctuations introduced by the positive film grain which add in quadrature, but these can be neglected when the positive film has a finer grain than the negative film.

2. Equivalent Optical and Electrical Channels for Random Fluctuations

The picture element a defined by a physical aperture of uniform transmission (square or round) for the purpose of a grain count or a scanning operation is not equivalent in size to the picture element defined by a sharply terminated electrical channel with uniform frequency response (See Part III, A1). The electrical channel Δf of the television system cuts off the uniformly distributed frequency components of random fluctuations at a frequency corresponding to the balanced line number $\overline{N}_{co}$ (See Part I, B2).

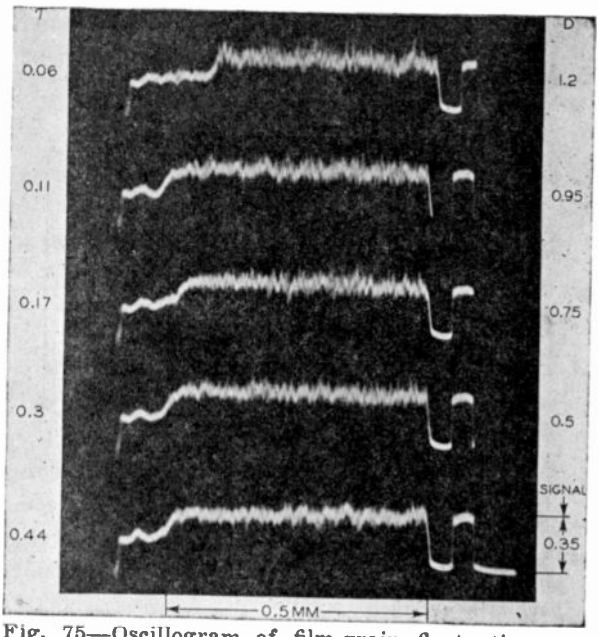

Fig. 75—Oscillogram of film-grain fluctuations at five different densities.

The size of the physical "aperture" duplicating the effect of a square-cutting electrical filter on the rms value of fluctuations can be established from the response characteristic of the scanning aperture to *sine-wave* flux patterns of constant amplitude. The "filter factor" m for random fluctuations is then determined as outlined in Part I, B2, pp29.* The sine-wave response of a square aperture is

* The filter factors given in Part I for the eye and kinescope were computed from the equivalent square-wave response ($r\Delta\bar{\gamma}$), because the sine-wave response was not known. The values m are, therefore, somewhat too low for channels near and beyond eye resolution. The filter factor computed from the equivalent square-wave response in the total pass band of the square aperture is $m' = 0.58$ as compared to the correct sine-wave value $m = 0.66$.

given by the $(\sin x)/x$ function (Figure 77). The filter factor computed from this "frequency response" curve has the value m of 0.66 for a channel extending to the first zero N_c. The equivalent electrical channel of constant frequency response ($m = 1$) extends, therefore, to the line number $\overline{N}_{co} = m\,N_c = 0.66\,N_c$ (87)

As the size of the square aperture is $\delta = V/(N_\delta) = 2V/N_c$ (See Part IIA) we obtain $\delta = V/(N_\delta) = 1.32\,V/\overline{N}_{co}$ (square aperture). (88)

The diameter of a round aperture of equal area is larger by $\sqrt{4/\pi}$. The equivalent round aperture is, hence, approximated by

$$\delta = 1.49\,V/\overline{N}_{co} \text{ (round aperture)}. \quad (89)$$

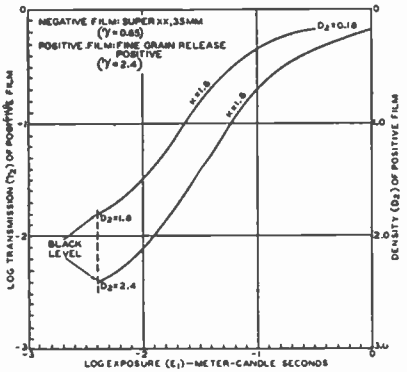

Fig. 76—Over-all transfer characteristic of motion picture film process.

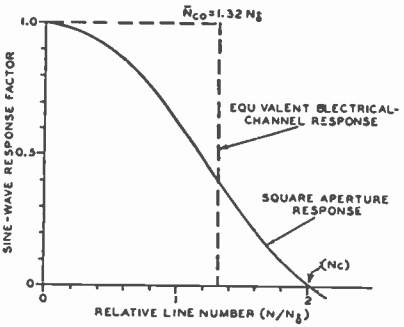

Fig. 77—Sine-wave response characteristics with equal filter effect on the RMS value of random fluctuations.

The filtering effect of a (standard) television channel ($\Delta f = 4.25$ megacycles) with the balanced line number $\overline{N}_{co}$ of 410 can, therefore, be duplicated on film by a grain count or a scanning operation with the equivalent round aperture given by equation (89). For 35-millimeter film with the vertical frame size of 15.7 millimeters, the aperture diameter is $\delta = 57$ microns.

Jones and Higgins[31] have measured rms fluctuation values by scanning with a round aperture $\delta' = 39$ microns. Their values (See Table VIII) multiplied by the aperture ratio $\delta/\delta' = 57/39$ furnish the rms

[31] L. A. Jones and G. C. Higgins, "Photographic Granularity and Graininess", *Jour. Opt. Soc. Amer.*, Vol. 36, No. 4, pp. 203-207, April, 1946.

value $|R|_1$ of negative film as modified by the filter effect of a standard television channel. The corresponding fluctuation ratios $|R|_1$ and $|R|_2$ of motion picture film processes using Super XX or Panatomic X negative film are established by multiplying the $|R|$-scale in Figure 74 by the respective ratios $34.1/6.5 = 5.25$ or $52.1/6.7 = 7.8$. The relative "graininess" of motion picture and television images as seen by the eye will be discussed later.

Table VIII—Signal-to-Fluctuation Ratios of Photographic Film.

Film Type	Density	τ_1	$\|R\|_1$* ($\delta = 39\mu$)	$\|R\|_1$ ($\delta = 57\mu$)
Super XX	0.43	0.37	23.3	34.1
Panatomic X	0.4	0.396	35.7	52.1

* Values from reference (31).

The equivalent grain number n'_{57} for a 57-micron circle on Super XX film can be computed by multiplying the number $n' = 100$ assumed for Figure 74 by 5.25^2. This furnishes $n'_{57} \simeq 2750$ for $D = 1$. A 10-micron *square* contains $n'_{10} \simeq 100$ average grains. The side of this elemental area is equal to one line width at the limiting resolution of this film ($N_c = 100$ lines per millimeter) and indicates five grain layers, each layer containing approximately 4.5×4.5 spaced grains, with an average grain diameter in the order of 1 micron.

Microphotometer measurements of grain structures confirm that finer grains and fewer layers result, in general, in a higher limiting resolution; while high signal-to-fluctuation ratios require a large number of preferably similar grains within the considered element size to form a more continuous layer of closely packed grains side by side or staggered in depth.

3. Resolving Power, Contrast, and Aperture Response Characteristics

The resolving power N_c and the aperture flux response characteristic $r\Delta\bar{\psi} = f(N)$ of film, depend on the size of its silver grains and the number of grain layers (thickness of emulsion). Observations on a number of film types indicate a line width $1/N_c$ at the limiting resolution in the order of 6 to 10 average grain diameters. When the test signals are large, the response characteristic $r\Delta\bar{\psi}$ of a single film process is distorted by the exponential light transfer characteristic. To establish a reference to *the rated resolving power* of film which is determined with large signals, i.e., a test pattern contrast $C = 20$ to 30, measurements with this contrast have been made on several film types with the television microphotometer (See Part III). Typical

oscillograms are shown in Figure 78. A correction for lens response errors according to Equation (30), Part II, is necessary when measuring film with a resolution $N_c > 100$ television lines per millimeter. The response curve for a test object contrast $C \simeq 25$ is approximated quite well in the range $N/N_c < 0.8$ by $r\Delta\overline{\psi} = e^{-3.5\,N/N_c}$ (80)

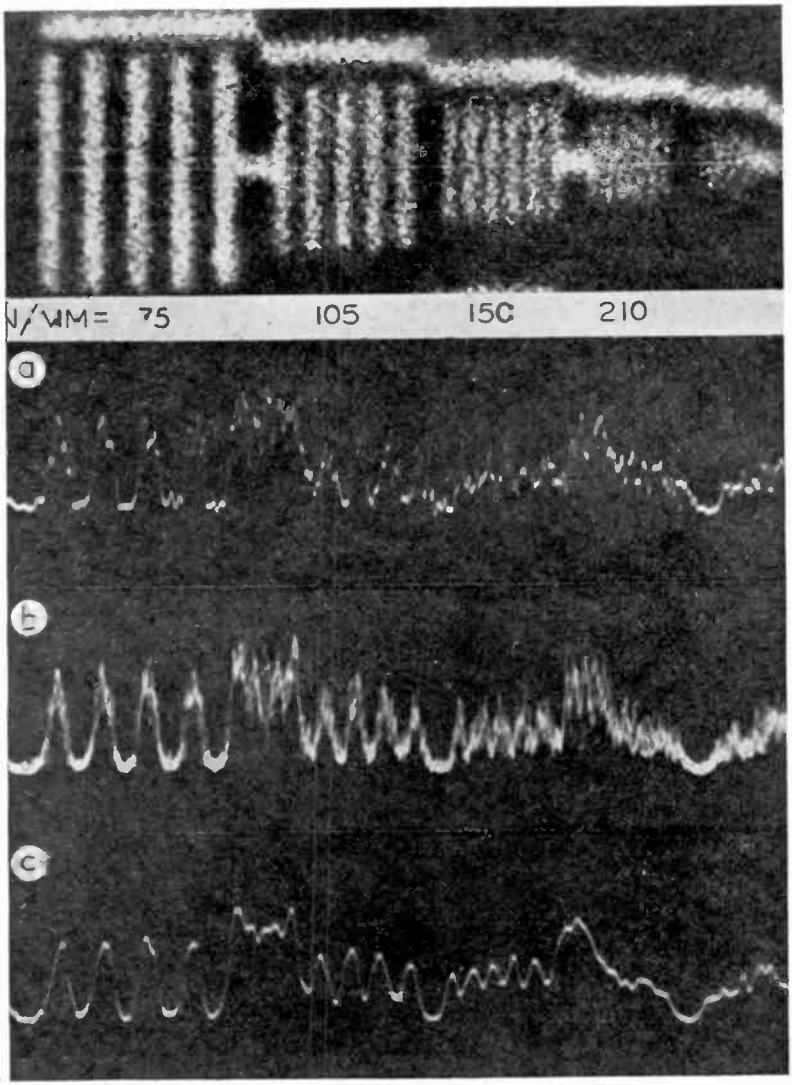

Fig. 78—Kinescope image and microphotometer traces showing limiting resolution of microfile film. a. Single line cross section. b. Six line cross sections superimposed. c. Single line cross section traced with larger scanning beam not resolving individual grains.

(Figure 79) where N_e is the rated resolving power* of the film type.

Response factors obtained with smaller signals, i.e., with a test object contrast $C = 2$, are more significant because the transfer characteristic is fairly linear for these increments. A series of measurements made with $C = 2$ on Super XX 35-millimeter film gave substantially the same values $r\Delta\bar{\psi}$ for exposures E_1 varied over a range of 20 to 1. The response curve, Figure 80, is a typical aperture response characteristic with a limiting resolution N_e equal to approximately 80 per cent of the rated value. Transfer of the negative test pattern into a positive causes further decrease of resolution due to the cascaded aperture effect of the second film. According to Equation (30), Part II, a positive film with double resolving power decreases the resolution by 10 per cent. This value is in substantial agreement with measured values (Figure 80). The signal distortion of the negative film is largely eliminated by the positive process. The response curves for $C = 25$ and $C = 2$ coincide in the positives except near cutoff which depends in visibility on the signal-to-fluctuation ratio. The flux response curves $r\Delta\bar{\psi}$ for positives made from negatives taken on Super XX film are representative of the performance of 35-millimeter motion picture film. The measurements furnish the values $N_e \simeq 75$ lines per millimeter and the value at 50-per cent response $N_{0.5} = 21$ lines per millimeter. For the 35-millimeter frame size $V = 15.7$ millimeters, the corresponding values are $N_e \cong 1175$ and $N_{0.5} = 330$ television lines.

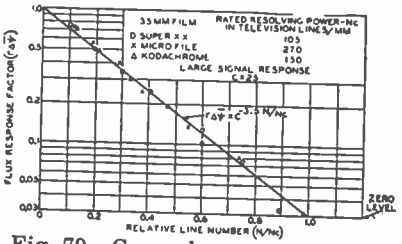

Fig. 79—General aperture response characteristics of photographic film for large signals.

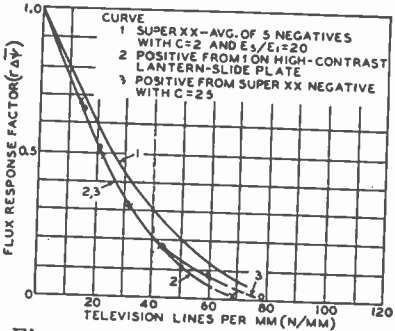

Fig. 80 — Aperture response of Super XX film before and after transfer on fine-grain positive film.

It is possible to obtain higher aperture-response factors with large signals because non-linear film characteristics can act as peak limiters, and, by properly adjusted exposures, can suppress grain and square up sinusoidal waveforms. A resolution test made in this manner is obviously not indicating a normal aperture response because such exposures

* This value N_e corresponds to $r\Delta\bar{\psi} \sim 0.03$: higher values correspond to lower response factors.

destroy normal gradation. The "clipping" action, however, can be used to advantage when making test patterns.

B. The Over-All Characteristics of Television and Motion Picture Systems

1. *Sensitivity and Scene Luminance*

The scene luminance B_o required for a normal "exposure" in a photographic or television camera is determined basically by the photosensitivity and storage capacity of the particular film type or photo surface of the camera tube (See Part III). The sensitivity of the imaging system (for a given photosensitivity or "quantum" efficiency) decreases inversely with the storage capacity, but the image quality increases because larger energies result in higher signal-to-fluctuation ratios $|R|$, better resolution $\overline{N}_{co}$, or both, depending on the particular system. The scene luminance must be increased as the square of $|R|$ or $\overline{N}_{co}$. (See Equation (44), Part III). The criterion for a normal photographic exposure is the rendition of tone values near the "black" level. The *exposure index* of film (Weston, G. E., or ASA Exposure Index) is based on a light range of 30 to 1 on the film curve (See B to W in Figure 73) so positioned that the slope of the curve at point B is ⅓ the slope of the straight line connecting points B and W. The "Kodak" speed $1/E$ is determined from the exposure E (meter candles $\times$ seconds) required for the black-level point B. Because Super XX film requires $E = 0.0025$, its Kodak speed is $1/E = 400$. Weston and G.E. speed ratings are obtained by multiplication with the factors 0.25 and 0.4, respectively, and have the values 100 and 160.

The speed index of camera tubes may be computed for comparison. The illumination E_i for point B on the characteristic of a high-capacitance image orthicon (Figure 67b, Part III) is $E_i = 0.008$ foot-candles for normal picture content. Because the exposure time T_f is 1/30 second, the exposure index (meter-candle seconds) is $1/E = 30/0.085 = 350$, corresponding to a Weston speed of 88. The close match with Super XX film in this example is incidental and misleading as high-capacitance tubes are not limited to the photosensitivity of the tube used for the example and have been built with higher photosensitivity. (See S for type 2P23 in Table VII, Part III). A more adequate basis for a comparison is the light flux required for equal performance, i.e., equal depth of focus, signal-to-fluctuation ratio, transfer range, and resolution. If this comparison is carried out, an image orthicon with seven times the intrinsic photosensitivity of the tube used for the example will be found to require approximately the same light flux as Super XX 35-millimeter motion picture film. (Com-

parisons of the over-all transfer characteristic, signal-to-fluctuation ratio, and resolution of the two systems are made in subsequent sections). Experimental tubes with even higher photosensitivity have been made.

A sensitivity rating of an image pickup device is frequently based on the light flux required for obtaining an image of reduced quality (lower $|R|$). When the scene luminance is reduced, the television system becomes increasingly more sensitive and surpasses the film camera, which ceases to function at light flux values considerably higher than the threshold value of the television camera.[26] The loss of sensitivity in high-quality operation of the image orthicon is caused partially by a loss of charge storage due to electron redistribution which is instrumental in obtaining a longer tone range.

A specification of the scene luminance required for a given fluctuation ratio $|R|$ and depth of focus is more informative than a "speed" rating. The high-light luminance $\hat{B}_o$ for the television camera may be computed in four steps:

1) Determine the lens diameter δ for the required depth of focus. (Equation (73), Part III)
2) Compute $|R|_{max}$ for the storage capacitance C of the camera tube. (For electron multiplier types, Equation (52), Part III)
3) Compute the image flux $\psi_{i(R)}$ (Equation (78) or (82) and Table VII, Part III)
4) The high-light luminance is then given by $\hat{B}_o = \psi_{i(R)}/g_o$ (Equation (61), Part III)

The light flux values plotted in Figure 68, Part III have been corrected for the decreasing transfer efficiency at higher light levels. Lens diameters and optical transfer factors g_o are given in Table VI, Part III for a depth of focus equal to the vertical scene dimension. The high-light luminance $\hat{B}_o$ (white card reading in foot-lamberts) for this depth of focus has been computed for various values $|R|$ and several camera tube types and is given in Table IX.

Table IX

$\lvert R\rvert_{max}$	Iconoscope $\hat{B}_o$ foot-lamberts for $\rho =$				Image Orthicon 5655 $\hat{B}_o$ foot-lamberts for $\rho =$				Image Orthicon 2P23 $\hat{B}_o$ foot-lamberts for $\rho =$			
	ψ_i	2.5	4.	8	ψ_i	2.5	4	8	ψ_i	2.5	4	8
150	0.8	720	190	7750	0.08	72	190.	775.				
100	0.15	360	950	3870	0.009	21.6	57	232				
50	0.05	120	317	1290	0.0018	4.3	11	464	0.0008	1.9	5.2	20.6
25									0.00015	0.36	0.95	3.9

The values $\hat{B}_o$ required for "close-ups" ($\rho = 8$) are prohibitive for the iconoscope, which has to be operated with a larger lens opening at a sacrifice of depth of field. (The lens stops for the conditions in Table IX can be found in Table VI, Part III for various camera plate sizes.) The high sensitivity of the image orthicon has permitted a considerable increase in the depth of the sharply imaged field at normal illumination levels.

2. Over-all Transfer Characteristics

The light transfer characteristics of modern television camera tubes cover a dynamic light range in the order of 100 to 1. This range increases somewhat for scenes with low average brightness but may decrease substantially due to electron redistribution effects and over-exposure when scenes with large high-light areas are transmitted (Compare Part III). Television camera tubes have a smaller latitude than photographic film and are perhaps more sensitive to errors in exposure when optimum performance is desired. This is particularly true of the type 2P23 image orthicon because of its relatively low storage capacitance and high photosensitivity. To illustrate the performance of image orthicons, a series of oscillograms, Figures 81 to 86, have been taken which show a signal cross-section from a photographic step tablet covering a light range of 100 to 1 (20 db) in 2 db steps. The linear time base corresponds, therefore, to a logarithmic step-exposure scale. Because the current scale is linear, the oscillogram is a transfer characteristic in semi-log coordinates. The step tablet is a film strip 8 millimeters wide and 85 millimeters long in an 8×10 inch viewing field. The end steps are opaque to produce black level pulses on the oscilloscope. The strip is placed vertically in front of an illuminator and the electrical response is observed with a vertical cross-section selector. Figures 81 and 82 show a composite photographic print of three transfer characteristics of the 2P23 and 5655 image orthicons obtained from the step tablet when surrounded by a high-light field.

The oscillograms illustrate clearly the black compression caused by redistributed electrons and secondaries from the collector screen when the "target bias" is too small (1 volt). In a dark background, the discharge of potentials is considerably reduced and confined to the step edges as shown by the sawtooth step shape in Figures 83 and 84. Shadow detail is found, in many cases, in darker sections of the scene and high-light detail in light sections. This condition is shown in Figure 85a, where the dark section of the step tablet was placed in a black field and the light section in a white field as indicated by the black and white level lines under and over the oscillogram trace. Figure

85b shows the reverse case. A comparison with Figures 82 and 84 indicates that the discharge by mesh secondaries (1-volt potential) from adjacent high-light regions does not extend over large distances. The effect of varying the exposure is illustrated by Figure 86 for a 2.7-volt potential limit and a two-level background. (The *f:* numbers of the camera lens indicate the relative exposure.) It should be noted that edge effects maintain visibility of the step contours even in over-exposures (sawtooth shape of steps) but do not reproduce the differences of actual tone values.

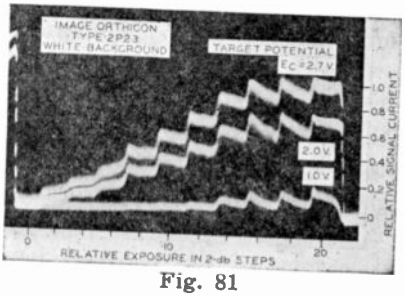

Fig. 81

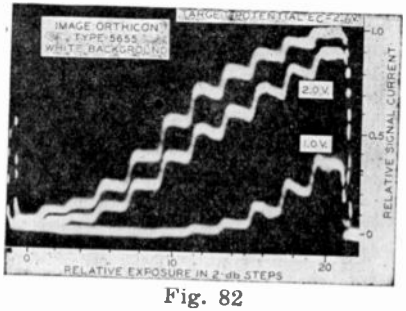

Fig. 82

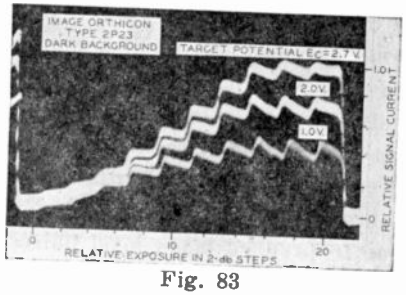

Fig. 83

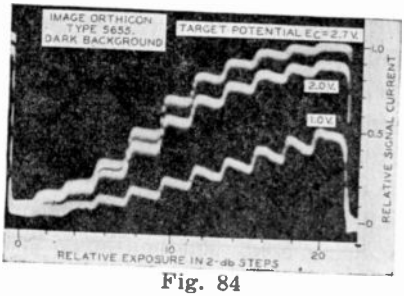

Fig. 84

Oscillograms of dynamic transfer characteristics of image orthicons (20 db = 100:1 range)

The oscillograms of the dynamic transfer characteristics give proof that the major difference between the 2P23 and 5655 camera tubes is their storage capacitance and photosensitivity, the 5655 giving a higher signal-to-fluctuation ratio but requiring a higher scene luminance (See Table IX). To prevent overexposure and undesirable relief effects and to obtain good shadow detail it is good practice in the studio to avoid too large a contrast range, (i.e., heavy shadows) by the use of soft "basic" lighting and by employing modeling lights of moderate intensity. In order to compute the over-all light transfer characteristic of the television system it is necessary to take into account optical effects modifying the static transfer characteristic of the kinescope, which otherwise follows essentially a 3rd power law.

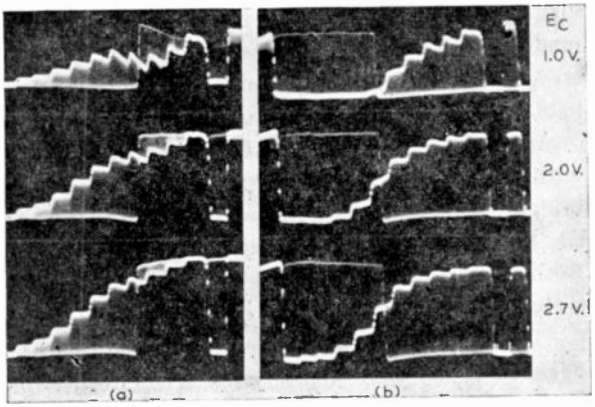

Fig. 85 — Oscillograms of dynamic transfer characteristics of a 5655 image orthicon with two-level background.

(a) Low light range in dark background, high light range in white background.

(b) Low light range in white background, high light range in dark background.

The range of the dynamic kinescope operating characteristic is reduced by a light bias of 1 or 2 per cent as shown in Figure 87. A light bias of this order can occur in a dark room because of light diffusion in the screen material and reflection on the glass surfaces. This "flare" light bias is actually not uniform and decreases in a manner similar to "lens flare" with distance from a high-light area (See B1*b*, Part III).

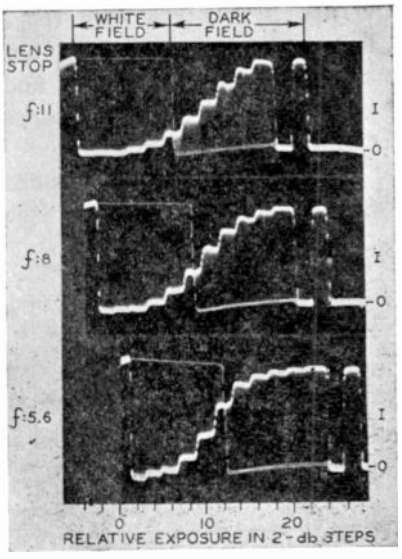

Fig. 86—Oscillograms of dynamic transfer characteristics of a 5655 image orthicon at target potential $E_c = 2.7$ volts with two-level background for three different exposures.

The over-all transfer characteristics in Figure 88 have been computed in the usual manner for the image orthicon operation shown in Figure 82, a *linear* amplifier characteristic, and the kinescope characteristic Figure 87. A simple

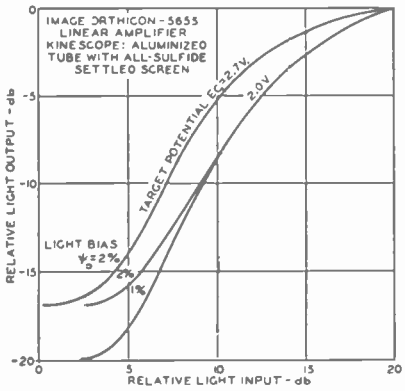

Fig. 88—Light-transfer characteristics of television process (ψ_b = combined ambient and flare light flux).

visual test for linearity of the over-all transfer characteristic can be made by reproducing a logarithmic step tablet and comparing it with an identical step tablet placed over a white background of the kinescope field parallel to the reproduced tablet. A direct measurement of the over-all characteristic can be made by covering the kinescope field with a black mask having a slit over the vertically positioned step tablet image and observing the oscilloscope trace (60-cycle sweep) of the modulated light output by means of a 931-A multiplier phototube. Both tests are in good agreement with the computed transfer characteristic.

The over-all transfer curve of a 35-millimeter motion picture system, Figure 89, has been constructed from Figure 76 by adding the effects of lens flare and ambient light. A light bias of 2 per cent is probably near the minimum value obtainable for the brightness levels in motion picture theaters. A comparison with the television transfer curve, Figure 88, reveals off-hand only minor differences. A slightly increased range in light input can be covered by the television system by introducing an amplifier transfer characteristic with moderate logarithmic compression, provided the camera tube is correctly adjusted and exposed. The corresponding reduction in contrast difference (lower slope), however, is not necessarily an advantage, and particularly not in the presence of ambient room light.

Camera tubes with constant transfer efficiency such as the

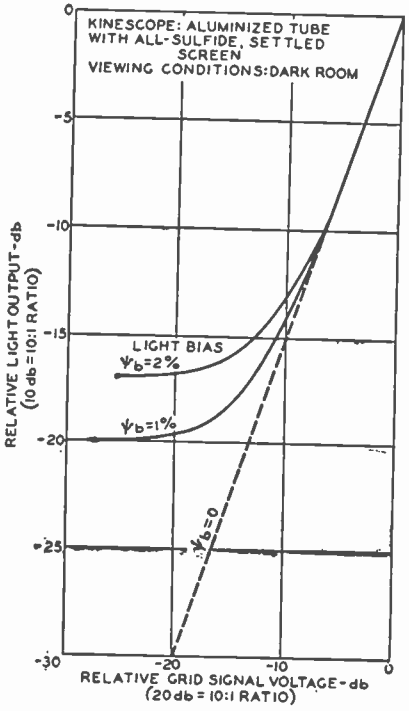

Fig. 87—Dynamic transfer characteristics of kinescope.

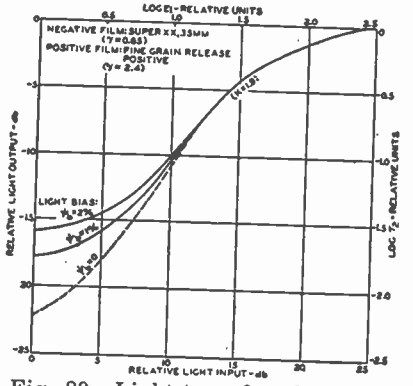

Fig. 89—Light-transfer characteristics of motion picture process (ψ_b = combined ambient and lens flare light flux).

orthicon, or a system generating video signals by a light-spot scanner (flying-spot systems), require a considerable compression of signals in the amplifier to obtain linearity in the over-all transfer curve. The amplifier is given a characteristic which is the inverse of the kinescope transfer curve inclusive of flare light bias (Figure 87) because the signal from these pickup devices is linearly related to the light input.

The contrast scale of normal television and motion picture systems falls somewhat short of a 100 to 1 range which has been considered a desirable standard (See Part I). Halation and light scattering in the kinescope or ambient light and lens flare are largely responsible for the reduction of image contrast. A gradual compression of signal values (low-"gamma" negative) is expedient in the film process to preserve a long tone scale when the object light range is large; but it does not produce similar effects in a television camera chain, because present storage-type camera tubes cannot reproduce a dynamic light range exceeding at best a ratio of 100 to 1. Upon further examination it is observed that the mechanism for obtaining a longer signal range in storage-type camera tubes (gradual saturation) causes redistribution effects, which are responsible for "shading" over larger areas or cause more localized deviations from normal signal levels (sawtooth shape of steps in oscillograms).

These "spurious signals" affect the smoothness or texture of the image. In image orthicons the redistribution and spurious effects decrease when the exposure is reduced, the shortened range resulting in a better tone quality. This limitation is, of course, not an inherent characteristic of a television system, but at present, the shorter latitude of the camera tube can be accommodated by advantageous and skillful lighting in the television studio.

3. *"Grain" Visibility, Brightness, and Optical Signal-to-Fluctuation Ratios*

The visibility of random brightness fluctuations as a function of the optical channel width $\overline{N}_{co}$ provided by a television system and taking into account the filtering action of the eye and kinescope has been discussed in Part I. The relatively high maximum values $|R|_{max} =$ 300 to 500 for the electrical signal given in Part II, page 283, are not obtainable with present camera tubes, nor are they realized by the motion picture process. These values were based on a peak brightness of 32 foot-lamberts. Because the visibility of "grain" fluctuations decreases with brightness, a comparison of the television image with motion pictures should be made at the brightness level of a 35-millimeter film projection which is less than 10 foot-lamberts. The threshold visibility of grain fluctuations in a 4.25-megacycle channel at a viewing

ratio $\rho = 4$ was, therefore, determined by measurements. The optical ratio $|R|_o$ for threshold grain visibility is plotted in Figure 90 as a function of brightness for an unmodulated viewing field (curve 0) and for fields containing a normal picture modulation (curves A and B). Curve 0 was obtained as follows: known electrical fluctuation ratios were generated with a light-spot scanner followed by a linear amplifier. The optical ratio from the kinescope screen is computed as one-third of the electrical values because of the 3rd-power expansion by the kinescope transfer characteristic (See Part III, A5). The amplifier gain was then adjusted to a screen brightness (with respect to the correct black level) for which threshold visibility occurs at $\rho = 4$. This

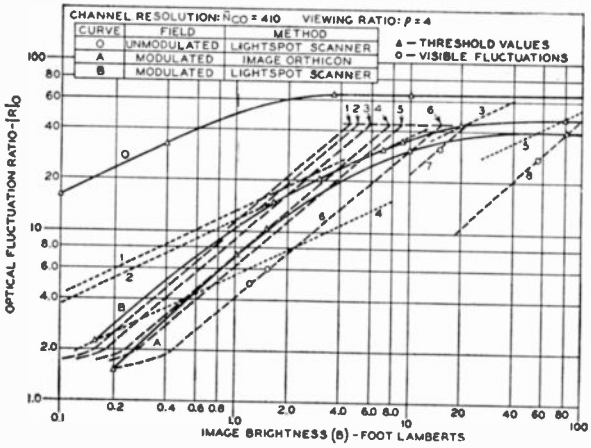

Fig. 90 — Development of characteristic curves of the optical signal-to-fluctuation ratio $|R|_o$ for threshold grain visibility at various brightness levels.

brightness was measured with an illuminometer. Curve 0 is in agreement with the value for $\overline{N}_{ro} = 410$ and $B > 2$ foot-lamberts shown on Table I, Part I, for the eye alone, because the kinescope used in the earlier computations (Figure 13, Part I, page 35) has been replaced by a tube with very high response ($r\Delta\bar{\psi} = 0.8$ at $N = 500$; curve 1 in Figure 42, Part I, page 282).

The visibility of random fluctuations is reduced considerably when the field is modulated by image signals and was measured as follows. Curve A was determined with a 5655 image orthicon giving the measured *electrical* fluctuation ratio $|R|_{max} = 130$. Four 8×10-inch Kodachrome transparencies were used as a source of picture signals, one being a high-key image, one a low-key image, the third one contained a large white area, and the fourth one contained well-distributed tone values in small areas. The optical signal-to-fluctuation ratio on the kinescope was computed for a linear amplifier from the transfer characteristic shown in Figure 88 and varies with signal as shown by the dashed lines (1 to 8) in Figure 90. The maximum *optical* fluctuation

ratio of the system was, therefore, one third of the electrical ratio, i.e., $|R|_{max}$ (optical) $\simeq 43$. By varying the signal strength (gain of the linear amplifier), the $|R|$ curve is displaced horizontally in Figure 90. Curves 1 to 8 yielded "noise"-free pictures; and curve 4 gave threshold visibility of fluctuations in the middle tone range, curve 6 gave visible fluctuation in the middle tone range and threshold visibility at a high and a low brightness value. The threshold ratio curve is thus determined by measurement of the brightness values giving threshold grain visibility. Variation of the image content disclosed no noticeable change in the observed threshold values. The low-key image was found to be reproducible without fluctuations at a higher peak brightness (See curve 5) because it contained middle tone values only in small detail areas.

Curve *B* was determined in a similar manner by slide pickup with a light-spot scanner. Because the amplifier was linear, the $|R|$-curves for this signal source retain substantially a ½-power slope over nearly the entire image-brightness range and the optical grain-fluctuation ratio is again reduced to ⅓ by the kinescope expansion. In view of the normal spread of data which is to be expected in observations of this type, the agreement of the two methods (A and B) is quite satisfactory.

The mean curve *M* shown in Figure 91 represents, in good approximation, the critical optical ratio $|R|_o$ for threshold visibility of grain fluctuations in a television channel or an equivalent optical channel with $\overline{N}_{co} = 410$. (The kinescope filter factor can be neglected.)

Fluctuation-free images are obtained at brightness values placing the $|R|$ curve of the imaging system to the left or tangent to the threshold curve. The tangent curve *A* represents a television system using a storage-type tube such as the image orthicon or iconoscope. Because the optical fluctuation ratio is very close to ⅓ of the electrical ratio produced by the camera tube, an electrical ratio of $|R|_{max} = 150$ permits a maximum image brightness $\hat{B} = 7$ foot-lamberts for a fluctuation-free kinescope image at $\rho = 4$. The brightness $\hat{B}$ may be increased by perhaps a factor of two without objectionable fluctuations (curve 1) which are visible in practically all tone values of the image.

Curve *B* of Figure 91 represents the condition for grain-free images from a linear signal source such as a light-spot scanner (no auxiliary currents causing fluctuations). When the over-all transfer characteristic is linearized by electrical compensation of the kinescope characteristic, the electrical and optical ratios $|R|$ coincide. A ratio $|R|_{max} = 75$ is easily obtainable with normal slide or motion picture densities and yields grain-free images with a peak brightness $\hat{B}$ near 50 foot-lamberts. An increase of $\hat{B}$ to 100 foot-lamberts (curve 2) causes

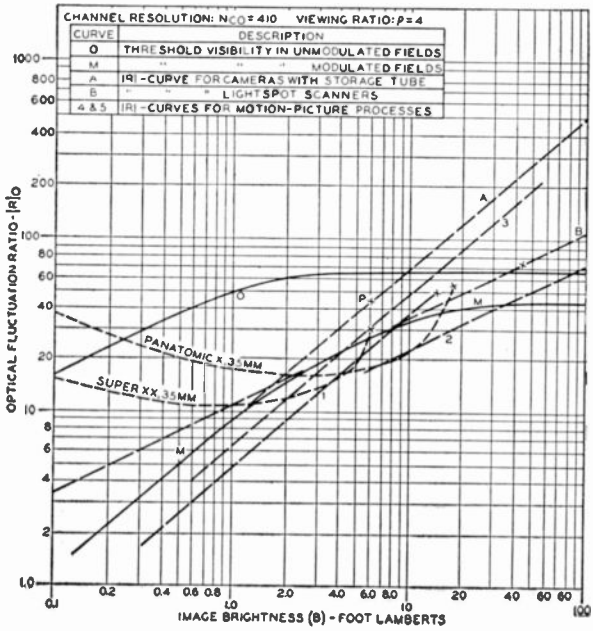

Fig. 91—Location of $|R|$-characteristics for various imaging processes with respect to threshold visibility curve of grain fluctuations.

visible fluctuations in the middle tone values. Substantially grain-free images at $\hat{B} = 50$ foot-lamberts from an image orthicon chain (curve 3) require high electrical ratios in the order $|R|_{max} = 600$ as indicated in Part I.

Reproduction of a 35-millimeter motion picture film at normal theater brightness over an ideal television channel with $\overline{N}_{co} = 410$ places the grain fluctuation characteristic $|R|_2$ (See Figure 74) in the position shown by the Super XX curve in Figure 91. A direct optical projection of the film results in practically the same positioning, because the increased bandwidth and the better storage factor ($s' = 1.5$, See Part III, page 494 et seq.) cancel each other. The characteristic computed for Super XX negative film appears to be in good agreement with visual observations in motion picture houses, because it indicates a grain-free reproduction of shadows and some graininess in the lighter middle tones and high lights. In comparison with an image orthicon camera chain ($\hat{B}$ = point P, curve A), the 35-millimeter motion picture Super XX offers no advantage at equal brightness values. At television brightness levels, the middle and lower tone values of the film move into the fluctuation region. A slower negative material with fine grain, such as Panatomic X film, permits a brightness increase to $\hat{B} \cong 17$ foot-lamberts as shown in Figure 91. The fluctuation curves for 16-millimeter motion pictures are lower by a factor of two on the $|R|$-scale unless the film is a reduction print made from 35-millimeter negative film.

It is quite apparent that the grain of motion picture film can be "seen" over a good standard television system and that it is nearly always controlling the fluctuation level in television reproductions of normal 16-millimeter film. In kinescope photography on 16-millimeter film[32], a relatively slow fine-grain negative or reversal film can be used because of the high brightness levels available. The fluctuation level can then be reduced and is not necessarily limiting the quality of the recording.

4. The Aperture Response Characteristics of Imaging Systems

a. An experimental proof of the theory for cascaded aperture processes

The theoretical analysis of aperture processes in cascade (Part II) has provided the rule that the over-all resolution number at a given response factor in a multi-stage process can be found by a quadrature addition of the individual resolution line numbers as expressed by the equation

$$1/N_p = \sqrt{(1/N_1)^2 + (1/N_2)^2 + \text{----} + (1/N_n)^2} \qquad (30)$$

It was pointed out that this rule does not apply accurately to response factors near zero, i.e., to line numbers near the limiting resolution, but that it is a good approximation for values $r\Delta\bar{\psi} > 0.3$. A quantitative proof by measurement of the response characteristics of two cascaded imaging processes is illustrated by Figure 92. A line-group test pattern is projected in sharp focus by lens 1 onto a diffuse reflecting screen. This image is picked up by the camera lens 2 of a television camera which is adjusted to an out-of-focus position causing a first zero at a relatively low line number N_c as observed on the kinescope viewing screen. The first image is now defocussed by lens 1 to the same cutoff N_c on the diffuse reflecting screen 1. The cascaded response of the two out-of-focus imaging systems is then measured by the methods described in Part III, and is shown by curve 1 + 2 in Figure 92.

The component characteristics (curves 1 and 2) of the system are measured similarly with one image in sharp focus and the other image defocussed to the previous value N_c. The measured characteristics 1 and 2 permit calculation of the cascaded response curve 3. The agreement between the measured and computed response characteristics 1 + 2 and 3 in Figure 92 is a quantitative proof that Equation (30) furnishes the cascaded aperture response of practical complex apertures in good approximation in the range $r\Delta\bar{\psi} > 0.2$.

---

[32] R. M. Fraser, "Motion Picture Photography of Television Images", *RCA Review*, Vol. IX, No. 2, pp. 202-217, June, 1948.

b. *The correction of aperture response characteristics and image sharpness by negative aperture processes*

The analysis and synthesis of complex apertures and aperture response characteristics as a sum of component apertures or characteristics has been discussed and verified by experiment in Part III. It is logical that subtraction of an undesired component (such as curve 2 in Figure 93) from a complex response characteristic, (curve 1) produces a simpler characteristic with higher (relative) response factors which result in a sharper image. Subtraction of a characteristic is equivalent to an addition of a "negative" response characteristic. The correction process, (photographic or electrical) may, hence, be considered as a "negative" aperture process. The apertures used in these processes are positive as well as the flux values which are positive quantities of light, silver grains or electrons. If phase-reversing or attenuating elements are inserted, however, flux changes or "signal" components can be generated which are negative with respect to the original signal. The amplitude range and shape of the negative-signal response curve is controlled by the "apertures" of the correcting process to provide the desired correction. These concepts are useful and necessary in coordinating optical and electrical processes. Negative aperture-processes are not used in cascade with the normal process but the correction "signals" are superimposed on the normal process. In overall response calculations made by applying Equation (30), the effect of an aperture correction stage is, therefore, not included as a negative cascaded aperture, but must be evaluated separately. It is important in a synthesis to include the spurious response of the correction aperture in the addition (See curve 2, Figure 93) and to select response characteristics which will add up to a smooth curve. Errors in this

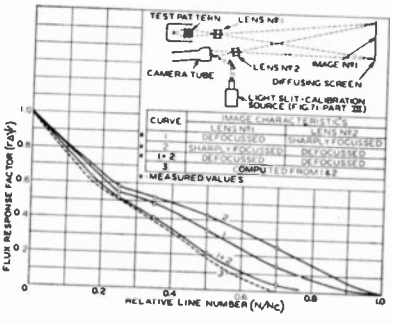

Fig. 92—Flux response characteristics of two cascaded imaging systems.

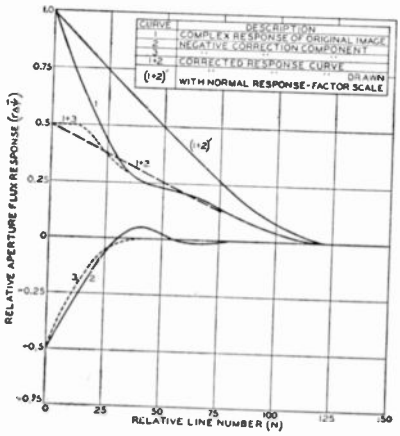

Fig. 93—Aperture response correction by "negative" response characteristics.

respect cause spurious signals or transients in both photographic and electrical processes.

The correction decreases the signal output or "gain" which would normally be obtained from the process (See curve $1 + 2$) and requires, therefore, a stage with increased amplication to restore normal signal amplitudes (curve $(1 + 2)'$ in Figure 93). In a photographic process the increased amplification is furnished by a film characteristic with higher slope (γ).

The correction process illustrated by response characteristics in Figure 93 can be duplicated by a photographic process employing optical two-dimensional apertures. The characteristic 1 is synthesized by two round apertures with equal flux and first zeros at $N_c = 30$ and $N_c = 120$. A test pattern is copied by out-of-focus projection (See Part II) on a photographic plate in a double exposure with two corresponding lens stops and the relative exposure times 1 to 16. A print from plate 1 is reproduced in Figure 94 and illustrates the poor aperture response of curve 1, Figure 93, which is to be corrected. An auxiliary plate 2a is made at the same enlarger setting by an exposure with the larger aperture only ($N_c = 30$). A positive plate 2b of proper density is then made by contact printing (phase reversal process) from 2a to obtain the "negative" response characteristic 2 in Figure 93, illustrated by the print Figure 95. The aperture correction of the image Figure 94 from plate 1 is made by printing plates 1 and 2b in contact and in register. The result is the considerably sharper image, Figure 96, representing curve $(1 + 2)'$ in Figure 93. Although giving a perfect correction, the described process requires an auxiliary image (plate

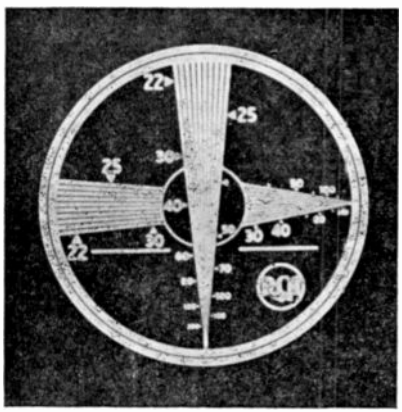

Fig. 94—Photograph of test pattern obtained by an optical aperture with characteristics given by curve 1, Figure 93.

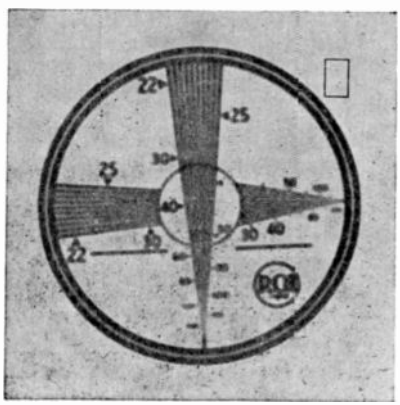

Fig. 95—Photograph of test pattern obtained from the correcting positive plate having the "negative" response characteristic given by curve 2, Figure 93.

2a) made from the original test pattern. If only the poor "signal" from plate 1 is available the correction signal must be derived from this plate by making the low-resolution correction positive directly from plate 1 by out-of-focus projection or diffuse copying with unity magnification. Because the copying process is a cascading operation, the copying aperture will always cause a widening of contours and produce an aperture response which contains a component having a cutoff N_c lower than any component ($N_c = 40$) of the original. A negative response curve obtained from a cascading operation (from 1) such as curve 3 in Figure 93 will, therefore, always cause a negative overshoot or "transient" in the corrected image. When the correction is not too large, the overshoot which appears as a relief effect is not disturbing. In the case of the example, an over-correction was made

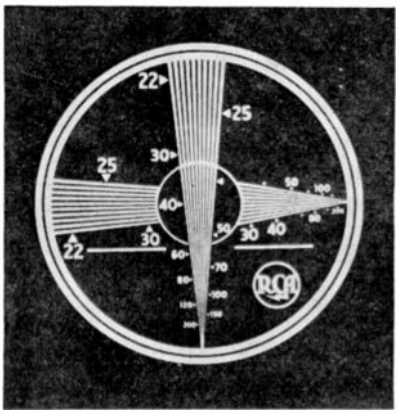

Fig. 96—Photograph of test pattern obtained with the photographically corrected aperture response given by curve 1 + 2, Figure 93.

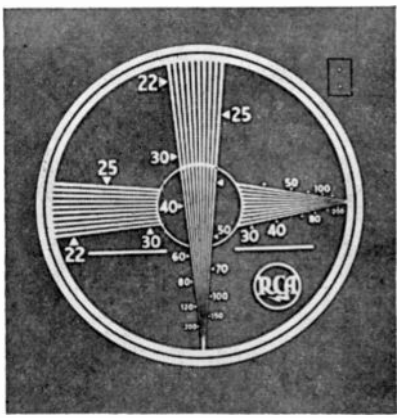

Fig. 97—Photograph of test pattern illustrating strong "transient" due to over-correction with a positive plate.

with a slightly larger correcting aperture than necessary to bring out the strong transient illustrated by Figure 97, as the normal effect was small and would probably be lost in the reproduction. It is evident that the two images must be accurately registered in the correction process because any error introducing a "phase shift" of the components causes strong transients as in electrical processes.

A television system is well suited for insertion of aperture correction processes. Its electrical characteristics, in particular, can easily be modified to subtract or add signal components in the range of the frequency response characteristic which determines the "horizontal" aperture response of the electrical channel. The aperture response signals from the television camera are corrected by inserting electrical

networks which cause a reduced amplification of low-frequency signals, i.e., a "negative" signal component with respect to low-frequency signals. If adequate phase correction is included, the *horizontal* aperture response of the television system may be raised to its maximum value (See Part II) provided the cutoff point of the over-all response of the uncorrected system occurs at a higher line number than the electrical channel cutoff.

The oscillograms in Figure 98 illustrate the electrical aperture correction of signals from a line-group test pattern. The uncorrected signal response in a 20-megacycle channel (trace 1) has decreased to a sine wave shape at $N = 100$. With aperture and phase correction the transition curve is considerably steepened and the response has become normal at $N = 350$ (trace 2). Insertion of a 3-section lowpass filter

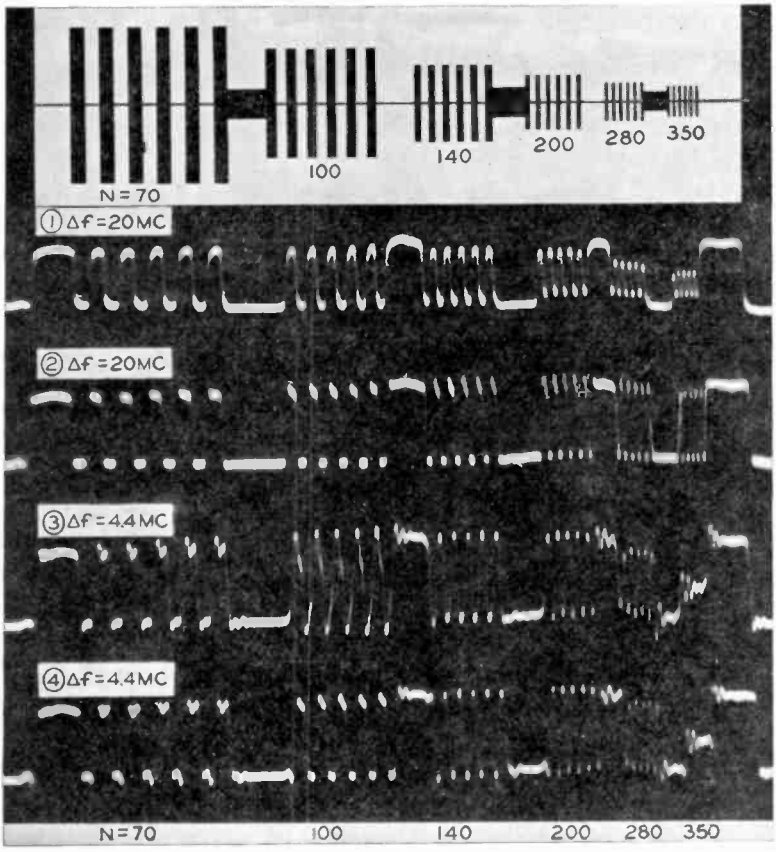

Fig. 98—Oscillograms of test pattern illustrating electrical aperture correction in the horizontal dimension and effects of limiting the frequency channel by a filter.

with sharp cutoff at $N_c = 350$ lines ($\Delta f = 4.4$ megacycles) resulted in trace 3 which demonstrates the incomplete phase correction of the filter by the one-sided transients from a unit function signal. Addition of a simple phase correcting circuit results in the trace 4, which approaches closely the theoretical response shown in Part II by Figure 36 and Figure 37, curve 5. The substantial increase of detail contrast obtained by electrical aperture correction in a 1000-line channel is demonstrated by the photographs Figures 99a and 99b which show the expanded center of a wedge test pattern before and after correction. (The pattern numbers are to be multiplied by ten. The horizontal expansion is obtained by a 4 to 1 expansion of the horizontal kinescope deflection.)

The electrical correction decreases the effective aperture width of the system but does not affect its height, forming a slit aperture with higher response in the horizontal direction. In over-all response calcu-

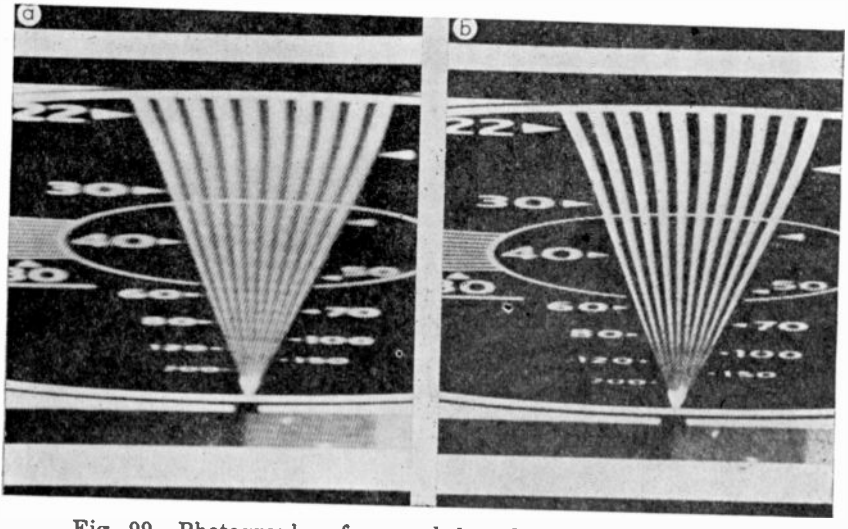

Fig. 99—Photographs of expanded wedge test-pattern image
a. without aperture correction
b. with electrical aperture correction in horizontal dimension.

lations, an asymmetric two-dimensional aperture can be treated as two one-dimensional apertures in cascade, with the horizontal and vertical resolution values multiplied by $\sqrt{2}$. For example, an aperture having the vertical resolution $N_v = 300$ lines and the horizontal resolution $N_H = 600$ lines at a given response factor is equivalent to an aperture with the cascaded values $N_v = 425$ and $N_H = 850$ which, according to Equation (30), is a symmetric aperture with the balanced resolution $\overline{N} = 380$.

According to this method the maximum increase in resolution obtainable by the one-dimensional horizontal aperture correction is limited to $\overline{N} = N_V \sqrt{2}$. The balanced resolution $\overline{N}$ is frequently evaluated by assuming that an asymmetric aperture may be replaced by a symmetric aperture of equal area as expressed by the geometric mean value $\overline{N} = \sqrt{N_H \times N_V}$. For a moderate unbalance of resolution values, both methods give similar values, but for larger differences of N_V and N_H, the geometric mean value $\overline{N}$ increases steadily indicating no limit to the maximum resolution obtainable by a one-dimensional aperture correction. It is obvious that the apparent sharpness of images with asymmetric resolution depends on the distribution of vertical and horizontal components in the subject material. For normal subjects and large unbalances of resolution the geometric mean value appears much too high while the cascading method furnishes more reasonable values which are perhaps somewhat conservative when compared with subjective observations (see ref. (5)).

Aperture correction processes increase the high-frequency components of random fluctuations by the same ratio as the detail signals.* The degree of correction is, therefore, limited in practical processes by the decrease in the signal-to-fluctuation ratio. Moderate "high peaking" (2 to 3 times at $N = 400$) increases the fluctuation visibility only slightly when the normal fluctuation energy is uniformly distributed in the frequency channel (See Part I).

c. *The aperture response of practical television and motion picture systems*

The aperture response of the various transducing processes in motion picture and television systems has been established in preceding parts of this paper. The component characteristics (1 to 3) of a typical 35-millimeter motion picture process are shown in Figure 100. The cascaded aperture response characteristics 4a and 4b, computed with Equation (30), show the relatively small difference in over-all response caused by decreasing the camera lens stop from f:2.8 to f:2.3 because the projection lens and film response are the main factors controlling the over-all response characteristic.

The response characteristics of a television system with standard channel are shown in Figure 101. The theoretical response of the system has been broken down into its vertical and horizontal components 3a and 3b (See Part II, B2, page 267 et seq.) which, in cascade, result in the theoretical curve 7 of the system. The response characteristics of the experimental camera tube (2) and kinescope (4) represent the best values obtainable in the laboratory.

* The fluctuation filter factor has values $m > 1$.

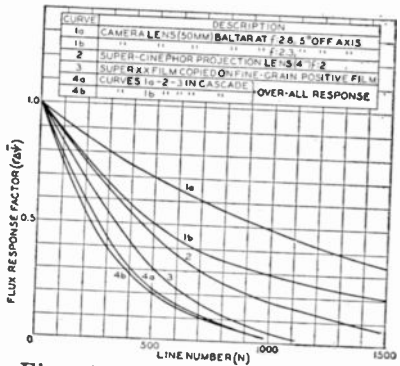

Fig. 100—Aperture response characteristics of 35-millimeter motion picture process.

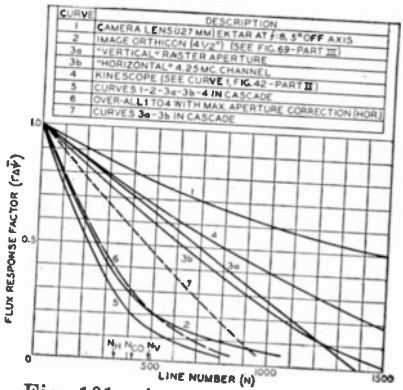

Fig. 101—Aperture response characteristics of television process with 4.25-megacycle channel width.

It is evident that the camera tube is the characteristic controlling the over-all response (5) of the system which is the cascaded value of curves 1, 2, 3a, 3b, and 4. The insertion of "horizontal" aperture correction circuits can eliminate the deterioration caused by the components 1, 2, and 4 in one dimension, resulting in the theoretical horizontal response component shown by curve 3b. The response of the system in the vertical dimension is given by the system curve 3a in cascade with the equivalent *vertical components* of the elements 1, 2, and 4, which are obtained by multiplying the resolution scales N of these characteristics by the cascading factor $\sqrt{2}$. The over-all response of the system with optimum aperture correction is then obtained by cascading the system curves 3b, 3a with the "stretched" curves $N_1\sqrt{2}$, $N_2\sqrt{2}$ and $N_4\sqrt{2}$. This process furnishes the corrected response curve 6.

The over-all aperture response characteristics of the television process (curves 5 and 6 of Figure 101) are *equivalent* characteristics because the real characteristics of the television raster and the electrical channel which have a higher response at $N < \overline{N}_{co}$ but no response beyond $N \geqq \overline{N}_{co}$, have been expressed by the optical equivalents (3a and 3b) derived in Part II. Because the equivalence is based on a varying picture content at a viewing ratio $\rho = 4$, the over-all characteristics are representative for a comparison with motion picture processes. *The equivalence for still pictures is expected to vary with picture content as repetitive detail beyond the value $\overline{N}_{co}$ is actually not reproduced, although fine single lines and contours may have a sharpness represented by the equivalent response curve.* It is interesting that the present 525-line television system ($N_v = 490$, and $N_H = 340$) results in a balanced contour sharpness even though the limiting

resolution values are unbalanced. However, it does not necessarily follow that this resolution ratio will produce balanced contour sharpness with other systems employing different line numbers. Such factors as viewing distance, scanning line number, and kind of subject material must be considered because they affect the visibility of the scanning lines and cutoff transients (See Part II).

A point-by-point comparison of the over-all response characteristics 4 in Figure 100 and 6 in Figure 101 reveals an almost perfect match for response factors $r\Delta\bar{\psi}$ greater than 0.1. This does not mean that a television system can *reproduce* a motion picture film without loss of quality because only a theoretically perfect imaging system can accomplish this feat. The equivalence applies rather to images obtained by a direct pickup of the same subject. In case of a motion picture reproduction over a television system, a comparison should, therefore, be made with a retake and reprojection of the original projected motion picture by means of a second motion picture process. It is quite apparent that the mechanical position and focus errors caused by film motion in cameras and projectors result in an additional degradation of sharpness which has been neglected and which does not occur in a television process where single stationary image surfaces are used.

A practical television system with sharp cutoff at $\overline{N}_{co} = 410$ lines can, therefore, produce an image sharpness approaching in effect the sharpness of a commercial 35-millimeter motion picture. This result appears optimistic by comparison with the best television transmissions made at this time. It must be remembered, however, that commercially available tubes have lower aperture response values than the experimental tubes of the example and that additional aperture effects may occur in modulating systems, radio links and receivers. Furthermore, when judging the sharpness of an image it is difficult to mentally exclude the distracting effects of fluctuations, contrast errors, and particularly defects due to spurious signals. Good detail response in a long contrast scale places severe requirements on the mechanical and electrical uniformity of image and multiplier surfaces and the fineness of the collector screens in the camera tube. It is, therefore, often preferable to operate present camera tubes somewhat out-of-focus until these problems have been solved. A long tone range in combination with good aperture response at all levels and freedom from blemishes are requirements for producing the smoothness, fine drawing, and "texture" of a good photograph.

5. *An evaluation of "sharpness" by including the process of vision*

The eye is the final judge in an evaluation of image sharpness. It is, however, an instrument which can be influenced by a number of

image properties other than resolution (See above). The eye does not analyze the exact cause and magnitude of a difference in the apparent sharpness of two images, but merely judges one image to be sharper, less sharp, or equally sharp than the other image or the original scene. If the eye judges these differences on a logarithmic basis the "minimum perceptible sharpness difference" should represent a constant increment on a scale plotted in decibels. The eye is an imaging system having a certain aperture response; it can, therefore, judge a sharpness difference only by the difference in retinal images which is technically the change in resolution caused by cascading an external imaging process with the process of vision. According to this reasoning, the relative sharpness of an image (or process) *as seen by the eye* can be expressed by the ratio of the decreased retinal resolution (N_{e+p}) obtained by cascading the visual process with an external process N_p, to the normal (retinal) resolution N_e, at a given response factor. The relative sharpness N_{e+p}/N_e is computed with Equation (30) and expressed by the relation

$$N_{e+p}/N_e = (N_e N_p)/\sqrt{N_e^2 + N_p^2}. \qquad (91)$$

A plot of Equation (91) as a function of the resolution ratio N_p/N_e in logarithmic coordinates (Figure 102) may be regarded as a basic function relating aperture response and line number of an external process to subjective sharpness impressions. Direct reading scales (such as scale A for $r\Delta\bar{\psi} = 0.5$) for the line number N_p of the external process can be located by the index number $N_p/N_e = 1$, which, for the desired response factor is given by the eye characteristic (Figure 20, Part II, page 253) for a viewing ratio $\rho = 4$.

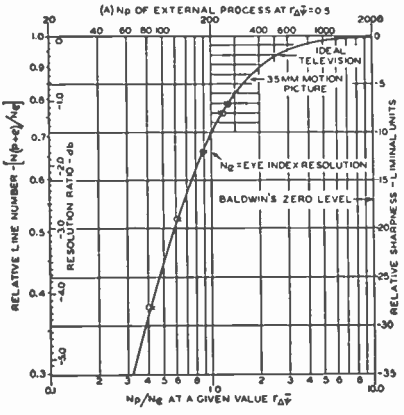

Fig. 102—Curve for evaluating the subjective sharpness of an imaging process.

The sharpness curve indicates that an increase in resolution from 150 to 200 lines (at $r\Delta\bar{\psi} = 0.5$) in an external imaging process causes a sharpness increase of 0.8 db; an equal increase of sharpness requiring progressively larger resolution differences at higher line numbers, such as a change from 260 to 600 lines. It is of considerable interest to determine the minimum perceptible sharpness difference, i.e., the "liminal" unit of the sharpness scale, to permit a quantitative interpretation of the sharpness of images.

This liminal unit has been determined by Baldwin[5] in a series of carefully made subjective observations on images with known resolution. Baldwin plotted sharpness in liminal units against the number n of square figures of confusion in out-of-focus motion picture projections. The balanced line number computed from n (Equation (38) Part III) furnishes the 50 per cent response value for the projector. The true value in the projected motion picture is obtained by cascading the value N (projector) with the film value for $r\Delta\bar{\psi} = 0.5$ (compare Figure 100). One set of corrected values is given in Table X.

Table X

Liminal units of sharpness	Number of figures of confusion n	Line number at $r\Delta\bar{\psi} = 0.5$ for $N_{film} = 350$
−11	10,000	84.2
−2	25,000	123.6
+5	61,000	182.
+9	130,000	223.
+10	160,000	246.

By adjusting the size of the liminal unit and varying the resolution index for the eye and the film, Baldwin's zero level had to be placed 17 liminal units below maximum sharpness (which is close to his estimate) to obtain the best fit of his values with the computed curve shape. (See Figure 102.) The graphic operation gives a simultaneous solution for the eye and film resolution at $r\Delta\bar{\psi} = 0.5$, which are in excellent agreement with the measured value.

The graphic experiment may be regarded as a proof that the visual process can be treated as an aperture process and that the sensory response to changes in sharpness follows substantially a logarithmic law. The liminal unit of sharpness represents a change of 0.15 db, i.e., a constant percentage (approximately 3 per cent) in the relative retinal resolution $N_{(p+e)}/N_e$ at a given response factor and viewing ratio.

The curve of sharpness shown in Figure 102 supplies an answer to many problems. It furnishes the difference in resolution N_p which can just be seen in a comparison of response characteristics; the effect of an improvement in the aperture response of a system; the number of sharpness units lost in the process of recording a television performance on motion picture film; the difference in sharpness between two imaging processes and many others.

According to Baldwin, one liminal unit is a barely perceptible difference, two units being required to make a definitely noticeable

change in the sharpness of an image. An imaging process reproducing a line number $N \geqq 700$ with a response of 50 per cent and $N \geqq 1050$ with a response of 30 per cent can thus be rated as absolutely "sharp" at a 4 to 1 viewing ratio. The limiting resolution of photographic processes having this sharpness is at least 3000 lines and in most cases over twice this value. The sharpness rating of a few processes of interest expressed in liminal units below the "zero level" of maximum subjective sharpness is listed in Table XI* for a viewing ratio $\rho = 4$. The motion picture process #1 rates —6.5 liminal units and is equalled by the television process #6 with aperture correction. The aperture correction causes a sharpness increase of 2.5 units which is a noticeable improvement. A light-spot slide scanning system #7 can produce

Table XI—Subjective Sharpness of Imaging Processes at $\rho = 4$.

#	Process	Camera Lens	Film	Sharpness Level liminal units
1	Commercial Motion Picture Process 35 mm (Figure 100)	f:2.5	Super XX or Plus X	—6.5
2	Commercial Motion Picture Process 16 mm	f:2.5	Super XX or Plus X	—15 (approx.)
3	Miniature Camera (High-quality Projector)	f:5 to f:11	Kodachrome	—8
4	Miniature Camera (High-quality Enlarger)	f:5 to f:11	Panatomic X	—2.6
5	2¼" x 3¼" Camera (High-quality Enlarger)	f:5 to f:11	Super XX or Plus X	—0.5
6	Standard Television Process (Image Orthicon)		best tubes	
	Figure 101, curve 5	f:8		—9
	Aperture corrected, curve 6	f:8		—6.5
7	Standard Television Process Light-Spot Slide Scanner		Miniature Slide	
	Aperture corrected	f:4.5		—5.
			Kodachrome	
8	Reproduction of Commercial 35-mm film by Standard Television Process with Light-Spot Film Scanner		35-mm positive from Super XX or Plus X	—9.5
9	Reproduction of Commercial 35-mm Film by an Identical Motion Picture Process	(repetition of process #1 with a second camera, film process and projector)		—11.5

a slightly sharper image (by 1.5 units). When a 35-millimeter motion picture is scanned, the light-spot scanner decreases the sharpness of process #1 by only 3 units (See #8) which is an excellent performance, because a repetition of the photographic 35-millimeter process (#9) would decrease the image sharpness to —11.5, i.e., by 5 units.

A 2¼ × 3¼-inch photographic camera can just produce a perfectly sharp picture with normal film types (for $\rho = 4$), while images from a good miniature camera rate approximately 2 units lower and do not attain "needle sharpness" with film types of normal speed and range.

* The over-all aperture response calculations are based on lens and film data obtained by measurement as described in this paper.

It will be of interest to briefly describe a series of tests made nearly two years ago to obtain information on the comparative sharpness of television and photographic processes. The tests were based on a visual comparison of photographs made over a television system, with direct photographs in which the limiting resolution ($\overline{N}_{co}$ or N_c) had been adjusted to various values. The purpose of the tests was to determine the relative cutoff ratio $\overline{N}_{co}/N_c$ of the two processes which gave images of equal sharpness. Television images of two of the three test objects selected as originals are reproduced in Figures 103 and 104. The objects were photographed on 3¼ × 4¼-inch negatives and enlarged by out-of-focus projection to 8 × 10-inch prints with varying degrees of sharpness. The cutoff N_c (indicated by the first "zero" on a resolution wedge) was adjusted to the values 200, 300, 450, 650, and 870 lines. Because a sharp enlargement had a limiting resolution $N_c = 4500$ lines, this print series (A) yielded grain-free images with the relatively sharp optical cutoff caused by a round aperture with substantially uniform flux distribution.

A second series (B) of 8 × 10-inch prints was made by "sharp" enlargements from selected miniature film negatives taken with a Contax Camera and Zeiss Sonnar Lens at its optimum stop, f:6.3, on Super XX film and Panatomic X film and developed in fine-grain developer. The vertical dimension of the image was adjusted to 4.5, 6, 8, 10, 12, 15, and 15.2 millimeters to obtain a series of cutoff values N_c caused predominantly by the aperture response of the film.

Finally, the test objects were reproduced over a high-quality television system containing a band-limiting filter which permitted sharp electrical cutoff at various bandwidths up to 20 megacycles. The scanning line numbers used were 525 and 637. The kinescope pictures obtained with this television chain were photographed on 3¼ × 4¼-inch film. A time exposure (½ second) eliminated fluctuations in the 8 × 10-inch enlargements. All prints were made as nearly alike in contrast as possible.

The test was conducted by arranging the prints of the photographic processes according to sharpness and asking ten observers to match the television prints with prints of equivalent sharpness.* The grain-free television prints with sharp cutoff at $\overline{N}_{co} = 420$ lines, for example, were found equivalent in sharpness to the substantially grain-limited photographs of series B having a limiting resolution $N_c = 850$ lines, and equivalent to grain-free defocussed photographs of series A having a (first zero) cutoff at $N_c = 600$ lines. The results of the tests are

* No reference numbers indicating N_c could be seen by the observer.

Fig. 103—Photograph of test object over a television system ($N_{oo} = 420$).

Fig. 104—Photograph of test object over a television system ($N_{oo} = 420$).

expressed by the cutoff ratios

$$\frac{\overline{N}_{co}\ \text{(grain-free television)}}{N_o\ \ \text{(grain-free film)}} \simeq 0.7 \quad \text{(Series A)}$$

$$\frac{\overline{N}_{co}\ \text{(grain-free television)}}{N_c\ \ \text{(grain-limited film)}} \simeq 0.5 \quad \text{(Series B)}$$

The aperture response characteristics of the television system and the photographic images, series A and B, were not known at the time of the tests, but can be established with fairly good accuracy from the characteristics of the system components. The television system characteristics were essentially those shown by Figure 101, except for a kinescope with somewhat lower response and a less complete phase correction. These differences are estimated to account for a decrease of not more than one liminal unit in the sharpness of the system, which is, therefore, —7.5, i.e., one unit less than given for the corrected system in Table IX.

The line number $N_{0.5}$ at $r\Delta\overline{\psi} = 0.5$ for the series A photographs obtained by out-of-focus projection can be established from the characteristics of the projection "aperture". The spurious response observed beyond the first zero point N_o indicated a round aperture with sharper cutoff than given by a cosine-square density, but not sharper than that obtained with uniform density. The ratio $N_{0.5}/N_c$ lies, therefore, between the values 0.40 and 0.48.* With the average value $N_{0.5} = 0.44\,N_c$ and the observed cutoff ratio $\overline{N}_{co}/N_c = 0.7$, the line number giving 50 per cent response in series A photographs is found to be $N_{0.5} = 0.63\ \overline{N}_{co}$, i.e., 63 per cent of the balanced line number of the equivalent television system. For $\overline{N}_{co} = 410$, we obtain $N_{0.5}$ (series A) $= 258$; and from Figure 102 the sharpness rating of —7 liminal units. The computed sharpness difference of only ½ unit agrees well with the observed equality of matched television and series A prints.

The series B prints were substantially grain limited in resolution as proven later by aperture response measurements of the particular camera lens which was used also in the enlarging process. The shape of the aperture response characteristic of series B images is, therefore, given with good approximation by the film curve 2 in Figure 80, which has the ratio $\overline{N}_{0.5}/N_o = 0.3$. With the ratio $\overline{N}_{co}/N_c = 0.5$ for series B images, we obtain for $\overline{N}_{co} = 410$ the value $N_{0.5}$ (series B) $=$ 246, and from Figure 102 a sharpness rating of —7.2 liminal units.

The close agreement and correlation of subjective sharpness ratings with the liminal number obtained by aperture response calculations

* See part II Appendix, Table III.

may be regarded as additional proof that resolution, detail contrast, and image sharpness are adequately and quantitatively interpreted by applying the "aperture" theory developed in this paper.

Conclusions

The quality of television and photographic images depends in a large measure on three basic characteristics of the imaging process: the ratio of signals to random fluctuations, the transfer characteristic, and the detail contrast response. These characteristics are measured and determined by objective methods which apply equally well to all components of photographic and electro-optical imaging systems. A unified system of specifying and measuring definition and detail contrast by the flux response of defining "apertures" has been demonstrated, permitting for the first time a practical analysis and rating of lenses, photographic film, television camera tubes, kinescopes, and other image-forming devices on an objective numerical basis. An interpretation of the numerical values obtained by calculation or measurement of the three characteristics which determine image quality requires correlation with the corresponding subjective impressions: graininess, tone scale, and sharpness. This correlation has been established by analyzing the characteristics of vision and by including these characteristics in an evaluation of the over-all process of seeing through an image-reproducing system.

Calculation and measurement have shown that, provided defects and non-uniformities in both processes are of comparable magnitude, a standard practical television system with a balanced resolution of 410 lines is technically capable of attaining an image equivalent in quality to commercial 35-millimeter motion pictures.

Acknowledgments

In the course of the several years through which these investigations have extended, the author has profited from the experience and helpful criticism of his associates, particularly Dr. Albert Rose of RCA Laboratories on the general subject of photosensitive devices and W. A. Harris of this company on the theory of random fluctuations.

The author also wishes to express his appreciation to the Bausch and Lomb Optical Company and the Eastman Kodak Company for their courtesy in supplying high-quality lenses for test purposes and special photographic material. Various discussions with Drs. T. G. Veal, R. Kingslake, C. D. Reid and other members of the Eastman Kodak Company have been stimulating and helpful in connection with lenses and the photographic process.

MOTION PICTURE PHOTOGRAPHY OF TELEVISION IMAGES*†

By

Robert M. Fraser

Television Development, National Broadcasting Company, Inc., New York, N. Y.

Summary—The permanent recording of television programs, for documentary, historical, legal, or critical purposes and as an aid to networking may be accomplished by motion picture photography of the television image, making use of the practical arts developed by motion picture engineers for recording the sight and sound of a television broadcast. This paper describes the apparatus and methods developed for the photographing of the television cathode-ray image. Development is traced from the first attempts in 1938 through the experimental cameras to the commercial camera system now in use. Subsequent sections deal in some detail with 16- and 35-millimeter equipment considerations, kinescope phosphors and film spectral characteristics, resolving power of films, exposure of film, processing and printing of kinescope film, the photographic monitor, and sound recording.

Introduction

A METHOD of permanently recording the otherwise transient video signal is desirable in the advancement of television art. Motion picture photography of the television image is a method of doing this. Use is made of the practical arts developed by the motion picture engineers in recording the sight and sound of a television broadcast. The reasons for recording television programs are manifold and are similar to the reasons for recording the sound of a standard broadcast program. Television recordings may be made for documentary purposes, to preserve an historical event, for legal purposes, and for critical purposes. These recordings may be used for a delayed or a repeat broadcast or for syndication to other television stations unable to obtain network programs because of the lack of coaxial cable or microwave relay connections with network sources. Television recordings of auditions are useful in the marketing of programs or talent.

It is the purpose of this paper to describe the apparatus and methods developed for the motion picture photography of the television cathode-ray image.

In 1938, the first attempts were made to photograph the television image on motion picture film. Kinescopes or cathode-ray tubes at that time used low efficiency phosphors and operated on relatively low

* Decimal Classification: R583 × R582.
† Reprinted from *RCA Review*, June, 1948.

second-anode voltages compared with present day practices. The amount of light obtainable from these cathode-ray tubes was not enough to produce a full exposure on the fastest films then obtainable with an exposure of one thirtieth of a second in a sixteen frame-per-second camera. By photographing the cathode-ray tube at eight frames per second with an exposure time of one fifteenth of a second, recognizable images were obtained on the motion picture film. Of course, these films when projected on a twenty-four frame projector show an unnatural rapidity of motion and are considered to have nothing more than historical interest.

The cameras used in these early experiments were spring-motor driven and the shutter rate was therefore nonsynchronous with the frame rate of the television system. This gave rise to phenomena termed "shutter bar", or banding — a black or a white bar which in a nonsynchronous system moves across the film image when projected, at a rate dependent on the difference in frequency between that of the television system and the frame rate of the motion picture camera. The width of the bar depends on the shutter angle of the camera. If the shutter angle and the frame rate of the camera combine to give an exposure time of less than one thirtieth of a second, less than a full television frame is photographed and a black or under-exposed section of the image results. If the exposure time is greater than one thirtieth of a second, there is an overlapping of the television image frame, i.e., a full frame plus part of the succeeding frame are photographed. This results in a white or over-exposed section on the film frame. It is apparent from this that the shutter speed of any camera used to photograph the television image should be precisely one thirtieth of a second or a multiple of one thirtieth such as one fifteenth or one tenth of a second if "shutter bar" is to be avoided. This rule applies to still cameras as well as to motion picture cameras. The degree of contrast between the under-exposed or over-exposed portion or banded section of the image and the correctly exposed portion decreases with the multiple increase in exposure in units of one thirtieth of a second. If the exposure is less than one thirtieth of a second, the error in exposure will be fifty per cent; for an exposure just under a fifteenth of a second, the error will be twenty-five per cent; and for an approximate tenth of a second exposure, the error will have decreased to twelve and one-half per cent. Since it is impossible to find still cameras with a shutter accuracy of the degree necessary to photograph the television image at a thirtieth of a second, better results can be obtained at the slower shutter speeds in respect to uniformity of the photograph. The problem of photographing rapid motion on the television screen with

a still camera is serious because of the distortion of motion, but no more so than in the case of direct photography.

Motion picture photography of television images was undertaken during the war to record television transmissions from cameras installed in aircraft and in guided missiles. Due to the conditions under which the television images generated by the Block[1] and Ring[2] equipment used in these tests were recorded, nonsynchronous cameras operated by batteries or spring motors at approximately sixteen or eight frames per second were used. "Shutter banding" was noticeable in these films which did not destroy their value in the studies then underway.

Some further work was done with an Eastman Cine-Special driven with a synchronous motor at fifteen frames per second. The shutter on this camera is open for 170 degrees which results in an exposure just under one thirtieth of a second. By phasing the motor drive so that the shutter opened and closed during the vertical blanking period of the television image, acceptable results without banding were obtained. When these fifteen frame-per-second recordings were projected through a standard silent projector at sixteen frames per second, no undesirable results due to change of speed were noticeable.

For a complete recording of a television program it is necessary to record the sound portion. Present day motion picture practice is to record sound at a twenty-four frame per second rate. It is desirable that recordings of television programs be capable of being played back on standard motion picture sound projectors. This necessitates the adoption of the standard twenty-four frame rate to record television programs.

Experimental Camera

A method has been devised of recording twenty-four frames of the standard thirty frame television signal.[3] The equipment now in use uses this method. A shutter driven by a sixty-cycle synchronous motor at twenty-four cycles per second is utilized. This shutter has a closing angle of 72 degrees and an opening of 288 degrees. At the twenty-four cycle per second rate these angles represent a closing time of 1/120 of a second and an opening time of 4/120 or 1/30 of a second, which is the time for one full television frame. Figure 1 shows the time sequence of such a shutter in relation to the television scanning cycle. The camera is driven by a synchronous motor from the same source of 60

[1] M. A. Trainer and W. J. Poch, "Television Equipment for Aircraft", *RCA REVIEW*, Vol. VI, No. 4, pp. 469-502, December, 1946.

[2] R. E. Shelby, F. J. Somers and L. R. Moffett, "Naval Airborne Television Reconnaissance System", *RCA REVIEW*, Vol. VI, No. 3, pp. 303-337, September, 1946.

[3] D. W. Epstein—U. S. Patent No. 2,251,786.

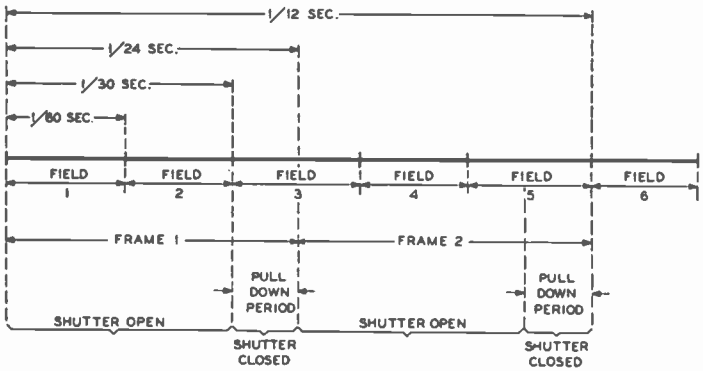

Fig. 1—Time sequence of exposure and pulldown timing of the camera in relation to the field rate of the television image.

cycle current as is used for the television synchronizing generator. If the phasing of the motor is such that the camera shutter opens on the beginning of one field, it remains open for that and the succeeding field, then closes. The shutter remains closed for 1/120 of a second or half the third field, while the film is advanced, then opens. It remains open for this last half of the third field, for the full succeeding fourth field, and for the top or first half of the fifth field. The shutter then closes at the same point that it opened in relation to the scan of

Fig. 2—"Breadboard" camera and photographic monitor.

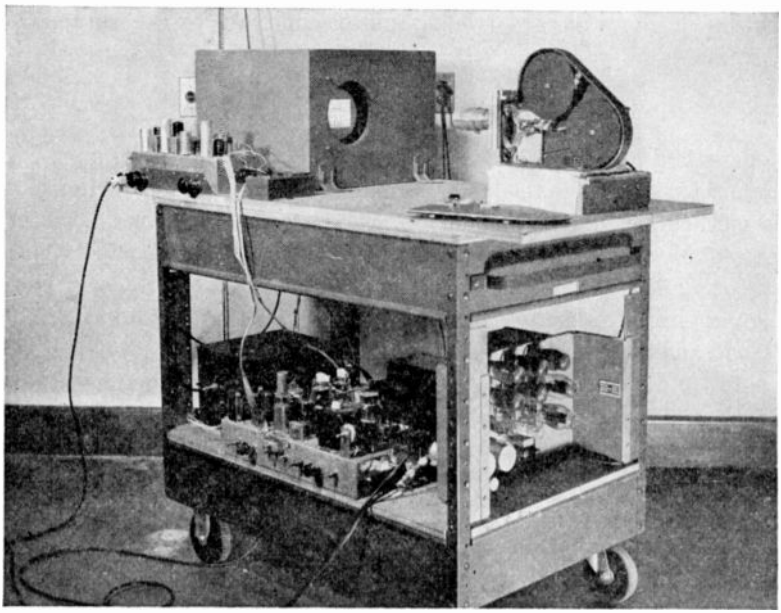

the image. A half field later the shutter opens completing the cycle. Pull-down of the film occurs during this time that the shutter is closed.

The one hundred twentieth of a second time allowed for pulldown is considerably less than is found in standard motion picture cameras. The normal pulldown time of a standard camera is between a fortieth and a fiftieth of a second. To achieve this high rate of pulldown in the television recording camera without undue strain on the film and to maintain registration of the film image is quite an undertaking. That it has been solved satisfactorily is to the credit of the motion picture engineers.

The Eastman Kodak Company constructed a "Breadboard" camera using the foregoing principles. This camera is shown in Figure 2. The camera was capable of a 200-foot load of 16-millimeter film, allowing the recording of 5½ minutes of program time. The satisfactory operation of this camera proved the 288-degree shutter to be practical in the photography of the thirty-frame television image at a twenty-four frame rate.

Commercial Camera

The Eastman Kodak Company in cooperation with the National Broadcasting Company, encouraged by the successful operation of the breadboard camera, began the design of a commercial recording camera capable of recording a half hour of program with a 1200-foot load of 16-millimeter film. The design of this camera was quite complicated by a number of factors. It had been determined through tests with the breadboard camera that the shutter has to rotate with a low flutter rate. A slight change in angular speed of the shutter results in banding of the film image. In severe cases this banding alternates from black to white on alternate film frames. It is therefore necessary to design the shutter drive to have the utmost constancy of angular speed. This is accomplished by using an 1800 revolutions-per-minute synchronous motor to drive the shutter at the necessary 1440 revolutions-per-minute rate through a set of precision gears. Another synchronous motor of larger capacity is employed to drive the film transport mechanism and the Geneva intermittent. The two motors are kept in step during the starting and stopping periods by a phase coupling device which allows the stronger of the two motors to assist the weaker until they both reach synchronous speed. The coupling then floats so that there is no physical connection between the motors.

The shutter motor then drives the shutter independently of any varying or intermittent change of load in the camera. The armature of this motor acts as a flywheel to damp out any tendency to flutter in the dynamically balanced shutter blade.

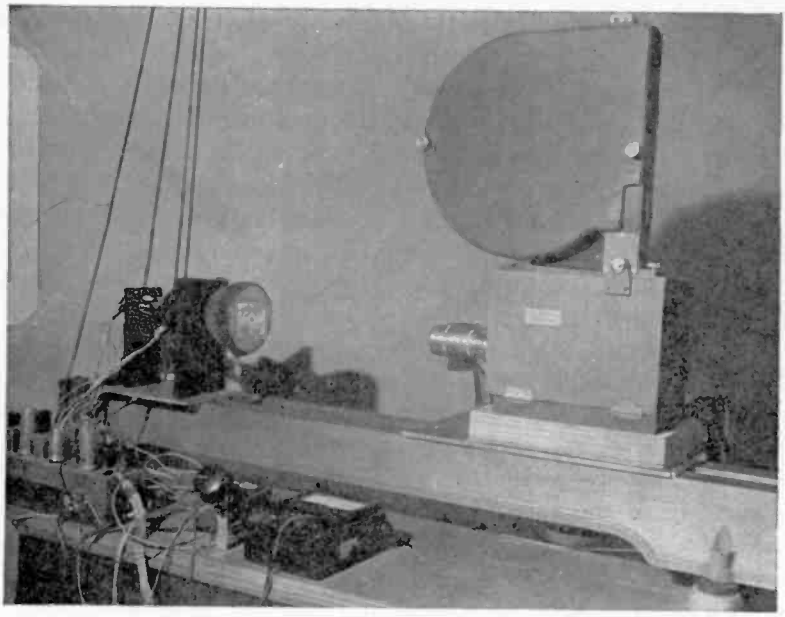

Fig. 3—The Eastman Kodak television recording camera.

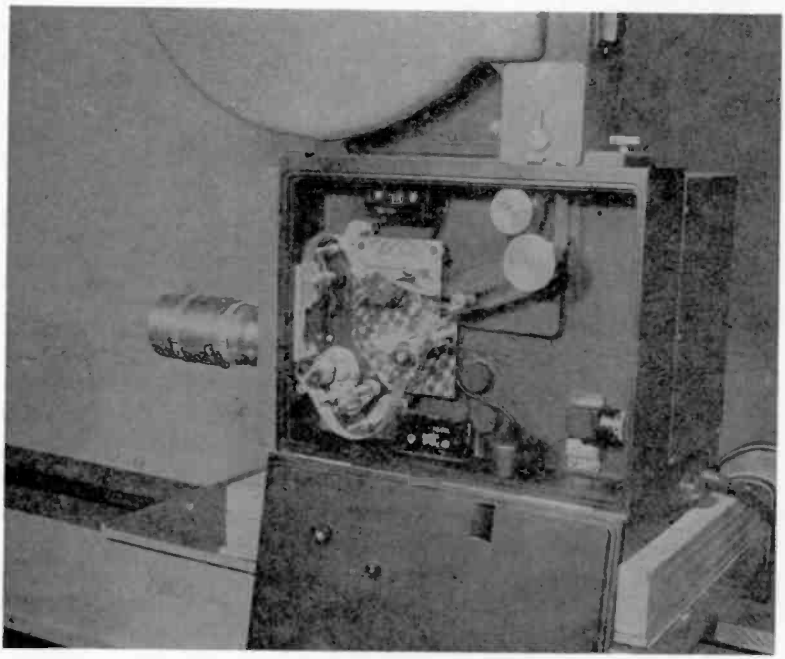

Fig. 4—Eastman Kodak camera interior showing film threading.

An eight tooth sprocket pulldown actuated by an accelerated Geneva star is employed for film pulldown. The pulldown angle of approximately 57 degrees is obtained by means of a spline-and-slot type of accelerator interposed between the constant speed shaft and the geneva driver.

The Eastman Kodak television recording camera is shown in Figures 3 and 4. Nylon is used in the film gate and pressure pad to minimize emulsion pile up, a potent source of trouble in motion picture cameras.

All friction points in the takeup side of the 1200-foot magazine are equipped with ball bearings so that take-up of film progresses smoothly from the two-inch core diameter to the full ten-inch diameter of the full 1200-foot roll. Loop loss indicators are provided and actuate microswitches in the event of loop loss, lighting a warning lamp mounted on the base of the camera.

Focussing and framing of the picture frame is done by means of a right-angle view finder equipped with a magnifying lens. This unit is snapped under the pad spring in place of the pressure pad. Visual focusing is done by means of this finder and checked by exposing film at several different settings about this visual optimum. The processed film is examined under a microscope to determine actual best focus.

The lens equipment of the camera is a 2-inch Eastman Anastigmat f1.6. Apertures of f2.0 to f2.8 are normally used to avoid sharpening the shadow of the shutter in the film plane during the opening and closing time, thereby reducing the possibility that a slight timing error may result in banding. It has been determined that at apertures of f5.6 and above, the cutoff of the shutter in the image field becomes abrupt and causes banding on the order of two or three television lines.

16- and 35-Millimeter Equipment Considerations

There are several reasons for the choice of 16-millimeter film for Kinescope recording rather than 35-millimeter. The main reason is that the cost of 35-millimeter is somewhat more than three times the cost of 16-millimeter for the same period of recording. The current quality of television images, which will undoubtedly undergo gradual refinement, is considered to be roughly equivalent to 16-millimeter home movies, although actually somewhat better with reference to contrast and detail. No marked improvement, however, is to be had by recording on 35-millimeter rather than 16-millimeter at the present time. With the use of fine grain high resolution 16-millimeter film emulsions, no loss of resolution in recording the television image is noticeable.

Fire regulations covering the use of 35-millimeter film, which apply regardless of whether the 35-millimeter film is acetate safety base or

the combustible nitrate base, are rigorous. The cost of providing space that meets these regulations for the use of 35-millimeter film is extremely high, and the changes needed in existing space are difficult to accomplish. 16-millimeter films are available only in acetate safety base which is classified by the Underwriter Laboratories as having a safety factor slightly higher than that of newsprint. The use of 16-millimeter films, therefore, are not restricted by fire regulations. It should be noted that in New York City these restrictions apply to space in which equipment capable of operating with 35-millimeter film is installed, so in order to forestall trouble, all equipment should be single purpose 16-millimeter equipment rather than dual purpose 35- or 16-millimeter equipment.

Another factor in the choice of 16-millimeter film is the high cost of 35-millimeter projection equipment. Most television stations are providing projection facilities for 16-millimeter film only for this reason. In order to service these stations with syndicated programs photographed from the kinescope, 16-millimeter prints will be needed.

Kinescope Phosphors and Film Spectral Characteristics

The spectral sensitivity of the film emulsion can be matched to the phosphor spectral characteristic for the greatest actinic efficiency. There are three general classifications of film emulsions in terms of their spectral characteristics:

1. *Panchromatic,* sensitive from the ultraviolet (4000 Angstrom Units (A°)) through the red (7000 A°). The spectral response of these emulsions correspond approximately to that of the eye and so are generally used for direct photography;

2. *Orthochromatic,* sensitive from the ultraviolet through green, (5700 A°) is used in direct photography where it is desirable to reduce the red sensitivity;

3. *"Ordinary"* or non-color sensitive emulsions, nonsensitized, responding to the ultraviolet and blue portions of the light spectrum. This type of emulsion is used in coating films and papers generally employed in making positive prints from negatives. In 16-millimeter form it is economical in comparison to the panchromatic and orthochromatic types. Another advantage is the ease of handling as relatively bright safelights may be used.

To match these film characteristics, kinescope phosphors are available with light output ranging from the ultraviolet through the entire visible spectrum. Three types of phosphors in common use in television techniques are as follows:

1. *P1, green fluorescence,* commonly used in oscillographic work.

It is the most efficient visually, but has poor actinic efficiency.

2. *P4, white fluorescence,* used for black and white reproduction of television images in most home receivers. This phosphor has a high output in the blue and green portions of the spectrum, but is down in the red. It has the advantage in kinescope photography that picture quality is most readily judged visually.

3. *P5 and P11,* these two phosphors are blue with high ultraviolet output. Photographically, they are very efficient. There is the difficulty in using a blue phosphor in judging the quality of image visually, due to the fact that the human eye has a low response in the blue region and cannot evaluate the quality of the ultraviolet component of the image light output at all.

Tests have been made on the P11, zinc sulphide, phosphor as to the relative actinic efficiency to the panchromatic, orthochromatic, and "ordinary" non-color sensitive emulsions. A Weston exposure meter was used to determine the light output of the aluminized P11 phosphor kinescope. A series of exposures were made of the image on the tube and the correct exposure as judged by visual inspection of the negative was chosen. The Weston meter was then set with this exposure data to find the Weston rating of the type of film for the P11 light output. This rating was then compared with the Weston rating for daylight as given by the manufacture of the film used. It was found that the exposure required for the P11 phosphor image for panchromatic film was one sixth that required for white light of equal intensity, for orthochromatic it was one twelfth, and for the ordinary or non-color sensitive stock, the exposure ranged from 1/16 to 1/32 of the exposure needed for white light.

With these facts it is apparent that for recording of television images a zinc sulphide, blue-fluorescing screen is desirable since it makes possible the use of high resolution, low cost, positive type of film stocks.

Resolving Power Of Films

Present day television systems operating on a 30-frame, 525-line standard, are capable of resolving 483 lines in the vertical direction, and inside the studio plant, before being transmitted on the 4.5 megacycle channel of the radio frequency transmitter, of resolving over 600 television lines horizontally.

Manufacturers of photographic film rate the resolution of their products in lines resolved per millimeter. By dividing the 7.2-millimeter height of the 16-millimeter frame, into 483 lines and dividing the result by two to convert from television lines to photographic lines per millimeter, it is found that in order to resolve the television scan-

ning lines, a resolving power of better than 33 lines per millimeter at contrast ranges below 1 to 10 is required. To resolve 600 television lines on 16-millimeter film, the emulsion must have a resolving power of 42 lines per millimeter.

The subject contrast of the test charts used to determine film resolution is of the order of 1 to several hundred times. Super X, a panchromatic emulsion, is rated by the manufacturer at 55 lines per millimeter. In television terms there would be resolved 792 television lines in the 16-millimeter frame. It might be thought that such a film would be suitable for photography of the television image. This is not so, for this film, used in photography of the television image, does not fully resolve the scanning lines.

The reason for this discrepancy lies in the different method used by the manufacturer to rate the film. As pointed out above, the resolution is determined by photographing a chart that has a contrast ratio between the black lines and the white spaces of several hundred times. Resolution is then determined by the point at which these lines are barely resolved on the film, or at a point where the contrast ratio is slightly greater than unity.

The resolving power of film, of television pickup tubes, and of image reproducing tubes, falls off with decrease in the subject contrast of the test target. A film rated at 55 lines per millimeter at a subject contrast of several hundred times may have only a resolving power of twenty lines per millimeter when the contrast is in the order of 1 to 10.

It has been pointed out in the literature[4,5] that the television image may have contrast ratios of fifty times in large areas, falling off to contrast ranges less than 1 to 10 in fine detail. A film emulsion rated at 90 lines per millimeter under normal test conditions has the necessary resolving power at the lower contrast ranges to resolve the required 42 lines per millimeter.

Suitable emulsions with resolving powers in excess of 90 lines per millimeter are to be found in the fine grain sound recording and print stocks. Both low and high gamma emulsions are available. For recording a positive image on the kinescope, the low gamma variable density type of emulsion is used. When recording from a reversed negative image on the cathode-ray tube, a high-gamma variable area or print type of emulsion is used.

Some improvement in the quality of resolution of the photographic

---

[4] A. Rose, "A Unified Approach to the Performance of Photographic Film, Television Pickup Tubes, and the Human Eye", *Jour. Soc. Mot. Pic. Eng.*, Vol. 48, No. 10, October, 1946.

[5] O. H. Schade, "Electro-Optical Characteristics of Television Systems: Introduction; Part I—Characteristics of Vision and Visual Systems", *RCA REVIEW*, Vol. IX, No. 1, pp. 5-37, March, 1948.

image is made by the use in the video feed of a phase and amplitude equalizer.* The increase in amplitude or contrast of fine detail that can be obtained by boosting the high frequencies in the kinescope image compensates somewhat for the normal falling off of fine detail contrast in the film image. Phase correction is used to reduce the transient white that follows black. The amount of high frequency peaking that can be used is limited by the noise component of the video signal.

Exposure Of Film

Present day aluminized kinescopes operating at high second-anode voltages in the order of 27 kilovolts are capable of brightness ratios of several hundred times in large areas. Most films used in normal photography can handle a range of this order. However, to make full use of such a latitude requires a very accurate exposure. Generally the object brightness range under controlled lighting arrangements never exceeds a ratio of 1 to 30 in direct photography. It is, therefore, necessary that the contrast of the photographic kinescope be maintained within the limits set by the latitude of the particular film used and that the brightness range be set to duplicate the 1 to 30 ratio used in direct photography so as to duplicate the printing contrast of a normal negative.

This is most conveniently achieved by the following method. A plain raster is used on the kinescope such as would be obtained by the use of the blanking signal or pedestal without picture modulation. The brightness of this raster is varied by means of the video gain control or kinescope grid bias control. The beam current of the kinescope is measured by means of a microammeter. Since the light output of the tube is dependent on the watts input to the screen, the measure of beam current affords a measure of the brightness of the tube. Film is exposed to this raster at beam currents varied by steps. The density of the film processed as a normal negative is measured and plotted against the logarithm of the beam current. A normal negative developed to a gamma of 0.65 which has been exposed to an object with a brightness range of 1 to 30 or in logarithmic units, a range of 1.5, should have a density range from 0.25 in the shadows to approximately 1.4 in the highlights. The change in beam current necessary to produce such a range on the kinescope can be read from the plot of the log beam current and film density. The average brightness of the kinescope with picture then would be set by using a beam current that produces a density in the middle of the above range. The video signal is adjusted

* Designed by E. D. Goodale, Television Development, NBC. It is planned that a paper on the equalizer will be published in the September 1948 issue of *RCA REVIEW*.

to a level that will put the blanking level of the composite signal just at visual cutoff of the kinescope. A picture signal judged to have an a-c axis of 50 per cent should be used for this adjustment. This method is largely empirical, but, with experience on the part of the operator, can be made to give consistent results.

Processing and Printing of Kinescope Film

A number of tests have been made in cooperation with the film manufacturers on the processing and printing of films exposed to the kinescope. Both reversal processing and negative processing of the original film were tried. Results show that standard processing methods result in optimum picture quality. Negatives exposed to television images originating in iconoscope cameras are developed to a gamma of 0.7 as determined by a standard IIB sensitrometric test. Film of orthicon pickups gives best results when processed to approximately 0.6 to 0.65. These are interim values as tests on the processing of films have not been completed.

Printing is done according to standard motion picture laboratory practice. Step printing in which the print stock and negative are exposed to the printing light a frame at a time is preferred over continuous printing, where the negative and print stock run past an illuminated slit at a continuous speed. There is a sufficient amount of slippage between the negative and print stock in the continuous printing process to degrade the resolution of the television image. Contrary to the opinion held by many workers, the fact that the film image of a television image is poorer in resolution than in the case of direct photography does not mean that less care in the handling of the film in printing and in projection can be used. The fact is that the utmost care must be taken to maintain the original quality inherent in the film negative throughout the printing process and in the projection of the resulting print.

Films of iconoscope programs can be printed at one printer light setting: i.e., the densities and contrast range of the film resulting from the recording of the outputs of a number of iconoscope cameras does not change sufficiently to warrant changes in the intensity of the printing light.

In film recordings of programs picked up by orthicon cameras the picture negative must be timed for printing. There is considerable difference in the contrast range between different orthicon cameras. Light changes in the order of 100 per cent are sometimes required when a switch between cameras occurs.

This is an undesirable condition as the timing of negatives is an

expensive, time consuming, procedure. The cure for this situation is in better control of the output levels of the various orthicon cameras in the studio. Much of this change can be charged to the fact that the spectral characteristics of the orthicon vary from tube to tube. An orthicon with excessive infrared response has a different tonal graduation as compared to an orthicon with no or little response in this region. If the spectral characteristics of the orthicon can be standardized within closer limits than is now done, much of this timing difficulty in the film recordings may disappear.

In kinescope recordings meant for retransmission through the television system a print gamma of 2.2 and a maximum density of 2.4 are recommended. Further tests may show the desirability of changing these recommendations, but to date the best results in the televising of release prints have been obtained under such conditions.

Emulsion position in the final print is of great importance in television because films may be spliced with other films for special purposes. The use of a non-standard emulsion position requires a change of focus in the film projector when interspliced with films using standard emulsion position. This would require the constant attention of the projectionist to maintain optimum focus throughout the spliced film, therefore it is advantageous to insist upon a standard emulsion position for all film to be used in television. The Society of Motion Picture Engineers' standard for 16-millimeter film is emulsion "toward the screen."

In the recording of television images there are several methods of obtaining the final print:

A. the use of reversible film stock in photographing a positive cathode-ray-tube image (A dupe negative is made of this material and prints are made from this negative. The final prints then have standard emulsion position.);

B. the photography of the cathode-ray-tube image using high contrast positive stock and a negative kinescope image resulting in a positive print from which dupe negatives are made for prints having standard position; and

C. the use of a positive image, photographing with a negative type of film from which final prints are made, resulting in a non-standard emulsion position (However, by reversing the direction of horizontal scanning the original negative may be made to have the same emulsion position as that of a dupe negative. Prints made from this negative, then have a standard emulsion position.)

Other factors must be considered in determining the method of recording. Where it is expected that a great number of prints will be

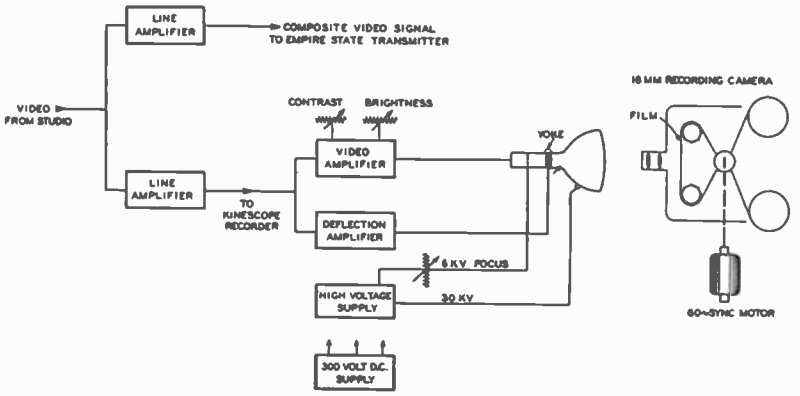

Fig. 5—Kinescope photographic monitor block diagram.

required, methods A or B would be desirable because of the protection of the original material.

Photographic Monitor

The various sizes of cathode-ray tubes may be used for television recordings. In order to insure adequate exposure on the fine grain positive type emulsions, the voltages used with these tubes should be on the order of 20,000 to 30,000 volts. All other factors being equal, such as relative spot size, uniformity of focus over the picture area, brightness and contrast, the smaller tubes offer advantages in the size of the photographic setup. A five-inch kinescope with a flat screen, aluminized P11 phosphor, and the same general type of electron gun

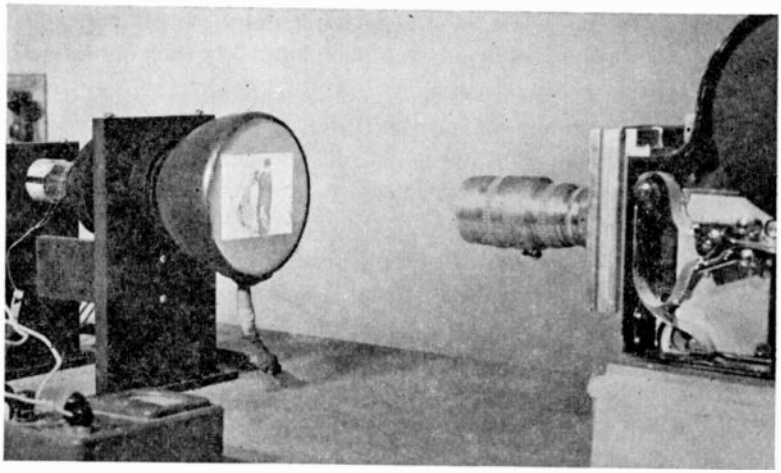

Fig. 6—Close-up of the kinescope with cover removed. (On the tube face is an actual television image of a baseball pickup.)

construction as is used in the 5TP4, gives adequate resolution, contrast and brightness.

A block diagram of the experimental photographic monitor setup is shown in Figure 5 and a photograph of the unit in Figure 6. The video amplifier is flat to eight megacycles, and down ten per cent at ten megacycles. A radio-frequency high voltage power supply delivers 29 kilovolts to the second anode of the kinescope. It should be mentioned that these tubes with the P11 phosphor have a high X-ray output at these voltages as compared with the 5TP4 at the same voltages, and that it is necessary to use more shielding than is evident in the photograph to safeguard personnel.

The deflection circuits follow conventional design. Provision is made to switch the direction of horizontal sweep in order to obtain a "dupe" negative emulsion position.

The camera is mounted on one end of a five-foot lathe bed isolated from the table with shock absorbers to absorb camera vibrations. The five-inch kinescope is mounted at the other end of bed. Isolation of the tube from vibrations transmitted through the lathe bed is accomplished by means of rubber shims around the deflection yoke and around the neck of the tube. The deflection chassis, the radio-frequency power supply, and the 285-volt regulated power supply are mounted on the lower shelf.

Sound Recording

Recording of the sound portion of a television program is done with standard 16-millimeter sound-on-film recording equipment operating with a synchronous drive at 24 frames per second. A switch operates both the motion picture cameras and the sound recorders simultaneously. Synchronizing marks are momentarily injected into both the sound and video channels by means of a remote switch. The marks are produced by a 420-cycle tone generated by an oscillator. The tone in the video channel produces bars in the kinescope image and an easily identified modulation of the sound track. The picture bars and the track tone are lined up for synchronization of the picture negative with the sound track negative.

Conclusion

A practical method of recording television programs, both sight and sound, has been developed. The recordings can be retransmitted through the television system with acceptable results. As the quality of the television image improves, the quality of recording in kinescope pho-

tography will be improved to a degree where the average viewer will be unable to tell if the program he is seeing is "live" or "canned." Certainly, these recordings made from wide-band channels available within the studio plant, unlimited by the restricted band width of the radio-frequency transmitter, will compare favorably with live programs as reproduced on the home television screen.

General References

G. L. Beers, E. W. Engstrom and I. G. Maloff, "Some Television Problems from the Motion Picture Standpoint", *Jour. Soc. Mot. Pic. Eng.*, Vol. 32, No. 2, February, 1939.

C. F. White and M. R. Boyer, "A New Film for Photographing the Television Monitor Tube", *Jour. Soc. Mot. Pic. Eng.*, Vol. 47, No. 2, August, 1946.

DEVELOPMENTS IN LARGE-SCREEN TELEVISION*†

By

RALPH V. LITTLE, JR.

RCA Victor Division,
Camden, N. J.

Summary

An experimental large-screen program is being carried on to determine the requirement for theater use. The governing factors: the light source, the optical system, and the screen are discussed. Photographs show equipment built for an experimental program.

(10 pages: 10 figures)

* Decimal Classification: R583.5.
† *Jour. Soc. Mot. Pic. Eng.*, July, 1948.

PHOTOMETRY IN TELEVISION ENGINEERING*†

By

D. W. EPSTEIN

RCA Laboratories,
Princeton, N. J.

Summary

This introduction to fundamental photometric concepts and measurements provides an understanding of principles and methods whereby performance of television receivers may be evaluated. Quantities needing measurement and their interrelations are explained.

(4 pages; 2 figures)

* Decimal Classification: R583.1.
† *Electronics*, July, 1948.

PLANNING RADIO AND TELEVISION STUDIOS*†

By

GEORGE M. NIXON

National Broadcasting Company,
New York, N. Y.

Summary

The problem of properly locating a television or radio studio is considered in relation to cast, convenience and technical aspects. The physical construction of studios is treated in detail, with emphasis being placed on acoustic insulation.

(12 pages; 22 figures)

* Decimal Classification: R583.3.
† *Broadcast News*, December, 1948.

TECHNICAL ASPECTS OF TELEVISION STUDIO OPERATION*†

By

R. W. Clark and H. C. Gronberg

Television Department, National Broadcasting Company, Inc., New York, N. Y. and Washington, D. C.

Summary

This article describes the operating procedures employed in a television studio for the presentation of a live talent program. It is divided into two parts, one covering the operation of the technical equipment and the other describing the improvements that have been incorporated in the equipment as a result of operating experience. This latter section includes discussion of camera dollies, lighting, microphones, microphone boom, iconoscope cameras, dialogue equalization, audio perspective, transcription turntables, communication and cue systems, and the control room.

(18 pages, 12 figures)

* Decimal Classification: R583.2 × R583.3.

† *RCA Review*, December, 1947.

THEATER TELEVISION — A GENERAL ANALYSIS*†

By

Alfred N. Goldsmith

Radio Corporation of America, New York, N. Y.

Summary

Excellent engineering progress has been made in the development of equipment and methods for the exhibition of television pictures in theaters. Considerable thought has been devoted to types of acceptable programs for theater television. However, the final design of commercial television equipment for theaters is not yet available, nor are proved and acceptable program methods as yet clearly defined.

Accordingly, theater television may be regarded at present as being, in some respects, in a partly developed state. Considering this situation, the following analysis is perforce a descriptive report, as of today. It contains as well as some analytical discussions of possible future trends. But the data and conclusions are of necessity subject to revision as further progress in theater television brings forth new methods and offers greater capabilities in this highly interesting field.

(27 pages)

* Decimal Classification: R583.

† *Jour. Soc. Mot. Pic. Eng.*, February, 1948.

SENSITOMETRIC ASPECT OF TELEVISION MONITOR-TUBE PHOTOGRAPHY*†

By

F. G. Albin

RCA Victor Division,
Hollywood, Calif.

Summary

The performances of the iconoscope and orthicon pickup tubes and kinescope monitor tubes constituting a television system are considered in regard to the response versus level characteristics. A nonlinear electrical network is advocated for combination with the iconoscope to equalize the gamma variations to a constant gamma approximately complementary with the monitor-tube gamma. Another nonlinear electrical network is advocated for combination with the orthicon to reduce the gamma of this camera to the same gamma as the corrected iconoscope camera.

A direct positive photographic technique is described using a negative monitor picture obtained by electrical phase reversal, and the toe region of the positive film characteristic. A general mathematical expression for the shape of the film toe as a function of the gammas of the television camera and monitor as required for linear over-all performance is derived.

The merits of such a photographic technique are economy, simplicity, rapidity of processing, and greater average screen brightness.

(18 pages; 6 figures)

* Decimal Classification: R583.1.

† *Jour. Soc. Mot. Pic. Eng.*, December, 1948.

OPTICAL PROBLEMS IN LARGE-SCREEN TELEVISION*†

By

I. G. Maloff

RCA Victor Division,
Camden, N. J.

Summary

Optical problems in large-screen television are enumerated and present-day solutions of these problems are discussed. Details of one prewar and two postwar models of RCA large-screen projectors are described.

(7 pages; 8 figures)

* Decimal Classification: R583.5.

† *Jour. Soc. Mot. Pic. Eng.*, July, 1948.